ISBN 978-82-471-4665-1 (printed version)
ISBN 978-82-471-4666-8 (electronic version)
ISSN 1503-8181

Jan Lindgård

Doctoral Thesis

Doctoral theses at NTNU, 2013:269

NTNU
Norwegian University of Science and Technology
Thesis for the degree of Philosophiae Doctor
Faculty of Natural Sciences and Technology
Department of Materials Science and Engineering

NTNU – Trondheim
Norwegian University of
Science and Technology

NTNU

Doctoral theses at NTNU, 2013:269

Jan Lindgård

Alkali-silica reaction (ASR) - Performance testing

NTNU – Trondheim
Norwegian University of
Science and Technology

Jan Lindgård

Alkali-silica reaction (ASR) – Performance testing

Thesis for the degree of doctor philosophiae

Trondheim, October 2013

Norwegian University of Science and Technology
Faculty of Natural Sciences and Technology
Department of Materials and Science Engineering

NTNU
Norwegian University of Science and Technology

Thesis for the degree of doctor philosophiae

Faculty of Natural Sciences and Technology
Department of Materials and Science Engineering

ISBN 978-82-471-4665-1 (printed ver.)
ISBN 978-82-471-4666-8 (electronic ver.)
ISSN 1503-8181

Doctoral Theses at NTNU, 2013:269
IMT-Report 2013:183

Acknowledgements

This PhD study has been performed at SINTEF Building and Infrastructure. Formally it has been connected to NTNU, department of Materials Science and Engineering, Faculty of Natural Sciences and Technology. The project is part of COIN, the COncrete INnovation centre (www.coinweb.no). I would like to acknowledge COIN and Norcem (part of Heidelberg) for the financial support to the work.

During the PhD study, several persons have given valuable support. First of all I would like to thank the positive staff at our concrete laboratory (Knut, Chris, Stig, Erik and Roger). Without their good support, the comprehensive laboratory program could not have been carried out. Improvement of laboratory testing methods needs active participation from experienced technicians. The good exactness of the measurements executed is also a premise to obtain reliable results and to perform a trustworthy parameter study. Their assistance is greatly appreciated, as well as the valuable experience transferred from Per Arne during the first part of the laboratory testing. Thanks also for the help with the measurements of alkali leaching (Kristin, Bente and Tone) and RH (Marius), the structural analyses and the petrographic analyses (Marit), the image analyses (Nelia Castro, NTNU) and the SEM analyses (Morten Raanes, NTNU). I am also thankful for the preparation of the thin sections at NTNU (Arild Monsøy) and the plane polished sections at VBM Laboratoriet (Klaus Haugsted), all with excellent quality. The RILEM AAR-2 testing and the chemical analysis of the cements performed by Norcem in Brevik are also appreciated.

My supervisors in the PhD study have also given invaluable support. In particular I am very grateful for professor (retired) Erik J. Sellevold's hospitality, great enthusiasm and "clear head" during all the discussions we have had at his kitchen table. The same goes for professor Mike D.A. Thomas's willingness to share his knowledge and experience in the field of ASR during our fruitful meetings in Texas, Canada, Iceland, England, the Azores, Switzerland and Norway. Special thanks to professor Harald Justnes for his contributions with respect to the "chemical part" of the study, and to my colleague Klaartje De Weerdt for her encouraging assistance during the courses I took at NTNU.

I am very grateful for the contributions from the co-authors of the six papers constituting the main part of the PhD thesis: Mike D.A. Thomas (paper III, IV, V and VI), Terje F. Rønning (paper II, III, IV and V), Bård Pedersen (paper II, IV and V), Erik J. Sellevold (paper IV and V), Özge Andiç-Çakır (paper III and V), Harald Justnes (paper IV and V), Marit Haugen (paper I and VI), Philip J. Nixon (paper I), Ingmar Borchers (paper I), Bjørn Schouenborg (paper I), Børge J. Wigum (paper I), Urban Åkesson (paper I), Sigrun K. Bremseth (paper II), Per A. Dahl (paper II), Isabel Fernandes (paper III) and Nelia Castro (paper VI).

I would like to give special thanks to my two sons, Anders and Øyvind, who have given me invaluable help during several "summer holidays" with development of work sheets, plotting laboratory data and preparing result tables and figures. Without their assistance, I have had to spend many more months on processing all the laboratory results. Finally, I would like to thank all my friends at SINTEF for an excellent collegiate relationship during my PhD Study and my wife for taking care of the home during my study.

Trondheim May 2013, Jan Lindgård

Abstract

Whether or not concrete prism tests developed for assessment of alkali-silica reactivity of aggregates is suitable for general ASR performance testing of concrete has been evaluated. The work has been part of the Norwegian COIN program (2007-2014), and has been performed in co-operation with the "performance testing" task group of RILEM TC 219-ACS. Thus, the RILEM aggregate concrete prism tests (CPTs) form the basis for the laboratory program.

As a foundation for the experimental work, an introductory study focused on the following:

- Summary and assessment of the main findings in the EU "PARTNER" project (2002–2006), in which the author participated actively.
- Summary and discussion of the experience gained from more than 15 years of performance testing in Norway.
- A comprehensive literature review, with the main objective to assess how various parameters might influence the laboratory/field correlation with respect to ASR performance testing.

Based on the introductory work, the experimental part of the study focused on the effect of specimen "pre-treatment", "ASR exposure conditions" and prism size on:

- Porosity and internal moisture state of the concrete prisms.
- Concrete transport properties (with respect to mobility of water and ions).
- Alkali leaching (rate and amount) from the concrete prisms during the ASR exposure.
- Concrete prism expansion (rate and ultimate expansion).

Additionally, the effect of water-to-cementitious-materials ratio (w/cm) and type of binder have been assessed.

The results clearly show that parameters of importance for the development of ASR are significantly influenced by the specimen "pre-treatment", "ASR exposure conditions" and prism cross-section. Most test conditions included are representative test procedures used in various "commercial" CPTs. The extent of the impact depends on the concrete quality, i.e. w/cm ratio and cement type. Consequently, the conclusion from a concrete performance test will differ depending on the test procedure used.

Generally, a high fraction of the in-mixed alkalis was leached out of the concrete prisms during the ASR exposure. In fact, the rate of alkali leaching during the first weeks of exposure is the parameter found to have the highest impact on the development of ASR expansion. When exposed to 60°C, it completely controls the prisms expansion. However, a modified test procedure was developed (cotton cloth with added alkalis) in the study which might be a promising tool to mitigate alkali leaching during accelerated laboratory testing.

For less permeable concretes, with a high degree of self-desiccation, the lower internal RH for the 38°C test series contributes together with the lower rate of diffusion to reduce the rate and extent of ASR.

The main part of the thesis is the papers enclosed. However, the summary gives an overview of the work and the main findings. Furthermore, some supplementary results are included together with an overview of a follow-up project initiated based on the results of the PhD study. The thesis also gives some general recommendations for performance testing.

Contents

List of enclosed papers

The main part of the PhD thesis is the following six papers enclosed in Appendix 1:

Paper I: J. Lindgård, P.J. Nixon, I. Borchers, B. Schouenborg, B.J. Wigum, M. Haugen, U. Åkesson, The EU "PARTNER" Project - European standard tests to prevent alkali reactions in aggregates: Final results and recommendations, Cement and Concrete Research, 40 (2010) 611-635.

Paper II: J. Lindgård, B. Pedersen, S.K. Bremseth, P.A. Dahl, T.F. Rønning, Experience using the Norwegian 38°C concrete prism test to evaluate the alkali reactivity of aggregates, concrete mixes and binder combinations, Nordic Concrete Research, 42 (2010) 31-50.

Paper III: J. Lindgård, Ö. Andiç-Çakır, I. Fernandes, T.F. Rønning, M.D.A. Thomas, Alkali–silica reactions (ASR): Literature review on parameters influencing laboratory performance testing, Cement and Concrete Research, 42 (2012) 223-243.

Paper IV: J. Lindgård, E.J. Sellevold, M.D.A. Thomas, B. Pedersen, H. Justnes, T.F. Rønning, Alkali-silica reaction (ASR) - Performance testing: Influence of specimen pre-treatment, exposure conditions and prism size on concrete porosity, moisture state and transport properties, Cement and Concrete Research 53 (2013) 145-167.

Paper V: J. Lindgård, M.D.A. Thomas, E.J. Sellevold, B. Pedersen, Ö. Andiç-Çakır, H. Justnes, T.F. Rønning, Alkali-silica reaction (ASR) - Performance testing: Influence of specimen pre-treatment, exposure conditions and prism size on alkali leaching and prism expansion, Cement and Concrete Research 53 (2013) 68-90.

Paper VI: J. Lindgård, M. Haugen, N. Castro, M.D.A. Thomas, Advantages of using plane polished section analysis as part of microstructural analyses to describe internal cracking due to alkali-silica reactions, in: T. Drimalas, J.H. Ideker, B. Fournier (Eds.) 14th International Conference on Alkali-Aggregate Reactions in Concrete, Austin, Texas, 2012.

Jan Lindgård has written the major part of all the papers. However, several co-authors contributed with a significant portion of the text to paper I and III. See the acknowledgement with respect to other contributions.

1 Introduction

1.1 Short introduction to alkali-silica reaction (ASR)

Several aggregate types in common use, particularly those with a siliceous composition, may be attacked by the alkaline pore fluid in concrete (the pH in the concrete pore water is normally in the range of 13.2-14.0). The attack, which essentially is a dissolution reaction where silica (SiO_2) is dissolved from the "alkali-silica reactive aggregates", requires a certain level of moisture and alkalis (Na^+ and K^+) within the concrete to take place. If the aggregate composition is "non-reactive" or the moisture state is too low or the pH of the pore water is below a critical limit ("alkali threshold"), no ASR will take place. During the reaction, a hygroscopic alkali-silica gel is produced (Figure 1). The overall expansion and cracking of the concrete is basically caused by sorption of water by the alkali–silica gel, which in turn swells and thereby causes the damage (Figure 2). The deterioration mechanism is denoted alkali–aggregate reaction (AAR) or, more specifically, for siliceous aggregates, alkali–silica reaction (ASR). The less common, so-called alkali–carbonate reaction (ACR), is not discussed further in this thesis. The ASR reaction mechanisms and the importance of various parameters are comprehensively discussed in paper III.

Figure 1. Alkali-silica gel present in an air void and in the interface between an aggregate particle and the cement paste in a concrete core drilled from a Norwegian dam structure.

Figure 2. Typical map cracking on the surface of a concrete foundation with alkali-silica reaction (ASR).

The reactivity of various aggregate types varies a lot depending on several factors [1]. Consequently, the time before damage is recognized on a concrete structure differs. Increased exposure temperature will also contribute to increase the rate of reaction. In the EU "PARTNER" project (paper I), the reactivity of the aggregates was divided into the following classes:

- "Non-reactive" aggregate combinations.
- "Fast" to "normally" reactive aggregate combinations *(damaging reactions occurring after 5 to 20 years. The terms “highly” or “rapidly” reactive aggregates are also frequently used in the literature instead of "fast" reactive).*
- ”Slowly” reactive aggregate combinations *(damaging reactions occurring after +15–20 years. Most Norwegian alkali-reactive aggregates belong to this group).*

1.2 Importance of the internal moisture state and the alkali content of the pore water

1.2.1 Moisture state

As stated above, moisture is generally accepted to be one of the main parameters affecting ASR. A comprehensive study looking into the influence of the moisture state on the extent of damage due to ASR was performed by Nilsson and Peterson in 1983 [2]. As they summarize, water is firstly a solvent for dissolved ions that takes part in the reaction. Secondly, water is a transport medium for these ions. Thirdly, water is important in the expansion stage where the ASR gel absorbs water and swell.

Most scientists seem to use relative humidity (RH) as the only measure of moisture state of the concrete in connection with ASR. RH describes the thermodynamic state of the pore water at a certain temperature, and is not a direct measure of the amount of water. At a given moisture content (e.g. expressed as weight-% water), the RH is a function of the pore structure (i.e. water-to-cement ratio, w/c), the temperature, the chemical composition of the pore water and the moisture history of the concrete. The relationship between the RH and the water content is given as absorption/desorption isotherms. High performance concrete (HPC) will normally have a limited content of capillary pores. One consequence of this, as discussed by Nilsson [3] and Relling [4] (see Figure 3), is that the degree of saturation of the concrete pores is always higher for a HPC at a given RH. Opposite, for a given saturation, the internal RH will always be lower in a HPC compared with a concrete with higher w/c. Furthermore, Nilsson [3] showed that also the cement type will influence the absorption/desorption isotherms, partly due to the influence on the alkalinity of the pore water (more alkalis dissolved will reduce the RH, maybe up to 5 % as shown by Hedenblad [5]) and partly due to different pore size distribution (that will influence the slope of the isotherm).

RH is easy to measure, also in situ and over time. However, such measurements require much care and experience to be meaningful. Many sources of errors exist, where temperature difference between the sensors and the concrete often is the cause of unreliable results [6]. One consequence of this is that RH measurements in the field are notoriously uncertain. A method that has shown to give more reliable results (frequently used at the University of Lund in Sweden for many years [7]) is to collect samples in the field (by drilling or sawing – but care must be taken during sampling for taking them to the laboratory in an "undisturbed" condition), split or crush the samples into smaller pieces, crush the pieces with a hammer and put them into slim glass tubes. Subsequently, a RH sensor is put into the glass tube before sealing it (this method was also used in this study for measuring the RH in the concrete prisms – paper IV). Thus, the RH can be performed under controlled and constant temperature (isothermal conditions). However, due to the influence of the temperature on the RH, corrections to the measured RH can be made to recalculate to the temperature in the structure in which the samples were collected from [6].

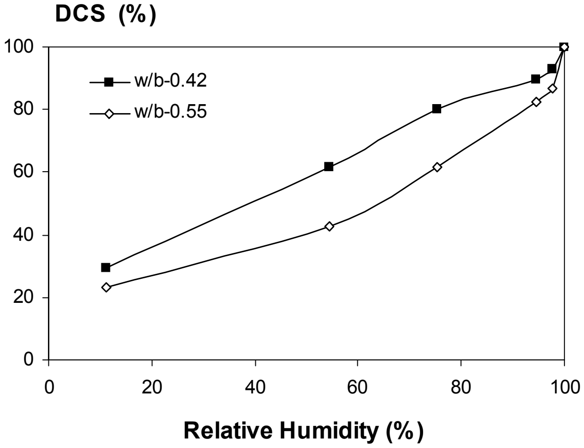

Figure 3. Desorption isotherms for concrete discs by the degree of capillary saturation (DCS) as a function of RH for two laboratory concretes of different w/c-ratio. (The concrete with w/c-ratio = 0.42 contained 5 % silica fume). From Relling (1999) [4].

Several researchers have performed tests with aim to detect the critical RH limit for initiating ASR, i.e. a limit in which ASR will not take place if the RH in the concrete is below this limit; Lenzner&Ludwig (1978) [8], Nilsson&Peterson (1983) [2], Ólafsson (1986) [9], Kurihara&Katawaki (1989) [10], Tomosawa et al. (1989) [11], Stark (1991) [12]. In these studies, mortar bars or concrete prisms are stored in various RH for a long time, and the expansion is measured periodically. It should be noted that the internal RH in the prisms is certainly not equal to the external environment, because a very long time is needed to reach equilibrium. In most studies, the critical limit for initiating ASR is reported to lie in the range of 80–90 % RH depending on several factors, among these the temperature (higher critical limit if the temperature increase) and the type of aggregate. However, in spite of this basic uncertainty, in general a critical lower limit of 80 % RH has been most frequently stated in the literature. Consequently, ASR must be taken into account for all outdoor concrete structures (that normally will have RH > 80 % in the interior, see for example Stark (1991)) and indoor concrete structures exposed to high humidity or water.

Furthermore, some studies have been performed with aim to find a possible "pessimum RH limit", i.e. if is exists a RH limit between the critical limit for initiating and sustaining ASR and 100 % RH in which the extent of ASR and/or the expansion is most severe, i.e. the swelling pressure of the ASR gel is maximum. For example showed Nilsson and Peterson (1983) [2] that RH close to 90 % at 20°C caused the most pop-outs in concrete floors when using aggregates from the Scania area (in the south west of Sweden) containing opaline flint and sandstone. They explained that if the humidity becomes too high, the viscosity of the ASR gel would be so low that the gel penetrates the cement paste without causing any expansion or pop-outs. By measuring water absorption of synthetic gels, Krogh (1975) [13] found a pessimum RH limit of about 90 % with respect to swelling of the gel.

Contradictory, most other laboratory studies have shown that the ASR expansion increases with increasing RH up to 95-100 %; Lenzner&Ludwig (1978) [8], Gudmundsson and Asgeirsson (1983) [14], Ólafsson (1986) [9], Chatterji et al. (1986) [15], Kurihara&Katawaki (1989) [10], Tomosawa et al. (1989) [11], Stark (1991) [12], Larive et al. (2000) [16]. This behaviour is principle illustrated in Figure 4.

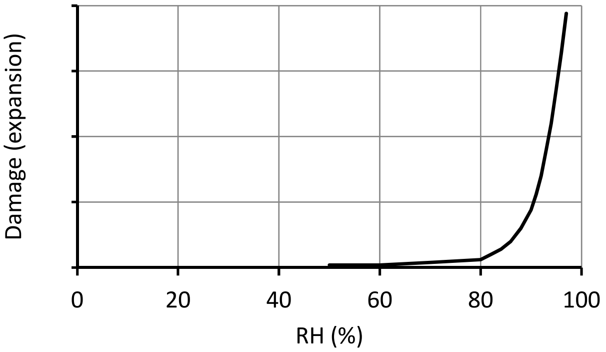

Figure 4. Principle illustration of the relation between RH and damage due to ASR.

Also some field surveys including RH measurements have shown that increased access to moisture will lead to more damage. For example measured Blight (1991) [17] RH above 97 % for the concretes cracked due to ASR. As Blights comments, the RH could have been lower when ASR initiated, but then later increased due to ASR (mainly because the alkali-silica gel will absorb water). Jensen (2000) [18] also found the most intensive map cracking in areas on bridges and dams where the RH was high, in the range of 93-100 %.

(Comment: As discussed later in this summary, the development of ASR is highly influenced by the alkali content of the concrete pore water. Knowing that increased access to water leads to more alkali leaching from concrete samples during laboratory testing, there is a "balance" between the possible increased expansion due to access to more water and the possible reduced expansion if more alkalis are leached out of the concrete. Some of the studies reported in the literature are assumed to be influenced by this fact).

In a review performed by Pedersen (2004) [19], he concluded that the relationship between the moisture state and expansion/cracking due to ASR is not well known. He also discussed whether the amount of water (expressed as mass-%) and/or the degree of capillary saturation (DCS) [20] might be more relevant parameters to describe the in situ moisture state if it is the amount of water that controls the ASR expansion. DCS expresses the % filling of the pores in concrete that are able to draw in water by capillary action (i.e. gel and capillary pores; not air entrained pores or voids). Measurement of DCS on samples cut from structures is done by weighing the samples immediately after unwrapping in the laboratory, after immersion in water for about 7 days and after drying at 105°C (paper IV). DCS measurements, in contradiction to RH measurements, are easy to perform accurately, but they are destructive and more cumbersome to do, involving cutting samples from the structure and taking them to a laboratory in an “undisturbed” condition. Thus, much care must be taken during sampling.

Based on a survey of a large number of Norwegian concrete bridges, Lindgård et al. [21] showed a rather good correlation between the presence of ASR and the DCS, see Figure 5. With only a few exceptions, the DCS of the concrete structures with pronounced ASR was higher than 90 %. The extent of damages generally increased with increasing water content above this level. They found that the extent of map cracking is considerably higher in structure members with abundant water supply compared with members periodically exposed to rain. For structure members totally sheltered from water/rain, normally no damaging ASR is found. This finding is in agreement with

Larive et al. (2000) [16] that states that the more water, the more severe is the degradation of the structure.

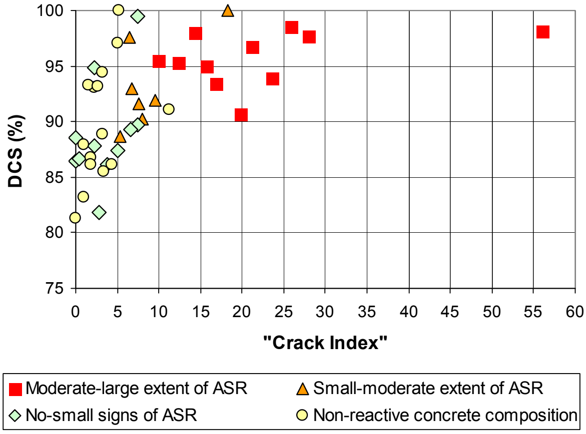

Figure 5. *Relation between the degree of damage in drilled concrete cores (expresses as increased "Crack Index) and the degree of capillary saturation (DCS). From Lindgård et al. (2006) [21].*

1.2.2 *Alkali content*

The main source of alkalis (Na^+ and K^+) to the concrete is normally the cement. Possible other sources might be alkali release from certain aggregate types or any ingress of alkalis from the surroundings, for example from de-icing salts (paper III). When Portland cement is mixed with water, the alkali sulphates go rapidly into the liquid phase converting to alkali hydroxides, thus increasing the hydroxyl ion concentration (i.e. the pH increases). Alkalis locked into the crystal structures of clinker minerals become available as the hydration proceeds [22]. Consequently, the alkali release rate varies from one cement type to another, depending on the distribution of alkalis between rapid-release and slow-release sources, and on the total alkali content in the cement. From early mortar bar studies, Hobbs [23] stated that considerably varying expansion results observed for mortars with various cements but with similar total alkali contents (kg/m^3) might be attributed to different alkali release rates of cements, variations in sodium/potassium ratio and different rates of strength development.

In order to assess the total content of available alkalis present in cement or concrete, it has become standard practice to express the alkali content in terms of “sodium oxide equivalent”: Na_2O_{eq}=Na_2O+ 0.658 K_2O (in weight percent). The more alkalis present in the concrete pore water, the higher is the pH (because more hydroxyl ions (OH^-) will be dissolved to balance the increased alkali content) and the more silica might be dissolved from the aggregates. Low-alkali cements and supplementary cementitious materials (SCMs; e.g. silica fume, fly ash, ground granulated blast furnace slag (ggbs), metakaolin and other pozzolans) are frequently used to allow alkali-silica reactive aggregate combinations to be used in concrete without damage. SCMs are known to control ASR expansion mainly by their capability to reduce the alkalinity of the pore solution by binding alkalis in the hydration products [24]. SCMs with a high (reactive) silica content and a low amount of CaO and alkalis will be the most effective [25]. Since the alkali reactivity of various aggregates varies greatly, no general “safe” lower concentration of hydroxyl ions in the pore solution can be stated. However, in the literature, this limit is reported by several authors to lie in the range of 200–300 mmol/l [1]. These OH^- concentrations correspond to pH-values in the range of approximately 13.3–13.5.

1.3 Development of reliable ASR performance test methods

The efficiency of SCMs depends on their characteristics and amount, the nature of the reactive aggregate and the availability of alkalis in the concrete. Consequently, to be able to utilise alkali–silica reactive aggregates (which constitute invaluable resources) for production of durable concretes, the effects of various measures must be correctly identified by accelerated laboratory performance tests (or ideally by relevant long-term field experience). Several performance tests have been used worldwide for at least 15 years. In principle, two groups of ASR performance test methods exist, one using mortar bars and the other using concrete prisms. However, the test conditions (e.g. temperature, alkali content, humidity) differ from one test method to another. Thus, the results and conclusions from different test methods may vary widely. *(Comment: The terms "ASR performance testing" and "ASR performance tests" are used frequently in this thesis and in some of the literature referred to. However, frankly speaking, a more precise term would have been "testing of expansion due to ASR as a performance test", since the measured expansions in the laboratory testing are taken directly as a measure of the assumed performance of the tested concrete in field. Of course this is a huge simplification, since the performance of a concrete in field among others will vary with type of structure, structural design, environment, exposure conditions and designed service life. Furthermore, the laboratory/field correlation for the various test procedures must also be taken into account, as is one of the aims of the follow-up study described in section 7).*

In 2006, Thomas et al. [26] provided a critical evaluation of different ASR performance test methods. One main problem reported for the Canadian concrete prism test (similar to ASTM C1293 - section 3.1) is that alkalis are leached out of the prisms during exposure in the humid environment and hence reduce the ultimate prism expansion. Another is the duration of some of the test methods (2 years). The authors concluded that none of the currently available or commonly used test methods meet all the criteria for an ideal performance test, which should be:

- rapid (calling for accelerated test conditions).
- capable of determining the “critical” alkali content for specific aggregates (i.e. the alkali leaching problem must be solved).
- capable of assessing all types of SCMs, lithium compounds and combinations of SCM and lithium, with cements of different alkali levels.
- suited to test job mixes identical to the concrete composition that will be used on actual projects (use of mortar bars is in conflict with this requirement).

As discussed in paper III, the development of accurate and reliable performance test methods for the production of durable concretes is a challenge. However, most of the currently used performance test procedures are simply adopted from the procedures used for assessment of the alkali-reactivity of aggregates. One example is the Norwegian 38°C concrete prism test (CPT) [27]. But, during assessment of aggregates, the alkali content of the mixture is normally boosted up to a high level. Consequently, the expansion is less influenced by alkali leaching during the exposure (the alkali content in the concrete will still be relatively high).

Research is thus on-going in several countries with the aim to improve current ASR performance test methods, develop alternative tests and document the reliability of the tests. The latter includes benchmarking of the test methods against real concrete structures or, as a surrogate, against large concrete blocks exposed outdoors to natural weathering conditions. As part of the international harmonization of ASR performance test methods, the "Performance testing" task group of RILEM TC 219-ACS (chaired by Terje F. Rønning, Heidelberg/Norcem, assisted by the author) is working on a performance testing concept aiming to develop one or more reliable ASR concrete performance test methods that might cover several applications/areas, ranging from combination of various aggregates with a standard CEM I binder up to the "ultimate goal" to document the alkali reactivity of any concrete mixture proportion.

1.4 PhD study – main focus

Whether or not concrete prism tests developed for assessment of alkali-silica reactivity of aggregates is suitable for general ASR performance testing of concrete has been evaluated. The work has been part of the Norwegian COIN program (2007-2014, www.coinweb.no), and has been performed in co-operation with the "performance testing" task group of RILEM TC 219-ACS. Thus, the RILEM aggregate concrete prism tests (CPTs) form the basis for the laboratory program

As a foundation for planning the experimental part of the PhD study and assessing the results, the introductory part of the study focused on the following:

- Summary and assessment of the main findings in the EU "PARTNER" project (2002–2006), in which the author participated actively (paper I) – section 2.1.
- Summary and discussion of the experience gained from more than 160 performance test series with the Norwegian CPT [27] (paper II) – section 2.2.
- A comprehensive literature review, with the main objective to assess how various parameters might influence the laboratory/field correlation with respect to ASR performance testing, either directly or indirectly (paper III) – section 2.3.

Based on the introductory work, the experimental part of the study focused on the effects of specimen "pre-treatment", "ASR exposure conditions" and prism size on:

- Porosity and internal moisture state of the concrete prisms.
- Concrete transport properties (with respect to mobility of water and ions).
- Alkali leaching (rate and amount) from the concrete prisms during the ASR exposure.
- Concrete prism expansion (rate and ultimate expansion).

Additionally, the effect of water-to-cementitious-materials ratio (w/cm) and type of binder have been assessed. In addition to the two Portland cements (CEM I), only one other binder with added SCM is included; a blended fly ash cement (CEM II/A-V) with approximately 20 % fly ash.

The term specimen "pre-treatment" includes the moisture conditions during pre-storage and the length of the pre-storage period at ambient temperature before taking the initial (zero) length measurements and exposing the prisms to elevated temperature. These conditions vary for various ASR CPTs used in different countries.

Also the "ASR exposure conditions" (i.e. moisture conditions, type of container, prism size, use of any wrapping, storage temperature, length of the storage period and addition of any external alkalis) might vary between various ASR test methods (section 3.1).

From an overall scientific point-of-view, the main aims of the study are:

- To assess how various parameters influence the laboratory/field correlation with respect to ASR performance testing, either directly or indirectly (paper III). *(Comment: Important input to the work in the "performance testing" task group of RILEM TC 219-ACS).*
- To quantify the rate and extent of alkali leaching depending on the exposure conditions (test procedure), the prisms size and the concrete composition.
- To document the effects of the rate and extent of alkali leaching on the prism expansion, and thus document the possible consequences of using various "commercial" CPTs (with, sometimes relatively small, diverging test details) for performance testing *(Comment: Even though the effect of alkali leaching has been known for a very long time, this source of error has not previously been an issue for research in most European countries. RILEM has not taken the alkali leaching problem into consideration in the draft RILEM CPTs AAR-3 (2000) [28] and AAR-4.1 (2006) [29]).*

- To increase the knowledge about the influence of the test details and the concrete composition on the internal moisture state of the test prisms, expressed by the RH and the DCS. *(Comment: One important question is whether the various test details are able to supply the volume of the concrete prisms with sufficient moisture for ASR to develop. This is a particularly relevant question when testing concretes with a high degree of self-desiccation, for example concretes with low w/c and/or high dosages of SCMs. This topic is a question of debate in the "performance testing" task group of RILEM TC 219-ACS).*
- Contribute to increase the knowledge about the influence of the internal moisture state on the ASR prisms expansion. *(Comment: Since the majority of the ASR literature claims that increased moisture state will increase the prism expansion, most ASR test procedures aims to give the prisms as much moisture as possible (i.e. close to 100 % RH by storing the prisms on grids over water; but of course not submerge the prisms in water due to the high extent of alkali leaching that would have been the result). In the test setups used in this study, most test procedures produce an environment inside the storage containers close to 100 % RH (section 3.2 and paper IV). Consequently, the laboratory program does not aim to document the critical RH for ASR to develop for the concrete compositions included, neither detect any "pessimum RH" (section 1.2.1). Furthermore, since the exposure temperature and the binder composition will influence the rate of diffusion and most likely the rate and extent of alkali leaching, it is not possible based on this study to sort out the pure influence of the internal moisture state on the development of ASR and on the ASR expansion).*

1.5 Outline of the thesis

The main part of the PhD thesis is the 5 published journal papers (I-V) enclosed in Appendix 1. Most results from the comprehensive laboratory program are presented and summarized in the papers IV and V. Furthermore, paper VI discusses the internal cracking in the concrete prisms after ending the ASR exposure. This latter paper is included in the proceedings from the 14th ICAAR in Texas in 2012.

This summary of the thesis (i.e. page 1-24);

- gives a short introduction to ASR, and discusses the importance of the internal moisture state and the alkali content of the pore water for development of ASR (section 1)
- gives the background and the objectives of the study (section 1)
- summarizes some important findings from the introductory part of the study (section 2)
- gives an overview of the test methods used and the modifications done with the various ASR test methods (section 3)
- gives an overview of the full laboratory test program (section 4)
- summarizes the most important findings in the comprehensive laboratory testing performed (section 5)
- gives recommendations for performance testing (section 6 plus Appendix 4)
- describes the follow-up project that has been initiated in response to the findings in this study (section 7 plus Appendix 5 and 6)

Furthermore, a brief description of some supplementary test methods and corresponding results (not included in any of the papers) are enclosed in Appendix 2 and 3, respectively, together with some detailed results not included in paper IV or V (Appendix 3).

2 Summary of the introductory part of the PhD study

2.1 The EU "PARTNER" project (paper I)

Paper I summarizes and assesses the main findings in the EU PARTNER Project (2002–2006) providing the basis for a unified European test approach for evaluating the potential alkali-reactivity of aggregates. The project evaluated the tests developed by RILEM and some regional tests (in total 9 laboratory test methods, including the Norwegian CPT [27]) for their suitability for use with the wide variety of aggregates and geological types found across Europe. Additionally, field exposure sites were established in 8 locations across Europe to document the laboratory/field correlation. The project had 24 partners from 14 countries. 22 different types of aggregates from 10 different European countries were evaluated. Among these, 6 aggregate types were supplied from Norway, including the two reference aggregate types used in this PhD study (section 4.1: the non-reactive fine aggregate was labeled "N3" in the "PARTNER" project, while the reactive coarse aggregate was labeled "N1").

Unfortunately, in the main work package most aggregate combinations were only tested by a very few laboratories. Consequently, the evaluation of the reproducibility of the various test methods remains somewhat limited. However, in another work packages the precision of the four RILEM methods was investigated in a proper round-robin testing program.

It was found that in most cases the four RILEM test methods could successfully identify the reactivity of the aggregates tested. They were most successful with "normally" reactive and non-reactive aggregates (section 1.1), but with aggregates that react very slowly an extended test period may be necessary for some of the RILEM methods. Overall, of the four RILEM methods, the accelerated 80°C mortar bar test (AAR-2 [28]) and the accelerated 60°C concrete prism test (AAR-4.1, wrapped version) [29] seemed most effective to identify the potential reactive aggregates and to have the best precision. Moreover, these methods have the advantage of producing (relatively) rapid results. *(Comment: For most of the RILEM test methods included in the study, there is a lack of field experience necessary to establish reliable critical laboratory expansion limits. Thus, in this study, the preliminary expansion limits suggested by RILEM [30] was used to evaluate the effectiveness of the various test methods compared with the reported field experience. However, whether exposure temperatures above 38°C are able to reflect field behavior of all aggregate types is still debated among scientists, as discussed in the literature survey (paper III) and in section 2.3).*

The Norwegian CPT [27] behaved almost exactly like the RILEM AAR-3 CPT [28]; identifying the “normally” reactive aggregate combinations and non-reactive combinations effectively, but giving marginal results with some of the “slowly” reactive combinations.

The project also illustrated large differences between the laboratories. Where laboratories were carrying out procedures with which they were very familiar, for example the Norwegian CPT carried out by NORCEM and SINTEF, the expansion values were very close.

2.2 Experience from 15 years of performance testing in Norway (paper II)

The Norwegian CPT [27] has, since 1996, been specified in the Norwegian guidelines [31] for performance testing. Until 2010, about 160 performance tests had been performed by the two most experienced and approved Norwegian laboratories at SINTEF (119) and Norcem (42). These tests include “job mixes” (i.e. real concrete recipes) and mixes to determine the critical alkali limit for different aggregate types. However, most of the performance tests have aimed at documenting different binder combinations ability to prevent ASR (mainly blended cements with various fly ashes).

In these tests, reference reactive aggregates have been used, including the two reference aggregate types used in this PhD study (section 4.1).

The main objective with paper II is to discuss experiences gained from the 15 years period of performance testing, rather than presenting detailed results. The paper also describes the Norwegian system for approval based on performance testing. Furthermore, precision data for the Norwegian CPT [27] is given, as well as results from mass measurements (all test series) and measurement of alkali leaching during exposure of the concrete prisms (30 test series).

Some conclusions from the assessment of the results:

- Despite the long testing time required (1-2 years), the Norwegian system for performance testing has proven to be an advantageous and flexible tool to document critical alkali limits for binders and aggregates and to be able to utilize alkali reactive aggregates. Such aggregates may be found in most parts of Norway.
- The repeatability obtained at SINTEF for the Norwegian CPT is in general very good.
- In all parallel tests, SINTEF and Norcem produce results that are very close.
- The review strengthens the importance of using mass measurements as a quality control of the moisture conditions within the storage containers.
- From 0.1 to 0.9 kg Na_2O_{eq} alkalis per m^3 of concrete are leached out of the concrete prisms after one year of exposure (not including any alkalis absorbed by the lining inside the storage containers), representing 2-17 % of the initial concrete alkali content. Consequently, the possible influence of alkali leaching on the measured expansions cannot be neglected, even when rather large concrete prisms (100x100x450 mm) are used. *(Comment: As comprehensively discussed in paper V, the typical "time versus alkali leaching profile" is a relatively high rate of alkali leaching during the first months of exposure, followed by a reduced rate with time. However, for some of the test series presented in paper II, the rate of alkali leaching seems to increase again in the period after one year of exposure. A similar behaviour was also detected for a very few test series in the main test program of the PhD study (paper V). The main reason for this is believed to be uncertainties in the measurements (in particular with respect to volume of water) – see further discussion in paper V).*

2.3 Literature survey on performance testing (paper III)

On the initiative and under the leadership of the author, a comprehensive literature review was performed within the task group “Performance testing” in RILEM TC 219-ACS. In total, 12 authors contributed to the report that included about 250 references [32]. The main objective was to assess how various parameters might influence the laboratory/field correlation with respect to ASR performance testing, either directly or indirectly. In this report, the procedure established within the PhD study for sampling and measurements of alkali leaching is enclosed (section 3.3).

The most important findings in the literature survey and preliminary recommendations for performance testing have been summarized in paper III. The recommendations include precautions when testing various aggregates and binders, important factors to take into account during mix design, as well as possible influences on ASR expansion of various conditions during the pre-storage and the ASR exposure. Furthermore, the literature survey has identified several issues that need further research in order to develop a reliable performance test procedure. For example, it is recommended to investigate the net influence of a reduced w/cm further as the basis to agree on a possible lower w/cm limit for performance testing.

Three parameters detected to be of particular importance for the outcome of a performance test were the internal humidity in the test specimens, the extent of alkali leaching and the exposure temperature (*comment: an essential question is for example whether decreased reliability is the payment for increased acceleration by elevating the exposure temperature*). Consequently, these parameters have been focused on in the PhD laboratory program (section 1.4). *(Comment: A more comprehensive review of the importance of internal humidity on ASR expansion is included in section 1.2 of this summary).*

3 Test methods **(paper IV, V and VI)**

3.1 ASR concrete prism tests

The majority of the ASR testing was performed with the draft RILEM aggregate concrete prism tests, AAR-3, 2000 (38°C) [28] and AAR-4.1, 2006 (60°C) [29]. For comparison, additional test series with the Norwegian CPT [27] (38°C) and the ASTM C1293-08b CPT (38°C) [33] were included. The main reason for incorporating the latter method was to establish a link to the comprehensive experience in North America with this method (this method is one of the most frequently used methods for ASR testing worldwide) and to document any batch to batch variation (several concrete batches were needed to cast all the concrete prisms with the reference "basis" binder – section 4.2 and 4.3).

The main differences between the selected CPTs are exposure temperature (38°C or 60°C), prism-cross-section (100x100 mm or 70x70 mm) and use of any wrapping (moist cotton cloth and polyethylene). Only the Norwegian CPT [27] uses the larger prisms. Table 3 in paper IV gives a detailed summary of the various concrete prism tests, including recommended critical limits for acceptance.

3.2 Modification of the ASR concrete prims tests

The standard versions of the concrete prism tests have been slightly modified in order to investigate the effect on concrete properties important for development of ASR, extent of alkali leaching and ASR expansion. The test procedure for the ASTM C1293 CPT [33] was not modified, apart from the use of prisms with 70x70 mm cross-section and not the prescribed 75x75 mm (*comment: In spite of this, the term "ASTM prisms" is used in this thesis*). The motivation for the modifications is given in paper III. A summary of the modifications is given below. More details are given in paper IV and V.

During all the testing only de-ionised water has been used as mixing water, in the moist cotton cloth wrapping (if any) and in the storage containers.

For all test series, each prism was always stored vertically in the storage container with the same prism end pointing upwards. Thus, it is possible to document any variation in internal moisture state, amount of alkali leaching and extent of internal cracking over the prism height.

For all standard versions of the CPTs, the readings of mass and length were taken after cooling the prisms for about 16 hours inside their storage container in a room kept at 20°C. However, all readings in the modified versions of the various concrete prism tests were taken without cooling the prisms. To avoid any influence of reduction in the internal prism temperature during the measurements, a detailed measuring procedure was established (Appendix 2).

The following "pre-treatment" parameters and/or ASR storage conditions have been varied when modifying the RILEM CPTs (see paper IV, Figure 1 and Table 4, for details and motivation):

- The wrapping procedure (if any) was slightly modified.

- The length of the "pre-storage" period at 20°C was varied (1, 7 or 28 days). However, for all test series, the prisms were prepared for final storage (e.g. wrapped) and put into the storage container immediately after de-moulding (and after the 0.5 h submersion where used) and the initial measurements of mass and length.
- Some prisms were pre-cured for 24h at elevated temperature (60°C) to simulate the curing temperature in a massive concrete structure.
- Some prisms were sealed in epoxy and aluminium foil after de-moulding to avoid any exchange of water with the environment.
- Some prisms were stored submerged in de-ionised water (to maximize the alkali leaching conditions).
- Some prisms were wrapped with cotton cloth saturated with a basic solution of strength pH 14.2 or 13.2 (instead of using de-ionised water), in order to try to reduce the amount of alkali leaching.

Most test conditions are by no means extreme, but are representative for test procedures used in various "commercial" CPTs.

3.3 Accompanying test methods

In order to document properties of importance for development of ASR, comprehensive complementary testing has been an important part of the study. The following tests have been included (for some, the background for selecting the particular test is given in paper IV and V):

- Alkali release from the aggregates (new procedure established – Appendix 2 in this thesis)
- Alkali leaching (rate and amount) from the concrete prisms (new procedure established – paper V, section 2.4)
- Concrete porosity ("PF-method" [34] – paper IV, section 2.4.2)
- Moisture state (degree of capillary saturation (DCS) [20] and relative humidity (RH - Vaisala sensors) [35] – paper IV, section 2.4.3)
- Relative diffusion coefficient [36] (new procedure established – paper IV, section 2.4.4, and Appendix 2)
- Electrical resistivity [37] , [38] (paper IV, section 2.4.5, and Appendix 2)
- Visual inspection (including photo documentation – paper V, section 2.5.2, paper VI and Appendix 3)
- Microstructural analysis of polished sections (paper V, section 2.5.2, and paper VI) and thin sections (paper VI and Appendix 2) and scanning electron microscopy (SEM) analysis (paper VI and Appendix 2)
- Dynamic E-modulus (Appendix 2)

The documentation was performed at two points in time: four weeks after starting the ASR exposure (in order to document concrete properties in the early stages of the ASR tests) and after ending the ASR exposure, i.e. after 39 weeks (all 60°C test series), 52 or 112 weeks (38°C test series). Some tests were only performed at one of these points in time. The measurements of alkali leaching and dynamic E-modulus were performed at every reading of length and mass of the ASR prisms in order to document the evolution over time (*comment: not including the wrapped prisms*).

For all test series, the testing initiated after four weeks of ASR exposure were performed on an "extra prism" exposed to identical pre-treatment and ASR exposure conditions as the three parallel prisms in the same test series. The complementary testing performed after ending the ASR exposure were executed on one of the three parallel prisms in each test series.

4 Laboratory test program (paper IV, V and VI)

4.1 Materials

Two CEM I Portland cements (EN-197-1), one high alkali (1.24 % Na_2O_{eq}) and one low alkali (0.60 % Na_2O_{eq}), and a CEM II/A-V cement containing 21.6 % of a class F fly ash (co-grinded with the clinker) were used in the study (Table 1 in paper IV and V).

A fixed aggregate combination (coarse:fine ratio 60:40) was used in all the test series. The aggregates are defined in the Norwegian ASR regulations ([31], [27]) as “reference Norwegian aggregates” and consist of a non-reactive natural sand from Årdal, mainly containing granites and gneisses, and an alkali-silica reactive coarse aggregate, a crushed cataclasite ("Ottersbo") with crypto- to microcrystalline quartz. A lot of experiences exist with these two aggregate types during more than 20 years of ASR testing at SINTEF and Norcem (paper II). They were also included in the EU "PARTNER" project (section 2.1)

Density and water absorption of the aggregates are given in paper IV (section 2.2). The petrographic analyses [27] (enclosed in Appendix 3) and testing according to the RILEM AAR-2 80°C accelerated mortar bar test [39] confirm that the ASR properties of the aggregates are in accordance with previous experience. The 14-day expansion of the sand and the coarse aggregate in the RILEM AAR-2 test [39] (prism size 40x40x160 mm) was measured to be 0.03 % (non-reactive) and 0.30 % (reactive).

4.2 Mixture proportions

Details of the concrete mixtures produced are given in paper IV and V (Table 2). The bulk of the testing was produced on a mixture containing 400 kg/m^3 of Portland cement with a water-to-cement ratio (w/c) of 0.45. The two CEM I cements were blended to produce an alkali content of 3.7 kg/m^3 Na_2O_{eq}. The alkali content was chosen (based on previous testing of the aggregates at SINTEF – paper II) with aim to reach an ultimate expansion of the reference test series lying on the steep (ascending) part of the “expansion-versus-alkali-level (S-shaped) curve”, so that a small loss of alkalis due to alkali leaching would be detectable in terms of reduced expansion.

To examine the impact of w/c, two additional concrete mixtures were cast with w/c of 0.30 and 0.60. The cement contents of these mixtures were modified to achieve the desired workability, but the alkali content of the mixes was maintained at 3.7 kg/m^3 Na_2O_{eq} by appropriate blending of the CEM I cements. *(Comment: Even if the total alkali content of the three concrete mixtures is equal, the concretes differ in porosity, pore size distribution and content of evaporable water, and hence with respect to concentration of alkalis and pH in the pore water. The diffusion properties are also influenced, as discussed in paper IV. Therefore, it was decided to keep the alkali content fixed and not to attempt to adjust it according to some arbitrary factors for the different water-binder ratios. This is in accordance with standard practise in many national codes).*

One mixture was produced with w/cm = 0.45 using the blended fly ash cement. The alkali content of this mixture was raised from 5.0 kg/m^3 Na_2O_{eq} (including all alkalis in the clinker and the fly ash) to 9.0 (boosted with NaOH) to obtain an ultimate expansion of the "fly ash concrete mix" on the ascending part of the “expansion-versus-alkali-level curve”.

4.3 Test series

The comprehensive laboratory program includes a total of 58 ASR test series. 40 of these were performed by use of modified versions of the two RILEM aggregate CPTs, 6 with modified versions of the Norwegian CPT and 12 with the ASTM C1293 CPT (section 3.1 and 3.2). Paper IV gives an overview of all the test series (Tables 5-8) and the notations used to identify them (Figure 2).

5 Summary of findings in the laboratory testing (paper IV, V and VI)

5.1 General

The results from the comprehensive laboratory program are presented and discussed in detail in the papers IV and V. In the conclusion part of these papers, it is stated which test conditions and procedures (section 3.1 and 3.2) have a significant impact on parameters of importance for the development of ASR (i.e. internal moisture state, transport properties and alkali leaching), and thus the prism expansion. Furthermore, effects of various binder compositions and w/cm are discussed and some detailed recommendations for performance testing are given.

A summary discussion of the findings in paper IV is included in Appendix 3 *(comment: based on advice from the reviewer of paper IV, this summary discussion was removed from the first draft of the paper in order to shorten it)*.

The main findings in the laboratory testing are briefly summarized in section 5.2, while some conclusions from the complementary testing are given in section 5.3.

5.2 Main findings

5.2.1 Overall findings

The results clearly show that parameters of importance for the development of ASR are significantly influenced by the specimen "pre-treatment", "ASR exposure conditions" and prism cross-section. Most test conditions included are representative test procedures used in various "commercial" CPTs. The extent of the impact depends on the concrete composition, i.e. w/cm and cement type.

Consequently, the conclusion from a concrete performance test will differ depending on the test procedure used. This is evident looking at the expansion curves in Figure 6. All the test series included in the figure have identical concrete composition; a non-reactive natural gneiss, granitic sand and a crushed reactive coarse cataclasite (section 4.1), "basis" binder (i.e. 400 kg/m^3 of CEM I, w/c of 0.45, alkali content of 3.7 kg/m^3 Na_2O_{eq}.- paper IV, Table 2). The figure includes unwrapped as well as wrapped prisms exposed to 100 % RH and either 38°C or 60°C. The 52-week expansion of the 38°C test series varies in the range of 0.17-0.31 %, while the 39 weeks expansion of the 60°C test series varies in the range of 0.04-0.22 %.

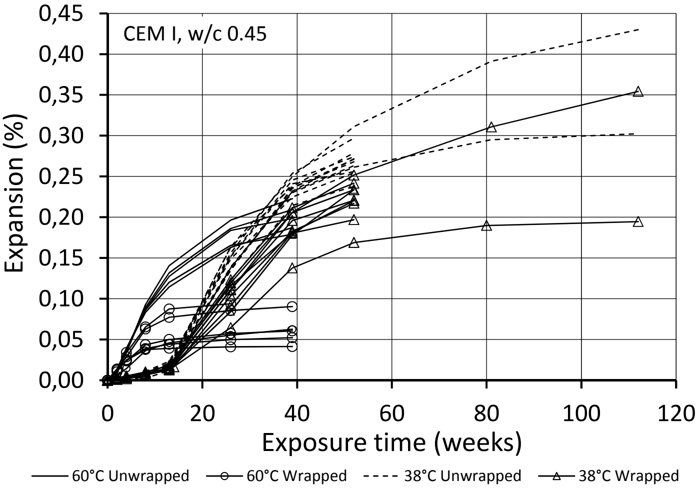

Figure 6 – Expansion versus time for 32 test series with the "basis" binder (CEM I, w/c 0.45).
(The figure includes unwrapped prisms (i.e. ASTM 38°C CPT, Norwegian 38°C CPT and RILEM AAR-4.1, 60°C CPT) as well as wrapped prisms (i.e. RILEM AAR-3, 38°C CPT and RILEM AAR-4.1 Alt., 60°C CPT) exposed to 100 % RH (i.e. stored on grids over water). Sealed and submerged test series are excluded. All the 60°C test series were ended after 39 weeks of exposure)

One of the most remarkable aspects of these differing results is that one of the testing variants that produced one of the lowest ultimate expansions was recommended by RILEM for a long period as an alternative test method to evaluate the alkali-reactivity of aggregates. *(Comment: That method, RILEM AAR-4.1 Alternative 60°C CPT (2006) using prisms wrapped with moist cotton cloth and plastic [29] is, however, not recommended by RILEM TC 219-ACS any longer due to the results of this study. For the same reason, the wrapping procedure is not recommended for the RILEM AAR-3 38°C CPT either. The revised version of RILEM AAR-3 [40] uses unwrapped prisms – the new test procedure is similar to the ASTM C 1293 38°C CPT [33]).*

The effect of wrapping is particularly pronounced for prisms exposed to 60°C, where the final expansion of unwrapped prisms was up to five times higher than for corresponding wrapped prisms (Figure 6). The main reason for the tremendous reduction in the prism expansion when the prisms are wrapped is the high rate of alkali leaching in the early stages of the test (section 5.2.3 and paper V). In fact, the rate of alkali leaching during the first weeks of exposure is the parameter found to have the highest impact on the development of ASR expansion. When exposed to 60°C, it completely controls the prism expansion (section 5.2.4).

Generally, a high fraction of the in-mixed alkalis was leached out of the concrete prisms during the ASR exposure (section 5.2.3). However, a modified wrapping procedure was developed (cotton cloth with added alkalis) in the study which might be a promising tool to mitigate alkali leaching during accelerated laboratory testing (paper V). Increasing the prism cross-section also decreases the rate and amount of alkali leaching considerably and consequently produced the highest expansions of all the test methods (the upper dotted curve in Figure 6), i.e. use of the larger Norwegian prisms is favoured.

For less permeable concretes, with a high degree of self-desiccation, the lower RH for the 38°C test series contributes together with the lower rate of diffusion to reduce the rate and extent of ASR (section 5.2.2).

Generally, the results from the various measurements are consistent, and the coefficient of variation between parallel samples within each test series is very low for most parameters measured. Where test series are repeated, the repeatability is good. More details are given in the papers IV and V.

5.2.2 Moisture state and transport properties

During the ASR exposure period, the concrete properties change. The general tendency is increased suction porosity and increased internal moisture state with increased ASR expansion, but the extent of any change depends on the binder composition. Moreover, a relation exists between water uptake and expansion, i.e. concrete expansion leads to increased porosity (i.e. cracks) that takes up water. However, more water is taken up than the volume corresponding to the increased porosity, implying that the DCS is increased (paper IV). Most of the water absorption is believed to be suction of water by the ASR gel in pores and cracks. Additionally, any very small cracks induced in the cement paste will absorb water due to capillary forces.

At all ages, the DCS varies far less than the corresponding RH. After 4 weeks of exposure (Figure 7), the DCS varies in the range of 91.5 to 96.5 vol-% (except for the two sealed test series). Thus, the DCS is higher than the "critical DCS" for development of ASR found based on an extensive field survey of Norwegian concrete structures, mainly bridges [21] (Figure 5 in section 1.2). The internal RH varies in the range of 82 to 97 %. Except for the sealed prisms, all the other pre-storage and exposure conditions are able to supply some water to the prisms leading to a higher internal RH than measured in the concrete sealed in plastic bottles (red points). Corresponding data at the end of the exposure period are given in paper IV.

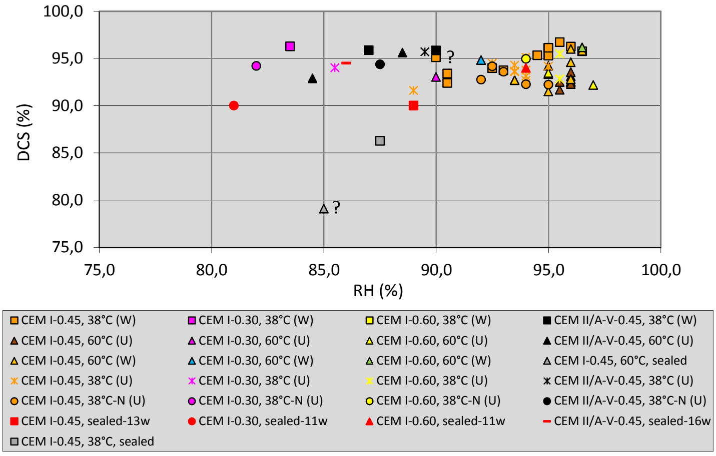

Figure 7 – Degree of capillary saturation (DCS) and relative humidity (RH) after 4 weeks of exposure
(The abbreviations for the various test series are given in the Tables 5-8 in paper IV; W = Wrapped prisms; U = Unwrapped prisms; N = larger Norwegian prisms; red points = sealed cured at 20°C in plastic bottles; w = weeks; ? = some uncertainty related to the RH measurement).

As expected, RH seems to depend strongly on the nature of the binder (w/cm and use of any additions). In contrast, no significant differences in the DCS are observed for the different binders. However, the amount of evaporable water is binder dependent; as expected decreasing with decreasing w/c due to less content of capillary pores. The spread in DCS and RH is in accordance with the expectations (see discussion in section 1.2). For a given RH, the DCS will normally be higher in more dense concretes compared to concretes with higher w/c due to the lower content of capillary pores. However, in the humid environment in the ASR storage containers most capillary pores for the concrete with higher w/c are also expected to be filled. Consequently, DCS are not expected to vary much between concretes with different w/c. On the other hand, the self-dessication and partly the ion concentration in the pore water will influence the RH, in particular for the densest concretes, and thus contribute to a larger spread in the RH (see below).

At both exposure temperatures, the internal RH for all test series with the CEM I binders with highest w/c (0.45 or 0.60) is always higher than 90 % after 4 weeks of exposure (except for the sealed test series), the majority in the range of 93.5-96 %.

Primarily due to increased self-desiccation and finer pore structure, and maybe partly due to higher ion concentration in the pore water, the "dense" CEM I binder (w/c of 0.30) test series obtain the lowest RH values after 4 weeks of exposure (Figure 7), ranging from 82-85.5 % for the 38°C test series. For corresponding test series exposed to 60°C, RH is higher; in the range of 90-92 %. This RH increase is probably related to the coarsening of the pore structure produced by exposure to elevated temperature as shown for cement pastes by Bray and Sellevold [41].

The presented values for RH were measured in a climate-controlled room at 20°C after cooling the prisms inside plastic foil (to avoid loss of moisture). As discussed in paper IV, the internal RH will increase during the ASR exposure compared with the results presented in Figure 7 by up to a maximum of 5 % when stored at 38°C and up to a maximum of 10 % when stored at 60°C. In other words, when the measured RH (at 20°C) for the "dense" binder is significantly lower for the 38°C test series compared with the corresponding 60°C test series, the difference will be even greater during the ASR exposure when the temperature is elevated. The practical importance of this temperature effect for the ASR reaction is not fully known, but it seems to be reasonable to assume that the higher RH at elevated temperature will contribute to accelerate the ASR expansion.

This assumption is strengthened by the fact that the expansion curves for the "dense" binder test series exposed to 60°C (paper V, Figure 14) are comparable with (i.e. not statistically different from) the corresponding results obtained for the CEM I test series with higher w/c (with the same initial alkali content – paper V, Figures 3 and 13), while the rate of expansion as well as the ultimate expansion for the "dense" binder test series exposed to 38°C (paper V, Figure 14) are dramatically reduced compared with the CEM I test series with w/c 0.45 or 0.60 (which produce comparable expansions - paper V, Figures 3 and 13). *(Comment: differences in alkali leaching cannot explain the diverging expansions observed for the "dense" binder at the two exposure temperatures (paper V). An assumed higher rate of dissolution of silica from the aggregate and the higher rate of diffusion (paper IV) at elevated temperature are also expected to contribute to the observed diverging expansions).*

To sum up: For all test series (except the two sealed), the DCS is higher than the "critical DCS" for development of ASR found in the extensive Norwegian field survey [21] (section 1.2). Assuming that the critical RH limit for developing ASR is in the range of 80-90 % depending on several factors (paper III and section 1.2), it appears that for the CEM I test series with w/c 0.45 or higher, all the test procedures provide sufficient moisture contents for ASR to initiate and proceed. However, it is likely that the lower RH measured for the "dense" binder (CEM I, w/c of 0.30) exposed to 38°C (Figure 7) and a considerably lower relative diffusion coefficient (paper IV) contribute to reduce the rate and extent of the ASR expansion (section 5.2.4) compared with the CEM I concretes with higher w/c and compared with the "dense" binder exposed to 60°C.

The "fly ash" binder (CEM II/A-V, w/cm of 0.45) gave RH in the range of 84.5-90 % after 4 weeks of exposure (Figure 7), i.e. almost as low as the "dense" CEM I binder. As for the "dense" binder, increased exposure temperature produces significantly higher expansion (paper V, Figure 15). Thus, the relatively "low" RH probably contribute to reduce the expansion of the "fly ash" binder test series as well, in particular when exposed to 38°C. However, one cannot rule out that also other parameters that might influence the development of ASR are slightly different at 60°C compared with 38°C (but the alkali leaching is comparable at both exposure temperatures), see discussion in paper V.

5.2.3 Alkali leaching

Generally, a very substantial proportion of the in-mixed alkalis is leached out of the concrete prisms during the ASR exposure. However, the rate and amount depend on the prism cross-section, specimen "pre-treatment", binder type and exposure conditions. During the early stages of the tests (4 weeks of exposure), alkalis in the range of 0.10-0.75 kg Na_2O_{eq} alkalis per m^3 of concrete are leached out (highest for wrapped prisms – section 5.2.1), constituting 3-20 % of the in-mixed alkalis for the CEM I binders with initial alkali content 3.7 kg Na_2O_{eq} per m^3 (even more for the test series submerged in de-ionised water). At the end of the exposure, from 14-37 % in total alkalis are leached out of the 60°C prisms (39 weeks – Figure 8), while corresponding numbers for the 38°C test series are in the range of 10-50 % (112 weeks – lowest for the larger Norwegian prisms). The highest number constitutes about 1.8 kg Na_2O_{eq} alkalis per m^3 of concrete for the CEM I binders. The total amount of alkali leaching is on a similar level as reported previously by Thomas et al. [26] for the ASTM C1293 CPT, Coté (M.Sc. thesis at Laval University (2009), samples exposed to 100 % RH and 38°C) [42] and by Bokern [43] for unwrapped concrete prisms exposed to high humidity at 60°C.

The mechanisms for alkali leaching are thoroughly discussed in paper V (section 3.2), including why the effect of increased exposure temperature and reduced w/c have far less influence on the rate and amount of alkali leaching than could be expected.

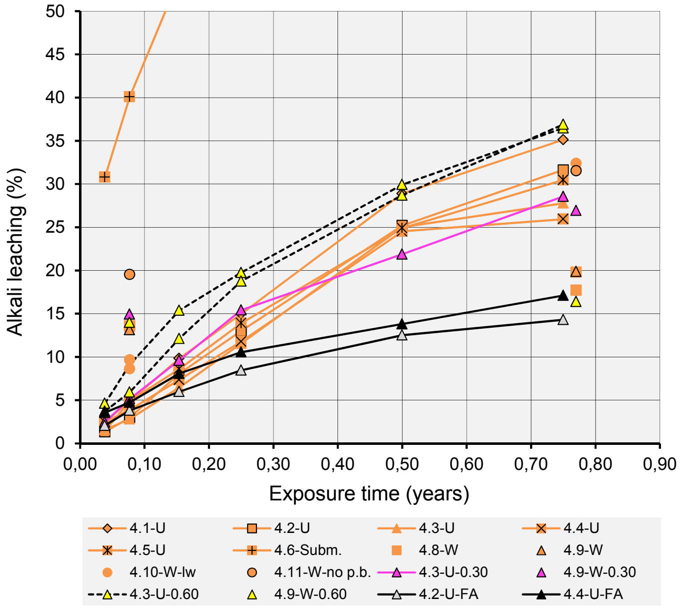

Figure 8 – Alkali leaching from the AAR-4.1 prisms (% of the initial concrete alkali content). (The single data points represent wrapped prisms (W). The accumulated curves represent unwrapped prisms (U). The abbreviations for the various test series are given in the Tables 5-8 in paper IV. The data points in the upper left corner represent the submerged test series.)

5.2.4 Correlation between alkali leaching and prism expansion

The statistical treatment of the expansion results (paper V, section 3.3.3, and Appendix 3) confirms the low spread and the consistency of the expansion measurements.

As stated in section 5.2.1 (and thoroughly discussed in paper V), the alkali leaching in the early stage of the test is the parameter found to have the highest impact on the final prism expansion. For the test series exposed to 60°C, with sufficient moisture content for ASR to develop and generally a higher relative diffusion coefficient than the 38°C test series (paper IV), the rate of alkali leaching in the first weeks of exposure completely controls the prism expansion. This finding is shown in Figure 9, demonstrating the good correlation between the remaining alkali content after 4 weeks of exposure and the expansion after 26 weeks for the 60°C CEM I test series *(comment: the reason for plotting the remaining alkali content after 4 weeks of exposure, is the fact that the alkali leaching from the wrapped test series is only measured after 4 weeks of exposure and in the end of the exposure – see section 3.3)*. For the "basis" binder (w/c of 0.45), the determination coefficient R^2 for the trend line is 0.94; excluding the submerged test series where, after just 4 weeks, rapid leaching results in the alkali content of the concrete being reduced to a value below the "alkali threshold" for the aggregate combination used. The impact of the early-age alkali leaching on expansion is similar also for the "open" binder (w/c of 0.60) and the "dense" binder (w/c of 0.30).

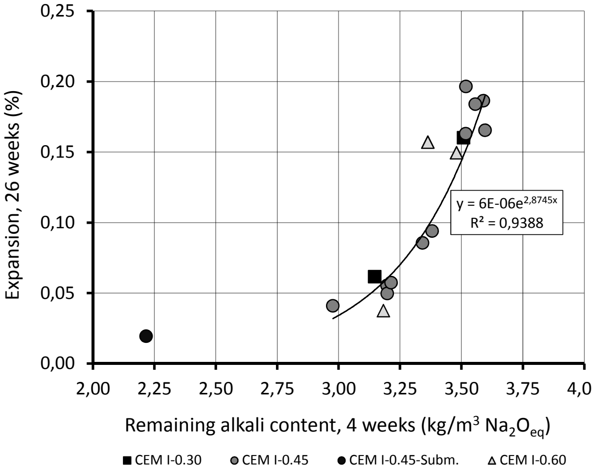

Figure 9 – Remaining alkali content after 4 weeks of exposure versus expansion at 26 weeks for wrapped and unwrapped AAR-4.1 60°C test series with CEM I binders (w/c of 0.30-0.60, initial alkali content 3.7 kg/m^3 Na$_2$O$_{eq}$). (The determination coefficient (R^2) is valid for the test series with the "basis" binder (w/c of 0.45), excl. the submerged test series. The abbreviations for the various test series are given in the Tables 5-8 in paper IV.)

One important reason for the good correlation found is that the alkali content was chosen with the aim to reach an ultimate (final) expansion of the reference test series lying on the steep (ascending) part of the "expansion versus alkali level (S-shaped) curve". Thus, loss of alkalis at early age has a considerable impact in terms of reduced expansion. If the CEM I concretes had contained surplus alkalis (i.e. lying on the plateau of the "expansion versus alkali level curve", as is the case for most aggregate testing), less influence of the alkali leaching on the expansion would have been expected.

The correlation between the total amount of alkali leaching and the final expansion is not particularly good for the prisms exposed to 60°C, most likely because significant alkali leaching occurs after the expansion has ceased. Furthermore, the wrapped prisms that reveal the highest rate of alkali leaching in the early stage of the test show little expansion beyond 8 weeks of exposure (Figure 6 in section 5.2.1).

The alkali leaching in the early stage of the test is also of high importance for the 38°C test series, even though the determination coefficient for the trend line for the "basis" binder test series in Figure 10 (R^2=0.77) is not as good as that found for the 60°C test series (Figure 9). The impact on expansion of alkali leaching is similar also for the "open" binder test series exposed to 38°C (Figure 10). In contrast, the "dense" binder (w/c of 0.30) test series do not fit into the same picture (Figure 10). The reason is most likely that the internal moisture state and the diffusion properties also influence the expansion, as discussed previously.

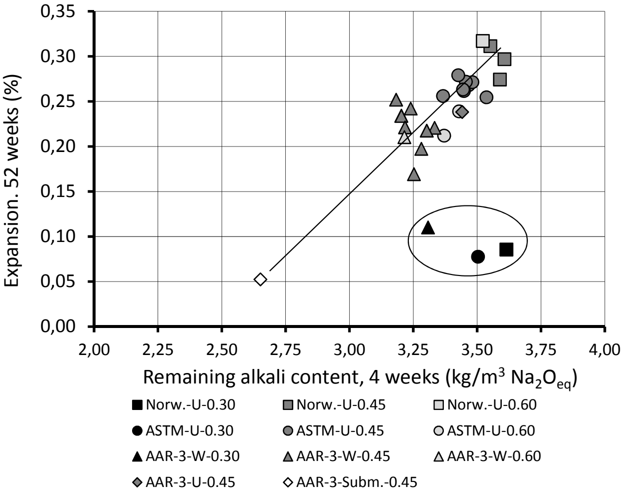

Figure 10 – Remaining alkali content after 4 weeks of exposure versus expansion at 52 weeks for wrapped (W) and unwrapped (U) 38°C test series with CEM I binders (w/c of 0.30-0.60, initial alkali content 3.7 kg/m^3 Na$_2$O$_{eq}$). (The determination coefficient (R^2) for the trend line for the "basis" binder test series is 0.77. The abbreviations for the various test series are given in the Tables 5-8 in paper IV.)

Generally, the determination coefficient for the trend line between the total amount of alkali leaching and the final expansion is not particularly good for the prisms exposed to 38°C, either. However, the tendency is that factors that reduce the amount of alkali leaching throughout the expansion period increase the final expansion for the CEM I test series with w/c of 0.45 and 0.60. Two examples illustrating this fact are the positive effect of increased prism cross-section (also found in the M.Sc. study at Laval University [42]) and the different expansion obtained between AAR-3 prisms pre-stored 1 day compared with 28 days at ambient temperature (paper V).

(Comment: For the "fly ash" binder, the test program does not include enough test series to produce a similar comparison as done for the CEM I binders in the Figures 9 and 10. Additionally, the internal moisture state most likely also influences the measured expansions for the "fly ash" binder, as discussed in section 5.2.2).

With respect to performance testing, where alkali contents close to the "alkali threshold" in many cases are used in the concrete mixtures (e.g. if the "alkali threshold" for an aggregate combination is of interest), the impact of alkali leaching is regarded to be high. Additionally, the exposure period is often extended (e.g. if SCMs are included) compared with pure aggregate testing. Thus, the total extent of alkali leaching might have higher influence than that found in the present study.

Consequently, to be able to mirror what will happen in a real concrete structure with minor or no alkali leaching (except in the outer layer), minimization of the rate and extent of alkali leaching during laboratory performance testing is crucial.

5.3 Complementary findings

5.3.1 Alkali release from the aggregates

Measurement of alkali release from the aggregates used (according to a new procedure established – Appendix 2) indicates that the sand and the coarse aggregate have contributed less than 0.2 kg Na_2O_{eq} alkalis per m^3 of concrete during the ASR exposure, constituting < 5 % of the initial "in-mixed" alkali content in the CEM I concretes (Appendix 3). This calculation is based on measurements of alkali release conducted on samples of the sand and coarse aggregate with the same particle-size distribution as that used in the concrete mixtures. When the aggregates were ground to a fine powder (< 0.125 mm), the amount of alkali release was substantially increased, as could be expected (Appendix 3). For comparison, results from alkali release measurements of more aggregate types are included in Appendix 3.

Consequently, the aggregate grading must be taken into account when developing a standardized test for measurement of alkali contributions from aggregates (as is the objective of one of the task groups in RILEM TC 219-ACS).

5.3.2 Microstructural analyses

A new method for the measurement of "cracking intensity" (given as area-% of cracks in an impregnated polished section) based on image analysis has been developed. This method has been used successfully to compare the extent of cracking in the concrete prisms caused by ASR, both internally within one plane polished section and between different test series (paper VI).

The image analyses of the 16 fluorescence impregnated plane polished sections confirm the results from the alkali leaching measurements. The main reason for the lower crack intensity in the outer/upper/lower parts of the prisms compared with the interior is assumed to be the higher amount of alkali leaching in these areas of the prisms (see paper VI and photos of the various plane polished sections in Appendix 3).

A good linear correlation is found between "cracking intensity" and prism expansion (R^2=0.89), and this seems valid for all strength levels tested (paper V and VI). This implies that the image analysing technique is potentially a useful tool to analyse the intensity of cracking induced by ASR, at least for post-documentation of the internal cracking in laboratory exposed samples. However, care should be taken when using the method. The image analysis method only measures the intensity of cracking, without reference to the origin of the cracking, neither differentiating cracking in the cement paste from that in the aggregate particles. Furthermore, it does not describe the "pattern of ASR" that typically involves cracking connecting reactive aggregate particles with generally important cracking within the aggregate particles. This is a critical feature of ASR that differentiates it from other pattern of cracking where most if not all cracking remains in the cement paste (as for example is the typical pattern for delayed ettringite formation (DEF) and freeze-thaw damage). Consequently, applying the method to a core extracted from an ASR-affected structure will allow determination, to some extent, of the condition of the concrete (intensity of cracking) without really be able to relate it specifically to ASR or another deleterious mechanism. One should also be aware of that any areas close to the cracks in the cement paste with significant higher porosity (as can be seen relatively frequently in drilled cores taken from real structures) might be miscalculated as part of the cracks. In such cases, special care must be taken. To conclude; the image analysis technique is essentially a tool to complement petrographic examination by allowing quantification of the degree of damage, but not to diagnose the source of the cracking. *(Comment: The application and the suitability of the method are intended to be investigated further in a planned R&D project at SINTEF).*

5.3.3 Dynamic E-modulus

The dynamic E-modulus, which was measured periodically for the unwrapped Norwegian prisms, is shown in Figure 11. The "initial" E-modulus (measured after 2 weeks of exposure) and the ranking between the various binders are as expected. All test series show a similar development during the ASR exposure; a slight increase in the dynamic E-modulus from 2 to 8 weeks (for a few test series from 2-13 weeks) of exposure; a slight reduction from 8-13 weeks; a considerable reduction in the E-modulus when the expansion and the internal cracking develops after about 13 weeks of exposure; a flattening tendency after a certain expansion, and finally a slight increase towards the end of the exposure period.

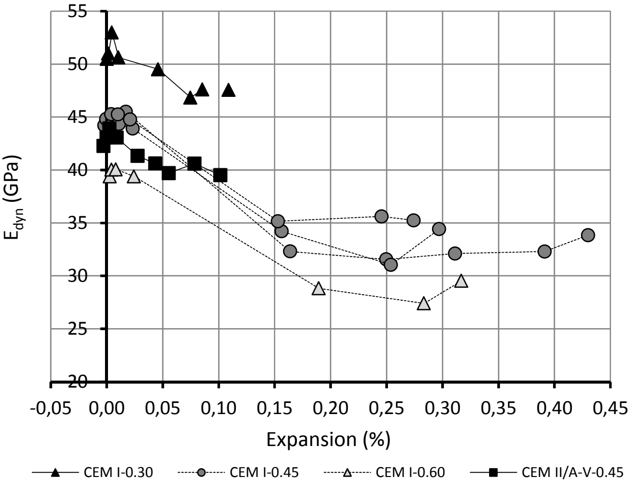

Figure 11 – Dynamic E-modulus for the Norwegian CPT series. (The first measurements were performed after two weeks of exposure. The abbreviations for the various test series are given in the Tables 5-8 in paper IV.)

The late increase in the dynamic E-modulus is assumed to be connected with filling of cracks with ASR gel. A similar behaviour has been previously observed by Verein Deutscher Zementwerke (VDZ) (unpublished results from the EU "PARTNER" project – paper I). The E-modulus of the ASR gel is also assumed to increase as the ASR gel picks up calcium (documented in the SEM analyses – Appendix 3), as shown by Leemann and Lura [44], and thus contributes to the observed increase in the concrete E-modulus towards the end of the exposure period.

The results clearly show that dynamic E-modulus measurements are very sensitive and able to detect the first internal cracking of the prisms; as soon as ASR initiates and the first internal cracks develop, the dynamic E-modulus slightly decreases. For some test series, this inflection point appears even before any noticeable expansion is measured. It thus seems promising to use dynamic E-modulus measurements to get an early indication if a concrete will develop ASR during accelerated laboratory testing. As expected, the results also show that the E-modulus will not decrease if no ASR takes place: There was no significant reduction in the dynamic modulus for the submerged 60°C test series that hardly expanded at all (Appendix 3). Similarly, in the EU "PARTNER" project (unpublished results), VDZ found no indication of any reduction in the concrete E-modulus for the non-reactive aggregates tested, confirming the consistency of the method.

Later in the exposure period, the dynamic E-modules measurements are less sensitive than the expansion measurements to describe the extent of ASR damage (relatively small differences in the E-modulus are observed between low-reacting and highly reacting test series).

Corresponding results for the ASTM C 1293 test series, the two unwrapped AAR-3 test series and all the unwrapped AAR-4.1 test series are included in Appendix 3. They show similar behaviour as the Norwegian prisms, except that the 60°C AAR-4.1 test series did not show a small increase in the dynamic E-modulus from two to eight weeks of exposure, rather a considerable reduction. The reason is probably that the internal cracking had initiated already at the first measurements after 2 weeks of exposure.

6 Recommendations

Based on the literature review, several general recommendations for ASR performance testing are given in paper III (section 6). The most important recommendations are:

- Concrete prism tests are recommended instead of mortar bar tests (allow testing of the aggregate fractions used in structures).
- Exposing the prisms to 60 °C during ASR testing might be questionable due to several reasons. More research is thus needed. Exposure of the test prisms to temperatures above 60 °C should be avoided, primarily because other deterioration mechanisms may occur (e.g. DEF).
- Extensive alkali boosting is not in general recommended for performance testing. More research is needed on this topic, as well.
- A laboratory performance test should be designed to subject the prisms to "worst-case humidity conditions", while considering the problems related to increased alkali leaching.
- As a quality control measure, the mass of prisms should always be measured, evaluated and reported.

Additionally, detailed recommendations based on the present work are given in the papers IV and V. The most important recommendations are:

- "Traditional" wrapping of concrete prisms with a damp cotton cloth, applied in some test methods primarily with the aim to secure a high moisture content surrounding the prisms, is not recommended due to a high extent of alkali leaching during the first weeks of exposure.
- One effective measure to reduce the amount of alkali leaching during performance testing is to increase the prism cross-section.
- A modified wrapping procedure developed (cotton cloth added alkalis) might be a promising tool to reduce the amount of alkali leaching during accelerated laboratory testing (this procedure might be a conservative approach, since the concrete alkali content might increase a little depending on the binder composition used and the concentration of the alkalis in the cotton cloth surrounding the prisms).
- To avoid any "false negative results" during accelerated performance testing, a fixed w/cm of 0.50 could be used (assumed to be conservative) until more research possibly documents that a lower (and more realistic) w/cm is safe to use; i.e. without resulting in a possible lower moisture state in the laboratory prisms compared with real concrete structures exposed to very high humidity.

According to the present work (stated in paper V, section 4.7), the major shortcoming of the various concrete prism tests is leaching of alkalis from the concrete during exposure. Consequently, the overriding recommendation is to develop test procedures that limit, compensate for or, preferably, eliminate alkali leaching during testing. The results of the present study have already been communicated to RILEM TC 219-ACS, and have resulted in withdrawal of one of the three draft RILEM CPTs and comprehensive revisions to a second one (section 5.2.1).

A number of practical details and recommendations on the test procedures are given in Appendix 4.

7 Research needs – follow-up project

The literature survey identified several issues that need further research in order to develop a reliable performance test procedure. The most important ones are summarized in paper III (section 7). Additionally, I want to address the following questions based on the findings in the PhD study:

1. Even if actions are taken, it is very difficult to totally hinder alkali leaching during accelerated laboratory testing. However, is it possible to account for this remaining alkali leaching in a reliable way (e.g. through alkali boosting)?
2. Testing of rather "dense" concretes at 60°C produces higher expansions compared with exposure to 38°C, opposite as that found for CEM I binders with w/c of 0.45 or higher. But, does the testing at 60°C reflect what will happen in field in a reliable way? *(Comment: Data on the laboratory/field correlation is in general lacking for the 60°C test procedures. Additionally, several scientists question the reliability of the 60°C CPT – paper III).*

Based on the findings in the laboratory program, the author has initiated a comprehensive follow-up project within the COIN program. In this study, the most promising test procedures used in the PhD study form the basis for the ASR testing. Aggregates from five sources are included, among them the reference Spratt aggregate from Canada. The binder types incorporated are two CEM I cements, one fly ash cement (CEM II/A-V) and one slag cement (CEM III/B). In total, 20 concrete mixtures and about 115 single ASR test series are included (Appendix 5).

To document the laboratory/field correlation, two field exposure sites have been established, one at SINTEF in Trondheim and one at LNEC in Lisbon, Portugal (Appendix 6). The test setup is the same as developed within the EU "PARTNER" project (paper I), using concrete cubes with dimension 300x300 x300 mm. The main experience from this project is that the various field exposure sites spread over Europe produce comparable results, but the ASR starts earlier in warmer climate.

The main aims with the follow-up project (Appendix 5 and 6) are to:

- Investigate whether some of the ASR test procedures used in the PhD study are able to produce expansion results that reflect the field behaviour, i.e. verify the laboratory/field correlation with the various test procedures included.
- Document various aggregate/binder combinations ("what is safe to use?")
- Continuously give input to the "Performance task group" of RILEM TC 219-ACS *(Comment: During 2014, a new RILEM committee will most likely take over the work from this TC).*
- Form the basis for any needed revisions of the Norwegian ASR regulations.

References

[1] J. Lindgård, Ö. Andiç-Çakır, I. Fernandes, T.F. Rønning, M.D.A. Thomas, Alkali–silica reactions (ASR): Literature review on parameters influencing laboratory performance testing, Cement and Concrete Research, 42 (2012) 223-243.

[2] L.-O. Nilsson, O. Peterson, Alkal-silica reactions in Scania, Sweden, Report TVMB-3014, Lund Institute of Technology, Div. of Building Materials, Lund, Sweden, 1983, pp. 106.

[3] L.-O. Nilsson, Long-term moisture transport in high performance concrete, Materials and Structures, 35 (2002) 641-649.

[4] R.H. Relling, Coastal concrete bridges: Moisture state, chloride permeability and aging effects, DrEng Thesis at Institute for Construction Technique, NTNU, Trondheim, 1999, pp. 244 + appendices.

[5] G. Hedenblad, Drying of building moisture in concrete, Svensk byggtjänst 17188 Solna, Sweden, 1995 (in Swedish).

[6] L.-O. Nilsson, Temperature effects in relative humidity measurements on concrete - some preliminary studies, in: Symposium and day of building physics, Lund, Sweden, 1987, pp. 456-462.

[7] L.-O. Nilsson, Hygroscopic moisture in concrete - drying, measurements and related material properties, Report TVBM-1003, Lund Institute of Technology, Lund, Sweden, 1980.

[8] D. Lenzner, U. Ludwig, The alkali aggregate reaction with opaline sandstone from Schleswig-Holstein, in: IVth International Conference on Effects of Alkalies in Cement & Concrete, Purdue University, W Lafayette, Ind. Publ. No. CE-MAT-1-78, 1978.

[9] H. Ólafsson, The effect of relative humidity and temperature on alkali expansion of mortar bars, in: P.E. Grattan-Bellew (Ed.) 7th International Conference on Alkali-Aggregate Reactions in Concrete, Noyes Publications, Ottawa, Canada, 1986, pp. 461-465.

[10] T. Kurihara, K. Katawaki, Effects of moisture control and inhibitation on alkali silica reaction, in: K. Okada, S. Nishibayashi, M. Kawamura (Eds.) 8th International conference on Alkali-Aggregate Reaction, Society of Materials Science, Kyoto, Japan, 1989, pp. 629-634.

[11] F. Tomosawa, K. Tamura, M. Abe, Influence of water content of concrete on alkali-aggregate reaction, in: K. Okada, S. Nishibayashi, M. Kawamura (Eds.) 8th International conference on Alkali-Aggregate Reaction, Society of Materials Science, Kyoto, Japan, 1989, pp. 881-885.

[12] J. Stark, The moisture condition of field concrete exhibiting alkali-silica reactivity, in: Second international conference on durability of concrete, ACI publication SP 126/52, Canada, 1991, pp. 973-987.

[13] H. Krogh, Examination of syntethic alkali-silica gels, in: Symposium on Alkali-Aggregate reaction Preventive Measures, Reykjavik, Iceland, 1975.

[14] G. Gudmundsson, H. Asgeirsson, Parameters affecting alkali expansion in Icelandic concretes, in: G.M. Idorn, S. Rostam (Eds.) 6th International Conference on Alkali-Aggregate Reaction in Concrete, Denmark, 1983.

[15] S. Chatterji, A.D. Jensen, N. Thaulow, P. Christensen, Studies of alkali-silica reaction. Part 3. Mechanisms by which NaCl and Ca(OH)2 affect the reaction, Cement and concrete research, 16 (1986) 246-254.

[16] C. Larive, A. Laplaud, O. Coussy, The role of water in alkali-silica reaction, in: M.-A. Bérubé, B. Fournier, B. Durand (Eds.) 11th International Conference on Alkali-Aggregate Reaction, Québec, Canada, 2000, pp. 61-69.

[17] G.E. Bligh, The moisture conditions in an exposed structure damaged by alkali-silica reaction, Magazine of concrete research, 43, No. 157 (1991) 249-255.

[18] V. Jensen, In-situ measurements of relative humidity and expansion of cracks in structures damaged by AAR, in: M.-A. Bérubé, B. Fournier, B. Durand (Eds.) 11th International Conference on Alkali-Aggregate reaction in Concrete, Quebec, Canada, 2000, pp. 849-858.

[19] B. Pedersen, Alkali-reactive and inert fillers in concrete. Rheology of fresh mixtures and expansive reactions. PhD-thesis, Norwegian University of Science and Technology, Trondheim, Norway, 2004, pp. 292.
[20] R.H. Relling, E.J. Sellevold, In situ moisture state of coastal bridges, in: Concrete repair, rehabilitation and retrofitting, Taylor & Francis, London, UK. ISBN 0415396549, Cape Town South Africa, 2005.
[21] J. Lindgård, E. Rodum, B. Pedersen, Alkali-silica reactions in concrete - Relationship between water content and observed damage on structures, in: V.M. Malhotra (Ed.) 7th CANMET/ACI International conference on Durability of Concrete, ACI, Montreal Canada, 2006, pp. 147-165.
[22] F.P. Glasser, Chemistry of the alkali-aggregate reaction, in: R.N. Swamy (Ed.) The Alkali-Silica Reaction in Concrete, Blackie and Son Ltd, London, 1992, pp. 333.
[23] D.W. Hobbs, Alkali-silica reaction in concrete, Thomas Telford Ltd, London, 1988.
[24] M.D.A. Thomas, The effect of supplementary cementing materials on alkali-silica reaction: A review, Cement and Concrete Research, 41 (2011) 1224-1231.
[25] M.D.A. Thomas, M.H. Shehata, Use of blended cements to control expansion of concrete due to alkali–silica reaction, in: 8th CANMET/ACI Int Conf on Fly Ash, Silica Fume, Slag and Natural Pozzolans in Concrete, Supplementary Papers, Las Vegas, 2004, pp. 591–607.
[26] M. Thomas, B. Fournier, K. Folliard, J. Ideker, M. Shehata, Test methods for evaluating preventive measures for controlling expansion due to alkali-silica reaction in concrete, Cement and Concrete Research, 36 (2006) 1842-1856.
[27] Norwegian Concrete Association: Alkali–aggregate reactions in concrete, Test methods and Requirements to Test Laboratories, NB32, 2005, pp. 39.
[28] RILEM TC 106-AAR, 'Alkali Aggregate Reaction' A. TC 106-2- Detection of Potential Alkali-Reactivity of Aggregates –The Ultra-Accelerated Mortar-Bar Test B. TC 106-3-Detection of Potential Alkali-Reactivity of Aggregates-Method for Aggregate Combinations Using Concrete Prisms, Materials and Structures, 33 (2000) 283-293.
[29] RILEM TC 219-ACS 'Alkali-silica reactions in Concrete Structures': RILEM AAR-4.1 - Detection of potential alkali-reactivity of aggregates: accelerated (60°C) concrete prism test, (unpublished draft, 2006).
[30] RILEM TC 191-ARP: 'Alkali-reactivity and prevention-Assessment, specification and diagnosis of alkali-reactivity', RILEM Recommended Test Method AAR-0: Detection of Alkali–Reactivity Potential in Concrete - Outline guide to the use of RILEM methods in assessments of aggregates for potential alkali-reactivity, Materials and Structures, 36 (2003) 472-479.
[31] Norwegian Concrete Association: Durable concrete containing alkali reactive aggregates, NB21, 2004, pp. 33.
[32] J. Lindgård, Ö. Andiç-Çakır, I. Borchers, M.T.A.M. Broekmans, E. Brouard, I. Fernandes, C. Giebson, B. Pedersen, C. Pierre, T.F. Rønning, M.D.A. Thomas, B.J. Wigum, RILEM TC219-ACS-P: Literature survey on performance testing, COIN project report 27, ISBN: 978-82-536-1209-6, 2011, pp. 164.
[33] ASTM C1293 - 08b Standard Test Method for Determination of Length Change of Concrete Due to Alkali-Silica Reaction, in, American Society for Testing and Materials, Annual Book of ASTM Standards, 2008, pp. 7.
[34] E.J. Sellevold, T. Farstad, The PF-method - A simple way to estimate the w/c-ratio and air content of hardened concrete, in: ConMat'05 and Mindness Symposium ISBN 0-88865-810-9, The University of British Colombia, Vancouver, Canada, 2005.
[35] Vaisala Instruments Catalog, Ref B210768EN rev. A (www.vaisala.com/HM44), 2009.
[36] E.J. Sellevold, D.H. Bager, E. Klitgaard Jensen, T. Knudsen, Silica fume cement pastes: Hydration and pore structure, in: Nordic miniseminar, Report BML 82-610 Norges Tekniske Høgskole, NTH, Trondheim, 1982, pp. 19-50.
[37] O. Skjølsvold, Hardened concrete. Measurment of electrical resistivity of concrete. Internal SINTEF test procedure KS 14-05-04-128, Trondheim, Norway, 2007.

[38] D.A. Whiting, M.A. Nagi, Electrical resistivity of concrete - A literature review. PCA R&D Serial No. 2457, 2003, pp. 56.

[39] RILEM TC 219-ACS, 'Alkali-silica reactions in Concrete Structures': RILEM recommended test method: AAR-2, Detection of potential alkali-reactivity - Accelerated mortar-bar test method for aggregates, (draft September, 2011).

[40] RILEM TC 219-ACS 'Alkali-silica reactions in Concrete Structures': RILEM recommended test method: RILEM AAR-3 - Detection of potential alkali-reactivity - 38°C test method for aggregate combinations using concrete prisms, (unpublished draft, 2011).

[41] W. Bray, E.J. Sellevold, Water sorption properties of hardened cement paste cured or stored at elevated temperatures, Cement and Concrete Research, 3 (1973) 723-728.

[42] T. Coté, GESTION DES OUVRAGES EN BÉTON AFFECTÉS DE RÉACTIVITÉ ALCALIS-SILICE : CONTRIBUTION À LA DÉTERMINATION DE L’EXPANSION ATTEINTE À CE JOUR ET DE L’EXPANSION RÉSIDUELLE À VENIR, M.Sc. thesis, Faculty of Civil Engineering, Laval, Quebec, Canada, 2009, pp. 130 (in French).

[43] J. Bokern, Concrete tests for ASR assessment: Effects of testing environment on preconditions for an ASR and transferability of test results, in: M.A.T.M. Broekmans, B.J. Wigum (Eds.) 13th International Conference on Alkali-Aggregate Reactions in Concrete, Trondheim, Norway, 2008, pp. 511-520.

[44] A. Leemann, P. Lura, E-modulus of the alkali-silica-reaction product determined by micro-indentation, Construction & Building Materials, 44 (2012) 221-227.

Appendices (overview)

Appendix 1 Enclosed papers

- Six papers: See list on page v.

Appendix 2 Complementary test procedures

- Alkali release from aggregates
- Dynamic E-modulus
- Alkali leaching: Procedure for sampling and measurement during concrete prism testing
- Relative diffusion coefficient: Supplementary test procedures plus calculation of results
- Electrical resistivity: Supplementary test procedures plus calculation of results
- Expansion: Detailed procedure for measuring length and weight without pre-cooling the prisms

Appendix 3 Complementary laboratory results

- Petrographic analysis of the two aggregate types
- Alkali release from aggregates
- Summary discussion of findings in paper IV
- Dynamic E-modulus
- Relative diffusion coefficient: Results from supplementary test procedures
- Electrical resistivity: Results from supplementary test procedures
- Supplementary comments to the "PF-measurements" and the DCS measurements
- Calculations based on the expansion measurements
  - Statistical analysis
  - Coefficient of thermal expansion
  - Length change in the "pre-reference phase"
- Mass increase of whole prisms: Supplementary results for the CEM I binders
- Microstructural analysis: Supplementary results, including WDS analysis of the ASR gel
- Photos
  - ASR test methods: ASR storage containers, wrapping of prisms and length measurements
  - Other measurements: DCS, RH and electrical resistivity
  - Visual inspection of prisms
  - Microstructural analyses
    - 16 plane polished sections (in UV-light)
    - Selected thin sections
    - Selected photos from the SEM analysis

Appendix 4 Comments on humidity and quality control during testing

Appendix 5 Follow-up project – laboratory testing

- Materials: Aggregates and cement types
- Mixture proportions: Aggregate and binder compositions
- ASR test procedures
- Photo: Casting of concrete prisms

Appendix 6 Follow-up project - field exposure sites

- Procedure for preparation and measuring of outdoor exposed cubes
- Photos: production of concrete cubes; two field exposure sites

References in Appendix 1-6

Appendix 1: Enclosed papers

Paper I

The EU "PARTNER" Project - European standard tests to prevent alkali reactions in aggregates: Final results and recommendations
J. Lindgård, P.J. Nixon, I. Borchers, B. Schouenborg, B.J. Wigum, M. Haugen, U. Åkesson,
Cement and Concrete Research, 40 (2010) pp. 611-635

Cement and Concrete Research 40 (2010) 611–635

Contents lists available at ScienceDirect

Cement and Concrete Research

journal homepage: http://ees.elsevier.com/CEMCON/default.asp

The EU "PARTNER" Project — European standard tests to prevent alkali reactions in aggregates: Final results and recommendations

Jan Lindgård [a,*], Philip J. Nixon [b], Ingmar Borchers [c], Björn Schouenborg [d], Børge Johannes Wigum [e], Marit Haugen [a], Urban Åkesson [d]

[a] SINTEF Building and Infrastructure, NO-7465 Trondheim, Norway
[b] Associate, Building Research Establishment, Watford, WD25 9XX, UK
[c] Verein Deutscher Zementwerke e.V., Düsseldorf, Germany
[d] SP Technical Research Institute of Sweden, Borås, Sweden
[e] Norwegian University of Science and Technology, NO-7491 Trondheim, Norway

ARTICLE INFO

Article history:
Received 24 November 2008
Accepted 5 September 2009

Keywords:
Aggregate
Alkali-silica reactions
Test methods

ABSTRACT

This paper presents the main findings in the EU PARTNER Project (2002–2006) providing the basis for a unified European test approach for evaluating the potential alkali-reactivity of aggregates. The project evaluated the tests developed by RILEM and some regional tests for their suitability for use with the wide variety of aggregates and geological types found across Europe. The project had 24 partners from 14 countries, covering most of Europe, from Iceland to Greece. 22 different types of aggregates from 10 different European countries were evaluated. It was found that in most cases the RILEM tests could successfully identify the reactivity of the aggregates tested. They were most successful with normally reactive and non-reactive aggregates, but with aggregates that react very slowly an extended test period may be necessary for some of the RILEM methods. Overall, the accelerated mortar bar test and the accelerated concrete prism test seemed most effective and to have the best precision.

1. Introduction

This paper presents the main results of PARTNER (2002–2006), a project partly funded by the European Community, which had the overall objective of establishing a unified test procedure for evaluating the potential alkali-reactivity of aggregates across the different European economic and geological regions. It is intended that the results of the project will be implemented by CEN, European Committee for Standardization, in the form of new standard methods of test and specifications.

In the project the tests developed by RILEM, and some established regional tests, were evaluated for their suitability for use with the wide variety of aggregate and geological types found across Europe. The results of the accelerated laboratory tests were calibrated against the behaviour of these aggregates in real concrete structures and in field test sites. The precision of the tests was then determined by inter-comparison trials using a common set of materials. Additionally, a petrographical atlas of the potentially alkali-reactive rocks in Europe was produced and published, an education programme undertaken and recommendations made to the relevant technical committees of CEN. The project had 24 Partners from 14 countries, covering most of Europe, from Iceland to Greece. Some of the participating laboratories had no/minor experience with the actual methods in advance.

2. The test programme

2.1. General

Details of the test programme, the aggregates, the methods of test and the results are given in a series of technical reports published by the Norwegian research institute SINTEF [1–5]. These reports may be freely downloaded (www.farin.no/english). Additionally, four papers covering parts of the project in more detail were submitted to the 13th ICAAR conference in Trondheim [6–9].

The main candidate methods of test were those developed by the RILEM committees TC106 and TC191-ARP. Additionally, several methods of test that were already established in particular European regions were included in order to see if these could be replaced by the RILEM methods for the particular geological types of aggregate for which they had been developed.

The field site tests were included to provide a means of calibrating the accelerated tests against behaviour in conditions closer to those experienced by actual structures.

2.2. The aggregates

The aggregates to be used for testing were chosen on the basis of a questionnaire completed by each partner regarding local potentially reactive materials. The final list contained 22 different types of aggregates

---

* Corresponding author.
E-mail address: jan.lindgard@sintef.no (J. Lindgård).

0008-8846/$ – see front matter © 2009 Elsevier Ltd. All rights reserved.
doi:10.1016/j.cemconres.2009.09.004

Table 1
Aggregate description and reactivity table.

Aggregate combination	Origin	Brief petrographic description	Reported alkali-reactivity
B1 (C + F)	Western Belgium	Crushed silicified, dark-grey argillaceous limestone with fossil debris; reactive mineral is crypto-microcrystalline quartz with sometimes fibrous habit.	Aggregate has caused damage in several concrete structures such as bridges and water structures.
D1 (C + F)	Denmark	Glaciofluvial gravel containing white to creamy opaline flint; reactive mineral is opal.	Aggregate has produced severe deterioration in all types of concrete structures (can occur quickly under severe conditions, clear pessimum effect).
D2 (C + F)	Denmark	Sea-dredged, polymictic gravel originally derived from glaciofluvial sediments; main component of interest is partly porous dense chalcedonic flint, in smaller amounts pure porous chalcedonic flint is included; reactive mineral is chalcedony.	Dense porous flint is considered to be non reactive, porous flint to be reactive. Aggregate has produced severe damage in all types of concrete structures (normally after 10–15 years). Not as severe as D1.
D3 (F)	Denmark	Non reactive siliceous sand.	No deterioration reported.
F1 (C)	France (Seine Valley)	Polymictic river gravel, mainly composed of flint/cherts; reactive mineral is micro-cryptocrystalline quartz.	In France is considered to be potentially reactive but with clear pessimum effect. No evidence of damage in structures.
F2 (C + F)	France	Fine-grained limestone with some fossils; no reactive minerals.	Non-reactive. No damage reported.
F3 (C + F)	France (Rhine Valley)	Polymictic river gravel (partly crushed), mainly composed of quartzite, alkali-reactive constituents are flint, greywacke and granitoids; reactive minerals are micro-cryptocrystalline quartz and strained, highly metamorphically sutured quartz.	No deterioration reported.
G1 (C)	Germany (Upper Rhine Valley)	Crushed polymictic river gravel, considerable variation in constituent lithologies; aggregates of interest are silicified limestone and chert; reactive minerals are micro- to cryptocrystalline quartz and chalcedony.	Considered to be reactive. Concrete pavements containing this aggregate have deteriorated due to ASR. (Damage observed after 10 years under very severe conditions).
G2 (C)	Northern Germany	Polymictic gravel from glaciofluvial deposit; alkali-reactive due to opaline sandstone (with tridymite/christobalite) and flint (with cryptocrystalline quartz and chalcedony).	Has produced severe deterioration, very quickly (<10 years), in concrete structures, clear pessimum effect [39,40].
It1 (C + F)	Italy (Marche region in central Italy)	Polymictic river gravel, containing mainly micritic limestone, but also silicified limestone, flint, chert and strained quartz; reactive minerals are micro- to cryptocrystalline quartz and strained, high metamorphically sutured quartz).	Quick reaction (5–10 years) observed in all types of concrete structures.
It2 (C + F)	Italy (Piemont region)	Polymictic river gravel; aggregate of interest is fine-grained quartzite with strained quartz; reactive mineral is strained highly metamorphically sutured quartz.	Considered to be “slowly” reactive, (one example is 50 years old water construction).
N1 (C)	Norway (middle)	Crushed cataclasite, homogeneous and fine-grained, feldspar particles lie scattered within a matrix of about 0.02 mm grain size; reactive mineral is crypto- to microcrystalline quartz.	Has caused severe damage in local areas (e.g. 11 years old airport pavement).
N2 (C)	Norway (south east)	Crushed sandstone, homogeneous and fine-grained, with a sediment grain size ranging between 0.05 and 0.5 mm. These variously sized particles are embedded in a fine-grained matrix; reactive mineral is crypto- to microcrystalline quartz.	Has caused severe damage in local areas (damage observed in bridges and dams after 15 to 20 years) [24].
N3 (C + F)	Norway (south western)	Natural gravel/sand from a glaciofluvial deposit, originally composed of Precambrian crystalline rocks, consists of granites and gneisses; no reactive constituents.	Non-reactive. No damage reported.
N4 (C + F)	Norway (south east)	Natural gravel/sand from a moraine deposit. Sandstones, siltstones and cataclastic rocks are reactive rocks; reactive mineral is crypto- to microcrystalline quartz.	The coarse fraction has caused moderate damage, if the humidity and the alkali content are high (e.g. 20–25 years old constructions, mainly bridges) [24].
N5 (C + F)	Norway (south)	Sand and coarse gravel from a glaciofluvial deposit. Rhyolite and fine-grained quartzite are reactive rocks; reactive mineral is microcrystalline quartz.	The coarse fraction has caused moderate damage, if the humidity and the alkali content are high (e.g. 20–25 years old constructions, mainly bridges) [24].
N6 (C + F)	Norway (south)	Sand and coarse gravel from a glaciofluvial deposit. The reactive rocks are mainly argillaceous rocks and sandstones in addition to small amounts of hornfels, rhyolite and mylonite. Reactive mineral is crypto- to microcrystalline quartz.	The coarse fraction has caused moderate damage, if the humidity and the alkali content are high (e.g. 20–25 years old constructions, mainly bridges) [24].
P1 (C)	Portugal	Crushed, poorly silicified limestone; reactive minerals could be micro- or cryptocrystalline quartz.	Similar limestone, probably with higher content of silica, has caused damage in several concrete structures like bridges and dams.
S1 (C + F)	Sweden	Polymictic glaciofluvial gravel and sand, primarily composed of meta-rhyolite and granite; aggregates of interest are meta-rhyolite and greywacke; reactive minerals are micro- or cryptocrystalline quartz or chalcedonic quartz.	Similar aggregate used as concrete material has caused moderate damage. The source is variable in composition.
UK1 (C + F)	United Kingdom	Crushed greywacke, poorly sorted; reactive minerals are micro- or cryptocrystalline quartz, possibly volcanic glass.	Concrete with this aggregate has demonstrated high damage at moderate to high alkali levels in many real structures (more than 20 years until observed damage).
UK2 (C + F)	United Kingdom	Polymictic mature river gravel and sand, composed primarily of metaquartzite, ortho-quartzite, quartz (vein) and chert, which is the reactive portion in the aggregate; reactive minerals are micro- or cryptocrystalline or chalcedonic quartz.	Both, fine and coarse constituents have demonstrated reactivity at moderately high alkali levels in many real structures, mainly bridges (damage after 10 to 15 years).
E1 (F)	Spain	Dolostone with prismatic dolomite crystals cemented with calcite, also opal and clay are apparent in considerable amounts; reactive mineral is opal.	Serious damage reported in 30 years old precast water pipe. Uncertainty if caused by ASR.

C = coarse aggregate (>4 mm); F = fine aggregate (≤4 mm).

from 10 different countries (Table 1). The aggregates were selected with the purpose of covering most types of reactive aggregates throughout Europe. Additionally, non-reactive reference aggregates were tested.

2.3. The test programme for testing the aggregates with the different methods

2.3.1. Laboratory test methods — general

The full list of methods, with brief descriptions, and references to the original published methods [10–17] are given in Table 2. The tests were performed according to these methods, amplified by detailed instructions prepared for each method. Some supplementary information about the methods is given below.

2.3.2. RILEM AAR-1 petrographic method

The petrographic method [10] is a test method used as a "first step" to assess the potential alkali-reactivity of concrete aggregates. The method is carried out by two mutually beneficial techniques; a standard petrographic examination of the aggregate particles and a detailed microscopical examination of thin sections which may incorporate point-counting. An initial inspection of the aggregate material should be undertaken to assess which technique(s) should be employed.

This RILEM AAR-1 petrographic method allows for three different technique(s)/procedure(s) to determine the potential alkali-reactivity of a particular aggregate sample:

1. Particle separation: After separation, selected particles can be thin sectioned to determine the microscopical reactivity related characteristics. The procedure is known to be somewhat uncertain and is not suited for unfamiliar or "complex" aggregate types.
2. Point counting technique: Considered to be the most accurate method for identification of the different rock types.
3. Whole rock petrography: If a crushed rock aggregate has uniform characteristics, then a thin section of the total aggregate particles can be produced for the determination of its potential alkali-reactivity.

All of these procedures are useful in establishing the potential alkali-reactivity of an aggregate, and none should be discounted as a technique of determining reactivity. The technique selected should be based on an initial macro-examination of the aggregate sample received. In reference to the RILEM AAR-1 method, it is not compulsory to use only one of these specified techniques. However, in the project report [1] and in the current paper only results from the point counting analyses are included.

When applying the point counting technique, an adequate number of representative particles must be included in the thin sections prepared. Guidance on minimum number of particles in the different fractions for thin sections of size 50×30 mm^2 is given in the method [10]. E.g. for the coarse fractions (>4 mm), two thin sections of the fraction 2/4 mm (after crushing) should be prepared (minimum 300 particles). For the sand fractions (≤4 mm) two thin sections of the fraction 2/4 mm (minimum 300 particles) and one thin section of the 1/2 mm fraction (minimum 800 particles) should be prepared. The method allows the analysis of one thin section of the fraction <2 mm (minimum 1500 particles) as an alternative to the 1/2 mm fraction. In the PARTNER project, one thin section of the 0.063/1 mm fraction was prepared for most fine aggregates (in addition to the 1/2 mm fraction).

The point counting technique is carried out along traverses in regular increments in two directions to form a virtual orthogonal grid. It is important that point-counting covers the whole thin section. During the point-counting, the operator must identify and group all rocks and minerals (i.e. provide an assessment of both the reactive and non-reactive ones) located under the cross hairs at each point on the grid. Note that a minimum of 1000 points (excluding points falling on to resin) should be counted for all the counted fractions. A statistically sound quantitative estimate of the various components can only be made if the entire thin section is covered and if the virtual grid is adapted to the size of the mineral crystals. Additionally, the number of points may significantly exceed the number of particles, as several points may be counted across some larger particles.

During the point counting process there are two different "procedures" in use. In some countries, it is common to determine the constituent and thus the reactivity assessment of the individual

Table 2
Summary of test methods.

Test method	Brief outline of method
RILEM AAR-1 Petrographic method [10]	The potential alkali-reactivity of the aggregate is classified on the basis of its petrographic composition. Depending on the nature of the aggregate, this can either be by hand separation, crushing and point counting under a microscope or by microscopic examination in thin section.
RILEM AAR-2 Accelerated mortar bar method [11]	Mortar bars made with the aggregate and a reference high alkali cement are stored in 1 M NaOH at 80 °C and their expansion monitored over a 14 days period.
TI-B51 — The Danish mortar bar test [12]	Mortar bars made with the aggregate are stored in saturated NaCl solution at 50 °C and their expansion is monitored for 52 weeks.
The Danish Chatterji method [13]	The degree of reaction between silica in the aggregate and KCl is determined by measuring the alkalinity after 24 h reaction to a non-reactive standard.
RILEM AAR-3 Concrete prism method [14]	Accelerated expansion test for 12 months. Wrapped concrete prisms, $(75 \pm 5) \times (75 \pm 5) \times (250 \pm 50)$ mm^3, made with the aggregate and a reference high alkali cement are stored over water in individual containers within a constant temperature room at 38 °C and measured at 20 °C.
RILEM AAR-4 Accelerated concrete prism method [15]	Accelerated expansion test for 20 weeks. Concrete prisms, $(75 \pm 5) \times (75 \pm 5) \times (250 \pm 50)$ mm^3, made with the aggregate and a reference high alkali cement are stored over water in individual containers within a reactor at 60 °C and 100 % relative humidity and measured at 20 °C.
RILEM AAR-4 Alt. Accelerated concrete prism method [15]	Accelerated expansion test for 20 weeks. Wrapped concrete prisms, $(75 \pm 5) \times (75 \pm 5) \times (250 \pm 50)$ mm^3, made with the aggregate and a reference high alkali cement are stored over water in individual containers within a constant temperature room at 60 °C and measured at 20 °C.
German concrete method [16]	Test duration of 9 months. Concrete prisms ($100 \times 100 \times 450$ mm^3) and one cube ($300 \times 300 \times 300$ mm^3) are stored in a fog chamber at 40 °C with measurements taken immediately with no cooling down period. The expansion of concrete prisms and the maximum crack width on the cube are determined.
Norwegian concrete prism method [17]	Accelerated expansion test for 12 months. Large concrete prisms ($100 \times 100 \times 450$ mm^3) made with the aggregate and a reference high alkali cement are stored over water in individual containers within a constant temperature room at 38 °C and measured at 20 °C.
Field site method [5]	$300 \times 300 \times 300$ mm^3 concrete cubes stored on outdoor exposure sites. Measurements of expansions and maximum crack widths.

point which is directly under the crosshairs rather than a determination of the reactivity of the entire aggregate particle. An evaluation of the reactivity of the whole particle is, however, common to use in other countries, e. g in Norway. An example; all cross hair points placed within a sandstone particle is recorded as sandstone. However, when particles consist of more than one type of rock e.g. sandstone with quartz vein, the cross hair point falling on to the sandstone should be recorded as sandstone, and cross hair points falling on to quartz vein should be recorded as quartz vein material. To determine which procedure is to be used, the experience with the aggregates within each country should be taken into account.

As a basis for calculating the total percentage of "reactive/possible reactive" rock types in an aggregate, each of the rock types detected should be placed, based on the petrographers experience, in one of the three "reactivity classes";

I. very unlikely to be alkali-reactive
II. alkali-reactive uncertain
III. very likely to be alkali-reactive.

Experience within some regions and with particular materials (i.e. highly metamorphic rocks) has shown that a determination of the quartz grain size within a particle is important in the assessment of the reactivity potential of that material. In such a rock (aggregate), the percentage of the material containing these varying sizes of quartz crystals is essential in the overall determination of the potential alkali-reactivity. However, at this stage the RILEM AAR-1 petrographic method should primarily attempt to report the reactivity potential of such constituents based on the petrographer's own experience, which, however, can result in significant variability in the test results.

RILEM has presented various acceptance criteria for RILEM test methods in assessments of alkali-reactivity potential [18]. The criteria are partly based upon the outcome of the PARTNER project. Regarding the petrographic method, RILEM points out that acceptance and experience with reactive constituents differ between countries, and thus, final assessment and classification should follow any national or regional experiences, recommendations and specifications. Assessments of alkali-reactivity potential of the petrographic results obtained in the current research project were based upon evaluations among petrographers gathering together at workshops within this project. In addition, Norwegian petrographic acceptance criteria were considered, as Norway have used the petrographic method for many years, and have published a set of critical requirements for the quantity of reactive constituents in aggregates [19].

2.3.3. RILEM AAR-2 accelerated mortar bar method

In the RILEM AAR-2 Accelerated mortar bar test [11], three mortar prisms are cast with the test aggregate and a reference high alkali cement. The aggregate is either natural sand or a crushed aggregate with a grading made to a certain specification. After demoulding, the prisms are stored for 24 h in water at 80 °C after which their initial length is measured. Then the prisms are submerged in 80 °C 1 M sodium hydroxide solution for 14 days during which at least three length measurements are taken. The expansion is calculated, and the mean of the expansions of the three prisms after 14 days are given as the result.

In this PARTNER test programme, in addition to testing the different aggregates, a comparison was made of the effects of using the short ($40\times40\times160$ mm^3 — RILEM-type) and long ($25\times25\times285$ mm^3 — ASTM-type) bars, and, for those aggregates where both coarse and fine fractions existed, the results of testing the crushed coarse fraction were compared with those of the fine fraction.

The RILEM acceptance criteria [18] for the interpretation of the results of AAR-2 have not yet been finally agreed. However, on the basis of trials carried out by RILEM on aggregate combinations of known field performance from various parts of the world, it seems that results in the test (after the standard 14-days exposure time, using 'long thin' $25\times25\times250$–300 mm^3 specimens) of less than 0.10% are likely to indicate non-expansive materials, whilst results exceeding 0.20% are likely to indicate expansive materials. It is not currently possible to provide interpretative guidance for results in the intermediate range 0.10% to 0.20% and, for all practical purposes in the absence of additional local experience, aggregates yielding AAR-2 results in this range will need to be regarded as being potentially alkali-reactive.

2.3.4. Concrete prism methods

In this programme, five concrete prism tests were evaluated [14–17]:

- RILEM AAR-3 Concrete prism method (storage at 38 °C)
- RILEM AAR-4 Accelerated concrete prism method (storage at 60 °C)
- RILEM AAR- 4 Alternative accelerated concrete prism method (storage at 60 °C)
- German concrete test method (storage at 40 °C)
- Norwegian concrete prism method (storage at 38 °C)

The details of the methods are given in the references, see Table 2. In general, all the methods monitor the expansion and the weight change of concrete specimens containing the test aggregate and made with high contents of a high alkali cement and which are stored in conditions of high humidity and elevated temperatures. For RILEM AAR-3 and the German and Norwegian methods, the storage period is quite long, 9 months or a year, but for the RILEM AAR-4 methods the exposure period is reduced to 20 weeks (or even 15 weeks) by use of the higher temperature of storage (60 °C). RILEM have recently renamed the AAR-4 method, and named it "AAR-4.1" when applied for testing aggregates [15]. However, in this paper, the method is consequently called "AAR-4".

The RILEM acceptance criteria [18] for the interpretation of the results of AAR-3 and AAR-4 have not yet been finally agreed. However, on the basis of trials carried out by RILEM on aggregate combinations of known field performance from various parts of the world, it seems that results in the AAR-3 test (usually after 12 months) of less than 0.05% are likely to indicate non-expansive materials, whilst results exceeding 0.10% indicate expansive materials (These suggested criteria apply only to results using the preferred prism size in AAR-3. The use of larger prism sizes, which is permitted as an alternative, is thought likely to produce different values). It is not currently possible to provide interpretative guidance for results in the intermediate range 0.05% to 0.10% and, for all practical purposes in the absence of additional local experience, aggregates yielding AAR-3 results in this range will need to be regarded as being potentially alkali-reactive. On the basis of an initial assessment of the AAR-4 trials carried out by TC 191-ARP on aggregate combinations of known field performance from various parts of the world, it seems that a maximum expansion in the RILEM AAR-4 test of 0.03% at 15 weeks indicates a non-reactive aggregate combination. It follows that, in the case of aggregate combinations producing AAR-4 results greater than 0.03% at 15 weeks, in the absence of local experience to the contrary, precautions should be taken to minimize the risk of ASR damage to any concrete in which the material is used.

The acceptance criterion for a non-reactive aggregate combination in the German test method [16], is expansion less than 0.06% after nine months of exposure. The zero readings are taken at 20 °C, while the other measurements are taken without cooling the prisms. Thus, the critical limit corresponds to a limit of approx. 0.04%, if the prisms had been cooled to 20 °C before measuring. In the Norwegian test method [17], the critical limit applied varies from 0.040% to 0.050% after one year of exposure depending on the aggregate combination tested [19].

2.3.5. Laboratory test programme

The test programme took into account the need for a sufficient number of tests on each aggregate type using each of the main (RILEM) methods and the experience and budgets of the participating laboratories. For the regional (i.e. Danish-, German- and Norwegian) methods, a reduced programme was undertaken in a few laboratories experienced with these methods.

The numbers of laboratories who participated in the evaluation of each method, the numbers of aggregate types tested according to the different methods, and the total numbers of single tests performed were as follows:

RILEM AAR-1	13[1] laboratories;	22 aggregate types;	in total 123 single analyses
RILEM AAR-2	16[2] laboratories;	22[3] aggregate types;	in total 75 single tests
RILEM AAR-3	10 laboratories;	19 aggregate combinations;	in total 48 single tests
RILEM AAR-4	6 laboratories;	18 aggregate combinations;	in total 59 single tests
RILEM AAR-4 Alt.	3 laboratories;	14 aggregate combinations;	in total 22 single tests
Norwegian	2 laboratories;	10 aggregate combinations;	in total 13 single tests
German	1 laboratory;	10 aggregate combinations;	in total 10 single tests
Danish TI-B51	3 laboratories;	25[4] aggregate types;	in total 37 single tests
Chatterji test	3 laboratories;	14 aggregate types;	in total 26 single tests

[1] Six of the laboratories classified themselves as experienced in performing petrographic analysis.

[2] Eight laboratories used the 40×40×160 mm^3 prisms (RILEM-type) and eight used the 25×25×285 mm^3 prisms (ASTM-type).

[3] For some of these, both the coarse and the fine fraction were tested separately.

[4] Included six extra aggregate types (five from Iceland and one from Norway).

In total, 413 individual tests were performed within the PARTNER project. The total amount of aggregate needed by the laboratories were calculated, collected by a partner in the particular country, grading, density and water absorption measured and appropriate amounts despatched to the participating laboratories. A reference high alkali cement (1.26% Na_2O-eqv.) was provided by Norcem who despatched the needed amounts to the laboratories.

2.3.6. The field site tests

These tests were undertaken as a means of evaluating the reliability of different laboratory test methods. Different climatic conditions representative for Europe were covered in order to take into account the influence of different environmental conditions. Furthermore, it is unclear if concrete that is partly immersed in water will exhibit faster and higher degrees of deterioration due to alkali–silica reaction (ASR) than a concrete that is only exposed to ambient rainfall. As a consequence, one cube was stored with its base in a tray filled with water (wet storage) and the other was exposed only to ambient rainfall (dry storage). In laboratory tests, it has earlier been found that samples containing reactive aggregates showed higher degrees of reaction if exposed to salt solutions instead of water [20–22]. Therefore, de-icing salts may trigger and/or accelerate a deleterious ASR in concrete with reactive aggregates. However, results show that the reaction could be different at normal temperatures as compared to elevated laboratory temperatures [23]. To study the influence of alkali supply by de-icing salts under realistic condition, specimens were stored in southwest of Sweden without salt at a field test site in Borås and with salt alongside a highway between Borås and Gothenburg.

For the field site tests, all the cubes representing one concrete mix (i.e. one aggregate type) were cast at one laboratory (generally in the country of origin of the aggregate) and transported to all the other laboratories (field test sites). Thirteen aggregate combinations (Table 3) produced at five laboratories were evaluated in this way on eight different field sites from Norway to Spain (Fig. 1). The mean monthly temperature and precipitations for each field site are given in Fig. 2.

For each site, two 300 mm concrete cubes were prepared with the aggregate combination used in the concrete prism tests. The concrete mixes were the same as those used in the RILEM AAR-3 and AAR-4 specimens, i.e. they were made with relatively high cement content (440 kg/m^3) and high alkali Portland cement (1.26% Na_2O-eqv.). No air entraining agent was added to the concrete mix. The cubes were kept for one day in the moulds, de-moulded and stored indoors for 6 days in a humid environment before being transported to the different field sites.

At the different field sites, two pairs of reference studs were glued on the top surface and on two adjacent side faces, before the cubes were exposed outdoors. All cubes were stored in the same direction in relation to the four cardinal points to minimize deviations between the labs resulting from different exposure to direct solar radiation.

During exposure, one cube was stored with its base in a tray filled with water (wet storage) and the other was exposed only to ambient rainfall (dry storage) (Fig. 3). The tray was filled with water to simulate a permanently wet concrete, so that the bottom of the first cube was immersed 50 to 60 mm in water during the whole testing time. The reference points at the bottom of the first cube were always above water level enabling length change measurements.

For the detection of possible deterioration due to ASR, the dimensions of the cubes at the top surface and two adjacent side faces as well as the crack width were determined periodically (first 2½ years every three months, afterwards every half year). Some laboratories have only measured once a year during the summer season. The measurements were done at the field site. Extreme temperatures should have been avoided, and in the procedure it is recommended to undertake the measurements at the same approximate time in the day, i.e. mid morning, and then at the same temperature as the reference measurements undertaken before exposure of the cubes.

3. Results

3.1. RILEM AAR-1 petrographic method

All the detailed results from the 123 single petrographic analyses were collected and evaluated. Tables 4A and 4B present the results from all the point counting analyses performed by the participating

Table 3
Aggregate combinations tested in the field site.

Sample number	Origin	Aggregate details	Combinations[a]
B1	Western Belgium	Silicified limestone	C + F
B1	Western Belgium	Silicified limestone	C + NRF
D2	Denmark	Sea-dredged gravel semi-dense flint	F + NRC
F1	France (Seine Valley)	Gravel with flint	C + NRF
F2	France	Non-reactive limestone	C + F
G1	Germany (Upper Rhine Valley)	Crushed gravel with siliceous limestone and chert	C + NRF
It2	Italy (Piemont region)	Gravel with quartzite and gneiss	C + F
N1	Norway (middle)	Cataclasite	C + NRF
N2	Norway (south east)	Sandstone	C + NRF
N4	Norway (south east)	Gravel with sandstone and catacl. rocks	C + F
S1	Sweden	Gravel with porphyritic rhyolite	C + F
UK1	United Kingdom	Greywacke	C + F
P1	Portugal	Silicified limestone	C + NRF

[a] C = coarse aggregate; F = fine aggregate; NRC = non-reactive coarse aggregate (= F2C, see Table 1); NRF = non-reactive fine aggregate (= N3F, see Table 1).

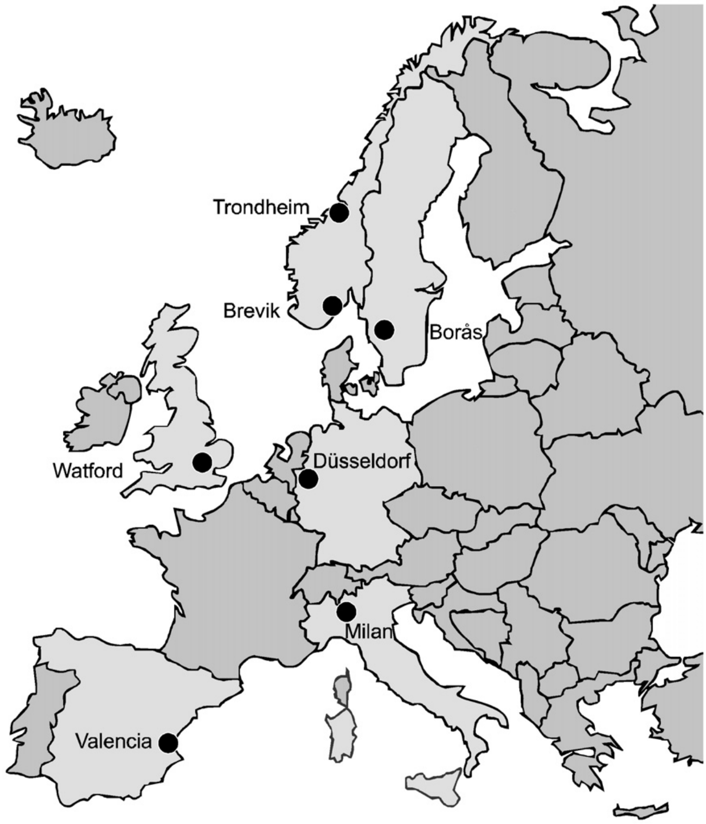

Fig. 1. Location of outdoor exposure sites.

laboratories. The following results are presented for each of the aggregate samples:

- Origin (country)/name of sample (see also Table 1)
- Type of aggregate (i. e. main rock type(s))
- Fraction investigated (e.g. 4/8 mm)
- Sum of suspicious rock types, i. e. the "reactivity classes" II and III (volume percentage within the aggregate fraction) [on the web page (www.farin.no/english) the detailed results for each of the three "reactivity" classes are available in an Excel file]
- Field performance (i. e. damage due to ASR documented?)
- Results in agreement with field performance?

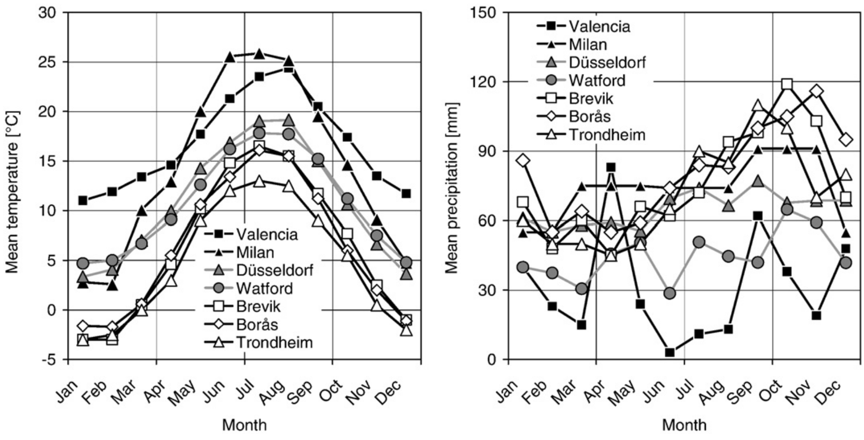

Fig. 2. Mean temperature and precipitation at different field sites.

Fig. 3. Concrete cubes located at the outdoor exposure site in Düsseldorf, Germany.

For fine aggregates (*F*; <4 mm) results from point counting of each of the fractions 2/4 mm, 1/2 mm and 0.063/1 mm were reported separately. However, this was not always the case by some laboratories. Some aggregates have been examined by up to eight different laboratories according to the same petrographic procedure.

3.2. RILEM AAR-2 accelerated mortar bar method

The detailed results of the testing and expansion graphs for each aggregate are given in the published report on the method [2] and are summarized in Table 5.

3.3. Concrete prism methods

The detailed results for all the methods and expansion graphs for each aggregate combination are given in the published report on the concrete methods [3]. Two examples of expansion graphs for a "normally" reactive and a "slowly" reactive aggregate combination are given in Figs. 4 and 5, respectively. The results are summarized in Table 6, where the aggregates are grouped into three categories according to their reported field behaviour (Table 1); aggregate combinations that react in "normal" timescales (5–20 years), "slowly" reactive aggregates (+15–20 years) and non-reactive aggregates.

The AAR-3 results obtained at two of the ten laboratories performing this test are omitted from the paper. The reason is that the one year values are missing from one of the laboratories (4 single tests). The other laboratory obtained zero expansion (i.e. 0.00%) after one year of exposure for all the three aggregates tested (B1, F3 and It2, respectively). Thus, they have probably not been able to completely follow the testing procedure.

3.4. The field site tests

In 2008, the samples had been exposed in the field sites for approximately four years. This time is too short for "slowly" reactive aggregates to cause a deleterious ASR in concrete. Thus, only preliminary conclusions are possible. The maximum expansion and the maximum crack width of the cubes are summarized for each aggregate combination and field site in Table 7 for cubes that were partly immersed in water and in Table 8 for cubes that were exposed only to ambient rainfall. After approx. one year of exposure, a new "zero" measurement was necessary because some laboratories had problems with the determination of dimension changes of the cubes or the use of the provided result files. Thus, the expansion values presented in the two tables represent approx. three years of outdoor exposure.

Extensive expansions >0.04% which have occurred since the new "zero" measurement in June 2005 and cracks ≥0.20 mm which occurred after four years of testing are highlighted (bold) in the Tables 7 and 8. Expansion in excess of these levels is an indication that a deleterious ASR might have taken place. The Figs. 6–11 show the mean expansions and crack widths for six of the reactive aggregates. In the Figs. 12–15, detailed expansions values (i.e. on the top and on two adjacent side faces) for two of these aggregate types measured at three field sites are presented. The figures also include measurements performed in 2009 at six of the eight field sites.

4. Discussion

4.1. RILEM methods and field site tests

4.1.1. RILEM AAR-1 petrographic method

4.1.1.1. Variation between laboratories with respect to evaluation of aggregate reactivity. Thirteen laboratories, both experienced and inexperienced, have performed petrographic analyses according to the AAR-1 method. Before the testing programme started, about one half of the petrographers had participated in one or two internal petrographic workshops in the PARTNER project, where selected European aggregate types were examined microscopically and the observations "discussed". No other co-ordination was made between the laboratories.

In the further discussion, focus is made on the variation between the laboratories with respect to the sum of rock types detected within the "reactivity classes" II+III (i.e. the suspicious rock types with respect to ASR).

The overall experience from the testing programme is that the spread in results between the laboratories for about half of the aggregate types is very high, also between some of the six laboratories performing the test on a regular basis. For 8 of the 22 aggregates types (D1, D2, G1, G2, It1, It2, UK2 and P1), the number of rock types detected by the participating laboratories within the "reactivity classes" II+III varies from less than 15% to more than 85% (Tables 4A and 4B). The rock names used also vary significantly.

However, for four of the six most experienced laboratories, the majority of the reported results seem to be more reliable. The cases where also these laboratories from time to time deviate from the average/median results, are mainly connected to the aggregate types D1, D2, It1 and UK2. These aggregate types are not familiar for most of these experienced petrographers, thus the importance of local knowledge about the reactivity of different alkali-reactive aggregates is obvious.

The majority of the results reported from the two remaining experienced petrographers deviates much from the average/median

Table 4A
Summary results of all the point counting analyses performed by the 13 participating laboratories [1].

Sample	Aggregate type	Fraction[1] (mm)	Statistics[2]	Point counting (%)						Field performance[6]	Results in agreement with field performance?
				TS 2/4 mm[5]		TS 1/2 mm[5]		TS 0.063/1 mm[5]			
				Sum II+III[3]	Comments	Sum II+III[3]	Comments	Sum II+III[3]	Comments		
B1 (F)	Silicified limestone	0/2	**"average"**					**97**	1 result (TS 0.125/2 mm)	**R?**	**Yes**
B1 (C)		4/20, "coarse"	**"average"**	**100**	1 result (1 lab., 1 frac.)[4]			**100**	1 result (TS 0.063/2 mm)	**R**	**Yes**
D1 (F)	Gravel with opaline flint	0/4	**average** Median minimum maximum	**36?** 16? 6 85	7 results (7 lab., 1 frac.)	**39** 44 7 87	5 results (5 lab., 1 frac.)	**48** 35 28 81	3 results (3 lab., 1 frac.)	**R (pessimum behavior)**	**Yes**
D2 (F)	Sea gravel semi-dense flint	0/4	**average** median minimum maximum	**38** 28 2 100	5 results (5 lab., 1 frac.)	**50** 40 9 100	3 results (3 lab., 1 frac.)	**53** -- 6 100	2 results (2 lab., 1 frac.)	**R**	**Yes**
D3 (F)	Non reactive silicious sand	0/2	**average** median minimum maximum			**2** -- 0 3	2 results (2 lab., 1 frac.)			**NR**	**Yes**
F1 (C)	Gravel with flint	6/20	**"average"** median minimum maximum	**96** -- -- --	1 result (1 lab., 1 frac.)	**96** -- -- --	1 result (1 lab., 1 frac.)	**86** -- -- --	1 result (0/1 mm)	**R (pessimum behavior)**	**Yes**
F2 (F)	Non reactive limestone	0/5	**"average"**	**0**	1 result (1 lab., 1 frac.)	**0**	1 result (1 lab., 1 frac.)	**0**	1 result (1 lab., 1 frac.)	**NR**	**Yes**
F3 (F)	Silicious gravel	0/4	**average** median minimum maximum	**53?** 42 37 94	5 results (5 lab., 1 frac.)	**54** 35/70 30 82	4 results (4 lab., 1 frac.)	**60** 76 25 78	3 results (3 lab., 1 frac.)	**NR?**	**No**
F3 (C)		4/20	**"average"** median minimum maximum	**26?** -- -- --	1 result (1 lab., 1 frac.) (TS > 4 mm)					**N R?**	**No**
G1 (C)	Crushed gravel with silicified limestone and chert	"4/22"	**"average"** median minimum maximum	**46** -- -- --	1 result (1 lab., 1 frac.)	**44** -- -- --	1 result (1 lab., 1 frac.)	**33** -- -- --	1 result (1 lab., 1 frac.)	**R**	**Yes**
G2 (C)	Gravel with opaline sandstone and flint	"2/8"	**average** median minimum maximum	**50?** 43 14? 92	3 results (3 lab., 2 frac.)					**R (pessimum behavior**	**Yes**
It1 (F)	Gravel with limestone, chert and flint	0/5	**average** median minimum maximum	**32?** 10 8 100	4 results (4 lab., 1 frac.)	**61** -- 21 100	2 results (2 lab., 1 frac.)	**55** -- 10 100	2 results (2 lab., 1 frac.)	**R**	**Yes**
It1 (C)		"5/30"	**"average"** median minimum maximum	**10?** -- -- --	1 result (1 lab., 1 frac.?)					**R**	**Yes**
It2 (F)	Gravel with quartzite and gneiss	0/5	**average** median minimum maximum	**51?** 24?/81 14 100	5 results (5 lab., 1 frac.)	**82** 86 60 100	3 results (3 lab., 1 frac.)			**R?**	**Yes**

For origin (country), see Table 1. (Regarding abbreviations: see footnotes to Table 4B).

results. For one of these laboratories, the sum of aggregate types classified in the "reactivity classes" II or III is in many cases somewhat lower than reported from the other laboratories. For the second of these laboratories, the percentage of aggregate types classified within the "reactivity classes" II or III is in most cases much higher than for all the other laboratories (also the inexperienced ones).

The other examined rock types were classified by different laboratories as follows:

- Sandstone: class I by several laboratories, class II or III by other laboratories
- Siltstone: class I by one laboratory, class II or III by other laboratories
- Flint: different types of flint detected/named by different laboratories (often named chert by several laboratories); the classification of reactivity also varies a lot — all three "reactivity classes" are used

This result is only valid for the examined aggregate sample of specific quarries. N.B. This is a general classification of rock types into reactivity classes according to RILEM AAR-1. However, a petrographer's detailed knowledge of local aggregates can change this classification. Having said this, it is important to bear in mind the results from the field exposure sites. Some aggregates react slowly in one climate and much quicker in another climate. The regional knowledge about reactivity can't therefore always be transferred to the use in another climate, e.g. when exporting aggregates.

Table 4B
Summary results of all the point counting analyses performed by the 13 participating laboratories [1].

Aggregate	Aggregate type	Fraction[1] (mm)	Statistics[2]	Point counting (%)						Field performance[6]	Results in agreement with field performance?
				TS 2/4 mm[5]		TS 1/2 mm[5]		TS 0.063/1 mm[5]			
				Sum II+III[3]	Comments	Sum II+III[3]	Comments	Sum II+III[3]	Comments		
N1 (C)	Cataclasite	4/16	**average** median minimum maximum	**90?** 98 71? 100	3 results (3 lab., 1 frac.)					**R**	**Yes**
N2 (C)	Sandstone	8/16	**"average"**	**100**	1 result (1 lab., 1 frac.)					**R**	**Yes**
N3 (F)	Non-reactive granitic sand	0/4	**average** median minimum maximum	**2** 1 0 6	3 results (3 lab., 1 frac.)	**2** 1 0 6	3 results (3 lab., 1 frac.)	**2** -- 0 4	2 results (2 lab., 1 frac.)	**NR**	**Yes**
N4 (F)	Gravel with sandstone and cataclastic rocks	0/7	**"average"** median minimum maximum	**27** -- 23 31	2 results (2 lab., 1 frac.)					**R?**	**Yes**
N4 (C)		7/16	**"average"** median minimum maximum	**25** -- 23 27	2 results (2 lab., 1 frac.)					**R**	**Yes**
N5 (F)	Gravel with rhyolite and quartzite	0/8	**"average"**	**22**	1 result (1 lab., 1 frac.)	**17**	1 result (1 lab., 1 frac.)			**R?**	**Yes**
N5 (C)		8/16	**"average"**	**22**	1 result (1 lab., 1 frac.)					**R**	**Yes**
N6 (F)	Gravel/sand with argillaceous rocks and sandstone	0/8	**"average"**	**37**	1 result (1 lab., 1 frac.)	**23**	1 result (1 lab., 1 frac.)			**R?**	**Yes**
N6 (C)		8/16	**"average"**	**33**	1 result (1 lab., 1 frac.)					**R**	**Yes**
S1 (F)	Gravel with porphyritic rhyolite	0/8	**average** median minimum maximum	**52?** 44 35? 100	5 results (5 lab., 1 frac.)	**61** 45 37 100	3 results (3 lab., 1 frac.)			**R?**	**Yes**
S1 (C)		4/16	**"average"** median minimum maximum	**43?** -- -- --	1 result (1 lab.,1 frac.) (TS > 4 mm)					**R?**	**Yes?**
UK1 (F)	Greywacke	0/5	**"average"**	**83**	1 result (1 lab., 1 frac.)	**66**	1 result (1 lab., 1 frac.)	**40**	1 result (1 lab., 1 frac.)	**R?**	**Yes**
UK2 (F)	Gravel with quartzite and chert	0/5	**average** median minimum maximum	**52** 54 15 89	5 results (5 lab., 1 frac.)	**27** 9 7 66	3 results (3 lab., 1 frac.)			**R**	**Yes**
UK2 (C)		5/20	**average** median minimum maximum	**54** 48 15 98	3 results (3 lab., 1 frac.)					**R**	**Yes**
P1 (C)	Silicified limestone	4/19	**"average"**	**100**	1 result (1 lab., 1 frac.)					**R**	**Yes**
E1 (F)	Silicified and clayed dolostone	0/4	**average** median minimum maximum	**3?** -- 0 8	3 results (3 lab., 1 frac.)	**3?** -- 0? 5	2 results (2 lab., 1 frac.)			**R?**	**No**

For origin (country), see Table 1.
1 The fraction investigated in the petrographic analyses.
2 The average represents the mean results of all the investigated fractions at all laboratories. "Average" means less than three results available.
3 The numbers represent the sum of the "reactivity classes" II and III, i.e. the sum of all the suspicious rock types.
4 Lab. = laboratories; frac. = fractions.
5 TS = thin sections.
6 R = proved to be alkali-reactive based on field performance ; NR = not observed damage due to ASR in real structures.
🟩 = something is not clear or uncertain.
🟧 = OK results (i.e. checked and found reasonable).

4.1.1.2. Link to field performance. Information about the field performance of the 22 "PARTNER aggregates" is given in the last column in Table 1. The averaged results from the petrographic analyses of almost all the 22 aggregate types (Table 4A and 4B) correlate very well with the reported field performance (Table 1), based upon acceptance criteria discussed previously in this paper. The French aggregate F3 and the Spanish aggregate E1 are two exceptions. The F3 aggregate contains many reactive rock types. Despite of this, the French partners were not aware of any deteriorated real concrete structures containing this aggregates type.

Table 5
Summarized results of the testing of the aggregates according to RILEM AAR-2, listed in order of expansion [2].

Aggregate	Results (14 days)		"S/L-ratio"	Reported reactivity in the field (see Table 1)
	Short (S) (40 × 40 × 160 mm^3)	Long (L) (25 × 25 × 285 mm^3)		
It1 (C) Gravel with limestone, chert and flint	X	0.62–1.06 (3)	X	Very high
G2 (C) Gravel with opaline sandstone and flint	0.51–0.56 (2)	0.68 (1)	0.75–0.82	Very high (pessimum)
It1 (F) Gravel with limestone, chert and flint	0.53 (1)	0.58–0.84 (2)	0.63–0.91	Very high
N1 (C) Cataclasite	0.42–0.46 (2)	0.42 (1)	1.00–1.10	High
UK1 (F) Greywacke	~0.43 (1)	X	X	High
G1 (C) Crushed gravel with silicified limestone and chert	0.27–0.41 (2)	0.46 (1)	0.59–0.89	High
B1 (F) Silicified limestone	0.20–0.28 (2)	0.42 (1)	0.47–0.67	High
F3 (F) Siliceous gravel	~0.17 (1)	0.36–0.42 (3)	0.40–0.47	No report
N2 (C) Sandstone	0.32 (1)	0.28 (1)	1.14	High
D1 (C) Gravel with opal,.flint	0.25 (1)	0.18 (1)	1.39	Very high (pessimum)
D2 (F) Sea gravel with semi-dense flint	0.25–0.27 (2)	0.32 (1)	0.78–0.84	High
D1 (F) Gravel with opal,.flint	0.23 (1)	X	X	Very high
N4 (F) Gravel with sandstone and cataclastic rocks	0.21–0.23 (2)	0.05 (1)	4.2–4.6	Moderate
D2 (C) Sea gravel semi-dense flint	0.13–0.31 (2)	0.25 (1)	0.52–1.24	High
It2 (F) Gravel with quartzite and gneiss	0.14 (1)	0.21–0.22 (2)	0.64–0.67	Moderate
It2 (C) Gravel with quartzite and gneiss	0.12 (1)	0.14–0.32 (2)	0.38–0.86	Moderate
N4 (C) Gravel with sandstone and cataclastic rocks	0.18–0.25 (2)	0.10–0.21 (2)	0.86–2.5	Moderate
S1 (F) Gravel with porphyritic rhyolite	0.20–0.27 (2)	0.08 (1)	2.5–3.38	Moderate
N5 (F) Gravel with rhyolite and quartzite	0.16 (1)	0.21 (1)	0.76	Moderate
UK2 (F) Gravel with quartzite and chert	0.18–~0.27 (2)	0.16 (1)	1.13–1.69	High
N5 (C) Gravel with rhyolite and quartzite	0.05–0.13 (2)	0.05–0.16 (2)	0.31–2.6	Moderate
P1 (C) Silicified limestone	0.06 (1)	0.07 (2)	0.86	Moderate
F1 (C) Gravel with flint	0.03 (1)	0.01–0.06 (2)	0.5–3	Low–Moderate (pessimum)
E1 (F) Dolomitic limestone	0.01 (1)	0.01–0.08 (3)	0.13–1	High, but uncertain
D3 (F) Non-reactive siliceous sand	0.07 (1)	X	X	Non-reactive
N3 (F) Non-reactive granitic sand	0.05 (1)	0.05–(0.10?) (2)	0.5–(1?)	Non-reactive
F2 (F) Non- reactive limestone	X	0.01 (1)	X	Non-reactive

The number of laboratories having tested each aggregate type is given in brackets. X = no data are available; ~ = data has been interpolated; C = coarse fraction; F = fine fraction.

The situation for the E1 aggregates is opposite. Only a minor amount of reactive constituents were detected, but serious damage is reported on a 30 years old precast concrete element. Several of the participating petrographers questioned whether E1 could lead to ASR.

In almost all known cases of Norwegian ASR-damaged structures, the damages are mainly caused by the coarse aggregate fractions (>8–10 mm) [24]. For several of the other European aggregate types included, there is a lack of information about which fractions that have proved to give ASR-problems in real concrete structures. This lack of information makes the evaluation of several of the fine aggregates uncertain.

4.1.1.3. Variation between aggregate fractions examined? Overall, the content of suspicious rock types ("reactivity class" II + III) detected within the different fractions examined (i.e. >4 mm, 2/4 mm and 1/2 mm) for a given aggregate type does not vary much compared to the variations revealed between the different laboratories participating (see above). The fraction 0.063/1 mm is tested for most fine aggregates. In particular, point counting of this small fraction did not give any complementary information about the potential alkali-reactivity of any of the aggregate types included in the test programme. For many of the aggregates types, e.g. N3 and N4, free minerals were also to a large extent detected within this fraction. Taking into account the time consuming examination of this small

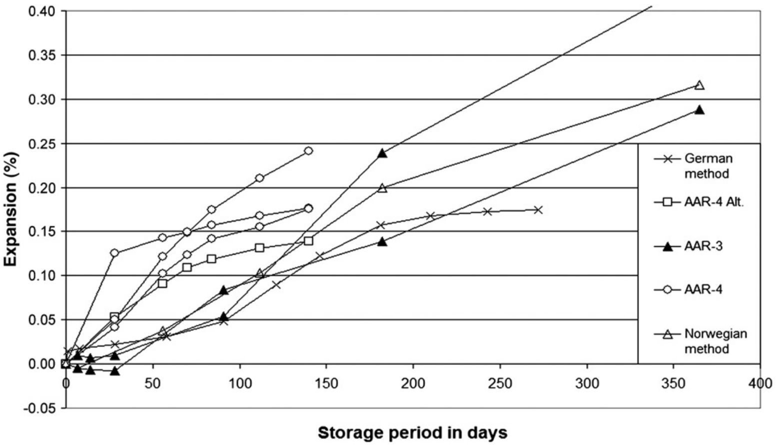

Fig. 4. Expansion of the coarse "normally" reactive aggregate N1 (cataclasite) in combination with the non-reactive fine aggregate N3 (granitic sand) in the various concrete prism methods.

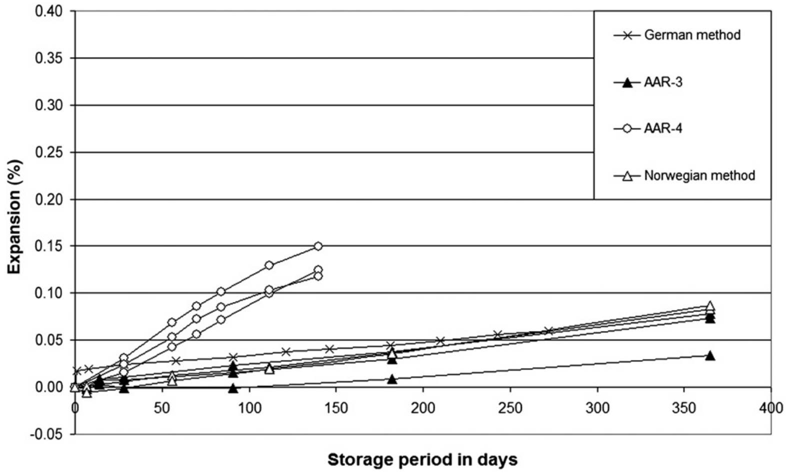

Fig. 5. Expansion of the “slowly” reactive aggregate N5 (fine/coarse gravel with the reactive rock types rhyolite and fine-grained quartzite) in the various concrete prism methods.

fraction, for most (all?) fine aggregate types one should consider only counting the fractions 1/2 and 2/4 mm, as has been done in Norway for the last 15 years [17,24].

4.1.1.4. Is the RILEM AAR-1 petrographic method a good tool to assess the potential alkali-reactivity of aggregates? The reported results from the test programme within task 3.1 in PARTNER have detected large inter-laboratory variations, and revealed the following main issues to be dealt with and solved if the RILEM AAR-1 method aims to be a widely used and reliable testing method to assess the potential alkali-reactivity of aggregates both within Europe and worldwide:

- The importance of education and round robin testing
- The importance of experience, both with the method and with the actual local aggregates
- The importance of calibrating the results with other RILEM methods and with field experience to be able to establish critical limits for acceptable content of suspicious rock types in different aggregate types.
- The importance of accuracy, quality control and system for certification of laboratories and petrographers.

4.1.1.5. Final remarks. Both the internal workshops and the testing within task 3.1 in the PARTNER project have shown that geological evaluations across the frontiers are difficult. However, the European petrographic atlas developed within the PARTNER project [25] and any national petrographic atlases will hopefully contribute to reduce the spread in the future. The PARTNER project and in particular the internal workshops have established a very good network of contacts between several experienced and less experienced petrographers that may be

Table 6
Average and range of expansion at end of test period for all concrete prism methods.

Aggregate[a] combination	RILEM AAR-3 (12 months)		RILEM AAR-4 (20 weeks)		RILEM AAR-4 alt. (20 weeks)		German (9 months)	Norwegian (12 months)
	Average	Range	Average	Range	Average	Range		(2 labs.)
Aggregates that react in “normal” timescales								
B1 (C+NRF)	0.254	0.146–0.362 (2)	0.136	0.084–0.170 (3)	0.149	0.120–0.178 (2)	–	–
B1 (C+F)	0.245	0.170–0.290 (3)	0.133	0.12–0.15 (3)	0.140	0.11–0.17 (2)	0.12 (1)	0.234 (1)
UK1 (C+F)	0.367	0.207–0.527 (2)	0.182	0.175–0.191 (3)	0.113	0.071–0.156 (2)	0.196 (1)	0.255 (1)
G1 (C+NRF)	0.564	0.164–0.963 (2)	0.143	0.140–0.168 (4)	0.141	0.121–0.162 (2)	0.166 (1)	–
It1 (C+F)	0.223	0.157–0.308 (3)	0.152	0.039–0.232 (3)	0.083	(1)	–	–
N1 (C+NRF)	0.361	0.288–0.435 (2)	0.197	0.175–0.241 (3)	0.139	(1)	0.174 (1)	0.316 (1)
UK2 (C+F)	0.090	0.073–0.118 (2)	0.098	0.058–0.157 (4)	0.054	0.050–0.058 (2)	–	–
D1 (C+F)	0.233	(1)	0.022	0.019–0.025 (3)	0.033	0.031–0.036 (2)	0.032 (1)	–
“Slowly”-reactive aggregate combinations								
D2 (F+NRC)	0.021	(1)	0.085	0.042–0.120 (3)	0.038	0.034–0.042 (2)	–	–
It2 (C+F)	0.036	0.036 (2)	0.067	0.045–0.097 (3)	0.071	(1)	–	–
N2 (C+F)	0.209	(1)	–	–	–	–	–	0.256/0.265 (2)
N4 (C+F)	0.052	0.040–0.066 (3)	0.100	0.097–0.105 (3)	–	–	0.056 (1)	0.061/0.068 (2)
N5 (C+F)	0.062	0.034–0.078 (3)	0.130	0.117– 0.149 (3)	–	–	0.060 (1)	0.083/0.087 (2)
N6 (C+F)	0.059	(1)	–	–	–	–	–	0.076 (1)
Non–reactive aggregate combinations								
F1 (C+NRF)	0.001	−0.0150–0.002 (3)	0.010	0.007–0.014 (4)	0.024	0.019–0.028 (2)	0.028 (1)	–
F2 (C+F)	0.008	0.001–0.012 (3)	0.006	−0.004–0.012 (3)	0.016	(1)	0.021 (1)	0.005 (1)
F3 (C+F)	0.015	−0.001–0.030 (2)	0.016	0.007–0.023 (4)	0.023	(1)	–	–
N3 (C+F)	0.012	(1)	0.036	0.032–0.039 (2)	–	–	–	0.012 (1)
S1 (C+F)	0.010	0.005–0.014 (2)	0.046	0.021–0.092 (4)	–	–	0.030 (1)	0.049 (1)
P1 (C+NRF)	0.018	0.011–0.027 (3)	0.023	0.003–0.034 (4)	0.036	(1)	–	–

The number of laboratories having tested each aggregate type is given in brackets.

[a] C = coarse aggregate; F = fine aggregate; NRC = non-reactive coarse aggregate (= F2C, see Table 1); NRF = non-reactive fine aggregate (= N3F, see Table 1).

Table 7
Maximum average values of expansion measured after three years of exposure at 6 sets of embedded reference points and crack width of cubes stored for four years partly immersed in water on different European outdoor exposure sites.

Storage: partly immersed in water			Location of outdoor exposure site/country/laboratory							
			Trondheim	Brevik	Borås Forest	Borås Road	Watford	Düsseldorf	Milan	Valencia
			N		S		GB	D	I	ES
Aggregate	Combination	Data	SINTEF	Norcem	SP		BRE	VDZ	CESI RICERCA	AIDICO
B1	C + F	Cracks		**0.40**	**0.20**	0.15		**0.35**		**2.20**
		Exp.		**0.167**	**0.138**	***0.106***		**0.186**		**0.171**
B1	C + NRF	Cracks	**0.70**		**0.20**		n. d.		**1.00**	**1.50**
		Exp.	**0.368**		**0.177**		**0.197**		**0.323**	***0.254***
D2	F + NRC	Cracks	0.10		0.05	0.05	n. d.			**1.30**
		Exp.	0.014		0.017	*0.008*	0.038			**0.420**
F1	C + NRF	Cracks					n. d.		0.05	
		Exp.					<0.0		0.006	
F2	C + F	Cracks		< 0.20	0.05	0.05		0.05		0.00
		Exp.		0.018	0.013	0.005		0.006		*0.007*
G1	C + NRF	Cracks	0.10					**0.20**	**0.30**	
		Exp.	**0.059**					**0.133**	**0.146**	
It2	C + F	Cracks		<0.20					0.05	
		Exp.		0.021					0.013	
N1	C + NRF	Cracks	0.05		0.05	0.10	n. d.	0.05		**0.25**
		Exp.	0.015		0.012	*0.014*	**0.052**	**0.118**		***0.160***
N2	C + NRF	Cracks		<0.20			n. d.			
		Exp.		0.016			0.018			
N4	C + F	Cracks		<0.2				0.05	0.00	
		Exp.		0.013				0.013	0.006	
S1	C + F	Cracks		<0.20	0.05	0.05		0.05		0.00
		Exp.		0.022	0.006	*0.007*		0.014		0.010
UK1	C + F	Cracks	0.15		0.05	0.05	n. d.			**0.20**
		Exp.	**0.117**		0.015	*0.013*	0.023			**0.146**
P1	C + NRF	Cracks			0.05				0.00	
		Exp.			0.008				0.028	

Exp. = maximum expansion of cubes in % after approx. three years of exposure (new "zero" measurement in June 2005).
Cracks = maximum crack width of cubes in mm that occurred after approx. 4 years of testing.
n. d. = no data provided; *Italic data* = Value is based only on 2 or 4 sets of embedded reference points.
C = coarse aggregate; F = fine aggregate; NRC = non-reactive coarse aggregate (= F2C, see Table 1); NRF = non-reactive fine aggregate (= N3F, see Table 1).

Table 8
Maximum average values of expansion measured after three years of exposure at 6 sets of embedded reference points and crack width of cubes stored for four years only exposed to ambient rainfall on different European outdoor exposure sites.

Storage: exposed only to ambient rainfall			Location of outdoor exposure site/country/laboratory							
			Trondheim	Brevik	Borås Forest	Borås Road	Watford	Düsseldorf	Milan	Valencia
			N		S		GB	D	I	ES
Aggregate	Combination	Data	SINTEF	Norcem	SP		BRE	VDZ	CESI RICERCA	AIDICO
B1	C + F	Cracks		**0.50**	**0.20**	**0.20**		**0.40**		**3.00**
		Exp.		**0.225**	**0.173**	**0.176**		**0.211**		**3.00**
B1	C + NRF	Cracks	**0.50**		**0.20**		n. d.		**1.00**	**0.90**
		Exp.	**0.299**		**0.248**		**0.208**		**0.420**	**0.220**
D2	F + NRC	Cracks	0.05		0.05	0.05	n. d.			**1.50**
		Exp.	0.014		0.018	0.015	**0.070**			**0.371**
F1	C + NRF	Cracks					n. d.		0.05	
		Exp.					<0.0		0.004	
F2	C + F	Exp.		<0.20	0.05	0.05		0.05		0.00
		Cracks		0.018	0.002	0.007		0.007		0.008
G1	C + NRF	Cracks	**0.30**					**0.25**	0.10	
		Exp.	**0.087**					**0.174**	**0.149**	
It2	C + F	Cracks		<0.20					0.00	
		Exp.		0.011					0.019	
N1	C + NRF	Cracks	0.10		0.10	0.10	n. d.	0.15		**0.30**
		Exp.	0.030		0.014	0.013	**0.046**	**0.143**		**0.151**
N2	C + NRF	Cracks		<0.20			n. d.			
		Exp.		0.011			0.012			
N4	C + F	Cracks		<0.20				0.05	0.00	
		Exp.		0.015				0.012	0.017	
S1	C + F	Cracks		< 0.20	0.05	0.05		0.10		0.00
		Exp.		0.022	0.006	0.005		0.014		*0.031*
UK1	C + F	Cracks	0.15		0.05	0.05	n. d.			**0.25**
		Exp.	**0.110**		0.032	0.014	**0.060**			**0.089**
P1	C + NRF	Cracks			0.05				0.00	
		Exp.			0.006				0.010	

(Regarding abbreviations: see legends to Table 7).

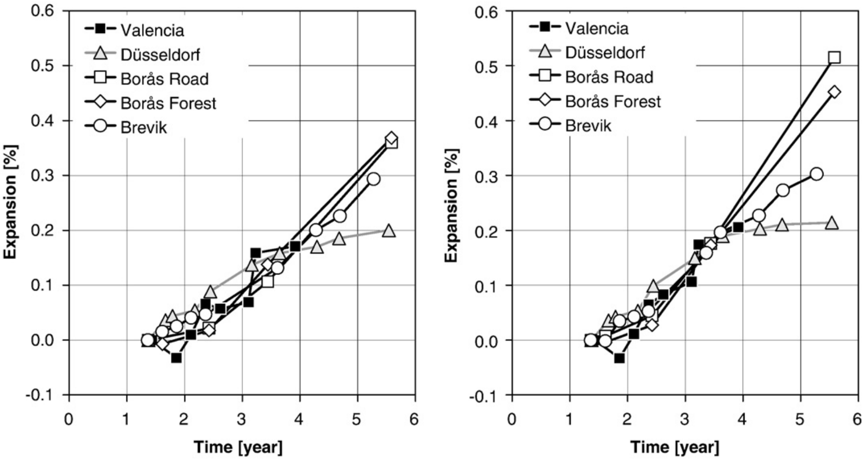

Fig. 6. Mean expansion of concrete cubes with aggregate combination B1(C + F); left: stored partly immersed in water; right: only exposed to ambient rainfall.

helpful in the future to an informal education and "flow of experience" across the frontiers.

4.1.2. RILEM AAR-2 accelerated mortar bar method

Overall, there is good agreement between the ranking of the expansion of the aggregates in the AAR-2 test method (Table 5) and their known reactivity in the field (Table 1), based upon acceptance criteria for AAR-2 presented by RILEM [18] and referred to previously in this paper. None of the non-reactive aggregates show any significant expansion. However, some of those aggregates which are reported to exhibit field reactivity also show very low expansions. The ambiguous aggregates are presented below, and in each case, there is some uncertainty in the reports of their reactivity in the field which can account for the anomaly:

- E1, "Dolomitic limestone"
- N5, "Gravel with rhyolite and quartzite"
- P1, "Silicified limestone"
- F1, "Gravel with flint"

In the case of E1 and P1, there are uncertainties about the aggregate samples tested compared with those found in the structures reported to suffer damage. Additionally, for E1, the cause of the field damage is not certain. F1 is known to exhibit a strong pessimum behaviour, while N5 has only been found to produce damage at long ages.

It can be seen in Table 5 that there is quite a wide spread in the results for some of those aggregates where more than one laboratory performed the test. This points to the fact that, even though the methodology was explained thoroughly in the method and an accompanying instruction, it is still necessary to build up experience before testing is done in earnest.

4.1.2.1. "S/L-ratio". An "S/L-ratio" of 0.54 between the expansion of $40 \times 40 \times 160$ mm^3 (S = short) and $25 \times 25 \times 285$ mm^3 (L = long) prisms (with the long prisms expanding more) has previously been given in the RILEM method [11], but the data obtained from this project does not support this. However, the data from this project suggests an "S/L-ratio" of 0.75 at 14 days, though with a large spread from 0.13 to 4.6. At 9 days and 28 days the mean ratios are 0.79 and 0.84, respectively. Although an "S/L-ratio" can be suggested from this data, the poor correlations means that for many of the aggregates the use of such a ratio would give a misleading result if used to extrapolate from one size of prism to another.

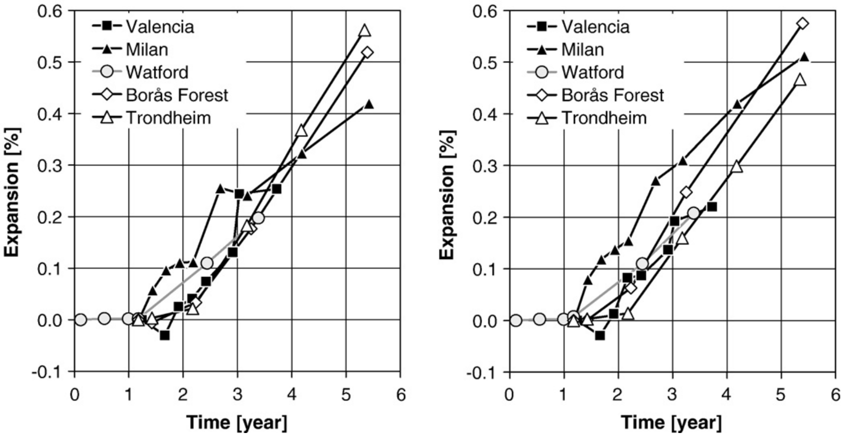

Fig. 7. Mean expansion of concrete cubes with aggregate combination B1(C + NRF); left: stored partly immersed in water; right: only exposed to ambient rainfall.

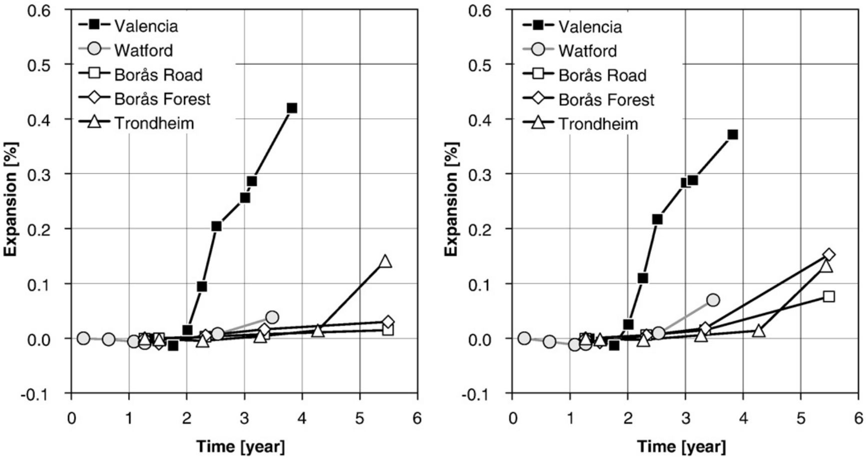

Fig. 8. Mean expansion of concrete cube with aggregate combination D2(F + NRC); left: stored partly immersed in water; right: only exposed to ambient rainfall.

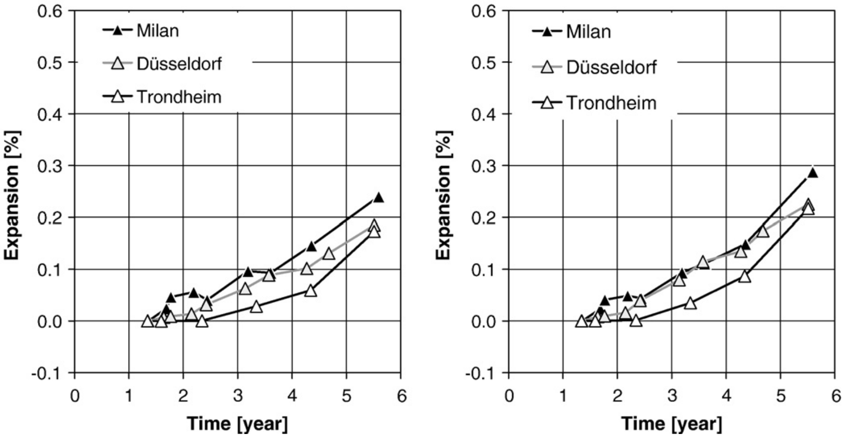

Fig. 9. Mean expansion of concrete cube with aggregate combination G1(C + NRF); left: stored partly immersed in water; right: only exposed to ambient rainfall.

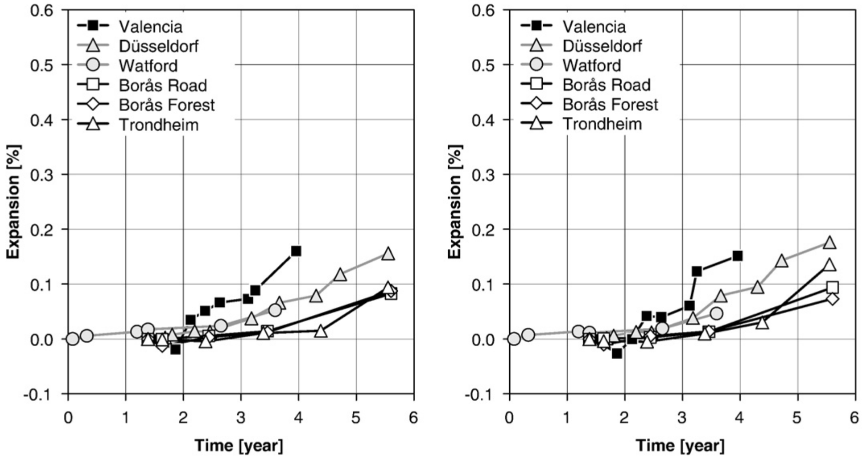

Fig. 10. Mean expansion of concrete cube with aggregate combination N1(C + NRF); left: stored partly immersed in water; right: only exposed to ambient rainfall.

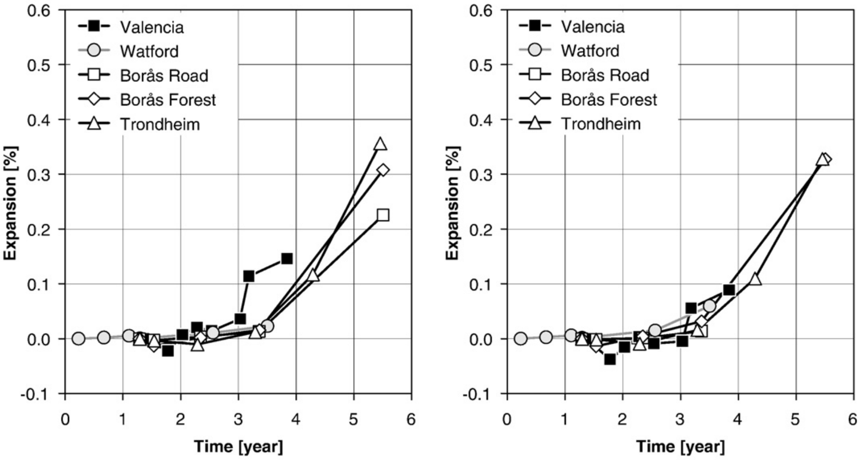

Fig. 11. Mean expansion of concrete cube with aggregate combination UK1(C + F); left: stored partly immersed in water; right: only exposed to ambient rainfall.

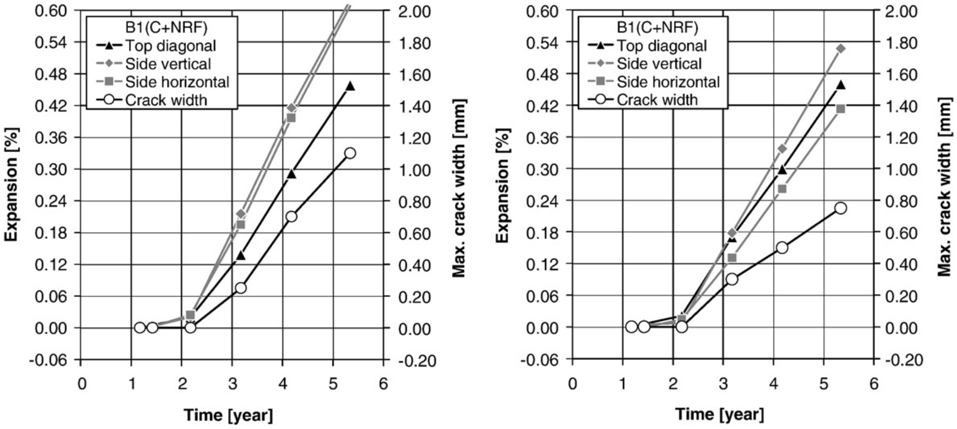

Fig. 12. Expansion of and max. crack width at concrete cubes with aggregate combination B1(C + NRF); field site Trondheim, Norway; left: stored partly immersed in water; right: only exposed to ambient rainfall.

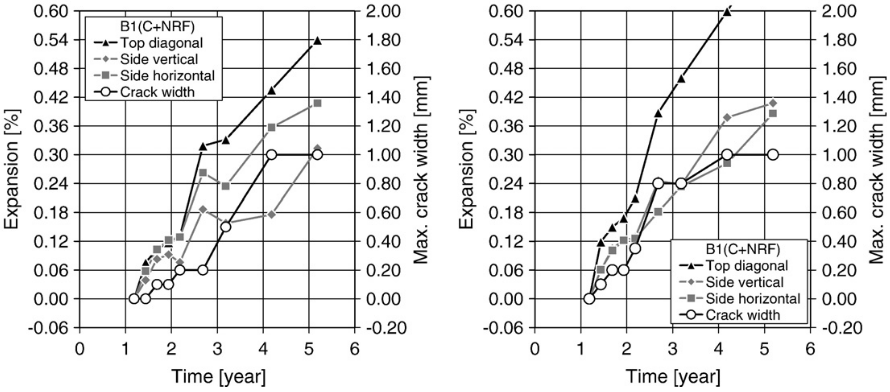

Fig. 13. Expansion of and max. crack width at concrete cubes with aggregate combination B1(C + NRF); field site Milan, Italy; left: stored partly immersed in water; right: only exposed to ambient rainfall.

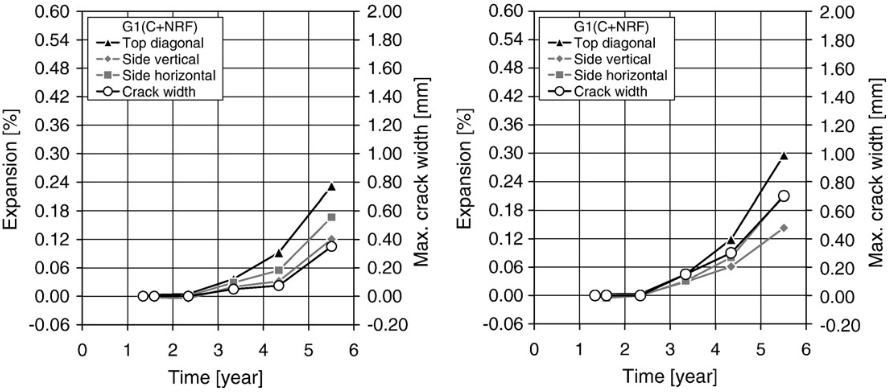

Fig. 14. Expansion of and max. crack width at concrete cubes with aggregate combination G1(C + NRF); field site Trondheim, Norway; left: stored partly immersed in water; right: only exposed to ambient rainfall.

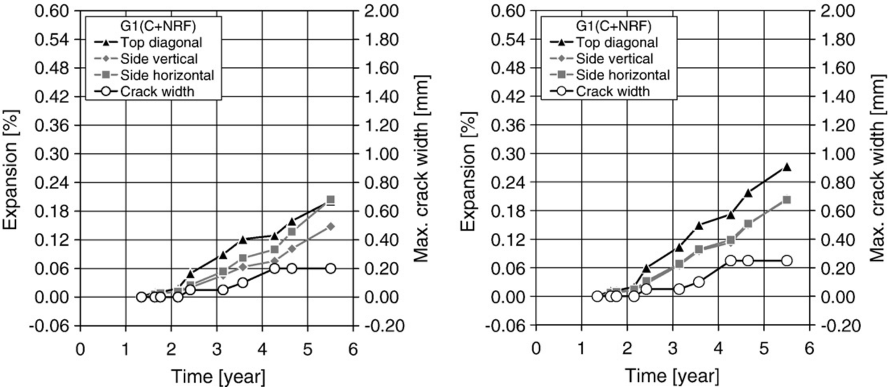

Fig. 15. Expansion of and max. crack width at concrete cubes with aggregate combination G1(C + NRF); field site Düsseldorf, Germany; left: stored partly immersed in water; right: only exposed to ambient rainfall.

4.1.3. RILEM AAR-3 (38 °C) and AAR-4 (60 °C) concrete prism methods

4.1.3.1. Identification of reactive aggregate combinations. In the overwhelming majority of cases, all the concrete prism methods correctly identified those aggregate combinations that had been shown by field experience to be involved in cases of damaging ASR, based upon acceptance criteria for the concrete prism methods presented by RILEM [18] and referred to previously in this paper.

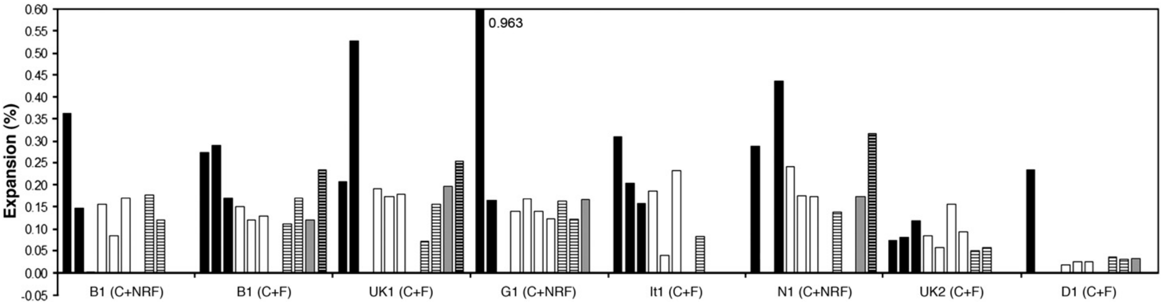

Fig. 16. “Normally” reactive aggregate combinations: % expansion at the end of the test period — all concrete prism methods. Order in chart is RILEM AAR-3 (black), RILEM AAR-4 (white), RILEM AAR-4 Alt. (white with stripes), German (grey), Norwegian (grey with stripes).

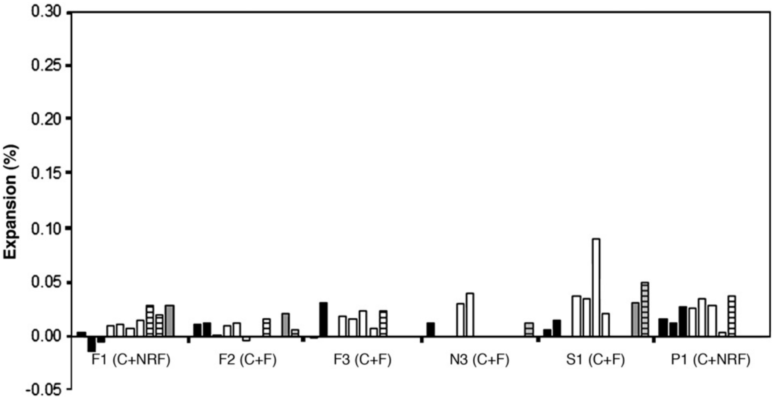

Fig. 17. Non-reactive aggregate combinations: % expansion at the end of the test period — all concrete prism methods. Order in chart is RILEM AAR-3 (black), RILEM AAR-4 (white), RILEM AAR-4 Alt. (white with stripes), German (grey), Norwegian (grey with stripes).

4.1.3.1.1. Aggregates that react in "normal" timescales. The methods were particularly effective in identifying aggregate combinations that caused damage in "normal" time scales; 5 to 20 years. This is shown in Fig. 16, where all the expansion results at the end of the test period for such aggregates are shown for all the methods.

The major exception was D1, where all the laboratories except one identified this aggregate combination as non-reactive, whereas it is known from field experience to cause rapid and severe damage to structures in Denmark. It is also known, however, that this aggregate type has a marked pessimum behaviour, and it is probable that the coarse and fine combination tested is well above the pessimum content of reactive silica.

4.1.3.1.2. Non-reactive aggregate combinations. Most methods correctly identified those aggregate combinations that were established from field experience as being non-reactive (Fig. 17), according to acceptance criteria presented by RILEM [18] and referred to previously in this paper. However, some exceptions were observed. For aggregate combination N3(C + F) and P1(C + NRF), some of the 60 °C test series by a small margin exceeded the critical limit. The 38 °C test series did not exceed the critical limit.

In the case of S1(C + F), all methods showed this combination to be on the margins of reactivity. Although this aggregate has been involved in known failures; its composition and reactivity is known to be variable.

4.1.3.1.3. "Slowly" reactive aggregate combinations. The one class of aggregates where some uncertainties showed up, were those where the damaging reactions were known to be slow, i.e. damaging reactions after + 15–20 years (Fig. 18). This was found in the following cases:

- D2(F + NRC); two of the three AAR-4 reactor test series (i.e. 60 °C) did correctly identify the reactivity potential of this aggregate combination. However, the expansions in the third AAR-4 reactor test and in the two AAR-4 Alt. test series were just above the critical limit (i.e. expansions of 0.03% after 20 weeks, as suggested below), whereas the expansion in the single AAR-3 test series was below the critical limit (i.e. 0.05% after one year).
- It2(C + F); the AAR-3 tests again did not identify the long term reactivity of this aggregate. The AAR-4 tests did identify its potential alkali-reactivity, although in one case only after the normal final test date.
- N4(C + F); again, the AAR-4 tests more clearly identified the reactivity of this combination. Two of the three AAR-3 results identified this combination as reactive, but only by the smallest of margins. The third AAR-3 laboratory obtained a one year expansion below the critical limit, probably due to lack of moisture (also the weight changes for the concrete prisms were measured, but these results will be discussed later in a separate paper). The reason for the "moisture problems", is that this laboratory did not follow the

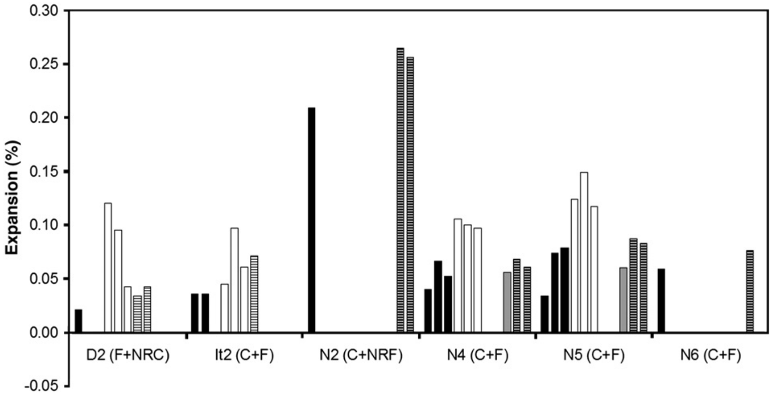

Fig. 18. "Slowly" reactive aggregate combinations: % expansion at the end of the test period —all concrete prism methods. Order in chart is RILEM AAR-3 (black), RILEM AAR-4 (white), RILEM AAR-4 Alt. (white with stripes), German (grey), Norwegian (grey with stripes).

instructions prepared for the test. The only AAR-3 expansion below the critical limit for the N5(C+F) combination in the Figs. 5 and 18, was also obtained at this laboratory.

4.1.4. Comments on the concrete prism methods

Comparison of test methods; as stated above, the various tests gave results that agreed in most cases. The main exceptions were the differences between the RILEM AAR-3 and RILEM AAR-4 results when very "slowly" reactive aggregates were tested. In these cases, the AAR-4 reactor method more clearly identified the potential alkali-reactivity (see Figs. 5 and 18), even though it did not necessarily show that the expansion would be slow.

The actual expansion values recorded were very variable for some aggregates, but quite consistent for others. The variability was greatest for the most expansive aggregates and least for the least expansive. The expansions in the RILEM AAR-3 method seemed particularly variable (Table 6). See also the results and discussion relating to the precision of the laboratory tests in section 5.

In general, amongst the RILEM methods, the results from the 60 °C AAR-4 methods, and in particular the AAR-4 reactor method, were the most consistent. The reactor version of this method was in all cases able to detect a potential alkali-reactivity of the "suspicious" aggregate combinations included in the test programme, also the "slowly" reactive aggregates. The only exceptions were for pessimum aggregate combinations. The AAR-4 Alt. method (wrapped prisms, no reactor; see Table 2) seems to be far more vulnerable with respect to keeping the moisture content high during the testing. The weight measurements (not included in this paper) showed in general a lower weight increase, and sometimes also a weight loss, for the aggregates tested according to the AAR-4 Alt. method compared to the reactor version.

There is also evidence that the experience of the laboratories with a particular method has a significant effect on the variability of results. Where laboratories were carrying out procedures with which they were very familiar, for example the Norwegian method carried out by NORCEM and SINTEF, the expansion values were very close.

4.1.5. The field site tests

After approximately 4 years of outdoor exposure, the cubes of aggregate combination B1(C+F) and B1(C+NRF) show high expansion >0.04% and cracks with maximum width ≥0.20 mm at all field sites from Norway to Spain independent of the type of storage (Tables 7 and 8, Figs. 6 and 7). B1(C+F) and B1(C+NRF) are in general the fastest reacting aggregate combinations. The concretes with the aggregates D2, G1, N1 and UK1 show in tendency higher expansions and large cracks when stored in medium (Düsseldorf, Watford) and hot climates (Milan, Valencia), whereas significant expansion and cracks developed later in colder climates (Figs. 8–11). The influence of the climate on the expansion development is for the aggregate combinations D2(F+NRC) and N1(C+NRF) stronger than for B1(C+F), B1(C+NRF), G1(C+NRF) and UK1(C+F). Fournier et al. [26] suggest that a deleterious expansion occurs 4 to 5 times faster in warm climates (Austin, Texas, USA) than in cool climates (Ottawa, Ontario, Canada). They compare the expansion of concrete block after three and four years. A general factor by which the ASR is accelerated cannot be derived in this study, because it differs for different aggregate combinations.

It can be assumed that the high expansions and crack widths can be attributed to a deleterious ASR that has taken place in the concrete cubes. Final confirmation will be given by the investigation of thin sections at the planned finalisation of the field site tests, i.e. when the slope of the expansion curves starts to flatten. Thus, the time depends on the reactivity of the aggregate combination.

All aggregate types (B1, D2, G1, N1 and UK1) that in advance were classified as "normally" reactive (Table 9A) and have caused damage in concrete structures, reacted at least at one outdoor exposure site in the timescale of 4 years. Except aggregate combination D2(F+NRC), all these aggregate combinations were identified as reactive with all laboratory methods. As discussed above, only two of the three AAR-4 reactor tests did clearly identify the reactivity potential of the D2 aggregate combination, whereas the single available 38 °C test result (AAR-3) did not. The relative fast reaction in the field site test, in particular in Valencia (Fig. 8) where the mean temperature is high

Table 9A
Comparison of results of test methods with behaviour in field sites and structures.

Aggregate	Fraction/ combination	Reactivity/evaluation							
		AAR-1	AAR-2	AAR-3	AAR-4/ AAR-Alt	TI-B51/ Chatterji	German/ Norwegian	Field site test after 4 years**	Reported reactivity in structures?
"Normally" reactive aggregate combinations									
B1 – Silicified limestone	F	R	R			R/R			Yes
	C	R							
	C+F			R	R/R		R/R	R	
	C+NRF			R	R/R			R	
UK1 – Greywacke	F	R	R			R/R			Yes, normally +20 years
	C	R							
	C+F			R	R/R		R/R	R	
G1 – Crushed gravel with siliceous limestone and chert	C	R	R			R/–			Yes, 10 years if severe conditions
	C+NRF			R	R/R		R/–	R	
G2 – Gravel with opaline sandstone and flint	C	R	R			R/–			Yes, <10 years but pessimum effect
It1 – Gravel with silicified limestone and flint	F	R	R			R/–			Yes, 5–10 years
	C	R	R						
	C+F			R	R/R				
N1 – Cataclasite	C	R	R			R/R			Yes, 10–15 years
	C+NRF			R	R/R		R/R	R	
UK2 – Gravel with quartzite and chert	F	R	R			R/R			Yes, 10–15 years
	C	R							
	C+F			R	R/R				
D1 – Gravel with opaline flint	F	R	R						Yes, quickly but pessimum effect
	C	R	R			R/R			
	C+F			?*	NR/NR		NR/–		
D2 – Sea gravel semi-dense flint	F	R	R			R/R			Yes, 10–15 years
	C	R	R						
	F+NRC			NR/MR?	R/MR			R	

(Regarding abbreviations: see legends to Table 9C).

(see Fig. 2), of this assumed relative "slowly" reactive aggregate, can be attributed to the high cement content and the high alkali content of the cement. However, this is seldom the practice in real concrete constructions where the lower alkali contents will result in a slower reaction.

It is also noteworthy and surprising that there are no obvious differences between the specimens exposed only to ambient rainfall and those stored partly immersed in water.

The concrete cubes with aggregate combination B1(C + F) stored in an open forest and alongside a highway in the southwest of Sweden show similar expansions and cracks after four years. So far, there is no measurable influence of an external alkali supply by de-icing salts on the performance of this concrete composition containing alkali-reactive aggregate.

B1(C + NRF) seems to have slightly higher expansion and sometimes larger cracks than B1(C + F) (Figs. 6 and 7). The latter contains reactive fines instead of non-reactive fines. The lower expansion of B1 (C + F) can probably be attributed to the reaction of fines, that may reduce the effective alkali content of the pore solution.

The Figs. 12–15 show the expansion on the top surface as well as on the side surfaces in horizontal and vertical direction for the aggregate combination B1(C + NRF) stored in Trondheim and Milan, as well as for G1(C + NRF) stored in Trondheim and Düsseldorf. Additionally, the development of the maximum crack width is given. The highest expansion occurred in most cases on the top surface, that is most exposed to solar radiation. The horizontal and vertical expansion was less, but a significant difference between them does not exist. This is independent of the climate. With increasing expansion, the maximum crack width is always increasing.

The "slowly" reactive aggregates It2, N2 and N4 and the non-reactive aggregates F1, F2, S1 and P1 did not show any noticeable expansion or cracking after 4 years of outdoor exposure. The small cracks with a width of 0.05 mm, visible in most cubes, are presumably due to shrinkage. However, the testing time of 4 years is too short to draw conclusions for these "slowly" reactive aggregate combinations. To get conclusive results, the tests will be continued.

The field site tests show that a deleterious ASR can take place in all European countries from Norway to Spain, and it occurs independently of the climate condition within the range represented in this study. However, the speed of the ASR is higher for some aggregates in hot climates (Valencia) than in medium (Düsseldorf, Watford) or cold climates (Borås, Trondheim). Special considerations may therefore be necessary when using some aggregates in warmer climates.

4.2. Comparison of test methods

The summarized results for the laboratory methods are compared in Table 9A, 9B and 9C with the preliminary results of the field site tests and with the reported reactivity in structures (see Table 1). They are presented in three groups according to whether their reported reactivity is;

- "normally" reactive (5–20 years)
- "slowly" reactive (+ 15–20 years)
- non-reactive

There are, however, some aggregates where the information on their reactivity is uncertain or where there is known variability in the source. Thus, the sample tested may not reflect the compositions in the reactive structures.

4.2.1. RILEM methods

In the first group, of "normally" reactive aggregates, all of the methods agreed with each other and with the field site results and the reported reactivity, except for D1. In this aggregate, there is a known strong pessimum effect and it is presumed that the results for the concrete methods reflect the presence of an amount of opaline flint that takes the combination past the pessimum amount when the fine and coarse aggregates are used together. The field site tests confirm that all "normally" reactive aggregate combinations can be reliably identified with all methods, if the critical limits suggested below are applied.

In the second group, of "slowly" reactive aggregates, the petrographic method (AAR-1), the accelerated mortar bar method (AAR-2) and the accelerated concrete prism method (AAR-4, 60°) successfully identified the potential alkali-reactivity, but did not necessarily show that the expansion would be slow. The concrete prism method (AAR-3, 38 °C) was better at demonstrating the slowness of the expansion of these aggregates, but in a few cases the expansion did not pass the critical limit within the one year timescale of the test. However, it can be seen from the expansion curves that the expansion in most of these cases is continuing, and more than a year may be needed for some "slowly" reactive aggregates to produce expansion over the critical limit in the conditions of this test [3]. In this respect therefore, the AAR-3 method, corresponds better with field experience for these "slowly" reactive aggregate types.

At the 12th ICAAR in China, Fournier et al. reported [27], based on data from various sources, a correlation of about 1-to-1 between 13 weeks at 60 °C and 1 year at 38 °C. According to Folliard [pers. comm.], the general experience in his laboratory in Austin, Texas, USA

Table 9B
Comparison of results of test methods with behaviour in field sites and structures.

Aggregate	Fraction/ combination	Reactivity/evaluation							
		AAR-1	AAR-2	AAR-3	AAR-4/ AAR-Alt	TI-B51/ Chatterji	German/ Norwegian	Field site test after 4 years**	Reported reactivity in structures?
"Slowly" reactive aggregate combinations									
It2 — Gravel with quartzite	F	R	R			NR/–			Yes, 50 years
	C	R	R						
	C + F			NR	R/R			n.r.	
N2 — Sandstone	C	R	R			NR/R			Yes, 15–20 years
	C + NRF			R			–/R	n.r.	
N4 — Gravel with sandstone and cataclastic rocks	F	R	R			R/R			Yes, 20–25 years
	C	R	R						
	C + F			MR	R/–		MR/MR	n.r.	
N5 — Gravel with rhyolite and quartzite	F	R	R			R/R			Yes, 20–25 years
	C	R	MR						
	C + F			MR	R/–		MR/MR		
N6 — Gravel with sandstone, rhyolite and mylonite	F	R							Yes, 20–25 years
	C	R							
	C + F			MR			–/MR		

(regarding abbreviations: see legends to Table 9C).

Table 9C
Comparison of results of test methods with behaviour in field sites and structures.

Aggregate	Fraction/ combination	Reactivity/evaluation							
		AAR-1	AAR-2	AAR-3	AAR-4/ AAR-Alt	TI-B51/ Chatterji	German/ Norwegian	Field site test after 4 years**	Reported reactivity in structures?
"Non-reactive" aggregate combinations									
F1 – Gravel with flint	C	R	NR			NR/R			No, but known pessimum effect
	C + NRF			NR	NR/NR		NR/–	n.r.	
F2 – Non-reactive limestone	F	NR	NR						No
	C	NR							
	C + F			NR	NR/NR		NR/NR	n.r.	
F3 – Gravel with quartzite, flint, greywacke and granitoids	F	R	R			NR/R			No, but likely pessimum effect
	C	R							
	C + F			NR	NR/NR				
S1 – Gravel with meta-rhyolite and greywacke	F	R	R			R/R			Yes, but source variable in composition
	C	R							
	C + F			NR	MR/–		NR/MR	n.r.	
P1 – Silicified limestone	C	R	NR			NR/–			Yes, but source and information uncertain
	C + NRF			NR	NR–MR/MR			n.r.	
N3 – Granitic sand	F	NR	NR			NR/NR			No
	C	NR							
	C + F			NR	MR/–		NR/NR		
E1 – Dolomitic limestone	F	NR	NR						Information uncertain
D3 – Siliceous sand	F	NR	NR			NR/–			No

F = fine aggregate; C = coarse aggregate.
NRF = non-reactive fine aggregate (= N3F, see Table 1); NRC = non-reactive coarse aggregate (= F2C, see Table 1).
R = reactive (according to the critical limits in the different testing methods).
NR = non-reactive (according to the critical limits in the different testing methods).
MR = marginally reactive (i.e. expansions just above the critical limits in the different testing methods).
n.r. = no rating yet possible.
* = one result strongly reactive, second non-reactive.
** = the evaluation of the preliminary results from the field sites is based on measurements of crack widths after about 4 years of exposure and of expansions during the last 3 years (the expansion measurements were re-started in 2005 due to problems with the zero measurements at some field sites).

is that the 20 weeks expansion in the 60 °C method is on average approx. 60% of the one year expansion in the 38 °C method. One main reason may be higher leaching in the 60 °C method compared to the 38 °C method [27,28]. In the PARTNER project (where unfortunately any leaching of alkalis was not measured), the corresponding ratio between the 20 weeks 60 °C expansion (reactor version of AAR-4) and the 1 year 38 °C expansion was on average approx. 0.5 (varying from 0.25 to 0.7) for the six "normally" reactive aggregate combinations (excl. D1) with a 1 year 38 °C expansion exceeding 0.20% (see Table 6 and Fig. 16). Most 60 °C expansion curves for these aggregate types had the similar characteristic shape, being rather steep in the beginning, before more or less flattening out after approx 8–12 weeks. Thus, the 13 weeks 60 °C expansion will almost be as high as the 20 weeks expansion.

In contrast to AAR-3, the AAR-4 method produced relatively higher expansions for "slowly" reactive aggregates compared with "normally" reactive aggregates. For the nine aggregate combinations with a 1 year 38 °C expansion in the range 0.010–0.10% (including both "slowly" reactive and non-reactive aggregates), the corresponding ratio between the 20 weeks 60 °C expansion (reactor version of AAR-4) and the 1 year 38 °C expansion was on average approx. 2.3 (varying from 1.1 to 4.6; see Table 6 and the Figs. 17 and 18). Most 60 °C expansion curves for these aggregate types were more linear (see Fig. 5) compared to the "normally" reactive aggregates. As a consequence, the 13 weeks 60 °C expansion will be significant lower than the 20 weeks expansion, a fact that has to be taken into account when critical limits are to be set (see discussion later in the paper).

On the other hand, the relatively high inter-laboratory variations make these comparisons somewhat uncertain. In the field site tests, the concrete compositions with "slowly" reactive aggregate combinations are not exhibiting any sign of expansion or cracking yet. The testing time of 4 years is too short to draw conclusions for these "slowly" reactive aggregate combinations. To get final results, the tests will be continued.

In the non-reactive group, the results of the concrete methods agreed with the reported reactivity in all cases where the information on reactivity in the field was clear cut. In the case of S1 and P1, there is uncertainty about the composition of the samples tested compared to the aggregates in the structures where damage was reported. Similarly, the accelerated mortar bar test (AAR-2) was effective in all cases, except with F3 (reactive in AAR-2, but no reports of any ASR in structures). This aggregate is reported to have a marked pessimum effect, and it is probable that the difference in result between the concrete and mortar methods reflects the fact that the proportion of reactive material in the fines is within the pessimum proportion, but when the coarse and fines are tested together in concrete, the amount of reactive material exceeds the pessimum, and limited expansion is obtained. The petrographic method (AAR-1) is effective in identifying those aggregates which contain either no or very low amounts of reactive material, but is unable to identify correctly those aggregate combinations where possibly pessimum effects lead to such aggregates being innocuous in structures.

Overall, the accelerated mortar bar test (AAR-2) and the accelerated concrete prism test (AAR-4, reactor version) seemed the most effective of the RILEM methods across the whole range of European aggregates tested in this study, including the identification of "slowly" reactive aggregate combinations. Additionally, these methods have the advantage of producing (relatively) rapid results.

The petrographic method (AAR-1) can produce an even quicker result. The averaged results for this method seem quite effective at identifying reactive materials, but can conflict with field experience when pessimum effects operate. The consistency of individual results for this method is the main issue, however. The spread in results between the laboratories for about half of the aggregate types tested was very high, and this high variability even applied to the results from some of the six laboratories which carry out petrographic analyses on a regular basis. As discussed, in relation to the precision test, below, there is a clear need for more education and inter-laboratory comparisons if the petrographic method is to be used on a European scale to evaluate the reactivity potential of an aggregate.

4.2.2. Other test methods

The German and Norwegian concrete prism tests behaved almost exactly like the AAR-3 method; identifying the "normally" reactive aggregate combinations and non-reactive combinations effectively, but giving marginal results with some of the "slowly" reactive combinations.

The two Danish methods were effective with most materials. However, the TI-B51 test appears to underestimate the reactivity of some "slowly" reactive materials when the standard 8 or 20 weeks are used, although at 26 or 52 weeks the method generally agrees well with the other concrete methods. The one exception is the result for Norwegian material N2, which was classified incorrectly by the TI-B51 method; so far no explanation for this discrepancy is obvious.

4.2.3. Critical limits

Final evaluation of the critical limits will need to be undertaken when longer term results for the field site tests are available. When evaluating and deciding the final critical limits, it is important to bear in mind the importance of degree of precisions for the various tests. When providing test results for clients, in order to classify an aggregate, it is however necessary that the critical limits are absolute values. But, when deciding critical limits, this must be done taking into account the tolerance and the uncertainty of measurement of the various tests. Critical limits should mainly be decided on the basis of field performance. It could, however, be interesting to compare the results of the various methods as it provides information about the appropriate test period for the methods. The correlation will, however, probably vary for various types of reactive aggregates, due to different shape of the expansion curves (see previous discussion). Based on the preliminary results of the field trials and comparison of the laboratory results with the reported reactivity in field structures, together with previous work by RILEM, the following critical limits can be suggested:

- AAR-2: Expansions of less than 0.10% after 14 days distinguishes a non-reactive and reactive aggregate when using the long thin prisms (ASTM-type). The short prisms (RILEM-type) initially expand more slowly, and either a lower limit (e.g. less than 0.08%) or a longer test period will be necessary with these test specimens (if a 0.10% limit should be applied also for this prism type).
- AAR-3: Expansions of less than 0.05% after 1 year indicate that the aggregate combination can be regarded as non-reactive. This limit will be effective for aggregates that react in normal timescales, but with some "slowly" reactive aggregates a longer test period may be necessary. The shape of the expansion curve will help to identify such aggregates.
- AAR-4: Expansions of less than 0.03% after 20 weeks indicate that the aggregate combination can be regarded as non-reactive. For this test, the standard time period of 20 weeks is sufficient for both normally and "slowly" reactive aggregates. The results of a separate RILEM inter-laboratory trial have suggested that the 15 weeks results can give an effective prediction of the potential alkali-reactivity of the aggregate. These PARTNER results support that assessment.

5. Precision trials

The precision of the four RILEM methods has been established in an inter-comparison trial in which the laboratories carried out the methods using samples of the same aggregates together with the reference cement. The procedures strictly follow ISO 5725-94 [29]. The organisation and results of the trial are described in detail in reference [30] and are outlined below. It is important to know and understand the differences between a strict precision trial according to ISO 5725 and a "less regulated" inter-comparison trial. Both the organisation and mathematical evaluation are strictly regulated in the ISO standard. Inter-comparison trials can have many different objectives, while the here presented work was strictly done to evaluate the precision of the amended RILEM methods. Several reported studies of the multi-laboratory variability focus on a specific part of the test procedure, e.g. storage conditions or influence of different aggregates, i.e. rock types [27,31], while those found in the standards [e.g. 32 and 33] focus on the precision in relation to the average expansion and critical limits.

The precision of AAR-4 Alternative method rather than the AAR-4 method was assessed, because too few laboratories had the reactor necessary to perform the test according to the original method. Earlier, the precision of the AAR-4 reference method, based on "reactor storage" of the prisms, has been evaluated within RILEM TC191-ARP [35].

5.1. Organisation

The laboratories and materials included in the precision trials were chosen based on the outcome of an enquiry, where the participants gave statements about their experience of the methods and the reactivity of the aggregates. Eight laboratories were chosen for each test along with three materials with expected low, medium and high reactivity, respectively. The low reactive material was a Norwegian natural gravel with rhyolite and quartzite (N5), fine and coarse from the same source. The medium reactive material was crushed Belgium silicified limestone (B1), fine and coarse from the same source. The expected high reactive material was a Norwegian crushed cataclasite (N1), mixed with non-reactive fines of Norwegian sand (N3: 0/4 mm). See Table 1 for more details of these aggregates.

Special instructions were prepared based on the outcome of other work packages. Templates for reporting were prepared, and no deviations from the instructions were accepted. All samples were divided by SP, Technical Research Institute of Sweden, given anonymous names and sent to the participants. The sample splitting procedure followed that of earlier EU-projects and EN 932-2 [34]. Rotary sample divider and fractional shovelling (Fig. 19) were used to minimize the difference between the samples.

5.2. Overall precision

The overall precision of the four RILEM methods assessed in the trial is set out in Table 10. For many other aggregate test methods, the precision can be expressed as a fixed percentage of the mean value or the characteristic value. As can be seen in Table 10, the precision of each method is varying within its working range. The mathematical relationships, e.g. the best fit curves, are therefore recommended to be

Fig. 19. Fractional shovelling, in accordance with EN 932-2.

Table 10
Precision statements for all assessed methods; *m* is the mean value.

Expected reactivity	Low to medium	Medium	High
AAR-2 Long prisms 14 days, 5 prisms, 1 recalculation			
General mean *m*	0.133	0.420	0.375
Repeatability COV(s_r)	6.80%	2.70%	1.9%
Reproducibility COV(s_R)	17.1%	22.0%	11.0%
AAR-2 Long prisms 28 days, 5 prisms, 2 recalculations			
General mean *m*	0.236	0.550	0.578
Repeatability COV(s_r)	2.5%	1.2%	3.0%
Reproducibility COV(s_R)	2.5%	6.6%	14.4%
AAR-2 Short prisms 14 days, 5 prisms, 1 recalculation			
General mean *m*	0.127	0.254	0.295
Repeatability COV(s_r)	5.5%	5.7%	4.2%
Reproducibility COV(s_R)	14.7%	19.8%	35.1%
AAR 2 Short prisms 28 days, 3 prisms, 2 recalculations			
General mean *m*	0.271	0.467	0.592
Repeatability COV(s_r)	3.4%	2.3%	2.5%
Reproducibility COV(s_R)	22.4%	24.3%	16.5%
AAR-3			
General mean *m*	0.059	0.181	0.260
Repeatability COV(s_r)	15.3%	13.8%	20.7%
Reproducibility COV(s_R)	49.3%	53.7%	54.3%
AAR-4 Alt.			
General mean *m*	0.107	0.130	0.170
Repeatability COV(s_r)	11.2%	9.1%	16.4%
Reproducibility COV(s_R)	33.1%	26.4%	24.2%

used instead of a fixed value. Another possibility is to give the precision value at each critical level, e.g. 0.10% after 14 days for the AAR-2 method using long prisms (ASTM-type) etc. This can easily be done by extrapolation of the test results down to that level.

The importance of a good repeatability mostly lies in the quality control of each laboratory. The importance of a good reproducibility lies in the fact that it should be possible to send similar samples to different laboratories and still get similar results. In case of dispute, it would otherwise be very difficult or impossible to state what result is correct. Both repeatability and reproducibility are crucial when requirement limits are chosen. A poor precision leads to problems of differentiating between aggregates of different qualities. Some laboratories will inevitably classify aggregates as belonging to a different reactivity class than other laboratories if the precision is poor.

5.2.1. General definitions (simplified and related to this project)

r = repeatability. This is a measure to determine the spread in results obtained between the individual prisms, tested at the same laboratory, same aggregate combinations and same concrete.

R = Reproducibility. This is a measure to compare the difference in the mean value obtained between the different laboratories.

COV(S_R) = Coefficient of variation for the Reproducibility. By using the coefficient of variation (COV) one relates the spread to the actual expansion. The COV is the standard deviation divided by the mean value. The COV(S_R) is thus used to compare the difference in the spread between the laboratories. Similarly, the COV (S_r) is used to compare the spread within one single test carried out at one laboratory. In this case, it is the spread between the three prisms and whether it is correct to average their results or if the test has to be remade or only two part results shall be averaged, all depending on the instructions in the test method.

5.3. AAR-1 petrography

The results from the AAR-1 petrography showed a large spread between the different laboratories. Their identification of the rocks and minerals is similar, but the classification of the degree of alkali–silica reactivity varies a great deal. This is probably due to the regional experience and inexperience of the different reactive rocks. Only porous/opaline flint and mylonite/cataclasite have been classified as reactive by all laboratories.

Overall, the results confirm the necessity of education. Petrographers need to get acquainted with the potentially reactive components in aggregates from different countries in order to use the most appropriate analytical techniques and to make a relevant assessment. Education, in combination with proficiency trials of individual laboratories, is therefore the way forward for future improvement in this area.

5.4. Expansion tests; RILEM AAR-2, AAR-3 and AAR-4 Alternative

Overall the precision is acceptable to good and it is possible to detect small differences in reactivity.

5.4.1. RILEM AAR-2

Both options, using the long and thin prisms (25 × 25 × 285 mm^3 — ASTM-type) and the short and thick prisms (40 × 40 × 160 mm^3 — RILEM-type) are working adequately. At the standard 14 days test age, the long and short prisms give different results, with the long prisms having the highest expansion. At 14 days, therefore, the short prisms would need a different (smaller) limiting requirement to differentiate

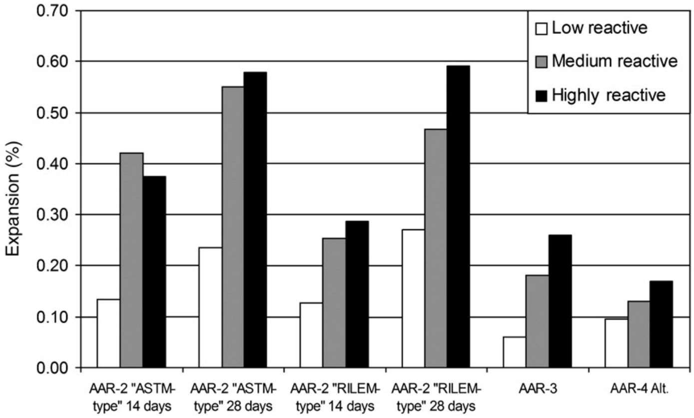

Fig. 20. Classification of the three test materials according to the RILEM methods evaluated in the precision trial. The white coloured columns indicate the results of the least expansive material combinations.

between reactive and non-reactive aggregates. However, the results are equalising after 20 days and even more so after 28 days (Fig. 20). The difference between laboratories is generally less than 1 standard deviation of the overall mean value. If the use of both prism sizes is still to be recommended in the same method, it seems necessary to continue the test for 28 days or to be able to determine a usable correlation factor. The precision trial also indicates that using 3 prisms instead of 5 actually improves the precision data, probably because with only 3 prisms they can all be stored in the same container. At the proposed limiting value for differentiating between reactive and non-reactive aggregates, 0.10% (for the long prisms), the band of uncertainty is less than 0.025%.

5.4.2. RILEM AAR-3

The results concerning this method indicated that the repeatability is good, whereas the reproducibility is quite poor, i.e. each laboratory produces results within a narrow range (i. e. between test prisms of the same set), but the difference in results between the laboratories is large. A coefficient of variation in the repeatability of up to 20% is acceptable, but the results indicate that AAR-3 does not achieve this with the most expansive material (i.e. the aggregate with approx. 0.26% expansion after 1 year of exposure — see Fig. 20). Equally, a coefficient of variation in reproducibility, COV(S_R), of above 50% is unacceptably high. It is therefore concluded that the precision of AAR-3 is not sufficient to discriminate between different levels of reactivity. The results of the precision trial do, however, confirm that the method can be used to discriminate between non-reactive and reactive materials. The reproducibility is shown to be about half of the expansion value. At the level of 0.05%, suggested as the limiting value to differentiate between reactive and non-reactive aggregate combinations when using AAR-3, there is therefore a band of uncertainty of 0.025%, and the lowest result for a reactive aggregate should exceed 0.075%. This was found to be the case for all the aggregates which react in normal timescales and where their record of field reactivity is well established. However, the AAR-3 method is not well suited to identifying "slowly" reactive aggregates. N.B! This statement relies on the assumption that all laboratories strictly followed the procedure described in the method and PARTNER amendments. During the prior test rounds in the project, important differences in the storage conditions were found.

5.4.3. RILEM AAR-4 alternative

Testing according to the AAR-4 Alt. method resulted in a better overall precision than AAR-3, and was able to detect smaller differences in reactivity than the AAR-3 method. The "overlap" between the different materials (e.g. categories of reactivity) is less, approximately half that of the AAR-3 test. The coefficient of variation in reproducibility, COV(S_R), is about one third of the mean test result, while the repeatability COV is about 10 to 15%, depending on the mean expansion. This is considered acceptable. In addition, this is an improvement over the figures reported by Sims and Nixon [35] from a RILEM initiated inter-comparison trial covering both AAR-4 reference method (reactor) and the Alternative wrapped version. It is obvious that participation in inter-comparison trials and practice will improve the precision. In some cases, there is no option but to use a mix of inexperienced and experienced laboratories despite the warning given in ISO 5725, simply because there are not enough laboratories available, and pre-test rounds are too expensive or time consuming.

Like AAR-3, the precision of the AAR-4 Alternative method is sufficient to distinguish between non-reactive and reactive materials, but not between smaller differences of reactivity. At the proposed limiting value for differentiating reactive and non-reactive aggregates, 0.03%, the band of uncertainty is less than 0.01%.

5.4.4. Precision statements from standards

For comparison, we have also compiled some information of precision data found in the most relevant national standards. According to the ASTM C-1260 [36] (similar to RILEM AAR-2). the within-laboratory COV is 2.94% at 0.1% 14-days expansion. The multi-laboratory COV at the same level of expansion is 15.2%. As regards the precision of the concrete methods, no directly comparable data has been found. The most similar method to RILEM AAR-3 is the Canadian CSA A23.2-14A (the main difference is that AAR-3 applies wrapped prisms), which is also referred to in the ASTM C-1293. However, the precision is reported in a different way which makes a direct comparison difficult. For expansion levels less than 0.014%, the expected difference between laboratories should generally not exceed 0.009% (absolute percent). This means that if you sample an aggregate, with an expected expansion of 0.014%, reduce it to several subsamples and send two of them to different laboratories, the expected expansion results (i.e. the average of three prisms) will most likely be between 0.023 and 0.005%. The multi-laboratory coefficient of variation for expansions greater than 0.014% is 23%. These data can be compared with the PARTNER results summarized in Table 10, e.g. the corresponding PARTNER data for AAR-3 is approximately between 15 and 20%. Since only the AAR-4 Alternative method was included in this study, we don't consider it relevant to compare with the precision statement of the French standard [37], based on the reactor type prism storage.

6. Petrographic atlas

As part of the PARTNER project, a petrographic atlas of the potentially alkali-reactive rocks in Europe was produced and published. The aim of this petrographic atlas is to assist geologists who work in the field of the concrete degradations and in particular in the field of alkali–silica reaction to recognise potentially reactive rock types and to differentiate these from rock types that will be resistant to alkali aggregate reactions. It will particularly be of assistance to petrographers who carry out the AAR-1 petrographic method on aggregates that are from a part of Europe with which they are unfamiliar.

A paper version of the atlas is published by the Belgian Geological Survey [25]. It is planned to maintain the electronic version under the auspices of RILEM. The current version of the atlas is accessible on www.farin.no/english.

The rocks are firstly classified under their origin (sedimentary, metamorphic or igneous) using the international nomenclatures. Secondly, they have been grouped under families of similar species. For each rock family, a general description is given in the header including the most particular characteristics of the different rock species from different countries. The reactive components are emphasized within the descriptions and, when possible, within the pictures which illustrate the type of aggregate. Despite the fact that this atlas is not exhaustive, it is nevertheless representative of the majority of the European alkali-reactive rocks.

7. State-of-art report

As part of the PARTNER project, a state-of-art report on key parameters influencing the alkali aggregate reaction was produced [38]. Annex A of the report includes a description of the existing national standards and requirements in the different European countries. The main objective of this report is to give an updated description of the mechanisms of AAR that can influence the results from the different test methods used in the PARTNER project. The ultimate challenge when testing for AAR in a laboratory, is to provide quick, reliable results regarding the potential alkali-reactivity of certain types of aggregate, or, even more important, an assessment of specific concrete job mixes (i.e. performance testing). The results are required to mirror the durability behaviour in real structures designed for a service life up to 100 years.

The report identified many parameters that will influence the alkali aggregate reactivity. Some of the parameters will only influence the reactivity in the laboratory, while others will have an overall contribution, both in the laboratory and in real structures. The following key parameters are discussed in the report in relation to AAR:

- Temperature
- Humidity, moisture and degree of saturation
- Content of alkalis
- Role of calcium hydroxide (CH)
- Types and content of reactive rock types
- Aggregate particle size/grading
- Size of test prisms
- Air entrainment, paste porosity and water/cement ratio
- Storage conditions — alkali leaching.

The influence of any changes in a parameter may vary a lot dependent of the situation, both when performing a laboratory test and in a real concrete structure. However, the experience has shown that in particular any variations in the humidity and/or the alkali content (due to leaching) in the test specimens can lead to incorrect results. It is also very important to bear in mind the influence of the different parameters when undertaking a performance test to reflect how a given concrete mix will behave in a real concrete structure over a long service life.

8. Conclusions

- In the majority of cases, all the RILEM test methods were able to correctly identify the potential alkali-reactivity of each of the individual aggregates or aggregate combinations (a total of 22) investigated in this study. The tests were particularly successful in identifying aggregates that react in "normal" time scales (i.e. 5 to 20 years) and in identifying non-reactive aggregates. There was less certainty in identifying "slowly" reactive aggregates, i.e. those that react in greater than 15–20 years. Whether these experiences can be applied to all European regions will have to be verified by additional local examinations.
- Where there were discrepancies between the results of the tests and field experience, these can usually be attributed to either uncertainties about the field results, to variability in the aggregate source or to pessimum effects.
- Overall, the accelerated mortar bar test (AAR-2) and the accelerated concrete prism test (AAR-4, reactor version) seemed the most effective of the RILEM methods across the whole range of European aggregates investigated, including the identification of "slowly" reactive aggregate combinations. Moreover, these methods have the advantage of producing (relatively) rapid results. To get comparable results from both prism sizes allowed for in AAR-2, it seems necessary to continue the test to 28 days. However, critical limits after 14 days are suggested.
- The petrographic RILEM AAR-1 method can produce an even quicker result. The averaged results for this method seem quite effective at identifying reactive materials, but can conflict with field experience when pessimum effects operate. The consistency of individual results for this method is the main issue, however, due to a rather large spread in results between many of the laboratories.
- Overall, the results from the petrographic analyses confirm the necessity of education and round robin testing. Petrographers need to get acquainted with the potentially reactive components in aggregates from different countries in order to use the most appropriate analytical techniques and to make a relevant assessment. Education, in combination with proficiency trials of individual laboratories, is therefore the way forward for future constructive development in this area. An improvement of the common understanding between petrographers really calls for extensive and repeated workshops, e.g. as arranged as part of the PARTNER project. The petrographic atlas developed in the project will also be a good tool to help the petrographers to recognise potentially reactive rock types and to differentiate these from rock types that will be resistant to alkali reactions.
- Precision statements for the four RILEM methods have been made. These confirm the poor precision of the petrographic method, unless the laboratories carrying out the test are familiar with the materials being evaluated. The precision of the expansion methods is much better, and the results confirm the conclusion that the AAR-2 and AAR-4 methods are the most repeatable and reproducible despite some non negligible within and between laboratory variations.
- The field site tests were carried out in various climate zones representative for Europe in order to take into account the influence of different environmental conditions. However, the results indicate that a deleterious ASR occurs in the same way in northern and in southern Europe with the difference that with some aggregates the reaction may occurs earlier in southern Europe, probably due to the higher mean temperature.
- Specimens were stored alongside a highway in Sweden to study the additional influence of alkali supply under severe conditions. So far, there is no difference in the performance of the concrete cubes stored in a nearby forest (without alkali supply) and alongside the highway (with alkali supply).

References

[1] J. Lindgård, M. Haugen, PARTNER Report No. 3.1. Experience from using petrographic analysis according to the RILEM AAR-1 method to assess alkali reactions in European aggregates, 2006 SINTEF Report SBF52 A06019 / ISBN 82-14- 04079-5/978-82-14-04079-5, p. 19 + appendices.

[2] J. Jensen, PARTNER Report No. 3.2. Experience from testing of the alkali reactivity of European aggregates according to the RILEM AAR-2 method, 2006 SINTEF Report SBF52 A06020 / ISBN 82-14-04080-9 / 978-82-14-04080-9, p. 43 + appendices.

[3] P. Nixon, S. Lane, PARTNER Report No. 3.3. Experience from testing of the alkali reactivity of European aggregates according to several concrete prism test methods, 2006 SINTEF Report SBF52 A06021 / ISBN 82-14-04081-7 / 978- 82-14-04081-7, p. 35 + appendices.

[4] B. Grelk, PARTNER Report No. 3.4. Experience from testing of the alkali reactivity of European aggregates according to two Danish laboratory test methods, 2006 SINTEF Report SBF52 A06022 / ISBN 82-14-04082-5 / 978- 82-14-04082-5, p. 18 + appendices.

[5] E. Siebel, J. Bokern, I. Borchers, PARTNER Report No. 3.5. Field test sites established in the PARTNER project for evaluating the correlation between laboratory tests and field performance, 2006 SINTEF Report SBF52 A06023 / ISBN 82-14-04083-3 / 978- 82-14-04083-3, p. 20 + appendices.

[6] P.J. Nixon, J. Lindgård, I. Borchers, B.J. Wigum, B. Schouenborg, The EU Partner Project—European Standard Tests to Prevent Alkali Reactions in Aggregates. Final results and Recommendations, in: M.A.T.M. Broekmans, B.J. Wigum (Eds.), Proceedings of the 13th International Conference on Alkali–Aggregate Reactions in Concrete, Trondheim, Norway, 2008, p. 10.

[7] M. Haugen, J. Lindgård, U. Åkesson, B. Schouenborg, Experience of using the RILEM AAR-1 petrographic method among European petrographers, in: M.A.T.M. Broekmans, B.J. Wigum (Eds.), Proceedings of the 13th International Conference on Alkali–Aggregate Reactions in Concrete, Trondheim, Norway, 2008, p. 10.

[8] I. Borchers, C. Muller, Field site tests established in the PARTNER project for evaluating the correlation between laboratory tests and field performance, in: M.A.T.M. Broekmans, B.J. Wigum (Eds.), Proceedings of the 13th International Conference on Alkali–Aggregate Reactions in Concrete, Trondheim, Norway, 2008, p. 10.

[9] B. Schouenborg, U. Åkesson, L. Liedberg, Precision trials can improve test methods for alkali aggregate reaction (AAR) — Part of the PARTNER Project, in: M.A.T.M. Broekmans, B.J. Wigum (Eds.), Proceedings of the 13th International Conference on Alkali–Aggregate Reactions in Concrete, Trondheim, Norway, 2008, p. 10.

[10] RILEM, AAR-1 - Detection of potential alkali-reactivity of aggregates — Petrographic method, Materials and Structures (36) (2003) 480–496.

[11] RILEM, AAR-2 - Detection of potential alkali-reactivity of aggregates — the ultra-accelerated mortar bar test, Materials and Structures (33) (2000) 283–289.

[12] TI B51, An accelerated method for the detection of alkali–aggregate reactivities of aggregates, Cement and Concrete Research (8) (1978) 647–650.

[13] K.A. Chatterji, Simple method for the detection of alkali–silica reaction, Cement and Concrete Research (18) (1988) 654–656.

[14] RILEM, AAR-3 - Detection of potential alkali-reactivity of aggregates — method for aggregate combinations using concrete prisms, Materials and Structures (33) (2000) 290–293.

[15] RILEM (to be published): AAR-4.1-Detection of potential alkali-reactivity of aggregates: accelerated (60 °C) concrete prism test.

[16] Deutscher Ausschuss für Stahlbeton, DAfStb (Ed.)(2001): Vorbeugende Maßnahmen gegen schädigende Alkalireaktion im Beton : Alkali-Richtlinie. Beuth, Berlin, (DAfStb-Richtlinie).

[17] Norwegian Concrete Association, NB, Alkali–aggregate reactions in concrete, Test methods and Requirements to Test Laboratories, 2005, NB Publication No. 32 (in Norwegian), p. 39.

[18] RILEM (to be published): RILEM recommended Test method AAR-0. Detection of Alkali-Reactivity Potential in Aggregates for Concrete. Draft 8 (version3). Outline Guide to the use of RILEM methods in assessments of Alkali-Reactivity Potential.

[19] Norwegian Concrete Association, NB, Durable Concrete with Alkali Reactive Aggregates, 2008, p. 38, NB Publication No. 21.

[20] S. Chatterji, A.D. Jensen, N. Thaulow, P. Christensen, Studies of alkali–silica reaction, Part 3. Mechanisms by which NaCl and $Ca(OH)_2$ affect the reaction, Cement and Concrete Research (16) (1986) 246–254.

[21] S. Chatterji, An accelerated method for the detection of alkali–aggregate reactivities of aggretates, Cement and Concrete Research (8) (1978) 647–649.

[22] R.G. Sibbick, C.L. Page, Mechanisms affecting the development of alkali–silica reaction in hardened concretes exposed to saline environments, Magazine of Concrete Research (50) (1998) 147–159.

[23] J.A. Larbi, P.P. Hudec, A study of alkali–aggregate reaction in concrete: measurement and prevention, Part II: AR in saturated hot and cold NaCl solutions, Cement and Concrete Research (20) (1990) 73–78.

[24] J. Lindgård, B.J. Wigum, Alkali aggregate reaction in concrete — field experiences, 2003 SINTEF report no. STF22 A02616, Trondheim, Norway, p. 127 + appendices. (In Norwegian).

[25] Geological Survey of Belgium, in: G. Lorenzi, J. Jensen, B. Wigum, R. Sibbick, M. Haugen, S. Guédon, U. Åkesson (Eds.), Petrographic Atlas of the Potentially Alkali-Reactive Rocks in Europe, 2006, Professional paper 2006/1-N.302, Brussels ISSN 0378-0902, p. 63 + 192 photographs.

[26] B. Fournier, J.H. Ideker, K.J. Folliard, M.D.A. Thomas, P.C. Nkinamubanzi, R. Chevrier, Effect of environmental conditions on expansion in concrete due to alkali–silica reaction (ASR), in: M.A.T.M. Broekmans, B.J. Wigum (Eds.), Proceedings of the 13th International Conference on Alkali–Aggregate Reactions in Concrete, Trondheim, Norway, 2008, p. 10.

[27] B. Fournier, R. Chevrier, M. de Grosbois, R. Lisella, K. Folliard, J. Ideker, M. Shehata, M.D.A. Thomas, S. Baxter, The accelerated concrete prism test (60 °C): variability of the test method and proposed expansion limits, in: M. Tang, M. Deng (Eds.), Proceedings of the 12th International Conference on Alkali–Aggregate Reaction in Concrete, Beijing, China, vol. 1, 2004, pp. 314–323.

[28] K.J. Folliard, J. Ideker, M.D.A. Thomas, B. Fournier, Assessing aggregate reactivity using the accelerated concrete prism testing, in: V.M. Malhotra (Ed.), Proceeding of the 7th CANMET/ACI International conference on recent advances in concrete technology (suppl. Papers), Las Vegas (USA), 2004, pp. 269–283.

[29] ISO 5725–94: precision of test methods — determination of repeatability and reproducibility for a standard test method by inter-laboratory tests (1994).

[30] Schouenborg, B (to be published): PARTNER Report No. 4.1. Precision Trial-Determination of repeatability and reproducibility of the amended RILEM methods; SINTEF report SBF52 A06024 / ISBN 82–14–04084–1 / 978–82–14–04084-1.

[31] M. De Grosbois, E. Fontaine, Performance of the 60 ºC-accelerated concrete prism test for the evaluation of potential alkali-reactivity of concrete aggregates, in: M.A. Bérubé, B. Fournier, B. Durand (Eds.), Proceedings of the 11th International Conference on Alkali–Aggregate Reactions in Concrete, Québec, Canada, 2000, pp. 277–286.

[32] C.A. Rogers, Multi-laboratory study of the accelerated mortar bar test (ASTM Test Method C 1260) for alkali–silica reaction, Cemant, Concrete and Aggregates (21) (1999) 185–194.

[33] CSA A23.2-14A-00, Potential Expansivity of Aggregates (Procedure for Length Change due to Alkali–Aggregate Reaction in Concrete Prisms at 38 °C), Methods of Testing for Concrete, Canadian Standards Association, Mississauga, Ontario, Canada, 2004, pp. 246–256.

[34] EN 932-2: tests for general properties of aggregates — Part 2: Methods for reducing laboratory samples. (European standard).

[35] I. Sims, P.J. Nixon, Assessment of aggregates for alkali–aggregate reactivity potential: RILEM international recommendations, in: Benoit Fournier (Ed.), Marc-Andre Berube Symposium on Alkali–Aggregate Reactivity in Concrete, part of the proceedings of the 8th CANMET International Conference on Recent Advances in Concrete Technology, Montreal, Canada, 31 May to 3 June 2006, 2006, pp. 71–91.

[36] ASTM C1260–07, Standard Test Method for Potential Alkali Reactivity of Aggregates (Mortar-Bar Method), 2007.

[37] AFNOR P18-454, Réactivité d'une formule de béton vis-à-vis de l'alcali-réaction (essaie de performance), Association Française de Normalisation, Paris, France, 2004.

[38] B.J. Wigum, L.T. Pedersen, B. Grelk, J. Lindgård, PARTNER Report No. 2.1. State-of-the art report: key parameters influencing the alkali aggregate reaction, 2007 SINTEF Report SBF52 A06018 / ISBN 82-14-04078-7 / 978-82-14-04078-7, p. 55 +appendices.

[39] J. Bonzel, J. Dahms, Alkalireaktion im Beton, Beton (23) (1973) 495–500 547-554 (in German).

[40] J. Dahms, Influences on the alkali–aggregate reaction under field conditions, in: A.B. Poole (Ed.), The effect of alkalis on the properties of concrete. Proceedings of the Symposium held in London, September 1976, 1976, pp. 277–290.

Paper II

Experience using the Norwegian 38°C concrete prism test to evaluate the alkali reactivity of aggregates, concrete mixes and binder combinations

J. Lindgård, B. Pedersen, S.K. Bremseth, P.A. Dahl, T.F. Rønning

Nordic Concrete Research, 42 (2010) pp. 31-50

Experience Using the Norwegian 38°C Concrete Prism Test to Evaluate the Alkali Reactivity of Aggregates, Concrete Mixes and Binder Combinations

Jan Lindgård
Senior Scientist
SINTEF Building and Infrastructure
Richard Birkelandsvei 3, NO 7465 Trondheim
E-mail: jan.lindgard@sintef.no

Bård Pedersen
Technology Manager
NorStone Heidelberg Cement
PO Box 60, NO 4301 Sandnes
E-mail: bard.pedersen@norstone.no

Sigrun K. Bremseth
Senior Engineer
Norcem Heidelberg Cement
NO 3950 Brevik
E-mail: sigrun.bremseth@norcem.no

Per Arne Dahl
Senior Scientist
SINTEF Building and Infrastructure
Richard Birkelandsvei 3, NO 7465 Trondheim
E-mail: per.dahl@sintef.no

Terje F. Rønning
R&D Manager
Norcem Heidelberg Cement
NO 3950 Brevik
E-mail: terje.ronning@norcem.no

ABSTRACT

Three test methods have been applied in Norway for 20 years to classify the alkali reactivity of concrete aggregates. The Norwegian 38°C concrete prism test was in 1996 also specified in the Norwegian guidelines for performance testing of concrete mixes and/or binders. Since then, more than 160 such performance tests have been carried out in Norway. The main objective with this paper is to discuss the experiences gained from these tests. The Norwegian concrete industry has successfully used the performance test as a flexible tool to be able to utilize alkali reactive aggregates.

Key words: alkali-silica reactions, performance testing, Norwegian experiences, critical alkali limit

1 INTRODUCTION

1.1 Background

Alkali-Silica Reaction (ASR) was recognized as a deterioration problem in Norway about 1990. Since then, several comprehensive national research projects have been carried out on this subject. These projects have strongly focused on test methods for aggregates and corresponding criteria for the prediction of ASR as observed on Norwegian concrete structures.

The research projects have resulted in reasonably reproducible test methods regarding ASR of Norwegian aggregates. Three methods have been applied since the early 90's, the *petrographic method* (similar to the RILEM AAR-1 method [1]), the *80°C accelerated mortar bar test* (AMBT, similar to the RILEM AAR-2 method [2]; exposure time 14 days; prism size 40x40x160 mm) and the *Norwegian 38°C concrete prism test* (NCPT; similar to the old Canadian CPT [3]; exposure time one to two years; unwrapped prisms of size 100x100x450 mm). These methods are included in the current Norwegian regulations for handling the alkali reactivity problem, see section 1.2 [4,5,6].

About 20 years of commercial testing of aggregates with respect to potential ASR have provided SINTEF a very good overview over the alkali reactivity of Norwegian aggregates. In most parts of Norway, alkali silica reactive rock types are present in varying quantities in many commonly used concrete aggregates. To be able to utilize these alkali-silica reactive aggregates for production of durable concretes, there is a need for a reliable performance test to evaluate the alkali reactivity of concrete mixes and/or binders resistant to alkali aggregate reactions. Several such performance tests have been used world wide for at least 15 years, mainly to evaluate supplementary cementing materials (SCMs) and lithium as means to avoid damaging ASR in concrete. Thomas et al. [7] have recently provided a critical evaluation of different test methods. The authors conclude that none of the currently available or commonly used test methods meet all the criteria for an ideal performance test. For example, the main shortcoming of the Canadian 38°C concrete prism test (prism size 75x75x250 mm) [8] is the duration of the test (2 years) and that addition of alkalis are required to compensate for alkali leaching effects. Thus the method cannot be used to determine the "critical" alkali content for an alkali reactive aggregate, nor determine how the minimum level of a SCM changes with the concrete alkali content. However, research are going on towards improving current test methods and to develop alternative tests, for instance within the RILEM technical committee "TC 219- ACS" (2007-2012). Similar work has also been initiated in USA by the U.S. Department of Transportation [9].

The NCPT [5] was in 1996 also specified in the Norwegian guidelines [10] for performance testing of concrete mixes and/or binders (i.e. various cements added any SCMs or other mineral admixtures). Since then, a large number of "job mixes" (i.e. real concrete recipes) and binders have been "performance tested", mainly on a commercial basis. The main objective with this paper is to discuss the experiences gained from these tests, rather than presenting detailed results. The Norwegian concrete industry has successfully used the performance test as a flexible tool to be able to utilize alkali reactive aggregates. Such aggregates may be found in most parts of Norway.

1.2 The Norwegian system for approval based on performance testing

In 1996, the Norwegian Concrete Association published a national guideline on ASR (“NB 21”) [10]. Based on knowledge gained after 1996, and the fact that the publication now is a harmonised normative reference document to the new concrete materials standard, NS-EN 206-1 [11], a revised version of the publication was provided in 2004 [4,6].

The 2004 edition of “NB21” is divided into two major parts. Part 1, “Specifications”, describes in formal terms the mandate and the use of the publication, and how concrete constituents and concrete recipes shall be tested and evaluated with respect to potential ASR. Individual aggregates and blends of aggregates shall be evaluated by the petrographic analysis as a first step. The evaluation based on results from these analyses can be reassessed by the 80°C AMBT, while the 38°C CPT can be used to reassess the evaluation from any of these tests. For the evaluation of binders and concrete compositions (incl. mortars and shotcrete), only the CPT can be used.

The three methods are described in detail in a corresponding publication from the Norwegian Concrete Association (“NB32”) [5]. “NB32” also gives rather detailed requirements to laboratories that aim to be approved to run the Norwegian ASR tests.

Part 2 of “NB21” gives advisory guidelines for how the concrete industry can fulfil the requirements given in part 1. It also provides a survey of binders and corresponding alkali contents documented to be suitable for production of ASR resistant concrete containing all types and amounts of Norwegian reactive aggregates. This survey is updated whenever new binders obtain satisfactory documentation – see www.betong.net (*comment: click on “Publikasjoner”*).

Based on extensive laboratory performance testing and comprehensive calibration of results against field behaviour [12,13], “NB21” states that all CEM I binders shall be considered to be suited for production of non-reactive concrete containing all types of alkali reactive Norwegian aggregates up to an alkali content of 3.0 kg Na_2O_{eq}/m^3 of concrete (see section 3.5). If alkali reactive aggregates are to be used in CEM I based concretes with a higher alkali content or in concretes containing other binders, the Norwegian regulations require performance testing of the actual “job mix” or the actual binder. In such general testing of different binders’ ability to prevent development of alkali silica reactions, the binders are tested in concrete containing a specified aggregate composition [5] (see Table 1) that for Norwegian conditions is considered to be “worst case” with respect to alkali reactivity (i.e. reacts at low alkali levels and gives a very high prism expansion when tested in the NCPT).

The validity of documentation supplied by performance testing is limited to concrete with composition considered to be no more reactive than was the concrete used for the testing. The reactivity is considered to increase if:

- The concrete alkali content increases *(comment: For performance tested materials, extra fly ash or silica fume may be added the cement or the concrete mix without any further documentation, even if these additions contribute with supplement alkalis).*
- The content of pozzolanic material or other SCMs decreases.
- The content of reactive rock types increases more than the upper limit specified in the publication *(comment: No pessimum effects have been documented for any Norwegian aggregate – opposite to the experience gained e.g. in Denmark with opaline flint [21]).*

The acceptance criteria for different types of binders and concrete recipes are differentiated when NCPT results are assessed. In general it can be said that:

- CEM I binders and CEM I based concrete compositions containing no pozzolans or other SCMs shall be considered non-reactive if showing 1 year expansion less than 0.050 %.
- CEM I based concrete compositions containing silica fume, concretes based on the fly ash blended CEM II/A-V cement produced by Norcem in Norway (co-grinding of PFA and clinker) and / or blends of this cement and CEM I shall be considered non-reactive if showing 1 year expansion less than 0.030 %.
- Concrete recipes based on other binders than those mentioned above shall be considered non-reactive if showing 1 year expansion less than 0.030 % and at the same time 2 years expansion less than 0.060 %.

A performance test shall be based on one or more mixes. If based on more than one mix, test results shall be plotted in an expansion versus alkali content-diagram as illustrated by Figure 1. Based on the assumption that a linear relation exists between expansion and alkali content, straight lines connecting the points shall be drawn. If a connecting line and the line illustrating the accepted limit for expansion cross each other, the alkali content limit value for acceptance of non-reactivity is given by the alkali content at the point of intersection subtracted a “safety factor” amounting to 0.2 kg Na_2O_{eq}/m^3 of concrete. If the above-mentioned crossing of lines does not occur, the alkali content limit value for acceptance of non-reactivity shall be:

- 3.0 kg Na_2O_{eq}/m^3 when all the mixes show expansions exceeding the acceptance value.
- Equal to the highest individual alkali content used within the mixes involved when all the mixes show expansions less than the acceptance value.

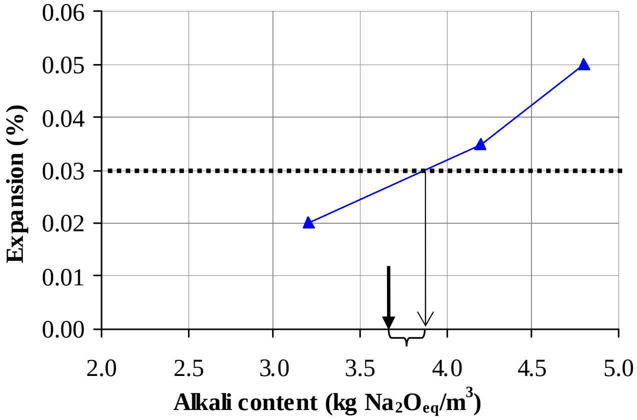

Figure 1 - Principle diagram for determination of acceptance limit for alkali content based on performance testing according to Norwegian regulations. The dotted line represents the critical expansion limit for PFA binders after one year of exposure. The bracket represents the “safety factor” amounting to 0.2 kg Na_2O_{eq}/m^3 of concrete. In the current example, the critical alkali limit is (3.85-0.20) 3.65 kg Na_2O_{eq}/m^3 of concrete.

Internationally, a too high extent of alkali leaching is reported to be one of the main sources of error in connection with accelerated performance testing (see e.g. Thomas et al. [7]), leading to a correspondingly reduced alkali content within the test prisms during the test. Consequently, a too low expansion may be obtained, negatively influencing the laboratory/field correlation. Despite this fact, no specific “safety factor” (beyond the 0.2 kg Na_2O_{eq}/m^3 alkalis of concrete discussed above) is included in the Norwegian regulations to compensate for the (so far undocumented) amount of alkalis that may leach out from the test prisms in the NCPT during the one to two years exposure period. However, alkali leaching is currently focused on in on-going national research activities, as well as in the RILEM task group 219-ACS-P “Performance testing”. This is also the case regarding the question if some aggregate types may release alkalis into the concrete pore water during the test period.

2 REVIEW OF NORWEGIAN PERFORMANCE TEST SERIES

2.1 Available test results

Since performance testing by use of the Norwegian 38°C CPT started in Norway in 1996, the detailed testing procedure has been unchanged [5]. Only a few testing laboratories are approved to perform such performance testing on a commercial basis. As part of the PhD study of Jan Lindgård, all available results from the performance test series performed by the two most experienced approved Norwegian laboratories, SINTEF Building and Infrastructure (Trondheim) and Norcem (Brevik) have been compiled and evaluated. SINTEF have primarily performed the testing on a commercial basis for the industry, while Norcem mainly have tested the performance of various cements in trade or under development [14,15,16,17,18]. All the about 30 concrete prisms test series being part of the PhD study of Bård Pedersen [19,20] are also included in the review. SINTEF performed all the test series in his study, focusing of the possible mitigating effects of different filler types on ASR.

In total, the review includes results from 161 performance test series. Table 1 and 2 give an overview of the different aggregate types and binder types tested. The duration for the 155 finalised test series have varied from one to twelve years.

Table 1 - Overview of aggregate types included in the reviewed performance test series executed in Norway in the period 1996-2010

Aggregate type		Number
Fine (0-5 mm)	Coarse (5-20 mm)	of tests [1]
Reference-I (NR) [2]	Reference-II (R) [3]	26
Reference-III R [4]	Reference-II (R) [3]	49
Reference-IV R [5]	Reference-II (R) [3]	7
Reference-IV R [5]	Reference-I (NR) [2]	26
Different types [6]	Different types [6]	50
Recycled glass (R)	Recycled glass (R)	3
	Sum	161

[1] 119 of the tests are performed at SINTEFs laboratory (include the 29 tests being part of Bård Pedersens PhD study [19, 20]). The remaining 42 tests are performed by Norcem.

[2] Non-Reactive (NR) natural gneiss/granite aggregate.

[3] Reactive (R) chrushed cataclasite.

[4] Natural aggregate (R) with claystone, siltstone and phyllite as the main reactive rock types.

[5] Natural aggregate (R) with mylonite, cataclasite, greywacke and phyllite as the main reactive rock types.

[6] Primary alkali silica reactive aggregate types. 27 of the mixes include a crushed mylonite [19, 20].

Table 2 - Overview of binder types included in the reviewed performance test series executed in Norway in the period 1996-2010

Binder type	Total number of tests	Number of the tests added CSF [5]
CEM I [1]	51	8
CEM I + CEM II Portland fly ash cement [2]	45	22
CEM II Portland fly ash cement [2]	26	9
CEM II Portland slag cement [3]	7	---
CEM I + fly ash added separately	5	---
CEM I + added LWA fines	4	---
CEM I + added different filler types [4]	22	---
CEM I + other admixture added	1	---
Sum	161	39

[1] All the cements, except the Portland slag cement, are produced by Norcem (part of the Heidelberg Cement Group). Different types of CEM I have been tested.

[2] CEM II/A-V including about 20 weight-% fly ash of the binder.

[3] CEM II/B-S including at least 32 % ggbfs.

[4] Most filler types were produced from alkali reactive aggregates [19, 20].

[5] CSF = Condenced Silica Fume.

The 161 test series include some “job mixes” and some mixes to determine the critical alkali limit for various aggregate types. However, most of the performance test series have aimed to document different binder combinations ability to prevent ASR. Reference reactive aggregates were used in these tests series. In addition to different CEM I cements, the binders tested included pulverized fly ash (PFA), condensed silica fume (CSF), ground granulated blast furnace slag (ggbfs), light weight aggregate fines and/or different filler types (mainly produced from alkali silica reactive rock types). The water/binder ratio in the test series varied mainly between 0.45 and 0.48. If needed to boost the alkali content, NaOH was added to the mixes.

2.2 Alkali leaching

Since 2007, SINTEF have systematically performed analyses to document the extent of alkalis leached out from the prisms in the NCPT during the one to two years exposure period. To avoid contamination, all testing equipment and storage containers are washed properly and a new lining is applied before new test series are started. At every standard measuring points of time, a 20 ml sample of the water in the bottom of each storage container is collected. Before each sampling, the total amount of water is calculated by measuring the depth of the water in the centre of each container. A depth versus volume ratio was earlier established for the applied type of storage container by successively adding a known quantity of water and measure the corresponding water depth. If some of the water has evaporated since the last measurement, water is added after sampling.

The content of alkalis, Na^+ and K^+, has been measured by use of flame atomic absorption spectroscopy (FAAS). Based on these measurements, the total content of alkalis leached out from the concrete prisms has been calculated. As a quality control, five samples were parallel tested in a laboratory at the Norwegian University of Science and Technology (NTNU) using inductively coupled plasma mass spectrometry (ICP-MS). A satisfactory correlation between the two methods was documented; on average about 5 % less alkalis were found by use of ICP.

3 RESULTS AND DISCUSSION

3.1 Repeatability and reproducibility of results

Spread in results obtained between individual prisms within one test series (repeatability)
To document the repeatability of the NCPT, standard deviations and coefficients of variation (c.o.v) for the measured expansions and the corresponding weight increases of the three prisms within one test series have been calculated. The outcome of these calculations is shown in Table 3 (mean results) and Figure 2 (detailed results for the expansion).

Two of the rows in Table 3 give the calculated mean standard deviations and c.o.v. for all 119 SINTEF test series included in the review (include 29 test series being part of the PhD study of Bård Pedersen [19,20]). In the other two rows and in Figure 2, all single test results with mean prism expansion lower than 0.010 % are left out, giving more meaningful results for the calculated c.o.v. for the expansion (calculation of c.o.v. becomes “meaningless” for very low expansion values; c.o.v. varies from about -200 to +200 %).

Table 3 - NCPT - three parallel prisms within one test series; calculated mean standard deviations and mean c.o.v. for measured expansions and weight increases. The data is based on 119 test series performed in SINTEFs laboratory.

	Expansion			Weight increase			Comments
Exposure time (months)	6	12	24	6	12	24	
Standard Deviation (%)	0.002	0.005	0.008	0.030	0.034	0.035	Included all SINTEF results
	0.003	0.006	0.008	0.032	0.034	0.035	Excl. tests with expansion < 0.010 %
Coefficient of variaton (%)	6.2	14.0	6.8	8.0	6.7	5.3	Included all SINTEF results
	6.3	7.8	6.8	6.8	6.3	5.3	Excl. tests with expansion < 0.010 %

For test series with expansion higher than approximately 0.025 %, c.o.v. for the expansion is lower than 10 % for most test series (Figure 2). The corresponding mean values for c.o.v. are in the range 6 to 8 % (Table 3). Normally, a coefficient of variation in the repeatability of up to 20 % is regarded acceptable [21]. The repeatability for the NCPT is thus in general very good. However, as can be seen from Figure 2, a few exceptions exist.

In the precision trials within the European research project PARTNER [21], eight laboratories took part for each of the four test methods incorporated. The two CPTs included, RILEM AAR-3 [23] and RILEM AAR-4 Alternative [24], applied wrapped prisms. Each laboratory tested the same three aggregates types, prepared at one laboratory, before being distributed. Identical cement type was applied in all mixes. Mean c.o.v. for the expansions measured was in the range 14-21 % for RILEM AAR-3 and 9-16.5 % for RILEM AAR-4 Alternative, respectively. For ASTM C 1293 (38°C CPT, same prism size as the RILEM CPTs, but no wrapping of the prisms), c.o.v. has been found to be 12 % for average expansions of more than 0.020 % [25].

As shown, the repeatability for the Norwegian CPT is in general much better than reported for ASTM C 1293 and as documented in the PARTNER project applying two draft RILEM CPTs. This is mainly assumed to be due to a good quality control in SINTEF laboratory, combined with long term experience in performing expansion tests.

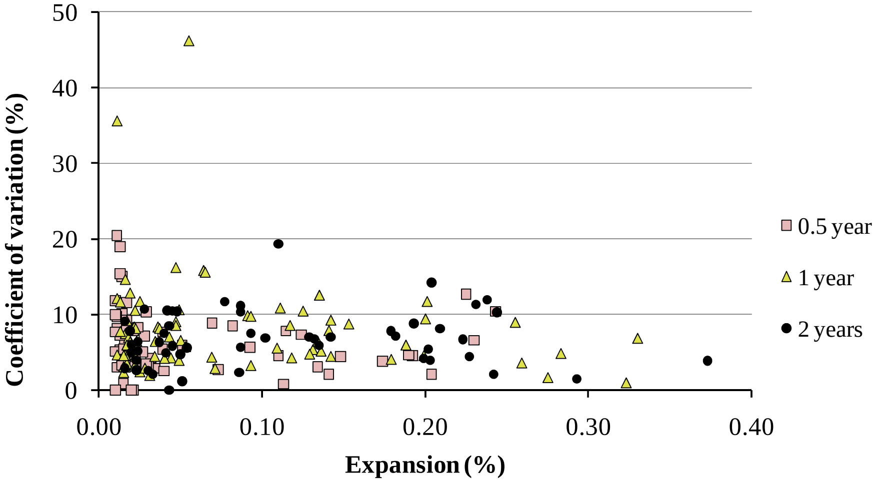

Figure 2 - NCPT; three parallel prisms within one test series; calculated c.o.v. for measured expansions versus corresponding mean expansions. The data is based on 119 test series performed in SINTEFs laboratory. All single test results with mean prism expansion lower *than 0.010 % are left out.*

Calculated c.o.v. for the weight increase is lower than 15 % for most test series (includes all SINTEF results). The corresponding mean values for c.o.v. are in the range 5.5-8 % (Table 3). The repeatability is thus acceptable with respect to measured weight increases, as well. In general, c.o.v. for the weight increase decreases with increasing weight increase.

Within laboratory – and multi laboratory variations (reproducibility)

Reproducibility of a concrete prism test is a measure to compare the difference in the mean value obtained between different laboratories when testing identical aggregate- and concrete compositions. In order to check the reproducibility of the NCPT, parallel tests have from time to time been performed by SINTEF and Norcem. Figure 3 shows the measured expansion versus exposure time for six such “pairs of concrete mixes” with identical concrete composition. For all these “pairs of mixes”, except one, one of the test series was performed by SINTEF and the other test was performed by Norcem.

As shown in Figure 3, the corresponding graphs for all the six “pairs of mixes” are close. However, if the expansion is very close to the critical expansion limit, also small deviations between the two laboratories may lead to different conclusions from the testing. In Figure 3, this is the case for one of the six “pairs of mixes”; one of test series for a concrete with a highly reactive aggregate, fly ash cement and a total alkali content of 6.6 kg Na_2O_{eq}/m^3 of concrete expanded just above the critical limit after one year of exposure at SINTEF (0.031 %), while the expansion at Norcem was just below (0.025 %) the critical expansion limit (0.030 %) (the mix is marked with an open rectangle). After two years of exposure, the expansion was a little bit below the critical expansion limit (0.060 %) at both laboratories (0.051 % and 0.044 %, respectively).

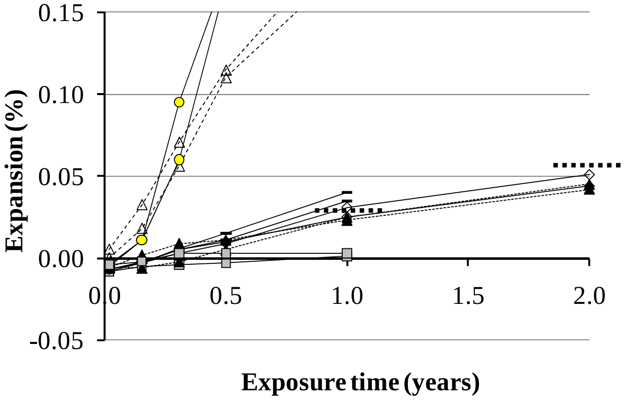

Figure 3 - NCPT; expansion versus exposure time for six parallel concrete mixes. Each "pair of mixes" is marked with identical bullets. The dotted lines drawn at 1 and 2 years, respectively, represent Norwegian critical expansion limits for concretes with binders containing fly ash, condensed silica fume or ggbfs.

Also other test series (not included in the figure) confirm that SINTEF and Norcem produce corresponding results, among these the parallel tests performed by the two laboratories within the PARTNER project [22]. In the paper summarizing the PARTNER findings [21], the importance of experience is highlighted: *"There is also evidence that the experience of the laboratories with a particular method has a significant effect on the variability of results. Where laboratories were carrying out procedures with which they were very familiar, for example the Norwegian method carried out by Norcem and SINTEF, the expansion values were very close".*

Due to a limited number of laboratories applying the NCPT, the precision of the method is not documented by round robin testing as in the PARTNER project, in which the procedure in ISO 5725-94 [26] was followed. In the PARTNER project, the reproducibility for the RILEM AAR-3 method was quite poor [21]. Calculated c.o.v. for the mean expansions measured by the eight laboratories taking part was in the range 49-54 %, i.e. unacceptably high. Corresponding values for RILEM AAR-4 Alternative, was in the range 24-33%, i.e. somewhat better. It was concluded [21] that the precision of both RILEM concrete prism tests is sufficient to distinguish between pronounced non-reactive and reactive materials, but not between smaller differences of reactivity.

The precision of the ASTM C 1293 CPT [25], which is similar to the NCPT except application of smaller prisms, is, as discussed in [21], reported in a way which makes a direct comparison with the PARTNER results difficult: *For expansion levels less than 0.014%, the expected difference between laboratories should generally not exceed 0.009% (absolute percent). This means that if you sample an aggregate with an expected expansion of 0.014%, reduce it to several subsamples and send two of them to different laboratories, the expected expansion results (i.e. the average of three prisms) will most likely be between 0.023 and 0.005%. The multi-laboratory coefficient of variation for expansions greater than 0.014% is 23%.*

3.2 Expansion versus exposure time – overall results

Tables 1 and 2 give an overview of the different aggregate types and binder combinations included in the review of the Norwegian performance test series performed in the period 1996-2010. In Figure 4, all the measured mean expansions are plotted versus exposure time (up to 12 years).

75 of the total 161 performance test series have run for at least 2 years. Out of these, 38 concrete mixes have been exposed for 3-12 years. As shown in Figure 4, the general tendency is that the rather constant expansion rates for the most alkali reactive mixes (mainly reference mixes with high alkali content) decrease after an exposure time of approximately 0.5 year. The expansion rates for the medium reactive mixes, however, have shown to be rather constant up to about 2-3 years of exposure, before decreasing. For most mixes, the increase in expansion is very low or even non-appearing after the first two years of exposure.

One of the main reasons for the reduced expansion rate with time are assumed to be alkali leaching (see section 3.6) combined with consumption of alkalis in the alkali silica reaction, both reducing the pH of the concrete pore water.

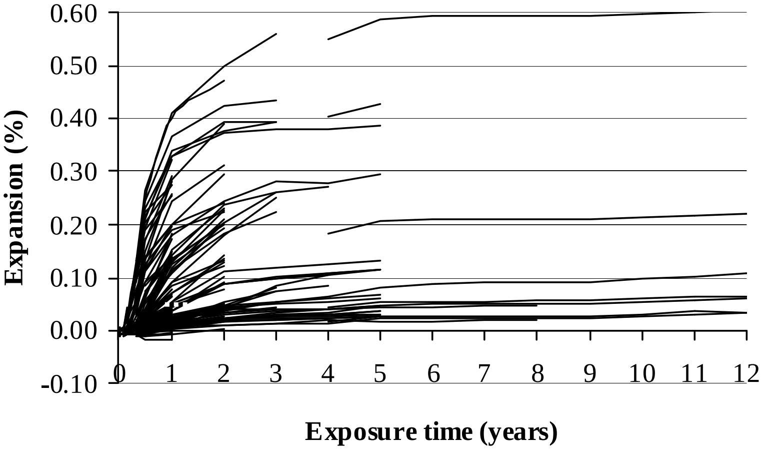

Figure 4 - NCPT; expansion versus exposure time for 161 performance test series. Criterion expansion limits are given in Figure 3.

Some of the approved non-reactive mixes, i.e. mixes with a lower expansion than the critical limits given in the Norwegian regulations [4], have expanded beyond the critical expansion level(s) at later ages. However, most mixes showing non-reactivity after one year of exposure still show an expansion below the critical expansion level(s) even up to 12 years of exposure. Due to more alkali leaching with time, no further significant expansion is expected for these concrete mixes.

3.3 Weight increase as a quality control

Standard procedure in the Norwegian CPT, as in most comparable test methods, is to measure both expansion and weight increase of the prisms. The weight increase is rarely reported, but should act as an important quality control of the moisture conditions within the storage containers.

As shown in Figure 5, the prism weight typically increases with increasing prism expansion. However, no good correlation exists. This is not surprisingly, since the review includes concrete mixes with various aggregate- and binder types. The calculated correlation factors R^2 between the measured weight increases and the expansions were approximately 0.80 at the ages 2, 3 and 4 years. R^2 was somewhat lower at the ages 0.5 and 1 year.

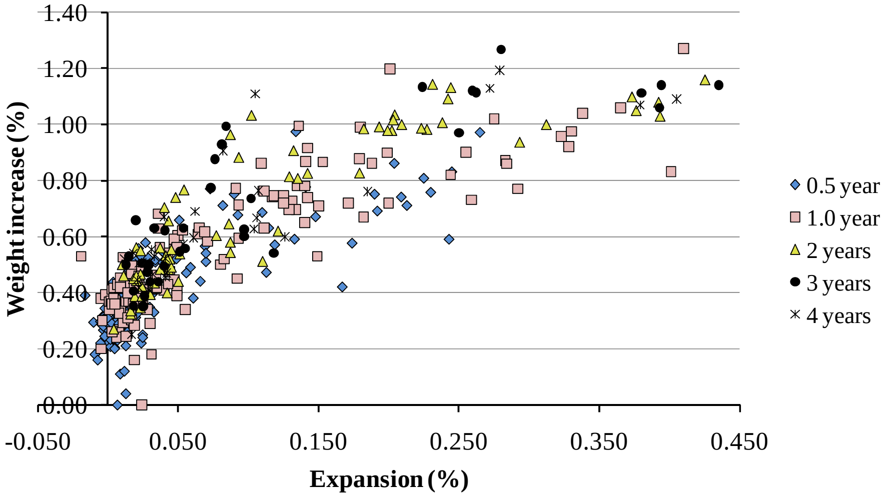

Figure 5 - NCPT; weight increase versus expansion at ages 0.5-4 years. The data is based on 161 test series.

All the 161 test series, except three, revealed a one year weight increase in the range 0.20-1.30 %, even though some of these test series exhibited a slight shrinkage. The weight increase due to ASR is the total weight increase of the prisms, subtracted the weight gain due to water absorption by the aggregates and by the cement paste (in particular due to the on-going hydration). The weight increases show a reduced rate with time, as the expansions do (see Figure 4). The three test series with lower weight increase, in the range 0-0.20 % after 0.5-1 year of exposure, was performed at Norcem. The reason for this low gain in weight is not known.

According to the comprehensive experience gained with the Norwegian CPT, a minor weight loss may for some binders be recorded in the first few weeks of exposure, limited to maximum 0.20 %. If the prisms still show a significant weight loss after a longer time of exposure, this is most likely due to insufficient water present in the system. Thus, a too low prism expansion will be recorded. Example; in one test series performed at SINTEF, all the three prisms in the storage container lost some weight from one to two years of exposure. At the same time the expansion of the prisms decreased somewhat. By control of the storage containers, a crack was observed in the cover, resulting in a moisture content within the storage container less than 100 % RH. Consequently, the test results had to be discarded.

In the RILEM CPTs, AAR-3 (38°C) [23] and AAR-4 (60°C) [24], a requirement is given to the recorded weight to ensure that sufficient water is present in the system. Until recently, the method descriptions stated that all the measurements related to a single test prism should be discarded if the weight loss recorded for the prism, with cross-section 75±5 mm and length 250±50 mm, was greater than 20 g. This means that a weight loss up to 0.4-0.8 % (depending on the prism size applied) compared to the starting reference weight should be accepted.

In light of the experience built up with the NCPT, where even prisms that exhibit shrinkage normally gain at least 0.2 % in weight after the first 0.5 year of exposure (Figure 5), this requirement seems far too little restrict. Based on a suggestion from SINTEF to the RILEM TC-219 ACS committee, the former requirement has now been sharpened. In the current method descriptions no weight reduction of the prisms, compared to the reference weight at start of testing, is allowed at the time of the final weight reading. If a net weight loss (i.e. without any cloth wrapping) is recorded at the time of executing the last length readings, the measurements relating to these prisms shall be discarded.

3.4 Performance testing of binders

As shown in Table 2, most of the performance test series have aimed to document different binder combinations ability to prevent ASR. About 70 of these test series have included Norcem “Standard FA” cement, a CEM II/A-V Portland - fly ash cement with a PFA content of approximately 20 % by weight of binder. All the fly ashes used the last 15 years are carefully selected in order to have good ASR mitigation properties. In contrast to usual CEM I - PFA combinations, the Norcem “Standard FA” cement is manufactured by co-grinding clinker and PFA, a process that has shown to enhance the well known ASR mitigating effect of fly ash [27]. An example of the effectiveness of this cement to suppress ASR is given in Figure 6. PFA constitutes about 80 kg/m^3 of the binder. All the alkalis in the fly ash are included in the calculated total alkali content of the concrete mixes. The expansion of these mixes increases with increasing alkali content from 5.0 to 8.5 kg Na_2O_{eq} /m^3 of concrete, obtained by boosting with NaOH. Based on such performance testing, all the Norcem “Standard FA” cements with various selected fly ashes have given acceptance alkali limits equal to or higher than 6.5 kg Na_2O_{eq}/m^3 of concrete, and may thus be used in combination with all Norwegian concrete aggregates up to this documented alkali limit.

The influence on ASR from addition of different filler types produced from alkali reactive rock types was the issue of the PhD work of Bård Pedersen [19,20]. Selected results are given in Figure 7. The alkali content in all mixes was 5.0 kg Na_2O_{eq}/m^3 of concrete (excl. alkalis in the fly ash, in which constitute about 0.9 kg Na_2O_{eq}/m^3 of concrete). As shown, addition of about 85 kg filler per m^3 (of concrete) produced from Icelandic Rhyolite (earlier proven to be pozzolanic and thus able to mitigate ASR [28]) or recycled bottle glass (mitigation effect on ASR debated [19]), as well as addition of about 75 kg fly ash per m^3 of concrete (constitutes about 16 % of the binder), were able to suppress ASR below the critical expansion limit. The fly ash applied is the same type as included in the Norcem fly ash cement (see Figure 6). In contrast, none of the Norwegian filler types were able to suppress ASR. They all led to higher expansion than the reference mix added filler made of a non-reactive gneiss/granite.

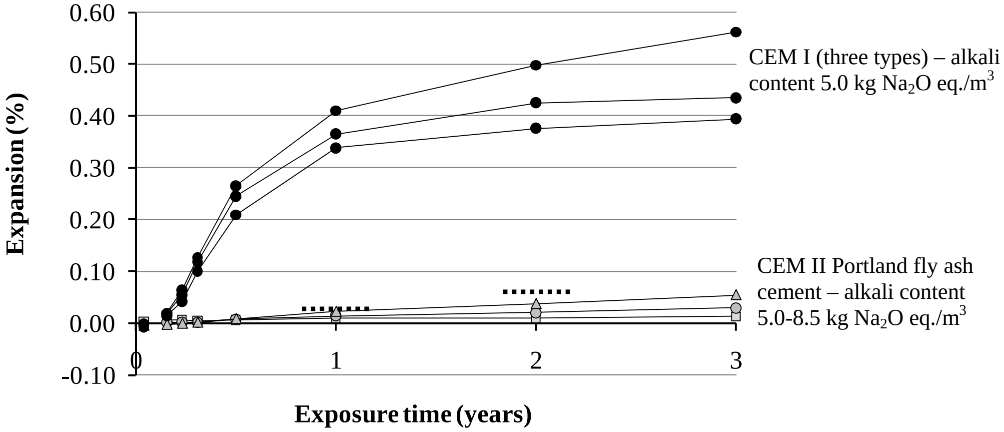

Figure 6 - Expansion versus exposure time for six binders tested with the aggregate combination Reference-I (non-reactive fine) + Reference-II (reactive coarse) - see Table 1. The CEM II Portland - fly ash cement contains 20 % PFA (80 kg/m^3 of concrete). The dotted lines drawn at 1 and 2 years, respectively, represent critical limits for concretes with binders containing fly ash, condensed silica fume or ggbfs.

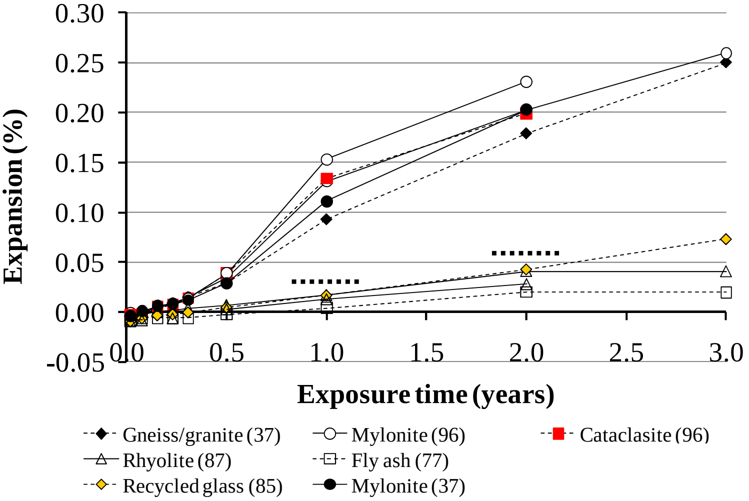

Figure 7 - Expansion versus exposure time for concretes containing different fillers (0/0.125 mm) and a reactive mylonite aggregate [19,20]. The number in ( ) is kg filler per m^3 of concrete. The alkali content in all mixes was about 5.0 kg Na_2O_{eq}/m^3 of concrete. The dotted lines drawn at 1 and 2 years, respectively, represent Norwegian critical limits for concretes with binders containing fly ash, condensed silica fume or ggbfs.

The Figures 6 and 7 show examples of application of the Norwegian performance test. Even though a one year testing time is required (two years for special binders – see section 1.2), Norwegian cement – and concrete producers have frequently performed such tests. The aim has been to achieve approval for using different binder combinations (e.g. a CEM II Portland – fly ash cement) and/or possible new pozzolanic material (e.g. fillers produced from reactive rock types) in combination with various alkali reactive Norwegian aggregates. In this way, a number of commercial concrete recipes may be pre-documented, giving the concrete producers flexibility with respect to fulfilling the ASR requirements in the Norwegian regulations.

Normally a reference "worst case" reactive aggregate combination is used in these performance tests [5], giving a general approval for using the tested binders in combination with all Norwegian alkali reactive aggregates, which in general are assumed to be less reactive than the reference reactive aggregate combinations (see Table 1) applied in the performance tests.

3.5 Critical alkali limit for different aggregate types

Some of the alkali reactive aggregate types in common use in Norway for concrete production, have been "performance tested" to determine the critical alkali limit in combination with CEM I binder. Results from such testing of four aggregate combinations are shown in Figure 8. The lines drawn in the figure at the alkali content 3.0 kg Na_2O_{eq}/m^3 of concrete and the expansion 0.050 %, respectively, represent the Norwegian critical limits for a fine/coarse aggregate combination combined with CEM I cements (see section 1.2).

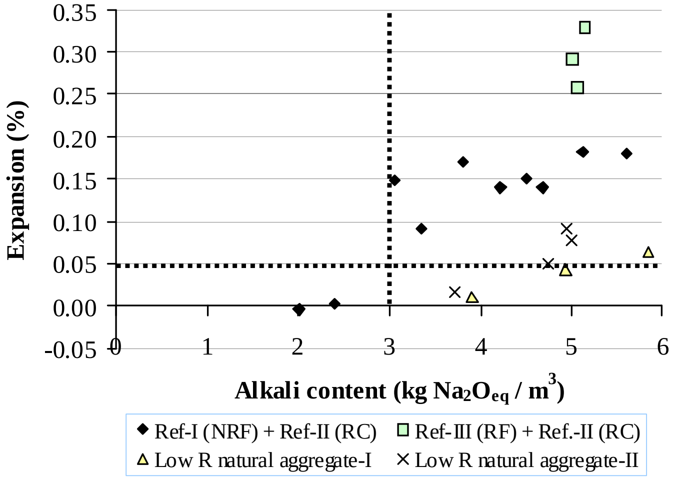

Figure 8 - Expansion versus alkali content for four Norwegian aggregate combinations after one year of exposure (R=Reactive, NR=Non-Reactive, F=Fine and C=Coarse aggregate). The dotted lines drawn at 3.0 kg Na_2O_{eq}/m^3 *of concrete and 0.050 %, respectively, represent Norwegian critical limits.*

One of the mixes with the highly reactive cataclasite ("Ref-II (RC)") revealed a disturbing high expansion at an alkali content of only 3.1 kg Na_2O_{eq}/m^3 of concrete. However, the cataclasite is very rarely used commercially in concrete, rather as a reference "worst case" coarse reactive aggregate [5]. Most alkali reactive aggregate types in common use in Norway are far less reactive than this cataclasite. Thus, the general Norwegian acceptance alkali limit of 3.0 kg Na_2O_{eq}/m^3 of concrete for CEM I binders has been regarded as safe. Two examples of more moderate reactive Norwegian aggregates, with critical alkali limits between 4.5 and 4.8 kg Na_2O_{eq}/m^3 of concrete, respectively, are also shown in Figure 8.

3.6 Alkali leaching

According to Thomas et al. [7], the problem with alkali leaching from specimens stored over water in sealed specimens was first reported by Blanks and Meissner in 1946 [29]. They detected a build up of alkali ions in the water at the bottom of the containers in which mortar bars were stored, and explained this based on water condensing on the surface of the bars and running down the bars into the reservoir below, thereby providing transport of the alkalis. Due to this alkali leaching, the alkali content within the test prisms is reduced, leading to a drop in the pH of the pore water. Consequently, less silica is being dissolved from the aggregates and the extent of ASR is reduced, resulting in a too low prism expansion.

Several parameters may influence the extent of alkali leaching, among them prism size, storage conditions and concrete composition.

Tests performed by Bakker in the early 80'ties [30] showed that the larger the cross-section of a concrete prism, the greater the expansion, which was interpreted as being caused by higher extent of alkali leaching for the smaller specimens.

According to Bokern [31], intensive alkali leaching occurs in extremely humid conditions like in a fog chamber, as applied in the German CPT [32]. Even though prisms with a 100x100 mm cross section is applied, a loss of 20 % of a concretes initial soluble alkali content after 28 days and more than 30 % after 90 days is possible. Bokern [31] also states that concretes made of OPC or cement with ggbfs (20 %) seem to be particularly vulnerable to alkali leaching.

Rivard et al. [33] showed that for the same reactive mixture, concrete alkali leaching seemed to be greater for specimens containing higher alkali level (5.25 kg Na_2O_{eq}/m^3 of concrete) compared with specimens with lower alkali level (4.0 kg Na_2O_{eq}/m^3 of concrete). In these tests, the ASTM C 1293 CPT [25] was applied.

Figure 9 and 10 show the cumulative extent of alkali leaching for 30 SINTEF NCPT series. In Figure 9, the alkali content measured in the water in the bottom of the storage containers is recalculated to represent the reduction in alkali content in kg Na_2O_{eq}/m^3 of concrete compared to the total alkali content in the concrete at the time of mixing (includes all alkalis in the cement and in any mineral - and chemical admixtures, but excludes any alkalis that possibly may be released from the aggregates). Figure 10 shows a corresponding graph, but the reduction in alkali content is given as %. As can be seen, the rate of alkali leaching is highest the first three to six months of exposure. After one year of exposure, from 0.1 to 0.9 kg Na_2O_{eq} alkalis per m^3 of concrete are leached out from the prisms with size 100x100x450 mm, representing 2-17 % of the original alkali content in the concrete. Correspondingly, Thomas et al. [7] reported that 35 % of the alkalis originally in prisms of size 75x75x300 mm were leached out after 1 year, and as much as 20 % after just 90 days, i.e. about twice as much as the highest values from the NCPT prisms.

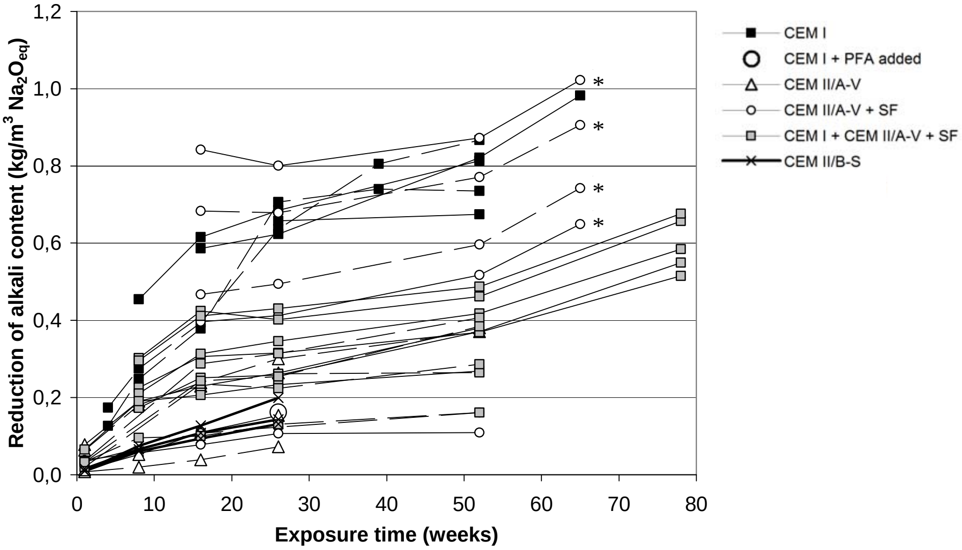

Figure 9 - NCPT; alkali content measured in the water in the bottom of storage containers, re-calculated to represent the reduction in alkali content in kg Na_2O_{eq}/m^3 of concrete compared to the total alkali content in the concrete at the time of mixing. The solid-drawn lines represent mixes in which NaOH is added to increase the alkali content. The dotted lines represent mixes without extra NaOH added. (= "shotcrete")*

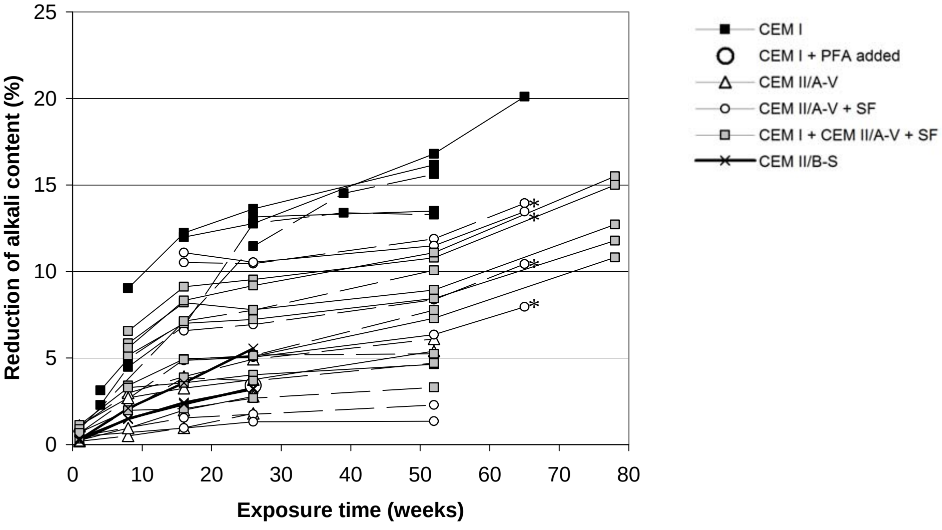

Figure 10 - NCPT; alkali content measured in the water in the bottom of storage containers, re-calculated to represent the reduction in alkali content in % compared to the total alkali content in the concrete at the time of mixing. The solid-drawn lines represent concrete mixes in which NaOH is added to increase the alkali content. The dotted lines represent concrete mixes without extra NaOH added. (= "shotcrete")*

Any alkalis absorbed by the lining inside the storage containers are not included in the presented results. Later tests performed at SINTEF show that the extent of alkalis absorbed by the lining after one year of exposure constitutes less than 2.5 % of the total alkali content in the concrete at the time of mixing (CEM I, w/c-ratio 0.45).

Similar as Bokern [31] reported, OPC (CEM I) seems to be most vulnerable to alkali leaching, while some of the mixes with fly ash cement (CEM II/A-V) show the lowest extent of alkali leaching. Also mixes with the CEM II/B-S cement containing 33 % ggbfs show a low extent of alkali leaching (3-5 %) after 26 weeks of exposure.

Primarily due to higher binder content, some mortar prisms (simulating a shotcrete - marked with *) liberate relatively large amounts of alkalis to the water in the bottom of the storage container during the first 26 weeks of exposure (Figure 9). The alkali content in these mixes varied in the range 4.9-8.2 kg Na_2O_{eq}/m^3 of concrete. No alkali based accelerator was used, but the alkali content in some mixes was boosted by adding NaOH. In generals for all tests, no obvious differences in extent of alkali leaching were observed between concretes with – and without added NaOH.

The total extent of alkali leaching increases with time (see Figure 9) as the expansion does (see Figure 4). However, no tests are performed with aim to correlate the extent of alkali leaching versus total prism expansion applying the same binder type. Based on the tests performed (not focusing on alkali leaching), it is thus not possible to draw any conclusions regarding this relation. But, the extent of alkali leaching may be significant also for low expanding concretes. In some test series, up to 10 % of the alkalis present in the cement were leached out after one year of exposure, even though the prism expansion was lower than the critical expansion limit.

Most concretes tested had a water/binder ratio in the area 0.45-0.48. Thus, too little data is available to document the influence of water/binder ratio (i.e. changed diffusion properties) on the extent of alkali leaching.

In contrast to many laboratory results, the pore solution in field concrete is mostly not subject to alkali leaching (Rivard et al. [33]), except close to the concrete surface or close to any cracks. The problem with alkali leaching in many laboratory test methods is thus a big challenge. However, the presented results show that use of relatively large concrete prisms in the NCPT secure a rather low extent of alkali leaching compared to corresponding concrete prism tests applying smaller prisms. Still, the possible influence of alkali leaching on the measured expansions in the NCPT can not be neglected. Thus, the leaching issue should be looked further into.

As mentioned in section 1.2, no specific “safety factor” (beyond the 0.2 kg Na_2O_{eq}/m^3 alkalis of concrete discussed above) is so far included in the Norwegian regulations to compensate for any alkalis that may leach out from the concrete prisms during the one to two years exposure period. However, some extra security is already built in these regulations when testing binders, since most alkali reactive aggregate types in common use in Norway are far less reactive than the reference “worst case” alkali reactive aggregate combinations applied for performance testing of binders. In addition, most commercial concretes containing SCMs will normally contain less alkalis than the critical alkali limits documented for various binders. Norcem has also declared “upper alkali limits” for their cements to be used for calculating the concrete alkali content according to the Norwegian regulations.

4 CONCLUSIONS

During the last 15 years, about 160 performance tests have been performed by the two most experienced approved Norwegian laboratories at SINTEF (119) and Norcem (42). These tests include “job mixes” (i.e. real concrete recipes) and mixes to determine the critical alkali limit for different aggregate types. However, most of the performance tests have aimed at documenting different binder combinations ability to prevent ASR. In these tests, reference reactive aggregates are used. Based on the review of the results from these tests, the following conclusions may be drawn:

- Despite the long testing time required (1-2 years), the Norwegian system for performance testing has proven to be an advantageous and flexible tool to document critical alkali limits for binders and aggregates.
- The repeatability obtained at SINTEF for the Norwegian CPT is in general very good.
- In all parallel tests, SINTEF and Norcem produce results that are very close.
- In general, the expansion rates for all concrete mixes are highest in the first 0.5-2 years of exposure, before decreasing considerable or for several mixes become non-appearing. The main reason for this is assumed to be alkali leaching, combined with consumption of alkalis during the ASR. The expansion rates decrease earliest for the most alkali reactive mixes.
- Most approved non-reactive mixes still show an expansion below the critical expansion level(s) even up to 12 years of exposure.
- The prism weight increases with increasing expansions. In all SINTEF test series, the mean weight increase after one year was higher than 0.20 %, even for concrete mixes that shrunk. However, some of the mixes revealed a small weight loss during the first weeks.
- The review strengthens the importance of using weight measurements as a quality control of the moisture conditions within the storage containers.
- Even though one of the mixes with the highly reactive reference cataclasite (not in commercial use in concrete) revealed a disturbingly high one year expansion at an alkali content of only 3.1 kg Na_2O_{eq}/m^3 of concrete, the general Norwegian acceptance alkali limit of 3.0 kg Na_2O_{eq}/m^3 of concrete for CEM I binders in combination with all Norwegian aggregate types in common use has been regarded as a safe tool.
- By using the Norcem Standard-FA cement (CEM II/A-V), containing about 20 % PFA, a general acceptance alkali limit of 6.5 kg Na_2O_{eq}/m^3 of concrete (including all the alkalis in the fly ash) is approved in combination with all Norwegian aggregate types in common use.
- From 0.1 to 0.9 kg Na_2O_{eq} alkalis per m^3 of concrete are leached out of the NCPT prisms after one year of exposure, representing 2-17 % of the original concrete alkali content. The highest extent of alkali leaching measured from these NCPT prisms represents about half as much as reported from smaller prisms, e.g. as applied in ASTM C 1293 [25].
- The possible influence of alkali leaching on the measured expansions in the Norwegian CPT can not be neglected, even though rather large concrete prisms are used.
- No specific “safety factor” (beyond a “general safety factor”) is included in the Norwegian regulations to compensate for any alkalis that may leach out from the prisms in the NCPT. However, some extra security is already built into these regulations when testing binders, since most alkali reactive aggregates in common use in Norway are far less reactive than the reference “worst case” alkali reactive aggregate combinations applied for performance testing of binders. In addition, most commercial concretes containing SCMs will normally contain less alkalis than the critical alkali limits documented for various binders. Norcem has also declared “upper alkali limits” for their cements to be used for calculating the concrete alkali content according to the Norwegian regulations.

5 ACKNOWLEDGEMENT

The authors would like to acknowledge COIN, the COncrete INnovation centre (www.coinweb.no) for the financial support.

6 REFERENCES

1. RILEM, "AAR-1 - Detection of potential alkali-reactivity of aggregates – Petrographic method", *Materials and Structures,* Volume 36, 2003, pp. 480-496.
2. RILEM, "AAR-2 - Detection of potential alkali-reactivity of aggregates - the ultra-accelerated mortar bar test", *Materials and Structures*, Volume 33, 2000, pp. 283-289.
3. *CSA Standard*, "CAN3-A.23.2-M77 – Potential Expansivity of Cement Aggregate Combinations (Concrete Prism Expansion Method)", Supplement NO.2, 1986.
4. Norwegian Concrete Association, NB, "Durable concrete containing alkali reactive aggregates", *NB Publication* No. 21, Oslo, 2004, 34 p. including appendices.
5. Norwegian Concrete Association, NB, "Alkali aggregate reactions in concrete. Test methods and requirements to laboratories", *NB Publ.* No. 32, 2005, 39 p. incl. appendices.
6. Dahl, P.A., Lindgård, J., Danielsen, S.W., Hagby, C., Kompen, R., Pedersen, B. & Rønning, T.F., "Specifications and guidelines for production of AAR resistant concrete in Norway", in: Tang, M. and Deng, M. (Eds.), *Proceedings of the 12th International Conference on Alkali–Aggregate Reaction in Concrete*, Beijing, China, vol. 1, 2004, pp. 499–504.
7. Thomas, M., Fournier, B., Folliard, K., Ideker, J. & Shehata, M., "Test methods for evaluating preventive measures for controlling expansion due to alkali-silica reaction in concrete", *Cement and Concrete Research*, Volume 36, Issue 10, 2006, pp. 1842-1856.
8. CSA Standard A23.2-27A, "Standard practice to identify degree of alkali-reactivity of aggregates and to identify measures to avoid deleterious expansions in concrete", *CSA A23.2-00 Methods of Test for Concrete, Canadian Standards Association*, Toronto, Canada, 2000.
9. Allen Jr., C.L. & Brumfield, J.W., "Final report. ASR Benchmarking Workshop, August 2006", *Federal Highway Administration*, Washington D.C., USA, 2006.
10. Norwegian Concrete Association, NB, "Durable concrete containing alkali reactive aggregates", *NB Publication* No. 21, 1996, 32 p. including appendices. (In Norwegian).
11. *Norwegian Committee for Standardization*, NS-EN 206-1:2001, "Concrete Part 1: Specification, performance, production and conformity", (Amendment, in Norwegian, prA1:2003 incorporated), 2003, 90 p.
12. Lindgård, J. & Wigum, B.J., "Alkali Aggregate Reaction in Concrete – Field experiences", *SINTEF report* no. STF22 A02616, 2003, 127 p. + appendices. (In Norwegian).
13. Lindgård, J., Wigum, B.J., Haugen, M. & Skjølsvold, O., "Field experience from investigation of more than 100 Norwegian bridges with respect to Alkali Aggregate Reactions (AAR)", *Nordic Concrete Research*, No. 2/2004, pp. 114-128.
14. Lundevall, G., "Ressursvennlig Kvalitetsbetong, Bestandighet av betong, Alkalireaktivitet – Alkaligrenser", *Report 9D4/R97018 Norcem R&D*, Brevik, 1997, 16 p. + 4 appendices. (In Norwegian).
15. Bremseth, S.K., "Resultater av funksjonsprøving av alkalireaktiv sand, ikke-reaktiv stein og bindemiddel av CEM I og Norcem StdFA-sement", *Report 9D4/R05015, Norcem R&D*, Brevik, 2005, 9 p. (In Norwegian).
16. Bremseth, S.K., "Funksjonstest av betongprismer ifm ny FA fra Vliegasunie", *Report 9D4/R06031, Norcem R&D*, Brevik, 2006, 7 p. + 4 appendices. (In Norwegian).

17. Bremseth, S.K., ”Resultater ifm langtidsforsøk i felt, sjø og 38°C i prosjektet Ressursvennlig Kvalitetsbetong”, *Report 9D4/R08001, Norcem R&D,* Brevik, 2008, 10 p. + 8 appendices. (In Norwegian).
18. Kjellsen, K.O., Rønning, T.F. & Meland, I., “Prevention of Deleterious Alkali Aggregate reactions by use of Norwegian Portland fly Ash Cement”, paper to the *Workshop “Durability of Exposed Concrete Containing Secondary Cementitious Materials”*, Hirtshals Denmark, 2001, 10 p. + 2 appendices.
19. Pedersen, B., “Alkali-reactive and inert fillers in concrete. Rheology of fresh mixtures and expansive reactions”, *Doctoral Theses at NTNU* 2004:92, Trondheim, Norway, 2004, 198 p. + appendices.
20. Pedersen, B., “Effect of alkali-reactive crushed fillers on expansions due to ASR”, in: Tang, M. and Deng, M. (Eds.), *Proceedings of the 12th International Conference on Alkali–Aggregate Reaction in Concrete*, Beijing, China, vol. 2, 2004, pp. 764–772.
21. Lindgård, J., Nixon, P.J., Borchers, I., Schouenborg, B., Wigum, B.J., Haugen, M. & Åkesson, U., “The EU “PARTNER” Project — European standard tests to prevent alkali reactions in aggregates: Final results and recommendations”, *Cement and Concrete Research* 40, 2010, pp. 611-635.
22. Nixon, P. & Lane, S., “PARTNER Report No. 3.3: Experience from testing of the alkali reactivity of European aggregates according to several concrete prism test methods”, *SINTEF Report* SBF52 A06021/ISBN 82-14-04081-7/978-82-14-04081-7, Trondheim, Norway, 2006, 35 p. + appendices.
23. RILEM, “AAR-3 - Detection of potential alkali-reactivity of aggregates - Method for aggregate combinations using concrete prisms”, *Materials and Structures* 33, 2000, pp. 290-293.
24. *RILEM*, “AAR-4 - Detection of potential alkali-reactivity of aggregates: Accelerated (60°C) concrete prism test”, draft 2006 (not published).
25. *ASTM International*, C 1293 – 08b, “Standard Test Method for Determination of Length Change of Concrete Due to Alkali-Silica Reaction”, United States, 2008, 7 p.
26. *ISO* 5725-94, “Precision of test methods – determination of repeatability and reproducibility for a standard test method by inter-laboratory testing”, 1994.
27. Internal Norcem results (not published yet).
28. Gudmundssson, G., “Investigations on Icelandic pozzolans”, proceedings of the *Symposium on Alkali-Aggregate Reactions, preventive measures*, Reykjavik, Iceland, 1975.
29. Blanks, R.F. and Meissner, H.S., “The expansion test as a measure of alkali-aggregate reaction”, *Journal of the American Concrete Institute* 17 (5), 1946, pp. 517–539.
30. Bakker, R.F.M., “The influence of test specimen dimensions on the expansion of alkali reactive aggregate in concrete”, in: Idorn, G.M. and Rostam, S. (Eds.), *Proceedings of the 6th International Conference on Alkali-Aggregate Reaction in Concrete*, Denmark, 1983, pp. 369-375.
31. Bokern, J., ”Concrete tests for ASR assessment: Effects of testing environment on preconditions for an ASR and transferability of test results”, in: Broekmans, M.A.T.M. and Wigum, B.J. (Eds.), *Proceedings of the 13th International Conference on Alkali-Aggregate Reactions in Concrete,* Trondheim, Norway, 2008, pp. 511-520.
32. *Deutscher Ausschuss für Stahlbeton*, DAfStb (ed.), “Vorbeugende Maßnahmen gegen schädigende Alkalireaktion im Beton: Alkali-Richtlinie”, Beuth, Berlin, 2001, (DAfStb-Richtlinie).
33. Rivard, P., Bérubé, M.A., Ollivier, J.P. and Ballivy, G., “Decrease of pore solution alkalinity in concrete tested for alkali-silica reaction”, *Materials and Structures* 40, 2007, pp. 909–921.

Paper III

Alkali–silica reactions (ASR): Literature review on parameters influencing laboratory performance testing
J. Lindgård, Ö. Andiç-Çakır, I. Fernandes, T.F. Rønning, M.D.A. Thomas
Cement and Concrete Research, 42 (2012) pp. 223-243

Cement and Concrete Research 42 (2012) 223–243

Contents lists available at SciVerse ScienceDirect

Cement and Concrete Research

journal homepage: http://ees.elsevier.com/CEMCON/default.asp

Alkali–silica reactions (ASR): Literature review on parameters influencing laboratory performance testing

Jan Lindgård [a,]*, Özge Andiç-Çakır [b], Isabel Fernandes [c], Terje F. Rønning [e], Michael D.A. Thomas [d]

[a] SINTEF Building and Infrastructure, NO-7465 Trondheim, Norway
[b] Ege University, Faculty of Engineering, Civil Engineering Department, Bornova, Izmir, Turkey
[c] University of Porto, DGAOT/Centro de Geologia, Porto, Portugal
[d] University of New Brunswick, Department of Civil Engineering, Fredericton, Canada
[e] Norcem Heidelberg Cement, NO-3950 Brevik, Norway

ARTICLE INFO

Article history:
Received 2 June 2011
Accepted 10 October 2011

Keywords:
Alkali–Aggregate reaction (C)
Performance testing
Pore solution alkalinity
pH (A)
Humidity

ABSTRACT

Utilisation of potentially alkali–silica reactive aggregates requires reliable performance tests to evaluate the alkali–silica reactivity of various aggregate combinations, including their alkali threshold dependence on binder type. Several such performance tests have been used worldwide for more than 15 years, but none of the methods have proven to be reliable for use with all aggregate types and all binders. One of the objectives of RILEM TC 219-ACS (2007–2012) is to develop and validate one or more of such performance tests.

Several parameters may influence the results obtained in an accelerated performance test compared to the field behaviour. Based on a state of the art literature review, this paper discusses which parameters must be considered to be able to develop reliable ASR performance testing methods and provides some tentative recommendations. The internal humidity in the test specimens, the extent of alkali leaching and the storage temperature are of particular importance.

Contents

---

* Corresponding author. Tel.: +47 73 59 68 59; fax: +47 73 59 71 36.
E-mail address: jan.lindgard@sintef.no (J. Lindgård).

0008-8846/$ – see front matter © 2011 Elsevier Ltd. All rights reserved.
doi:10.1016/j.cemconres.2011.10.004

1. Introduction

1.1. Background

National regulations for preventing alkali–silica reaction (ASR) in concrete structures are based on various principles that have to take into account a range of material properties and local experience. In order to improve flexibility, extend material selection criteria and optimise concrete mix design, some countries have incorporated the option of performance testing in their provisions. Such options are meant partly to replace technically and commercially restrictive prescriptive requirements by performance-oriented requirements (see e.g. EN 206-1 [1]).

In order to identify a general international ASR performance based testing concept, one of the objectives of RILEM TC 219-ACS 'Alkali–aggregate reactions in Concrete Structures' (2007–2012) is to develop and validate one or more ASR performance tests. In order to maintain the relevance to field structures when testing in the laboratory, it is crucial that the basic conditions do not change to an extent where the correlation of performance ranking under the two different conditions is not maintained. Hence, performance testing in the present context is not about predicting an exact level of deterioration with the selected materials and design, but to determine a relative level of performance with the perception that test results conforming to certain acceptance criteria will assure acceptable field performance.

Setting up a performance test will require both theoretical considerations and practical verification. As a base for the work within RILEM TC 219-ACS a literature survey on influencing parameters has recently been completed [2]. The main objective of the review was to assess which parameters must be considered to be able to develop reliable performance testing methods, i.e. to identify parameters and limitations for accelerating ASR under elevated moisture and temperature conditions. These concerns will be taken into account by the RILEM committee, whereby identified challenges should be dealt with in one of the following ways:

- Research needs (i.e. the performance test will not cover the specific issue until further research has been accomplished).
- Experience based convention for agreed, unified approach.
- The phenomenon discussed can be dealt with within the level of the chosen safety margin.
- Scatter introduced by the specific or collective phenomena of concern can be determined by a precision test.

All authors of this paper are members of the "Performance testing" task group of RILEM TC 219-ACS.

1.2. Technical background

Several aggregate types in common use, particularly those with a siliceous composition, may be attacked by the alkaline pore fluid in concrete. This attack, essentially a dissolution reaction, requires a certain level of moisture and alkalis (leading to high pH) within the concrete to take place. During the reaction, a hygroscopic gel is produced. When imbibing water, the gel will swell and thus cause expansion, cracking, and in worst case disruption of the concrete. The deterioration mechanism is denoted alkali–aggregate reaction (AAR) or, more specifically, for siliceous aggregates, alkali–silica reaction (ASR). The less common, so-called alkali–carbonate reaction (ACR) is not discussed in this paper.

Since ASR was recognised as a durability challenge more than 70 years ago by Stanton [3], several comprehensive research projects have focused on test methods for determining the reactivity of aggregates and corresponding acceptance criteria. As part of the international harmonisation of such test methods, the main aim of RILEM TC 106-AAR (1998–2000) and RILEM TC 191-ARP (2001–2006) was to propose and validate test methods for classifying the alkali reactivity of concrete aggregates. The committees have proposed several RILEM aggregate test methods (AAR-1, 2003 [4]; AAR-2, 2000 [5]; AAR-3, 2000 [5]; AAR-4.1, 2006 [6]; AAR-5, 2005 [7]), in addition to recommendations for how to use these test methods and interpret the results (RILEM AAR-0, 2003 [8]) and how to ensure durable non-reactive concrete (RILEM AAR-7.1, 2008 [9]). All the draft RILEM methods have been developed further by RILEM TC 219-ACS (2007–2012) and are planned to be published in a special issue of Materials and Structure during 2012. In USA and Canada, corresponding ASTM and CSA test methods exist (ASTM C 1260-07 [10]; ASTM C1293-08b [11]; ASTM C 295-08 [12]; CSA A23.2-14A-04 [13]; CSA A23.2-25A-09 [14]; CSA A23.2-15A [15]).

In a concrete containing reactive aggregates the potential for a damaging alkali–silica reaction is to a great extent influenced by the composition of the concrete pore solution with its function as a reaction partner for the reactive silica and as a supplier of moisture. In particular the content of alkalis, i.e. sodium (Na^+) and potassium (K^+), in the concrete pore solution plays a major role for development of ASR. The main contributor of alkalis to the concrete pore solution is usually the cement. In the first place, more Na^+ and K^+ lead to dissolution of more hydroxyl ions (OH^-) from $Ca(OH)_2$ to maintain equilibrium with the increased alkali concentration. For high pH pore solutions and at 20 °C, $[Na^+]+[K^+]\approx[OH^-]$ because the quantity of other ions is insignificant compared to the concentration of alkali ions beyond the first 24 h ([16,17]). The pH of the pore solution will thus increase. This higher alkalinity again leads to dissolution of more reactive silica (SiO_2) from alkali–reactive aggregates. Secondly, alkalis will react with the dissolved silica (and calcium) forming alkali–silica gel [18]. As discussed further in Section 3.2.1, the alkali–silica reaction is very similar to pozzolanic reactions.

Thus, the degree of reaction of an aggregate is a function of the alkalinity of the pore solution. For a given aggregate, a critical lower pH-value exists below which the aggregate will not react. Consequently, ASR will be prevented by lowering pH of the pore solution beneath this critical level where the dissolution of alkali-reactive constituents (silica) in the aggregates will be strongly reduced or even prevented, as discussed by Böhm and Baetzner [19]. This pH-value corresponds to a certain alkali threshold that several have reported to exist for initiating and sustaining ASR in concrete [20]. No "absolute" limit is defined, because the critical alkali content largely depends on the aggregate reactivity [21]. For most alkali-reactive aggregates, the alkali threshold when applying CEM I cements in 38 °C concrete prism tests (CPTs) is in the range 3–5 kg Na_2O_{eq} per m^3 concrete, but may be lower for some rapidly reactive aggregates. However, due to alkali leaching (see Section 5.4.1) from laboratory exposed samples, the true field alkali threshold may be significantly lower than the limit measured in the laboratory. The majority of existing concrete prism tests apply alkali contents in the range of 5.0–5.5 kg Na_2O_{eq} per m^3 when testing the alkali reactivity of aggregates. If the alkalinity is changed during the test, the expansion of the concrete prisms will be influenced.

Internationally, various ways of controlling ASR are suggested (in addition to use of non-reactive aggregates): utilization of low-alkali cement, limiting the alkali content of the concrete, incorporation of supplementary cementitious materials (SCMs; e.g. silica fume, fly ash, ground granulated blastfurnace slag (ggbs), metakaolin) or use of lithium salts. SCMs control expansion due to ASR by binding alkalis and limiting their availability for reaction with alkali–silica reactive aggregates [22]. The efficiency of the SCMs depends on their composition. Consequently, to be able to utilise alkali–silica reactive aggregates for production of durable concretes, the effects of various measures must correctly be identified by accelerated performance tests (or alternatively by relevant long term field experience). Several such of accelerated laboratory performance tests have been used worldwide for at least 15 years, mainly to evaluate various SCMs and lithium salts (e.g. ASTM C-1293-08b [11] and the Norwegian CPT [23]). In principle two groups of performance test methods exist, one using mortar bars and the other using concrete prisms. However, the test conditions (e.g. temperature, alkali content, humidity) used within these two groups might vary widely from one test method to another. Thus, the results/conclusions from different test methods may vary.

In 2006, Thomas et al. [24] provided a critical evaluation of different test methods. The authors concluded that none of the currently available or commonly used test methods meet all the criteria for an ideal performance test. For example, the main shortcoming of the Canadian 38 °C concrete prism test (CPT) [13] is the duration of the test (2 years) and that the addition of alkalis is required to compensate for alkali leaching effects, i.e. the fact that alkalis are leached out of the prisms during exposure in the humid environment (see Section 5.4.1). Thus, the authors concluded that the method cannot be used to determine the "critical" alkali content for an alkali–reactive aggregate, nor determine how the minimum level of a SCM changes with the concrete alkali content. Thus, research is going on in many countries with the aim to improve current test methods and develop alternative tests.

1.2.1. Main challenges

The development of accurate and reliable performance tests for the production of durable concretes is a challenge. Several requirements must be fulfilled, some being somewhat contradictory. On the one hand the test methods should be inexpensive and rapid, calling for extremely accelerated test conditions. On the other hand a performance test should mirror the field performance of the actual concrete for more than 50 years lifetime. Another important requirement is the possibility to test job mixes with identical aggregate and concrete composition that will be used on actual projects. Use of mortar bars is in conflict with this latter requirement.

According to Thomas et al. [24], other important requirements for an ideal performance test for ASR are:

- The test should be capable of evaluating the "critical" alkali contents, i.e. the alkali leaching problem must be solved to avoid the need for a boosted alkali level.
- The test should be capable of assessing all types of SCMs, lithium compounds and combinations of SCM and lithium, with cements of different alkali level.

1.2.2. Crucial parameters to ensure a good laboratory/field correlation

As stated by Thomas et al. [24], the only suitable benchmarking of a laboratory performance test is against real concrete structures (if available) or, as a surrogate, against large concrete blocks exposed outdoors and exposed to natural weathering conditions. However, such long-term field experience is available only for a limited number of commercial SCMs, e.g. some class F fly ashes and some slag cements. When developing an accelerated performance test, it is thus crucial theoretically to evaluate fundamental questions in order to ensure a satisfactory laboratory/field correlation. Consequently, the main focus needs to be put on the three parameters known to have the primary influence on the rate and extent of alkali–silica reactions (for a given alkali–reactive aggregate type). These are ([25,26]):

- Humidity
- Alkali content ("controls" the concentration of OH^- in the pore solution)

- Temperature

Additionally, other parameters may influence the laboratory/field correlation, for instance by affecting the humidity or the alkali content of the test samples. This is further discussed in the paper (see Section 1.3).

1.3. Assessment of influencing parameters

The main objective of the comprehensive literature review performed within the task group "Performance testing" in RILEM TC 219-ACS, where 12 authors contributed to the report that included about 250 references [2], was to assess how various parameters might influence the laboratory/field correlation with respect to ASR performance testing, either directly or indirectly. More exactly the aim was to evaluate how various aggregate and binder types, the mix design and the laboratory exposure conditions might influence the following important ASR related parameters and thus the laboratory/field correlation:

- Internal humidity of the concrete prisms.
- Composition of the concrete pore solution during testing.
- Properties of hydration products formed during hydration/exposure.
- Aggregate reactivity.
- Type and properties of reaction products, i.e. primarily ASR-gel, formed during exposure.

This paper summarises the main findings in the literature survey. Firstly, precautions when testing various aggregates types (Section 2) and binder types (Section 3) are discussed. Secondly, any influences of mix design parameters (e.g. water-to-cementing-materials ratio (w/cm ratio) and type of any chemical admixtures added) are assessed (Section 4). The last part of the paper (Section 5) evaluates the influence of exposure conditions on ASR expansion, i.e. pre-curing conditions and storage conditions (incl. addition of any external alkalis). In the concluding part (Section 6), the authors have given some recommendations for what is considered the best approach for performance testing. Finally, some important issues needing further research are summarised (Section 7).

2. Aggregate type

Since the alkali–silica reaction was first identified, a great number of rock types have been classified as potentially reactive. There is evidence that apparently similar rock types can vary greatly in reactivity in practice depending on their geological history and geographical location. For several rock types, there are reactive and non-reactive varieties according to differences in the detailed mineralogical composition or texture [4]. There are two generalised classes of siliceous minerals that are known to be expansively reactive with the alkalis in concrete: the metastable types of silica (opal, chalcedony, tridymite, cristobalite) including some disordered forms of quartz, and alumina–silicate glasses mainly in the matrix of intermediate to acid volcanic rocks [27]. Although the classification has a strong regional component, there are minerals and rock types containing minerals generally considered as potentially reactive. Lists are present in literature and usually on standards (e.g. ASTM C294-05 [28]; CSA A23.2-15A [15]; BS 7943, 1999 [29]; RILEM AAR-1, 2003 [4]).

The first step in the assessment of potential alkali reactivity should be the petrographic characterization of the rock types in thin sections under optical microscope ([30,31,32]). In RILEM AAR-1 [4], the list of potentially reactive rock types includes the reference to the countries where deleterious reaction was recognised with each rock. It has been verified that the generic classification of a rock type is not reliable in respect of alkali reactivity. Due to different geological histories, a rock type might be innocuous in one country or region and reactive in another, and therefore the final classification based on the petrographic assessment must follow national or regional experience. The petrographic examination, based on the RILEM AAR-1 [4], allows that an aggregate is classified as very unlikely to be alkali-reactive (Class I), alkali-reactivity uncertain (Class II) or very likely to be alkali-reactive (Class III). The petrographic examination is therefore usually followed by laboratory tests performed on mortars or concretes in order to confirm the results obtained.

2.1. Dissolution of silica

Silica is a material which dissolves in strongly acidic or alkaline conditions, and less around neutral pH. The laboratory tests for evaluating the potential reactivity of siliceous aggregates are based on the concept that the free energy of quartz, which determines its solubility, is related to the amount of defects in the lattice and degree of crystallinity [33]. Under ambient conditions, fine-grained amorphous silica dissolves much easier in high-pH solvents than crystalline quartz [34]. The alkali reactivity is affected by a number of factors and is related with the qualities of quartz from different geological environments [35]; e.g. deformed quartz is confirmed to be highly reactive owing to distorted crystal structure and small grain size due to increased surface area.

The presence of alkalis influences the reactivity of aggregates and the extent of the reaction. Therefore, for a specific aggregate, more alkalis available means more expansion, due to a higher concentration of OH^- in the concrete pore solution and thus more silica dissolved. Fournier et al. [36] have shown that "non-reactive" sands can have components which are activated by high alkali content.

2.2. Aggregate properties

2.2.1. Mineralogy

The rate at which the rocks containing potentially reactive forms of silica react is variable. In consequence of the results obtained by laboratory tests as well as from field performance, the aggregates might be classified regarding alkali-reactivity as "fast" to "normal" reactive (5 to 20 years), "slow/late" reactive (+15 to 20 years) and "non-reactive" [37]. The terms "highly" or "rapidly" reactive and "low" reactive are also frequently used in the literature. Rocks containing opal are examples of rapidly reactive aggregates for which the accelerated laboratory tests usually give reliable results. By contrast, there are rocks containing strained quartz with strain lamellae for which the field performance shows the occurrence of ASR after some decades and for which some of the laboratory tests (e.g. RILEM AAR-2 [5]) might be ineffective ([38,39]). The reverse may happen with non-reactive aggregates, which may be classified as reactive because the conditions in the test are too severe for some types of aggregates ([30,39]). Ideker et al. [40] and Shayan et al. [39] verified that tests performed with different "non-reactive" natural sands mixed with the same coarse reactive aggregate show different results depending on the test method applied. Also the variation between laboratories was high.

2.2.2. Other aggregate properties

The mineralogy is, however, not the only parameter to consider in the potential reactivity of a rock type. Increased permeability of aggregates with higher porosity may enhance the alkali reactivity, due to easier access to concrete pore fluids ([27,41]). Wenk et al. [42] tested a deformed granitic rock and concluded there is a relationship between the aggregate microstructure and the mortar expansion due to grain size reduction, development of foliation in the rock and dislocation density of quartz, confirming former findings by other authors ([43,44]).

2.2.3. Pessimum

Laboratory tests performed with different types of aggregates have shown that there is not always a linear relationship between the content of potentially reactive constituents and the measured prism expansions. A maximum level of expansion might occur at a particular content of the reactive constituent known as the ‘pessimum’. Decreasing levels of expansion will develop for contents of the reactive constituents above or below the pessimum ([45,25,46,47,33,48,4]). Expansion increases with an increase in the amount of reactive constituents up to the pessimum, beyond which it decreases due to the lack of alkalis available for the formation of expansive gel [49]. The pessimum may differ for differing potentially reactive constituents. For fast reactive aggregates, such as those containing opal, maximum expansion occurs for low contents of reactive silica ([49,50]), usually below 10%, whilst for slowly reactive aggregates the percentage will be much higher, even up to 100% (i.e. they do not show a pessimum effect).

The implication when dealing with aggregates showing a possible pessimum is that several concrete mixes have to be performed with different percentages of reactive constituents in order to document the pessimum. It is also important to be able to evaluate such aggregates in a performance test.

Use of a sufficient amount of SCMs has shown to be effective to prevent development of ASR in concrete with aggregates showing a pessimum. However, Buck and Mather [51] showed that some fly ashes when used at a too low replacement level actually caused more expansion, especially with low-alkali cement. They believed it was caused by the additional water-soluble alkalis provided by the fly ash to the system.

2.2.4. ASR gel composition

The chemical composition and the texture of alkali– silica gel have been studied by a number of researchers and it is recognised that it varies widely with time and with the location in the concrete. These results are based mainly in qualitative analyses carried out by SEM/EDS ([52,53,54,55,56,57]), and show that gel has high and varying contents of silica, lower and varying contents of calcium and low and relatively constant contents of alkalis, in agreement with other workers ([58,59]). If not extremely low in total alkali content, the K_2O/Na_2O ratio of the cement clinker is normally in the range of 1 (unusually low) to 3, which may be reflected in the gel composition. Any addition of Na_2O or K_2O into the concrete mixture for accelerating the reaction [60] or exposure to external alkalis, e.g. from de-icing salts, seawater or in laboratory tests, may also affect this ratio and also the relative content of calcium and alkalis [59].

The formation of ASR products depends on the nature, texture and composition of the aggregate [61], and on whether the aggregate is slowly reactive, rapidly reactive or showing pessimum content [62]. However, the composition of gel seems not to be dependent on the nature of aggregates. Gel with varied composition regarding the Ca content was identified in the same sample, with different composition from one grain to another and also in the same grain ([53,54,63,64]). Calcium content is more prevalent in cracks found in the cement paste [52] than inside aggregates, developing a reverse trend to that of silicon. In cracks, Ca-rich gel is found at larger distance from the coarse aggregates, due to exchanges of alkalis with Ca in the cement paste. It has been verified that expansion does not necessarily increase proportionally to the reaction degree or the amount of gel produced, but it seems to be dependent on Ca content ([52,56,65]).

2.3. Grading and size

The influence of aggregate grading on mortar bar or concrete prism expansion has been studied since Stanton [3] in 1940 concluded that the aggregate particles (siliceous magnesium limestone containing opal and chalcedony) in the 170–600 μm range yielded greater expansion than coarser sizes. Diamond and Thaulow [62] tested opal aggregates in the range of 20– 125 μm, and found that the smaller fractions expanded faster than the coarser material, which needed a prolonged exposure, but the total expansions were of the same order. Lu et al. [66] state that within a certain size range, the finer the aggregate particles of argillaceous dolomite limestone, the faster and higher the alkali– silica reaction rate and the expansion.

However, Multon et al. [67] state that the aggregate size causing the highest ASR expansion is dependent on the nature and composition of the aggregate. For rapidly reactive aggregates, it was found that the amount of soluble silica was similar for different particle sizes of a certain aggregate, but the expansion varied for different size fractions, being larger for coarser particles [68]. In an apparently contradictory finding, Zhang et al. [69] concluded that for siliceous aggregates the smaller the particle size, the greater the ASR expansion when aggregate size is within the range of 0.15– 10 mm. They also state that the aggregate grading can affect the expansion of ASR: when there are larger aggregates in the specimen, the expansion is smaller at early ages, but will increase continuously at later ages. Hobbs and Gutteridge [70] concluded that for opaline rocks, expansion increases as the particle size decreases, when the reaction occurs at the surface of the particles. However, when the reaction occurs within the particle, the rate of gel formation will be independent of the particle size.

Barisone and Restivo [71] and Lu et al. [72] showed that the use of very fine aggregates can destroy the original microstructure characteristic of the rocks, and thus under-estimating the alkali reactivity of the rocks in accelerated mortar bar tests (e.g. RILEM AAR-2 [5]).

Wigum and Lindgård [73] state that slowly reactive Norwegian coarse aggregates have proven to be more harmful in the field than fine aggregates. This has been accounted for in the Norwegian regulations [74] by differentiating the critical limits in the Petrographic method and the accelerated mortar bar test [23].

Another parameter to consider, although there is limited literature on the subject, is the shape of the particles. Ramyar et al. [75] found that the angularity of the particles had an effect on the mortar bar expansion for intermediate size fractions, and that the effect of size of the particles was more pronounced in crushed aggregate when compared to rounded gravels of the same aggregate type. Work developed in the UK [60] showed that some greywacke aggregates can give rise to cracking at lower alkali levels than occurs with other aggregates. Therefore, aggregates and aggregate combinations which contain crushed greywacke or crushed greywacke-type aggregates have been classified as highly reactive whilst natural gravel aggregates are considered as having “normal” reactivity.

The accelerated mortar bar test failed to detect the reactivity of glass aggregates at 14-days [76], but the expansions were rising suddenly after an initiation period. This behaviour was not observed in concrete prism tests. The effect is probably due to increased pozzolanicity of filler-sized fine particles at high temperatures during the early testing period. Pedersen [77] also detected that some reactive aggregates showed a similar pozzolanic behaviour when ground to filler size.

The implication to reliably test the ASR performance of aggregates, including size effects, is that the fractions used in structures should preferably also be used in the laboratory tests. It should also be kept in mind that, crushing certain types of aggregates for laboratory testing may change some of their characteristics.

2.4. Alkali release

Some aggregate types containing certain minerals, e.g. micas, clay minerals, alkali feldspars, zeolites and volcanic glass may gradually release significant quantities of alkalis, i.e. sodium (Na^+) and potassium ($K+$), to the concrete pore water ([78,79,80,81,82]). Temperature has an influence on the extraction of alkalis, as concluded by Lu et al. [83], which varies with the type of rocks as well as with the fineness of the rock particles and the type of solution. Wang et al. [84] report that the factors that influence the maximum alkali release include the types of alkali minerals, the pore solution/aggregate ratio, the pH and the type of alkali ions in pore solution from sources other than the alkaline minerals.

Bérubé et al. [80] tested the extent of alkali release for 17 aggregate types from Canada. Most of these aggregates contributed alkalis in the range 0.45 to 0.70 kg Na_2O_{eq} per m^3 of concrete, but the amount varied from about 0.1 to 1.6 kg Na_2O_{eq} alkalis per m^3 of concrete dependent on the aggregate type.

The most common tests to evaluate alkali release are based on the immersion of alkali-bearing aggregates in alkaline solutions such as of calcium hydroxide, potassium hydroxide and sodium hydroxide ([85,86,87,81]), whilst the hot-water extraction method uses distilled water [87]. In Bérubé et al. [81] a summary is presented of the procedures used by different authors to evaluate the alkali contribution by aggregates. The task group “Releasable alkalis” in RILEM TC 219-ACS is presently developing a reliable test procedure to measure the extent of alkali release from various aggregate types, including corresponding interpretation criteria.

2.5. Lightweight aggregates (LWA)

Lightweight aggregates (LWAs) have been used in several important structures, e.g. in some bridges and oil platforms. Most of these LWAs contain silica, often in a poorly crystalline, glassy condition, making them potentially alkali-reactive. In tests performed at SINTEF, four commonly used LWAs have also developed ASR in the ultra accelerated mortar bar test [5]. However, there is a gap in knowledge internationally whether these and other LWAs may give deleterious ASR in real structures. In a review in 2000, no cases of ASR were found in LWAC [88]. However, instances of ASR in LWAC have later been reported in Japan (PC girders of a bridge and PC sleepers) by Matsuda et al. [89]. There are no international agreed requirements regarding how to test and evaluate the alkali reactivity of a LWA or a LWA Concrete (LWAC). Even though some ASR test methods allow testing of LWAs (e.g. ASTM C-1293-08b [11], where the LWA concrete mixes are designed on a volume basis which is necessary for such low-density aggregates), the interpretation criteria may be questioned. The main reason for this is that most test methods for ASR apply only expansion criteria, which cannot be applied uncritically for LWA, since experiences show that the ASR gel (if developed) initially accumulates in voids in the LWAs and primarily contributes to a weight increase but only a moderate length increase. After the gel has accumulated in and partly filled the voids in the LWAs, the rate of expansion might increase [90]. More research is therefore needed to be able to develop suitable laboratory test procedures and corresponding acceptance criteria for LWA and LWAC. The acceptance criteria should include evaluation of the measured weight increase (since an increased weight of the LWAC may alter structural design parameters), and they also need to be correlated with long time field experiences with use of LWAC in various concrete structures.

3. Binder type

Type and amount of various binders (i.e. different cements and SCMs) significantly affect the concrete pore solution alkalinity. The concentration of Na^+, K^+ and OH^- is dependent on the quantity of sodium and potassium compounds in the anhydrous Portland cement clinker and in the supplementary cementitious materials (SCMs). Any significant change in the pore solution composition caused by a change in the binder type and composition is discussed in this section. Any other contributors of alkalis, e.g. any chemical admixtures (alkali boosting), de-icing salts or any alkalis released from aggregates, are discussed in other sections in the paper.

3.1. CEM I-type of clinker

When Portland cement is mixed with water, the alkali sulphates go rapidly into the liquid phase converting to alkali hydroxides, thus increasing the hydroxyl ion concentration. Alkalis locked into the crystal structures of clinker minerals become available as the hydration proceeds [26]. Consequently, the alkali release rate varies from one cement type to another, depending on the distribution of alkalis between rapid-release and slow-release sources, and on the total alkali content in the cement. Since alkali–aggregate reaction proceeds slowly under site exposure conditions, it is possible that most of the cement alkalis are released for reaction at a constant time. Under accelerated conditions in a laboratory performance test, it is important to ensure a rate of alkali release from the binder (more important for blended cements) corresponding to that in the field.

From early mortar bar studies, Hobbs [25] stated that considerably varying expansion results observed for mortars with various cements but with similar total alkali contents (kg/m^3) might be attributed to different alkali release rates of cements, variations in sodium/potassium ratio and different rates of strength development.

In order to assess the total content of available alkalis present in cement or concrete, it has become standard practice to express the alkali content in terms of “sodium oxide equivalent”: $Na_2O_{eq} = Na_2O + 0.658\ K_2O$ (in weight percent). Leemann and Lothenbach ([91,92]) stated that concrete mixtures produced with cements having similar Na_2O_{eq} but different K/Na ratios can expand considerably differently in accelerated laboratory tests. However, there are also contradictory findings in the literature [93]. Hou et al. [94] stated that K and Na ions behave similarly in the ASR reaction, but the rate of reaction is higher with K than with Na. In contrast, Borchers and Műller [95] found that Na produced a higher reaction rate in laboratory tests compared to K. Considering these, it is possible to obtain misleading conclusions if two cements having equal sodium oxide equivalent but extreme variations of Na_2O and K_2O levels are assumed to act similarly in a performance test. In other words, if one CEM I cement is used in a performance test in order to determine the critical alkali limit for the aggregate in question, the test result will not necessarily be valid for all types of CEM I cements.

Within the cement paste, the ASR gel becomes richer in calcium with time, releasing alkalis to the pore water ([96,97,98]). This alkali recycling during ASR reveals that the reaction may theoretically continue until all the reactive silica is transformed into alkali–silica gel. The swelling capacity of ASR gel is also related to the calcium ions present in the ASR gel, which depends on the amount of Ca^{2+} available in the pore solution. The latter varies with the type of binder used. It is also known that the process of ASR reduces the alkalinity of pore solution by binding some alkalis in the alkali–silica gel [99]. Then the question arises as to how the time-dependent alkali recycling phenomenon might affect the concrete performance during its service life?

In hardened concrete, the alkalis supplied by the binder (i.e. the cement or any SCM incorporated) may be dissolved in the pore solution, bound by the hydration products or adsorbed either by aggregates or the ASR gel in different amounts [20]. At a given age, the presence of alkalis still bound in unhydrated binders (important especially for SCMs that release alkalis slowly into the system) and the availability of alkalis from alkali releasing aggregates should also be considered.

The type of cement and the type and amount of any SCMs incorporated alter the permeability of concrete, thereby influencing water uptake, leaching of alkalis, the resistivity to drying during exposure and the extent of self-desiccation. This should be taken into account while testing the concrete performance, because field structures might be less affected from some of these parameters when compared with laboratory samples. Consequently, the paper also discusses these parameters comprehensively.

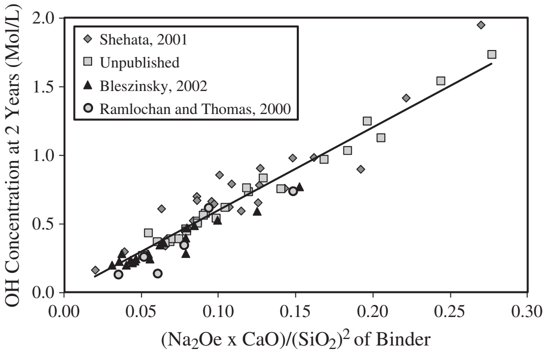

Fig. 1. Relationship between pore solution composition and the chemical composition of the binder ([108,109,100,101,22]).

3.2. Supplementary cementitious materials (SCMs)

3.2.1. Role of SCMs in prevention of ASR

SCMs are known to control ASR expansion mainly by their capability to reduce the alkalinity of the pore solution by binding alkalis in the hydration products. The SCMs that are low in calcium and high in silica are most effective in reducing pore solution alkalinity, thereby ASR expansions. As summarised by Thomas et al. ([100,101]), after the analysis of extracted pore solutions from 79 cement pastes of different binders, a direct linear relationship between the OH^- concentration of the pore solution and the “chemical index” $(Na_2O_{eq} \times CaO)/(SiO_2)^2$ of the binders (Fig. 1) were observed after 2 years of exposure. In other words, SCMs with a high (reactive) silica content and a low amount of CaO and alkalis will be the most effective in terms of lowering the pore solution alkalinity and preventing expansion due to ASR. Since the alkali reactivity of various aggregates varies greatly, no general “safe” lower concentration of hydroxyl ions in the pore solution can be stated. However, in the literature this limit is reported by several authors to lie in the range of 200–300 mmol/l ([102,103,104,20,105,24,106]). These OH^- concentrations correspond to pH-values in the range of approximately 13.3–13.5. There is also evidence that alumina might play in important role in the alkali binding capacity of SCMs [107].

However, the empirical relationship between the 2 years expansion of 132 concrete mixes tested in accordance with ASTM C-1293-08b [11] revealed a different chemical index $[(Na_2O_{eq})^{0.33} \times CaO]/(SiO_2)^2$, see Fig. 2 [22], compared with the empirical relationship derived from the pore solution analyses. The cementing materials used to produce these concretes were the same as those used for the pore solution study discussed above. The reactive coarse aggregate was siliceous limestone (Spratt). According to Thomas [22], the relationship is likely quite different if a different reactive aggregate or, even, a different test method is used. When comparing the two chemical indices, the author concludes that the alkali content of the binder appears to play a less important role in expansions when compared with the pore solution composition owing to leaching of alkalis during the concrete prism test (while no alkali leaching occurred for the cement pastes stored separately in sealed bottles) and this may reduce the apparent importance of the initial alkali content. This effect can be observed when looking at the expansion data for the concrete mixes produced with low-alkali cement. The expansion is lower than that expected based on the chemical composition. However, it is known that the concrete prism test will likely underestimate the expansion with low-alkali cement because of alkali leaching [24].

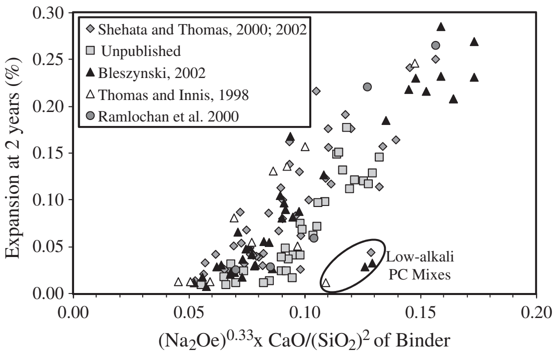

Fig. 2. Effect of binder composition on the expansion of concrete containing siliceous limestone ([110,111,108,112,109,100,22]).

Duchesne and Bérubé [113] state that the mean Ca/Si molar ratio ($=CaO/SiO_2$ ratio $=$ C/S ratio) of non-blended samples was 2.0, while this value ranged between 1.24 and 1.46 for blended types independent on the type of SCM. The reduction of pH of the pore solution is mainly attributed to the incorporation of alkalis by low Ca/Si hydration products in the presence of SCMs.

In addition to these main effects, when SCMs are used partially to replace the Portland cement, there is a dilution of the alkalis available from the clinker, a lower rate of alkali release, a decrease in the pH of the pore solution owing to the reduction of $Ca(OH)_2$ in the paste, restricted ingress of water into the concrete caused by reduced permeability and an increase in the resistance to cracking by increasing the strength of concrete [26]. The decreased permeability will also decrease the ion mobility and thus possibly reduce the rate of ASR. Finally, the extent of self-desiccation might also be increased by incorporating SCMs, resulting in a lowered internal RH in the test prisms (unpublished results from Jan Lindgård's PhD study (2007–2012) at NTNU). Thus, at a constant testing temperature, the type, amount and fineness of SCMs and reactivity of aggregates are among the most important factors that control pore solution alkalinity and consequent ASR expansions.

Some authors revealed that ASR is very similar to pozzolanic reactions, pozzolanic reactions proceeding before ASR ([114,94,22]). The reactive silica present in finely-divided SCMs reacts rapidly with the alkali hydroxides in the pore solution forming an alkali–silica gel containing small amounts of calcium. Over time calcium exchanges for alkalis in the gel and the resulting gel will have relatively low Ca/Si ratio when compared with that formed in Portland cement paste. The main difference between the pozzolanic reaction and ASR is not only the characteristics of resulting products (C–S–H formed by the pozzolanic reaction is rigid, whereas ASR gel can imbibe water and swell), but also (owing to the fineness of SCMs) that the products formed through the pozzolanic reaction are homogenously distributed throughout the binder paste instead of accumulating around the weaker Interfacial Transition Zones (ITZ) or cracks within the aggregate as is the case of ASR.

This is mostly important when testing the performance of binders by exposing mortars or concretes to high temperatures; the acceleration of the pozzolanic reaction and ASR might not be at the same level. At high temperatures, the pore structure at early stage is altered, the capillary porosity is decreased and the transport of alkalis and water to the reaction sites is thus hindered. Mortar bar tests also show that, at a given age, the fineness of SCMs affects ASR expansion ([115,116]). These results may be attributed to the acceleration of pozzolanic reactions by increasing SCM fineness. At high temperatures, finer SCMs will react even faster. Thus, in a performance test method the pozzolanic reaction and the ASR should preferably be accelerated to the same extent.

3.2.2. Fly ash (FA)

In FA-containing binders, the alkali fixation in the resulting reaction products starts at the same time as the pozzolanic reaction, i.e.

after a period of approximately 28 days, which results in a successive reduction of the dissolved alkali content. Low-CaO FA reduces the pore solution alkalinity beyond just dilution [117]. Due to the pozzolanic reaction, the C–S–H phases are low in calcium, i.e. they have a low CaO/SiO_2 ratio, and have thus a high alkali binding capacity. The fly ashes that were found to be most effective in reducing the alkalinity of the pore solution expressed from paste samples were also found to be the best for controlling ASR expansion [118].

Sibbick and Page [119] stated that the effectiveness of the FAs in suppression of ASR was dependent on the initial alkali content of the mix and on the alkali content of the FA, but the results of pore solution analysis did not provide a simple explanation for the corresponding expansion data showing that the differences in expansions cannot *only* be explained by changes in the pore solution chemistry. Thomas et al. [120], following an overall survey, differentiate with respect to quality parameters of the SCM: limiting the total alkali content of the ggbs and fly ash to 1.0% and 4.5%, respectively (and some additional limitations), the alkali contribution from the SCM may be assumed to be zero, in spite of some contradicting laboratory conditions test results.

Shayan et al. [121] investigated the long-term results of concrete prisms at various alkali levels. It was shown that the two Australian fly ashes studied were effective in preventing deleterious ASR damage in concretes with alkali contents as high as 7.0 kg Na_2O_{eq}/m^3, but they produced only a delaying effect (up to two and six years depending on the type of aggregate) in concretes containing extreme amounts of alkalis; 12.5 kg Na_2O_{eq}/m^3. These results indicate that the effectiveness of fly ashes is dependent on the alkalinity of the mixtures as well as the type of the aggregates.

Exposure site studies up to 16–18 years [122] show that fly ash used at replacement levels of 25% and 40% was effective in significantly reducing expansion and cracking with all three flint aggregates at all alkali levels. The authors state that there is no evidence of alkali contribution by the fly ash. It was also indicated that the laboratory concrete prism test expansions did not confirm the field performance of blocks from the same mix. Significantly greater levels of alkalis are required to produce expansion in laboratory-stored concrete prisms compared with field-exposed blocks. Thus, the suitability of present performance tests is questionable due to alkali-leaching problems.

3.2.3. Silica fume (SF)

Being a highly effective pozzolanic material, silica fume (SF) is among the most efficient SCMs for reducing ASR expansions even when used at rather low replacement levels (8–10%). However, the quantity of silica fume needed to prevent ASR is dependent on the aggregate reactivity. Depending on the level of replacement, silica fume decreases the Na^+, K^+ and OH^- ion concentrations in the pore solutions of cement pastes and concretes due to binding of alkalis. Silica fume inclusion thus increases the Na^+ and K^+ content of C–S–H of the hydrated cement paste [123].

Silica fume rapidly binds alkalis probably due to a reaction very similar to ASR [111]. Thus, the alkali concentration in the pore solution decreases within the first two days of hydration [117]. The alkali–silica gel at the border of the silica grain reacts with available calcium to form C–S–H phases that have a low Ca/Si ratio. Most alkalis are bound by the alkali–silica gel in the silica fume particles and low-calcium C–S–H phases. At later ages the alkali–silica gel reacts with calcium, and alkalis will be released into the pore solution and increase the alkalinity of the pore solution after 28 days up to 2 or 3 years [111]. Alkali recycling starts after a fixation phase, at least part of the alkalis eventually become available for alkali–silica reaction.

As a consequence, performance testing of silica fume containing concretes need a prolonged testing time in order to detect the possible increased alkali level with time. However, a challenge is that more alkalis will be leached out of the test prisms with time, reducing the alkali level in the concrete pore solution. Due to its extreme fineness, the pozzolanic reaction rate of silica fume is higher than that of other SCMs (e.g. fly ash).

3.2.4. Ground granulated blastfurnace slag (ggbs)

Similar to other SCMs, hydration products of slag (ggbs)-incorporating cementitious systems have decreased Ca/Si ratios, ranging between 1.55 and 1.79 [114]. The extent of alkali release is much less than that of clinker, and is almost independent of the alkali content of the ggbs. The alkalinity of the pore solution of ggbs containing cements is mainly attributed to the reduced clinker content of the cement. In cements with ggbs, alkalis are mainly absorbed by the C–S–H phases. Up to 40% ggbs, the Ca/Si ratio of the C–S–H phases and therefore the sorption properties are similar to that of OPC [117].

Arano and Kawamura [124] stated that at the early stages of ASR, the amount and composition of the gel produced does not seem to be affected by ggbs addition; however, decreased expansions may be due to the decreased mobility of ions and reduced OH^- concentration of the pore solution. Hester et al. [125] observed that 50% replacement of Portland cement with ggbs significantly reduced the expansion of concrete in laboratory expansion tests. The authors indicate that the alkali level of the ggbs was not a contributory factor at this replacement level.

However, Zhao et al. [126] analysed the pore solution chemistry of mortar samples and suggest that the effect of ggbs is to produce a delaying effect by changing the gel composition for a temporary period.

Bleszynski et al. [127] investigated the ASR performance of ternary and binary mixtures incorporating ggbs by using concrete prism test and outdoor exposure site studies. Binary mixtures contained 35% and 50% ggbs replaced with Portland cement, respectively. Concrete prism tests revealed that the mixtures with blastfurnace slag were also capable of limiting expansion to below the CSA threshold 0.04% at 2 years. However, at a replacement level of 35%, the prisms still showed an increasing expansion trend beyond two years. A ternary blend mixture (3.8% SF and 25% ggbs) showed the most effective measure against ASR expansion in field studies.

Studies on the mechanism of ggbs in reducing ASR expansions are still far from elucidating the role of slag in controlling ASR expansion. Regardless, numerous field and laboratory studies confirm the efficiency of ggbs in elimination damaging expansion at replacement levels of 50% or more.

3.2.5. Other SCMs

Some other SCMs have been found to be effective in reducing ASR expansions, e.g. metakaolin and other calcined clays, rice husk ash, zeolites and siliceous fillers. Incorporation of 20% metakaolin was found significantly to reduce the long-term OH^-, Na^+, and K^+ ion concentrations in pore solutions [109]. Burned and ground rice husk ash becomes quite pozzolanic (similar to microsilica), owing to its amorphous silica content and high surface area. The pozzolanic reaction depletes the CH content of tricalcium silicate pastes to about 1% at 28 days, and the hydration product C–S–H has Ca/Si ratio of about 1.3 [128]. Zeolites are found to be effective in reducing the alkali–aggregate reactions. Naiqian and Tingyu [129] explain the effectiveness of zeolites in reducing ASR as the decrease of pore solution alkalinity in concrete through ion exchange and pozzolanic reaction.

Pozzolanic behaviour of certain rock fillers may also mitigate the alkali–silica reaction, as discussed by Pedersen [77] and Pedersen et al. [130]. Examples of highly reactive materials being very effective pozzolans when crushed down to fines (finer than 63 μm) are Icelandic rhyolite and crushed bottle glass. These materials have a distinct amorphous silica phase. Fines from slowly reactive materials, such as Norwegian cataclasite and mylonite are not pozzolanic at normal curing temperatures, because the silica phase in these slowly reactive materials is well crystalline.

4. Mix design

4.1. Water/binder ratio

4.1.1. Pore solution alkalinity

By decreasing w/cm ratio the hydration products tend to become more homogeneous and contain less crystalline hydrates, particularly portlandite. At very low w/cm ratios, some of the portlandite may occur in nanometre dimensions rather than in well-crystallised form ([131,132]). Decreased w/cm ratio will lead to increased OH^- concentration in the pore solution and vice versa [133]. With decreasing w/cm ratio, the pH increases and thus the dissolution of silica increases. Additionally, the release of alkalis from aggregates increases due to the increased solubility of alkali-minerals at high pH. On the other hand, in a dense paste (low w/cm ratio), transport and ingress of water or solutions, respectively, is reduced as well as the release of alkalis from aggregates [84].

4.1.2. Self-desiccation– relative humidity

4.1.2.1. The role of water in the alkali– silica reaction. Moisture is generally accepted to be one of the main factors affecting ASR. Water is important as a transport media for ions. The role of water is also important in the expansion stage. The overall expansion and cracking of concrete is basically caused by sorption of water by the alkali– silica gel, which in turn swells and thereby causes damage.

The water content in ASR-affected structures is normally expressed as relative humidity (RH), which is a measure of the thermodynamic state of the pore water. However, measurement of RH is notoriously very difficult and uncertain, particularly in the field. The critical limit for developing ASR is reported to lie in the range of 80– 90% RH depending on several factors, as discussed by Larive et al. [134].

4.1.2.2. Mechanisms causing self-desiccation. The hydration process of cement gives a reduction in the overall volume of the paste. This is due to the fact that the reaction products (i.e. C– S– H gel and CH) have a smaller volume than that of the original reactants (cement + water). This phenomenon is referred to as chemical shrinkage, and has some major effects:

1) It causes autogenous shrinkage, which is a volume contraction of the total concrete body. In the plastic phase, the chemical shrinkage equals the autogenous shrinkage.
2) In the hardening phase, the chemical shrinkage results in empty pores within the concrete. These pores will remain empty if no water is supplied from the surroundings. This leads to a lowering of the RH in the concrete, a phenomenon called self-desiccation. Generally, the extent of self-desiccation increases with decreasing w/cm ratio.
3) When water is gradually consumed during the hydration process and the chemical shrinkage pores are left empty, the remaining water will be in a state of "tension stress". This is the mechanism explaining the autogenous shrinkage in the hardening state.

4.1.2.3. Practical implications. For practical purposes the effects of self-desiccation might become important for concretes with w/cm ≤ 0.45. At low w/cm ratios this effect is large and may reduce the RH even below 80% over a period of time, provided there is no water supply from the surroundings. Consequently, a minimum limit should be considered for the w/cm. If such test limitations are not introduced, the internal RH in laboratory test prisms might be lower than in structures exposed to water in service. This could lead to incorrect test conclusions, i.e. some potentially alkali-reactive mixes could be classified as non-reactive based on performance testing because of the lack of water. A suggestion for such a minimum limit could be w/cm ≥ 0.40— in other words, performance tests should not be conducted at w/cm less than 0.40. However, the type of binder, in particular the type and amount of any SCM used, will influence the extent of self-desiccation. More research is thus needed as basis to agree on a possible lower w/cm limit for performance testing.

Additionally, the aggregate porosity and the aggregate moisture state at the time of mixing might significantly influence the RH within the concrete. If rather porous (≥ 0.8%) normal density pre-wetted aggregates are used, they may theoretically totally counteract the effect of self-desiccation. This is due to supply of water from the aggregates to the cement paste during the curing period ([135,136,137]). As a consequence, it might be conservative to use pre-wetted aggregates in laboratory performance testing. Conversely, if dry porous aggregates are used, this will likely exacerbate self-desiccation.

The shrinkage due to self-desiccation of a concrete with w/cm ratio 0.35 might be in the order of 0.01% after one week curing [138], and in extreme cases up to 0.02% [139]. Consequently, it may significantly influence the measured prism length in the early age, in particular the reference readings if the concrete prisms are prolonged pre-cured at 20 °C for e.g. one week as in the RILEM AAR-3 concrete prism test [5]. One important question needs further research or at least detailed and informed discussion within RILEM TC 219-ACS to achieve consensus: *What is the most correct "reference length" to apply in ASR expansion testing; the length after de-moulding, the shortest length after some shrinkage has occurred or the length after a pre-curing period*? The magnitude of the irreversible shrinkage will also influence the reference length, as will the internal prism temperature during the reference readings.

4.1.3. Transport properties

Increasing w/cm ratio will result in a higher and more continuous porosity (more capillary pores), and consequently internal transport processes will be accelerated, the rate of alkali leaching will increase and water or possibly other solutions will penetrate more easily ([140,141]). All these mechanisms might influence the rate and extent of ASR during laboratory performance testing, calling for similar concrete quality to be used in laboratory performance testing as in the actual field structures. If deviations are necessary, laboratory testing should aim to give conservative results.

Several authors, e.g. Stark [142] and Sellevold [143], have shown that moisture fluctuations in the field basically take place in the outer layer (some centimetres thick) of the concrete. The depth of the influenced zone will decrease with decreasing w/cm ratio, as shown by Yang et al. [144], as the result of a reduced permeability. As a consequence, the residual concrete mix water, depending on the w/cm ratio (influencing the extent of self-desiccation), rather than ambient wetting and drying, determines the prevailing moisture content in the interior of massive concrete structures, as discussed by Stark [145]. For such structures the extent of self-desiccation, mainly controlled by the w/cm ratio, may govern the interior RH level of the concrete. Also during laboratory testing, there is a probability for development of a moisture profile through the prism cross-section, with lowest RH in the mid part, in particular if the size of the concrete specimens is rather large (≥ 100 mm cross-section) combined with a rather low w/cm ratio (≤ 0.40).

The type of binder will also influence the permeability of the concrete, and thus the permeability related ASR mechanisms, i.e. internal transport processes, alkali leaching, water uptake and sensitivity to drying during exposure and measuring in the laboratory. Furthermore, increased permeability in aggregates may enhance the alkali reactivity due to easier access to concrete pore fluids [41].

4.2. Binder content

Unless alkalis are added during mixing, the cement content directly controls the alkali content of concrete mixes and, hence, the rate and amount of expansion due to ASR. However, changing the cement content can also modify the water/binder ratio as discussed above and this can influence transport properties, including alkali leaching, the concentration of ions in the pore solution, and self-desiccation. Differences in the cement-to-aggregate ratio, within the range usually encountered with typical concrete mixes, are unlikely to have a significant impact on the outcome of the test unless an aggregate exhibits a pronounced pessimum behaviour.

4.3. Alkali boosting

The alkali content of the concrete is a critical factor in determining both the rate and amount of expansion induced by ASR. Fig. 3 (produced from unpublished data from the Building Research Establishment, U.K.) shows the expansion of concrete prisms as a function of the alkali content of the concrete, for concrete with a range of cement contents (and w/cm), cement alkali levels and with and without alkali boosting (by the addition of K_2SO_4 to the mix water in this case). The data indicate that expansion is primarily a function of the alkali content and to some extent independent of the cement content, the alkali content of the cement and whether or not the alkali content was boosted.

The alkali content of the concrete is often boosted to ensure that there are sufficient alkalis present to identify reactive aggregates and to compensate for alkali leaching. However, extensive alkali boosting is not recommended for performance testing as it masks the critical role of the alkali content of the job mixture. Other concerns regarding alkali boosting include the following:

- The effect of alkali boosting on expansion also depends on the type of aggregate [146].
- The alkali compound added might influence the behaviour of the concrete [147].
- For a binder with 7.5% silica fume, Pedersen [77] documented that alkali boosting significantly increased the concrete permeability and reduced the compressive strength up to one year of standard curing. The capillary porosity was also increased, but less pronounced.
- The addition of alkalis may accelerate the release of alkalis from certain aggregates ([81,148,83,84]).
- Also the type of the alkali ions (Na^+ or K^+) and the source influence the release of the alkalis.
- The addition of alkalis may change the K/Na ratio, which could impact the expansion ([91,92]).
- The increased pH will reduce the concentration of calcium in the pore solution and some Ca^{2+} is required for the formation of swelling gels ([149,133,150]).
- Experiences with mortar bar tests at the FIB (unpublished data— information received from Colin Giebson) show clearly that alkali boosting mortars with cements (CEM I) different in Na_2O_{eq} to the same alkali level by adding NaOH does not result in the same expansion. This finding appears to contradict the observations at BRE shown in Fig. 3.

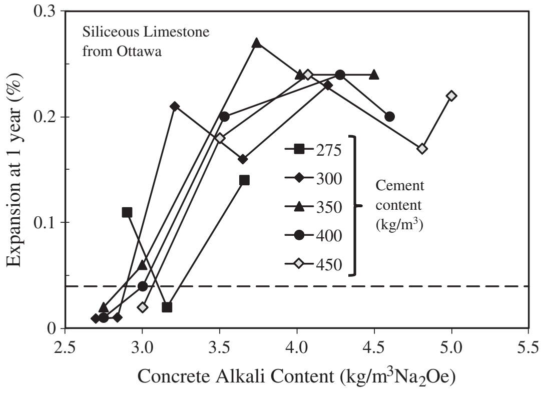

Fig. 3. Expansion of concrete prisms as a function of alkali content (produced from unpublished data from the Building Research Establishment, U.K.). The dashed line represents the critical 1 year expansion limit.

The effect of extensive alkali boosting is currently subject to further research within RILEM TC 219-ACS.

4.4. Chemical admixtures

There are no indications in the literature that chemical admixtures that are added either to modify the workability or the set behaviour of the concrete either in the laboratory or the field significantly influence ASR, unless the admixtures contain significant quantities of alkalis including sodium, potassium and lithium. The latest generation of admixtures normally do not contribute to the alkali content of concrete, but an exception is still shotcrete accelerators ([151,152]), available in both high and low alkali level versions.

The use of air-entraining admixtures is unlikely to have a direct effect on ASR, but the presence of an air-void system may impact the amount of expansion. There is some conflicting evidence in the literature regarding the role of air content on ASR expansion. Whereas it is generally agreed that air will not prevent ASR expansion, there is some evidence that it can reduce or delay expansion with some aggregates by accommodating ASR gel ([153,154]). However, there are some other findings in the literature that air entrainment is not beneficial in reducing ASR expansions ([60], [155]). It is recommended that the air content of the performance test is the same as that intended for the job mixture. However, alternatively it may be recommended to use lower air content in the laboratory test prisms, since this is a conservative approach.

Lithium-containing admixtures are effective in controlling expansion with some aggregates. Feng et al. [156] summarised the findings in the literature about the effect of lithium salts on the reaction products formed, and stated that the efficiency of lithium salts in suppressing the ASR expansions depends on the nature and reactivity of the aggregate, the form of lithium, the amount of alkalis in the pore solution and the dosage of lithium salt added (lithium to alkali molar ratio). It is essential that the lithium to alkalis (sodium and potassium) ratio, [Li]/[Na + K], in the performance test is equal to that of the job mixture being tested.

5. Exposure conditions

5.1. Pre-storage conditions

The “pre-storage period” is defined as the period from casting of the concrete prisms up to the point of the initial (zero) length comparator readings. The “pre-storage conditions”, i.e. the storage conditions during the pre-storage period, vary for different concrete prism tests. After casting, most test methods describe storage of the moulds at 18–23 °C and minimum 90–95% RH in the surroundings, while other describe more humid storage of the moulds, e.g. in a fog room with 100% RH. After de-moulding the day after casting, some test methods describe direct exposure of the prisms to the actual storage temperature, e.g. ASTM C-1293-08b [11]. Other methods describe 0.5 h submergence of the prisms in water after de-moulding, before further preparation for final storage. Finally, the length of the pre-storage period at 18–23 °C normally varies from 1 day (e.g. as in ASTM C-1293-08b [11] and RILEM AAR-4.1 [6]) to 7 days (e.g. as in RILEM AAR-3 [5]). For performance testing, some laboratories use an even more prolonged pre-storage period, up to 28 days, dependent on the type of binder [157].

Possible influences of the variations in pre-storage conditions and ASR exposure conditions on vital "ASR parameters" (i.e. prism internal humidity, composition of the concrete pore solution, aggregate reactivity, properties of hydration products formed and properties of any reaction products formed) and thus on the outcome of a performance test are discussed in this section.

5.2. ASR exposure conditions

The result of a performance test is strongly dependent on the ASR storage conditions and thus on the initiation and progress of ASR. The following parameters are evaluated and discussed:

- Moisture conditions
- Type of container
- Prism size
- Wrapping (if any)
- Storage temperature
- Storage period
- Any external alkalis added

5.3. Internal humidity

During laboratory performance testing, the internal moisture content within the concrete prisms is aimed to be very high, i.e. higher than in many real concrete structures. Thus, the prisms should be subjected to "worst-case humidity conditions". The pre-storage and storage conditions might also significantly influence the interior RH of the prisms.

The following parameters may increase the influence of self-desiccation when using a relatively low w/cm ratio, and thus contribute to maintain a "rather low" internal RH in the concrete prisms: prism size (worse when increased), micro climate in the storage containers (worse the lower the RH is inside the containers), length of the pre-storage period (reduced internal RH if prolonged storage period due to a higher degree of hydration), permeability (less water uptake if low) and storage temperature (the degree of influence may vary dependent on the micro climate in the storage container). Any possibility for drying of the prisms due to evaporation, e.g. if they are pre-stored in a climate with less than 100% RH in the air, will also naturally influence the prism interior RH.

The curing temperature might influence the concrete porosity and permeability. For an OPC, a higher curing temperature in the early age will normally lead to a coarser porosity and consequently an increased permeability, as reported by Kjellsen et al. [158], Kjellsen and Detwiler [159] and Lothenbach et al. [160]. Somewhat contradictory, Schmidt et al. [161] found that the total capillary porosity measured after three months on concrete samples cured at 20, 40 and 60 °C, respectively, decreased with increasing storage temperature. The influence of curing temperature was most pronounced for the concrete containing 30% fly ash compared with the OPC concrete. However, in these tests all concretes were presumably pre-cured at approximately 20 °C until de-moulding (not stated specifically in their study), i.e. in the early hydration period the curing temperature was equal. This implies that their measured lower capillary porosity at elevated temperature primarily reflects a higher degree of hydration and that more fly ash reacts earlier at elevated temperature.

In general, a concrete subjected to prolonged pre-curing period at 20 °C will have a lower permeability when starting the ASR test compared with a concrete exposed to the ASR storage conditions directly after de-moulding. The time at which the temperature is elevated and the magnitude of the elevated temperature (normally in the range 38 to 60 °C) will consequently influence the concrete water uptake, the water transport properties, as well as the drying properties, and thus also the internal concrete moisture content during the accelerated ASR testing.

In order to maintain a high internal RH in the test prisms during the entire test period, the ambient humidity during storage must be very high ($\approx$100%). The micro climate in the storage containers is thus of great importance. Important parameters are size and design of storage containers, type of lining (if any) and application of a watertight seal. Large containers may lead to an inhomogeneous distribution of moisture. For example, the experience gained with the Norwegian 38 °C CPT [23] indicated that when large storage containers holding several concrete prisms were replaced by smaller containers holding only 3 prisms in each, there was a general increase in expansion. Also a Norwegian sandstone, proven to be reactive in the field, showed expansions above the critical limit in the smaller containers, but not in the larger ones [73].

The sorption properties and the internal RH in concrete are to a certain degree dependent on the storage temperature. A raised temperature in part of a concrete sample/structure will lead to increased local vapour pressure. This will initiate moisture transport from warmer to colder regions and, eventually, reduce the local moisture content, and as a consequence lead to a decrease in RH, as discussed by Nilsson [162]. This phenomenon will take place during cooling of concrete prisms overnight, before the prisms are measured the day after. During cooling, moisture will move from the warmer inner part to the colder outer parts of the specimen.

On the other hand, if the moisture content within a concrete is rather constant (as one can assume for small concrete prisms stored over water in a sealed container, at least if the w/cm ratio is not too low), a general increase in the temperature will give rise to a small increase in the internal RH. For example, according to tests reported by Sjöberg et al. [163], the RH within a concrete with w/cm 0.40 and internal RH 90% will increase approximately 0.25% per °C. Thus, an increase of the concrete temperature from 20 °C to 40 °C might increase the internal RH by approximately 5%. The effect decreases with increasing w/cm ratio ([163,162]). The effect is max in the middle RH-range (around 50–60%), and decreases to zero in very dry and in saturated concrete [164]. One consequence of this phenomenon is that the internal RH in concrete prisms will increase with increasing storage temperature, provided there is no change in the concrete internal water content.

The susceptibility to loss of moisture during the exposure period will increase with increasing storage temperature. The extent of any weight loss is controlled by the relative humidity in the surroundings and the type of container. If concrete prisms are stored over water in containers placed in a dry and hot room, as is the case for several concrete prism tests (Norwegian CPT [23], ASTM C1293-08b [11], CSA A23.2-14A-04 [13], RILEM AAR-3 [5]), the risk of drying is high compared to storage in containers placed in a humid environment—e.g. in a reactor, as in the RILEM AAR-4.1 CPT [6]. If the lid is broken or not made watertight, the risk of evaporation of the water in the bottom of the container is significant provided storage in a dry room or an oven. Also the storage period influences the sensitivity to loss of water. For instance, SINTEF have experienced that RILEM AAR-3 containers [5] are particularly vulnerable to drying due to the small amount of water in the bottom of the containers (only 350 ml) combined with a long testing time (one year for aggregate testing).

As a consequence, the test set up and the test procedures must aim to avoid loss of water during storage and measuring. Important parameters in this respect are quality control (e.g. control of the water level and use of watertight lids), strict measuring procedures (measure quickly with as low moisture loss as possible), evaluation if the prisms should be pre-cooled or not before measuring (the prisms will dry during cooling, because moisture will move from the warmer inner part to the colder outer parts) and storage temperature (the higher storage temperature, the more drying during cooling). As a quality control, the mass of prisms should always be measured, evaluated and reported.

As several have experienced, e.g. Lindgård et al. [165], after a possible weight loss in the first one to two weeks, the weight of the prisms normally increases with increasing expansion and with time. However, if the prisms show too low mass increase with time or in extreme cases weight loss over time, this is most likely due to insufficient water present in the system, and consequently the test results might be questioned. Another reason for a decrease in prism weight might be connected to the ambient humidity the first day of curing. Unpublished data from the PARTNER project [37] showed that storage in a fog chamber with 100% RH the first day after casting lead to a higher reference prism weight compared with storage at approximately 95% RH (as required in the method). When testing some non-reactive aggregates in the 60 °C AAR-4.1 reactor [6], the prisms pre-stored in the fog chamber showed a slight weight loss in the end of the test period, while the prisms stored at 95% RH showed a slight weight increase. However, the expansion test results were comparable.

Submerged storage of the prisms will give rise to high internal water content, unless large test specimens and a low w/cm ratio are applied. One consequence of the likely higher moisture content in submerged concrete prisms, compared to most field concrete structures, is development of a less swelling gel due to a reduced viscosity [166]. However, an essential consequence of any submergence in water is extensive leaching of alkalis [167], and such storage is not recommended.

Wrapping of concrete prisms, by use of moist cotton cloths and plastic sheets, are applied in some test methods primarily with the aim to secure a high moisture content surrounding the prisms, but some have also expected less leaching of alkalis from wrapped prisms. On the other hand, wrapping might reduce the access to ambient moisture in the air. If the wrapping effectively hinders contact between the ambient moisture content in the storage container and the prisms (e.g. as in the RILEM AAR-3 CPT [5], where the wrapped prisms are stored in plastic bags), the amount of water added during the wrapping procedure and on top of the prisms at every measuring point of time may have large influence on the internal moisture content within the concrete prisms. Unpublished data from Jan Lindgård's PhD study (2007–2012) at NTNU reveals that wrapping significantly reduces the extent of evaporation during cooling (provided cooling of the prisms before each length reading) and during measuring.

Another important factor is to keep the internal prism temperature constant during all measurements. Several methods state that the maximum allowed variation in the room temperature where the prisms are being stored before and during the measurements is ±2 °C, e.g. RILEM AAR-3 [5]. *But how sensitive is the recorded expansion of a moderately deviating prism temperature at measuring compared with the temperature during the reference readings*? A concrete will expand approximately 0.001% if the temperature increases 1 °C [168]. This means that a 5 °C temperature change corresponds to approximately 0.005% length change. When the critical expansion limit for several concrete prism methods is in the range of 0.030–0.040%, a 5 °C temperature deviation constitutes 1/6 to 1/8 of the critical expansion limit, i.e. the influence of a deviating internal prism temperature might be significant.

An aspect that significantly can influence the recorded reference length of the prisms (being the basis for calculating the expansion) is whether the initial length readings are taken immediately after de-moulding or after 30 min submergence in water. Without submergence, the internal prism temperature may be somewhat higher than 20 °C due to the cement hydration. If the prisms are submerged, the water temperature will control the internal prism temperature. If the quality control in some laboratories is not satisfactory, a temperature variation up to 5 °C is likely to occur.

5.4. Composition of the concrete pore solution

As discussed previously, the content of alkalis (i.e. Na^+ and K^+) in the concrete pore solution plays a major role in development of ASR. Thus, all conditions during pre-storage and storage that may contribute to change the alkali content in the pore solution, either reduce it (e.g. due to alkali leaching or binding of alkalis) or increase it (e.g. due to alkali release from aggregates or ingress of any external alkalis e.g. from de-icing salts) will consequently influence the rate and extent of ASR during laboratory performance testing.

In several studies, results from pore solution analyses are reported. However, there is no consensus on the procedure on how to extract pore solution, analyse it and interpret the results. In particular for low w/cm ratios (e.g. <0.50), it is very difficult and in many cases impossible to press any pore water from the concrete, even though high pressures are applied. If extremely high pressures are used, there is also a question over whether the pressed pore water is representative for the pore water within the concrete. Some researchers have thus used alternative methods to detect the soluble alkali content in the concrete pore water. One example is the “hot water extraction method” that Berubé et al. [87] used to measure the extent of alkali release from various aggregate types.

5.4.1. Alkali leaching

The problem of alkali leaching from specimens stored over water in sealed containers was first reported by Blanks and Meissner in 1946 [169]. The authors detected a build up of alkali ions in the water at the bottom of the containers in which mortar bars were stored, and explained this based on water condensing on the surface of the bars and running down the bars into the reservoir below, thereby providing transport of the alkalis. The mechanism for alkali leaching is further explained by Rivard et al. [20] to be excessive condensation of water on the prism surfaces, leading to an outward diffusion of alkalis from the interior of the concrete. The degree of alkali leaching depends strongly on the storage conditions. Additionally, the conditions during pre-storage might significantly influence the rate and extent of alkali leaching. A prolonged pre-storage period at a moderate storage temperature (18–23 °C) is assumed to reduce the early extent of alkali leaching due to a lower permeability when the concrete prisms are exposed to the ASR storage environment. On the other hand, early exposure of the prisms to a very humid environment, e.g. a fog chamber with 100% RH or even more extreme storage conditions, e.g. submerging the prisms in water after de-moulding for a long period, are expected to increase the extent of alkali leaching.

Thomas et al. [24] found that specimen size clearly has a large impact on expansion and this effect can be largely ascribed to more leaching of the alkalis from smaller specimens. In their study they found that the impact of alkali leaching will be less for larger concrete prisms, but is still significant. Three concrete prisms ($75 \cdot 75 \cdot 300\ mm^3$) containing a reactive siliceous limestone (Spratt) were stored over water at 38 °C in a container. By assuming a constant reservoir volume of 1.8 l and neglecting any alkalis that may wick up the absorbent material lining in the container, it was estimated that approximately 35% of the alkalis originally in the concrete found their way into the water reservoir after 1 year, and as much as 20% after just 90 days. Also tests performed by Bakker [170] and Lindgård [167] showed that the larger the cross-section of a concrete prism, the greater the expansion, which was interpreted as being caused by higher extent of alkali leaching for the smaller specimens. However, even for larger concrete prisms (cross-section $100 \cdot 100\ mm^2$) alkali leaching cannot be neglected [165].

Rogers and Hooton [171] found that concrete prisms (assumed size $75 \cdot 75\ mm^2$ cross section) stored in a moist room showed the least expansion, as well as the greatest amount of alkali leaching. Storage in a polyethylene bag resulted in less leaching of alkalis and more expansion. Results of percent change in alkalis at 130 weeks of exposure exhibited;

- 22% decrease for prisms stored at 23 °C in plastic bags with 100 ml of water
- 42% decrease for prisms stored at 38 °C over water in a sealed box
- 63% decrease for prisms stored at 23 °C in a moist room

Fournier et al. [36] studied deviations between the 38 °C concrete prism test and the 60 °C accelerated concrete prism test. They verified that in the 60 °C test, the ultimate expansion was considerably lower, probably due to higher extent of alkali leaching and changes in pore solution composition (more sulphate dissolved—see later). The increased alkali leaching at elevated temperature is expected, since the diffusion increases with increasing temperature.

According to Bokern [166], under extremely humid conditions, like in a fog chamber with temperature 40 °C, intensive alkali leaching occurs. A loss of 20% of the initial soluble alkali content after 28 days and more than 30% after three months is possible for a concrete with OPC and w/cm ratio 0.55. In these tests, 100 mm cubes were used. Comparable values were also reached in the 60 °C RILEM AAR-4.1 CPT [6] after three months storage of the concrete prisms with cross section $70 \cdot 70$ mm^2 on grids over water in the small containers inside the reactor.

Submergence of test prisms in water will remove most soluble alkalis from the concrete pore water, thus substantially slow down or stop any potential ASR, as shown e.g. by Lindgård [167].

Wrapping in cotton cloth and plastic has sometimes been applied in order to decrease alkali leaching, but there are also references showing that wrapping may decrease the expansion ([30,172]). Lindgård [167] documented that wrapped concrete prisms stored at 60 °C showed significantly lower expansion than unwrapped prisms due to increased alkali leaching in the early age.

Nixon et al. [173] and Åhs [174] have shown that alkalis can diffuse towards the surface of concrete on wetting and drying. The alkali concentrated regions are generally located in the outermost regions of concrete structures after drying of concrete. Thus, even for concrete containing low alkali cement, local ASR formation might become possible [175]. As a consequence, drying/wetting cycles during cooling of concrete prisms overnight (before each measurement) might transport alkalis to the prism surface and thus enhance the extent of alkali leaching (compared to measuring the prisms without pre-cooling).

Rivard et al. [176] showed by chemical analysis of the water beneath test prisms that the alkalinity reduction of the concrete pore solution with time was mostly associated with alkali leaching. It was shown that for the same reactive mixture, concrete alkali leaching seemed to be greater for the specimens containing higher alkali level (5.25 kg/m^3 Na_2O_{eq}) compared with specimens with lower alkali level (4.00 kg/m^3 Na_2O_{eq}).

The cement type or binder combination also influences the rate of alkali leaching due, among other things, to the influence on the concrete permeability. According to Bokern [166], concrete made of OPC or cement with ggbs (20%) seems to be particularly vulnerable to alkali leaching compared with cement with silica fume or fly ash. Recent investigations by Schmidt [177] also show (Fig. 4) that the extent of alkali leaching during ASR-testing in a 40 °C fog chamber is influenced by the binder combination. Naturally, this will influence the measured expansions.

In contrast to many laboratory results, pore solutions in field concrete are mostly not subject to alkali leaching, according to Rivard et al. [176], probably due to the higher volume to surface ratio compared with laboratory specimens. The problem of alkali leaching is thus a big challenge in laboratory tests.

5.4.2. Alkali release from aggregates

The storage conditions during ASR testing might also influence the rate and extent of alkali release from aggregates. Ideker et al. [178] showed that the contribution of alkalis from a "non-reactive" sand resulted in increased concentration of K^+ in the pore solution, elevated pore solution pH and a higher rate of expansion at early age compared with other "non-reactive" sands tested. The difference was most pronounced for the 60 °C CPT compared with the 38 °C CPT.

5.4.3. Storage temperature

Fournier et al. [36], Lothenbach et al. [160] and Schmidt et al. [161] have documented that the concentration of sulphates in the pore solution is increased when the storage temperature is elevated, see Fig. 5. Consequently, the concentration of OH^- in the pore solution, and thus the pH, is correspondingly decreased resulting in a lower solubility of SiO_2. The cause of the higher concentration of sulphates in the pore solution at elevated temperature is higher solubility of ettringite [36]. If the pre-storage of ASR concrete prisms at approximately 20 °C is prolonged e.g. from 1 day to 7 days, less ettringite will be available in the concrete prisms (more is transformed to mono-sulphate), and probably less ettringite will be dissolved when the ASR test is started (i.e. the temperature is elevated). Consequently, the pH of the concrete pore solution will be increased.

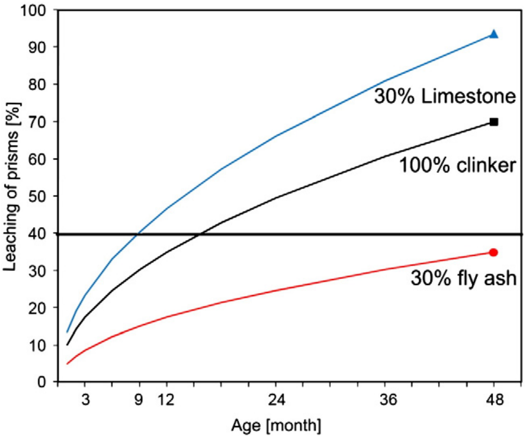

Fig. 4. Estimated development of alkali leaching of concrete prisms with different binders, 400 kg/m³ of binder, w/cm = 0.45, storage at 40 °C and 100% RH in a fog chamber [177].

Partly as a result of the drop in OH^- concentration (Fig. 5), the addition of only 10% fly ash to the binder was apparently able to suppress the expansion below the critical expansion limit for a highly reactive aggregate when exposed to 60 °C one day after casting [161]. When pre-stored at 20 °C for at least 28 days before starting the 60 °C CPT, the concrete prisms with 10% fly ash expanded far beyond the critical limit. Also when adding 20% fly ash, the length of the pre-storage period affected the measured prism expansion significantly, but the effect was less pronounced. When adding 30% fly ash, no expansion was revealed for any of the three pre-curing periods applied (1, 28 and 90 days, respectively).

Schmidt et al. [161] believe that the accelerated rate of reaction of the fly ash when exposed to elevated temperature after 1 day also contributes to reduce the expansion of the concrete prisms exposed at early ages (see further discussion later). However, the extent of alkali leaching was not discussed in the paper, but might according to our experience also have influenced the results presented, since the rate of alkali leaching is expected to be highest in the concrete prisms exposed to the ASR storage at earlier ages (i.e. at age 1 day).

5.4.4. External alkalis

According to Nixon et al. [179], the introduction of sodium chloride to cement paste, mortar or concrete at the mixing stage, results in an elevation of the hydroxyl ion concentration of the pore solution to a level similar to that produced by a Portland cement with an equivalent alkali level. This will increase the likelihood of damaging ASR in concrete with alkali-reactive aggregates. Correspondingly, various external alkalis may influence the concrete pore solution chemistry. Thus, when testing the influence of various de-icing salts on ASR in a performance test, similar "alkali-conditions" (i.e. identical type and amount of cement, admixtures and any external alkalis; etc.) should preferably be used as will be used in the field.

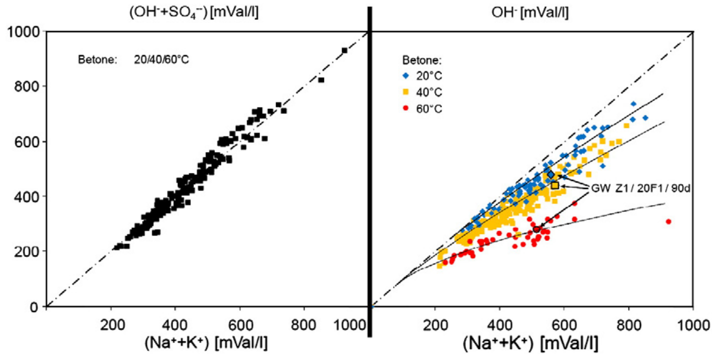

Fig. 5. Concentration of anions OH^- and SO_4^{2-} vs. concentration of cations (Na^+ and K^+) of pore solutions at different temperatures [161].

Additionally, alkali leaching from the test samples during expansion testing should be considered when fixing testing conditions, considering threshold levels or conforming to acceptance criteria.

Information on the influence of external alkalis on the alkali binding capacity of the hydration products formed with OPC, ggbs, FA and SF was not found in the literature study.

5.5. Aggregate reactivity

The solubility of silica species is controlled by pressure, temperature, particle size, pH and by dissolved species in the solute [35]. Dove [180] concluded that the net dissolution rate of quartz in aqueous solutions containing mixtures of cations is dominated by the ions with the stronger surface interaction ($Ba^{2+} > K^+ \approx Na^+ \approx Li^+ \approx Ca^{2+} > Mg^{2+}$).

Regarding the effect of temperature, experiments show that the exposure temperature influences the aggregate reactivity. The solubility of SiO_2 increases with the temperature (Fig. 6), but the effect is different for different forms of silica. High exposure temperature also seems to activate some apparently “non-reactive” aggregates [39]. A greater amount of gel is formed and higher expansion is observed at a given time since the reaction rate is accelerated by temperature. However, the temperature should not be analysed in isolation, as it works simultaneously with other factors.

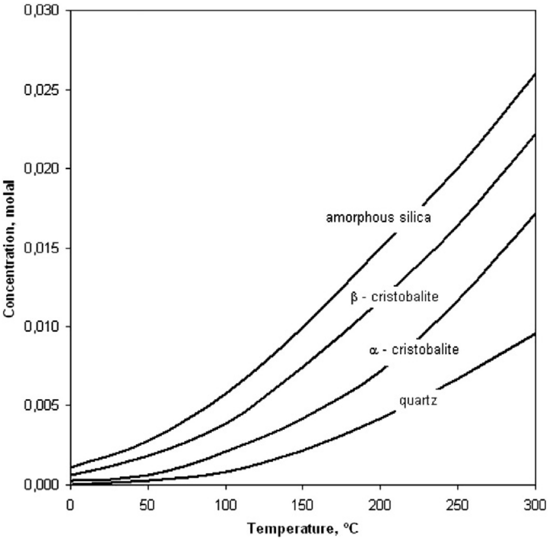

Fig. 6. Solubility of polymorphs of silica regarding temperature based on equations from Rimstidt and Barnes [181,182].

The effect of temperature is mirrored in the experimental results of tests with different temperatures. Fournier et al. [146] performed field tests on concrete blocks in two different locations, one in Texas and one in Canada, to study the effect of ambient temperature. Those authors concluded that the expansion is faster and higher for the place with highest exposure temperature, but it depends on the type of aggregate selected. The difference in expansion increases with decreasing reactivity level. Additionally, Iler [183] concluded that with testing at 60 °C, more siliceous material from the aggregate is likely to be dissolved, compared with that at 38 °C or at ambient conditions.

Very fine particles of certain rock types have the capability to react pozzolanicly and hence increase the C–S–H phase, as suggested by Pedersen [77]. An important finding by Pedersen [77] was a significant temperature effect. Some rock fillers that were not pozzolanic at ordinary curing temperature may be highly pozzolanic at a temperature of 80 °C. This fact is of high significance when using test regimes with very high temperatures. Testing of mortar or concrete mixes with significant amounts of fines from alkali-reactive rocks may then give a “false negative” result if tested at very high temperatures. This arises from the fact that the pozzolanic reactivity increases with increasing temperature. Pedersen [77] examined exposure temperatures of 20, 38 and 80 °C, and concluded that methods using 80 °C should not be used for performance testing of real mixes.

5.6. Properties of hydration products formed

The rate of hydration of Portland cement increases with increasing temperature, which is more pronounced at lower degrees of hydration. The composition of C–S–H does not differ from that formed at ambient temperature up to about 50 °C, but beyond this temperature Ca/Si ratios increase moderately. At high temperature curing, the paste might have a higher porosity and/or coarser pore structure, even decreasing the strength at long hydration times [184]. According to the authors' experience, the effect of curing temperature is more pronounced at the early period of hydration.

The effect is even more complicated when SCMs are present in the cementitious system. The average Ca/Si ratio of hydration products of fly ash (FA) increases with increasing storage period and increasing temperature, which results in a decreased alkali sorption capacity [185]. Up to 40% ggbs, the Ca/Si ratio of the C–S–H phases and therefore also the alkali sorption properties are similar to that of OPC [117]. By contrast, for ggbs, higher temperatures may lead to a higher degree of condensation of the silicate anions in the C–S–H phases, and therefore to a lower Ca/Si ratio [186]. Thus, the C–S–H phases formed can absorb more alkalis. Additionally, De Weerdt and Justnes [187] have documented that not only the C–S–H phases are changed when elevating the temperature from 20 °C to 80 °C, but also the aluminium containing phases. However, more hydration products of fly ash are formed at 40 °C and 60 °C than at 8 °C and 20 °C, thus more alkalis can be bound [185]. The two opposite trends indicate that there may be an optimum temperature for the highest alkali binding capacity of FA. Baetzner and Böhm [188] found that, in the presence of FA, the alkali concentration in the pore solution often was lowest at 40 °C. Thus, testing of FA containing concretes at this temperature will not be conservative.

In order to access the alkali reactivity potential of specific concrete compositions in a relatively short time, mortar or concrete samples are often exposed to high temperatures at very early ages. Bokern [166] assumes that ASR takes place within 28 to 56 days in very accelerated laboratory conditions (temperature 60 °C), when maximum alkalinity in the pore solution usually is achieved. Under normal conditions (20 °C), the pozzolanic reaction of FA starts after the age of 28 days [117]. If the concrete with FA is exposed to high temperatures at an early age, alkalis may be bound by the accelerated pozzolanic reaction that takes place before the ASR. This means that the pore solution has a lowered alkali hydroxide content when the ASR is about to start. To reduce this impact on the alkalinity of the pore solution, Bokern [166] thus recommends storing the concrete samples under normal temperatures to allow a normal development of the pore solution composition. This is confirmed by Schmidt et al. [161], where the accelerated concrete prism test at 60 °C is extended by a pre-storage period of 28 and 90 days at 20 °C before the samples are tested at 60 °C.

Temperature effects on laboratory test expansions vary with respect to the alkali content of the system. If a fixed amount of alkalis is available, maximum expansions are observed at a pessimum level of temperature (38–40 °C) [189], i.e. the expansions are reduced for lower and higher temperatures. Tests carried out with an unlimited amount of alkalis show that for particular aggregates, total expansion decreases with increasing temperature [190]. The latter case might be connected to the behaviour of calcium hydroxide as the solubility of calcium hydroxide decreases by increasing temperature. For many field structures, the tendency is that the higher temperature, the higher the rate of alkali–silica reaction [173].

Diamond et al. [102] tested opal-containing sealed mortar specimens at 20 °C and 40 °C, respectively. It was observed that the rate of reaction and expansion is higher at 40 °C, however, the ultimate expansion and the percent of alkalis reacted become higher at 20 °C at later ages [99]. This should be kept in mind while evaluating the laboratory versus field expansions.

The implications of the findings discussed above are that the time of starting the ASR exposure as well as the exposure temperature might significantly influence the outcome of a performance test. This is due both to accelerated pozzolanic reactivity if the concrete is exposed to elevated temperature at early ages and to the temperature-dependence of the alkali binding capacity of various SCMs.

5.7. Properties of reaction products formed

5.7.1. ASR-products

The expansive forces caused by gel depend on the gel composition as well as of the amount of gel present in the concrete [27]. Time seems to have an effect on the development of the products of reaction. With extended exposure time, a larger amount of ASR gel is produced, leading to a higher expansion ([56,191]). The composition of gel evolves with time; initially the gel absorbs water without taking in Na^+ and K^+ ions [56]. In later stages, due to the evolution of the reactions, the Ca content increases and the gel becomes more viscous and expansive than the original alkali-rich gel. Kawamura et al. [56] also observed that higher temperature results in a greater amount of Ca^{2+} in the gel, assumed to be a pre-requisite for the formation of expansive gel ([57,59,65]). However, there is no general agreement in the literature regarding the influence of the Ca content in the ASR gel on its expansion ([65,192]).

Additionally, the Ca content is reported to be a function of the place where gel occurs inside the concrete; Knudsen and Thaulow [52], Kawamura et al. [56] and Fernandes [64]. Among others, Kawamura and Iwahori [193] and Bokern [166] have shown that an increase in the alkali content in ASR gel (i.e. high Na_2O/SiO_2 ratio) decreases the viscosity. Thus, the viscosity of alkali-rich gels may be so low that they cannot produce sufficiently high expansive pressure to crack mortar or concrete specimens, but lead to exudation of ASR gel on the surface of the exposed test samples. This exudation limits the gel content inside the specimens and probably results in reduced expansion. Struble and Diamond [194] measured swelling properties of alkali–silica gels of various Na_2O/SiO_2 ratios. Under “free-swelling conditions” they recorded swelling ranging from 0.1 MPa to almost 11 MPa. Gels with Na_2O/SiO_2 ratio of 0.33 and less exhibited the lowest swelling pressures.

In field concretes, the alkali content is often limited, while calcium is continuously brought into the pore solution due to portlandite dissolution. Additionally, in laboratory test specimens, the high level of sodium content (resulting from the NaOH enrichment of the mixing water or storage in alkaline solution) leads to increasingly sodium-rich gel with lower viscosity. Furthermore, Bokern [166] showed that the addition of SCMs may hinder deleterious ASR in laboratory tests, but not always in the field, partly because the viscosity of the gel decreases at elevated temperature and at a higher RH level. Thus, in the field, ASR-related expansion can be more intense, but slower.

Regarding properties of ASR gel, it was found that products obtained in laboratory tests are similar to those identified in field concretes (amorphous and crystalline) ([195,196,197]). If so, this fact is important as it means that temperature is probably not as important to the morphology of the alkali–silica gel as it is for the reactivity, rate and amount of gel produced [197]. Davies and Oberholster [198] compared alkali–silica products formed in field concretes with those formed during the 80 °C NBRI test [199]. They showed that, compared to the field, the NBRI test does not modify the naturally occurring process. Nevertheless, during the test they noticed fluid gels exuding into the NaOH solution, in the form of thin filaments. SEM examinations of gel conducted at the completion of such accelerated laboratory tests have revealed that morphologies were very similar to those found in field concretes [63] irrespective of whether NaOH or KOH solutions were used (massive gels, sponge-like texture and rosette-like phase).

By contrast, Fernandes et al. [38] observed that gel formed in mortar bar specimens showed an amorphous structure whilst the gel from old concrete structures is partly crystalline. Gavrilenko et al. [191] compared concrete cores taken from Spanish dams and mortar bars made up with the same aggregates (crushed granitic mylonite and quartzite) by scanning electron microscopy and semi-quantitative analysis of gels performed by EDX. In both cases they found large varieties of gel: compact smooth gel (amorphous), lepispheres and sheet sponge or clot morphology (crystalline/porous). However, field and laboratory reaction products had very different chemical compositions. Gels formed in mortars (alkali-boosted) were highly enriched in Na and poor in Ca, with often more silica than in the field concretes.

The alkali–silica reaction product has initially low fluidity and considerable swelling capacity in the presence of water. There is also evidence, at least under laboratory conditions, that dehydrated gel can be rehydrated and will re-expand when additional water is added to the specimen [134]. However, dried and carbonated gels are unlikely to regain their expansive properties, and they are not soluble in water [99].

Tests on specimens submerged in different salt solutions in ASR storage containers led to the conclusion that the ASR products formed differ in composition. NaOH is the more aggressive and produces a greater amount of gel, but KOH produces more crystalline gel [200]. In the literature, it is reported that the expansion increases until a certain level of alkalis is reached and then decreases for higher alkali contents, concluding that there is a "pessimum" effect of external alkalis (probably related to available silica) [201].

5.7.2. Delayed ettringite formation (DEF)

Delayed ettringite formation (DEF) is attributed to high temperature during early age curing [202]. At elevated temperature there is an incongruent dissolution of ettringite with much of the sulphate going into solution and being encapsulated by the rapidly forming C–S–H. During subsequent storage at ambient temperatures the sulphate is slowly released from the C–S–H and ettringite forms at later ages. Under certain conditions this delayed formation of ettringite can lead to expansion and cracking of the concrete. Expansion due to DEF has not been demonstrated for concrete cured below 65 °C, motivating temperature limits in many concrete standards. Hence, it is strongly recommended to consider this curing temperature limit for any ASR performance test.

6. Conclusions and recommendations

Based on the literature survey, the authors have provided recommendations for performance testing. These recommendations include precautions when testing various aggregates and binders, important factors to take into account during mix design, as well as possible influences on ASR expansion of various conditions during pre-storage and the ASR exposure.

6.1. Precautions dependent on type of aggregate

- When dealing with aggregates showing a possible pessimum, this must be accounted for during performance testing, e.g. by performing several concretes mixes with different percentages of reactive constituents.
- The aggregate fractions used in structures should also be used in the laboratory tests, since the aggregate size causing the highest ASR expansion is dependent on the nature and composition of the aggregate. Concrete prism tests are thus recommended instead of mortar bar tests. It should also be kept in mind that crushing some certain types of aggregates may affect their reactivity.
- Testing and assessment of alkali release from aggregates should preferably be taken into account during performance testing, since the extent of alkali release might vary with the test conditions, e.g. with the exposure temperature. However, the first and urgent step is to agree on a test method for measurement of alkali release representative of that occurring in practice and corresponding interpretation criteria.
- The ASR aggregate test methods and the corresponding interpretation criteria (maximum allowed expansion) have been developed for normal weight aggregates and are not necessarily applicable for lightweight aggregates (oven dry particle density less than 2000 kg/m^3) or heavy weight aggregates (oven dry particle density greater than 3500 kg/m^3). Also the weight increase should be taken into consideration since experiences show that the ASR gel (if developed) initially accumulates in voids in the LWAs and primarily contributes to a weight increase but only a moderate length increase. After the gel has accumulated in and partly filled the voids in the LWAs, the rate of expansion might increase

6.2. Precautions dependent on type of binder

- The same type of OPC cement should be used in performance testing as planned to be used in the structure. The reason is that some concrete mixtures produced with cements having similar Na_2O_{eq} but different K/Na ratios have been observed to expand considerably differently in accelerated laboratory tests. However, there are contradictory findings in the literature about this issue.
- The type of cement and the type and amount of any SCMs incorporated influence the parameters related to ASR, including composition of hydration products, pore water composition and permeability. This should be taken into account when testing the concrete performance, during mix design, pre-curing and exposure, as further discussed below.
- It is recommended to test the actual binder composition in combination with the actual aggregate to be used in the structure. Even though the chemical composition of e.g. two fly ashes is quite similar, their ASR mitigation properties might differ significantly.
- If the aim is to document the ability of a commercial binder (e.g. a fly ash cement) to prevent ASR for a number of aggregate types within a region, a possible alternative approach is to test the binder in combination with an assumed "worst case reference aggregate" (e.g. as described in the Norwegian ASR regulations [74]).
- An acceptable performance test method requires an approach that accelerates the pozzolanic reaction and the ASR to the same extent, since an extensive acceleration of the pozzolanic reaction might lead to less ASR expansion in the laboratory testing (not conservative). This might be of particular interest when testing fly ash containing cements, in which the pozzolanic reaction and thus the alkali binding starts after a period of approximately 28 days when cured at 20 °C.
- Performance testing of silica fume containing concretes needs a prolonged testing time (at least two years) in order to detect a possible increased alkali level with time when the alkali–silica gel continuously reacts with calcium. Thus, at least part of the alkalis becomes available for alkali–silica reaction.

6.3. Important factors to take into account during mix design

- The w/cm ratio influences the concrete properties, and thus the outcome of an ASR performance test. Decreasing the w/cm ratio on the one hand might lead to increased ASR expansions (due to increased OH^- concentration in the pore solution), while on the other hand may reduce the ASR expansions (due to a denser paste, and thus slower and less transport and ingress of water or solutions, and due to a higher degree of self-desiccation and thus a reduced internal RH). As a consequence, the authors suggest that the net influence of a reduced w/cm ratio should be investigated further, before executing commercial accelerated laboratory performance testing of concretes with w/cm ratio below 0.40.
- As a conservative approach, pre-saturated aggregates might be used to counteract self-desiccation to a certain extent (might be particularly effective for highly porous aggregates).
- The alkali content of the concrete is often boosted to ensure that there are sufficient alkalis present to identify reactive aggregates and to compensate for alkali leaching. Nonetheless, extensive alkali boosting is not in general recommended for performance testing because it masks the critical role of the alkali content of the job mixture. Additionally, there are several other concerns regarding alkali boosting (e.g. added alkalis might influence the behaviour of the concrete and thus affect the ASR properties). However, there are contradictory findings in the literature on the influence of some alkali boosting, thus calling for more research.
- It is recommended that the entrained air content of the performance test is the same as that intended for the job mixture. Alternatively, one might use lower air content in the laboratory test prisms, since this is a conservative approach. Whereas it is generally agreed that entrained air will not prevent or delay ASR expansion, there is some evidence that it can reduce expansion with some aggregates by accommodating ASR gel.
- In the case of using lithium to reduce the risk of ASR, it is essential that the lithium to alkalis (sodium and potassium) molar ratio, $[Li]/[Na+K]$, in the performance test is equal to that of the job mixture being tested.

6.4. Influence of conditions during pre-storage and ASR exposure

- The “pre-storage conditions” (i.e. moisture conditions during pre-storage and the length of the pre-storage period at ambient temperature) and the ASR exposure conditions (i.e. moisture conditions, type of container, prism size, wrapping (if any), storage temperature, storage period and any external alkalis added) might have significant influence on vital “ASR parameters” (i.e. prism internal humidity, composition of the concrete pore solution, aggregate reactivity, properties of hydration products formed and properties of any reaction products formed) and thus on the outcome of a performance test.
- A laboratory performance test should be designed to subject the prisms to “worst-case humidity conditions”, while considering the problems related to increased alkali leaching. As a quality control measure, the mass of prisms should always be measured, evaluated and reported.
- When using a relatively low w/cm ratio, e.g. as in high performance concrete, the self-desiccation will increase and, as a consequence, the internal RH will decrease. Several parameters might increase the influence of self-desiccation (e.g. the prism size and the micro climate in the storage containers) and thus contribute to maintain a “rather low” internal RH in the concrete prisms. A good laboratory performance test should take into account these parameters to avoid a too low internal RH in the concrete prisms.
- It is essential to keep the internal prism temperature constant during all measurements, because the recorded expansion is rather sensitive to a moderately deviating prism temperature at the time of measuring compared with the temperature during the reference readings. The time of reading the prism reference length might also be of importance, in particular for concretes showing some shrinkage in the early age (e.g. when testing binders with high extent of self-desiccation).
- The extent of alkali leaching, one of the biggest challenges during accelerated ASR testing in the laboratory, should be minimised. It is important to account for alkali leaching when drawing conclusions based on a performance test.
- The rate and extent of alkali leaching are heavily influenced by the storage and exposure conditions. The following parameters are of particular importance:
  - ○ Reduced alkali leaching occurs with larger prism size, lower concrete permeability, lower exposure temperature and less moisture condensing on the prism surfaces.
  - ○ Increased alkali leaching occurs when prisms are submerged in water or exposed to extreme moisture conditions (e.g. fog chamber), prisms wrapped in wet cotton cloth or prisms subjected to drying and wetting cycles (e.g. during cooling before measuring).
- To make a performance test more practical, there is a need to find a way to accelerate the reaction, e.g. by elevating the storage temperature. However, exposing the prisms to 60 °C during ASR testing might be questionable due to several reasons:
  - ○ Lack of experience with respect to laboratory-field correlation.
  - ○ Higher rate of silica dissolution and alkali release from aggregates.
  - ○ The concentration of sulphates in the concrete pore water increases with increasing temperature, and thus the concentration of OH^- is reduced correspondingly.
  - ○ The influence of the pre-curing conditions (e.g. length of curing at ambient temperature before starting the ASR test) on the prism expansion might be of higher importance, dependent on the type of binder.
  - ○ The alkali binding capacity is influenced by the exposure temperature.
  - ○ The pozzolanic reactivity of the SCM or the ggbs used might be accelerated significantly, and thus contribute to a poorer laboratory/field correlation.
- To build up experience with ASR testing at 60 °C and collect data for evaluation of the laboratory/field correlation, research laboratories are encouraged to keep on testing various concretes by use of the RILEM AAR-4.1 test method and cast concrete cubes for outdoor exposure. Also the extent of alkali leaching should be documented.
- In a performance test, exposure of the test prisms to temperatures above 60 °C should be avoided. At such high temperatures, some other deterioration mechanisms may occur, e.g. DEF.

7. Further research

The literature survey has identified several issues that need further research in order to develop a reliable performance test procedure. Among the most important ones are:

- Among current test procedures, a variant of a 38 °C concrete prism test seems to be the best candidate to be developed as a performance test method. However, the period of testing is a major drawback. More research is thus needed to find a reliable way of accelerating a performance test method to make it more practical.
- Testing and assessment of alkali release from aggregates is a matter of extensive dispute for their use in concrete. The task group “Releasable alkalis” in RILEM TC 219-ACS is presently developing a reliable test procedure for such measurements.
- There is a gap in knowledge internationally whether LWAs might give deleterious ASR in real structures. There are no internationally agreed requirements regarding how to test and evaluate the alkali reactivity of a LWA or a LWAC in the laboratory.
- More research is needed to investigate whether test results obtained with one type of OPC are also valid for other types of OPCs or if each OPC has to be tested separately, because there are contradictory findings in the literature about the influence of the Na/K ratio on the ASR expansion.
- More research is needed to evaluate the effect of alkali boosting with different binder types and/or OPCs with different alkali levels, because some alkali boosting might be needed to compensate for small changes in the cement alkali content.
- The net influence of a reduced w/cm ratio should be investigated further as the basis to agree on a possible lower w/cm limit for performance testing.
- It is of urgent importance to try to reduce the rate and extent of alkali leaching in future performance test methods.
- Further research is necessary to test the performance of special concrete mixtures, e.g. self compacting concrete and fibre-reinforced concrete, because the design considerations (restricted aggregate size, high filler content, inclusion of other ingredients), in addition to physical (e.g., permeability, unit weight) and mechanical (e.g., strength, toughness) properties of these special concretes might differ from ordinary concrete.

Acknowledgement

We greatly acknowledge all RILEM TC 219-ACS members and the TC Chairman and Secretary. We are particularly thankful to the authors that took part in the literature survey report performed within the task group “Performance testing”, in which has formed the basis for this review paper. The authors would also like to acknowledge COIN, the COncrete INnovation centre (www.coinweb.no) for the financial support to the PhD study of the principle author.

References

[1] EN 206–1 Concrete—Part 1: Specification, performance, production and conformity, 2001.
[2] J. Lindgård, Ö. Andiç-Çakır, I. Borchers, M. Broekmans, E. Brouard, I. Fernandes, C. Giebson, B. Pedersen, C. Pierre, T.F. Rønning, M.D.A. Thomas, B.J. Wigum, RILEM TC 219-ACS-P: Literature survey on performance testing, COIN project report 27, ISBN: 978-82-536-1209-6, 2011, p. 164.

[3] D.E. Stanton, The expansion of concrete through reaction between cement and aggregate, American Society of Civil Engineers, 66, 1940, pp. 1781–1811.

[4] RILEM TC 191-ARP: 'Alkali-reactivity and prevention—assessment, specification and diagnosis of alkali-reactivity', RILEM recommended test method AAR-1: detection of potential alkali-reactivity of aggregates—petrographic method, Mater. Struct. 36 (2003) 480–496.

[5] RILEM TC 106-AAR, 'Alkali aggregate reaction' A. TC 106-2—Detection of potential alkali-reactivity of aggregates—the ultra-accelerated mortar-bar test B. TC 106-3—Detection of potential alkali-reactivity of aggregates—method for aggregate combinations using concrete prisms, Mater. Struct. 33 (2000) 283–293.

[6] RILEM TC 219-ACS 'Alkali–silica reactions in Concrete Structures': RILEM AAR-4.1—Detection of potential alkali-reactivity of aggregates: accelerated (60°C) concrete prism test, (unpublished draft), (2006).

[7] RILEM TC 191-ARP: 'Alkali-reactivity and prevention—assessment, specification and diagnosis of alkali-reactivity', AAR-5: Rapid preliminary screening test for carbonate aggregates, Mater. Struct. 38 (2005) 787–792.

[8] RILEM TC 191-ARP: 'Alkali-reactivity and prevention—assessment, specification and diagnosis of alkali-reactivity', RILEM recommended test method AAR-0: Detection of alkali-reactivity potential in concrete—outline guide to the use of RILEM methods in assessments of aggregates for potential alkali-reactivity, Mater. Struct. 36 (2003) 472–479.

[9] RILEM TC 219-ACS 'Alkali–silica reactions in concrete structures': recommended specification: AAR-7.1 International Specification to minimise damage from alkali reactions in concrete Part 1, Alkali–silica reaction, (unpublished draft), (2008).

[10] ASTM C1260—07 Standard Test Method for Potential Alkali Reactivity of Aggregates (Mortar-Bar Method), American Society for Testing and Materials, Annual Book of ASTM Standards, 2007, p. 5.

[11] ASTM C1293—08b Standard Test Method for Determination of Length Change of Concrete Due to Alkali–Silica Reaction, American Society for Testing and Materials, Annual Book of ASTM Standards, 2008, p. 7.

[12] ASTM C295—08 Standard Guide for Petrographic Examination of Aggregates for Concrete, American Society for Testing and Materials, Annual Book of ASTM Standards, 2008, p. 8.

[13] CSA, CSA A23.2-14A-00, Potential expansivity of aggregates (procedure for length change due to alkali–aggregate reaction in concrete prisms at 38 °C), Methods of Testing for Concrete, Canadian Standards Association, Mississauga, Ontario, Canada, 2004, pp. 246–256.

[14] CAN/CSA-A23, 2-25A-09 Test Method for Detection of Alkali–Silica Reactive Aggregate by Accelerated Expansion of Mortar Bars, Canadian Standards Association, 2009.

[15] CSA A23.2-15A, Petrographic examination of aggregates, Canadian Standards Association, 2004.

[16] M.D.A. Thomas, R.F. Bleszynski, The use of silica fume to control expansion due to alkali–aggregate reactivity in concrete—a review, in: J. Skalny, S. Mindess (Eds.), Materials Science of Concrete VI, American Ceramics Society, 2000, pp. 377–433.

[17] J. Duchesne, M.-A. Bérubé, Long-term effectiveness of supplementary cementing materials against alkali–silica reaction, Cem. Concr. Res. 31 (2001) 1057–1063.

[18] ACI, State of the art report on alkali aggregate reactivity, ACI Committee 221, ACI 221.1R-98, 1998, p. 31.

[19] M. Böhm, S. Baetzner, The effect of the alkalinity of the pore solution on ASR, in: M.A.T.M. Broekmans, B.J. Wigum (Eds.), 13th International Conference on Alkali–Aggregate Reactions in Concrete, Trondheim, Norway, 2008, pp. 501–510.

[20] P. Rivard, M.-A. Bérubé, J.-P. Ollivier, G. Ballivy, Alkali mass balance during the accelerated concrete prism test for alkali–aggregate reactivity, Cem. Concr. Res. 33 (2003) 1147–1153.

[21] R.G. Sibbick, C.L. Page, Threshold alkali contents for expansion of concretes containing British aggregates, Cem. Concr. Res. 22 (1992) 990–994.

[22] M.D.A. Thomas, The effect of supplementary cementing materials on alkali–silica reaction: a review, Cem. Concr. Res. 41 (2011) 1224–1231.

[23] Norwegian Concrete Association: Alkali–aggregate reactions in concrete, Test methods and Requirements to Test Laboratories, NB32, 2005, p. 39.

[24] M. Thomas, B. Fournier, K. Folliard, J. Ideker, M. Shehata, Test methods for evaluating preventive measures for controlling expansion due to alkali–silica reaction in concrete, Cem. Concr. Res. 36 (2006) 1842–1856.

[25] D.W. Hobbs, Alkali–silica Reaction in Concrete, Thomas Telford Ltd, London, 1988.

[26] F.P. Glasser, Chemistry of the alkali–aggregate reaction, in: R.N. Swamy (Ed.), The Alkali–Silica Reaction in Concrete, Blackie and Son Ltd, London, 1992, p. 333.

[27] D.A. St John, A.B. Poole, I. Sims, Concrete Petrography—A Handbook of Investigative Techniques, Arnold, U.K, 1998, p. 474.

[28] ASTM C294—05 Standard Descriptive Nomenclature for Constituents of Concrete Aggregates, American Society for Testing and Materials, Annual Book of ASTM Standards, 2005, p. 10.

[29] BS 7943:1999, Guide to the Interpretation of Petrographical Examinations for Alkali–Silica Reactivity, ISBN: 0580282732, 1999, p. 20.

[30] M.-A. Bérubé, B. Fournier, Canadian experience with testing for alkali–aggregate reactivity in concrete, Cem. Concr. Compos. 15 (1993) 27–47.

[31] B. Fournier, M.-A. Bérubé, Alkali–aggregate reaction in concrete: a review of basic concepts and engineering implications, Can. J. Civ. Eng. 27 (2000) 167–191.

[32] I. Sims, P. Nixon, Assessment of aggregates for alkali–aggregate reactivity potential: RILEM International Recommendations, in: B. Fournier (Ed.), Marc-André Bérubé Symposium on Alkali–Aggregate Reactivity in Concrete, Canada, 2006, pp. 71–91.

[33] P.E. Grattan-Bellew, Petrographic and Technological Methods for Evaluation of Concrete Aggregates, in: V.S. Ramachandran, J.J. Beaudoin (Eds.), Handbook of analytical techniques in concrete science and technology Principles, Techniques, and Applications, Noyes Publications, 2001, pp. 63–98.

[34] P.M. Dove, J.D. Rimstidt, Silica–water interactions, in: P.J. Heaney, C.T. Prewitt, G.V. Gibbs (Eds.), Silica: physical behaviour, geochemistry and materials applications Reviews in Mineralogy, Mineralogical Society of America, 1994, pp. 259–308.

[35] M.A.T.M. Broekmans, Structural properties of quartz and their potential role for ASR, Mater. Charact. 53 (2004) 129–140.

[36] B. Fournier, R. Chevrier, M. DeGrosbois, R. Lisella, K. Folliard, J. Ideker, M. Shehata, M. Thomas, S. Baxter, The accelerated concrete prism test (60°C): variability of the test method and proposed expansion limits, in: M. Tang, M. Deng (Eds.), 12th International Conference on Alkali–Aggregate Reaction in Concrete, International Academic Publishers—World Publishing Corporation, Beijing, China, 2004, pp. 314–323.

[37] J. Lindgård, P.J. Nixon, I. Borchers, B. Schouenborg, B.J. Wigum, M. Haugen, U. Åkesson, The EU "PARTNER" Project—European standard tests to prevent alkali reactions in aggregates: Final results and recommendations, Cem. Concr. Res. 40 (2010) 611–635.

[38] I. Fernandes, F. Noronha, M. Teles, Microscopic analysis of alkali–aggregate reaction products in a 50-year-old concrete, Mater. Charact. 53 (2004) 295–306.

[39] A. Shayan, A. Xu, H. Morris, Comparative study of the concrete prism test (CPT 60°C, 100% RH) and other accelerated tests, in: M.A.T.M. Broekmans, B.J. Wigum (Eds.), 13th International Conference on Alkali–Aggregate Reactions in Concrete, Trondheim, Norway, 2008, pp. 391–400.

[40] J.H. Ideker, K.J. Folliard, B. Fournier, M.D.A. Thomas, The role of "non-reactive" aggregates in the accelerated (60 °C) concrete prism test, in: B. Fournier (Ed.), Marc-André Bérubé Symposium on Alkali–Aggregate Reactivity in Concrete, Montreal, Canada, 2006, pp. 45–70.

[41] M.A.T.M. Broekmans, The alkali–silica reaction: mineralogical and geochemical aspects of some Dutch concretes and Norwegian mylonites, PhD. Thesis, in, University of Utrecht, 2002, pp. 144.

[42] H.R. Wenk, P.J. Monteiro, K. Shomglin, Relationship between aggregate microstructure and mortar expansion. A case study of deformed granitic rocks from the Santa Rosa mylonite zone, J. Mater. Sci. 43 (2008) 1278–1285.

[43] B.S. Gogte, An evaluation of some common Indian rocks with special reference to alkali–aggregate reactions, Eng. Geol. 7 (1973) 135–153.

[44] D.M. Kerrick, R.D. Hooton, ASR of concrete aggregate quarried from a fault zone: results and petrographic interpretation of accelerated mortar bar tests, Cem. Concr. Res. 22 (1992) 949–960.

[45] J.E. Gillott, Alkali–aggregate reactions in concrete, Eng. Geol. 9 (1975) 303–326.

[46] P.H. Besem, P. Demars, Reactions alkalis-granulats dans le beton, Annales des Travaux Publics de Belgique, 4, Ministère des Travaux Publics, Belgique, 1989.

[47] The Institution of Structural Engineers, Structural effects of alkali–silica reaction, Technical guidance on the appraisal of existing structures, London, 1992, p. 48.

[48] A. Le Roux, Les mécanismes mis en jeu dans les dégradations dues à l'alcali-réaction, Seminário Degradação de Estruturas por Reacções Expansivas de Origem Interna, LNEC, Lisbon, 2001.

[49] A. Shayan, The pessimum effect in an accelerated mortar bar test using 1 M NaOH solution at 80 °C, Cem. Concr. Compos. 14 (1992) 249–255.

[50] F. Bektas, L. Turanli, T. Topal, M.C. Goncuoglu, Alkali reactivity of mortars containing chert and incorporating moderate-calcium fly ash, Cem. Concr. Res. 34 (2004) 2209–2214.

[51] A.D. Buck, K. Mather, Methods for controlling effects of alkali–silica reaction in concrete, Army Engineer Waterways Experiment Station Vicksburg MS Structures Lab, Accession no ADA178479, 1987, p. 69.

[52] T. Knudsen, N. Thaulow, Quantitative microanalyses of alkali–silica gel in concrete, Cem. Concr. Res. 5 (1975) 443–454.

[53] M. Regourd, H. Hornain, Microstructure of reaction products, in: P.E. Grattan-Bellew (Ed.), 7th International Conference on Alkali–Aggregate Reactions in Concrete, Ottawa, 1986, pp. 375–380.

[54] M. Regourd-Moranville, Products of reaction and petrographic examination, 8th International Conference on Alkali–Aggregate Reactions in Concrete, Kyoto, 1989, pp. 445–456.

[55] N. Thaulow, U.H. Jakobsen, B. Clark, Composition of alkali silica gel and ettringite in concrete railroad ties: SEM-EDX and X-ray diffraction analyses, Cem. Concr. Res. 26 (1996) 309–318.

[56] M. Kawamura, N. Arano, T. Terashima, Composition of ASR gels and expansion of mortars, in: M. Cohen, S. Mindess, J. Skalny (Eds.), Materials Science of Concrete: Special Volume—The Sidney Diamond Symposium, American Ceramic Society, Westerville, OH, 1998, pp. 261–276.

[57] S. Diamond, Chemistry and other characteristics of ASR gels, in: M.-A. Bérubé, B. Fournier, B. Durand (Eds.), 11th International Conference on Alkali Aggregate Reactions in Concrete, Québec, Canada, 2000, pp. 31–40.

[58] M.-A. Bérubé, B. Fournier, Les produits de la réaction alcali-silice dans le béton: étude de cas de la région de Québec, Can. Mineral. 24 (1986) 271–288.

[59] M. Brouxel, The alkali–aggregate reaction rim: Na2O, SiO2, K2O and CaO chemical distribution, Cem. Concr. Res. 23 (1993) 309–320.

[60] BRE Digest 330, Alkali–silica reaction in concrete—Background to the guidance notes, Part 1, 2 and 3, BRE Press, 2004.

[61] D. Lu, B. Fournier, P.E. Grattan-Bellew, Evaluation of accelerated test methods for determining alkali–silica reactivity of concrete aggregates, Cem. Concr. Compos. 28 (2006) 546–554.

[62] S. Diamond, N. Thaulow, A study of expansion due to alkali–silica reaction as conditioned by the grain size of the reactive aggregate, Cem. Concr. Res. 4 (1974) 591–607.

[63] K. Peterson, D. Gress, T. Van Dam, L. Sutter, Crystallized alkali–silica gel in concrete from the late 1890s, Cem. Concr. Res. 36 (2006) 1523–1532.

[64] I. Fernandes, Composition of alkali–silica reaction products at different locations within concrete structures, Mater. Charact. 60 (2009) 655–668.

[65] M.D.A. Thomas, The role of calcium in alkali–silica reaction, in: M. Cohen, S. Mindess, J. Skalny (Eds.), Materials Science of Concrete: The Sidney Diamond Symposium, American Ceramic Society, Westerville, OH, 1998, pp. 325–337.

[66] D. Lu, B. Fournier, P. Grattan-Bellew, Y. Lu, Z. Xu, M. Tang, Expansion behaviour of Spratt and Pittsburg limestones in different test procedures, in: M.A.T.M. Broekmans, B.J. Wigum (Eds.), 13th International Conference on Alkali–Aggregate Reactions in Concrete, Trondheim, Norway, 2008, pp. 619–627.

[67] S. Multon, M. Cyr, A. Sellier, P. Diederich, L. Petit, Effects of aggregate size and alkali content on ASR expansion, Cem. Concr. Res. 40 (2010) 508–516.

[68] S. Multon, M. Cyr, A. Sellier, N. Leklou, L. Petit, Coupled effects of aggregate size and alkali content on ASR expansion, Cem. Concr. Res. 38 (2008) 350–359.

[69] C. Zhang, A. Wang, M. Tang, B. Wu, N. Zhang, Influence of aggregate size and aggregate size grading on ASR expansion, Cem. Concr. Res. 29 (1999) 1393–1396.

[70] D.W. Hobbs, W.A. Gutteridge, Particle size of aggregate and its influence upon the expansion caused by the alkali–silica reaction, Mag. Concr. Res., Cem. Concr. Assoc. 31 (1979) 235–242.

[71] G. Barisone, G. Restivo, Alkali–silica reactivity of some Italian opal and flints tested using a modified mortar bar test, in: M.A. Bérubé, B. Fournier, B. Durand (Eds.), 11th International Conference on Alkali–Aggregate reaction in Concrete, 2000, pp. 239–245.

[72] D. Lu, B. Fournier, P. Grattan-Bellew, Effect of aggregate particles size on determining alkali–silica reactivity by accelerated tests, J. ASTM Int. 3 (2006) 11.

[73] B. Wigum, J. Lindgård, AAR: Testing, mitigation & recommendations. The Norwegian approach during two decades of research, in: M.A.T.M. Broekmans, B.J. Wigum (Eds.), 13th ICAAR—International Conference on Alkali–Aggregate Reactions, Trondheim, 2008, pp. 1299–1309.

[74] Norwegian Concrete Association: Durable concrete containing alkali reactive aggregates, NB21, 2004, p. 33.

[75] K. Ramyar, A. Topal, Ö. Andiç-Çakır, Effects of aggregate size and angularity on alkali–silica reaction, Cem. Concr. Res. 35 (2005) 2165–2169.

[76] H. Zhu, W. Chen, W. Zhou, E.A. Byars, Expansion behaviour of glass aggregates in different testing for alkali–silica reactivity, Mater. Struct. 42 (2009) 485–494.

[77] B. Pedersen, Alkali-reactive and inert fillers in concrete, Rheology of fresh mixtures and expansive reactions, PhD-thesis, Norwegian University of Science and Technology, Trondheim, Norway, 2004, p. 292.

[78] J.H.P. van Aardt, S. Visser, Reaction of Ca(OH)2 and of Ca(OH)2 + CaSO4 2H2O at various temperatures with feldspars in aggregates used for concrete making, Cem. Concr. Res. 8 (1978) 677–681.

[79] P.E. Grattan-Bellew, Alkali contribution from limestone aggregate to pore solution of old concrete, ACI Mater. J., Am. Concr. Inst. 91 (1994) 173–177.

[80] M.-A. Bérubé, J.F. Dorion, M. Rivest, Distribution of alkalis in concrete structures affected by alkali–silica reactivity and contribution by the aggregates, in: M.-A. Bérubé, B. Fournier, B. Durand (Eds.), 11th International Conference on Alkali–Aggregate Reaction in Concrete, Canada, 2000, pp. 139–148.

[81] M.-A. Bérubé, J. Duchesne, J.F. Dorion, M. Rivest, Laboratory assessment of alkali contribution by aggregates to concrete and application to concrete structures affected by alkali–silica reactivity, Cem. Concr. Res. 32 (2002) 1215–1227.

[82] D. Constantiner, S. Diamond, Alkali release from feldspars into pore solutions, Cem. Concr. Res. 33 (2003) 549–554.

[83] D. Lu, X. Zhou, Z. Xu, X. Lan, M. Tang, B. Fournier, Evaluation of laboratory test method for determining the potential alkali contribution from aggregate and the ASR safety of the Three-Gorges dam concrete, Cem. Concr. Res. 36 (2006) 1157–1165.

[84] Y. Wang, G. Yu, M. Deng, M. Tang, D. Lu, The use of thermodynamic analysis in assessing alkali contribution by alkaline minerals in concrete, Cem. Concr. Compos. 30 (2008) 353–359.

[85] M. Kawamura, M. Koike, K. Nakano, Release of alkalies from reactive andesitic aggregates and fly ashes into pore solution in mortars, in: K. Okada, S. Nishibayashi, M. Kawamura (Eds.), 8th International conference on Alkali–Aggregate Reaction, Society of Materials Science, Kyoto, Japan, 1989, pp. 271–278.

[86] LCPC, Essai de granulats, Détermination des alcalins solubles dans l'eau de chaux, Méthod D'Essai LPC nº 37, Paris, 1993.

[87] M.-A. Bérubé, J. Frenette, M. Rivest, D. Vézina, Measurement of the active alkali content of concrete using hot-water extraction, in: M.-A. Bérubé, B. Fournier, B. Durand (Eds.), 11th International Conference on Alkali–Aggregate reaction in Concrete, Canada, 2000, pp. 159–168.

[88] STRUCTURAL LWAC Specification and guideline for materials and production, The European Union—Brite EuRam III, EuroLightCon, Economic Design and Construction with Light Weight Aggregate Concrete, Contract BRPR-CT97-0381, Project BE96-3942, Document BE96-3942/R14, ISBN: 90 376 0108 1, 2000, p. 69.

[89] Matsuda, et al., Investigation of structures using lightweight aggregate, Upgrade Symposium on Concrete Repair and Reinforcement, Kyoto, Japan, 2004.

[90] J. Lindgård, H. Justnes, M. Haugen, P.A. Dahl, Alkali aggregate reactions in LWAC —introductory laboratory testing, SINTEF report SBF52 F06004, Trondheim, Norway, 2006.

[91] A. Leemann, B. Lothenbach, The influence of potassium–sodium ratio in cement on concrete expansion due to alkali–aggregate reaction, Cem. Concr. Res. 38 (2008) 1162–1168.

[92] A. Leemann, B. Lothenbach, The Na2O-equivalent of cement: a universal parameter to assess the potential alkali–aggregate reactivity of concrete? in: M.A.T.M. Broekmans, B.J. Wigum (Eds.), 13th International Conference on Alkali–Aggregate Reactions in Concrete, Trondheim, Norway, 2008, pp. 909–919.

[93] S. Bremseth, Perfomance testing of laboratory made and full scale production of fly ash cement at the Kjøpsvik plant, Norcem AS internal R&D project report no 9RD4/R10034, Brevik, Norway, 2010, p. 35.

[94] X. Hou, L.J. Struble, R.J. Kirkpatrick, Formation of ASR gel and the roles of C–S–H and portlandite, Cem. Concr. Res. 34 (2004) 1683–1696.

[95] I. Borchers, C. Müller, Einfluss von Natrium und Kalium auf eine schädigende AKR in Abhängigkeit von der Gesteinskörnung, Bauhaus-Universität Weimar (Hrsg): Proceedings at the 17 Internationale Baustofftagung : (Weimar 23-26092009), Weimar, Germany, 2009, pp. S. 2-0211-0212-0216.

[96] T.C. Powers, H.H. Steinour, An interpretation of some published researches on the alkali–aggregate reaction part I—the chemical reactions and mechanism of expansion, J. Am. Concr. Inst. 51 (1955) 497–516.

[97] W.J. French, Maintenance of mobile alkali concentration in cement paste during alkali–aggregate reactions, in: K. Okada, S. Nishibayashi, M. Kawamura (Eds.), Paper distributed at the 8th International conference on Alkali–Aggregate Reaction, Kyoto, Japan, 1989.

[98] B. Lagerblad, J. Trägårdh, Slowly reacting aggregates in Sweden—mechanism and conditions for reactivity in concrete, in: A.B. Poole (Ed.), 9th International Conference on Alkali–Aggregate Reaction in Concrete, Concrete Society Publication CS.104, London, 1992, pp. 570–578.

[99] A.B. Poole, Chemistry of the alkali–aggregate reaction, in: R.N. Swamy (Ed.), The Alkali–Silica Reaction in Concrete, Blackie and Son Ltd, London, 1992, p. 333.

[100] M.D.A. Thomas, M.H. Shehata, Use of blended cements to control expansion of concrete due to alkali–silica reaction, 8th CANMET/ACI Int Conf on Fly Ash, Silica Fume, Slag and Natural Pozzolans in Concrete, Supplementary Papers, Las Vegas, 2004, pp. 591–607.

[101] M.D.A. Thomas, K.J. Folliard, Concrete aggregates and the durability of concrete, in: C.L. Page, M.M. Page (Eds.), Durability of Concrete and Cement Composites, Woodhead, Cambridge, UK, 2007, pp. 247–281.

[102] S. Diamond, R.S. Barneyback, L.J. Struble, On the physics and chemistry of alkali–silica reactions, 5th International Conference on Alkali–Aggregate Reaction, Cape Town, 1981, p. S252/222.

[103] J.J. Kollek, S.P. Varma, C. Zaris, Measurement of OH^- concentrations of pore fluids and expansion due to alkali–silica reaction in composite cement mortars, 8th International Congress on the Chemistry of Cement, Rio de Janeiro, 1986, pp. 183–189.

[104] M.D.A. Thomas, Review of the effect of fly ash and slag on alkali–aggregate reaction in concrete, BRE Report, Building Research Establishment Report, BR 314, Construction Research Communications, Watford, UK, 1996, p. 117.

[105] H. Kagimoto, I. Inoshita, M. Kawamura, Threshold OH^- concentration in pore solution of mortar using alkali reactive aggregates, in: M. Tang, M. Deng (Eds.), 12th International Conference on Alkali–Aggregate Reaction in Concrete, Beijing, China, 2004, pp. 728–735.

[106] M.H. Shehata, M.D.A. Thomas, Alkali release characteristics of blended cements, Cem. Concr. Res. 36 (2006) 1166–1175.

[107] S.Y. Hong, F.P. Glasser, Alkali sorption by C–S–H and C–A–S–H gels: Part II. Role of alumina, Cem. Concr. Res. 32 (2002) 1101–1111.

[108] R.F. Bleszynski, The performance and durability of concrete with ternary blends of silica fume and blast-furnace slag, PhD thesis, University of Toronto, 2002.

[109] T. Ramlochan, M. Thomas, K.A. Gruber, The effect of metakaolin on alkali–silica reaction in concrete, Cem. Concr. Res. 30 (2000) 339–344.

[110] M.H. Shehata, M.D.A. Thomas, The effect of fly ash composition on the expansion of concrete due to alkali–silica reaction, Cem. Concr. Res. 30 (2000) 1063–1072.

[111] M.H. Shehata, M.D.A. Thomas, Use of ternary blends containing silica fume and fly ash to suppress expansion due to alkali–silica reaction in concrete, Cem. Concr. Res. 32 (2002) 341–349.

[112] M.D.A. Thomas, F.A. Innis, Effect of slag on expansion due to alkali–aggregate reaction in concrete, ACI Mater. J. 95 (1998) 716–724.

[113] J. Duchesne, M.-A. Bérubé, Effect of supplementary cementing materials on the composition of cement hydration products, Adv. Cem. Based Mater. 2 (1995) 43–52.

[114] H.F.W. Taylor, Cement Chemistry, Academic Press, London, 1990, p. 491.

[115] F. Naiqian, J. Hongwei, C. Enyi, Study on the suppression effect of natural zeolite on expansion of concrete due to alkali–aggregate reaction, Mag. Concr. Res. 50 (1998) 17–24.

[116] S. Nagataki, H. Ohga, T. Inoue, Evaluation of fly ash for controlling alkali–aggregate reaction, 2nd International Conference on Durability of Concrete, Montreal, Canada, 1991, pp. 955–972.

[117] E. Schäfer, Einfluss der Reaktionen verschiedener Zementhauptbestandteile auf den Alkalihaushalt der Porenlösung des Zementsteins, Schriftenreihe der Zementindustrie (TU Clausthal, Dissertation 2004), 69 (2006).

[118] M.H. Shehata, M.D.A. Thomas, R.F. Bleszynski, The effects of fly ash composition on the chemistry of pore solution in hydrated cement pastes, Cem. Concr. Res. 29 (1999) 1915–1920.

[119] R.G. Sibbick, C.L. Page, Effects of pulverized fuel ash on alkali–silica reaction in concrete, Constr. Build. Mater. 9 (1995) 289–293.

[120] M.D.A. Thomas, R.D. Hooton, C.A. Rogers, Prevention of damage due to alkali–aggregate reaction (AAR) in concrete construction—Canadian approach, Cem. Concr. Aggregates 19 (1997) 26–30.

[121] A. Shayan, R. Diggins, I. Ivanusec, Effectiveness of fly ash in preventing deleterious expansion due to alkali–aggregate reaction in normal and steam-cured concrete, Cem. Concr. Res. 26 (1996) 153–164.

[122] M. Thomas, A. Dunster, P. Nixon, B. Blackwell, Effect of fly ash on the expansion of concrete due to alkali–silica reaction—exposure site studies, Cem. Concr. Compos. 33 (2011) 359–367.

[123] H. Cheng-yi, R.F. Feldman, Influence of silica fume on the microstructural development in cement mortars, Cem. Concr. Res. 15 (1985) 285–294.

[124] N. Arano, M. Kawamura, Comparative consideration on the mechanism of ASR suppression due to different mineral admixtures, in: M.A. Bérubé, B. Fournier, B. Durand (Eds.), 11th International Conference on Alkali–Aggregate reaction in Concrete, Quebec, Canada, 2000, pp. 553–562.

[125] D. Hester, C. McNally, M. Richardson, A study of the influence of slag alkali level on the alkali–silica reactivity of slag concrete, Constr. Build. Mater. 19 (2005) 661–665.

[126] Q. Zhao, J. Stark, E. Freyburg, M. Zhou, The mechanism of GBFS preventing AAR: a discussion, in: M.A.T.M. Broekmans, B.J. Wigum (Eds.), 13th International Conference on Alkali–Aggregate Reactions in Concrete, Trondheim, Norway, 2008, pp. 410–411.

[127] R. Bleszynski, R.D. Hooton, M.D.A. Thomas, C.A. Rogers, Durability of ternary blend concrete with silica fume and blast-furnace slag: laboratory and outdoor exposure site studies, ACI Mater. J. (2002 September–October) 499–508.

[128] M.H. Khan, K. Mohan, H.F.W. Taylor, Pastes of tricalcium silicate with rice husk ash, Cem. Concr. Res. 15 (1985) 89–92.

[129] F. Naiqian, H. Tingyu, Mechanism of natural zeolite powder in preventing alkali–silica reaction in concrete, Adv. Cem. Res. 10 (1998) 101–108.

[130] B. Pedersen, E. Mørtsell, V. Jensen, Effects of alkali-reactive crushed fillers on expansions due to ASR, in: T. Mingshu, D. Min (Eds.), 12th International Conference on Alkali–Aggregate Reactions in Concrete, Beijing, China, 2004, pp. 764–772.

[131] F.W. Locher, Zement—Grundlagen der Herstellung und Verwendung, Verlag Bau + Technik GmbH, Düsseldorf, 2000.

[132] T. Slamecka, F. Skvara, The effect of water ratio on microstructure and composition of the hydration products of portland cement pastes, Ceramics-Silikaty 46 (2002) 152–158.

[133] J. Stark, D. Erfurt, E. Freyburg, C. Giebson, K. Seyfarth, B. Wicht, Alkali-Kieselsäure-Reaktion (Alkali–Silica Reaction), Series of publications No. 3, Bauhaus-University, F.A. Finger Institute for building materials science, Weimar, 2008.

[134] C. Larive, A. Laplaud, O. Coussy, The role of water in alkali–silica reaction, in: M.-A. Bérubé, B. Fournier, B. Durand (Eds.), 11th International Conference on Alkali–Aggregate Reaction, Québec, Canada, 2000, pp. 61–69.

[135] T.A. Hammer, Ø. Bjøntegaard, E.J. Sellevold, Internal curing—role of absorbed water in aggregates, in: J.P. Ries, A. H.T. (Eds.), ACI SP-218 High-performance structural lightweight concrete, Farmington Hills, Michigan, 2004, pp. 131–142.

[136] P. Lura, O.M. Jensen, S.I. Igarashi, Experimental observation of internal water curing of concrete, Mater. Struct. 40 (2007) 211–220.

[137] M.S. Meddah, R. Sato, Effect of curing methods on autogenous shrinkage and self-induced stress of high-performance concrete, ACI Mater. J., Am. Concr. Inst. 101 (2010) 65–74.

[138] Ø. Bjøntegaard, Volume changes and cracking tendency of concrete, Compendium, Norwegian University of Science and Technology, Department of Structural Engineering, Trondheim, Norway, 2004, p. 34.

[139] G. Toma, M. Pigeon, J. Marchand, B. Bissonnette, L. Barcelo, Early age restrained shrinkage: stress build up and relaxation, International research seminar: Self-desiccation and Its Importance in Concrete Technology, Lund, Sweden, June 18., 1999, pp. 61–71.

[140] S. Kamali, B. Gérard, M. Moranville, Modelling the leaching kinetics of cement-based materials—influence of materials and environment, Cem. Concr. Compos. 25 (2003) 451–458.

[141] S. Kamali, M. Moranville, S. Leclercq, Material and environmental parameter effects on the leaching of cement pastes: experiments and modelling, Cem. Concr. Res. 38 (2008) 575–585.

[142] D. Stark, The moisture condition of field concrete exhibiting alkali–silica reactivity, Second International Conference on Durability of Concrete, 126/52, ACI Publication SP, 1991, pp. 973–987.

[143] E. Sellevold, Resistivity and humidity measurements of repaired and non-repaired areas in Gimsøystraumen bridge, International Conference: Repair of concrete structures, from theory to practice in a marine environment, Svolvær, Norway, 1993.

[144] Y. Yang, X. Zhenjian, C. Weizhong, C. Min, Distribution of water content in self-compacted high strength concrete due to water evaporation and self-desiccation, RILEM Proceedings PR042, First International Symposium on Design, Performance and Use of Self-Consolidating Concrete, SCC'2005, Changsha, Hunan, China, 2005, pp. 173–180.

[145] D. Stark, Effects of water–cement ratio on expansion due to ASR, Concrete Technology Today, Portland Cement Association, Skokie, Illinois, 1995, pp. 3–5.

[146] B. Fournier, J. Ideker, K. Folliard, M.D.A. Thomas, P.C. Nkinamubanzi, R. Chevrier, Effect of environmental conditions on expansion in concrete due to alkali–silica reaction (ASR), in: M.A.T.M. Broekmans, B.J. Wigum (Eds.), 13th International Conference on Alkali–Aggregate Reactions in Concrete, Trondheim, Norway, 2008, pp. 637–646.

[147] S. Chatterji, N. Thaulow, A.D. Jensen, Studies of alkali–silica reaction. Part 4. Effect of different alkali salt solutions on expansion, Cem. Concr. Res. 17 (1987) 777–783.

[148] M.-A. Bérubé, B. Fournier, Alkalis releasable by aggregates in concrete—significance and test methods, in: M. Tang, M. Deng (Eds.), 12th International Conference on Alkali–Aggregate reaction in Concrete, International Academic Publishers—World Publishing Corporation, Beijing, China, 2004, pp. 17–30.

[149] H. Wang, J.E. Gillott, Mechanism of alkali–silica reaction and the significance of calcium hydroxide, Cem. Concr. Res. 21 (1991) 647–654.

[150] J. Stark, E. Freyburg, K. Seyfarth, C. Giebson, D. Erfurt, 70 years of ASR with no end in sight? ZKG International, No. 4-2010, pp. 86–95 (part 1) and No. 5-2010, 2010, pp. 55–70, (part 2).

[151] P.K. Mehta, Studies on chemical resistance of low water/cement ratio concretes, Cem. Concr. Res. 15 (1985) 969–978.

[152] R. Rixom, N. Mailvaganam, Chemical Admixtures for Concrete, Taylor & Francis, 1999, p. 437.

[153] A.D. Jensen, S. Chatterji, P. Christensen, N. Thaulow, Studies of alkali–silica reaction—part II effect of air-entrainment on expansion, Cem. Concr. Res. 14 (1984) 311–314.

[154] P. Hagelia, Origin of map cracking in view of the distribution of air voids, strength and ASR-gel, in: M. Tang, M. Deng (Eds.), 12th International Conference on Alkali–Aggregate reaction in Concrete, International Academic Publishers—World Publishing Corporation, Beijing, China, 2004, pp. 870–881.

[155] B. Fournier, J.H. Ideker, K.J. Folliard, M.D.A. Thomas, P.-C. Nkinamubanzi, R. Chevrier, Effect of environmental conditions on expansion in concrete due to alkali–silica reaction (ASR), Mater. Charact. 60 (2009) 669–679.

[156] X. Feng, M.D.A. Thomas, T.W. Bremner, B.J. Balcom, K.J. Folliard, Studies on lithium salts to mitigate ASR-induced expansion in new concrete: a critical review, Cem. Concr. Res. 35 (2005) 1789–1796.

[157] Personal communication with Colin Giebson, Bauhaus-Universität Weimar Fakultät Bauingenieurwesen, F.A. Finger-Institut für Baustoffkunde, 2011.

[158] K.O. Kjellsen, R.J. Detwiler, O.E. Gjørv, Pore structure of plain cement pastes hydrated at different temperatures, Cem. Concr. Res. 20 (1990) 927–933.

[159] K.O. Kjellsen, R.J. Detwiler, Reaction kinetics of portland cement mortars hydrated at different temperatures, Cem. Concr. Res. 22 (1992) 112–120.

[160] B. Lothenbach, F. Winnefeld, C. Alder, E. Wieland, P. Lunk, Effect of temperature on the pore solution, microstructure and hydration products of Portland cement pastes, Cem. Concr. Res. 37 (2007) 483–491.

[161] K. Schmidt, L. Urbonas, A. Dressler, D. Heinz, AKR-Performance-Prüfung von flugaschehaltigen Betonen—Einfluss der Temperatur auf die Porenlösung und Möglichkeiten zur zielsicheren Bewertung, in: B.-U. Weimar (Ed.), 17 Internationale Baustofftagung, 23–26 September 2009, Tagungsbericht; Band 1 und 2 (Internationale Baustofftagung : 16 Weimar 23-26092009), Weimar, 2009, pp. 2-0267-0262-0276.

[162] L.-O. Nilsson, Modelling moisture conditions in cementitious materials—some present challenges, 2nd International Symposium on Advances in Concrete through Science and Engineering, Quebec City, Canada, 2006.

[163] A. Sjöberg, L.-O. Nilsson, T. Rapp, Moisture measurements in floors with heating pipes. Part I. (in Swedish), publication P-02:1, dept. of Building Materials, Chalmers, University of Technology, Gothenburg, 2002.

[164] E.J. Sellevold, Ø. Bjøntegaard, Coefficient of thermal expansion of cement paste and concrete: mechanisms of moisture interaction, Mater. Struct. 39 (2006) 809–815.

[165] J. Lindgård, B. Pedersen, S. Bremseth, P.A. Dahl, T.F. Rønning, K. Kjellsen, Experience using the Norwegian 38°C concrete performance test evaluating the alkali reactivity of concrete mixes and different binder combinations, in: M.A.T.M. Broekmans, B.J. Wigum (Eds.), 13th International Conference on Alkali–Aggregate Reactions in Concrete, Trondheim, Norway, 2008, pp. 931–940.

[166] J. Bokern, Concrete tests for ASR assessment: effects of testing environment on preconditions for an ASR and transferability of test results, in: M.A.T.M. Broekmans, B.J. Wigum (Eds.), 13th International Conference on Alkali–Aggregate Reactions in Concrete, Trondheim, Norway, 2008, pp. 511–520.

[167] J. Lindgård, Are the RILEM AAR-3 and AAR4.1 concrete prism tests suited for performance testing? Presentation at the RILEM AAR seminar "Recent development in AAR", 11th March, Azores, 2010.

[168] A.D. Herholdt, C.F.P. Justesen, P. Nepper-Christensen, A. Nielsen, Beton-Bogen, Aalborg Portland, Cementfabrikkernes tekniske Oplysningskontor, 1979, p. 719.

[169] R.F. Blanks, H.S. Meissner, The expansion test as a measure of alkali–aggregate reaction, J. Am. Concr. Inst. 17 (1946) 517–539.

[170] R.F.M. Bakker, The influence of test specimen dimensions on the expansion of alkali reactive aggregate in concrete, in: G.M. Idorn, S. Rostam (Eds.), 6th International Conference on Alkali–Aggregate Reaction in Concrete, Denmark, 1983, pp. 369–375.

[171] C.A. Rogers, R.D. Hooton, Reduction in mortar and concrete expansion with reactive aggregates due to alkali leaching, Cem. Concr. Aggregates 13 (1991) 42–49.

[172] M.-A. Bérubé, D. Chouinard, L. Boisvert, J. Frenette, M. Pigeon, Influence of wetting–drying and freezing–thawing cycles and effectiveness of sealers on ASR, in: A. Shayan (Ed.), 10th International Conference on Alkali–Aggregate Reaction in Concrete, Australia, 1996, pp. 1056–1063.

[173] P.J. Nixon, R.J. Collins, P.L. Rayment, The concentration of alkalies by moisture migration in concrete—a factor influencing alkali aggregate reaction, Cem. Concr. Res. 9 (1979) 417–423.

[174] M. Åhs, Redistribution of moisture and ions in cement based materials, PhD thesis, Division of Building Materials, Lund University, Lund, Sweden, 2011.

[175] J.A. Farny, S.H. Kosmatka, Diagnosis and control of alkali–aggregate reactions in concrete, Concrete Information, Portland Cement Association, 1997, p. 23.

[176] P. Rivard, M.-A. Bérubé, J.-P. Ollivier, G. Ballivy, Decrease of pore solution alkalinity in concrete tested for alkali–silica reaction, Mater. Struct. 40 (2007) 909–921.

[177] K. Schmidt, Verwendung von Steinkohlenflugasche zur Vermeidung einer schädigenden Alkali-Kieselsäure Reaktion im Beton, Fak f Bauingenieur- u Vermessungswesen, München, 2009.

[178] J.H. Ideker, B.L. East, K.J. Folliard, M.D.A. Thomas, B. Fournier, The current state of the accelerated concrete prism test, Cem. Concr. Res. 40 (2010) 550–555.

[179] P.J. Nixon, C.L. Page, I. Canham, R. Bollinghaus, Sodium chloride and alkali aggregate reaction, Concrete alkali–aggregate reactions, 7th International Conference, Noyes Publications, Ottawa, Canada, 1986, pp. 110–114.

[180] P.M. Dove, The dissolution kinetics of quartz in aqueous mixed cation solutions, Geochim. Cosmochim. Acta 63 (1999) 3715–3727.

[181] J.D. Rimstidt, H.L. Barnes, The kinetics of silica–water reactions, Geochim. Cosmochim. Acta 44 (1980) 1683–1699.

[182] P.M. Dove, Kinetic and thermodynamic controls on silica reactivity in weathering environments, in: A.F. White, S.L. Brantley (Eds.), Chemical weathering rates of silicate minerals Reviews in Mineralogy, Mineralogical Society of America, , 1995, pp. 235–290.
[183] R.K. Iler, The Chemistry of Silica, Wiley-Inter science, New York, USA, 1979.
[184] P.C. Hewlett, Chemistry of cement and concrete, LEA'S, chapter 6Fourth Ed., 1988, p. 1057.
[185] F.d. Zementindustrie (Ed.), Activity Report 2007–2009, Verein Deutscher Zementwerke (VDZ), Düsseldorf, 2009.
[186] F.W. Locher, Cement: principles of production and use, Verlag Bau + Technik GmbH, Düsseldorf, 2005.
[187] K. De Weerdt, H. Justnes, Microstructure of binder from the pozzolanic reaction between lime and siliceous fly ash, and the effect of limestone addition, 1st International Conference on Microstructure Related Durability of Cementitious Composites, Nanjing, China, 2008, pp. 107–116.
[188] S. Baetzner, M. Böhm, Vermeidung einer schädigenden AKR durch den Einsatz von Steinkohlenflugasche, VGB-Forschungsprojekt, 272, 2009.
[189] F.W. Locher, Ursache und Wirkungsweise der Alkalireaktion, Vorbeugende Massnahmen gegen Alkalireaktion im Beton, VDZ, Schriftenreihe der Zementindustrie Heft, 40, 1973.
[190] S. Chatterji, P. Christensen, Studies of alkali–silica reaction. Part 7. Modelling of expansion, Cem. Concr. Res. 20 (1990) 285–290.
[191] E. Gavrilenko, D. Garcia del Amo, B. Calvo Pérez, E. Garcia Garcia, Comparison of ASR-gels in concretes against accelerated mortar bar test samples, Mag. Concr. Res. 59 (2007) 483–494.
[192] M.D.A. Thomas, The role of calcium hydroxide in alkali recycling in concrete, in: J. Skalny, J. Gebauer, I. Odler (Eds.), Materials Science of Concrete Special Volume on Calcium Hydroxide in Concrete, American Ceramic Society, Westerville, OH, 2001, pp. 225–236.
[193] M. Kawamura, K. Iwahori, ASR gel composition and expansive pressure in mortars under restraint, Cem. Concr. Compos. 26 (2004) 47–56.
[194] L. Struble, S. Diamond, Unstable swelling behaviour of alkali silica gels, Cem. Concr. Res. 11 (1981) 611–617.
[195] S. Sachlová, R. Prikryl, Z. Pertold, Alkali–silica reaction products: comparison between samples from concrete structures and laboratory test specimens, Mater. Charact. 61 (2010) 1379–1393.
[196] M. Moranville-Regourd, Products of reaction and petrographic examination, in: K. Okada, S. Nishibayashi, M. Kawamura (Eds.), 8th International Conference on Alkali–Aggregate Reaction, Kyoto, Japan, 1989, pp. 445–456.
[197] B. Fournier, M.-A. Bérubé, G. Bergeron, A rapid autoclave mortar bar method to determine the potential alkali–silica reactivity of St. Lawrence lowlands carbonate aggregates, Cem. Concr. Aggregates 13 (1991) 953–957.
[198] G. Davies, R.E. Oberholster, Alkali–silica reaction products and their development, Cem. Concr. Res. 18 (1988) 621–635.
[199] G. Davies, R.E. Oberholster, An interlaboratory test programme on the NBRI accelerated test to determine the alkali reactivity of aggregates, National Building Research Institute, Council for Scientific and Industrial Research, South Africa, 1987, p. 16.
[200] D. Lu, L. Mei, Z. Xu, M. Tang, B. Fournier, Alteration of alkali reactive aggregates autoclaved in different alkali solutions and application to alkali–aggregate reaction in concrete: (I) Alteration of alkali reactive aggregates in alkali solutions, Cem. Concr. Res. 36 (2006) 1176–1190.
[201] T. Kuroda, S. Inoue, A. Yoshino, S. Nishibayashi, ASR expansion characteristics of mortar bars immersed in NaOH solution by autoclave method, in: M.-A. Bérubé, B. Fournier, B. Durand (Eds.), 11th International Conference on Alkali–Aggregate Reaction, Québec, Canada, 2000, pp. 375–384.
[202] Internal sulphate attack and delayed ettringite formation, International RILEM TC 186-ISA workshop, Villars, Switzerland, 2002, p. 300.

Paper IV

Alkali-silica reaction (ASR) - Performance testing: Influence of specimen pre-treatment, exposure conditions and prism size on concrete porosity, moisture state and transport properties
J. Lindgård, E.J. Sellevold, M.D.A. Thomas, B. Pedersen, H. Justnes, T.F. Rønning
Cement and Concrete Research 53 (2013) pp. 145-167

Cement and Concrete Research 53 (2013) 145–167

Contents lists available at SciVerse ScienceDirect

Cement and Concrete Research

journal homepage: http://ees.elsevier.com/CEMCON/default.asp

Alkali–silica reaction (ASR)—performance testing: Influence of specimen pre-treatment, exposure conditions and prism size on concrete porosity, moisture state and transport properties

Jan Lindgård [a,*], Erik J. Sellevold [b], Michael D.A. Thomas [c], Bård Pedersen [d], Harald Justnes [a,b], Terje F. Rønning [e]

[a] SINTEF Building and Infrastructure, NO-7465 Trondheim, Norway
[b] Norwegian University of Science and Technology, NO-7491 Trondheim, Norway
[c] University of New Brunswick, Fredericton, Canada
[d] Norwegian Public Roads Administration, NO-0033 Oslo, Norway
[e] Norcem Heidelberg Cement, NO-3950 Brevik, Norway

ARTICLE INFO

Article history:
Received 15 November 2012
Accepted 30 May 2013
Available online 12 July 2013

Keywords:
Alkali–aggregate reaction (C)
Performance testing
Humidity (A)
Transport properties (C)
Permeability (C)

ABSTRACT

Whether or not concrete prism tests (CPTs) developed for assessment of alkali–silica reactivity of aggregates might be suitable for general ASR performance testing of concrete has been evaluated. This paper presents the background for the choice of test procedures and results on how variations in specimen pre-treatment, ASR exposure conditions and prism size influence concrete porosity, moisture state and transport properties. Results from measurements of alkali leaching and prism expansions during the ASR exposure are presented in a separate paper, together with discussion of consequences for ASR test procedures.

For ordinary Portland cements and with water-to-cementitious-materials ratio (w/cm) 0.45 and higher it was found that the internal moisture state is sufficiently high in all the assessed procedures to produce ASR expansion. However, for less permeable concretes lack of internal moisture and lower rate of diffusion can significantly reduce the rate and extent of ASR expansion during laboratory performance testing.

1. Introduction

1.1. Background

Since ASR was recognised as a concrete durability problem more than 70 years ago by Stanton [1], several comprehensive research projects have focused on test methods for determining the alkali reactivity of aggregates and corresponding acceptance criteria. In Europe, only national ASR aggregate tests are available today. As part of the international harmonisation of such aggregate tests, two previous RILEM technical committees (TC 106-AAR, 1998–2000 and TC 191-ARP, 2001–2006) have proposed and validated several RILEM aggregate test methods for classifying the alkali reactivity of aggregates: petrographic method (AAR-1, 2003 [2]), accelerated mortar bar tests (AAR-2, 2000 [3] and AAR-5, 2005 [4]) and concrete prism tests, CPTs (AAR-3, 2000 [3] and AAR-4.1, 2006 [5]), in addition to recommendations for how to use these test methods and interpret the results (RILEM AAR-0, 2003 [6]). These draft RILEM methods have been developed further by RILEM TC 219-ACS (2007–2013), partly based on findings in the EU funded "PARTNER" research project where all the RILEM aggregate test methods were evaluated [7]. In USA and Canada, corresponding ASTM and CSA test methods exist (ASTM C 1260-07 [8]; ASTM C1293-08b [9]; ASTM C 295-08 [10]; CSA A23.2-14A-04 [11]; CSA A23.2-25A-09 [12]; CSA A23.2-15A [13]).

Internationally, various ways of controlling ASR are suggested (in addition to use of non-reactive aggregates): utilisation of low-alkali cement, limiting the alkali content of the concrete, incorporation of supplementary cementing materials (SCMs; e.g. silica fume, fly ash, ground granulated blast furnace slag (ggbs), metakaolin and other pozzolans) or use of lithium salts. For example RILEM TC 219-ACS has prepared a document with recommendations on how to ensure durable non-reactive concrete (RILEM AAR-7.1, 2008 [14]). This document is scheduled for publication together with the RILEM aggregate test methods in a special issue of Materials and Structures during 2013.

SCMs control expansion due to ASR by binding alkalis and limiting their availability for reaction with alkali–silica reactive aggregates [15]. The efficiency of the SCMs depends on their characteristics and amount, the nature of the reactive aggregate and the availability of alkali in the concrete. Chappex and Scrivener [16] also showed that the aluminium present in certain SCMs (e.g. metakaolin) may limit the dissolution of silica from reactive aggregates. Consequently, to be able to utilise alkali–silica reactive aggregates for production of durable concretes, the effects of various measures must be correctly identified by accelerated laboratory performance tests (or ideally by relevant long-term field experience). Several performance tests have been used worldwide for

---

[*] Corresponding author. Tel.: +47 93 05 86 89.
E-mail address: jan.lindgard@sintef.no (J. Lindgård).

0008-8846/$ – see front matter © 2013 Elsevier Ltd. All rights reserved.
http://dx.doi.org/10.1016/j.cemconres.2013.05.020

at least 15 years. In principle two groups of ASR performance test methods exist, one using mortar bars and the other using concrete prisms. However, the test conditions (e.g. pre-curing, temperature, alkali content, humidity) differ from one test method to another. Thus, the results and conclusions from different test methods may vary widely.

The most frequently used concrete performance test is ASTM C1293-08b [9], where concrete prisms are stored at high humidity over water in sealed containers at 38 °C. Other examples of concrete performance tests are the French 60 °C CPT [17] and the Norwegian 38 °C CPT [18].

1.2. Development of reliable ASR performance test methods

1.2.1. Main challenges

In 2006, Thomas et al. [19] provided a critical evaluation of different ASR performance test methods. The authors concluded that none of the currently available or commonly used test methods meet all the criteria for an ideal performance test. For example, the main shortcoming of the Canadian 38 °C CPT [11] (similar to ASTM C-1293-08b [9]) is the duration of the test (2 years) and that addition of alkalis is required to compensate for alkali leaching effects, i.e. the fact that alkalis are leached out of the prisms during exposure in the humid environment. Thus, the authors concluded that the method neither can be used to determine the “critical” alkali content for an alkali–reactive aggregate, nor to determine how the level of a SCM required to control expansion varies with the concrete alkali content.

In 2010, Lindgård et al. [20] assessed about 15 years of experience with use of the Norwegian 38 °C CPT [18]. This method is similar to ASTM C 1293-08b [9], but larger prisms are used (100 mm cross section compared with 75 mm in the ASTM method). The method has been specified in the Norwegian guidelines [21] for performance testing of concrete mixes and/or binders since 1996. Despite the long testing time required (1–2 years), the Norwegian system for performance testing has proven to be an advantageous and flexible tool to document critical alkali limits for binders and aggregates. However, even though the extent of alkali leaching is less for the Norwegian CPT with larger prisms than used in the ASTM C-1293 CPT, Lindgård et al. [20] recommended that the influence of alkali leaching on the measured expansions in the Norwegian CPT should be investigated further.

The development of accurate and reliable performance test methods for the production of durable concretes is a challenge. Several requirements must be fulfilled, some being somewhat contradictory. On the one hand the test methods should be inexpensive and rapid, calling for extremely accelerated test conditions. On the other hand a performance test should mirror the field performance of the actual concrete for more than 50 years lifetime. Another important requirement is the possibility to test job mixes identical to the concrete composition that will be used on actual projects. Use of mortar bars is in conflict with this latter requirement. According to Thomas et al. [19], other important requirements for an ideal performance test for ASR are:

- The test should be capable of determining the “critical” alkali content for specific aggregates, i.e. the alkali leaching problem must be solved.
- The test should be capable of assessing all types of SCMs, lithium compounds and combinations of SCM and lithium, with cements of different alkali levels.

1.2.2. RILEM TC 219-ACS

Today, research is on-going in several countries with the aim to improve current ASR performance test methods and develop alternative tests. As part of the international harmonisation of ASR performance test methods, the “Performance testing” task group of RILEM TC 219-ACS is working on a performance testing concept aiming to develop one or more reliable ASR concrete performance test methods that might cover several applications/areas, ranging from combination of various aggregates with a standard CEM I binder up to the “ultimate goal” to document the alkali reactivity of any concrete mix design (“job mix”).

1.3. PhD study on ASR

The main objective of the PhD study by Jan Lindgård, being part of the Norwegian COIN program (2007–2014, www.coinweb.no), has been to evaluate whether concrete prism tests developed for assessment of alkali–silica reactivity of aggregates might be suitable for general ASR performance testing of concrete. This paper is one of several from the PhD study, which has been performed in close co-operation with the “Performance testing” task group of RILEM TC 219-ACS (all authors of this paper, except one, are members of this RILEM task group).

1.3.1. Literature review—assessment of parameters influencing laboratory performance testing

As stated by Thomas et al. [19], the only suitable benchmarking of a laboratory performance test is against real concrete structures or, as a surrogate, against large concrete blocks exposed outdoors to natural weathering conditions. However, long-term field experience is available only for a limited number of commercial SCMs, e.g. some class F fly ashes and some slag cements. When developing an accelerated performance test method, it is thus crucial as a first step to evaluate fundamental questions theoretically in order to ensure a satisfactory laboratory/field correlation.

As a collaborating work between the PhD study and the work within the task group “Performance testing” in RILEM TC 219-ACS, a comprehensive literature review has recently been performed. In total, 12 authors contributed to the report that included about 250 references [22]. The main objective was to assess how various parameters might influence the laboratory/field correlation with respect to ASR performance testing, either directly or indirectly. The most important findings in the literature survey and recommendations for performance testing have recently been summarised by Lindgård et al. [23]. These recommendations include precautions when testing various aggregates and binders, important factors to take into account during mix design, as well as possible influences on ASR expansion of various conditions during pre-storage and the ASR exposure. Additionally, the literature survey has identified several issues that need further research in order to develop a reliable performance test procedure.

1.3.2. Parameters focused on in the PhD study

Based on the most important findings from the literature review ([22,23]), the PhD study has focused on the effect of various specimen “pre-treatments”, “ASR exposure conditions” as well as prism size on:

- Porosity and internal moisture state of the concrete prisms.
- Concrete transport properties (with respect to mobility of water and ions).
- Alkali leaching (rate and extent) from the concrete prisms during the ASR exposure.
- Concrete prism expansion (rate and final expansion).

Additionally, the effect of water-to-cementitious-materials ratio (w/cm) and type of binder is assessed.

The specimen “pre-treatment”, defined as the moisture conditions during pre-storage and the length of the pre-storage period at ambient temperature (up to the point of the initial (zero) length comparator reading), vary for different concrete prism tests used in the different countries. After casting, most test methods prescribe storage of the moulds at 18–23 °C and minimum 90–95% RH in the surroundings, while others prescribe more humid storage of the moulds, e.g. in a fog room with 100% RH. After de-moulding the day after casting, some test methods prescribe direct exposure of the prisms to the actual exposure temperature, e.g. ASTM C-1293-08b [9]. Other methods prescribe 0.5 h submersion of the prisms in water after de-moulding, before further preparation for final exposure. Finally, the length of the pre-storage period at 18–23 °C normally varies from 1 day (e.g. as in ASTM C-1293-08b [9] and RILEM AAR-4.1 [5]) to 7 days (e.g. as in RILEM AAR-3 [3]). Some laboratories use an even more prolonged pre-storage period, up to 28 days, dependent on the type of binder [24].

Also the "ASR exposure conditions" (i.e. moisture conditions, type of container, use of any wrapping, exposure temperature, length of the storage period, addition of any external alkalis) and prism size varies between various performance test methods used in the different countries.

In the PhD study, an extensive laboratory program has been performed. The test series cover the variations in test conditions in the most commonly used ASR test methods. Additionally, some test series include measures intended to reduce the extent of alkali leaching. This paper presents the technical background for the choice of test procedures and gives an overview of the laboratory programme (see Section 2), that in total has included 58 ASR test series (see Section 2.3) and comprehensive complementary testing for documentation (see Section 2.4). Furthermore, the paper presents and evaluates the results from measurements of concrete porosity, internal moisture state and transport properties. As a basis for this evaluation, some important findings in the literature review [23] regarding concrete internal moisture state and concrete transport properties, in particular with respect to influence on development of ASR, are briefly discussed in Sections 1.4 and 1.5, respectively.

In a separate paper [25], results from the periodic measurements of alkali leaching from the concrete prisms and concrete prism expansion are presented and evaluated, together with main findings from some of the supplementary tests (see Section 2.4). Additionally, consequences for ASR test procedures are discussed.

1.4. Importance of the internal moisture state

1.4.1. Description of the moisture state in concrete

The moisture conditions in concrete can be described in two different ways ([26,27]):

1. Relative humidity (RH) at a certain temperature.
2. The pore water content expressed either as the percentage of mass or volume, or as the degree of saturation. The degree of capillary saturation (DCS) expresses the % filling of the pores in concrete that are able to draw in water by capillary action (i.e. gel and capillary pores; not air entrained pores or voids).

It is important to note that the RH is a measure of the thermodynamic state of the pore water, and is not a direct measure of the amount of water [28]. At a fixed moisture content, the RH is a function of the pore structure, the temperature, the chemical composition of the pore water and the moisture history of the concrete. Hedenblad [29] reported that the chemical effect on the pore water can be as much as 4% reduction of the RH, i.e. a fully saturated concrete may only exert 96% RH.

In general, the relation between the RH in concrete and the DCS varies a lot depending on several factors, where the w/cm is the most important one [27]. High w/cm concretes have a steeper desorption isotherm than low w/cm concretes [26]. In other words, for a given loss of moisture, RH decreases less in open concretes compared with denser concretes. Note also that the RH–DCS relation depends on whether a given moisture state is obtained during adsorption or desorption.

RH is easy to measure, also in situ and over time. However, such measurements require much care and experience to be meaningful. Many sources of errors exist, where temperature difference between the sensors and the concrete often is the cause of unreliable results. RH measurements in the field are notoriously uncertain.

Measurement of DCS on samples cut from structures is done by weighing the samples immediately after unwrapping in the laboratory, after immersion 7 days in water and after drying [30] (see Section 2.4). DCS measurements, in contradiction to RH measurements, are easy to perform accurately, but they are destructive and more cumbersome to do, involving cutting samples from the structure and taking them to a laboratory in an "undisturbed" condition. Thus, much care must be taken during sampling.

1.4.2. The role of water in the alkali–silica reaction

Moisture is generally accepted to be one of the main factors affecting ASR. Water is important as a transport medium for ions. The role of water is also important in the expansion stage. The overall expansion and cracking of concrete is basically caused by sorption of water by the alkali–silica gel, which in turn swells and thereby causes damage. In a review by Pedersen [31], very few discussions of the fundamental aspects of moisture state in concrete in connection with ASR were found in the literature, and most scientists seem to use relative humidity as the only measure of moisture. The critical limit for developing ASR is reported to lie in the range of 80–90% RH depending on several factors, as discussed by Larive et al. [32]. In general, the 80% RH limit has been most frequently used in the literature.

DCS is, however, a more relevant parameter to describe the in situ moisture state if it is the amount of water that is controlling the expansion. Based on a survey of a large number of Norwegian concrete bridges, Lindgård et al. [27] showed a rather good correlation between the presence of ASR and the DCS. With only a few exceptions DCS of the concrete structures with pronounced ASR was higher than 90 %. The extent of damages generally increased with increasing water content above this level.

The concrete moisture state might also influence the expansion properties of the alkali–silica gel ("ASR-gel"). Bokern [33] showed that the viscosity of the ASR gel decreased at higher RH levels and thus decreased the expansive pressure exerted.

1.4.3. Consequences of self-desiccation

The hydration process of cement gives a reduction in the volume of the reacted cement and water. This phenomenon is referred to as chemical shrinkage, and has some major effects:

1) In the hardening phase, the chemical shrinkage results in partly empty pores within the concrete. These pores will remain partly empty if no water is supplied from the surroundings. This leads to a lowering of the RH in the concrete, a phenomenon called self-desiccation. Generally, the extent of self-desiccation increases with decreasing w/cm. The type of binder, in particular the type and amount of any SCM used, will also influence the extent of self-desiccation.
2) The reduced RH implies (capillary) tension in the pore water. This tension produces autogenous shrinkage, which is a bulk volume contraction of the paste and consequently of the entire concrete body.

For practical purposes the effects of self-desiccation becomes more important as w/cm is reduced. For example at w/cm 0.40, RH may be less than 90% after a few weeks. At lower w/cm the effect is larger and may reduce the RH to below 80% over a period of time, provided there is no water supplied from the surroundings. Thus, for massive concrete structures the residual concrete mix water, depending on the w/cm, rather than ambient wetting and drying, determines the prevailing interior moisture content ([26,30,34–36]). The depth of the surface layer that is influenced by external moisture fluctuations will normally be in the range of about 2–10 mm ([35,37]). This depth will be less with decreasing w/cm as the result of reduced permeability [38].

Even during laboratory testing, a moisture profile through the prism cross-section often develops, with lowest RH in the mid part, in particular if the size of the concrete specimens is relatively large (≥100 mm cross-section) combined with a rather low w/cm. Consequently, a minimum limit should be considered for the w/cm for ASR testing. If such limitations are not introduced, the internal RH in laboratory test prisms might be lower than in slim structures exposed to water in service. This could lead to incorrect test conclusions, i.e. some potentially alkali-reactive mixes could be classified as non-reactive based on performance testing because of the lack of water. For this reason, Lindgård et al. [23] suggested that the net influence of a reduced w/cm (<0.40) should be investigated further.

Additionally, the aggregate porosity and the aggregate moisture state at the time of mixing might significantly influence the RH within the concrete. For example might use of pre-wetted aggregates with relatively high porosity supply additional water to the cement paste during the curing period and thereby reducing the self-desiccation ([39,40]).

1.5. Factors effecting transport properties

Increasing w/cm will result in a higher and more continuous (capillary) porosity, consequently internal transport processes will be accelerated, the rate of alkali leaching will increase and water loss/uptake will take place more easily ([41,42]).

Furthermore, addition of any SCMs will influence the permeability of the concrete and thus the permeability-related ASR mechanisms, i.e. internal transport processes, alkali leaching, water uptake and sensitivity to drying during exposure and measuring in the laboratory. Additionally, increased permeability in aggregates may enhance the alkali reactivity due to easier access to concrete pore fluids [43].

2. The test programme

2.1. General

The PhD laboratory test programme has included four concrete mixtures (see Section 2.2) and in total 58 ASR test series, most of them using modified versions of the draft RILEM aggregate concrete prism tests; AAR-3, 2000 (38 °C, wrapped prisms) [3] and AAR-4.1, 2006 (60 °C, unwrapped and wrapped procedure) [5]—see details in Section 2.3. For comparison, six test series with slightly modified versions of the Norwegian 38 °C CPT [18] and 12 test series with the ASTM C1293-08b CPT [9] (38 °C, unmodified version) were included. The main reason for incorporating the latter method was to establish a link to the comprehensive experience in North America with this method and to document any batch to batch variation; 8 concrete batches were needed to cast all the concrete prisms with the "basis" binder and two batches were prepared with the "open" binder (see Section 2.2).

In addition to the ASR testing, a comprehensive complementary testing program for documentation of concrete properties of importance for development of ASR has been performed. The main parameters include internal moisture state, transport properties (of water and ions) and alkali leaching (see Section 2.4). Additionally, fresh concrete properties (slump, density and air content), 28 days compressive strength of 100 mm cubes and porosity/density properties were measured.

Before the laboratory testing started, a "pilot testing" program was carried out in order to develop detailed laboratory procedures to improve the reliability of the measurements.

The selected components and the concrete mix design used, including the technical background for the choices made, are described in Section 2.2.

2.2. Materials and mixture proportions

Two CEM I Portland cements (EN-197-1), one high alkali (1.24% Na_2Oeq) and one low alkali (0.60% Na_2Oeq), and a CEM II/A–V cement containing 21.6% of a siliceous fly ash (class F, co-grinded with the clinker) were used in the study, see Table 1 (*comment: The CEM II/A–V cement normally contains 17–20% fly ash*). This type of blended cement has been widely used for years in Norway, partly in order to avoid ASR in combination with alkali–silica reactive aggregates.

The aggregates used are defined in the Norwegian ASR regulations ([18,21]) as "reference Norwegian aggregates" and consist of a non-reactive natural sand (mainly containing granites and gneisses, saturated surface-dry density 2660 kg/m^3, water absorption 0.1%) and an alkali–silica reactive crushed coarse aggregate (cataclasite with crypto- to microcrystalline quartz, saturated surface-dry density 2760 kg/m^3, water absorption 0.4%). In all the test series, the aggregates were blended to produce a 60:40 coarse:fine ratio (by mass). This is in agreement with the grading prescribed in the RILEM CPTs ([3,5]).

Details of the concrete mixtures are given in Table 2. Based on a series of considerations, the bulk of the testing was produced using a mixture containing 400 kg/m^3 of Portland cement and water-to-cement ratio (w/c) of 0.45 (denoted "basis" binder). The two CEM I cements were blended to produce an alkali content of 3.7 kg/m^3 Na_2Oeq. The alkali content was chosen (based on previous testing of the aggregates at SINTEF [20]) with aim to reach a final expansion of the reference test series lying on the steep part of the "expansion versus alkali level (S-shaped) curve", so that a small loss of alkalis due to alkali leaching would be detectable in terms of reduced expansion. If a high alkali level had been chosen, most of the test series would probably show a rather high expansion (i.e. lie on the plateau of the "expansion versus alkali level curve"), even if significant quantities of alkalis were leached out during the ASR exposure. Then only minor differences in expansion would have been expected between the different test series.

To examine the impact of w/c, two additional concrete mixtures were cast with CEM I cement and w/c of 0.30 and 0.60 (denoted "dense" and "open" binder, respectively). The cement contents of these mixtures were modified to achieve the desired workability, but the alkali content of the mixtures was maintained at 3.7 kg/m^3 Na_2Oeq by appropriate blending of the CEM I cements, see Table 2.

Additionally, one mixture was produced with w/cm of 0.45 using the blended cement containing about 20% fly ash (denoted "fly ash" binder, see Table 2). The alkali content of this mixture was raised from 5.0 kg/m^3 Na_2Oeq (alkalis originating from the blended cement) to 9.0 kg/m^3 Na_2Oeq by adding NaOH to obtain a final expansion of the "fly ash" concrete mixture on the steep part of the "expansion versus alkali level curve".

To achieve an appropriate consistency, a minor quantity of a low-alkali superplasticiser was added to some of the concrete mixes. To avoid any influence on the ASR expansion of varying air content in

Table 1
Chemical composition (EN 196-2) of the three cements used in the study.

	SiO_2	Al_2O_3	Fe_2O_3	CaO	MgO	SO_3	K_2O	Na_2O	Na_2O_e	P_2O_5	LOI[a]
High alkali CEM I	19.61	4.87	3.48	61.03	2.83	3.81	1.11	0.51	1.24	0.15	2.44
Low alkali CEM I	20.06	4.67	3.31	63.06	2.01	3.40	0.39	0.34	0.60	0.16	2.24
CEM II/A–V[b]	26.61	8.73	4.24	50.34	2.37	3.28	1.04	0.56	1.25	0.33	1.20

[a] Loss-Of-Ignition.

[b] Blended cement with a class F fly ash content of 21.6 wt.%. Manufactured by co-grinding clinker and fly ash. Normally, the content of fly ash is in the range of 17–20%.

Table 2
Composition of the four concrete mixtures included in the study.

Materials (kg/m^3)			Binder composition			
			CEM I, 0.45 “basis” binder	CEM I, 0.30 “dense” binder	CEM I, 0.60 “open” binder	CEM II/A–V, 0.45 “fly ash” binder
Cement	High alkali CEM I		200	60	285	–
	Low alkali CEM I		200	490	30	–
	CEM II/A–V		–	–	–	400
Aggregates (SSD[a])	Årdal (gneiss/granite)	0/4	735	700	755	725
	Ottersbo (cataclasite)	4/8	185	175	190	180
		8/11	365	350	375	360
		11/16	550	525	565	540
Deionised water (free) (excl. any water in the superplasticizer)			180	165	189	180
NaOH (solids)			–	–	–	5.2
Alkali content (kg Na_2Oeq per m^3)			3.7	3.7	3.7	9.0
Superplasticizer (SIKA SSP 2000)			If necessary, add until workable and stable concrete (aimed slump 120 mm)			
De-foaming agent (SIKA)			If measured air content is >3.0%, add until air content is reduced to <3.0%			

[a] Saturated surface dry condition.

the different test series, a minor quantity of a de-foaming agent was added to the concrete mix if the air content was measured to be higher than 3.0%. The concrete samples were compacted manually.

2.3. ASR test procedures—test series

2.3.1. ASR concrete prism tests

All the CPTs included in the study (see Table 3) are designated for testing alkali–silica reactivity of concrete aggregates. Additionally, the ASTM C-1293 CPT [9] and the Norwegian CPT [18] are frequently used for ASR performance testing. The main differences between the CPTs are *exposure temperature* (38 °C or 60 °C; only RILEM AAR-4.1, 2006 [5] uses 60 °C), *prism cross section* (100 × 100 mm (only the Norwegian CPT [18]) or 70–75 × 70–75 mm) and *use of any wrapping* (damp cotton cloth and polyethylene; only RILEM AAR-3, 2000 [3] and RILEM AAR-4.1 “Alternative”, 2006 [5]). Except for the “Standard” RILEM AAR-4.1 CPT, 2006 (unwrapped prisms) [5] where small containers are stored inside a larger container (“reactor”) over water, the other storage containers are stored in a hot, dry room or an oven (thus being more vulnerable for evaporation of the water in the bottom if the seal of the container is compromised).

> *(Comment: Based on results from this study, the RILEM AAR-4.1 “Alternative” CPT (2006)* [5] *(wrapped prisms) is no longer considered suitable within the RILEM TC 219-ACS. Furthermore, the RILEM AAR-3 CPT 2000* [3] *(wrapped prisms) was significantly revised during 2010. In the 2011 draft version of the AAR-3 CPT, the exposure conditions are similar to ASTM C-1293* [9]*, i.e. no wrapping is applied. The reason for the revisions made was the disturbingly high extent of alkali leaching from the wrapped concrete prisms at early age—further discussed in* [25,44]*).*

2.3.2. Modification of the test procedures

The standard versions of the concrete prism tests, except the ASTM C-1293 CPT [9], have been slightly modified in order to investigate the effects of these modifications. The motivation for the modifications is given in the recently published literature review [23].

During all the testing only deionised water has been used as mixing water, in the moist cotton cloth wrapping (if any) and in the storage containers.

For all test series, the moulds were stored at ambient temperature in the laboratory under plastic foil from casting until de-moulding the following day.

For all test series, each prism was always stored vertically in the storage container with the same prism end pointing upwards (marked with an arrow). This is in contrast to the description for the three RILEM CPTs ([3,5]) and the ASTM C-1293 CPT [9] that prescribe that each prism should be turned at every reading. The reason for this modification was to be able to document any variation in internal moisture state, extent of alkali leaching and extent of internal cracking over the prism height.

For all standard versions of the CPTs the mass and length were taken after cooling the prisms for about 16 h inside their storage container in a room kept at ~20 °C (see Table 3). However, during cooling some water will evaporate from the prisms and the extent of alkali leaching might increase [23]. As an example, “pilot tests” showed that each prism in the RILEM AAR-4.1 Standard CPT (unwrapped prisms) [5] lost 8–11 g water during cooling from 60 to 20 °C inside the container. This mass loss constitutes about 5–6% reduction in degree of capillary saturation for this concrete quality (CEM I, w/c 0.45). For this reason, all measurements in the modified versions of the various concrete prism tests were taken without pre-cooling the prisms (i.e. similar to what is the normal procedure in the accelerated mortar bar tests RILEM AAR-2 [3] and ASTM C-1260 [8]). To secure accurate measurements, i.e. reduce the influence of any mass loss and temperature variations from reading to reading, a detailed measuring procedure was developed. The reference readings of the prisms measured without pre-cooling were taken the day after the prisms were exposed to their ASR exposure temperature (see Fig. 1).

The following specimen “pre-treatment” and/or ASR exposure conditions have been varied when modifying the RILEM AAR-3 CPT (2000, [3]) and the RILEM AAR-4.1 CPT (2006, [5])—see Fig. 1 and Table 4 for details and motivation:

- The wrapping procedure (if any) was modified, either by adding only half of the water content prescribed or by removing the prescribed polyethylene bag.
- The length of the “pre-storage” period was varied. The prisms were kept at ambient temperature until 1, 7 or 28 days after casting before being exposed to the ASR exposure temperature. However, for all test series, the prisms were prepared for final exposure (e.g. wrapped) and put into the storage container immediately after de-moulding (and any 0.5 h submersion) and the initial measurements of mass and length.
- Some prisms were pre-cured 24 h at elevated temperature (60 °C) to simulate the curing temperature in a massive concrete structure.
- Some prisms were sealed to avoid any exchange of water with the environment.
- Some prisms were stored submerged in deionised water (to maximise the alkali leaching conditions).
- Some prisms were wrapped with cotton cloth saturated with a basic solution with pH 14.2 (1.5 M OH^-) or 13.2 (0.15 M OH^-), respectively (instead of the usual deionised water), in order to try to reduce the

Table 3
Overview of the concrete prism tests (CPTs) included in the laboratory test program.

Method[a]	Notation (Fig. 2)	Pre-treatment[b]	Storage conditions			Testing time (weeks)	Acceptance criteria	Binder composition (for aggregate testing)
			Temp. (°C)	Humidity[c,d]	Readings[e] (weeks)			
RILEM AAR-3	3	No submersion after de-moulding, but directly wrapping[f]. Ref. readings ~48 h after casting	38 ± 2 (from 7 days)	Each prism wrapped[f] in damp cotton cloth and polyethylene (prism ends not covered)	2,4,13,26,52	52	Single aggregate: b0.03% (15 weeks). (Not allowed for measurement of alkali threshold for CEM I)	440 kg/m^3 CEM I (0.9–1.2% Na_2O_{eq}), w/c-ratio 0.50, 5.5[g]kg/m^3 Na_2O_{eq} alkalis
RILEM AAR-4.1	4	Ref. readings directly after de-moulding, then 0.5 h submersion in water	60 ± 2 (from ~24 h)	Unwrapped prisms stored in a metal container (no lining). Several small containers stored in a larger container ("reactor") on grids over water	5,10,15,20	20	Single aggregate: <0.03% (15 weeks). (Not allowed for measurement of alkali threshold for CEM I)	
RILEM AAR-4.1 Alt.	4	No submersion after de-moulding, but directly wrapping[f] before ref. readings are taken	60 ± 2 (from ~24 h)	Each prism wrapped[f] in damp cotton cloth and polyethylene (prism ends not covered). RILEM AAR-4.1 Alternative is similar to AAR-3, except the exposure temp.	5,10,15,20	20	Single aggregate: <0.03% (15 weeks). (Not allowed for measurement of alkali threshold for CEM I)	
ASTM C-1293	ASTM	No submersion after de-moulding, but directly ref. readings	38 ± 2 (from ~24 h)	Unwrapped prisms stored in a plastic container—inside wall covered with a lining with lower part immersed in the deionised water in the bottom	1,4,8,13,26,39,52 (78,104)[h]	52 (104)[h]	Single aggregate: <0.04% (52 weeks) Pozzolans/slag: [h] <0.04% (104 weeks)	420 ± 10 kg/m^3 CEM I (0.9 ± 0.1% Na_2O_{eq}), w/c-ratio 0.42–0.45, 5.25[g]kg/m^3 Na_2O_{eq} alkalis
Norwegian CPT	N	Prisms submerged 0.5 h in water after de-moulding, before ref. readings are taken	38 ± 2 (from ~24 h)	Unwrapped prisms stored in a plastic container—inside wall covered with a lining with lower part immersed in the deionised water in the bottom	1,8,16,26,52 (104)[i]	52 (104)[i]	Single aggregate: <0.040% (52 weeks) Pozzolans/slag:[i] <0.030% (52 weeks)	400 ± 10 kg/m^3 CEM I (1.15 ± 0.10% Na_2O_{eq}), w/c-ratio 0.48 ± 0.02, 5.0[g]kg/m^3 Na_2O_{eq} alkalis

[a] Three concrete prisms cast for each test series. Prism size ~75 × 75 × 250 mm^3 (RILEM CPTs and ASTM C-1293) and 100 × 100 × 450 mm^3 (Norwegian CPT), respectively.

[b] All prisms stored at ~20 °C under a plastic sheet the first 24 h, before de-moulding. Subsequent pre-treatment before exposed to elevated temp. is described below.

[c] In all CPTs, the prisms are stored vertically on grids above water, without being in direct contact with the water. A humid environment close to 100% RH is aimed.

[d] Except the RILEM AAR-4.1 CPT ("reactor"), the storage containers are stored in a hot, dry room or an oven.

[e] For all methods the readings are taken after cooling the prisms inside their storage container in a room kept at ~20 °C. Any wrapping is not removed.

[f] ~80 g deionised water added to each cotton cloth before wrapping. Each wrapped prism sealed inside a separate polyethylene bag. 5 ml deionised water poured on top surface before sealing the bag and after each reading. Each bag is placed in a separate container (plastic tube with inside lining in contact with the bottom water).

[g] For all test methods, NaOH may be added to reach the aimed alkali content of the binder: 1.25% Na_2O_{eq}.

[h] For testing of combinations of aggregates and pozzolans or slag, a 104 weeks testing time is required. Not allowed for measurement of alkali threshold for CEM I.

[i] Other binders than CEM I (alkali threshold), pozzolans or slag must be tested for two years. An extra criterion must then be fulfilled: Expansion <0.060% (104 weeks).

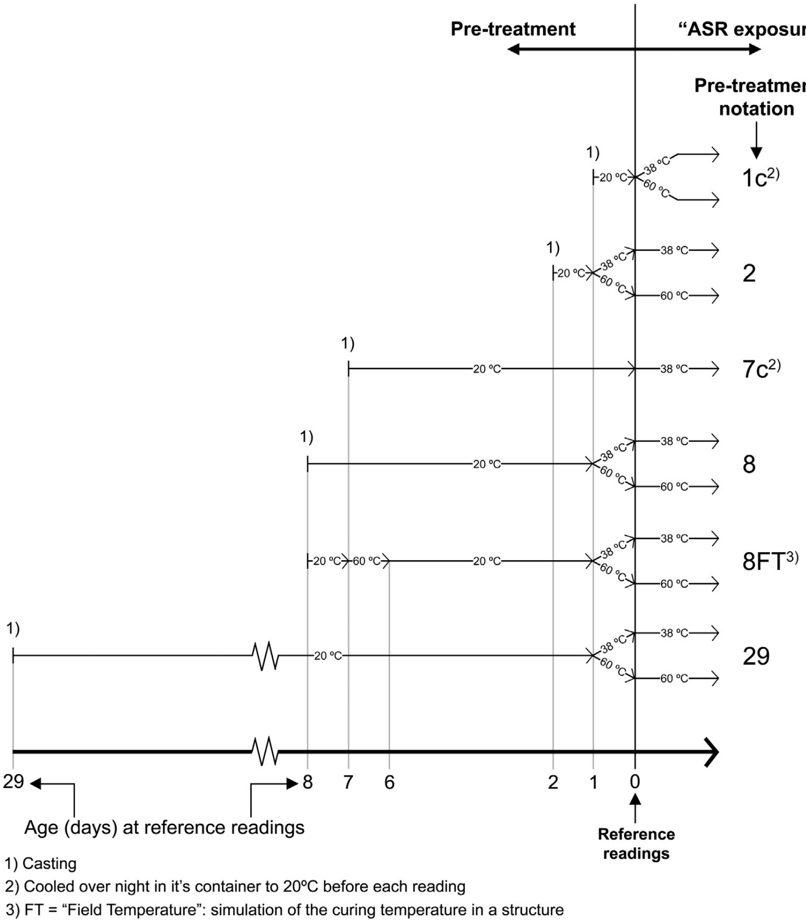

Fig. 1. Pre-treatment of the various test series, included notations. For all test series, the prisms were prepared for final storage and put into their storage container immediately after de-moulding (and after the 0.5 h submersion period where used—see Fig. 2 and Tables 5–8).

extent of alkali leaching. The lowest pH level corresponds to the typical pH found in water filtered from fresh cement paste with a high alkali Norwegian CEM I after half an hour. The highest pH level corresponds to the calculated pH level in the pore water in the concrete with the "basis" binder after about one month of curing when most of the water has been consumed by hydration and concentrated up the salt solution about ten times. *(Comment: Some may find it strange with a pH above 14, but the pH scale from 0 to 14 is just the common range corresponding to 1 M* H^+ *and 1 M* OH^-*, respectively, and is not "limits").*

To be able to document the effect of raising the exposure temperature from 38 °C to 60 °C, similar pre-treatment variants were applied for both ASR exposure temperatures as far as possible.

Also the Norwegian CPT was slightly modified by increasing the length of the "pre-storage" period from 1 to 7 days.

During the "pre-storage" period and the ASR exposure all the prisms were stored in containers prepared as prescribed in the "standard" test procedures (see Table 3), but with the following exceptions: For the "Alternative" version of RILEM AAR-4.1 CPT (wrapped prisms) [5] the three prisms from each test series were stored in the same metal container as prescribed for the "Standard" version of RILEM AAR-4.1 (unwrapped prisms) [5], instead of being stored in separate containers.

2.3.3. Overview of test series

Fig. 2 shows the notations used to label the various test series. The full notations give a complete description of the pre-treatment and ASR exposure of the prisms. However, to simplify, short names are used in some figures and tables when presenting the results.

Tables 5–8 give an overview of all 58 test series included in the test programme.

2.4. Complementary tests

2.4.1. Overview

In order to document properties of importance for initiation and progress of ASR, comprehensive complementary testing has been an important part of the study. Fig. 3 gives an overview of the following tests performed on concrete prisms during and after the ASR exposure (the abbreviations used in Fig. 3 are quoted in the brackets below):

- Concrete porosities ("PF-method"—Section 2.4.2)
- Moisture state ("in-situ" (evaporable) water content, "DCS" and "RH"—Section 2.4.3)
- Relative diffusion coefficient ("Relative D"—Section 2.4.4)
- Electrical resistivity (Section 2.4.5)
- Visual inspection (photo)—see [44])

Table 4
Specimen environment during testing.

Notation	Specimen environment[a]	Comments
A	Three unwrapped prisms stored inside each container	Standard procedure for RILEM AAR-4.1, ASTM C-1293 and Norwegian CPT (see Table 3)
B[b]	Each prism was wrapped[c] in damp cotton cloth and poly-ethylene (prism ends not covered). Before wrapping, each cotton cloth was submerged for minimum 10 min in 80 g deionised water. Excess water not absorbed by the cotton cloth during submersion (~35–45 g) was poured on the top surface before sealing the bag. This lead to a "water reservoir" in the bottom of each polyethylene bag, that after four weeks of exposure was measured to be in the range of 4–25 g for 38 °C exposure and 0–2.5 g for 60 °C exposure	Standard procedure for RILEM AAR-3 and RILEM AAR-4.1 Alternative, including addition of 5 ml deionised water on the top surface after every reading (see Table 3)
C[b]	Equal to "B", except that each cotton cloth was submerged in half the amount of deionised water (i.e. 40 g). All the water was absorbed by the cotton cloth	Motivation: Investigate the importance of the amount of water added to the wrapping
D	Equal to "B", except that each wrapped prism was not sealed inside a separate polyethylene bag, but was placed on a grid inside the "AAR-3 container". Neither was 5 ml deionised water poured on the top surface at any time	Motivation: Investigate the importance of storing each wrapped prism in a separate polyethylene bag
E	After de-moulding, each prism was coated with epoxy. The next day the prisms were further sealed by packing them in aluminium foil. Further storage in dry containers	Motivation: Try to totally hinder any moisture exchange with the surroundings
F	After de-moulding, the unwrapped prisms were totally submerged in deionised water. After every reading, the water was exchanged with new deionised water	Motivation: Give the prisms the maximum alkali leaching conditions
G[b]	Equal to "B", except each cotton cloth was submerged for minimum 10 min in a basic solution with pH 14.2 (Na/K-ratio ≈ 1/3) simulating the pH in the pore water of the "basis CEM I binder" after ~28 days of curing. No extra solution was poured on the top surface, beyond the ~60 g absorbed by the cotton cloth when it was submerged	Motivation: Investigate if application of a similar pH in the cotton cloth as in the concrete pore water is able to hinder alkali leaching from the concrete prisms
H[b]	Equal to "G", except each cotton cloth was submerged in a basic solution with pH 13.2 (Na/K-ratio ≈ 1/3) simulating a less basic pore solution. No extra solution was poured on the top surface, beyond the ~50 g absorbed by the cotton cloth when it was submerged	Motivation: Investigate if application of a somewhat lower pH in the cotton cloth compared to the concrete pore water is able to reduce the extent of alkali leaching

[a] In all CPTs, the prisms are stored vertically on grids above water, without being in direct contact with the water. A humid environment close to 100% RH is aimed. See more details about the storage containers in Table 3.

[b] For 60 °C storage, three wrapped prisms were stored in an "AAR-4.1 metal container" instead of single "AAR-3 containers".

[c] Each wrapped prism was sealed inside a separate polyethylene bag. 5 ml deionised water was poured on the top surface before sealing the bag and after each reading. Each bag was placed in a separate "AAR-3 container" with a tight lid.

- Microstructural analysis (on polished sections ("PS") and thin sections ("TS"), in addition to use of scanning electron microscope (SEM)—see [25] and [44])

The tests were performed at two ages: four weeks after starting the ASR exposure (in order to document concrete properties in the early stage of the ASR test) and after ending the ASR exposure, i.e. after 39 weeks (all 60 °C test series), 52 or 112 weeks (38 °C test series).

The tests initiated after four weeks of ASR exposure were performed on an "extra prism" exposed to identical pre-treatment and ASR exposure conditions as the three parallel prisms in the same test series. The tests performed after ending the ASR exposure were executed on one of the three parallel prisms in each test series.

In both cases, the prisms were removed from their container and immediately sealed in polyethylene foil to avoid loss of moisture. After being cooled to ambient laboratory temperature the next day, each prism was unwrapped before the test samples (six samples after four weeks of the ASR exposure and four samples after ending the ASR exposure) with height about 40 mm were split immediately (to avoid loss of moisture) from the prism by use of a rock splitter. Each of the split samples represents a given height from the bottom of the prism.

This paper presents results from the measurements described in Sections 2.4.2–2.4.5. Results from the visual inspections and the microstructural analyses are presented in the PhD thesis [44] together with measurements of alkali release from the aggregates and the dynamic

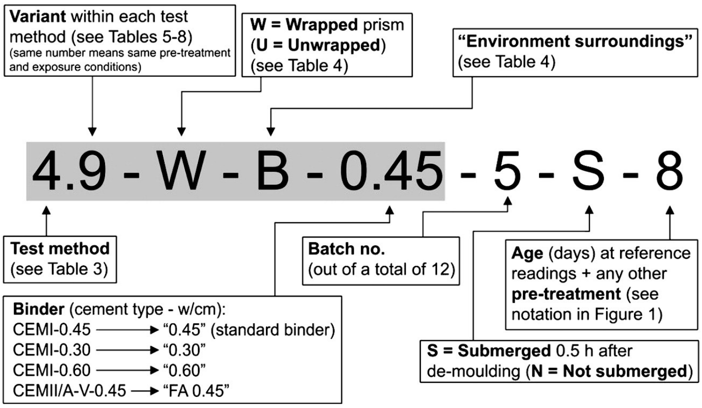

Fig. 2. Notations used to name the various test series. The short names (see Tables 5–8) used in some figures and tables when presenting results are marked with grey shadow. For repeated test series, the batch no. is additionally included in the short name.

Table 5
Overview of the 18 test series with modified versions of the RILEM AAR-3 38 °C CPT (2000) [3].

Test series		Comments
Short name[a]	Full notation[b]	
3.1-W-B-0.45	3.1-W-B-0.45–3-N-7c	Standard RILEM AAR-3 test procedure (wrapped prisms, 7 days pre-storage at 20 °C, prisms cooled before every reading)[c]
3.2-W-B-0.45	3.2-W-B-0.45–4-N-8	As 3.1-W-B-0.45, but readings taken without pre-cooling
3.3-W-C-0.45	3.3-W-C-0.45–4-N-8	As 3.2-W-B-0.45, but less water in wrapping
3.4-W-B-0.45	3.4-W-B-0.45–4-S-8	As 3.2-W-B-0.45, but prisms 0.5 h submerged after de-moulding
3.5–E-0.45	3.5–E-0.45–5-N-8	Sealed storage (epoxy and aluminium foil) after de-moulding (no water in the bottom of the storage containers)
3.6-W-D-0.45	3.6-W-D-0.45–6-S-8	As 3.4-W-B-0.45, but no polyethylene bag
3.7-U- A-0.45	3.7-U-A-0.45–6-S-8	As 3.4-W-B-0.45, but no wrapping (one prism in each container)
3.8-W-B-0.45	3.8-W-B-0.45–3-S-2	As 3.4-W-B-0.45, but 1 day pre-storage at 20 °C
3.9-W-B-0.45	3.9-W-B-0.45–2-S-29	As 3.4-W-B-0.45, but 28 days pre-storage at 20 °C
3.10-W-B-0.45–2	3.10-W-B-0.45–2-S-8FT	As 3.4-W-B-0.45, but simulating “field curing temperature” (see Fig. 1)
3.10-W-B-0.45–10	3.10-W-B-0.45–10-S-8FT	As 3.10-W-B-0.45–2, but repeated test series
3.11-U- F-0.45	3.11-U-F-0.45–5-S-8	Stored submerged in deionised water after de-moulding
3.12-W-G-0.45	3.12-W-G-0.45–12-S-8	As 3.4-W-B-0.45, but pH 14.2 in wrapping at start
3.13-W-H-0.45	3.13-W-H-0.45–12-S-8	As 3.4-W-B-0.45, but pH 13.2 in wrapping at start
3.4-W-B-0.30	3.4-W-B-0.30–7-S-8	As 3.4-W-B-0.45, but lower w/c ratio
3.4-W-B-0.60	3.4-W-B-0.60–8-S-8	As 3.4-W-B-0.45, but higher w/c ratio
3.8-W-B-FA-0.45	3.8-W-B-FA-0.45–9-S-2	As 3.8-W-B-0.45, but fly ash binder with boosted alkali level
3.9-W-B-FA-0.45	3.9-W-B-FA-0.45–9-S-29	As 3.9-W-B-0.45, but fly ash binder with boosted alkali level

[a] Used in figures and tables when presenting results.
[b] See details in Fig. 2.
[c] See details in Table 3.

E-modulus (measured for all unwrapped prisms at the same point in time as the expansion measurements).

Additionally, the rate and amount of alkali leaching from concrete prisms (measured for all test series at the same point in time as the expansion measurements) are properly discussed in [25].

2.4.2. Concrete porosity

After splitting, each sample was brushed with a wire brush to remove loose particles. The measurements were performed according to the “PF-method” (named “PF” in Fig. 3) as described by Sellevold and Farstad [30] by weighing each sample at the following moisture stages:

- Immediately after splitting and brushing the sample.
- After submersion of the sample in water for seven days assumed to saturate the gel and capillary porosity (also submerged mass to obtain volume).
- After drying the samples at 105 °C in an oven for seven days.
- After submersion of the sample in water for seven days.

Table 6
Overview of the 22 test series with modified versions of the RILEM AAR-4.1 60 °C CPT (2006) [5].

Test series		Comments
Short name[a]	Full notation[b]	
4.1-U-A-0.45	4.1-U-A-0.45–1-S-1c	Standard RILEM AAR-4.1 test procedure (unwrapped prisms, “reactor”, 1 day pre-storage at 20 °C, prisms 0.5 h submerged after de-moulding and cooled before every reading)[c]
4.2-U-A-0.45	4.2-U-A-0.45–1-S-2	As 4.1-U-A-0.45, but readings taken without pre-cooling
4.3-U-A-0.45	4.3-U-A-0.45–6-S-8	As 4.2-U-A-0.45, but 7 days pre-storage at 20 °C
4.4-U-A-0.45	4.4-U-A-0.45–2-S-29	As 4.3-U-A-0.45, but 28 days pre-storage at 20 °C
4.5-U-A-0.45	4.5-U-A-0.45–2-S-8FT	As 4.3-U-A-0.45, but simulating “field curing temperature” (see Fig. 1)
4.6-U-F-0.45	4.6-U-F-0.45–5-S-8	Stored submerged in deionised water after de-moulding
4.7–E-0.45	4.7–E-0.45–5-N-8	Sealed storage (epoxy and aluminium foil) after de-moulding (no water in the bottom of the storage container)
4.8-W-B-0.45–1	4.8-W-B-0.45–1-S-2	Standard RILEM AAR-4.1 Alt. test procedure (wrapped prisms[c], 1 day pre-storage at 20 °C), except prisms 0.5 h submerged after de-moulding and readings taken without pre-cooling
4.8-W-B-0.45–10	4.8-W-B-0.45–10-S-2	As 4.8-W-B-0.45–1, but repeated test series
4.9-W-B-0.45	4.9-W-B-0.45–5-S-8	As 4.8-W-B-0.45-1, but 7 days pre-storage at 20°C
4.10-W-C-0.45–6	4.10-W-C-0.45–6-N-8	As 4.9-W-B-0.45, but less water in wrapping
4.10-W-C-0.45–12	4.10-W-C-0.45–12-N-8	As 4.10-W-B-0.45–6, but repeated test series
4.11-W-D-0.45	4.11-W-D-0.45–3-S-8	As 4.9-W-B-0.45, but no polyethylene bag
4.12-W-G-0.45	4.12-W-G-0.45–12-S-8	As 4.9-W-B-0.45, but pH 14.2 in wrapping at start
4.13-W-H-0.45	4.13-W-H-0.45–12-S-8	As 4.9-W-B-0.45, but pH 13.2 in wrapping at start
4.3-U-A-0.30	4.3-U-A-0.30–7-S-8	As 4.3-U-A-0.45, but lower w/c ratio
4.9-W-B-0.30	4.9-W-B-0.30–7-S-8	As 4.9-W-B-0.45, but lower w/c ratio
4.3-U-A-0.60-I	4.3-U-A-0.60–8-IS-8	As 4.3-U-A-0.45, but higher w/c ratio
4.3-U-A-0.60-II	4.3-U-A-0.60–8-IIS-8	As 4.3-U-A-0.60-I, but repeated test series
4.9-W-B-0.60	4.9-W-B-0.60–11-S-8	As 4.9-W-B-0.45, but higher w/c ratio
4.2-U-A-FA-0.45	4.2-U-A-FA-0.45–9-S-2	As 4.2-U-A-0.45, but fly ash binder with boosted alkali level
4.4-U-A-FA-0.45	4.4-U-A-FA-0.45–9-S-29	As 4.4-U-A-0.45, but fly ash binder with boosted alkali level

[a] Used in figures and tables when presenting results.
[b] See details in Fig. 2.
[c] See details in Table 3.

Table 7
Overview of the 6 test series with modified versions of the Norwegian 38 °C CPT [18].

Test series		Comments
Short name[a]	Full notation[b]	
N.1-U-0.45	N.1-U-A-0.45-3-S-1c	Standard Norwegian CPT procedure (1 day pre-storage at 20 °C, prisms 0.5 h submerged after de-moulding and cooled before every reading)[c]
N.2-U-0.45	N.2-U-A-0.45-1-S-2	As N.1-U-0.45, but readings taken without pre-cooling
N.3-U-0.45	N.3-U-A-0.45-4-S-8	As N.2-U-0.45, but 7 days pre-storage at 20 °C
N.3-U-0.30	N.3-U-A-0.30-7-S-8	As N.3-U-0.45, but lower w/c ratio
N.3-U-0.60	N.3-U-A-0.60-8-S-8	As N.3-U-0.45, but higher w/c ratio
N.3-U-FA-0.45	N.3-U-A-FA-0.45-9-S-8	As N.3-U-0.45, but fly ash binder with boosted alkali level

[a] Used in figures and tables when presenting results.
[b] See details in Fig. 2.
[c] See details in Table 3.

Table 8
Overview of the 12 test series with the ASTM C-1293 38 °C CPT [9].

Test series		Comments
Short name[a]	Full notation[b]	
ASTM-U-0.45–1	ASTM-U-A-0.45–1-N-1c	Standard ASTM C-1293 test procedure (1 day pre-storage at 20 °C, prisms cooled before every reading)[c]
ASTM-U-0.45–2	ASTM-U-A-0.45–2-N-1c	As ASTM-U-0.45–1, but new batch
ASTM-U-0.45–3	ASTM-U-A-0.45–3-N-1c	As ASTM-U-0.45–1, but new batch
ASTM-U-0.45–4	ASTM-U-A-0.45–4-N-1c	As ASTM-U-0.45–1, but new batch
ASTM-U-0.45–5	ASTM-U-A-0.45–5-N-1c	As ASTM-U-0.45–1, but new batch
ASTM-U-0.45–6	ASTM-U-A-0.45–6-N-1c	As ASTM-U-0.45–1, but new batch
ASTM-U-0.45–10	ASTM-U-A-0.45–10-N-1c	As ASTM-U-0.45–1, but new batch
ASTM-U-0.45–12	ASTM-U-A-0.45–12-N-1c	As ASTM-U-0.45–1, but new batch
ASTM-U-0.30–7	ASTM-U-A-0.30–7-N-1c	As ASTM-U-0.45–1, but lower w/c ratio
ASTM-U-0.60–8	ASTM-U-A-0.60–8-N-1c	As ASTM-U-0.45–1, but higher w/c ratio
ASTM-U-0.60–11	ASTM-U-A-0.60–11-N-1c	As ASTM-U-0.60–8, but repeated test series
ASTM-U-FA-0.45–9	ASTM-U-A-FA-0.45–9-N-1c	As ASTM-U-0.45–1, but fly ash binder with boosted alkali level

[a] Used in figures and tables when presenting results.
[b] See details in Fig. 2.
[c] See details in Table 3.

- After submersion of the sample in water in a pressure tank with 50 bar for two days.

The following parameters were measured:

- "In-situ" (evaporable) water content (see Section 2.4.3).
- Degree of capillary saturation, DCS = "in situ" water content/water content after saturation (see Section 2.4.3).
- Gel + capillary porosity (suction porosity [45]) and macro porosity (taken directly as the air content in the hardened concrete) (volume-%).
- Dry-, saturated surface dry (SSD)—and solid densities.

The "PF-method" is frequently used at SINTEF and NTNU as a quality control of a concrete, including estimating the w/cm based on Powers model [30]. Some experiences with the method are summarised in [30]. For equal cement paste contents, a higher suction porosity reflects a more porous concrete with a higher content of capillary pores. The concrete pore system and the content of capillary pores strongly depend on the mix design (in particular on cement type and w/cm), on the degree of hydration and also on the pre-storage conditions (in particular temperature and access to moisture) and the ASR exposure conditions (temperature and access to moisture) [23].

2.4.3. Moisture state

The moisture state of the samples split from each prism was documented by the following three parameters (see further description in Sections 1.4.1 and 2.4.2):

- "In-situ" (evaporable) water content (mass-% of dry concrete).
- Degree of capillary saturation, DCS (%).
- Relative humidity, RH (%).

As discussed in Section 1.4.1, measurement of RH is connected with fairly large uncertainties. To improve the accuracy of the measurements, efforts were put into selecting humidity sensors and measuring procedures that had proven to be reliable. Based on "pilot testing" with two RH sensors that had been frequently used at SINTEF and discussions with experienced colleagues at the University of Lund in Sweden, the following measuring procedure was used:

- Use of Vaisala sensors "HMP44" with reported accuracy ±2% in the range of 0–90% RH and accuracy ±3 % in the range of 90–100% RH [46].
- Each sensor was carefully calibrated before and after each measurement.
- One of the concrete samples split from each prism were split into smaller pieces by use of the splitter, before these pieces were crushed with a hammer. The pieces of crushed cement mortar (some being stuck to small aggregate particles) with diameter from about 5–10 mm were collected and put into slim glass tubes (inner diameter 18 mm) until about ¾ of the glass tube was filled. The top of the glass tube was then immediately sealed with putty. Cement mortar particles from the outer about 15–20 mm of the concrete samples were not used. The collected crushed particles thus represent the "inner part" of each prism at the following levels from the bottom of the prisms: 100–160 mm (prisms of length 280 mm) and 120–240 mm (prisms of length 450 mm). Throughout the crushing and sampling procedure care was taken to avoid loss of moisture.

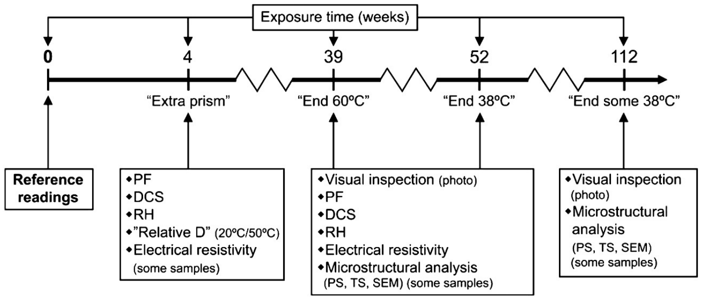

Fig. 3. Tests performed on the concrete prisms after start ASR exposure.

- For some of the large concrete prisms (100 × 100 mm) used in the Norwegian CPT, cement mortar particles were also collected from the outer 0–25 mm in order to check if there were any moisture gradients.
- A Vaisala sensor was installed in each glass tube before placing the glass tubes in a conditioning room with temperature 20 °C and 50% RH.
- For 4–5 days readings of RH were taken early every morning, before any other activity took place in the room (in order to secure a stable temperature in the samples and thus improve the accuracy of the measurements).
- The readings taken after 2–4 days (when they had stabilised) are presented in Section 3.3.

2.4.4. Relative diffusion coefficient

The rate of drying of concrete samples with identical geometries may be used to calculate relative diffusion coefficients, as done by Relling [26]. This parameter is used to characterise the transport properties of the various ASR test series in the early period of the ASR exposure. Since the diffusion coefficient strongly depends on the internal moisture content, the calculated relative diffusion coefficients (named “Relative D” in Fig. 3) are really average values over a certain drying time at isothermal conditions [26].

After 4 weeks of ASR exposure, one of the six samples split from each “extra prism” (as described in Section 2.4.1) were given special treatment during the “PF test procedure” (see Section 2.4.2). After the initial submersion (i.e. before drying the samples at 105 °C), this sample was placed in a conditioning room at 20 °C and 50 % RH in order to dry out slowly during the following 6 months.

The relative diffusion coefficient (“RelD”) was calculated by comparing the time ($t_{c/2}$) various concrete samples need to dry out to a moisture state representing half of the amount of water lost (*c*) from saturated state to a moisture state in equilibrium with the surrounding environment relative to a reference sample. The mean calculated drying time for the ASTM samples (7 parallel test series) with the “basis” binder was chosen as a universal reference sample ($t_{ref.c/2}$). The relative diffusion coefficient (*RelD*) could then be calculated according to Eq. (1).

$$RelD = t_{ref.c/2}/t_{c/2} \tag{1}$$

After six months of drying in the conditioning room, most samples were still drying slowly, in particular the concretes with lowest w/cm. Thus, an estimation of the total water loss at equilibrium (*c*) was made by simply assuming that the samples had reached a moisture state in equilibrium with the surrounding environment by extrapolation to 400 days.

2.4.5. Electrical resistivity

The electrical resistivity of concrete depends on the porosity, the continuity of the pore system and the degree of water filling of pores (i.e. “physics”). Additionally, it depends on type and amount of ions dissolved in the pore water (i.e. “chemistry”) [47]. Several authors have reported a reasonable correlation between electrical resistivity and chloride diffusion for saturated concrete [48]. Hopefully, electrical resistivity might also be used as an indirect measure for concrete transport properties in the present laboratory testing, i.e. as a measure for the ability for water and ions to move to the “reaction site” during the ASR exposure—at least for concrete with the same cement.

After 4 weeks of ASR exposure, supplementary “pilot” measurements of electrical resistivity were performed on five parallel “PF-samples” split from each prism from ten test series. Due to the good correlation obtained between relative diffusion coefficient and electrical resistivity for CEM I cement with similar chemistry (see Section 3.4.1), this simpler and less time consuming test method was chosen to describe the transport properties of the concrete prisms from all test series after ending the ASR exposure (instead of measuring relative diffusion coefficients). The measurements were performed on samples with “in-situ” moisture state by applying current at 1000 Hz at 20 °C [49]. Electrical resistivity is sensitive to DCS ([35,50]), but the procedure chosen was later justified by the fact that DCS maximally varied 5% between various test series. The following test procedure was established (results from measurements according to two additional procedures are included in the coming PhD thesis [44]): After unpacking the prism from the tight polyethylene foil, but before splitting the “PF-samples” (see Section 2.4.1), the electrical resistance (*R*, in *ohm*) across the prism cross section was measured by placing two 100 × 100 mm metal plates on two opposite sides (not the casting surface) of the mid part of the prism. A conductive gel was evenly distributed on the two plates to ensure good contact, before the readings of the electrical resistance (*R*, in *ohm*) were taken.

When calculating the electrical resistivity (ρ) according to Eq. (2) ([47,49]), the width of the metal plates (100 mm) was as a simplification used as the cross section widths (*t*).

$$\varrho = A \cdot R/L = L \cdot t \cdot R/L = t \cdot R(ohm \cdot m) \tag{2}$$

where

A $L \cdot t$ = area of each of the two opposite sides of the sample (m^2)
L length between the metal plates = length of the prism side (m)

Even though the results presented in Section 3.4.3 are somewhat lower than the “true” electrical resistivity (since some current can be transported through the concrete prisms outside the 100 mm zone used in the calculations), the internal ranking between the various test series is believed to be correct.

Table 9
Quality control of the 12 concrete mixes.

Binder composition	Density[a] ρ_{mean} (kg/m^3)	Compr. strength, cubes 28 days		Suction porosity[b], 4 weeks of exposure		Macro porosity[b], 4 weeks of exposure		Solid density[b], 4 weeks of exposure	
		$f_{c\text{-}mean}$ (MPa)	c.o.v. (%)	$\varepsilon_{suc\text{-}mean}$ (vol.%)	c.o.v. (%)	$\varepsilon_{air\text{-}mean}$ (vol.%)	c.o.v. (%)	ρ_{mean} (kg/m^3)	c.o.v. (%)
CEM I, w/c 0.60[c]	2450	49.7	1.6	13.3	4.8	1.9	15	2715	0.3
CEM I, w/c 0.45[d]	2450	70.0	2.1	12.0	3.2	1.8	22	2720	0.2
CEM I, w/c 0.30	2520	103.4	–	10.4	–	1.9	–	2725	–
CEM II/A–V, w/cm 0.45	2450	44.4	–	14.0	–	1.4	–	2735	–

[a] Saturated surface dry condition, measured on the compressive strength cubes.
[b] Measured on “PF-samples” cut from the ASTM test series (see Section 2.4.2).
[c] Two batches prepared.
[d] Eight batches prepared.

Table 10
Porosity and internal moisture state for the 18 RILEM AAR-3 38 °C CPT series (numbers in brackets are somewhat uncertain).

Test series	Suction porosity (%)		Macro porosity (%)		Water content ("in-situ") (mass-%)			DCS (%)			RH (%)		
	4 weeks	$\Delta_{4-52\ \text{weeks}}$	4 weeks	$\Delta_{4-52\ \text{weeks}}$	4 weeks	52 weeks	$\Delta_{4-52\ \text{weeks}}$	4 weeks	52 weeks	$\Delta_{4-52\ \text{weeks}}$	4 weeks	52 weeks	$\Delta_{4-52\ \text{weeks}}$
3.1-W-B-0.45–3- N-7c	11.9	1.3	1.9	0.5	4.9	6.0	1.1	93.7	97.2	3.4	93.0	97.0	4.0
3.2-W-B-0.45–4- N-8	11.5	2.1	1.4	0.1	4.9	6.0	1.1	96.3	97.7	1.4	96.0	96.5	0.5
3.3-W-C-0.45–4- N-8	11.9	1.1	1.5	0.1	4.9	5.6	0.6	95.1	95.3	0.2	(90.0)	96.5	(6.5)
3.4-W-B-0.45–4- S-8	11.7	1.4	1.5	0.0	5.0	5.8	0.8	96.0	97.7	1.7	95.0	96.5	1.5
3.5- –E-0.45–5- N-8	12.0	−0.3	2.1	−0.1	4.5	3.9	−0.6	86.3	77.9	−8.4	87.5	(75.0)	(−12.5)
3.6-W-D-0.45–6- S-8	12.1	0.8	2.3	−0.4	5.1	5.8	0.7	95.3	97.4	2.1	94.5	97.0	2.5
3.7-U -A-0.45–6- S-8	12.2	0.6	2.1	0.3	4.9	5.7	0.8	93.7	96.7	3.0	93.5	97.5	4.0
3.8-W-B-0.45–3- S-2	12.2	1.3	1.8	0.3	5.1	6.0	0.9	96.7	96.2	−0.5	95.5	97.5	2.0
3.9-W-B-0.45–2- S-29	11.7	1.3	1.1	0.6	4.9	5.9	1.0	94.0	97.2	3.2	92.5	97.5	5.0
3.10-W-B-0.45–2- S-8FT	11.8	0.9	1.2	0.2	4.9	5.6	0.7	95.3	97.7	2.4	95.0	98.0	3.0
3.10-W-B-0.45–10- S-8FT	12.4	0.1	1.8	−0.5	5.3	5.6	0.3	96.1	97.9	1.8	95.0	96.0	1.0
3.11-U -F-0.45–5- S-8	12.2	1.0	1.7	0.1	5.1	5.6	0.5	95.1	96.8	1.7	94.0	97.0	3.0
3.12-W-G-0.45–12- S-8	11.6	0.6	1.5	−0.2	4.7	5.3	0.6	92.4	96.0	3.6	90.5	95.5	5.0
3.13-W-H-0.45–12- S-8	11.8	0.3	1.5	0.1	4.9	5.4	0.5	93.4	97.8	4.4	90.5	95.5	5.0
3.4-W-B-0.30–7- S-8	10.2	−0.3	1.8	0.0	4.1	4.4	0.2	96.3	97.4	1.1	83.5	(90.5)	(7.0)
3.4-W-B-0.60–8- S-8	12.5	2.5	1.7	0.4	5.4	6.6	1.2	95.8	98.6	2.8	96.5	97.5	1.0
3.8-W-B-FA-0.45–9-S-2	13.9	−0.9	1.4	−0.4	5.6	5.4	−0.2	95.9	97.5	1.6	90.0	88.5	−1.5
3.9-W-B-FA-0.45–9-S-29	14.0	−0.4	1.2	−0.4	5.8	5.7	−0.1	95.9	97.8	1.9	87.0	88.5	1.5

3. Results and discussion

3.1. Overall concrete properties—control of mix design and concrete mixes

In order to cast the prisms for all the 58 test series, 12 concrete mixes of about 50 liters were prepared; eight of the "basis" binder, two of the "open" binder and one of each of the two remaining binders (see Table 9). All the 12 concrete mixes showed good workability properties. The slump varied from 120 to 150 mm.

The air (macro) pores might act like evacuation chamber for the ASR gel produced, but the influence of increased air content on the expansion is not fully agreed in the literature [23]. However, the fresh air content was rather low and in the target range (<3.0%) for all concrete mixes, except one (3.1%). Consequently, the expansions can be compared without consideration of the slightly varying air contents.

Table 9 shows overall hardened concrete properties for the 12 concrete mixes. All the 8 batches with the "basis" binder (CEM I, w/c of 0.45) attain nearly identical hardened concrete properties. The 8 parallel ASTM test series with this binder (see Table 8) also obtain very similar prism expansions (mean 52 weeks expansion of 0.266%, c.o.v. of 3.2%). The variation between the mean prism expansions for these 8 parallel test series is in fact lower than the internal variation between the three parallel prisms within each of the test series (typical c.o.v. is in the range of 4–10%). Furthermore, the suction porosities (Section 2.4.2) measured for the 8 parallel ASTM test series with the "basis" binder after 4 weeks of exposure are comparable (mean value of 11.9%, c.o.v. of 3.2%). Based on these 8 parallel suction porosities and by assuming a realistic degree of hydration ($\alpha = 0.85$ [51]), w/c is estimated to be in the range from 0.44 to 0.47 applying Powers model [30], with a mean w/c of 0.45, agreeing with the mix design.

The two batches with the "open" binder (CEM I, w/c of 0.60) also obtain nearly identical hardened concrete properties, with internal

Table 11
Porosity and internal moisture state for the 22 RILEM AAR-4.1 60 °C CPT series (numbers in brackets are somewhat uncertain).

Test series	Suction porosity (%)		Macro porosity (%)		Water content ("in-situ") (mass%)			DCS (%)			RH (%)		
	4 weeks	$\Delta_{4-39\ \text{weeks}}$	4 weeks	$\Delta_{4-39\ \text{weeks}}$	4 weeks	39 weeks	$\Delta_{4-39\ \text{weeks}}$	4 weeks	39 weeks	$\Delta_{4-39\ \text{weeks}}$	4 weeks	39 weeks	$\Delta_{4-39\ \text{weeks}}$
4.1-U -A-0.45–1- S-1c	11.7	1.2	2.1	−0.5	4.6	5.6	1.0	92.7	95.2	2.5	95.5	98.0	2.5
4.2-U -A-0.45–1- S-2	11.9	0.9	2.0	−0.3	4.8	5.6	0.8	93.5	94.7	1.1	96.0	97.0	1.0
4.3-U -A-0.45–6- S-8	12.5	−0.3	2.1	−0.2	5.1	5.3	0.2	92.6	95.1	2.5	96.0	97.0	1.0
4.4-U -A-0.45–2- S-29	11.7	0.8	1.2	0.2	4.8	5.4	0.6	92.4	95.0	2.5	96.0	97.5	1.5
4.5-U -A-0.45–2- S-8FT	11.6	1.2	1.1	0.2	4.6	5.5	0.9	92.5	94.6	2.1	95.5	98.0	2.5
4.6-U -F-0.45–5- S-8	12.0[a]	–	2.3[a]	–	–	4.9	–	–	93.9	–	–	97.0	–
4.7- -E-0.45–5- N-8	11.7	0.0	2.0	0.3	4.1	4.3	0.2	79.1	84.8	5.7	(85.0)	–	–
4.8-W-B-0.45–1- S-2	12.0	−0.4	1.9	−0.2	5.0	5.1	0.1	95.8	95.9	0.0	96.5	96.0	−0.5
4.8-W-B-0.45–10- S-2	12.1	−0.2	1.5	−0.2	5.2	5.1	−0.1	96.0	95.1	−0.9	96.0	95.5	−0.5
4.9-W-B-0.45–5- S-8	12.0	−0.2	1.6	0.1	5.0	4.8	−0.2	94.2	93.8	−0.4	95.0	97.0	2.0
4.10-W-C-0.45–6- N-8	11.9	0.3	2.1	0.0	4.9	5.3	0.4	92.8	94.8	2.0	96.0	97.0	1.0
4.10-W-C-0.45–12- N-8	10.8	1.3	1.5	−0.3	4.4	5.1	0.7	91.5	96.6	5.1	95.0	94.0	−1.0
4.11-W-D-0.45–3- S-8	11.5	−0.1	1.8	0.6	4.8	5.0	0.2	94.6	96.5	1.8	96.0	97.5	1.5
4.12-W-G-0.45–12- S-8	11.1	1.8	1.4	−0.2	4.6	5.6	1.0	92.7	97.5	4.8	93.5	94.0	0.5
4.13-W-H-0.45–12- S-8	10.5	1.1	1.4	−0.2	4.4	4.9	0.4	92.7	96.6	3.8	93.5	94.0	0.5
4.3-U -A-0.30–7- S-8	10.2	−0.2	1.8	−0.1	4.1	4.4	0.2	93.0	93.9	0.9	90.0	95.0	5.0
4.9-W-B-0.30–7- S-8	9.7	−0.4	1.7	0.0	4.0	3.8	−0.2	94.8	92.9	−2.0	92.0	92.0	0.0
4.3-U -A-0.60–8-I S-8	13.2	1.6	1.6	0.2	5.4	6.3	0.9	93.5	95.2	1.7	95.0	99.0	4.0
4.3-U -A-0.60–8-II S-8	12.9	1.4	1.8	−0.2	5.2	5.9	0.7	92.2	94.8	2.6	97.0	98.0	1.0
4.9-W-B-0.60–11- S-8	13.4	−0.1	2.3	−0.7	5.7	5.9	0.2	96.2	97.4	1.2	96.5	96.5	0.0
4.2-U -A-FA-0.45–9-S-2	14.0	−0.5	1.3	−0.3	5.6	5.8	0.1	95.6	96.8	1.2	88.5	88.0	−0.5
4.4-U -A-FA-0.45–9-S-29	12.6	−0.5	1.1	0.0	5.1	4.9	−0.3	92.9	94.5	1.6	84.5	89.0	4.5

[a] 39 weeks of exposure.

Table 12
Porosity and internal moisture state for the 6 Norwegian 38 °C CPT series.

Test series	Suction porosity (%)		Macro porosity (%)		Water content ("in-situ") (mass%)			DCS (%)			RH (%)		
	4 weeks	$\Delta_{4–52\ weeks}$	4 weeks	$\Delta_{4–52\ weeks}$	4 weeks	52 weeks	$\Delta_{4–52\ weeks}$	4 weeks	52 weeks	$\Delta_{4–52\ weeks}$	4 weeks	52 weeks	$\Delta_{4–52\ weeks}$
N.1-U- A-0.45–3- S-1c	12.2	0.7	2.1	−0.1	4.8	5.5	0.7	92.3	93.3	1.0	94.0	96.5	2.5
N.2-U- A-0.45–1- S-2	11.9	1.0	2.1	−0.1	4.8	5.6	0.8	93.9	94.7	0.8	93.0	96.5	3.5
N.3-U- A-0.45–4- S-8	12.1	1.3	1.7	−0.2	4.9	5.8	0.9	92.7	94.7	1.9	93.0	96.5	3.5
N.3-U- A-0.30–7- S-8	10.1	−0.3	2.0	0.1	3.8	4.1	0.3	94.2	95.2	1.0	82.0	88.0	6.0
N.3-U- A-0.60–8- S-8	13.6	2.0	2.1	0.4	5.8	6.6	0.8	95.0	95.9	1.0	94.0	98.0	4.0
N.3-U- A-FA-0.45–9-S-8	13.9	−0.6	1.4	−0.2	5.5	5.5	−0.1	94.4	95.2	0.8	87.5	83.0	−4.5

variations for the various parameters tested in the same range as for the "basis" binder (Table 9). The mean prism expansions are also comparable (mean 52 weeks expansion of 0.225%, c.o.v. of 8.5%). Furthermore, based on the suction porosities after 4 weeks of exposure (mean of 13.2 vol.%) and by assuming a realistic degree of hydration ($\alpha = 0.95$ [51]), w/c is estimated to be 0.55 and 0.60, with a mean w/c of 0.58, i.e. a fairly good agreement with the mix design.

Based on the suction porosity after 4 weeks of exposure (10.4 vol.%) and by assuming a realistic degree of hydration ($\alpha = 0.65$ [51]), w/c for the ASTM test series with the "dense" CEM I binder (w/c of 0.30) is estimated to be 0.30, i.e. agreeing with the mix design.

Based on the suction porosity after 4 weeks of exposure (13.7 vol.%) and by assuming a realistic degree of hydration ($\alpha = 0.60$ [51]), w/c for the ASTM test series with the "fly ash" binder (CEM II/A–V, w/cm of 0.45) is estimated to be 0.44, i.e. agreeing with the mix design.

Since most of the fly ash still has not reacted after 4 weeks of exposure, the suction porosity for the "fly ash" binder is significantly higher than for the "basis" binder even though w/cm is equal. Note that the differences in concrete suction porosity do not directly reflect the variation in "binder porosity", since the cement paste content varies somewhat from binder to binder (see Table 2).

Based on the discussion above, we conclude that the produced concretes are of designed quality and that test series cast from different batches can be compared.

3.2. Change in porosity and mass during the ASR exposure

3.2.1. Porosity

Tables 10–13 show the suction and macro porosities for all the test series after 4 weeks of exposure based on suction and submersion after drying. Additionally, the change in porosities from 4 weeks to the end of the exposure period is given.

As shown in Fig. 4, the suction porosity (before drying) for most test series are significantly altered when ASR develops during the exposure period from 4 weeks to 39 weeks (60 °C test series) or 52 weeks (38 °C test series) of exposure, as are the "in-situ" water contents (see Section 3.2.3). It appears that the suction porosity increases (up to 2.2 vol.% = 22 l/m^3) for most test series with the CEM I binders with w/c of 0.45 and 0.60, in particular for those revealing high expansion, a natural consequence of the expansion producing cracks that hold ASR-gel and water. However, alteration of the suction porosity also depends on the type of binder (in addition to the magnitude of expansion). For four of the five "fly ash" test series, the suction porosity is reduced in the range of 0.4 to 0.9 vol.%, while being almost unchanged for the remaining "fly ash" test series. Also the test series with the "dense" CEM I binder reveal rather small alterations of the suction porosity (from 0.3 vol.% reduction to 0.6 vol.% increase). One reason for the observed reduction in suction porosity is assumed to be further hydration, in particular of the fly ash, making the paste denser. Additionally, the final expansions are less for these two binders compared with the two CEM I binders with higher w/c (discussed in [25]).

The average changes in macro porosity (air content) during the ASR exposure from 4 to either 39 or 52 weeks of exposure are negligible, in the range of −0.3 to 0.1 vol.%. This is somewhat surprising, since ASR also leads to formation of cracks that are too large to build up capillary forces [52]. One should thus expect an increase in the macro porosity corresponding to the formation of such "coarse" cracks. However, the microstructural analysis showed that ASR gel was present in several air voids and cracks at the end of the ASR exposure period. In the "PF-analysis", the macro porosity filled with ASR gel (that probably will suck even more water when the concrete samples are submerged), will be part of the measured increase in suction porosity. Since the measured macro porosity did not change significantly, the reduced air void content due to filling with ASR gel seems to be of the same magnitude as the increase in macro porosity due to formation of "coarse" cracks. However, one should not exclude another possible explanation that might have some influence: Some of the cracks formed may be so large that water is running into the cracks when the concrete samples are submerged (i.e. without any capillary forces present). If this water is not released again before the samples are weighed, the water will contribute to an increase in the

Table 13
Porosity and internal moisture state for the 12 ASTM C-1293 38 °C CPT series (numbers in brackets are somewhat uncertain).

Test series	Suction porosity (%)		Macro porosity (%)		Water content ("in-situ") (mass%)			DCS (%)			RH (%)		
	4 weeks	$\Delta_{4–52\ weeks}$	4 weeks	$\Delta_{4–52\ weeks}$	4 weeks	52 weeks	$\Delta_{4–52\ weeks}$	4 weeks	52 weeks	$\Delta_{4–52\ weeks}$	4 weeks	52 weeks	$\Delta_{4–52\ weeks}$
ASTM-U-A-0.45–1- N-1c	12.3	0.6	2.2	−0.2	5.0	5.6	0.6	92.7	95.3	2.6	94.0	95.5	1.5
ASTM-U-A-0.45–2- N-1c	12.1	0.5	1.4	−0.1	4.8	5.5	0.7	94.3	96.9	2.6	(93.5)	96.0	(2.5)
ASTM-U-A-0.45–3- N-1c	11.9	1.1	1.9	0.3	4.7	5.6	0.9	94.2	94.7	0.5	95.0	96.0	1.0
ASTM-U-A-0.45–4- N-1c	11.6	1.1	1.4	0.1	4.6	5.5	0.9	93.1	96.4	3.3	94.0	96.5	2.5
ASTM-U-A-0.45–5- N-1c	12.6	0.6	1.9	0.3	5.2	5.8	0.6	93.6	95.1	1.5	93.5	96.5	3.0
ASTM-U-A-0.45–6- N-1c	12.3	1.2	2.5	−0.4	5.1	5.8	0.7	93.8	94.9	1.1	94.0	96.5	2.5
ASTM-U-A-0.45–10- N-1c	11.5	1.3	1.5	−0.1	4.7	5.6	0.9	94.5	96.8	2.3	92.5	96.5	4.0
ASTM-U-A-0.45–12- N-1c	11.8	0.8	1.6	0.0	4.7	5.7	1.0	91.6	97.5	5.9	89.0	96.0	7.0
ASTM-U-A-0.30–7- N-1c	10.4	−0.9	1.9	−0.2	4.2	4.1	−0.1	94.0	96.4	2.4	85.5	(84.5)	(−1.0)
ASTM-U-A-0.60–8- N-1c	12.8	1.7	1.7	0.7	5.3	6.4	1.1	95.5	95.6	0.1	95.5	98.0	2.5
ASTM-U-A-0.60–11- N-1c	13.7	0.6	2.1	−0.1	5.6	6.4	0.8	92.8	97.1	4.3	95.5	98.5	3.0
ASTM-U-A-FA-0.45–9- N-1c	14.0	−1.3	1.4	−0.3	5.7	5.3	−0.4	95.7	96.7	1.0	89.5	87.0	−2.5

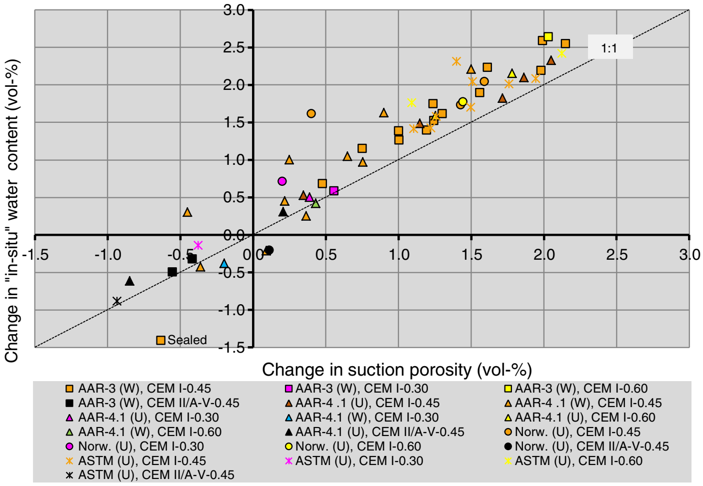

Fig. 4. Change in evaporable "in-situ" water content in cut samples versus change in suction porosity from 4 weeks to 39 weeks (60 °C) or 52 weeks (38 °C) of exposure (W = Wrapped prisms; U = Unwrapped prisms).

measured suction porosity. One observation supporting this theory is that the mass increased a little for the (few) samples being submerged longer than the prescribed one week in the "PF-procedure"; 14 days of prolonged submersion raised the suction porosity with about 0.3 vol.% (CEM I, w/c of 0.45) and 0.5 vol.% (CEM I, w/c of 0.60), respectively.

3.2.2. Mass change of whole prisms

Extensive ASR testing has shown that the concrete will absorb water during the exposure period, see for example study by Lindgård and co-workers [20]. The main mechanisms for the water uptake are: 1) Water is absorbed because of self-desiccation; 2) Any cracks developed during the ASR exposure that are able to suck water and any ASR-gel in cracks and pores will absorb water if available.

In addition to document internal moisture state of one prism from each test series (Sections 2.4.3 and 3.2.3), the net mass change of the whole prisms from de-moulding has been recorded. To avoid loss of moisture, these prisms were cooled inside polyethylene foil before being split. Thus, the net increases in prism mass are assumed to represent the "true" water absorptions at these ages (neglecting the minor influence on the prism mass of alkali leaching). Based on this assumption, the increase in mass might be recalculated from mass % to volume % (vol.%) water absorbed, as done in several figures (1 vol.% water corresponds to 10 l/m^3 of concrete). *(Comment: The mass of the three parallel*

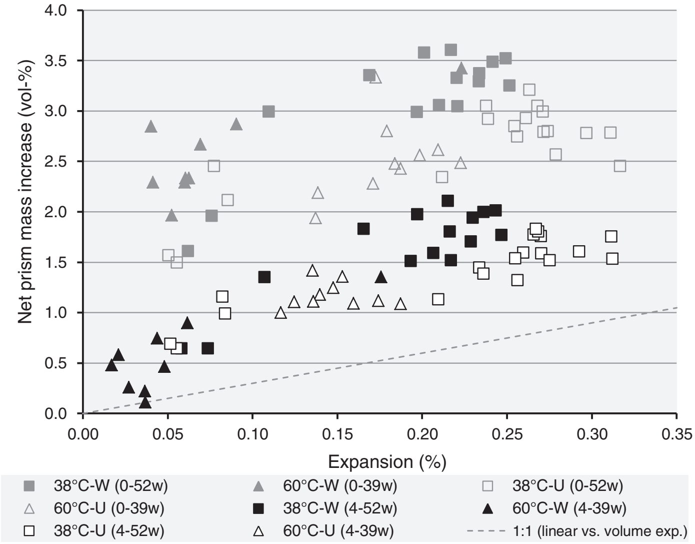

Fig. 5. Increase in net mass of whole prisms (in vol.%) versus corresponding prism expansion in various time intervals; upper points (grey symbols) represent mass increase from de-moulding and prism expansion from reference readings until 39/52 weeks of exposure; lower points (black symbols) represent the time interval 4 weeks to 39/52 weeks of exposure. The sealed and submerged test series (see Tables 5 and 6) are not included. (1 vol.% constitutes about 0.40 mass%; W = Wrapped prisms; U = Unwrapped prisms; w = weeks).

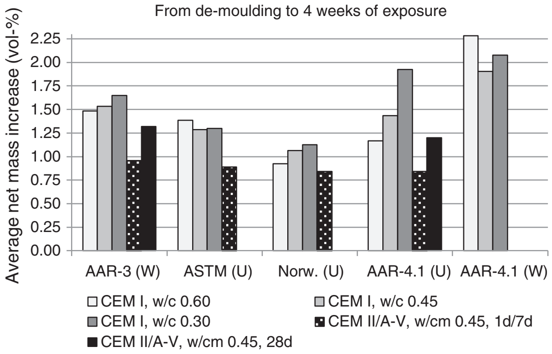

Fig. 6. Increase in net mass of whole prisms (re-calculated to vol.% water absorption) from de-moulding to 4 weeks of exposure (W = Wrapped prisms; U = Unwrapped prisms; d = age (days) at exposure to elevated temperature).

prisms used for expansion readings has additionally been recorded at every measuring point in time, but these results are not presented in this paper. For the wrapped prisms, these periodic mass readings include any water absorbed by the cotton wrapping during the ASR exposure.)

The fact that concrete will absorb water when ASR develops is evident from Fig. 5. A fair correlation exists between the water uptake and the expansion in the period beyond 4 weeks of exposure. When adding trend lines, R^2 is calculated to be about 0.90 for the wrapped prisms and about 0.83 for the unwrapped prisms. At high expansions, the “mass versus expansion trend line” seems to flatten out more for unwrapped prisms compared with wrapped prisms, indicating that wrapped prisms absorb slightly more water during the ASR exposure compared with unwrapped prisms for comparable expansions. Some of the wrapped prisms absorb up to 0.80–0.85 mass % of water in the period beyond 4 weeks of exposure, corresponding to about 20 litres of water per m^3 of concrete.

The dotted line in Fig. 5 represents the linear expansion of the prisms recalculated to volume expansion, assuming a uniform expansion in all directions and that the increased volume is filled with water. Thus, this line represents the new volume generated due to the ASR expansion. As seen, all the test series absorb more water in the period beyond 4 weeks of exposure than the amount representing the new volume generated. A part of this absorption is water entering partly empty pores (i.e. increased DCS—see later). Additionally, this indicates that during the ASR exposure, water is able to enter space that was not available before the ASR started; for instance ASR gel in air voids.

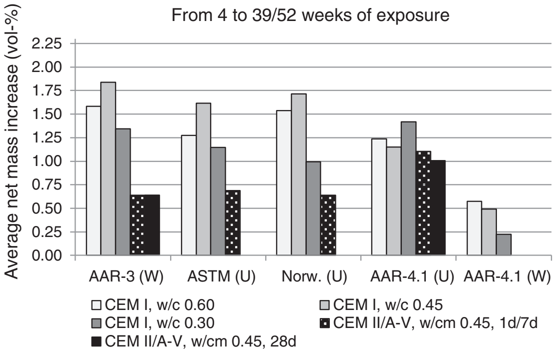

Fig. 7. Increase in net mass of whole prisms (re-calculated to vol.% water absorption) from 4 weeks to 39 weeks (60 °C) or 52 weeks (38 °C) of exposure (W = Wrapped prisms; U = Unwrapped prisms; d = age (days) at exposure to elevated temperature).

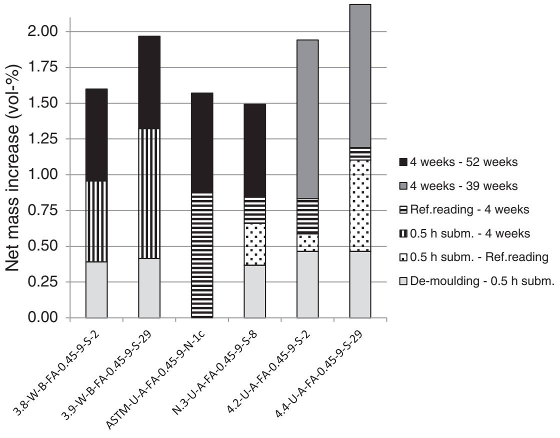

Fig. 8. Increase in net mass of whole prisms (re-calculated to vol.% water absorption) from de-moulding to 39 weeks (60 °C) or 52 weeks (38 °C) of exposure for the six test series with the binder CEM II/A–V, w/cm of 0.45 (W = Wrapped prisms; U = Unwrapped prisms; see Fig. 2 for explanations of notations for various test series).

The correlation between the total water absorption from de-moulding and the total prism expansion from the reference readings is less good than the correlation beyond 4 weeks (Fig. 5). A possible reason could be that during the first 4 weeks the water uptake is mainly caused by hydration/self-desiccation, while beyond 4 weeks the ASR creates cracks and ASR-gel absorbs water.

> *(Comment: Fig. 5 clearly indicates that wrapped prisms absorb more water compared with unwrapped prisms for comparable expansions. In the summary of findings in the EU-PARTNER project [7], it was stated that: “The weight measurements showed in general a lower weight increase, and sometimes also a weight loss, for the aggregates tested according to the AAR-4 Alt. method (i.e. wrapped prisms) compared to the reactor version (i.e. unwrapped prisms)”. Apparently, the conclusion from the PARTNER tests with respect to effect of wrapping on the mass change of the 60 °C prisms was contradictory to the findings discussed above. However, in the PARTNER project the weight results discussed were not net mass of the prisms, rather total mass including any wrapping. Additionally, the prisms were cooled over night to ambient temperature before the readings were taken, and thus some water had evaporated, and then significantly more for the unwrapped prisms—documented in pilot testing in this study).*

Figs. 6 and 7 show the average net mass increase of prisms depending on binder type, prism size, test method and time interval. The results for all test series with similar exposure conditions are averaged, irrespective of the length of the pre-storage period at 20 °C (see Tables 5–8). However, one exception is made for the “fly ash” binder, where the RILEM AAR-3 and AAR-4.1 results are shown for both 1 and 28 days of pre-storage at 20 °C. Fig. 8 provides details of the progression of water uptake from de-moulding to the end of the exposure period for the “fly ash” concrete prisms. Similar figures for the other CEM I binders are included in Lindgård's PhD thesis [44]. *(Comments to Fig. 8: For the wrapped prisms, the net mass of the prisms is not known at the time of the reference readings. For the unwrapped prisms measured without being pre-cooled to 20 °C (i.e. all unwrapped test series except the ASTM test series), the measured reference mass have been corrected (based on results from pilot testing) for the mass loss from the prisms were removed from their containers until the mass measurements 60 s later.)*

The following main trends are observed with respect to average water absorption from de-moulding to 4 weeks of exposure (Fig. 6):

- The water absorption varies with binder type, prism size, pre-treatment and exposure conditions. The prisms absorb from 8 to 23 l of water per m^3 of concrete, corresponding to about 0.35 to 0.95 mass%.
- In general, prisms with the "fly ash" binder absorb significantly less water compared with prisms with the CEM I binders. One reason could be that the hydration products incorporating fly ash bind less water than hydration products of pure OPC, [53,54]. For similar pre-storage period at 20 °C, the mass gain of the prisms with the "fly ash" binder seems to be independent of test method and exposure temperature.
- The two "fly ash" test series pre-stored in the containers at 20 °C for 28 days absorb significantly more water compared with the corresponding test series exposed to elevated temperature after 1 day.
- In general for CEM I binders, exposure to 60 °C leads to considerably higher water absorption compared with corresponding test series exposed to 38 °C (one exception is unwrapped prisms with w/c of 0.60). Two obvious reasons can explain this higher mass increase when the temperature raises; 1) Some of the 60 °C test series have already started to expand somewhat during the first 4 weeks of exposure (up to 0.03 %), leading to suction of water; 2) The relative diffusion coefficient in general increases with increasing exposure temperature (Section 3.4.2), making ingress of water easier.
- In general for the CEM I binders, wrapped prisms absorb significantly more water than corresponding unwrapped prisms (documented by weighing the prisms after unwrapping). It is expected that wrapping the prisms in saturated cloth will increase water availability.
- In general for CEM I binders, the larger Norwegian prisms absorb less water per m^3 of concrete compared with the smaller ASTM prisms, indicating that the interior of the concrete prisms have less access to water when the prism cross section is increased from 70 to 100 mm. An internal moisture gradient is also observed in the larger Norwegian prisms (Section 3.3).
- After 4 weeks of exposure, no significant differences in total water absorption was observed between prisms submerged in water for 0.5 h after de-moulding compared with prisms not submerged.

The following additional main trends with respect to average water absorption from 4 weeks to 39/52 weeks of exposure can be drawn from Fig. 7:

- The extent of water absorption during the ASR exposure varies with binder type, prism size, pre-treatment and exposure conditions, and is closely connected to extent of ASR expansion; higher expansion in general leads to increased water uptake (see also Fig. 5).
- Prisms with the "fly ash" binder exposed to 60 °C absorb considerably more water than corresponding prisms exposed to 38 °C, primarily due to significantly higher prism expansion. The 38 °C "fly ash" test series reveal equal mass increase, independent of prism size and use of any wrapping.
- At 38 °C exposure, prisms with the "dense" CEM I binder (w/c of 0.30) absorb significantly less water compared with the prisms with higher w/c. The main reason for this is assumed to be the lower ASR expansion for these "dense" test series, combined with a lower relative diffusion coefficient (Section 3.4.2). Even less water absorption is observed for the "fly ash" test series.
- As expected, the extreme environments "sealed prisms" and "submerged prisms" (Table 4) significantly influence the water uptake at all ages by respectively reducing it (elimination it for the 38 °C prisms) and increasing it.

3.2.3. Mass change of split samples

After 4 weeks of exposure, the evaporable "in-situ" water content varies from approximately 90–135 l/m^3 (3.8–5.8 mass%), primarily depending on binder type and exposure conditions (Tables 10–13). As expected, the "dense" binder test series contain least evaporable water, while the test series with the "fly ash" binder and the "open" CEM I binder reveal the highest "in-situ" water contents.

In the period beyond 4 weeks, the change in "in-situ" water content varies from 14 l/m^3 reduction (sealed 38 °C test series) to 26 l/m^3 increase (Fig. 4). A fairly good correlation exists between the change in suction porosity and the corresponding change in evaporable "in-situ" water content, with a linear correlation (R^2) of 0.85 (excluding the sealed samples). The interpretation of a point lying on the 1:1 line in the figure is that the increased suction porosity due to ASR is filled up with a corresponding amount of water (and as discussed earlier also some ASR gel that absorbs water). Most data points, except for the "fly ash" binder and the sealed 38 °C prism (lowest data point), lie slightly above the 1:1 line, indicating that DCS increase during the ASR exposure (Section 3.3).

For all test series with the "fly ash" binder and the "dense" CEM I binder, the change in evaporable water content beyond 4 weeks is generally small. In fact, most "fly ash" test series reduce the "in-situ" water content. However, whole prisms with these binders absorb significantly more water in the same period (Figs. 6 and 7), indicating that some of

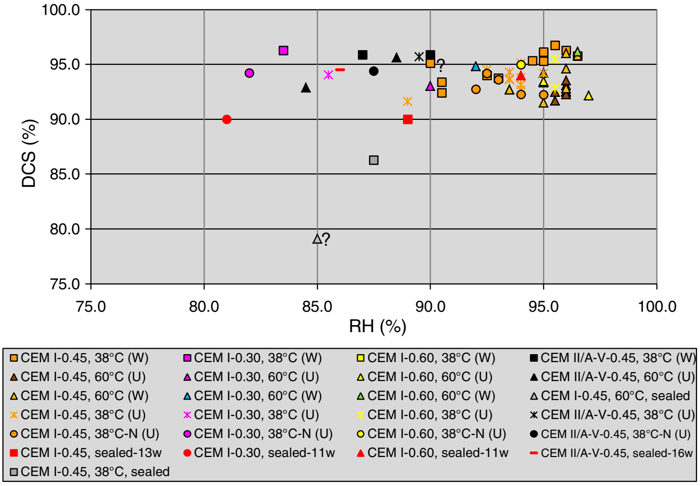

Fig. 9. Degree of capillary saturation (DCS) and relative humidity (RH) after 4 weeks of exposure (W = Wrapped prisms; U = Unwrapped prisms; N = larger Norwegian prisms; red points = sealed cured at 20 °C in plastic bottles; w = weeks; ? = some uncertainty related to the RH measurement).

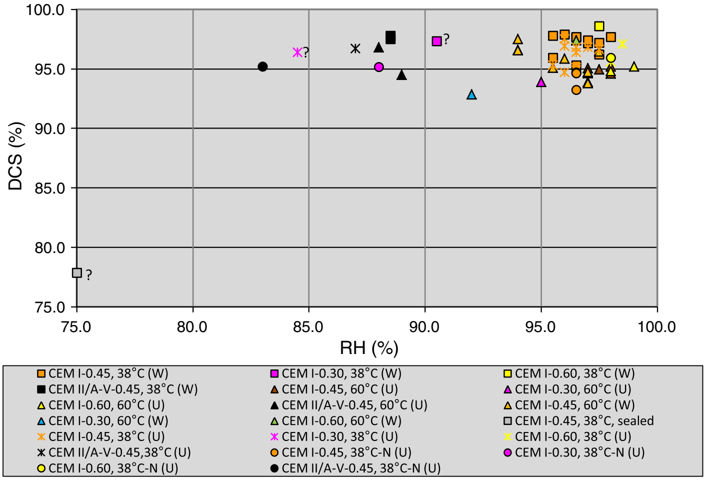

Fig. 10. Degree of capillary saturation (DCS) and relative humidity (RH) after 39 weeks (60 °C) or 52 weeks (38 °C) of exposure (W = Wrapped prisms; U = Unwrapped prisms; N = larger Norwegian prisms; ? = some uncertainty related to the RH measurement).

the absorbed water has been bound in the cement hydrates during further hydration and is not released when the "PF-samples" are dried at 105 °C.

For CEM I test series with higher w/c, the change in "in-situ" water content primarily depends on the expansion. With increasing expansion, the suction porosity and the evaporable water content increase due to formation of internal cracks and growth of ASR gel in cracks and macro pores. At the end of the exposure period, the evaporable water content is still lowest for the "dense" binder (95–110 l/m^3), in the range of 120–145 l/m^3 for the "fly ash" binder and the "basis" binder, while the test series with the "open" binder contain the most evaporable water (140–155 l/m^3).

3.3. DCS and RH of split samples

3.3.1. Samples split from ASR test prisms

The relation between DCS and internal RH is given in Figs. 9 and 10. Detailed results are shown in Tables 10–13, including changes of DCS and RH during the ASR exposure.

DCS is relatively easy to measure accurately and is regarded as a reliable measure for the percentage of water filling the gel and capillary pores [30]. A low spread is also documented, both between parallel test series (mean c.o.v. is about 1% for 8 parallel ASTM test series) and over the prism height (mean c.o.v. for the three parallel "PF-samples" split from various heights of each prism (58 test series) after 4 weeks of exposure is 0.5–0.8%). An implication of the latter is that no distinct variation in DCS can be observed over the prism height, even though all the prisms have been stored vertically with the same end facing upwards during the whole ASR exposure period.

Due to the test setup and the actions taken to try to minimise the known sources of errors (Section 2.4.3), the RH measurements are generally regarded to be reliable. Parallel measurements generally showed comparable results, being well within the reported accuracy of the sensors. However, for five of the more than 120 RH measurements the sensors drifted, hence the points are uncertain.

At all ages, DCS varies far less than the corresponding RH. After 4 weeks (Fig. 9), DCS varies in the range of 91.5–96.5 vol.% (except for the two sealed test series), while the RH varies in the range of 82–97%. At the end of the exposure period (Fig. 10), DCS ranges from about 93–98.5 vol.%. The corresponding RH varies in the range of 83–99% (except for the sealed 38 °C test series).

RH seems to depend strongly on the nature of the binder (w/cm and use of any additions), and for the "dense" binder also on the exposure temperature. In contrast, no significant differences in DCS are observed for the different binders, but the amount of evaporable water is binder dependent.

Primarily due to increased self-desiccation and finer pore structure, and maybe partly due to higher ion concentration in the pore water, the "dense" CEM I binder (w/c of 0.30) reveals the lowest RH values after 4 weeks of exposure (Fig. 9), ranging from 82 to 85.5% for the 38 °C test series (lowest for the larger Norwegian prisms). For corresponding test series exposed to 60 °C, RH is higher; in the range of 90–92%. This RH increase is probably related to the coarsening of the pore structure produced by exposure to elevated temperature (60 °C) as shown for cement pastes by Bray and Sellevold [55].

The "fly ash" test series obtain RH in the range of 84.5–90% after 4 weeks (Fig. 9), i.e. almost as low as the "dense" binder. The lowest RH is obtained for the prisms pre-stored at 20 °C for 28 days, in particular those later exposed to 60 °C. This latter test series also attain the lowest DCS of the "fly ash" test series. Note that these test series are 4 weeks older than the other "fly ash" test series, and consequently more fly ash has reacted and the degree of self-desiccation is thus higher.

At both exposure temperatures, the internal RH in the test series with the CEM I binders with higher w/c (0.45 or 0.60) is always higher than 90 % after 4 weeks of exposure, the majority in the range of 93.5–96%. During the whole ASR exposure, test series with the most "open" binder always reveal slightly higher or as high RH as the test series with the "basis" binder with highest RH.

The presented values for RH were measured in a climate-controlled room at 20 °C after cooling the prisms inside plastic foil (to avoid loss of moisture). As discussed by Lindgård et al. [22,23], a general increase in the temperature will give rise to a small increase in the internal RH provided the moisture content within the concrete is kept constant. For example, Sellevold and Bjøntegaard [28] and Nilsson [56] reported that the RH within a concrete will increase in the range of 0.2–0.3% RH per °C with a starting RH around 70–90%. The effect decreases with increasing w/cm ratio and is RH dependent. The effect is most marked in the middle RH-range (around 50–60%), and decreases to zero in very dry and in saturated concrete [28]. For the present test series with RH in the range of 82–97% RH (measured after cooling to 20 °C), the internal RH will increase during the ASR exposure compared with the results presented in Figs. 9 and 10 by up to a maximum of 5% when stored at 38 °C and up to a maximum of 10% when stored at 60 °C. In other words, when the measured RH (at 20 °C) for the "dense" binder is significantly lower for the 38 °C test series compared with the corresponding 60 °C test series, the difference will be even greater during the ASR exposure when the temperature is elevated. The practical importance of this temperature effect for the ASR reaction is not known, but it seems to be reasonable to assume that the higher RH at elevated temperature will contribute to accelerate the ASR expansion.

Knowing that the critical RH limit for developing ASR is in the range of 80–90%, depending on several factors as discussed by Larive et al. [32], it is likely that the rather low RH revealed for the "dense" binder after 4 weeks of exposure and maybe also for the "fly ash" binder contributes to reduce the rate and extent of ASR, in particular for the test series exposed to 38 °C (further discussed in [25]). For all test series with the CEM I binders with higher w/c (0.45 or 0.60), except for the sealed test series, RH is regarded to be sufficient for ASR to develop. Thus, it appears that for these concretes all the test procedures provide sufficient moisture contents for ASR to proceed.

In contrast to the findings by Lindgård et al. [27], no good correlation has been found in the present tests between the rate and extent of ASR and the DCS. However, DCS is higher than 91.5% for all the test series, while the "critical DCS" for the field concretes was found to be about 90% DCS [27]. On the other hand, not only the degree of pore filling but also the total amount of evaporable water in the concrete might influence the extent of ASR. One can thus not rule out that the less amount of available (evaporable) water in the "dense" concrete (w/c of 0.30) might contribute to lower extent of ASR compared with the CEM I concretes with higher w/c.

For all binders and all test methods, DCS generally increases during the ASR exposure as water is taken in (only a few exceptions exist). However, the observed changes in RH during the exposure period depend on type of binder, pre-treatment and exposure temperature.

In general, RH increases beyond 4 weeks of exposure for the test series with the CEM I binders, irrespective of w/c (with only a few exceptions). The main trend is that most test series with the "dense" binder (that reveal the lowest RH after 4 weeks of exposure) and those test series with the "basis" binder that obtain "relative low" RH values after 4 weeks of exposure (except the sealed test series) show the highest increase in RH (+5–7%).

On the contrary, the internal RH decreases (up to 4.5%) for most of the "fly ash" test series, despite a small increase in DCS.

At the end of the exposure (Fig. 10), the CEM I test series with w/c 0.45 or 0.60 obtain highest RH, the majority lying in the range of 95.5–98%. The 38 °C "dense" binder test series attain RH in the range of 84.5–90.5%. For corresponding 60 °C test series, RH is higher; in the range of 92–95%. For the "fly ash" binder, RH varies in the range of 83–88.5% for test series exposed to 38 °C, significantly lowest for the larger Norwegian prisms, and in the range of 88–89% for test series exposed to 60 °C.

In general at 38 °C exposure, wrapped prisms obtain slightly higher DCS and internal RH compared with corresponding unwrapped prisms at all ages (Figs. 9 and 10, Tables 10 and 13). This is valid for all binder types and for all test series (with only a few minor exceptions).

After 4 weeks of exposure to 60 °C (Fig. 9 and Table 11), wrapped prisms with the CEM I binders obtain slightly higher DCS compared with corresponding unwrapped prisms. This corresponds to the observed higher water uptake for wrapped prisms (Fig. 6). Regarding RH, wrapped prisms with the "dense" binder attain slightly higher values than corresponding unwrapped prisms. For higher w/c (0.45 and 0.60), no significant difference in RH is observed between wrapped and unwrapped prisms.

After 39 weeks of exposure to 60 °C (Fig. 10), no systematic differences in DCS or RH between wrapped and unwrapped prisms are observed. However, a tendency is that RH is slightly less for some of the wrapped test series that reveal significantly lower expansion compared with corresponding unwrapped test series. The assumed reason for this is that more ASR gel is produced for test series that reveal higher expansion, and thus the internal RH is increased.

Except use of any wrapping (or sealed or submerged samples), no systematic differences in DCS or RH are detected between test series with the "basis" binder where other pre-treatments are varied.

During the entire exposure period, the test series submerged in de-ionised water obtain DCS and RH values on the same level as corresponding wrapped test series. *(Comment: no results are available for submerged samples after 4 weeks of exposure to 60 °C).*

After 4 weeks (Fig. 9), the sealed prisms stored in tight, dry containers placed in the dry 38 °C room obtain DCS of about 86.5 vol.% and RH of 87.5%. After 52 weeks (Fig. 10), DCS is reduced to 78 vol.%, while RH is reduced to about 75% (some uncertainty is related to this latter RH measurement). However, some water is assumed to have evaporated from the prisms during the one year exposure in the dry 38 °C room.

After 4 weeks, sealed prisms stored in airtight, dry containers placed inside the humid 60 °C reactor obtain DCS of about 79 vol.% and RH of 85% of exposure (Fig. 9; some uncertainty is related to this RH measurement). At 60 °C, the sealing with epoxy and aluminium foil is not completely watertight, and some water is taken up beyond age 4 weeks. Thus, no reliable "sealed humidity data" is available for the 60 °C test series at the end of the exposure period.

In general for all binders and at all ages, the larger Norwegian prisms (cross section 100 × 100 mm) obtain slightly lower (or equal) DCS and internal RH compared with the smaller ASTM prisms (70 × 70 mm) (when excluding the few uncertain RH measurements). This agrees with the observed lower water uptake for the larger prisms in the early period of exposure (Fig. 6). After 4 weeks of exposure of the Norwegian prisms,

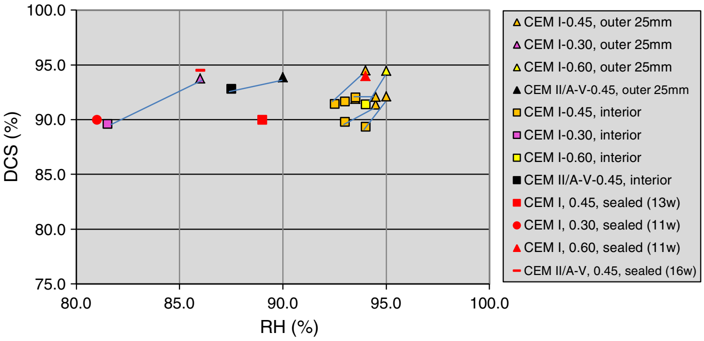

Fig. 11. Degree of capillary saturation (DCS) and relative humidity (RH) in the outer 25 mm versus the interior of Norwegian concrete prisms after 4 weeks of exposure (red points = sealed cured at 20 ° C in plastic bottles; w = weeks). (For interpretation of the references to color in this figure legend, the reader is referred to the web version of this article.)

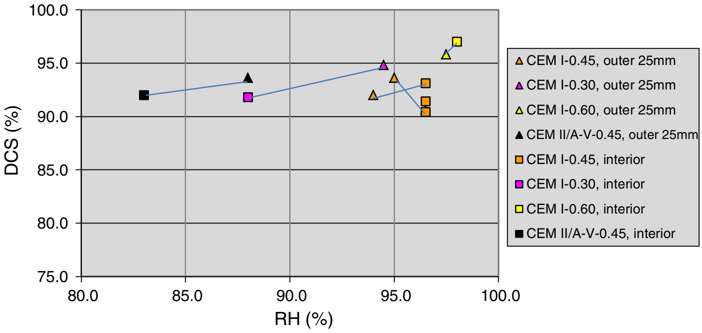

Fig. 12. Degree of capillary saturation (DCS) and relative humidity (RH) in the outer 25 mm versus the interior of Norwegian concrete prisms after 52 weeks of exposure.

DCS and in particular the corresponding RH are always higher in the outer 25 mm compared with the interior of the prism (Fig. 11). The RH gradient is most pronounced for the "dense" binder, where DCS and RH in the interior of the large Norwegian prism are equal to DCS and RH of sealed samples stored in airtight plastic bottles at 20 °C until age 11–16 weeks (Fig. 11). After 52 weeks of exposure, a substantial RH gradient is observed for the "dense" CEM I binder and the "fly ash" binder (Fig. 12). For both binders, the RH gradient is higher than the corresponding gradients after 4 weeks of exposure.

3.3.2. Pilot tests with more porous aggregates

Any supply of water from aggregate pores to the cement paste during the curing period will reduce the self-desiccation ([39,40]) and thus significantly increase the RH compared with use of relatively dry aggregates, in particular for low w/cm binders (see Section 1.4.3). If rather porous (≥0.8%) normal density pre-wetted aggregates are used, they may theoretically totally counteract the effect of self-desiccation [39]. As a consequence, it might be conservative to use pre-wetted aggregates in laboratory performance testing instead of dry aggregates that is the practice in some laboratories.

To verify this theory, pilot tests have been performed with two additional aggregates with different porosity and moisture state at the time of mixing. The water absorption of the coarse aggregate fractions was about 1% (in the upper range for Norwegian aggregates) and 6.5% (Icelandic basalt), somewhat lower for the fines. Two mixtures were prepared with each of these aggregates, one with dry aggregates and one with moist aggregates (pre-wetted overnight). The same binder with cement CEM I and effective w/c of 0.30 was used in all the mixtures (the amount of extra water added to the mixtures with the dry aggregates was calculated based on the 1 h water absorption of the aggregates). The four concretes were stored sealed in tight plastic bottles at three temperatures (20, 38 and 60 °C) for 2, 3 and 6 weeks (shorter storage when the temperature is increased). Two independent RH measurements were performed on crushed samples (Section 2.4.3) from each of the 12 bottles. The results clearly show the impact on RH of aggregate porosity and aggregate moisture state:

- RH in the concretes containing pre-wetted highly porous Icelandic aggregates was 8–14 % higher compared with the corresponding concrete with dry aggregates. Corresponding differences for the Norwegian less porous aggregate were in the range of 5–10%. *(Comment: Even though the spread in RH measured on parallel crushed samples from the same bottle was rather high, the tendency was clear).*

3.4. Transport properties

3.4.1. Assessment of methods used for estimation of transport properties

In general, the internal spread for the relative diffusion coefficient between parallel test series is much higher compared with the other parameters measured (Sections 3.1–3.3). For example, the c.o.v. of RelD for parallel test series (Table 14) is in the range of 0–24%. The internal spread for the electrical resistivity is low (c.o.v. for 5 parallel "PF-samples" split from each prism during the pilot testing was about 4.5%).

Fig. 13 shows mean results from this "pilot" testing of electrical resistivity (Section 2.4.5) plotted against the calculated relative diffusion coefficient measured on the same samples. The figure only includes CEM I cement with w/c in the range of 0.30–0.60, i.e. binders with comparable pore water composition. As seen, a good correlation is obtained between relative diffusion coefficient and electrical resistivity. R^2 for the linear trend line is 0.96 when removing the outlier with a relatively high RelD compared with the other samples. This indicates that both methods can be used for assessment of transport properties of the various test series, provided the binders have equal chemistry, i.e. as long as that the electrical resistivity is not too much influenced by varying chemistry of the pore water. Note that changes in pore water chemistry, DCS or internal cracking (see later) will significantly influence the electrical resistivity.

Results from measurements of RelD after 4 weeks of exposure and electrical resistivity at the end of the exposure period are presented in Sections 3.4.2 and 3.4.3, respectively.

3.4.2. Relative diffusion coefficient

Calculated relative diffusion coefficients (RelD) after 4 weeks of exposure are presented in Table 14. The following main trends can be drawn from the results:

- The relative diffusion coefficient varies significantly with binder type, exposure conditions, prism size and pre-treatments. RelD for the different test series varies in the range of 0.1–4.1 (RelD = 1.0 for the reference ASTM samples with the "basis" binder).
- RelD for the "fly ash" test series varies far less (in the range of 0.4 to 0.6) compared with the values for the CEM I "basis" binder with equal w/cm (in the range of 0.5–4.1). In other words, the "fly ash" binder is more "robust" against any changes in pre-treatments and exposure conditions compared with the CEM I "basis" binder.
- RelD for various binders exposed to 38 °C: "dense" binder < "fly ash" binder < "basis" binder < "open" binder. For all the three CPTs the differences between the binders are significant, and the internal ranking is in accordance with our expectations.
- RelD for various binders exposed to 60 °C: "fly ash" binder < ≈"dense" binder ≪ "basis" binder < ≈"open" binder. In general, the internal differences between the two densest binders and the two most open binders, respectively, are less pronounced compared with exposure to 38 °C.
- Test series with CEM I binders (w/c of 0.30–0.60) exposed to 60 °C for 4 weeks have significantly higher RelD compared with corresponding 38 °C test series. One reason is the coarser pore structure when

Table 14
Relative diffusion coefficient (RelD) after 4 weeks of exposure for 56 test series. *(Comment: The two test series in brackets are epoxy coated on the side faces, and thus reveal lower RelD than comparable test series).*

Relative diffusion coefficients (RelD). Reference = Mean of seven ASTM samples of the basis binder (in bold).							
Test series RILEM AAR-4.1	RelD	Test series RILEM AAR-3	RelD	Test series ASTM C-1293	RelD	Test series Norwegian CPT	RelD
4.1-U-A-0.45–1- S-1c	3.75	3.1-W-B-0.45–3- N-7c	0.70	ASTM-U-A-0.45–1- N-1c	**1.10**	N.1-U-A-0.45–3- S-1c	0.52
	2.81	3.2-W-B-0.45–4- N-8	0.90	ASTM-U-A-0.45–2- N-1c	**0.96**		0.64
	4.09	3.3-W-C-0.45–4- N-8	0.98	ASTM-U-A-0.45–3- N-1c	**1.50**	N.2-U-A-0.45–1- S-2	0.73
4.2-U-A-0.45–1- S-2	3.46	3.4-W-B-0.45–4- S-8	0.80	ASTM-U-A-0.45–4- N-1c1	**0.98**		0.92
4.3-U-A-0.45–6- S-8	2.37	3.5- -E-0.45–5- N-8	(0.46)	ASTM-U-A-0.45–5- N-1c	**0.76**	N.3-U-A-0.45–4- S-8	0.58
4.4-U-A-0.45–2- S-29	2.25	3.6-W-D-0.45–6- S-8	0.54	ASTM-U-A-0.45–6- N-1c	**1.22**	N.3-U-A-0.30–7- S-8	0.11
	2.05	3.7-U-A-0.45–6- S-8	0.85	ASTM-U-A-0.45–10- N-1c	**0.82**	N.3-U-A-0.60–8- S-8	0.78
4.5-U-A-0.45–2- S-8FT	1.22	3.8-W-B-0.45–3- S-2	0.82	ASTM-U-A-0.30–7- N-1c	0.27	N.3-U-A-FA-0.45–9-S-8	0.39
4.7- -E-0.45–5- N-8	(0.70)	3.9-W-B-0.45–2- S-29	0.69	ASTM-U-A-0.60–8- N-1c	1.50		
4.8-W-B-0.45–1- S-2	1.88	3.10-W-B-0.45–2- S-8FT	0.90	ASTM-U-A-0.60–11- N-1c	1.41		
4.8-W-B-0.45–10- S-2	1.29	3.10-W-B-0.45–10- S-8FT	1.15	ASTM-U-A-FA-0.45–9- N-1c	0.56		
4.9-W-B-0.45–5- S-8	1.32	3.11-U-F-0.45–5- S-8	0.71				
4.10-W-C-0.45–6- N-8	1.61	3.4-W-B-0.30–7- S-8	0.16				
4.11-W-D-0.45–3- S-8	1.32	3.4-W-B-0.60–8- S-8	0.98				
4.3-U-A-0.30–7- S-8	0.52	3.8-W-B-FA-0.45–9-S-2	0.60				
4.9-W-B-0.30–7- S-8	0.44	3.9-W-B-FA-0.45–9-S-29	0.41				
4.3-U-A-0.60–8-I S-8	3.00						
4.3-U-A-0.60–8-II S-8	3.00						
4.9-W-B-0.60–11- S-8	2.32						
4.2-U-A-FA-0.45–9-S-2	0.40						
4.4-U-A-FA-0.45–9-S-29	0.41						

“cured” at a higher temperature [55]. The influence of “curing temperature” (higher permeability) is however, as demonstrated in [55], expected to be even more pronounced when exposed to elevated temperatures directly after casting compared with exposure to elevated temperatures after some time (as in this case, where all test series were cured at 20 °C the first day). Still, there is a tendency that exposure to 60 °C after 7 or 28 days leads to a somewhat lower RelD compared with exposure to elevated temperature directly after de-moulding. Another factor that might have higher influence on the observed differences in RelDs between the two exposure temperatures is the fact that some of the test series exposed to 60 °C already have expanded significantly during the first 4 weeks of exposure (up to 0.03%). Thus, expected incipient internal micro-cracking have most likely contributed to an increase of RelD already after 4 weeks of exposure to 60 °C. Since no test series exposed to 38 °C have started to expand significantly after 4 weeks, the influence on any micro-cracking on the revealed RelDs for these test series are assumed to be negligible.

- RelD for test series with CEM I binders (w/c of 0.30–0.60) tested according to various 38 °C CPTs (W = Wrapped; U = Unwrapped): Norwegian CPT (U) < RILEM AAR-3 (W) < ASTM C-1293 (U). The main reason for the lowest RelDs for the Norwegian CPT test series is assumed to be that the larger Norwegian concrete prisms dry out more slowly than the smaller prisms (similarly as a dense binder dry out more slowly than a more open binder). The fact that the ASTM test series in general reveal slightly higher RelDs compared with the AAR-3 test series might be due to several reasons, among them earlier exposure to elevated temperature (1 day versus 7 days).

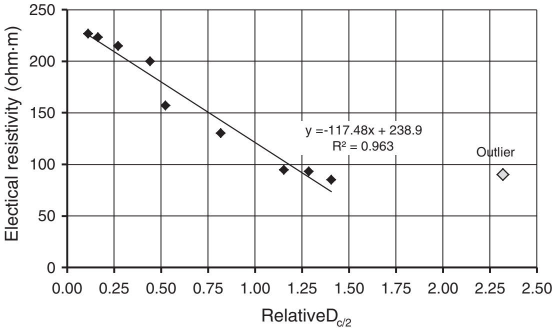

Fig. 13. Results from “pilot” testing of electrical resistivity *(measured on split “PF-samples”—procedure given in* [49]*)* plotted against the corresponding relative diffusion coefficients after 4 weeks of exposure to 38 or 60 °C. One outlier is removed when calculating the linear correlation (R^2). The figure only includes CEM I cement with w/c in the range of 0.30–0.60.

3.4.3. Electrical resistivity

Experiences show that 1% increase in DCS will give approximately 3% reduction in electrical resistivity [50]. However, DCS values are comparable for all test series, and should thus not influence the measured electrical resistivity too much. In Fig. 14, the “in-situ” electrical resistivity measured on whole prisms at the end of the exposure period is plotted against the corresponding expansion. The following main trends can be drawn from the figure:

- The electrical resistivity is influenced by binder type, exposure conditions, pre-treatments and prism expansion. The calculated values vary in the range 40–635 Ω m.
- As expected [48], the test series with the “fly ash” binder had much higher values (ranging from 330 to 635 Ω m) compared with the CEM I binders (ranging from 40 to 190 Ω m, except one test series with the “dense” binder with electrical resistivity of 335 Ω m). Furthermore, the “fly ash” test series exposed to 60 °C reveal higher values (540–635 Ω m) compared with the 38 °C test series (330–490 Ω m), even though the latter test series reveal lower expansions (see later discussion). A similar influence of curing temperature is also observed for the CEM I test series. Possible reasons for this might be higher degree of hydration of the clinker (for the “dense” binder) and reaction of more fly ash at the highest temperature, and thus a denser concrete (the ion concentration in the pore water could also have been slightly reduced).
- There is a tendency that the electrical resistivity decreases when the ASR expansion increases. The reason might be that cracks generated during the ASR exposure are partly filled with ASR gel and water, making the transport of current easier than through concrete with less internal cracking. In particular it can be observed that the wrapped 60 °C test series that reveal significantly less expansion than corresponding unwrapped test series, obtain significantly higher

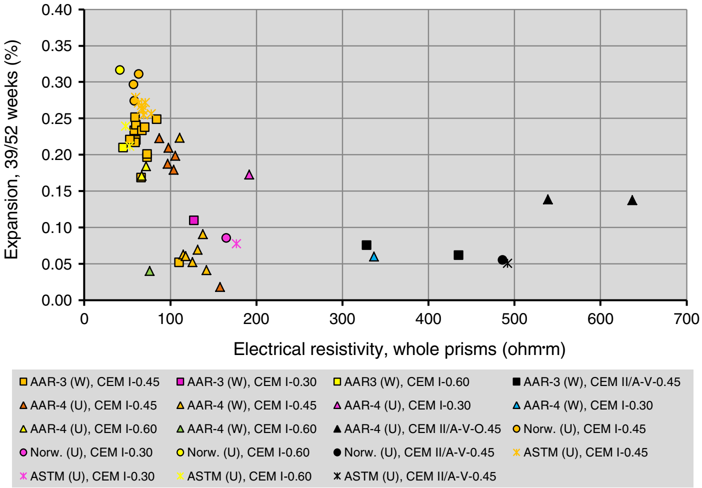

Fig. 14. Relation between electrical resistivity and expansion after 39/52 weeks of exposure. Sealed test series are excluded.

electrical resistivity than the unwrapped test series (despite that more alkalis are leached out from the unwrapped prisms at the end of the ASR exposure compared with the wrapped prisms, and consequently less ions are present in the concrete pore water).

- As expected, the test series with the “dense” CEM I binder reveals higher electrical resistivity than the “basis” binder, while test series with the “open” binder reveal the lowest values for comparable expansions.
- For the CEM I binders, a good correlation is revealed after 4 weeks of exposure between the relative diffusion coefficient ($RelD_{4\ weeks}$) and the electrical resistivity (Fig. 13). However, no correlation exists between $RelD_{4\ weeks}$ and the electrical resistivity at the end of the exposure period (except that similar internal ranking is obtained between the CEM I binders). The main reason is assumed to be that the internal cracking due to ASR influence the continuity of the pores (i.e. “opens up” the pore structure), and thus dominates the measured electrical resistivity (for similar binder qualities) late in the exposure period.

4. Conclusions

Based on the comprehensive laboratory study, including 58 test series with modified versions of five concrete prisms tests (CPTs), the following conclusions can be drawn:

- The internal moisture state and the transport properties of a given concrete may be significantly influenced by the specimen “pre-treatment”, “ASR exposure conditions” and prism cross-section. The influence depends on the concrete composition, i.e. w/cm and cement type. Consequently, the results of applying a performance test to a given concrete might differ depending on the details of the test method.
- During the ASR exposure, the concrete properties are altered. The general tendency is increased suction porosity and increased internal moisture state with increased ASR expansion, but the alteration depends on the binder composition. The change in macro porosity is negligible. Moreover, a relation exists between water uptake and expansion, i.e. concrete expansion leads to increased porosity that takes up water. However, more water is taken up than the volume corresponding to the increased porosity.
- With respect to the specimen ”pre-treatment”, the main findings are:
  - ✓ From a “moisture point of view”, the 0.5 h submersion after de-moulding described in several CPTs seems unnecessary (has little effect beyond the first weeks of exposure).
  - ✓ The length of pre-storage at 20 °C before exposure to elevated temperature might marginally influence the internal moisture state in the first period of exposure, but not at later ages. However, exposure to 60 °C directly after de-moulding significantly increase the relative diffusion coefficient (RelD) for CEM I binders, making the internal transport of water and ions easier.
  - ✓ Prisms wrapped in moist cotton cloth and plastic sheets absorb significantly more water than unwrapped prisms displaying similar expansions in ASR tests. During the first weeks of exposure, this behaviour is particularly pronounced at 60 °C. For prisms exposed to 38 °C, the wrapping also leads to slightly higher DCS and internal RH after 4 weeks of exposure.
- With respect to the “exposure conditions” and prism cross-section, the main findings are:
  - ✓ The “exposure parameter” confirmed to have the highest impact on the internal moisture state and the transport properties of concrete is the temperature. The prism cross-section can also significantly influence the internal moisture state. For both parameters, the influence depends on the binder composition.
  - ✓ Generally for CEM I binders, exposure to 60 °C leads to considerably higher water absorption during the first weeks compared with corresponding test series exposed at 38 °C. The internal RH is also significant higher for the test series exposed to 60 °C, both at early age and later. This RH-increase is probably primarily related to the coarsening of the pore structure produced by the elevated temperature and, of course, more water.
  - ✓ At the end of the ASR exposure, the total prism water uptake and the internal moisture state is to a high extent influenced by the extent of ASR and thus the extent of internal cracking and amount of ASR-gel produced. Also the electrical resistivity is influenced—increased ASR expansion tends to decrease the electrical resistivity.
  - ✓ In general for CEM I binders exposed to 38 °C, increased prism cross-section leads to less absorbed water in the interior of the prisms, in particular during the first period of the exposure. A pronounced RH gradient is present for test series with the “dense”

binder (w/c of 0.30) during the entire exposure period. A similar, but less distinct, gradient is observed in prisms with the “fly ash” binder (w/cm of 0.45).

- With respect to influence of binder composition (i.e. w/cm and cement type), the main findings are:
  - ✓ No systematic difference in the degree of capillary saturation (DCS) between binders of different composition can be found, neither at 4 weeks nor at the end of the exposure.
  - ✓ For the CEM I test series, one of the most important properties of the “dense” binder (w/c of 0.30) compared with higher w/c is the much lower internal RH, in particular when exposed to 38 °C (RH in the range of 82–90%). The reason is primarily the higher extent of self-desiccation. Furthermore, the relative diffusion coefficient is substantially lower also due to a finer pore structure so that the water uptake is slower. Additionally, an assumed higher concentration of ions in the pore water might contribute to reduce the RH.
  - ✓ Several concrete properties of the test series with the “fly ash” binder deviate from the CEM I series. Firstly, most concrete properties for the “fly ash” binder seem to be more or less independent of both the specimen pre-treatment and the storage conditions during testing. Secondly, concrete prisms with the “fly ash” binder generally absorb less water compared with prisms with the CEM I binders at the same w/cm, presumably due to the lower “permeability” (measured as a low RelD and a higher electrical resistivity) and less water bound by the hydration products incorporating fly ash. Thirdly, the internal RH is considerably lower in the “fly ash” test series compared with CEM I series with equal w/cm. Fourthly, the general increase in RH seen for the CEM I binders during the ASR exposure is not observed for the “fly ash” binder. Note that all test series are subjected to elevated temperature which is very favourable for the pozzolanic reaction.
- It is likely that the comparatively low RH found for the “dense” binder and probably also for the “fly ash” binder after 4 weeks of exposure contributes together with the measured lower relative diffusion coefficients to reduce the rate and extent of ASR. This is particularly true for the test series exposed to 38 °C. Additionally, less amount of available (evaporable) water in the “dense” CEM I concrete (w/c of 0.30) might contribute to the lower extent of ASR observed compared with the CEM I concretes with higher w/c.
- For all test series with the CEM I binders with higher w/c (0.45 or 0.60), RH is regarded to be sufficient for ASR to initiate (well over 90% RH after 4 weeks). Thus, it appears that for these binders all the specimen pre-treatment and test procedures provide sufficient moisture contents for ASR to proceed.

The consequences of the present results for alkali leaching and prisms expansion are treated in a separate paper [25].

A number of practical details and recommendations on the test procedures are given in the appendix to the thesis [44].

Acknowledgements

The authors would also like to acknowledge COIN, the COncrete INnovation centre (www.coinweb.no) and Norcem (part of Heidelberg Cement Group) for the financial support to the PhD study of the principle author. Furthermore, the comprehensive and accurate work performed at the laboratory staff at SINTEF is greatly appreciated.

References

[1] D.E. Stanton, The expansion of concrete through reaction between cement and aggregate, Am. Soc. Civ. Eng. 66 (1940) 1781–1811.

[2] RILEM TC 191-ARP: ‘Alkali-reactivity and prevention—assessment, specification and diagnosis of alkali-reactivity’, RILEM Recommended Test Method AAR-1: Detection of potential alkali-reactivity of aggregates—petrographic method, Mater. Struct. 36 (2003) 480–496.

[3] RILEM TC 106-AAR, ‘Alkali aggregate reaction’ A. TC 106-2—Detection of potential alkali-reactivity of aggregates—The ultra-accelerated mortar-bar test B. TC 106-3-Detection of potential alkali-reactivity of aggregates-method for aggregate combinations using concrete prisms, Mater. Struct. 33 (2000) 283–293.

[4] RILEM TC 191-ARP: ‘Alkali-reactivity and prevention—assessment, specification and diagnosis of alkali-reactivity’, AAR-5: Rapid preliminary screening test for carbonate aggregates, Mater. Struct. 38 (2005) 787–792.

[5] RILEM TC 219-ACS ‘Alkali–silica reactions in concrete structures’: RILEM AAR-4.1—Detection of potential alkali-reactivity of aggregates: accelerated (60 °C) concrete prism test, 2006. (unpublished draft).

[6] RILEM TC 191-ARP: ‘Alkali-reactivity and prevention—assessment, specification and diagnosis of alkali-reactivity’, RILEM Recommended Test Method AAR-0: detection of alkali-reactivity potential in concrete—outline guide to the use of RILEM methods in assessments of aggregates for potential alkali-reactivity, Mater. Struct. 36 (2003) 472–479.

[7] J. Lindgård, P.J. Nixon, I. Borchers, B. Schouenborg, B.J. Wigum, M. Haugen, U. Åkesson, The EU “PARTNER” Project—European standard tests to prevent alkali reactions in aggregates: final results and recommendations, Cem. Concr. Res. 40 (2010) 611–635.

[8] ASTM C1260—07 Standard Test Method for Potential Alkali Reactivity of Aggregates (Mortar-Bar Method), Annual Book of ASTM StandardsAmerican Society for Testing and Materials, 2007, p. 5.

[9] ASTM C1293—08b Standard Test Method for Determination of Length Change of Concrete Due to Alkali–Silica Reaction, Annual Book of ASTM Standards, American Society for Testing and Materials, 2008. p. 7.

[10] ASTM C295—08 Standard Guide for Petrographic Examination of Aggregates for Concrete, Annual Book of ASTM Standards, American Society for Testing and Materials, 2008, p. 8.

[11] CSA, CSA A23.2-14A-00, Potential Expansivity of Aggregates (Procedure for Length Change due to Alkali–Aggregate Reaction in Concrete Prisms at 38 °C), Methods of Testing for Concrete, Canadian Standards Association, Mississauga, Ontario, Canada, 2004, pp. 246–256.

[12] CAN/CSA-A23.2-25A-09 Test Method for Detection of Alkali-Silica Reactive Aggregate by Accelerated Expansion of Mortar Bars, Canadian Standards Association, 2009.

[13] CSA A23.2-15A Petrographic Examination of Aggregates, Canadian Standards Association, 2009.

[14] RILEM TC 219-ACS ‘Alkali–silica reactions in Concrete Structures’: Recommended Specification: AAR-7.1 International Specification to Minimise Damage from Alkali Reactions in Concrete Part 1, Alkali–Silica Reaction, 2008. (unpublished draft).

[15] M.D.A. Thomas, The effect of supplementary cementing materials on alkali–silica reaction: a review, Cem. Concr. Res. 41 (2011) 1224–1231.

[16] T. Chappex, K. Scrivener, Controlling alkali silica reaction by understanding the contribution of aluminium provided by supplementary cementitious materials, in: T. Drimalas, J.H. Ideker, B. Fournier (Eds.), 14th International Conference on Alkali–Aggregate Reactions in concrete, Austin, Texas, 2012.

[17] AFNOR NF P 18-454, Reactivity of a Concrete Formula with Regard to the Alkali–aggregate Reaction, Association Française de Normalisation, Paris, France, 2004.

[18] Norwegian Concrete Association: Alkali–aggregate Reactions in Concrete, Test methods and Requirements to Test Laboratories, NB32, 2005, p. 39.

[19] M. Thomas, B. Fournier, K. Folliard, J. Ideker, M. Shehata, Test methods for evaluating preventive measures for controlling expansion due to alkali–silica reaction in concrete, Cem. Concr. Res. 36 (2006) 1842–1856.

[20] J. Lindgård, B. Pedersen, S.K. Bremseth, P.A. Dahl, T.F. Rønning, Experience using the Norwegian 38 °C concrete prism test to evaluate the alkali reactivity of aggregates, concrete mixes and binder combinations, Nord. Concr. Res. 42 (2010) 31–50.

[21] Norwegian Concrete Association: Durable Concrete Containing Alkali Reactive Aggregates, NB21, 2004, p. 33.

[22] J. Lindgård, Ö. Andiç-Çakır, I. Borchers, M.T.A.M. Broekmans, E. Brouard, I. Fernandes, C. Giebson, B. Pedersen, C. Pierre, T.F. Rønning, M.D.A. Thomas, B.J. Wigum, RILEM TC219-ACS-P: Literature survey on performance testing, COIN project report, 27, ISBN: 978-82-536-1209-6, 2011, p. 164.

[23] J. Lindgård, Ö. Andiç-Çakır, I. Fernandes, T.F. Rønning, M.D.A. Thomas, Alkali–silica reactions (ASR): literature review on parameters influencing laboratory performance testing, Cem. Concr. Res. 42 (2012) 223–243.

[24] Personal communication with Colin Giebson, Bauhaus-Universität Weimar Fakultät Bauingenieurwesen, F.A. Finger-Institut für Baustoffkunde, 2011.

[25] A.J. Lindgård, M.D.A. Thomas, E.J. Sellevold, B. Pedersen, Ö. Andiç-Çakır, H. Justnes, T.F. Rønning, Alkali-silica reaction (ASR)-performance testing: influence of specimen pre-treatment, exposure conditions and prism size on alkali leaching and prism expansion, Cem. Concr. Res. 53 (2013) 68–90.

[26] R.H. Relling, Coastal concrete bridges: moisture state, chloride permeability and aging effects, DrEng Thesis at Institute for Construction Technique, NTNU, Trondheim, 1999, p. 244, (+ appendices).

[27] J. Lindgård, E. Rodum, B. Pedersen, Alkali–silica reactions in concrete—relationship between water content and observed damage on structures, in: V.M. Malhotra (Ed.), 7th CANMET/ACI International conference on Durability of Concrete, ACI, Montreal Canada, 2006, pp. 147–165.

[28] E.J. Sellevold, Ø. Bjøntegaard, Coefficient of thermal expansion of cement paste and concrete: mechanisms of moisture interaction, Mater. Struct. 39 (2006) 809–815.

[29] G. Hedenblad, Drying of building moisture in concrete, Svensk byggtjänst 17188 Solna, Sweden, 1995, (in Swedish).

[30] E.J. Sellevold, T. Farstad, The PF-method—a simple way to estimate the w/c-ratio and air content of hardened concrete, ConMat'05 and Mindness Symposium, The University of British Colombia, Vancouver, Canada, ISBN: 0-88865-810-9, 2005.

[31] B. Pedersen, Alkali-reactive and inert fillers in concrete. , PhD-thesis Rheology of Fresh Mixtures and Expansive Reactions, Norwegian University of Science and Technology, Trondheim, Norway, 2004, p. 292.

[32] C. Larive, A. Laplaud, O. Coussy, The role of water in alkali–silica reaction, in: M.-A. Bérubé, B. Fournier, B. Durand (Eds.), 11th International Conference on Alkali–Aggregate Reaction, Québec, Canada, 2000, pp. 61–69.

[33] J. Bokern, Concrete tests for ASR assessment: effects of testing environment on preconditions for an ASR and transferability of test results, in: M.A.T.M. Broekmans, B.J. Wigum (Eds.), 13th International Conference on Alkali–Aggregate Reactions in Concrete, Trondheim, Norway, 2008, pp. 511–520.

[34] R.H. Relling, E.J. Sellevold, In situ moisture state of coastal bridges, Proceeding of the International conference: Concrete, Repair, Rehabilitation and Retrofitting, Taylor & Francis, London, ISBN: 0415396549, 2006, (Cape Town, South Africa).

[35] E. Sellevold, Resistivity and humidity measurements of repaired and non-repaired areas in Gimsøystraumen bridge, International Conference: Repair of concrete structures, from theory to practice in a marine environment, Svolvær, Norway, 1993.

[36] D. Stark, Effects of water–cement ratio on expansion due to ASR, Concrete Technology Today, Portland Cement Association, Skokie, Illinois, 1995, pp. 3–5.

[37] D. Stark, The moisture condition of field concrete exhibiting alkali–silica reactivity, Second International Conference on Durability of Concrete, ACI Publication SP 126/52, 1991, pp. 973–987.

[38] Y. Yang, X. Zhenjian, C. Weizhong, C. Min, Distribution of water content in self-compacted high strength concrete due to water evaporation and self-desiccation, RILEM Proceedings PR042, First International Symposium on Design, Performance and Use of Self-Consolidating Concrete, SCC'2005, Changsha, Hunan, China, 2005, pp. 173–180.

[39] T.A. Hammer, Ø. Bjøntegaard, E.J. Sellevold, Internal curing—role of absorbed water in aggregates, in: J.P. Ries, H.T. A. (Eds.), ACI SP-218 High-performance structural lightweight concrete, Farmington Hills, Michigan, 2004, pp. 131–142.

[40] P. Lura, O.M. Jensen, S.I. Igarashi, Experimental observation of internal water curing of concrete, Mater. Struct. 40 (2007) 211–220.

[41] S. Kamali, B. Gérard, M. Moranville, Modelling the leaching kinetics of cement-based materials-influence of materials and environment, Cem. Concr. Compos. 25 (2003) 451–458.

[42] S. Kamali, M. Moranville, S. Leclercq, Material and environmental parameter effects on the leaching of cement pastes: experiments and modelling, Cem. Concr. Res. 38 (2008) 575–585.

[43] M.A.T.M. Broekmans, The alkali–silica reaction: mineralogical and geochemical aspects of some Dutch concretes and Norwegian mylonites. , PhD. Thesis University of Utrecht, 2002, p. 144.

[44] J. Lindgård, Alkali–silica reactions (ASR)—Performance testing (draft title for the PhD thesis), NTNU, Norwegian Universiy of Science and Technology Trondheim, (to be published during 2013).

[45] T.C. Powers, T.L. Brownyard, Research Lab Portland Cement Association, Bull, 22, 1948.

[46] Vaisala Instruments Catalog, Ref B210768EN rev. A, www.vaisala.com/HM44 2009.

[47] D.A. Whiting, M.A. Nagi, Electrical Resistivity of Concrete—A Literature Review, PCA R&D Serial No. 2457, 2003, p. 56.

[48] K.D. Stanish, R.D. Hooton, M.D.A. Thomas, Prediction of Chloride Penetration in Concrete, US Department of Transportation, Federal Highway Administration, Publication No. FHWA-RD-00-142, 2001.

[49] SINTEF internal procedure KS 14-05-04-128, Hardened concrete, Measurement of electrical resistivity, 2007.

[50] W. Elkey, E. Sellevold, Electrical Resistivity of Concrete, Publication no. 80, Directorate of Public Roads, Norwegian Road Research Laboratory, 1995, p. 33.

[51] H. Justnes, E.J. Sellevold, G. Lundevall, High strength concrete binders, in: V.M. Malhotra (Ed.), Part A: Reactivity and Composition of Cement Pastes With and Without Condences Silica Fume, Fly Ash, Silica Fume, Slag, and Natural Pozzolans in Concrete, Istanbul, Turkey, 1992, pp. 132–147.

[52] J. Lindgård, M. Haugen, N. Castro, M.D.A. Thomas, Advantages of using plane polished section analysis as part of microstructural analyses to describe internal cracking due to alkali–silica reactions, in: T. Drimalas, J.H. Ideker, B. Fournier (Eds.), 14th International Conference on Alkali–Aggregate Reactions in Concrete, Austin, Texas, 2012.

[53] K. De Weerdt, K.O. Kjellsen, E. Sellevold, H. Justnes, Synergy between fly ash and limestone powder in ternary cements, Cem. Concr. Compos. 33 (2011) 30–38.

[54] K. De Weerdt, M. Ben Haha, G. Le Saout, K.O. Kjellsen, H. Justnes, B. Lothenbach, The effect of temperature on the hydration of composite cements containing limestone powder and fly ash, Mater. Struct. 45 (2012) 1101–1114.

[55] W. Bray, E.J. Sellevold, Water sorption properties of hardened cement paste cured or stored at elevated temperatures, Cem. Concr. Res. 3 (1973) 723–728.

[56] L.-O. Nilsson, Modelling moisture conditions in cementitious materials—some present challenges, 2nd International Symposium on Advances in Concrete through Science and Engineering Quebec City, Canada, 2006.

Paper V

Alkali-silica reaction (ASR) - Performance testing: Influence of specimen pre-treatment, exposure conditions and prism size on alkali leaching and prism expansion
J. Lindgård, M.D.A. Thomas, E.J. Sellevold, B. Pedersen, Ö. Andiç-Çakır, H. Justnes, T.F. Rønning
Cement and Concrete Research 53 (2013) pp. 68-90

Cement and Concrete Research 53 (2013) 68–90

Contents lists available at SciVerse ScienceDirect

Cement and Concrete Research

journal homepage: http://ees.elsevier.com/CEMCON/default.asp

Alkali–silica reaction (ASR)—performance testing: Influence of specimen pre-treatment, exposure conditions and prism size on alkali leaching and prism expansion

Jan Lindgård [a,*], Michael D.A. Thomas [b], Erik J. Sellevold [c], Bård Pedersen [d], Özge Andiç-Çakır [e], Harald Justnes [a,c], Terje F. Rønning [f]

[a] SINTEF Building and Infrastructure, NO-7465 Trondheim, Norway
[b] University of New Brunswick, Department of Civil Engineering, Fredericton, Canada
[c] Norwegian University of Science and Technology, NO-7491 Trondheim, Norway
[d] Norwegian Public Roads Administration, NO-0033 Oslo, Norway
[e] Ege University, Faculty of Engineering, Civil Engineering Department, Bornova, Izmir, Turkey
[f] Norcem Heidelberg Cement, NO-3950, Brevik, Norway

ARTICLE INFO

Article history:
Received 17 February 2013
Accepted 28 May 2013
Available online xxxx

Keywords:
Alkali–aggregate reaction (C)
Performance testing
Alkalis (D)
Expansion (C)
Microstructure (B)

ABSTRACT

Whether or not concrete prism tests developed for assessment of alkali–silica reactivity of aggregates might be suitable for general ASR performance testing of concrete has been evaluated. This paper discusses how variations in specimen pre-treatment, ASR exposure conditions and prism size influence the rate and amount of alkali leaching and prism expansion, together with a discussion of consequences for ASR test procedures. Furthermore, results from some complementary tests are included.

Generally, a remarkably high proportion of the in-mixed alkalis were leached out of the concrete prisms during the ASR exposure. For prisms exposed to 60 °C, the rate and amount of alkali leaching is the main controlling factor for the prism expansion. For less permeable concretes exposed to 38 °C, lack of internal moisture and lower rate of diffusion contributes to reduce the rate and extent of ASR expansion (reported in a separate paper).

1. Introduction

1.1. Background

Supplementary cementing materials (SCMs; e.g. silica fume, fly ash, ground granulated blast-furnace slag (ggbs), metakaolin and other pozzolans) control expansion due to alkali–silica reaction (ASR) by binding alkalis and limiting their availability for reaction with alkali–silica reactive aggregates [1]. The efficiency of the SCMs depends on their composition and amount, the nature of the reactive aggregate and the availability of alkali in the concrete. Chappex and Scrivener [2] also showed that the aluminium present in certain SCMs (e.g. metakaolin) may limit the dissolution of silica from reactive aggregates. Consequently, to be able to utilise alkali–silica reactive aggregates for production of durable concretes, the effects of various measures must correctly be identified by accelerated laboratory performance tests (or ideally by relevant long-term field experience). Several such performance tests have been used worldwide for at least 15 years, but the test conditions (e.g. pre-curing, temperature, alkali content, humidity) differ from one test method to another. Thus, the results and conclusions from different test methods may vary widely.

In 2006, Thomas et al. [3] provided a critical evaluation of different ASR performance test methods. The authors concluded that none of the currently available or commonly used test methods meet all the criteria for an ideal performance test. One main problem discovered is that alkalis are leached out of the prisms during exposure in the humid environment and hence reduce the final prism expansion, e.g. as documented for the Canadian 38 °C concrete prism test (CPT) [4] (similar to ASTM C1293 [5]). Thus, the authors concluded that this most frequently used CPT world-wide cannot be used to determine the "critical" alkali content for an alkali–reactive aggregate, nor to determine how the level of a SCM required to control expansion varies with the concrete alkali content. The "critical" or "threshold" alkali content is defined here as the lowest amount of alkali that will cause deleterious expansion with a particular aggregate.

Today, research is on-going in several countries with the aim to improve current ASR performance test methods and develop alternative tests. As part of the international harmonisation of ASR performance test methods, the "Performance testing" task group of RILEM TC 219-ACS is working on a performance testing concept aiming to

---

* Corresponding author. Tel.: +47 93 05 86 89.
E-mail address: jan.lindgard@sintef.no (J. Lindgård).

0008-8846/$ – see front matter © 2013 Elsevier Ltd. All rights reserved.
http://dx.doi.org/10.1016/j.cemconres.2013.05.017

develop one or more reliable ASR concrete performance test methods that might cover several applications/areas, ranging from combination of various aggregates with a standard CEM I binder up to the "ultimate goal" to document the alkali reactivity of any concrete recipe.

1.2. PhD study on ASR

1.2.1. General

The main objective of the PhD study by Jan Lindgård, being part of the Norwegian COIN program (2007–2014, www.coinweb.no), has been to evaluate whether concrete prism tests developed for assessment of alkali–silica reactivity of aggregates might be suitable for general ASR performance testing of concrete. This paper is one of several from the PhD study.

As part of the background study, a comprehensive literature review has recently been performed in close collaboration with the task group "Performance testing" in RILEM TC 219-ACS [6] (all authors of this paper, except one, are members of this RILEM task group). The main objective was to assess how various parameters might influence the laboratory/field correlation with respect to ASR performance testing, either directly or indirectly. The most important findings in the literature survey and recommendations for performance testing have recently been summarised by Lindgård et al. [7]. Additionally, the literature survey identified several issues that need further research in order to develop a reliable performance test procedure.

1.2.2. Parameters focused on in the PhD study

The experimental part of the study has focused on the effect of specimen "pre-treatment" and "ASR exposure conditions" as well as prism size on:

- Porosity and internal moisture state of the concrete prisms.
- Concrete transport properties (with respect to mobility of water and ions).
- Alkali leaching (rate and amount) from the concrete prisms during the ASR exposure.
- Concrete prism expansion (rate and final expansion).

Additionally, the effect of water-to-cementitious-materials ratio (w/cm) and type of binder is assessed.

The specimen "pre-treatment" is defined as the moisture condition during pre-storage and the length of the pre-storage period at ambient temperature (up to the point of the initial (zero) length comparator reading). The "ASR exposure conditions" include various moisture conditions, type of container, use of any wrapping (damp cotton cloth and plastic foil), exposure temperature, length of the storage period and addition of any external alkalis. These conditions as well as prism size varies between various performance test methods used in the different countries.

An extensive laboratory program has been performed, including 58 ASR test series and comprehensive complementary testing for documentation (Section 2.5). The test series cover the variations in test conditions in the most commonly used ASR concrete prism test methods. Additionally, some test series include measures to try to reduce the amount of alkali leaching. A separate paper [8] presents the technical background for the choice of test procedures.

As a basis for the evaluation of alkali leaching, some important findings on this topic in the recently published literature review [7] are summarised in Section 1.3.

1.3. Alkali leaching from concrete prisms during the ASR exposure

The problem of alkali leaching from specimens stored over water in sealed containers, leading to reduced prism expansion, was first reported by Blanks and Meissner in 1946 [9]. The authors detected an increasing concentration of alkali ions in the water at the bottom of the containers in which mortar bars were stored, and explained this as water condensing on the surface of the bars and running down the bars into the reservoir below, thereby transporting the alkalis. The mechanism for alkali leaching is further explained by Rivard et al. [10] to be excessive condensation of water on the prism surfaces, leading to an outward diffusion of alkalis from the interior of the concrete. The following parameters of importance for the rate and amount of alkali leaching are discussed in the literature review [7]:

- Pre-storage conditions (assumed less alkali leaching when pre-stored longer at 20 °C due to the higher degree of hydration when exposed to the extreme storage environments).
- Prism size (documented higher fraction of alkali leaching (i.e. higher % of the total alkalis leached out) for specimens of smaller cross-section [3,11]).
- Use of any wrapping (might reduce alkali leaching [12], or the opposite, decrease the expansion [13,14]).
- ASR exposure temperature (assumed more alkali leaching at higher exposure temperature [15] due to higher diffusivity).
- Humidity (fog chamber assumed to give more alkali leaching (due to increased condensation of water on the prism surfaces) compared with storage of prisms in a humid container [12,16].
- Drying/wetting cycles (does cooling of the prisms prior to length measurements enhance the amount of alkali leaching?).
- Alkali content (amount of alkali leaching assumed to increase with increased concrete alkali level [17]).
- Cement type (could be of high importance [16,18]).
- w/cm (assumed increased alkali leaching with increasing w/cm due to higher permeability [19,20]).

In contrast to laboratory testing, where the whole cross-section of the prisms is exposed to alkali leaching, field concrete structures are, according to Rivard et al. [17], mostly not subject to significant alkali leaching (documented by pore solution analysis), probably due to the much higher volume to surface ratio compared with laboratory specimens. Some alkali leaching is, though, expected in the surface layer of concrete structures exposed to moisture. The problem of alkali leaching (leading to reduced prism expansion) is thus a big challenge in accelerated ASR laboratory tests, and is consequently an important issue to focus on in the PhD study.

2. The test programme

2.1. General

The PhD laboratory test programme has included four concrete mixtures (Section 2.2) and in total 58 ASR test series, most of them using modified versions of the draft RILEM aggregate concrete prism tests; AAR-3, 2000 (38 °C, wrapped prisms) [21] and AAR-4.1, 2006 (60 °C, unwrapped and wrapped procedure) [22]. For comparison, six test series with slightly modified versions of the Norwegian 38 °C CPT [23] and 12 test series with the ASTM C1293 CPT [5] (38 °C, unmodified version) were included. Details for the various CPTs are given in a separate paper [8] (Table 3). An overview of modifications made in this study is given in Section 2.3.

The main reason for incorporating the ASTM C1293 CPT [5] was to establish a link to the comprehensive experience in North America with this method and to document any batch-to-batch variation; 8 concrete batches were needed to cast all the concrete prisms with the "basis" binder and two batches were prepared with the "open" binder (Section 2.2). In a separate paper [8] it was concluded that all the concretes produced are of the desired quality and that test series cast from different concrete mixtures can be compared. Furthermore, it was concluded that the prism expansions can be compared without consideration of the slightly varying, but generally low (<3.0%) air contents between the test series.

Except for the ASR testing, focus has been on alkali leaching measurements (Section 2.4) and documentation of moisture state in the concrete prisms (reported in a separate paper [8]). Additionally, a comprehensive complementary testing program for documentation of other concrete properties of importance for development of ASR has been performed (Section 2.5).

2.2. Materials and mixture proportions

Two CEM I Portland cements (EN-197-1), one high alkali (1.24% Na_2O_{eq}) and one low alkali (0.60% Na_2O_{eq}), and a CEM II/A-V cement containing 21.6% of a class F fly ash (co-grinded with the clinker) were used in the study, see Table 1 (comment: The CEM II/A-V cement normally contains 17–20% fly ash). This type of blended cement has been widely used for years in Norway, partly in order to avoid ASR in combination with alkali–silica reactive aggregates.

A non-reactive natural gneiss/granitic sand from Årdal and an alkali–silica reactive crushed coarse aggregate, a cataclasite with crypto- to microcrystalline quartz from Ottersbo, were used in all mixtures, blended to produce a 60:40 coarse:fine ratio (by mass)—more details are given in [8]. The 14-day expansion of the sand and the coarse aggregate in the RILEM AAR-2 80 °C accelerated mortar bar test [24] was measured to be 0.03% (non-reactive) and 0.30% (reactive), respectively (prism size 40 × 40 × 160 mm).

Details of the concrete mixtures are given in Table 2. Based on a series of considerations, the bulk of the testing was produced on a mixture containing 400 kg/m^3 of Portland cement and water-to-cement ratio (w/c) of 0.45 (denoted “basis” binder). The two CEM I cements were blended to produce an alkali content of 3.7 kg/m^3 Na_2O_{eq}. The alkali content was chosen (based on previous testing of the aggregates at SINTEF [25]) with aim to reach a final expansion of the reference test series lying on the steep (ascending) part of the “expansion-versus-alkali-level (S-shaped) curve”, so that a small loss of alkalis due to alkali leaching would be detectable in terms of reduced expansion. If a high alkali level had been chosen, most of the test series would probably show a rather high expansion (i.e. lie on the plateau of the “expansion-versus-alkali-level curve”), even if significant quantities of alkalis were leached out during the ASR exposure. Then only minor differences in expansion would have been expected between the different test series.

To examine the impact of w/c, two additional concrete mixtures were cast with CEM I cement and w/c of 0.30 and 0.60 (respectively denoted “dense” and “open” binder). The cement contents of these mixtures were modified to achieve the desired workability, but the alkali content of the mixtures was maintained at 3.7 kg/m^3 $Na_2O_{eq.}$ by appropriate blending of the CEM I cements (Table 2).

Additionally, one mixture was produced with w/cm of 0.45 using the blended fly ash cement (denoted “fly ash” binder, see Table 2). The alkali content of this mixture was raised from 5.0 kg/m^3 Na_2O_{eq} (alkalis originating from the blended cement) to 9.0 kg/m^3 Na_2O_{eq} by adding NaOH to obtain a final expansion of the “fly ash” concrete mixture on the steep (ascending) part of the “expansion-versus-alkali-level curve”, as well.

2.3. ASR test procedures—test series

2.3.1. Modification of the test procedures

The standard versions of the concrete prism tests have been slightly modified in order to investigate the effects of these modifications. The test procedure for the ASTM C1293 CPT [5] was not modified, apart from the use of prisms with 70 × 70 mm cross-section and not the prescribed 75 × 75 mm (comment: In spite of this, the term “ASTM prisms” is used in this paper). A summary of the changes is given below. The motivation for the modifications is given in the recently published literature review [7].

During all the testing only de-ionised water has been used as mixing water, in the moist cotton cloth wrapping (if any) and in the storage containers.

For all test series, the moulds were stored at ambient temperature in the laboratory under plastic foil from casting until de-moulding the following day. Furthermore, each prism was always stored vertically in the storage container with the same prism end pointing upwards.

For all standard versions of the CPTs, the mass and length were measured after cooling the prisms for about 16 h inside their storage container in a room kept at ~20 °C. For these test series, the reference readings where performed at de-moulding (and after the 0.5-h submersion period where used). However, all measurements in the modified versions of the various concrete prism tests were performed without pre-cooling the prisms. To secure accurate measurements, i.e. reduce the influence of any weight loss and temperature variations from reading to reading, a detailed measuring procedure was developed. The reference readings of the “warm” prisms were taken the day after the prisms were exposed to their ASR exposure temperature (see Fig. 1). The least reading of the length comparator was 0.001 mm.

The following specimen “pre-treatment” parameters and/or ASR exposure conditions have been varied when modifying the RILEM AAR-3 CPT (2000, [21]) and the RILEM AAR-4.1 CPT (2006, [22])—see Fig. 1 and Table 3 for details and motivation:

- The wrapping procedure (if any) was slightly modified, either by adding only half of the water content prescribed or by removing the prescribed polyethylene bag.
- The length of the “pre-storage” period was varied. The prisms were kept at 20 °C until 1, 7 or 28 days after casting before being exposed to the ASR exposure temperature. However, for all test series, the prisms were prepared for final storage (e.g. wrapped) and put into the storage container immediately after de-moulding (and after the 0.5-h submersion period where used) and the initial measurements of weight and length.
- Some prisms were pre-cured for 24 h at elevated temperature (60 °C) to simulate the curing temperature in a massive concrete structure.
- Some prisms were sealed in epoxy and aluminium foil after de-moulding to avoid any exchange of water with the environment.
- Some prisms were stored submerged in deionised water (to maximise the alkali leaching conditions).
- Some prisms were wrapped with cotton cloth saturated with a basic solution of strength pH 14.2 (1.5 M OH^-) or 13.2 (0.15 M OH^-), respectively (instead of the usual de-ionised water), in order to try to reduce the amount of alkali leaching. The lowest pH level corresponds to the typical pH found in water filtered from fresh cement paste with a high alkali Norwegian CEM I after half an hour. The highest pH level corresponds to the calculated pH level in the pore water in the concrete with the “basis” binder after about one

Table 1
Chemical composition (EN 196–2) of the three cements used in the study.

	SiO_2	Al_2O_3	Fe_2O_3	CaO	MgO	SO_3	K_2O	Na_2O	Na_2O_e	P_2O_5	LOI[a]
High alkali CEM I	19.61	4.87	3.48	61.03	2.83	3.81	1.11	0.51	1.24	0.15	2.44
Low alkali CEM I	20.06	4.67	3.31	63.06	2.01	3.40	0.39	0.34	0.60	0.16	2.24
CEM II/A-V[b]	26.61	8.73	4.24	50.34	2.37	3.28	1.04	0.56	1.25	0.33	1.20

[a] Loss-Of-Ignition.

[b] Blended cement with a class F fly ash content of 21.6 wt.%. Manufactured by co-grinding clinker and fly ash. Normally, the content of fly ash is in the range of 17–20%.

Table 2
Composition of the four concrete mixtures included in the study.

Materials (kg/m^3)			Binder composition			
			CEM I, 0.45 “basis” binder	CEM I, 0.30 “dense” binder	CEM I, 0.60 “open” binder	CEM II/A-V, 0.45 “fly ash” binder
Cement	High alkali CEM I		200	60	285	–
	Low alkali CEM I		200	490	30	–
	CEM II/A-V		–	–	–	400
Aggregates (SSD[a])	Årdal (gneiss/granite)	0/4	735	700	755	725
	Ottersbo (cataclasite)	4/8	185	175	190	180
		8/11	365	350	375	360
		11/16	550	525	565	540
Deionised water (free) (excl. any water in the superplasticiser)			180	165	189	180
NaOH (solids)			–	–	–	5.2
Alkali content (kg Na_2Oeq per m^3)			3.7	3.7	3.7	9.0
Superplasticiser (SIKA SSP 2000)			If necessary, add until workable and stable concrete (aimed slump 120 mm)			
De-foaming agent (SIKA)			If measured air content is >3.0%, add until air content is reduced to <3.0%			

[a] Saturated surface dry condition.

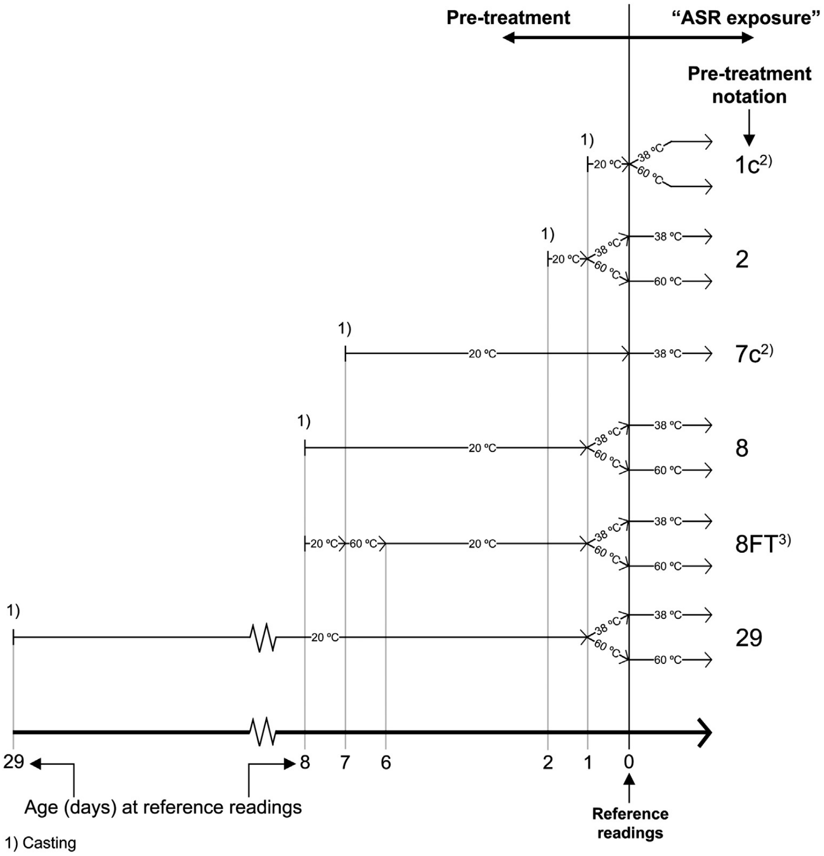

1) Casting
2) Cooled over night in it's container to 20ºC before each reading
3) FT = “Field Temperature”: simulation of the curing temperature in a structure

Fig. 1. Pre-treatment of the various test series, included notations. For all test series, the prisms were prepared for final storage and put into their storage container immediately after de-moulding (and after the 0.5 h submersion period where used—see Fig. 2 and Tables 4–7).

Table 3
Specimen environment during testing.

Notation	Specimen environment[a]	Comments
A	Three unwrapped prisms stored inside each container	Standard procedure for RILEM AAR-4.1, ASTM C-1293 and the Norwegian CPT
B[c]	Each prism was wrapped[b] in damp cotton cloth and poly-ethylene (prism ends not covered). Before wrapping, each cotton cloth was submerged for minimum 10 minutes in 80 g deionised water. Excess water not absorbed by the cotton cloth during submersion (~35–45 g) was poured on the top surface before sealing the bag. This lead to a "water reservoir" in the bottom of each polyethylene bag, that after four weeks of exposure was measured to be in the range of 4–25 g for 38 °C exposure and 0–2.5 g for 60 °C exposure	Standard procedure for RILEM AAR-3 and RILEM AAR-4.1 Alternative, including addition of 5 ml deionised water on the top surface after every reading
C[c]	Equal to "B", except that each cotton cloth was submerged in half the amount of deionised water (i.e. 40 g). All the water was absorbed by the cotton cloth	Motivation: Investigate the importance of the amount of water added to the wrapping
D	Equal to "B", except that each wrapped prism was not sealed inside a separate polyethylene bag, but was placed on a grid inside the "AAR-3 container". Neither was 5 ml deionised water poured on the top surface at any time	Motivation: Investigate the importance of storing each wrapped prism in a separate polyethylene bag
E	After de-moulding, each prism was coated with epoxy. The next day the prisms were further sealed by packing them in aluminium foil. Further storage in dry containers	Motivation: Try to totally hinder any moisture exchange with the surroundings
F	After de-moulding, the unwrapped prisms were totally submerged in deionised water. After every reading, the water was exchanged with new deionised water	Motivation: Give the prisms the maximum alkali leaching conditions
G[c]	Equal to "B", except each cotton cloth was submerged for minimum 10 min in a basic solution with pH 14.2 (Na/K-ratio ≈ 1/3) simulating the pH in the pore water of the "standard CEM I binder" after ~28 days of curing. No extra solution was poured on the top surface, beyond the ~60 g absorbed by the cotton cloth when it was submerged	Motivation: Investigate if application of a similar pH in the cotton cloth as in the concrete pore water is able to hinder alkali leaching from the concrete prisms
H[c]	Equal to "G", except each cotton cloth was submerged in a basic solution with pH 13.2 (Na/K-ratio ≈ 1/3) simulating a less basic pore solution. No extra solution was poured on the top surface, beyond the ~50 g absorbed by the cotton cloth when it was submerged	Motivation: Investigate if application of a somewhat lower pH in the cotton cloth compared to the concrete pore water is able to reduce the extent of alkali leaching

[a] In all CPTs, the prisms are stored vertically on grids above water, without being in direct contact with the water. A humid environment close to 100% RH is aimed.
[b] Each wrapped prism was sealed inside a separate polyethylene bag. 5 ml deionised water was poured on the top surface before sealing the bag and after each reading. Each bag was placed in a separate "AAR-3 container" with a tight lid.
[c] For 60 °C storage, three wrapped prisms were stored in an "AAR-4.1 metal container" instead of single "AAR-3 containers".

month of curing when much of the water has been consumed by hydration resulting in an increase in the concentration of alkali hydroxides in the pore solution (Comment: Some may find it strange with a pH above 14, but the pH scale from 0 to 14 is just the common range corresponding to 1 M H^+ and 1 M OH^-, respectively, and is not "limits").

2.3.2. Overview of test series

Fig. 2 shows the notations used to label the various ASR test series. The full notations give a complete description of the specimen "pre-treatment" and "ASR exposure" of the prisms. However, to simplify, short names are used in most figures and tables when presenting the results.

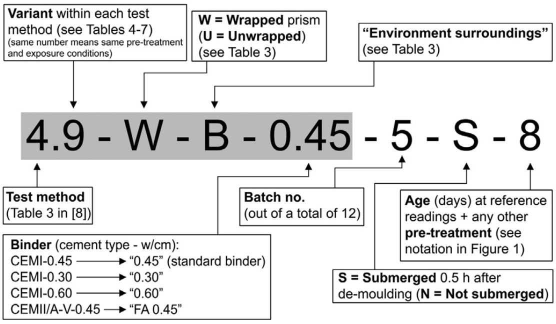

Fig. 2. Notations used to name the various test series. The short names given in the Tables 4–7 are marked with grey shadow. For repeated test series, the batch no. is additionally included in the short name.

Tables 4–7 give an overview of all 58 test series included in the test programme.

2.4. Alkali leaching measurements

To avoid any contamination, all the storage containers and any equipment used were washed thoroughly in a mild acid solution and de-ionised water. Additionally, a new lining was always used in each of the 38 °C storage containers (no lining was used in any of the 60 °C storage containers). Furthermore, "dummy" tests were performed with each type of container used (including any lining, the bottom grid, any separate sealing, any cotton wrapping and any plastic foil). After storing these containers up to one year at 38 or 60 °C, no significant quantity of alkalis was measured in samples taken out from the de-ionised water in the bottom of these storage containers. Consequently, any alkalis sampled during the ASR exposure originated from the concrete prisms.

During the ASR exposure, a 20-ml sample was periodically extracted from the bottom of each of the storage containers at the same time that expansion measurements were made. Before sampling, the water in the bottom of each storage container was stirred. The sample was stored in alkali-resistant plastic bottles before being analysed ("dummy" tests documented no alkali supply from the plastic bottles). Simultaneously, the height of the water was measured as basis for calculating the volume of water in each container (for each type of container, several "pilot measurements" were performed in order to prepare a volume vs. height curve). At the end of the ASR exposure period, the total amount of water in the bottom of each of the storage containers was measured by weighing the water, improving the accuracy of the final "container reservoir measurements". The detailed sampling procedure developed in the pilot study is included in the recently published RILEM TC 219-ACS literature review report (Appendix 8) [6]. For the wrapped prisms, sampling the water in

Table 4
Overview of the 18 test series with modified versions of the RILEM AAR-3 38 °C CPT (2000) [21].

Test series		Comments
Short name[a]	Full notation[b]	
3.1-W-B-0.45	3.1-W-B-0.45-3-N-7c	Standard RILEM AAR-3 test procedure (wrapped prisms, 7 days pre-storage at 20 °C, prisms cooled before every reading)
3.2-W-B-0.45	3.2-W-B-0.45-4-N-8	As 3.1-W-B-0.45, but readings taken without pre-cooling
3.3-W-C-0.45	3.3-W-C-0.45-4-N-8	As 3.2-W-B-0.45, but less water in wrapping
3.4-W-B-0.45	3.4-W-B-0.45-4-S-8	As 3.2-W-B-0.45, but prisms 0.5 h submerged after de-moulding
3.5- - E-0.45	3.5- -E-0.45-5-N-8	Sealed storage (epoxy and aluminium foil) after de-moulding (no water in the bottom of the storage containers)
3.6-W-D-0.45	3.6-W-D-0.45-6-S-8	As 3.4-W-B-0.45, but no polyethylene bag
3.7-U- A-0.45	3.7-U-A-0.45-6-S-8	As 3.4-W-B-0.45, but no wrapping (one prism in each container)
3.8-W-B-0.45	3.8-W-B-0.45-3-S-2	As 3.4-W-B-0.45, but 1 day pre-storage at 20 °C
3.9-W-B-0.45	3.9-W-B-0.45-2-S-29	As 3.4-W-B-0.45, but 28 days pre-storage at 20 °C
3.10-W-B-0.45-2	3.10-W-B-0.45-2-S-8FT	As 3.4-W-B-0.45, but simulating "field curing temperature" (see Fig. 1)
3.10-W-B-0.45-10	3.10-W-B-0.45-10-S-8FT	As 3.10-W-B-0.45-2, but repeated test series
3.11-U- F-0.45	3.11-U-F-0.45-5-S-8	Stored submerged in deionised water after de-moulding
3.12-W-G-0.45	3.12-W-G-0.45-12-S-8	As 3.4-W-B-0.45, but pH 14.2 in wrapping at start
3.13-W-H-0.45	3.13-W-H-0.45-12-S-8	As 3.4-W-B-0.45, but pH 13.2 in wrapping at start
3.4-W-B-0.30	3.4-W-B-0.30-7-S-8	As 3.4-W-B-0.45, but lower w/c ratio
3.4-W-B-0.60	3.4-W-B-0.60-8-S-8	As 3.4-W-B-0.45, but higher w/c ratio
3.8-W-B-FA-0.45	3.8-W-B-FA-0.45-9-S-2	As 3.8-W-B-0.45, but fly ash binder with boosted alkali level
3.9-W-B-FA-0.45	3.9-W-B-FA-0.45-9-S-29	As 3.9-W-B-0.45, but fly ash binder with boosted alkali level

[a] Used in figures and tables when presenting results.
[b] See details in Fig. 2.

the bottom of the containers was only performed in the end of the ASR exposure.

After ending the ASR exposure, the alkali content in any cotton wrapping and in any lining inside the storage containers was also measured. The alkali content in the cotton wrappings was likewise measured after four weeks of exposure (on the "extra prism" made of each test series—see [8]). The linings and the cotton wrappings were cut in smaller pieces, submerged in 1500 ml of de-ionised water in plastic bottles that was shaken once a day for one week before 20-ml samples were extracted after stirring the solution.

The concentration of alkalis, sodium [Na] and potassium [K] (in mg/l), in all the samples collected was analysed by flame atomic absorption spectroscopy (FAAS) of type "SpectrAA-400".

Based on the volume of the concrete prisms stored within each container and the in-mixed alkali content of the different concrete mixes (only alkalis from the cement and the fly ash was included, i.e. the insignificant quantity of alkalis supplied from the minor amount of superplasticiser added to some of the concrete mixes was neglected), the total amount of alkalis leached out from the prisms (i.e. sum of alkalis in the bottom of the containers and alkalis

Table 5
Overview of the 22 test series with modified versions of the RILEM AAR-4.1 60 °C CPT (2006) [22].

Test series		Comments
Short name[a]	Full notation[b]	
4.1-U-A-0.45	4.1-U-A-0.45-1-S-1c	Standard RILEM AAR-4.1 test procedure (unwrapped prisms, "reactor", 1 day pre-storage at 20 °C, prisms 0.5 h submerged after de-moulding and cooled before every reading)
4.2-U-A-0.45	4.2-U-A-0.45-1-S-2	As 4.1-U-A-0.45, but readings taken without pre-cooling
4.3-U-A-0.45	4.3-U-A-0.45-6-S-8	As 4.2-U-A-0.45, but 7 days pre-storage at 20 °C
4.4-U-A-0.45	4.4-U-A-0.45-2-S-29	As 4.3-U-A-0.45, but 28 days pre-storage at 20 °C
4.5-U-A-0.45	4.5-U-A-0.45-2-S-8FT	As 4.3-U-A-0.45, but simulating "field curing temperature" (see Fig. 1)
4.6-U-F-0.45	4.6-U-F-0.45-5-S-8	Stored submerged in deionised water after de-moulding
4.7- -E-0.45	4.7- -E-0.45-5-N-8	Sealed storage (epoxy and aluminium foil) after de-moulding (no water in the bottom of the storage container)
4.8-W-B-0.45-1	4.8-W-B-0.45-1-S-2	Standard RILEM AAR-4.1 Alt. test procedure (wrapped prisms, 1 day pre-storage at 20 °C), except prisms 0.5 h submerged after de-moulding and readings taken without pre-cooling
4.8-W-B-0.45-10	4.8-W-B-0.45-10-S-2	As 4.8-W-B-0.45-1, but repeated test series
4.9-W-B-0.45	4.9-W-B-0.45-5-S-8	As 4.8-W-B-0.45-1, but 7 days pre-storage at 20 °C
4.10-W-C-0.45-6	4.10-W-C-0.45-6-N-8	As 4.9-W-B-0.45, but less water in wrapping
4.10-W-C-0.45-12	4.10-W-C-0.45-12-N-8	As 4.10-W-B-0.45-6, but repeated test series
4.11-W-D-0.45	4.11-W-D-0.45-3-S-8	As 4.9-W-B-0.45, but no polyethylene bag
4.12-W-G-0.45	4.12-W-G-0.45-12-S-8	As 4.9-W-B-0.45, but pH 14.2 in wrapping at start
4.13-W-H-0.45	4.13-W-H-0.45-12-S-8	As 4.9-W-B-0.45, but pH 13.2 in wrapping at start
4.3-U-A-0.30	4.3-U-A-0.30-7-S-8	As 4.3-U-A-0.45, but lower w/c ratio
4.9-W-B-0.30	4.9-W-B-0.30-7-S-8	As 4.9-W-B-0.45, but lower w/c ratio
4.3-U-A-0.60-I	4.3-U-A-0.60-8-IS-8	As 4.3-U-A-0.45, but higher w/c ratio
4.3-U-A-0.60-II	4.3-U-A-0.60-8-IIS-8	As 4.3-U-A-0.60-I, but repeated test series
4.9-W-B-0.60	4.9-W-B-0.60-11-S-8	As 4.9-W-B-0.45, but higher w/c ratio
4.2-U-A-FA-0.45	4.2-U-A-FA-0.45-9-S-2	As 4.2-U-A-0.45, but fly ash binder with boosted alkali level
4.4-U-A-FA-0.45	4.4-U-A-FA-0.45-9-S-29	As 4.4-U-A-0.45, but fly ash binder with boosted alkali level

[a] Used in figures and tables when presenting results.
[b] See details in Fig. 2.

Table 6
Overview of the 6 test series with modified versions of the Norwegian 38 °C CPT [23].

Test series		Comments
Short name[a]	Full notation[b]	
N.1-U-0.45	N.1-U-A-0.45-3-S-1c	Standard Norwegian CPT procedure (1 day pre-storage at 20 °C, prisms 0.5 h submerged after de-moulding and cooled before every reading)
N.2-U-0.45	N.2-U-A-0.45-1-S-2	As N.1-U-0.45, but readings taken without pre-cooling
N.3-U-0.45	N.3-U-A-0.45-4-S-8	As N.2-U-0.45, but 7 days pre-storage at 20 °C
N.3-U-0.30	N.3-U-A-0.30-7-S-8	As N.3-U-0.45, but lower w/c ratio
N.3-U-0.60	N.3-U-A-0.60-8-S-8	As N.3-U-0.45, but higher w/c ratio
N.3-U-FA-0.45	N.3-U-A-FA-0.45-9-S-8	As N.3-U-0.45, but fly ash binder with boosted alkali level

[a] Used in figures and tables when presenting results.
[b] See details in Fig. 2.

in any wrapping and any lining) was calculated (expressed as kg Na_2O_{eq} per m^3 of concrete and as % of in-mixed alkalis). In these calculations it was assumed that all the three prisms within one storage container leached out the same quantity of alkalis (except for the RILEM AAR-3 CPT, where only one prism was stored inside each container).

2.5. Complementary tests

2.5.1. Overview

In order to document properties of importance for development of ASR, comprehensive complementary testing has been an important part of the study (Section 1.2.2). A separate paper [8] presents and evaluates the results from measurements of concrete porosity, moisture state and transport properties. In addition to the rate and amount of alkali leaching (Sections 2.4 and 3.2) and prism expansion (Section 3.3), this paper includes results from visual inspections and microstructural analysis of prisms after the ASR exposure (Sections 2.5.2 and 3.4). Some further complementary tests (alkali release from aggregates and dynamic E-modulus) are included in the PhD thesis [26].

Before the laboratory testing started, a "pilot testing" program was carried out in order to develop detailed laboratory procedures to improve the reliability of the measurements.

Table 7
Overview of the 12 test series with the ASTM C-1293 38 °C CPT [5].

Test series		Comments
Short name[a]	Full notation[b]	
ASTM-U-0.45-1	ASTM-U-A-0.45-1-N-1c	Standard ASTM C-1293 test procedure (1 day pre-storage at 20 °C, prisms cooled before every reading)
ASTM-U-0.45-2	ASTM-U-A-0.45-2-N-1c	As ASTM-U-0.45-1, but new batch
ASTM-U-0.45-3	ASTM-U-A-0.45-3-N-1c	As ASTM-U-0.45-1, but new batch
ASTM-U-0.45-4	ASTM-U-A-0.45-4-N-1c	As ASTM-U-0.45-1, but new batch
ASTM-U-0.45-5	ASTM-U-A-0.45-5-N-1c	As ASTM-U-0.45-1, but new batch
ASTM-U-0.45-6	ASTM-U-A-0.45-6-N-1c	As ASTM-U-0.45-1, but new batch
ASTM-U-0.45-10	ASTM-U-A-0.45-10-N-1c	As ASTM-U-0.45-1, but new batch
ASTM-U-0.45-12	ASTM-U-A-0.45-12-N-1c	As ASTM-U-0.45-1, but new batch
ASTM-U-0.30-7	ASTM-U-A-0.30-7-N-1c	As ASTM-U-0.45-1, but lower w/c ratio
ASTM-U-0.60-8	ASTM-U-A-0.60-8-N-1c	As ASTM-U-0.45-1, but higher w/c ratio
ASTM-U-0.60-11	ASTM-U-A-0.60-11-N-1c	As ASTM-U-0.60-8, but repeated test series
ASTM-U-FA-0.45-9	ASTM-U-A-FA-0.45-9-N-1c	As ASTM-U-0.45-1, but fly ash binder with boosted alkali level

[a] Used in figures and tables when presenting results.
[b] See details in Fig. 2.

2.5.2. Visual inspection and microstructural analysis

In order to confirm the presence and amount of ASR after the exposure, microstructural analyses have been performed on 15 selected concrete prisms. These examinations have included analysis of 16 fluorescence impregnated plane polished sections and 25 fluorescence impregnated and polished thin sections, as well as scanning electron microscopy (SEM) analysis of 11 of the thin sections. Additionally, a visual inspection including photo documentation of any surface cracking and precipitation was performed on one prism from each of the 58 test series. As part of this inspection, cut faces of the prism ends were carefully examined to search for any internal gel accumulation in cracks and pores.

The extent of internal cracking in the concrete prisms (Section 3.4.2) was documented in the plane polished sections that cover the whole prism (70 × 280 mm; two half prisms for the larger Norwegian prisms). In the photos taken in UV-light, the crack patterns appear clearly. By use of image analysis, the crack patterns were analysed to quantify the extent and spread in cracking in the concrete prisms.

Results from the thin section and SEM analyses are included in the PhD thesis [26]. A paper presenting some important findings from all the microstructural analyses was presented at the 14th ICAAR in 2012 [27].

3. Results and discussion

3.1. General

Before presenting the detailed results from the study (Sections 3.2–3.4), some astonishing expansion results are presented in Fig. 3 to demonstrate the substantial impact of the test procedure used on the prism expansion, and consequently on the outcome of a performance test. All the test series included in the figure have identical concrete composition ("basis" binder, Table 2). The figure covers unwrapped as well as wrapped prisms exposed to 100% RH and either 38 °C or 60 °C. Several of the testing variants represent test procedures used in various "commercial" CPTs (Section 2.3.1), i.e. they are by no means extreme. The 52 weeks expansion of the 38 °C test series varies in the range of

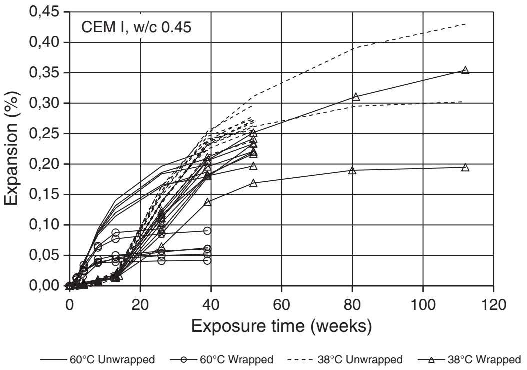

Fig. 3. Expansion versus time for 32 test series with the "basis" binder (CEM I, w/c 0.45, 3.7 kg/m^3 Na_2O_{eq} alkalis).

0.17–0.31%, while the 39 weeks expansion of the 60 °C test series varies in the range of 0.04–0.22%.

One of the most remarkable aspects of these differing results is that one of the testing variants that produced one of the lowest final expansions was recommended by RILEM for a long period as an alternative test method to evaluate the alkali-reactivity of aggregates (Comment: That method (RILEM AAR-4.1 Alternative 60 °C CPT (2006) with wrapped prisms [22]) is, however, not recommended by RILEM TC 219-ACS any longer due to the results of this study).

3.2. Alkali leaching from concrete prisms

3.2.1. General

The results from the alkali leaching measurements are presented in the following sub-sections. Firstly, the distribution of the alkalis leached out are discussed, i.e. relative quantities found in the water at the bottom of the containers, in the cotton cloth (for wrapped prisms) and in the lining inside the containers. Secondly, the general findings are evaluated, before a more detailed discussion about the effect of prism size, specimen "pre-treatment", exposure temperature and binder type follows. Subsequently, the rate of leaching of Na compared with K is discussed. Finally, the effect of the measures taken to try to reduce the amount of alkali leaching is assessed.

3.2.2. Presentation of results—location of the alkalis leached out

The accumulated amount of alkali leaching is presented in Figs. 4, 6, 7 and 8 expressed as a percentage of the in-mixed alkalis, i.e. 3.7 kg/m^3 Na_2O_{eq} for the CEM I binders (w/c ranging from 0.30 to 0.60, alkalis originating from the cement) and 9.0 kg/m^3 Na_2O_{eq} for the "fly ash" binder (CEM II/A-V, w/cm of 0.45, included the alkalis originating from the cement, the fly ash and the added 4.0 kg Na_2O_{eq} NaOH per m^3 of concrete)—see Tables 1 and 2. In Fig. 5, the alkali leaching from the ASTM prisms is alternatively expressed as kg Na_2O_{eq} per m^3 of concrete. However, this way of presenting the results does not influence the relative differences between the various test series with the CEM I binders. But, due to the higher alkali content in the "fly ash" binder, the relative values between the CEM I test series and the "fly ash" test series is drastically changed. When expressed as a percentage of the in-mixed alkalis, the "fly ash" test series leach considerably less alkalis than the CEM I test series, while the "fly ash" binder leaches most alkalis when expressed as kg Na_2O_{eq} per m^3 of concrete (see Section 3.2.7).

For the unwrapped test series (Tables 4–7), the accumulated contents of alkalis measured in the bottom of the various storage containers are shown as continuous lines in Figs. 4–8. Fig. 7 (RILEM AAR-4.1) and Fig. 8 (RILEM AAR-3) include the alkalis measured in the cotton cloth for the wrapped test series (Tables 3–5) at two ages: four weeks after starting the ASR exposure (measured on the "extra prism") and after ending the ASR exposure (mean of three prisms).

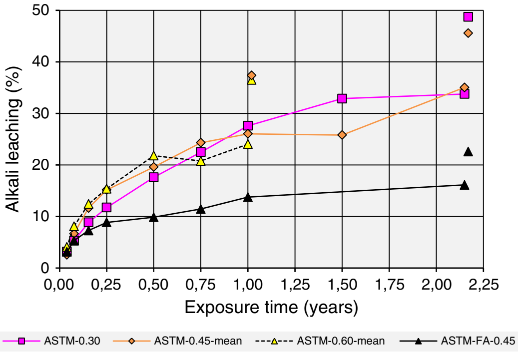

Fig. 4. Alkali leaching from the unwrapped ASTM prisms (% of the initial concrete alkali content). The single data points include alkalis absorbed by the lining—added to the accumulated alkali content in the bottom of the storage containers at the end of the exposure period. See Fig. 2 and Table 7 for abbreviations.

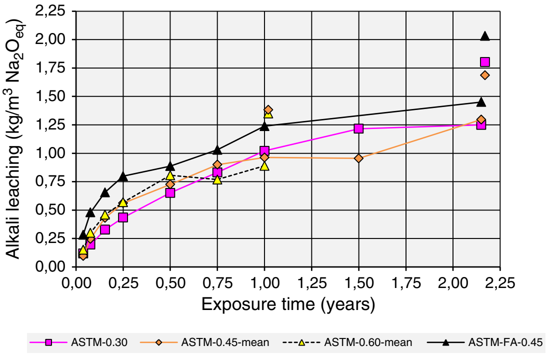

Fig. 5. Alkali leaching from the unwrapped ASTM prisms (expressed as kg/m^3 Na_2O_{eq}). The single data points include alkalis absorbed by the lining—added to the accumulated alkali content in the bottom of the storage containers at the end of the exposure period. See Fig. 2 and Table 7 for abbreviations.

Furthermore, at the end of the ASR exposure of the 38 °C test series, the content of alkalis absorbed by the linings used inside the various storage containers has been added to the accumulated content of alkalis measured in the bottom of the storage containers. Moreover, the accuracy of the final "container reservoir measurements" was improved compared with the interim measurements (Section 2.4). These "true" final quantities of alkalis leached out are shown as single data points in Figs. 4 and 5 (ASTM C1293 CPT) and in Fig. 6 (Norwegian CPT) at ages 52 and 112 weeks. For both CPTs, 25 to 30% of the total amounts of alkalis leached out from the concrete prisms have been absorbed by the lining (same type of cotton cloth) during the exposure period. Consequently, for these two CPTs the "true" accumulated amount of alkalis leached out throughout the ASR exposure period is significantly higher (up to 25–30%?) than shown in Figs. 4–6 (since only the final measurements include the alkalis absorbed by the lining).

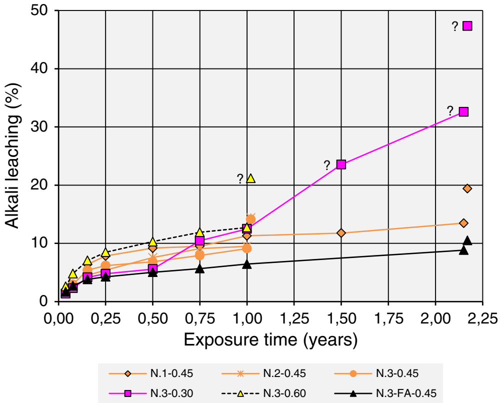

Fig. 6. Alkali leaching from the unwrapped Norwegian CPT prisms (% of the initial concrete alkali content). The single data points include alkalis absorbed by the lining—added to the accumulated alkali content in the bottom of the storage containers at the end of the exposure period. See Fig. 2 and Table 6 for abbreviations. The four data points with a question mark are uncertain (due to uncertain volume of water).

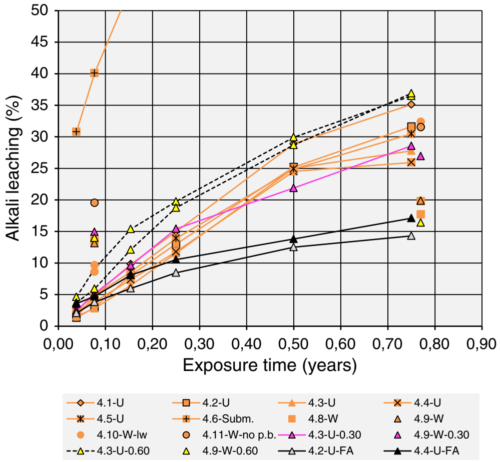

Fig. 7. Alkali leaching from the AAR-4.1 prisms (% of the initial concrete alkali content). The single data points represent wrapped prisms (W). The accumulated curves represent unwrapped prisms (U). See Fig. 2 and Table 5 for abbreviations (Remark: Different scaling on the x-axes compared with Figs. 4–6 and 8, 9).

For the AAR-3 test series (Fig. 8), the presented results at ages 52 and 112 weeks express the "true" content of alkalis leached out (i.e. sum of alkalis from any wrapping, the container reservoir and the lining). For this CPT, the relative amount of alkalis absorbed by the lining was only about 1/8 to 1/10 of what was found for the test series with the ASTM C1293 CPT and the Norwegian CPT (see above). The main reasons for this is believed to be that the wrapped AAR-3 prisms have a plastic sheet covering the cotton cloth (only the top and bottom faces are uncovered), the prisms are stored inside a polyethylene bag inside the storage container and a less absorbing lining was used. Consequently, on average about 90% of the alkalis leached out are trapped in the cotton cloth. The remaining (about 6%) of the total quantity of alkalis leached out was found in the water in the bottom of the containers. Corresponding numbers for the wrapped AAR-3 test series stored without any polyethylene bag were as follows: about 40% were trapped in the cotton cloth wrapping, about 55% were found in the container reservoir and about 5% were absorbed by the lining.

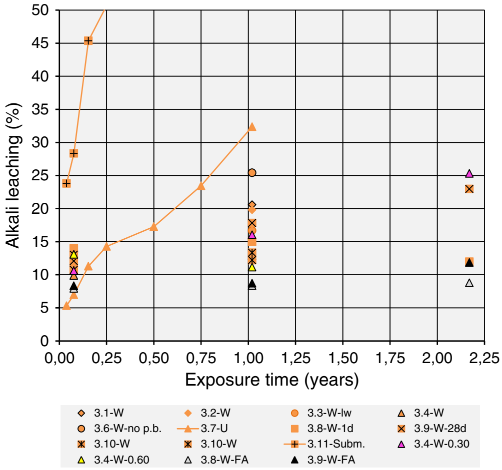

Fig. 8. Alkali leaching from the AAR-3 prisms (% of the initial concrete alkali content). The single data points represent wrapped prisms (W). The accumulated curves represent unwrapped prisms (U). See Fig. 2 and Table 4 for abbreviations.

For the 60 °C AAR-4.1 test series, no lining was used. Thus, the accumulated results for the unwrapped test series presented in Fig. 7 express the "true" quantity of alkalis leached out throughout the full ASR exposure. Another consequence of not using any lining inside these rectangular shaped steel containers is that the accuracy of the interim volume estimations of the amount of water in the container (based on height measurements) is even better than for the other circular containers in which the lower part of the lining was submerged in the reservoir.

The average distribution of leached alkalis for the wrapped 60 °C AAR-4.1 test series was as follows:

- Prisms stored inside a polyethylene bag: 55–65% of the total amount of alkalis leached out (0.7 kg Na_2O_{eq} per m^3 of concrete) was trapped in the cotton cloth wrapping and 35–45% were found in the container reservoir.
- Prisms stored without any polyethylene bag: About 25% of the total amount of alkalis leached out (1.2 kg Na_2O_{eq} per m^3 of concrete) was trapped in the cotton cloth wrapping and about 75% were found in the container reservoir.

One of the reasons for measuring a relatively higher portion of alkalis in the container reservoir in the 60 °C AAR-4.1 containers compared with the 38 °C AAR-3 containers might be that most polyethylene bags were broken (leakage in the joints) when exposed to 60 °C for some time. Additionally, considerably more water vapour is observed inside the containers stored at 60 °C compared with 38 °C exposure when opening the containers during the exposure. Thus, the wrapped 60 °C prisms are most likely exposed to relatively more "moisture movements" compared with exposure to 38 °C.

3.2.3. General evaluation of the alkali leaching results

Figs. 4–8 show that considerable quantities of alkalis are leached out of the concrete prisms during the ASR exposure. However, the rate and amount depend strongly on the prism cross-section, specimen "pre-treatment", binder type and exposure conditions. During the first 4 weeks of exposure, alkalis in the range of 3–20% are leached out, constituting 0.10–0.75 kg Na_2O_{eq} alkalis per m^3 of concrete for the CEM I binders (even more for the test series submerged in de-ionised water—see later). At the end of the exposure, from 14 to 37% are in total leached out of the 60 °C prisms (39 weeks), while corresponding numbers for the 38 °C test series are in the range of 10–49% (112 weeks). The highest number constitutes about 1.8 kg Na_2O_{eq} alkalis per m^3 of concrete for the CEM I binders.

Before presenting the detailed results, the following remarks are considered relevant regarding the consistency of the results:

- The accumulated alkali leaching curves are smooth, indicating a satisfactory accuracy of the interim measurements.
- In general, similar ranking is obtained between the various binder types when tested according to different concrete prism tests.
- The distribution of alkalis between various locations inside the storage containers (i.e. in the container reservoir, in the wrapping or lining) is similar for comparable CPTs (Section 3.2.2).
- C.o.v. for the alkali leaching between parallel test series (i.e. repeated test series) and between comparable test series (i.e. with identical binder composition, but slightly different specimen "pre-storage") is acceptable. For the eight ASTM test series with the "basis" binder, the c.o.v. is in the range of 10–20% (lowest at age 52 weeks). A similar c.o.v. is found for the three Norwegian test series with the "basis" binder. If test series N.1 (pre-cooled before measuring, which has some influence—see later) is excluded, the c.o.v. is reduced to 1–10% (lowest at age 52 weeks). The c.o.v. for the five unwrapped AAR-4.1 test series with the "basis" binder is in the range of 7–15% at ages

8–39 weeks. If the pre-cooled test series (4.1) is excluded, the c.o.v. is reduced to 1–12%.

- The total amount of alkali leaching is on a similar level as reported previously by Thomas et al. [3] for the ASTM C-1293 CPT and by Bokern [16] for unwrapped concrete prisms exposed to high humidity at 60 °C.
- A very good correlation is found between the amount of alkali leaching at early age and prism expansion, in particular for the test series exposed to 60 °C (Section 3.3.7).
- The extent and distribution of internal cracks in the concrete prisms correspond well with the amount of alkali leaching (see further discussion in Section 3.4.2).

(Comment: In addition to measurements of alkalis leaching, it was of interest to measure the remaining alkali content within the prisms. However, the results from the performed "pilot" tests were considered to be too uncertain to be included in this paper.)

As a basis to assess the parameters influencing the rate and amount of alkali leaching, the following general consideration of the mechanisms for alkali leaching is made: Alkali leaching consists of two steps: internal transport of the alkalis (to the prism surface) and external reception of the alkalis ("sink capacity"). The internal transport is dependent on diffusion properties, the distance the alkalis have to diffuse through the concrete pore water (dependent on the prism cross-section) and the "driving force" for alkali leaching (i.e. the difference in alkali concentration in the concrete pore water compared with the alkali concentration in any water (liquid) present on the prism surface [10]). The diffusion properties are primarily controlled by the permeability (dependent on binder type, w/cm and specimen "pre-treatment"), the water content and the exposure temperature. The "driving force" for alkali leaching is influenced by the "sink capacity" (see below) and the concentration of alkalis in the concrete pore water. Rivard et al. [17] has, for example, shown that increased alkali content in the concrete, and consequently higher concentration of alkalis in the concrete pore water, increases the alkali leaching. The concentration of alkalis in the concrete pore water further depends on the binder type and the w/cm, the moisture state and any reduction of the alkali content over time due to binding of alkalis in the ASR gel and/or alkali leaching. The fact that the alkali content in the concrete pore water is reduced with time is assumed to be one of the main reasons for the observed reduced rate of alkali leaching with time for most test series.

The "sink capacity" is dependent on the storage environment. The more water surrounding the prisms, the more leached alkalis can be absorbed by the water. The most extreme storage condition in this respect is prisms totally submerged in de-ionised water that is replaced with new de-ionised water at every periodic measurement of length and mass of the prisms. Opposite, if only a limited number of water drops condense on the surface of the prisms stored on grids over water and run down the prisms into the water reservoir below, the "sink capacity" might be the limiting factor for alkali leaching. If that is the case, less influence of the parameters influencing the internal transport is expected (e.g. less influence of increased storage temperature, even if higher temperature gives higher mobility of ions and thus higher diffusivity).

3.2.4. Influence of prism size

For all binders, increasing the prism cross-section from 70 × 70 mm (ASTM size, Fig. 4) to 100 × 100 mm (Norwegian size, Fig. 6) decreases the rate and amount of alkali leaching considerably (the cross-sectional area of the latter is double of the former). As a result of this, the final expansion increases substantially (Sections 3.3.4 and 3.3.5). For each of the binders, the "alkali leaching ratio" between the two prism sizes is rather constant throughout the full exposure period. On average the ratio is in the range of 1.8–2.5. The surface/volume ratio for the two prism sizes are 0.64 (ASTM) and 0.44 (Norwegian), respectively, giving a relative ratio of 1.45. For test series with equal concrete composition (with assumed similar concentration of alkalis in the concrete pore water) and comparable diffusion properties, it is logical that the rate and amount of alkali leaching decreases when the prism cross-section is increased, since the alkalis have to diffuse a longer distance. The advantage of increasing the prism size is previously reported by several scientists, e.g. Bakker [11], Thomas et al. [3] and Lindgård et al. [25]. An obvious consequence of this finding is that one effective measure to reduce the amount of alkali leaching during performance testing is to increase the prism cross-section.

3.2.5. Influence of cotton cloth wrapping

One important, but somewhat surprising, finding is that from prisms wrapped with a wet cotton cloth considerable quantities of alkalis are leached out during the first 4 weeks of exposure, significantly more than that measured for the unwrapped prisms (Figs. 7 and 8). However, later in the exposure period, the rate of alkali leaching from the wrapped prisms is considerably less compared with the unwrapped prisms (for some of the wrapped prisms exposed to 38 °C hardly any more alkalis are leached out beyond 4 weeks of exposure). When exposed to 38 °C for 4 weeks, the wrapped AAR-3 prisms with CEM I binders stored inside the prescribed polyethylene bags lose from 10 to 14% of alkalis due to leaching (Fig. 8) compared with 5–9% for the unwrapped ASTM prisms of similar size (Fig. 4). Corresponding numbers are 11–21% (wrapped prisms) compared with 30–40% (unwrapped prisms) after 52 weeks of exposure and 12–25% (wrapped prisms) compared with 45–49% (unwrapped prisms) after 112 weeks of exposure.

When exposed to 60 °C for 4 weeks, the wrapped AAR-4.1 prisms (stored inside polyethylene bags) with CEM I binders lose 9–15% of alkalis due to leaching compared with 3–9% for corresponding unwrapped prisms (Fig. 7). After 39 weeks of exposure, the wrapped AAR-4.1 prisms lose 16–32% of alkalis compared with 26–37% for unwrapped prisms.

The wrapping procedure is of high importance for the amount of alkali leaching and consequently influences the prism expansions (Section 3.3). When adding only half of the prescribed 80 g of water to the cotton cloth, a significant drop in the early-age alkali leaching (and a corresponding increase in the prism expansion) was observed for the 60 °C test series; reduced from 13.0–13.5% to 8.5–9.5% (Fig. 7). On the other hand, a considerably increased amount of alkali leaching was observed in the end of the exposure period (32%) compared with comparable test series where the prescribed quantity of water was added to the wrapping (20%). Reducing the amount of water added to the cotton cloth had less influence on the rate of alkali leaching from the AAR-3 prisms exposed to 38 °C.

Furthermore, whether each wrapped prism was stored inside the prescribed polyethylene bag or not also had high influence on the amount of alkali leaching (Figs. 7 and 8). When removing the bag, prisms exposed to 60 °C for 4 weeks lost as much as 20% of the in-mixed alkalis, and throughout the full exposure period about 1.5 times more alkalis were leached out from these prisms compared with prisms stored inside a bag. The influence was less at 38 °C. Not surprisingly, the 60° test series without the polyethylene bag obtained the lowest expansion of all the wrapped 60 °C test series (Section 3.3.4).

The reason for the increased amount of alkali leaching at early age when wrapping the prisms with a wet cotton cloth is believed to be increased "sink capacity" (see Section 3.2.3). For unwrapped prisms, some condensed water is present on the prism surfaces, running down from the top into the reservoir below [9]. These water drops pick up and transport the alkalis leached out from the prisms. For wrapped prisms, when adding the prescribed 80 g of water to the cotton cloth, the cotton wrapping is dripping wet with de-ionised water (some of the water was added on top of the prisms before closing the polyethylene bag—see Table 3). Consequently, the “sink capacity” is high, able to maintain the difference in alkali concentration between the concrete surface and the concrete pore water for a relatively long time, since more water has to reach a certain concentration before the diffusion is slowed down. However, over time, alkalis are gradually accumulated in the cotton cloth wrapping, thus reducing the “driving force” for alkali leaching. Additionally, the alkali concentration in the concrete pore water is decreased with time due to the alkali leaching and binding of alkalis in any ASR gel, e.g. as reported by Rivard et al. [28]. Therefore, the wrapped prisms leach out less alkalis later in the exposure period compared with the unwrapped prisms, where constantly more “pure water drops” are condensing and running down the prism surfaces.

When adding only half of the water to the cotton cloth, the cotton wrapping is not fully wetted and hence a reduced reservoir of de-ionised water is present on the prism surface and in the cotton cloth “pores” (i.e. less “sink capacity”). Consequently, less alkali leaching is measured at early age. In contrast, when removing the polyethylene bag, the wrapped prisms have access to more “moisture movements” as water is condensing and dripping from the underside of the lid down on the top surface of the wrapped prisms (i.e. increased “sink capacity”). The result is increased rate of alkali leaching throughout the full exposure period.

3.2.6. Influence of exposure temperature

In general, elevating the exposure temperature from 38 °C to 60 °C did not influence the amount of alkali leaching at early age (4 weeks), neither for wrapped nor for unwrapped prisms (Figs. 7–9). This is surprising, since the rate of diffusion increases somewhat as the temperature increases, since temperature is a measure of molecular movement. One possible explanation might be that most test series exposed to 60 °C have already developed some ASR gel during the first 4 weeks of exposure. Consequently, some of the alkalis have been bound by the ASR gel and are thus less available for leaching [10,28], i.e. the “driving force” for alkali leaching is reduced for the 60 °C test series and thus counteracts the higher diffusion rate compared with the 38 °C test series. Another possibility is that the “sink capacity” is limiting the rate of diffusion, not the internal diffusion of ions (see above).

However, a few exceptions were found; for example, the rate of alkali leaching was significantly increased for the 60 °C test series submerged in de-ionised water (Fig. 7) compared with submerged prisms exposed to 38 °C (Fig. 8). Similarly, the early-age alkali leaching from the wrapped test series stored without the polyethylene bag increased with the temperature. In both cases, the “sink capacity” is high. Consequently, the rate of diffusion more controls the rate of alkali leaching, and a higher influence of the elevated temperature is thus observed. Furthermore, these latter test series with the highest rate of alkali leaching only develop minor expansion (Section 3.3.4), meaning that less ASR gel is produced at early age. Thus, less alkalis are bound in the ASR gel [28], and consequently a high “driving force” for alkali leaching is maintained.

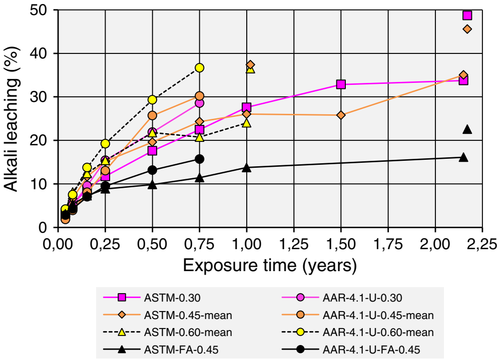

Fig. 9. Temperature dependency of alkali leaching; accumulated mean results for the ASTM C 1293 CPT (38 °C) and the AAR-4.1 CPT (60 °C)—all unwrapped prisms. The alkalis absorbed by the lining in the ASTM CPT are not included, except for the single points at ages 52 and 112 weeks (upper points). See Fig. 2, Tables 5 and 7 for abbreviations.

Fournier et al. [15] also documented a low influence of the exposure temperature on the rate of alkali leaching. They did not find a pronounced increase in the amount of alkali leaching after 3 weeks of exposure of unwrapped prisms when elevating the temperature from 38 °C to 60 °C (only a tendency to a little more alkali leaching at 60 °C).

Throughout the full exposure period, the rate and amount of alkali leaching from the unwrapped AAR-4.1 prisms (60 °C) and the unwrapped ASTM prisms (38 °C) is comparable for almost all corresponding test series, see Fig. 9 (after adding the assumed amount of alkalis absorbed by the lining in the ASTM containers (25–30% of the total amount of leached alkalis, see Section 3.2.2) to the shown accumulated curves). The main reason for this could be the same as discussed above; the “sink capacity” is limiting the rate of diffusion for these unwrapped prisms, reducing the influence of the increased rate of diffusion with increasing exposure temperature. Only one (minor) exception is observed; for the unwrapped prisms with the CEM I “open” binder (w/c of 0.60), the rate of alkali leaching is somewhat higher at 60 °C compared with 38 °C in the period beyond 8 weeks of exposure.

In contrast, the temperature dependency for the alkali leaching is more evident (and more as expected) for wrapped prisms in the period beyond 4 weeks of exposure; those exposed to 60 °C have a considerably higher rate of alkali leaching compared with those exposed to 38 °C (Figs. 7 and 8). This is most probably due to a higher “sink capacity” for the wrapped prisms, and thus the diffusion properties are of greater importance for the rate of alkali leaching. Furthermore, the rate of expansion reduces for the wrapped 60 °C test series beyond 8 weeks of exposure (Section 3.3.4), i.e. less alkalis are bound in the ASR gel and consequently a higher “driving force” for alkali leaching is maintained.

3.2.7. Influence of binder type

The third somewhat surprising observation is that the rate and amount of alkali leaching is less dependent on the w/c of the CEM I binders than expected (Figs. 4–9), despite the huge differences between the measured relative diffusion coefficients of water (RelDs) (reported in a separate paper [8]). However, generally for both exposure temperatures, no good correlation is found between the RelD and the amount of alkali leaching when comparing CEM I test series with different w/c (Fig. 10). The reason for this is assumed to be that not only “internal” diffusion properties, but also other parameters (e.g. concentration of alkalis in the pore water and “sink capacity”) influence the rate and amount of alkali leaching (discussed further below). Additionally, water (vapour) can move differently than alkalis (that can only diffuse through water-filled pores), i.e. the relative diffusion coefficients measured cannot directly be transferred into diffusion rates of alkalis.

For unwrapped prisms exposed to 38 °C, the “open” binder (w/c of 0.60) and the “basis” binder (w/c of 0.45) exhibit a similar degree of alkali leaching throughout the first year of exposure (Figs. 4–6), though slightly more for the “open” binder when tested in the Norwegian CPT (Fig. 6). The rate of alkali leaching is as expected a little less for the “dense” binder (w/c of 0.30) during the first 6 months of exposure, probably due to the lower rate of diffusion. The lower rate of diffusion is not just due to a more refined pore structure, but also because the limited amount of larger pores (that dominate transport of ions by diffusion) are to a high extent empty in the “dense” binder (which is unsaturated due to self-desiccation). However,

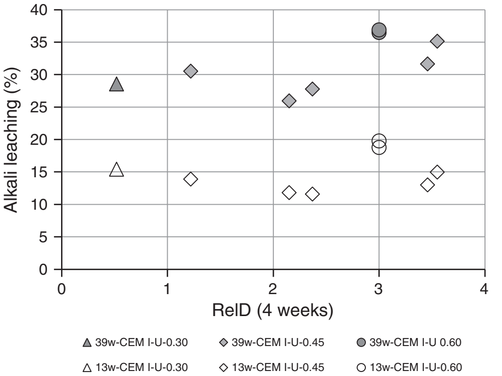

Fig. 10. Relative diffusion coefficient (RelD) vs. alkali leaching at two ages (13 and 39 weeks) for unwrapped test series with the RILEM AAR-4.1 60 °C CPT. See Fig. 2 and Table 5 for abbreviations.

relatively more alkalis are leached out from the "dense" 38 °C test series with time (comment: please note that the measurements of alkali leaching from the Norwegian CPT after 1.5 and about 2 years of exposure (Fig. 6) are uncertain due to a rather low water content in the container). Thus, after two years of exposure the total amount of leached alkalis is higher for the test series with the "dense" binder than for the "basis" binder test series (comment: the "open" binder test series were only exposed for one year). This finding is assumed to primarily be connected to differences in the "driving force" for alkali leaching; the lower w/c ratio and the lower evaporable water content in the prisms with the "dense" binder both lead to higher concentration of alkalis in the pore water [29,30], and thus an enhanced "driving force" for alkali leaching. For example, Rivard et al. [28] measured a considerably higher concentration of alkalis in the pore solution expressed from prism with CEM I cement and w/c of 0.40 (about 800 mmol/l after 4 weeks of exposure to 38 °C) compared with corresponding prisms with w/c of 0.55 (about 400 mmol). Additionally, the lower amount of alkalis leached out from the "dense" binder test series in the first stage of the ASR exposure and the fact that less ASR-gel is produced in the "dense" binder test series due to a lower extent of ASR (see later), contributes to increase the differences in "driving force" between the "dense" binder test series and the CEM I test series with higher w/c and increased expansion. Furthermore, the slightly increased moisture state of the "dense" binder test series during the ASR exposure [8] will contribute to increase the rate of diffusion with time.

For unwrapped prisms exposed to 60 °C, the rate of alkali leaching is significantly higher for the "open" binder compared with the two CEM I binders with lower w/c, which showed comparable alkali leaching throughout the full exposure period (Figs. 7 and 9).

For wrapped prisms (Figs. 7 and 8), the rate of alkali leaching during the first 4 weeks of exposure seems to be independent of the w/c ratio for both exposure temperatures. However, at the end of the exposure, the wrapped test series with the "open" binder showed the least amount of alkali leaching (no significant alkali leaching from 4 to 39 weeks), while the two CEM I binders with lower w/c still revealed a comparable amount of alkali leaching.

The ratio between alkali leaching from the "fly ash" binder (boosted with NaOH to raise the alkali content from 5.0 to 9.0 kg Na_2O_{eq} per m^3 of concrete) and the CEM I binders (with 3.7 kg Na_2O_{eq} alkalis per m^3 of concrete) is rather similar for all the concrete prism tests. After two years of exposure, the total amount of alkali leaching for the "fly ash" test series is in the range of 10–22%, constituting 0.9–2.0 kg Na_2O_{eq} alkalis per m^3 of concrete. As a consequence of the higher alkali content of the "fly ash" binder, the relative alkali leaching ratio between the CEM I test series and the "fly ash" test series "seemingly contradicts" depending on how the results are presented (as a percentage of the total amount or as an absolute measure in kg Na_2O_{eq} alkalis per m^3 of concrete).

3.2.8. Rate of leaching of Na compared with K

The Na/K of the alkalis leached out (K recalculated to Na_{eq}) has been calculated after 4 weeks of exposure and at the end of the exposure period in order to assess the following questions:

1. Is the rate of leaching of Na and K comparable throughout the exposure period?
2. Is there any binder dependency?
3. Is the Na/K the same for various exposure conditions?
4. Does the added Na (when boosting with NaOH) leach out in the same rate as the alkalis in the fly ash cement?

The initial Na/K of the various CEM I binders (based on values analysed by our laboratory by FAAS) was as follows: 1.01 ("open" binder), 1.44 ("basis" binder) and 1.85 ("dense" binder). The corresponding Na/K for the "fly ash" binder was 3.37 including the added alkalis (1.19 excluding the added alkalis). The ratio between the Na/K of the alkalis leached out and the Na/K of the various binders is denoted "leached out vs. binder Na/K ratio". A ratio <1.0 means that relatively less Na than K is leached out compared with the Na/K of the binder. In this comparison, as a simplification it is assumed that all alkalis in the cement minerals are released to the pore water since the degree of hydration is rather high in most binders.

The Na/K of the alkalis leached out is consistent, i.e. for each of the binders the Na/K varies similarly for comparable exposure conditions. However, the Na/K of the alkalis leached out is dependent on binder type, exposure temperature, whether any cotton cloth wrapping is used and on exposure time.

After 4 weeks of exposure to both exposure temperatures, the average "leached out vs. binder Na/K ratio" for unwrapped test series with the "basis" binder and the "dense" binder is in the range of about 0.55 (c.o.v. is in the range of 2.0–2.5% between test series with identical concrete composition and exposure conditions). The interpretation of this is that less Na than K is leached out in the first weeks of exposure. This is somewhat surprising, since the Na ion is considerably smaller than the K ion. However, the Na ion coordinates more water molecules (6) around itself and interacts more strongly with them due to its stronger polarisation power (smaller ion with same charge) compared with the K ion. Thus, a possible explanation of the observed differences in the rate of diffusion between Na ions and K ions is that Na and K "molecules" (that interact with different amounts of water and thus have different "size") are diffusing through the concrete pore water rather than "single" Na and K ions. In free water, the ratio between diffusion of Na^+ compared with K^+ is according to a physics handbook [31] reported to be about 0.70.

For the "open" binder, the "leached out vs. binder Na/K ratio" is about 0.75 after 4 weeks of exposure of the unwrapped prisms. The corresponding value for the "fly ash" binder is about 0.70 (when including the alkalis added to boost the alkali level). If assuming that the alkalis originating from the fly ash cement are leached out with a similar Na/K as the "basis" binder (with equal w/cm), the higher "leached out vs. binder Na/K ratio" for the "fly ash" binder compared with the "basis" binder could be due to the fact that the added alkalis are leached out more quickly compared with the alkalis originating from the fly ash cement. This is to be expected as the added alkalis are immediately soluble whereas a significant portion of the alkalis in fly ash are bound in the glass and are not immediately available to the concrete pore solution.

Corresponding "leached out vs. binder Na/K ratios" for wrapped test series (in the range of 0.65–0.95 after 4 weeks of exposure) are always considerably higher than measured for comparable unwrapped test series (0.55–0.75). The difference is highest for the test series exposed to

60 °C. When the rate of alkali leaching increases (wrapped prisms leach out considerably more alkalis than unwrapped prisms at early age—see above), it thus seems like relatively more Na is leached out compared with the test series with lower rate of alkali leaching. A similar observation is made for the submerged test series with the "basis" binder ("leached out vs. binder Na/K ratios" in the range of 0.70–0.80 after 4 weeks of exposure vs. about 0.55 for comparable unwrapped test series).

Beyond the first months of exposure, considerably more Na compared with K is leached out from the concrete prisms with the "basis" binder and the "dense" binder (valid for both exposure temperatures). Consequently, at the end of the exposure period, the "leached out vs. binder Na/K ratio" is in the range of 0.60–0.90 (vs. about 0.55–0.70 after 4 weeks of exposure). The reason for this could partly be that the larger hydrated Na ions (i.e. 6 water molecules surrounding Na^+ moves with it) need longer time than the smaller K ions with less polarised water to diffuse out of the concrete prisms. Another contributing factor could be connected to binding of alkalis in the ASR gel during the ASR exposure. The composition of the ASR gel was analysed by WDS analyses as part of the SEM analyses (see [26]). The average Na/K (both recalculated to Na_2O_{eq}) of the ASR gel was 0.80 (mean of 97 analyses). Since the Na/K of the "basis" and "dense" binder is considerably higher (1.44 and 1.85, respectively) than the Na/K in the ASR gel, a surplus of Na might occur in the concrete pore water with time. This could again lead to leaching out of more Na ions with time.

A corresponding increase in the Na/K with time is not observed for unwrapped test series with the "open" binder and the "fly ash" binder exposed to 38 °C. Since the Na/K of the "open" binder (1.01) is closer to the mean Na/K of the ASR gel (0.80), this finding supports the theory of a surplus of Na ions with time for the CEM I binders with lower w/c due to alkali binding in the ASR gel (i.e. a considerable less surplus of Na ions will occur for the "open" binder). However, the fact that the Na/K of the "fly ash" binder (included added alkalis) is as high as 3.37, does not support this theory. If so, a surplus of Na ions should have occurred for the "fly ash" binder, and thus enhanced leaching of Na ions with time. On the other hand, only a limited amount of ASR gel is produced in the 38 °C test series with the "fly ash" binder (see later). Furthermore, the pozzolanic reaction itself consumes much of the alkalis added as NaOH to the mix water, reducing the expected surplus of Na ions with time.

Contradictory to the unwrapped test series with the "open" binder and the "fly ash" binder exposed to 38 °C, the Na/K increases 20–30% during the ASR exposure for the unwrapped test series exposed to 60 °C and the wrapped test series exposed to both temperatures. The reason for this contradiction is not clear. One contributing factor can be that the fly ash reaction product (C—(A)—S—H) might be slightly different when exposed to 60 °C compared with exposure to 38 °C [32]. On the other side, the "fly ash" test series exposed to 60 °C expanded considerably more than those exposed to 38 °C, a fact that might support the theory of alkali binding in the ASR gel introduced above.

3.2.9. Influence of other "pre-treatment" conditions

During the 0.5 h submersion period in water after de-moulding (standard procedure for some of the CPTs), 3–4% of the alkalis mixed in the 70 × 70 × 280 mm concrete prisms with the CEM I binder with w/c of 0.45 and 0.60 (constituting up to 0.15 kg Na_2O_{eq} per m^3) leached out to the water, most from the prisms with highest w/c (measured on liquid samples collected from the de-ionised water after submerging selected prisms for 0.5 h). Since this submersion period had little effect on the internal moisture state of the prisms beyond the first weeks of exposure [8], it is recommended to skip this submersion sequence from the ASR testing procedures.

Another "pre-treatment" parameter that has been varied is the length of pre-storage at ambient temperature before exposing the prisms to elevated temperature; 1, 7 or 28 days, respectively (Tables 4–6). For most test series exposed to 38 °C, the pre-storage length did not significantly influence the alkali leaching properties, neither at early age nor later during the exposure period. However, one exception was noticeable: The wrapped AAR-3 test series pre-stored for 28 days at 20 °C (denoted "3.9-W-28d" in Fig. 8) leached out considerably more alkalis after two years of exposure than the corresponding test series exposed to 38 °C directly after de-moulding (denoted "3.8-W-1d"). A corresponding decrease in expansion was also measured (Section 3.3.4).

For test series exposed to 60 °C, no influence on the rate of alkali leaching at early age was observed for the unwrapped prisms when varying the length of pre-storage at ambient temperature. However, pro-longed pre-storage tends to decrease the final amount of alkali leaching from these prisms (about 20% less for test series pre-stored 28 days compared with the one exposed to elevated temperature at age 1 day). This finding is in contrast to the finding for the wrapped AAR-3 prisms. One explanation could be that the moist wrapping applied on the AAR-3 prisms directly after de-moulding immediately contributes to leach out alkalis from the prisms, while the unwrapped AAR-4.1 prisms are less prone to alkali leaching during the pro-longed storage at 20 °C. The latter prisms are thus allowed to become relatively dense before the ASR exposure and the increased alkali leaching attributed "ASR exposure" begins. However, the measured differences in the total amount of alkalis leached long term did not directly influence the expansion of the AAR-4.1 prisms. One reason could be that also the diffusion properties were influenced by the length of pre-storage at ambient temperature. The RelD was considerably reduced when the length of pre-storage was increased (see [8]), thus it contributes to decrease the expansion (due to reduced moisture and ion mobility, slowing down the ASR process) while the decreased alkali leaching does the opposite.

Pre-cooling the prisms before each measurement (of length and mass) should theoretically increase the rate of alkali leaching, see Section 1.3 and [7]. This study confirms this hypothesis. The influence varies depending on test conditions, but the same tendency is observed for all concrete prisms tests (i.e. for wrapped and unwrapped prisms and for both temperatures, see Figs. 6–8 and Tables 4–6); pre-cooling before measuring increase the amount of alkali leaching. The influence is greatest after 4 weeks of exposure (increase of 8–60%) compared with the end of the exposure period (increase of 4–20%). The assumed mechanism is that cooling results in drying which again concentrates alkalis near the surface [33]—making them easier to be washed away.

The special "pre-treatment" given to some test series in order to simulate the curing temperature in a massive concrete structure, i.e. pre-curing for 24 h at 60 °C (Fig. 1 and Tables 4 and 5), did not significantly influence the rate of alkali leaching for the test series later exposed to 38 °C. With respect to total amount of alkali leaching, the test series later exposed to 60 °C performed similarly as the other test series exposed to high temperature directly after de-moulding (i.e. slightly increased alkali leaching compared with longer pre-storage at ambient temperature).

Finally, the extreme exposure condition where the prisms were submersed in de-ionised water from de-moulding in order to maximise the alkali leaching conditions behaved as expected. However, a surprisingly high amount of alkali leaching was measured (probably due to the very high "sink capacity"—see Section 3.2.3), with a slightly higher rate for the test series exposed to the highest exposure temperature (Figs. 7 and 8). At the end of the exposure period, the measured amount of alkali leaching was as high as 80% when exposed to 38 °C and close to 100% when exposed to 60 °C. Consequently these test series exhibited minor levels of expansion (Section 3.3.4).

3.2.10. Modifications trying to reduce the alkali leaching

To try to reduce the amount of alkali leaching, some prisms were wrapped with a cotton cloth saturated with a basic solution of strength pH 14.2 or 13.2 (see Table 3 and the background for the selection of the basic solutions in Section 2.3.1). For the test series with pH 14.2 in the wrapping, about 2.7 g of Na_2O_{eq} alkalis was present in the cotton cloth used to wrap each of the prisms (based on calculations), corresponding to about 50% of the in-mixed alkalis in the CEM I concretes. The measured alkali content in the cotton cloth before wrapping the prisms (measured on "dummy samples"—see procedure in Section 2.4) was practically the same as the calculated value, confirming the consistency of the alkali leaching measurements. For the less alkaline wrapping (pH 13.2), one tenth of the alkali content in the "pH 14.2 wrapping" was present in the cotton cloth, corresponding to only about 5% of the in-mixed alkalis in the CEM I concretes.

During the first 4 weeks of exposure, the alkali content in the "pH 14.2 wrapping" was reduced from about 2.7 g to about 1.3 g (60 °C) and 1.5 g (38 °C). At the end of the exposure, the alkali content in these cotton cloth wrappings was even more reduced (to about 0.5 g and 1.1 g, respectively), while the alkali content in the water in the bottom of each storage container correspondingly increased. The movement of moisture inside each of the polyethylene bags in which each wrapped prism was stored was thus able to gradually dilute the alkali concentration in the cotton cloth wrapping during the ASR exposure, most when exposed to 60 °C. At the end of the exposure of the "pH 14.2 test series", the sum of alkalis measured in the wrapping of the three prisms within each container and in the container reservoir was a little lower than the alkali content added to the wrappings when preparing the test series. This indicates an uptake of alkalis by the concrete prisms from the "pH 14.2 wrapping" during the exposure period, corresponding to about 15% (60 °C) and 20% (38 °C), respectively, of the in-mixed alkali content of the "basis" binder concrete. However, one cannot rule out that even more alkalis have been absorbed by the concrete during the first period of the ASR exposure (despite the amount of liquid in the cotton cloth was moderate—see Table 3), before some alkali leaching has occurred later in the exposure period when the concentration of alkalis in the cotton cloth wrapping was gradually reduced.

A result of the gradually reduced alkali content in the "pH 14.2 cotton cloth wrappings" during the ASR exposure is that the preventing effect (i.e. low "driving force" for alkali leaching) is correspondingly gradually reduced. However, the amount of alkali leaching during the first weeks of exposure has proven to be of greater importance for the final prism expansion than the total amount of alkali leaching (Section 3.3.7). It is thus not surprising that a considerable increased prism expansion is measured for these prisms compared with corresponding test series with de-ionised water in the cotton cloth wrapping, in particular when exposed to 60 °C (Section 3.3.6).

For the "pH 13.2 wrapping", the alkali content in the cotton cloth wrappings increased considerably from start testing up to 4 weeks of exposure. This confirms that the wrapping with the reduced alkali content is not able to prevent alkali leaching from the concrete prisms during the ASR exposure. As discussed in Section 3.3.6, the effect on the prism expansions is also practically insignificant.

3.3. Prism expansion

3.3.1. General

Any change of length in the period from de-moulding to the reference readings (see Fig. 1 and Section 2.3.1), primarily connected to the cement hydration, is discussed separately in Section 3.3.2 (denoted "pre-reference phase"). Of particular importance in this respect is the question; "when to take the reference readings"?

The periodic measurements of length change of the prisms from the reference readings up to exposure time either 39 weeks (60 °C test series), 52 weeks or 112 weeks (38 °C test series) are presented in the Sections 3.3.4–3.3.7. The corresponding mass increase is discussed in a separate paper [8]. That paper also gives details about the various concrete prism tests (Table 3), included recommended critical expansion limits, ranging from 0.030% after 20 weeks of exposure for the 60 °C RILEM AAR-4.1 CPT [34] up to 0.060% after two years of exposure for the 38 °C Norwegian CPT [35].

In order to document if the measured differences in prism expansion are statistically significant, all the expansion results are treated statistically as described in Section 3.3.3.

3.3.2. Length change in the "pre-reference phase"

Length changes in the "pre-reference phase" (i.e. the period from de-moulding to the reference readings) may be in the form of shrinkage or swelling, depending on the composition of the concrete and the surrounding environment. Generally, continued hydration of concrete cured in water leads to minor swelling/expansion due to absorption of water by the cement hydrates [36]. The magnitude on the swelling might be in the order of 0.005% or slightly higher according to Aítcin [37]. On the other hand, if the moisture supply to the hydrating cement paste is insufficient, shrinkage occurs due to withdrawal of water from capillary pores caused by the self-desiccation process. These effects are clearly shown by comparing the sealed prisms (Table 3), giving a net shrinkage of −0.011% during the 6 days of pre-storage at 20 °C after de-moulding, with the prisms stored in de-ionised water during the same period giving an expansion of 0.001%. Both values are for CEM I concrete with w/c ratio of 0.45 ("basis" binder).

Early-age shrinkage of a reversible nature may represent an "error" due to a resulting higher expansion when the prisms are placed in the ASR environment, provided the reference readings are taken after the pre-storage period at ambient temperature. However, if we assume that most of the early phase length changes may be reversible, a net shrinkage in the early phase may represent a "conservative approach", i.e. a phenomenon that is likely to increase the amount of expansion that is attributed to ASR and vice-versa.

The maximum "conservative error" (if we exclude the extreme sealed variant) is 0.006% ("dense" binder: CEM I, w/c of 0.30, Norwegian prism size). Consequently, if we use an acceptance criterion (critical expansion limit) of 0.040%, this maximum "conservative error" constitutes about 15% of the expansion limit (compared with taking the reference readings directly after de-moulding). However, most test series reveal less shrinkage than the "dense" binder test series, which in general reveal the highest shrinkage. The average length change during the 6 days of pre-storage is −0.002% (when excluding the sealed prisms), i.e. insignificant shrinkage, constituting about 5% of a critical expansion limit of 0.040%. We can conclude that the time of the reference readings is of minor importance for the final prisms expansion compared with the huge influence of alkali leaching (Section 3.3.7). Moreover, the time of the reference readings will only influence the conclusion from a performance test if the final expansion is very close to the acceptance criterion.

3.3.3. Statistical treatment of results

In order to evaluate the concrete prism expansion results statistically, arithmetic mean, standard deviation and c.o.v. of all test series were calculated. The multi-specimen c.o.v. for the ASTM C1293 test series ranged between 1 and 12% at 52 weeks, with a mean of 7%, i.e. lower than the reported multi-specimen, within-laboratory c.o.v of 12% [5]. Furthermore, the c.o.v. for the mean expansion of the eight ASTM test series with the "basis" binder (expansion ranging from 0.254 to 0.279%, Fig. 11) was as low as 3.2%, confirming the consistency of the expansion measurements. In order to test the equality of mean expansion for these eight series, one-way ANOVA was performed. The null hypothesis (H_o) was constructed so that all group means assuming equal to each other. With a significance level of $\alpha = 0.05$, the critical f value ($f_{0.05,7,16}$) was computed as 2.6572. The f-value calculated from ANOVA was 0.8871. Given that $f < f_{critical}$ in this level of significance, there is no strong evidence to reject the

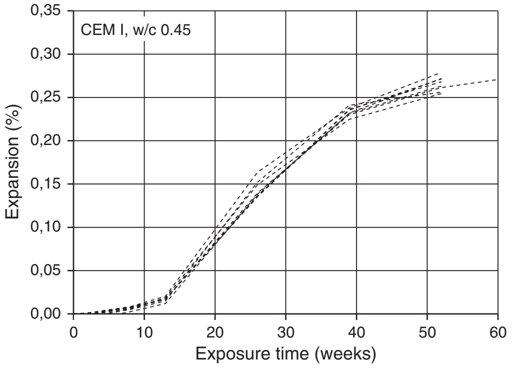

Fig. 11. Expansion versus time for the eight ASTM test series with the "basis" binder (CEM I, w/c 0.45, 3.7 kg Na_2O_{eq} alkalis per m^3 of concrete).

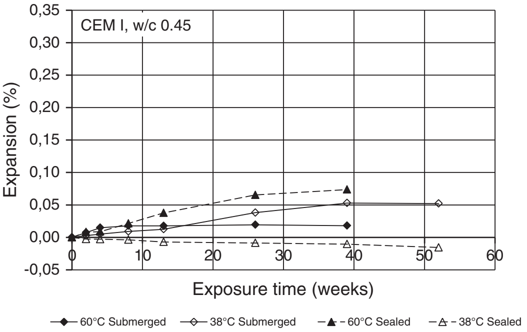

Fig. 12. Expansion versus time for four test series with the "basis" binder (CEM I, w/c 0.45, 3.7 kg Na_2O_{eq} alkalis per m^3 of concrete) given "extreme" exposure conditions.

null hypothesis. In other words, the difference between the mean of the eight test series were found insignificant with a p-value of 0.5384. Thus, the mean of parallel test series (8 different ASTM test groups) may be considered identical. Consequently, the test series prepared from various batches can be compared (see Section 2.1).

Likewise, all the Norwegian concrete prism test series revealed multi-specimen c.o.v. less than 13% at 52 weeks (mean of 6%), while the corresponding c.o.v. was less than 12% for all the 18 RILEM AAR-3 test series (mean of 7%), except one (18%). Based on these results, it can be concluded that the precision (repeatability) of the measurements performed with the three CPTs conducted at 38 °C is good (average multi-specimen c.o.v. was in the range of 6–7%).

For comparison, the repeatability in the round robin testing performed in the PARTNER project [38] with the RILEM AAR-3 method (wrapped prisms) was not as good (mean multi-specimen c.o.v. in the range of 14–21% depending on the final expansion), but was still regarded as satisfactory. The corresponding mean c.o.v. obtained with the RILEM AAR-4.1 Alternative CPT (wrapped prisms) was lower, in the range of 9–16%.

In the present study, the c.o.v. of the different AAR-4.1 test series was calculated after 13, 26 and 39 weeks of exposure, respectively. Except the sealed test series (with higher c.o.v.), all the c.o.v. values were <22% after 13 weeks (mean of 7%), <20% after 26 weeks (mean of 9.5%) and <22% after 39 weeks (mean of 10%). The precision is thus satisfactory, but not as good as that obtained for the CPTs conducted at 38 °C.

Additional statistical analyses, e.g. t-test, ANOVA and f-test, were performed for the evaluation of expansion test results and for the comparison of different test series. The detailed results from these analyses are included in the thesis [26]. In this paper, we only state in the discussion of results whether one test series expand significantly more or less than another.

Furthermore, the statistical analyses showed that the mean of all parallel test series cast in this study was found to be equal to each other at all ages.

3.3.4. "Basis" binder—effect of specimen "pre-treatment", prism size and exposure conditions

As discussed in Section 3.1, Fig. 3 demonstrates the substantial impact on the rate of expansion and the final expansion (ranging from 0.04 to 0.31% within the first year of exposure) of varying specimen "pre-treatment", prism size and exposure conditions. The figure covers all unwrapped and wrapped test series with the "basis" binder stored over water in sealed containers exposed to either 38 °C or 60 °C (comment: documented by pilot measurements to give 100% RH inside the "dummy" storage containers without concrete prisms), except the test series with the most extreme exposure conditions (sealed and submerged storage), the results of which are included in Fig. 12 (see later).

The early age (<13 weeks) rate of expansion for the test series exposed to 60 °C is, as expected, considerably higher than those exposed to 38 °C. At later ages, the opposite is observed, still as expected based on previous experiences. However, for similar exposure temperature, the "pre-treatment" of the concrete prisms highly influence the rate and level of expansion.

The parameter shown to have the highest impact on the final prism expansion, by reducing it, is the use of any moist cotton cloth wrapping. The reduction is dramatic for exposure to 60 °C, but far less pronounced (not statistically significant) for exposure to 38 °C (Fig. 3). The final expansion of unwrapped prisms exposed to 60 °C is up to five times higher than for corresponding wrapped prisms. The increase in expansion for the unwrapped prisms from 13 to 26 weeks is significant (about 0.05%), while the expansion from 26 to 39 weeks is low (0.015–0.025%), giving final expansions in the range of 0.18–0.22%. For all the wrapped prisms exposed to 60 °C, the expansion curves almost flatten out after 8–13 weeks of exposure, giving final expansions in the range of 0.04–0.09%.

When exposed to 38 °C, all the "basis" binder test series still expand after one year of exposure, giving 1 year expansions in the range of 0.17–0.25% for wrapped RILEM AAR-3 prisms (Fig. 3) compared with an average expansion of 0.27% for corresponding unwrapped ASTM prisms (Fig. 11). The effect of wrapping on the expansion at 2 years is less clear (see later).

Another parameter that significantly influences the final prism expansion is the prism size. Generally, increased prism cross-section increases the ASR expansion, on average by about 10% after one year of exposure of the test series with the "basis" binder (Fig. 3). The test series with the 100 × 100 × 450 mm Norwegian prisms continue to expand throughout two years of exposure. The increase from one to about two years is about 0.12%. Corresponding 70 × 70 × 280 mm ASTM prisms practically flatten after about 1.5 years of exposure, resulting in about 40% higher expansion after about 2 years of exposure for the larger Norwegian prisms compared with the smaller ASTM prisms. Note that ASTM C 1293 specifies a prism with a 75 × 75 mm cross section and one might expect slightly smaller differences in expansion between prisms of this size and the 100 × 100 mm Norwegian prisms; however, the differences would still be significant.

The main reason for the remarkable reduced prism expansion when either wrapping the prisms or reducing the prisms cross-section is the considerable high impact these parameters have on the rate and amount of alkali leaching (see Sections 3.2.4 and 3.2.5). In particular the rate and amount of alkali leaching during the first weeks of exposure have shown to be very important for the development of ASR expansion. The effect is most pronounced for test series exposed to 60 °C. Three examples clearly illustrate this finding:

1) The early age alkali leaching is significantly reduced when adding only half of the prescribed water content to the cotton cloth wrapping (Fig. 7), resulting in an increase in the final expansion by more than 60% (shown as the two upper "60 °C Wrapped" curves in Fig. 3; two parallel test series with comparable expansion) compared with the use of the prescribed water content in the cotton cloth;

2) About 50% more alkalis are leached out when removing the polyethylene bag from the wrapped test series exposed to 60 °C (compared with use of the polyethylene bag). This test series reveals the lowest expansion of all the test series shown in Fig. 3;

3) The test series permanently submerged in de-ionised water at 60 °C, that leads to leaching of most of the in-mixed alkalis (Fig. 7 and Section 3.2.9), hardly shows any expansion at all, see Fig. 12. The corresponding test series permanently submerged in de-ionised water at 38 °C, and that reveals about 20% less alkali leaching (Fig. 8 and Section 3.2.9), expands slightly more before the expansion curve flattens (Fig. 12).

Furthermore, for the wrapped 38 °C test series, the final expansion is generally reduced with increasing length of the pre-storage period at 20 °C (1, 7 and 29 days, respectively). In particular, the expansion of the two test series exposed for slightly more than 2 years differs remarkably (Fig. 3). The test series represented with the upper expansion curve was exposed to 38 °C after 1 day, while the test series that expanded less was stored at ambient temperature for 28 days before being exposed to 38 °C. As shown in Fig. 8, considerably more alkalis were leached from the latter test series (denoted "3.9-W-28d") than the one that expanded considerably more (denoted "3.8-W-1d"). It should also be mentioned that the "3.9" test series additionally had slightly lower internal moisture content than the more expansive "3.8" test series (discussed in a separate paper [8]), a fact that might have contributed somewhat to the lower measured final expansion. A similar effect of prolonging the pre-storage up to 28 days is not observed for the unwrapped 60 °C test series (see Section 3.2.9).

The correlation between alkali leaching and prism expansion is further discussed in Section 3.3.7.

Fig. 12 additionally shows the expansion of the two sealed test series. The one stored in the dry 38 °C room reveals a little shrinkage (−0.02%) after one year of exposure. As discussed in a separate paper [8], this test series lost some water during the exposure even though it was sealed. On the other hand, the sealed test series stored at 60 °C did increase slightly in weight due to a minor uptake of water through the sealing of epoxy and aluminium foil. Consequently, the prism started to expand slowly, giving a final expansion slightly higher than the wrapped test series (Fig. 3).

3.3.5. Other binders—effect of exposure temperature, wrapping and prism size

Fig. 13 presents the expansion data for all the test series with the "open" binder (CEM I, w/c of 0.60). In principle, the expansion curves and the internal ranking between the various "open" binder test series are comparable with the "basis" binder test series (Fig. 3 and Section 3.3.4). This is not surprising, since the alkali content is identical in both binders (as discussed in the literature review report [7], the ASR expansion primarily seems to be a function of the alkali content of the concrete and to some extent independent of the cement content), the moisture state is sufficient high in the concrete prisms prepared with both binders [8] and the rate and amount of alkali leaching are similar (Section 3.2.7).

Fig. 14 shows the expansion data for all the test series with the "dense" binder (CEM I, w/c of 0.30). In principle, the expansion curves for the "dense" binder test series exposed to 60 °C are comparable with (i.e. not statistically different from) the corresponding results obtained for the "basis" and "open" binders with higher w/c (Figs. 3 and 13). However, one small deviation observed is that the expansion curve for the wrapped 60 °C test series with the "open" binder (Fig. 13) flattens earlier and has slightly less (statistically lower) final expansion compared with the two CEM I test series with lower w/c (Figs. 3 and 14), even if the amount of alkali leaching is comparable after four weeks of exposure for these wrapped prisms with w/c ratio varying from 0.30 to 0.60.

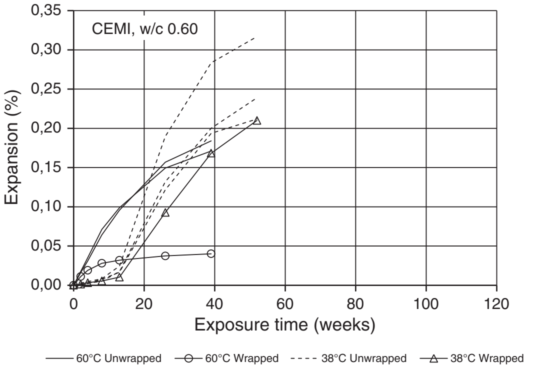

Fig. 13. Expansion versus time for the seven test series with the "open" binder (CEM I, w/c 0.60, 3.7 kg Na_2O_{eq} alkalis per m^3 of concrete).

The rate of expansion as well as the final expansion for the "dense" binder test series exposed to 38 °C is, however, dramatically reduced compared with the CEM I test series with higher w/c (Figs. 3, 13 and 14). Nevertheless, they all still expand beyond the critical expansion limits. The main reason for this reduction is assumed to be less access to water (i.e. considerably lower internal relative humidity (RH) and evaporable water content), together with the substantially lower relative diffusion coefficient (RelD) for the "dense" binder test series compared with the test series with higher w/c (reported in a separate paper [8]). For the 60 °C test series, the reduction in the internal RH and the RelD is less when w/c is lowered to 0.30. Additionally, the increase in internal RH during the ASR exposure (compared with the measured RH, performed at 20 °C after cooling the prisms inside polyethylene foil) will be higher for the 60 °C test series than for the 38 °C test series (discussed in [8]). Thus, a relatively high RH is still obtained internally in the 60 °C test series with the "dense" binder, securing sufficient moisture for the ASR to develop.

Another observation made, is that the wrapped "dense" binder test series exposed to 38 °C expands somewhat more than the corresponding unwrapped test series in the period after 26 weeks of

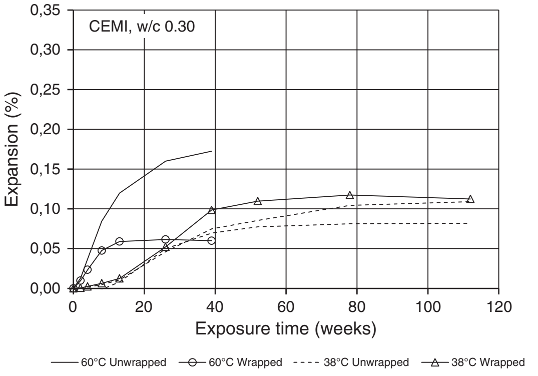

Fig. 14. Expansion versus time for the five test series with the "dense" binder (CEM I, w/c 0.30, 3.7 kg Na_2O_{eq} alkalis per m^3 of concrete).

exposure (Fig. 14), while the opposite was found for the CEM I test series with higher w/c (Figs. 3 and 13). This finding contradicts that the wrapped test series leach out more alkalis in the first period of the ASR exposure. The main reason for this inconsistency is assumed to be that the internal moisture state is slightly higher in the wrapped "dense" binder test series than in the unwrapped prisms (discussed in [8]).

Furthermore, the expansion curves for the 38 °C "dense" binder test series with the Norwegian CPT and the RILEM AAR-3 CPT practically flatten after about 1–1.5 years of exposure (Fig. 14), in contrast to the still expanding "basis" binder test series (Fig. 3). The ASTM test series flatten for both w/c ratios. Increasing alkali leaching with time (Figs. 6 and 8), together with low diffusion coefficient and limited access to water during the ASR exposure (see above) are probably the reasons for these observations.

The "dense" binder test series with the Norwegian CPT still expand more than the test series with the ASTM C-1293 CPT with smaller prism cross-section, primarily due to less alkali leaching throughout the full ASR expansion period. In other words, the effect of the prism cross-section on expansion (see discussion above) is noticeable for all w/c ratios with the CEM I cement, as well as for the "fly ash" binder (see later). The difference in expansion between the two prism sizes, though, seems to increase with increasing w/c. The reason for this is not clear.

The shape of the expansion curves and the internal ranking between the various concrete prism test procedures are comparable for the "fly ash" binder (CEM-II/A-V, w/cm of 0.45, boosted from 5.0 to 9.0 kg/m^3 Na$_2$O$_{eq}$ alkalis—see Fig. 15) and the "dense" binder (Fig. 14), except that the 38 °C "dense" binder test series expand a little more during the first year of exposure before flattening, while the corresponding "fly ash" test series expand more linearly. This analogue behaviour indicates that it is not only the alkali leaching that controls the prism expansion when these two binders are exposed to 38 °C, but the internal moisture state and the diffusion properties also play a role. When exposed to 60 °C, the internal RH is a little higher during the ASR exposure (compared with 38 °C), contributing to the higher measured expansion. One cannot rule out that also other parameters that might influence the development of ASR are slightly different at 60 °C compared with 38 °C. For example might the fly ash reaction product (C—(A)—S—H) be slightly different [32], the rate of reaction of the fly ash compared with the rate of development of ASR might differ [7] and the pore solution chemistry might differ [7]. An example of the latter was recently presented by Matthias Böhm internally at Verein Deutscher Zementwerke (VDZ) (personal communication with Matthias Böhm): Measurements of alkali content of pore water pressed from cement paste (w/cm 0.50) cured at temperatures ranging from 8 to 60 °C up to one year in tight plastic bottles showed that at 60 °C the amount of alkalis released into the pore water from cement paste with 30% fly ash content was about 20% higher than at 40 °C.

The "fly ash" test series exposed for either 1 day or 28 days at ambient temperature prior to ASR exposure show comparable expansions for both temperatures (Fig. 15). There is, however, a tendency that prolonged storage at 20 °C leads to marginally higher expansion during most of the exposure period (only statistically different for the test series exposed to 38 °C), despite the fact that the alkali leaching is a little bit higher.

The effect of binder type and exposure temperature on prism expansion for unwrapped test series with the Norwegian 38 °C CPT and the 60 °C RILEM AAR-4.1 CPT are summarised in Fig. 16. The figure clearly shows that the CEM I binders with w/c ranging from 0.30 to 0.60 expand similarly when exposed to 60 °C (documented to be statistically equal at age 26 and 39 weeks), somewhat more than the "fly ash" binder. Also when exposed to 38 °C, the "fly ash" test series reveal the least expansion during the first 2 years of exposure. This is remarkable taking into account that the in-mixed alkali content is 9.0 kg/m^3 Na$_2$O$_{eq}$ for the "fly ash" binder (after boosting it from the initial 5.0 kg/m^3) compared with only 3.7 kg/m^3 for the other CEM I binders. This finding demonstrates the huge effect on the development on ASR of substituting cement by only about 20% of a class F fly ash. The favourable effect of fly ash with respect to ASR is in accordance with previous findings [1,25] (Comment: Pedersen [39] has previously documented the impact of alkali boosting on the concrete properties (reduced compressive strength). The possible effect of this on the expansion results obtained for the "fly ash" test series is not further evaluated).

3.3.6. Effect of modifications trying to reduce the alkali leaching

As discussed in Section 3.2.10, the use of a cotton cloth wrapping saturated with a basic solution with pH = 14.2 seems to be able to prevent alkali leaching from the concrete prisms, at least in the first period of exposure, while the solution with pH 13.2 has little influence on the rate of alkali leaching. The effect on the prism expansion of these measures is shown in Fig. 17. The effect of wrapping the prisms with cotton cloth saturated with the pH 14.2 solution is remarkable for prisms exposed to 60 °C. During the full exposure period, these wrapped prisms expand about 25% more than the corresponding unwrapped prisms after 26 and 39 weeks of exposure and up to 3.5 times more than the prisms wrapped with de-ionised water. The effect of wetting the cotton cloth with the pH 13.2 solution

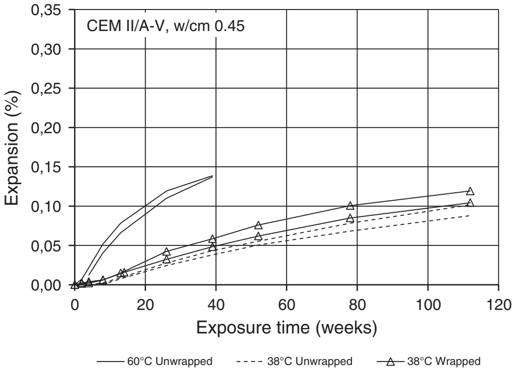

Fig. 15. Expansion versus time for the six test series with the "fly ash" binder (CEM II/A-V, w/cm 0.45, boosted from 5.0 to 9.0 kg Na$_2$O$_{eq}$ alkalis per m^3 of concrete).

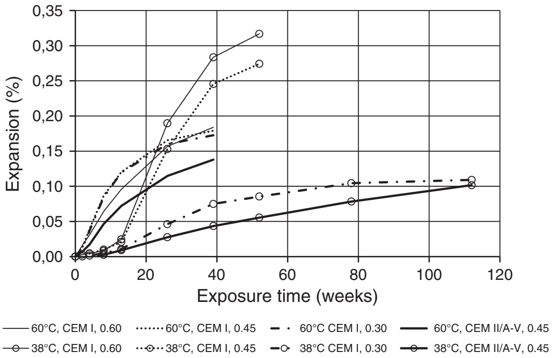

Fig. 16. Expansion versus time for unwrapped test series with four different binders (three CEM I binders with 3.7 kg/m^3 Na$_2$O$_{eq}$ alkalis and one "fly ash" binder with 9.0 kg/m^3 Na$_2$O$_{eq}$ alkalis) exposed to either 38 °C (Norwegian CPT) or 60 °C (AAR-4.1). Except the 60 °C test series with the "fly ash" binder (mean of the two test series in Fig. 15), the test series were pre-stored 7 days at 20 °C before being exposed to elevated temperature.

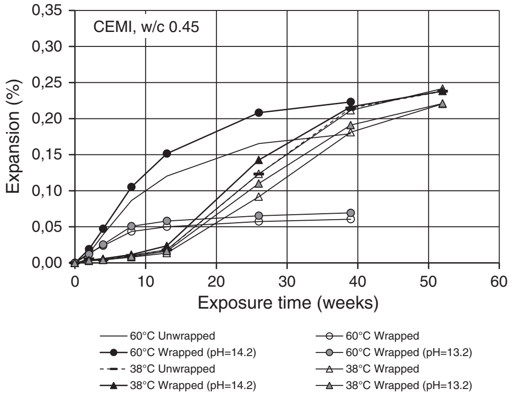

Fig. 17. Expansion versus time for various wrapped AAR-3 and AAR-4.1 test series with the "basis" binder (CEM I, w/c 0.45, 3.7 kg/m^3 Na$_2$O$_{eq}$ alkalis). Either de-ionised water (standard procedure) or a solution with pH 13.2 or 14.2 was added to the cotton cloth wrapping. All the eight test series were pre-stored 7 days at 20 °C before being exposed to elevated temperature.

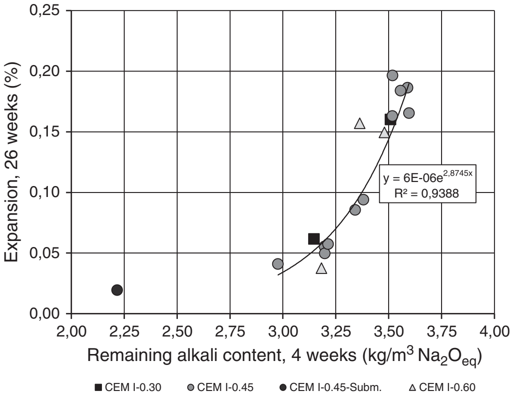

Fig. 18. Remaining alkali content after 4 weeks of exposure versus expansion at 26 weeks for wrapped and unwrapped AAR-4.1 60 °C test series with CEM I binders (w/c of 0.30–0.60, initial alkali content 3.7 kg/m^3 Na$_2$O$_{eq}$). The determination coefficient (R^2) is valid for the test series with the "basis" binder (w/c of 0.45), excl. the submerged test series.

is negligible, i.e. those wrapped prisms exhibit similar expansion as the prisms wrapped with de-ionised water.

For prisms exposed to 38 °C, the effect on the expansion of wrapping the prisms with cotton cloth saturated with the pH 14.2 solution is not statistically significant (but still slightly positive). No effect could be seen when using the pH 13.2 solution. However, the difference between wrapped and unwrapped prisms is generally less pronounced at 38 °C (see Section 3.3.4).

Even if the alkali leaching is prevented (or minimised) when applying the pH 14.2 wrapping, the expansion curve for the 60 °C practically flattens after about 26 weeks of exposure. This could be due to several reasons, in which reduction of the pH in the pore solution is assumed to be the most important one. The pH is reduced partly due to growth of ASR gel that contains alkalis [10]. Furthermore, Fournier et al. [15] found that the solubility of ettringite increases with increasing exposure temperature, leading to an increase in the concentration of sulphate ions in the pore water and a corresponding decrease in the concentration of OH$^-$ ions to maintain electroneutrality. Consequently, pH is reduced with time when exposed to 60 °C. Another influencing factor could be connected to the ASR gel itself. After many ASR cracks have been induced in the concrete prisms, much gel must be produced to fill up and increase the width of these cracks. Thus, the rate of expansion might decrease due to "lack of" ASR gel. Additionally, Bokern [16] showed that the ASR gel is less viscous when the exposure temperature and the water content increase, which is the case for the 60 °C prisms. This contributes to reduce the "expanding force" and increase the mobility of the ASR gel.

3.3.7. Correlation between alkali leaching and prism expansion

As discussed previously, alkali leaching has a very significant impact on the expansion of the CEM I concretes with an initial alkali content of 3.7 kg Na$_2$O$_{eq}$. For the test series exposed to 60 °C, with sufficient moisture content for ASR to develop and generally a higher relative diffusion coefficient than the 38 °C test series [8], the amount of alkali leaching is totally controlling the prism expansion. In particular, the rate of alkali leaching in the first weeks of exposure is of high importance as shown in Fig. 18 in which the remaining alkali content after 4 weeks of exposure is plotted against the expansion after 26 weeks. (Comment: The reason for plotting the remaining alkali content after 4 weeks of exposure is the fact that the alkali leaching from the wrapped test series is only measured at this age and in the end of the exposure—see Section 2.4). For the "basis" binder (w/c of 0.45), the determination coefficient R^2 for the trend line is 0.94, (excluding the submerged test series where, after just 4 weeks, rapid leaching results in the alkali content of the concrete being reduced to a value below the "alkali threshold" for the aggregate combination used). The impact on expansion of the early-age alkali leaching is similar also for the "open" binder (w/c of 0.60) and the "dense" binder (w/c of 0.30) (Fig. 18).

One important reason for the very high impact of the early-age alkali leaching is that the alkali content of the concrete was deliberately selected such that small changes in alkali would have a significant impact on the expansion. This was done by considering the relationship between long-term expansion and alkali content for the reference test series, and selecting an alkali content that lay on the steep, ascending part of the s-shaped curve. Thus, the loss of alkalis at early age has a considerable impact in terms of reduced expansion. If the CEM I concretes had contained a surplus of alkalis (i.e. lying on the plateau of the "expansion versus alkali level curve", instead of the steep part—see Section 2.2), it is expected that alkali leaching would have a much lower impact on expansion. This is probably the reason for the contradictory findings in the RILEM round robin testing with the AAR-4 CPT (unwrapped prisms) and the AAR-4 Alternative CPT (wrapped prisms). The round robin testing program, using various aggregates and a binder with CEM I cement and about 5.5 kg Na$_2$O$_{eq.}$ of alkalis, concluded that the two alternative 60 °C aggregate test methods produced comparable expansions [40]. This conclusion is clearly in conflict with the observations from the present study.

The correlation between the total amount of alkali leaching and the final expansion is not particularly good for the prisms exposed to 60 °C, most likely because most of the expansion has occurred already after 13–26 weeks of exposure. Furthermore, the prisms revealing the highest rate of alkali leaching show little expansion beyond 8 weeks of exposure.

The early age alkali leaching is also of high importance for the 38 °C test series, even though the determination coefficient for the trend line for the "basis" binder test series in Fig. 19 ($R^2 = 0.77$) is not as good as that found for the 60 °C test series (Fig. 18). The impact on expansion of alkali leaching is similar also for the "open" binder test series exposed to 38 °C (Fig. 19). In contrast, the "dense" binder (w/c of 0.30) test series do not fit into the same picture. The reason is most likely that the internal moisture state and the diffusion properties also influence expansion, as discussed previously.

Generally, the determination coefficient (R^2) for the trend line between the total amount of alkali leaching and the final expansion is not particularly good for the prisms exposed to 38 °C. However, the

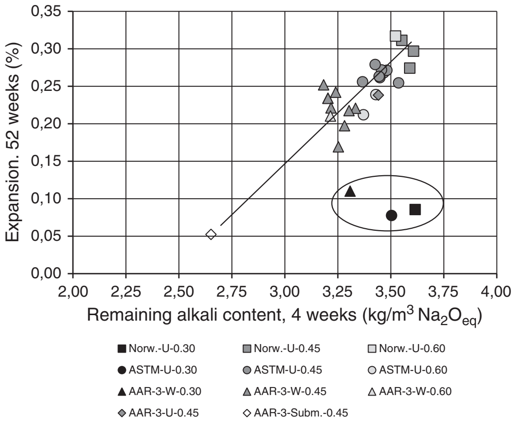

Fig. 19. Remaining alkali content after 4 weeks of exposure versus expansion at 52 weeks for wrapped (W) and unwrapped (U) 38 °C test series with CEM I binders (w/c of 0.30–0.60, initial alkali content 3.7 kg/m^3 Na$_2$O$_{eq}$). The determination coefficient (R^2) for the trend line for the "basis" binder test series is 0.77.

tendency is that factors that reduce the amount of alkali leaching throughout the expansion period increase the final expansion for the CEM I test series with w/c of 0.45 and 0.60. Two examples illustrating this fact are the positive effect of increased prism cross-section and the different expansion obtained between AAR-3 prisms pre-stored 1 day compared with 28 days at ambient temperature (see Section 3.3.4).

With respect to performance testing, where alkali contents close to the "alkali threshold" normally are used in the concrete mixes, the impact of alkali leaching is regarded to be high. Additionally, the exposure period is normally extended compared with pure aggregate testing. Thus, the total amount of alkali leaching might have even greater influence than found in the present study. Consequently, to be able to mirror what will happen in a real concrete structure with minor or no alkali leaching, minimisation of the rate and amount of alkali leaching during laboratory performance testing is crucial.

3.4. Visual inspection and microstructural analysis

3.4.1. Visual inspection

The visual inspections performed on one prism from all series after ending the ASR exposure confirmed the expansion measurements, i.e. those prisms that obtained high expansions also showed the highest extent of surface cracking and internal gel exudation in cracks and pores. The amount of surface precipitation (assumed to primarily be calcium carbonate resulting from the carbonation of portlandite leached from the concrete) varied dependent on exposure temperature and use of any wrapping. The extent of precipitation was generally higher for unwrapped prisms exposed to 60 °C compared with corresponding prisms exposed to 38 °C. Hardly any precipitation was visible on the surface of the wrapped prisms after unwrapping them, indicating that any precipitation was absorbed by the cotton cloth.

3.4.2. Plane polished section analysis

3.4.2.1. Internal cracking. The analyses of the 16 fluorescence impregnated plane polished sections (Section 2.5.2) confirmed the results from the expansion measurements as well as the alkali leaching measurements. A huge spread in the extent of internal cracking was observed both internally within most of the prisms and between prisms from various test series. One example of the internal variation of crack intensity is presented in Fig. 20, showing a UV-photo of a prism from a 60 °C test series with the "open" binder (CEM I, w/c 0.60). The extent of cracking is very low in the bottom part (0–30 mm) and the upper part (80–100 mm) of the prism, while the medium section is more heavily cracked. The main reason for the lower crack intensity in the lower and upper part of the prism is assumed to be higher amount of alkali leaching in these areas. After 39-weeks, a total of 37% of the in-mixed alkalis leached out during the ASR exposure (Section 3.2.5). This finding is valid for most prisms, except those prisms which showed the least amount of alkali leaching. An example of the latter is presented in Fig. 21, showing the lower part of a Norwegian prism with the "basis" binder. In total about 20% of the in-mixed alkalis leached out during the 112 weeks of ASR exposure. In this prism, the cracks seem to be rather homogenously distributed in the prism.

Corresponding results for the 14 remaining polished sections are presented in the PhD thesis [26] and in a paper presented at the 14th ICAAR in 2012 [27].

3.4.2.2. Measurement of "cracking intensity" by image analysis. At the 14th ICAAR, Lindgård et al. [27] presented a method where image analysis was used to quantify the "cracking intensity" in the concrete prisms, expressed as area-% occupied by cracks in each image (covering the whole prisms). During the transformation of the pictures of the fluorescence impregnated polished sections taken in UV-light to the images analysed, any air voids were removed (if not, these air voids filled with the fluorescence liquid will be miscounted as part of the cracking area). To measure any spread in internal "cracking intensity" over the prisms, each image was divided in crosswise slices of height 25 mm (from the bottom to the top of each prism) or alternatively lengthwise slices of width 14 mm (12.5 mm in the larger Norwegian prisms). The area-% occupied by cracks in each slice was analysed, before the values were normalised to the total area-%.

The measurements of "cracking intensity" over the prism height confirm the findings discussed in Section 3.4.2.1; the upper 25 mm of the prisms exhibited least cracking for most test series, followed by the lower 25 mm of the prisms. Furthermore, in most cases the slices located 25–50 mm from the top of the prisms obtained less cracking than the slices located in correspondent distance from the bottom of the prisms. For some samples with a high amount of alkali

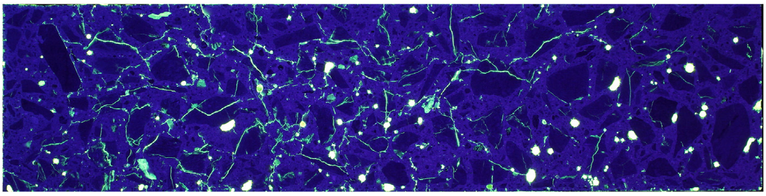

Fig. 20. Photo in UV-light of the plane polished section prepared from a prism from test series "4.3-U-A-0.60-I" (see Table 5) with expansion 0.18%. The bottom of the prism is to the left. Length 280 mm.

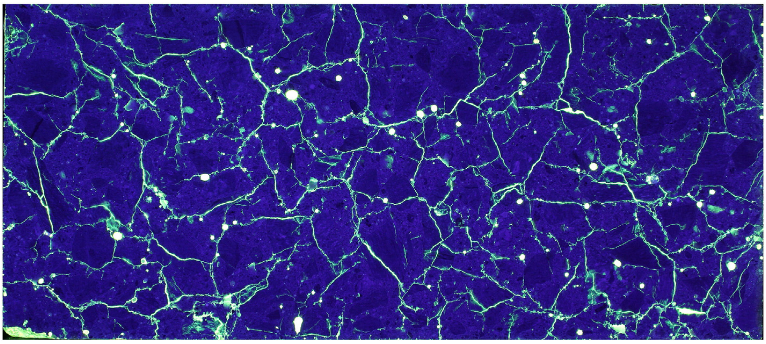

Fig. 21. Photo in UV-light of the plane polished section prepared from the lower part of a prism from test series "N.1-U-0.45" (see Table 6) with expansion 0.43%. The bottom of the prism is to the left. Length 225 mm.

leaching (e.g. the prism shown in Fig. 20), a larger area of the upper half of the prism had very low "cracking intensity" compared with the mid part, which undoubtedly revealed the highest "cracking intensity" [27].

Also the measurements of "cracking intensity" over the width of the prisms show a "cracking gradient"; the cracking was somewhat less in the outer 10–15 mm of most prisms compared with the interior of the prisms [27]. This indicates that less ASR is taking place in this outer layer, probably due to a higher amount of alkali leaching.

The results from the measurements of total "cracking intensity" (area-%) of all the 16 plane polished sections are presented in Fig. 22. In this figure, the cracking intensities, ranging from about 0.3 to 6.7 area-%, are plotted against the measured prism expansions. A very good linear correlation is found ($R^2 = 0.89$), even though four different binder qualities were used (Table 2), giving concretes with 28 days compressive strength ranging from 44 to 103 MPa. The aggregate composition was, however, identical in all test series. The good correlation found indicates that the cracks developed due to ASR lead to a corresponding increase in the prism expansion. Or conversely, if a prism expands during the ASR exposure, you will find a corresponding internal crack pattern in the prism.

Furthermore, the promising results indicate that the accuracy of the image analysing technique is sufficiently good to use the method as a tool to analyse the degree of ASR damage in larger concrete samples, at least for post-documentation of the internal cracking in laboratory exposed samples, but probably also for drilled cores taken from real structures. Rivard and Ballivy [41] have also previously found a relatively good correlation between the measured expansion caused by ASR on laboratory concrete prisms and the damage to concrete, as quantified by the Damage Rating Index (DRI) on polished sections prepared from these prisms. If various aggregate types are included in the same diagram, the correlation between prism expansion and internal cracking is assumed to be somewhat poorer (e.g. as is the case for the measurements performed by Rivard and Ballivy [41]).

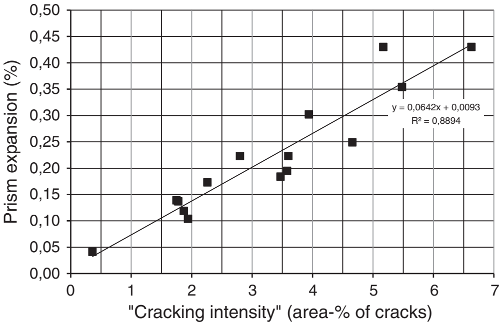

Fig. 22. Total "cracking intensity" (area-%) in the 16 plane polished sections plotted against the corresponding prism expansions.

The thin section and SEM analyses confirmed that ASR was the cause of expansion of the prisms. Further results from these analyses are included in the PhD thesis [26] and the ICAAR 2012 paper [27].

4. Conclusions and recommendations

4.1. Main findings

Based on the comprehensive laboratory study, including 58 test series with modified versions of five concrete prisms tests (CPTs), the following conclusions can be drawn:

- The rate of alkali leaching during the first weeks of exposure is the parameter shown to have highest impact on the prism expansion.
- A modified wrapping procedure developed (cotton cloth added alkalis) might be a promising tool to reduce the amount of alkali leaching during accelerated laboratory testing. Increasing the prism cross-section also decreases the rate and amount of alkali leaching considerably.
- The results clearly show that the amount of alkali leaching and the prism expansion is significantly influenced by the specimen "pre-treatment", "ASR exposure conditions" and prism cross-section. Most test conditions are by no means extreme, but represent test procedures used in various "commercial" CPTs. The extent of the impact depends on the concrete quality, i.e. w/cm and cement type. Consequently, the conclusion from a concrete performance test will differ depending on the test procedure used.
- Generally, a very substantial proportion of the in-mixed alkalis was leached out of the concrete prisms during the ASR exposure; 3–20% during the first 4 weeks of exposure and 10–50% at the end of the exposure of the CEM I test series (w/c of 0.30–0.60) with an initial alkali content 3.7 kg Na_2O_{eq} per m^3 of concrete. For the test series submerged in de-ionised water, a substantial higher portion of alkalis was leached out of the concrete during exposure.
- A very good correlation is found between the amount of alkali leaching during the first 4 weeks and the final prism expansion, in particular for the test series exposed to 60 °C. At this exposure temperature, the rate and amount of alkali leaching is the main controlling factor for the prism expansion. Consequently, to be able to mirror what will happen in a real concrete structure with minor or no alkali leaching, minimisation of the rate and amount of alkali leaching during accelerated laboratory performance testing is crucial.

- In principle, the expansion curves and the internal ranking between the various "open" binder test series (CEM I, w/c of 0.60) are comparable with the "basis" binder test series (CEM I, w/c of 0.45) with equal alkali content. This is valid for both exposure temperatures.
- For less permeable concretes (i.e. the "dense" binder (CEM I, w/c of 0.30) and the "fly ash" binder (CEM II/A-V, w/cm of 0.45)) exposed to 38 °C, it is not only the alkali leaching that controls the prism expansion, but the internal moisture state and the diffusion properties also play a role [8]. Thus, the two exposure temperatures produce different expansions. When exposed to 60 °C, the internal RH is a little higher during the ASR exposure, contributing to the higher measured expansion (compared with 38 °C). In a follow-up project [26], the field behaviour of some of these test series will be evaluated: one main aim is to assess which test procedure is best able to foresee the field behaviour of various concrete mixtures.

4.2. Effect of varying the specimen "pre-treatment"

With respect to variations in the specimen "pre-treatment", the main findings are:

- During the 0.5 h submersion period in water after de-moulding (standard procedure for some of the CPTs), 3–4% of the alkalis mixed in the concrete prisms leached out into the water. Since this submersion period had little effect on the internal moisture state of the prisms beyond the first weeks of exposure, it is recommended to eliminate this submersion sequence from the ASR testing procedures.
- Wrapping of concrete prisms by use of moist cotton cloths and plastic sheets caused leaching of considerable quantities of alkalis during the first 4 weeks, significantly more than measured for the unwrapped prisms. The result was a dramatic reduction of the prisms expansion for the wrapped test series exposed to 60 °C, while the effect was far less pronounced (not statistically significant) for the wrapped test series exposed to 38 °C. "Traditional" wrapping of concrete prisms with a damp cotton cloth, applied in some test methods primarily with the aim to secure a high moisture content surrounding the prisms, is thus not recommended. (Comment: This advice is already adopted by RILEM TC 219-ACS based on this study; the Alternative wrapped version of the AAR-4.1 CPT (60 °C) is no longer recommended, and the revised version of the RILEM AAR-3 CPT (38 °C) use unwrapped prisms similar as the ASTM C 1293 CPT).
- The wrapping procedure is also of high importance for the amount of alkali leaching, in particular for test series exposed to 60 °C. Less water added to the cotton cloth significantly reduced the early age alkali leaching and correspondingly increased the expansion. Opposite, removal of the polyethylene bag increased the alkali leaching and reduced the expansion.
- To try to reduce the amount of alkali leaching, some prisms were wrapped with a cotton cloth saturated with a basic solution of either pH = 14.2 or 13.2. For both exposure temperatures, the measurements indicates a small uptake of alkalis by the concrete prisms from the "pH 14.2 wrapping" during the exposure period, corresponding to about 15% (60 °C) and 20% (38 °C), respectively, of the in-mixed alkali content of the "basis" binder concrete. During the full exposure period, the wrapped prisms exposed to 60 °C consequently expanded about 25% more than the corresponding unwrapped prisms after 26 and 39 weeks of exposure and up to 3.5 times more than the prisms wrapped with de-ionised water. This "modified wrapping procedure" might thus be a promising tool to reduce the amount of alkali leaching during accelerated laboratory testing (will be followed up [26]).
- The less alkaline wrapping (pH 13.2) was not able to significantly prevent alkali leaching from the concrete prisms during the ASR exposure. Consequently, the effect on the prism expansions was practically negligible.
- With a few exceptions, neither the pre-storage length at ambient temperature nor the "simulated field curing" did significantly influence the alkali leaching properties of the test series exposed to 38 °C, neither at early age nor later during the exposure period. Likewise for the test series exposed to 60 °C, no general influence on the rate of alkali leaching at early age was observed when varying the length of pre-storage at ambient temperature. However, pro-longed pre-storage tends to somewhat decrease the final amount of alkali leaching from unwrapped prisms. However, none of these small differences in amount of alkali leaching directly influenced the expansion of the AAR-4.1 prisms.

4.3. Effect of varying the exposure conditions

With respect to variations in the "exposure conditions", the main findings are:

- In general, elevating the exposure temperature from 38 °C to 60 °C does not influence the amount of alkali leaching during the first 4 weeks, neither for wrapped nor for unwrapped prisms. Furthermore, throughout the full exposure period, the rate and amount of alkali leaching from the unwrapped AAR-4.1 prisms (60 °C) and the unwrapped ASTM prisms (38 °C) are comparable for almost all corresponding test series, even though the relative diffusion coefficient is considerably increased with increasing temperature. The main reason for this is assumed to be that the "sink capacity" is the limiting factor, not the rate of diffusion.
- In contrast, the temperature dependency for the alkali leaching is more evident (and more as expected) for wrapped prisms in the period beyond 4 weeks of exposure; those exposed to 60 °C have a considerably higher rate of alkali leaching compared with those exposed 38 °C, probably due to higher "sink capacity" for wrapped prisms (compared with unwrapped prisms) and thus more influence of differences in diffusion properties.
- For all binders, increasing the prism size cross-section from 70 × 70 mm (RILEM size) to 100 × 100 mm (Norwegian size) decreases the rate and amount of alkali leaching considerably. For many test series, the amount of alkali leaching is practically halved. As a result of this, the final expansion increases substantially. An obvious consequence of this finding is that one effective measure to reduce the amount of alkali leaching during performance testing is to increase the prism cross-section.
- Pre-cooling the prisms before every periodic reading of length and mass increases the amount of alkali leaching. The assumed mechanism is that cooling results in drying which again concentrates alkalis near the surface—making them easier to be washed away. However, no significant differences in expansion were found between pre-cooled test series and corresponding test series measured "warm".
- For the Norwegian CPT and the ASTM C 1293 CPT, both using an absorbing lining inside the storage containers in order to maintain a high humidity, 25 to 30% of the total amounts of alkalis leached out from the concrete prisms have on average been absorbed by the lining (same type of cotton cloth) during the exposure period. The remaining alkalis were found in the water in the bottom of the containers. Thus, it is important to measure all alkalis that have leached out from the concrete prisms.

4.4. Influence of binder composition on alkali leaching

The binder composition, i.e. cement type and w/cm, have different effects on alkali leaching and prism expansion. Thus, the summary part is split into two sub-sections (Sections 4.4 and 4.5). With respect to the influence of binder composition on alkali leaching, the main findings are:

- At both exposure temperatures, the rate and amount of alkali leaching are less dependent on the w/c of the CEM I binders than expected, despite the huge differences between the measured relative diffusion coefficients of water vapour (RelD). This demonstrates that not only diffusion properties, but also other parameters, for example concentration of alkalis in the pore water and "sink capacity", influence the rate and amount of alkali leaching.

- For unwrapped prisms exposed to 38 °C, the rate of alkali leaching is as expected a little less during the first 6 months of exposure of test series with the "dense" binder (CEM I, w/c of 0.30) compared with corresponding test series with higher w/c (0.45 and 0.60), probably due to the lower rate of diffusion. However, relatively more alkalis are leached out from the "dense" 38 °C test series with time, assumed to primarily be caused by higher concentration of alkalis in the pore water and thus a higher "driving force" for alkali leaching.
- For unwrapped prisms exposed to 60 °C, the rate of alkali leaching is significantly higher for the "open" binder compared with the two CEM I binders with lower w/c, which exhibit comparable alkali leaching throughout the full exposure period.
- For wrapped prisms, the rate of alkali leaching the first 4 weeks of exposure seems to be independent of the w/c for both exposure temperatures.
- As a consequence of the higher alkali content of the "fly ash" binder (9.0 kg Na_2O_{eq} per m^3 of concrete, after boosting it from the initial 5.0 kg/m^3), the relative alkali leaching ratio between the CEM I test series (3.7 kg Na_2O_{eq} per m^3 of concrete) and the "fly ash" test series depends on how the results are presented. In absolute terms (e.g. in kg/m^3 of alkalis) more alkalis are leached from the "fly ash" test series. However, when expressed as a proportion of the initial alkali content, the alkali leaching for the "fly ash" test series is considerably less than that for the CEM I test series.
- The ratio between alkali leaching from the "fly ash" binder and the CEM I binders is similar for all the concrete prism tests.

4.5. Influence of binder composition on prism expansion

With respect to the influence of binder composition (cement type and w/cm) on prism expansion, the main findings are:

- At both temperatures, corresponding test series with the "basis" binder and the "open" binder show comparable expansion (see Section 4.1).
- Similarly, the expansion curves for the "dense" binder test series (w/c of 0.30) exposed to 60 °C are comparable with the corresponding results obtained at higher w/c. Furthermore, the "fly ash" binder test series expand almost as much as the CEM I test series at this exposure temperature, in contrast to what is observed at 38 °C. One assumed reason for this behaviour is that a higher internal RH is obtained for these less permeable concretes when exposed to 60 °C compared with 38 °C (see [8]). One cannot rule out that also other parameters that might influence the development of ASR are slightly different at 60 °C compared with 38 °C, e.g. the properties of the fly ash reaction product and the pore solution chemistry (see Section 3.3.5).
- When exposed to 38 °C, the rate of expansion and the final expansion for the less permeable test series with the "dense" binder and the "fly ash" binder are dramatically reduced relative to 60 °C and compared with the CEM I test series with higher w/c exposed to 38 °C. This behaviour indicates that it is not only the alkalinity of the pore solution and the alkali leaching that controls the prism expansion when exposing these less permeable binders to 38 °C, but also the internal moisture state and the diffusion properties (see [8]). To avoid any "false negative results" during accelerated performance testing, a fixed w/cm of 0.50 could be used (assumed to be conservative) until more research possibly documents that a lower (and more realistic) w/cm is safe to use; i.e. without resulting in a possible lower moisture state in the laboratory prisms compared with real concrete structures exposed to very high humidity.
- Another observation supporting the "lack of moisture theory" is that the wrapped "dense" binder test series exposed to 38 °C expands a little more than the corresponding unwrapped test series in the period after 26 weeks of exposure, the opposite to what was found for the CEM I test series with higher w/c. This finding contradicts the observation that the wrapped test series results in more alkalis being leached out during the first period of the ASR exposure. The main reason for this inconsistency is assumed to be that the internal moisture state is slightly higher in the wrapped "dense" binder test series than in the unwrapped prisms (see [8]).
- The "fly ash" test series exposed to either 1 day or 28 days at ambient temperature prior to ASR exposure produce comparable expansions at both exposure temperatures.
- When exposed to 60 °C, the CEM I binders expand a little more than the "fly ash" binder. Also when exposed to 38 °C, the "fly ash" test series exhibit the least expansion after 2 years of exposure. This is remarkable taking into account that the in-mixed alkali content is 9.0 kg/m^3 Na_2O_{eq} for the "fly ash" binder (after boosting it from the initial 5.0 kg/m^3) compared with only 3.7 kg/m^3 for the other CEM I binders. However, this finding is as expected and demonstrates the favourable effect on the development on ASR of substituting cement by only about 20% of class F fly ash.

4.6. Complementary testing

The main conclusions from the complementary testing are:

- Measurement of alkali release from the aggregates indicated that only a minor (insignificant) amount of alkalis would be released from the aggregates under the conditions of the tests (further discussed in [26]).
- A new method for the measurement of "cracking intensity" (given as area-% of cracks in an impregnated polished section) based on image analysis has been developed. This method has been used successfully to compare the extent of cracking due to ASR in concretes, both internally within one plane polished section and between different test series.
- The image analyses of the 16 fluorescence impregnated plane polished sections confirm the results from the alkali leaching measurements. The main reason for the lower crack intensity in the outer/upper/lower parts of the prisms compared with the interior is assumed to be the higher amount of alkali leaching in these areas of the prisms.
- A very good linear correlation is found between "cracking intensity" and prism expansion ($R^2 = 0.89$), and this seems valid for all strength levels tested. This implies that the image analysing technique is sufficiently good to use the method as a tool to analyse the degree of ASR damage in larger concrete samples, at least for post-documentation of the internal cracking in laboratory exposed samples.

4.7. Some recommendations

Collectively, the data presented in this study indicate that the major shortcoming of the various concrete prisms tests is the loss of alkalis from the concrete during exposure. Consequently, the overriding recommendation to RILEM and those involved in the development of performance tests for evaluating the ASR potential of "job mixes" is to develop test procedures that limit, compensate for or, preferably, eliminate alkali leaching during testing. Further details on improvements in test procedures are given in the thesis [26] and in the literature paper [7].

Acknowledgement

The authors would also like to acknowledge COIN, the COncrete INnovation centre (www.coinweb.no) and Norcem (part of Heidelberg) for the financial support to the PhD study of the principal author. Furthermore, the comprehensive and accurate work performed at the laboratory staff at SINTEF is greatly appreciated.

References

[1] M.D.A. Thomas, The effect of supplementary cementing materials on alkali–silica reaction: a review, Cem. Concr. Res. 41 (2011) 1224–1231.
[2] T. Chappex, K. Scrivener, Controlling alkali silica reaction by understanding the contribution of aluminium provided by supplementary cementitious materials, in: T. Drimalas, J.H. Ideker, B. Fournier (Eds.), 14th International Conference on Alkali–Aggregate Reactions in concrete, Austin, Texas, 2012.
[3] M. Thomas, B. Fournier, K. Folliard, J. Ideker, M. Shehata, Test methods for evaluating preventive measures for controlling expansion due to alkali–silica reaction in concrete, Cem. Concr. Res. 36 (2006) 1842–1856.
[4] CSA, CSA A23.2-14A-00, Potential expansivity of aggregates (procedure for length change due to alkali–aggregate reaction in concrete prisms at 38 °C), Methods of Testing for Concrete, Canadian Standards Association, Mississauga, Ontario, Canada, 2004, pp. 246–256.
[5] ASTM C1293—08b Standard Test Method for Determination of Length Change of Concrete Due to Alkali–Silica Reaction, Annual Book of ASTM Standards, American Society for Testing and Materials, 2008, p. 7.
[6] J. Lindgård, Ö. Andiç-Çakır, I. Borchers, M.T.A.M. Broekmans, E. Brouard, I. Fernandes, C. Giebson, B. Pedersen, C. Pierre, T.F. Rønning, M.D.A. Thomas, B.J. Wigum, RILEM TC219-ACS-P: Literature Survey on Performance Testing, COIN project report, 27, ISBN: 978-82-536-1209-6, 2011, p. 164.
[7] J. Lindgård, Ö. Andiç-Çakır, I. Fernandes, T.F. Rønning, M.D.A. Thomas, Alkali–silica reactions (ASR): literature review on parameters influencing laboratory performance testing, Cem. Concr. Res. 42 (2012) 223–243.
[8] J. Lindgård, E.J. Sellevold, M.D.A. Thomas, B. Pedersen, H. Justnes, T.F. Rønning, Alkali–silica reactions (ASR)—performance testing: influence of specimen pre-treatment, exposure conditions and prism size on concrete porosity, moisture state and transport properties, Cem. Concr. Res. 53 (2013) 145–167.
[9] R.F. Blanks, H.S. Meissner, The expansion test as a measure of alkali–aggregate reaction, J. Am. Concr. Inst. 17 (1946) 517–539.
[10] P. Rivard, M.-A. Bérubé, J.-P. Ollivier, G. Ballivy, Alkali mass balance during the accelerated concrete prism test for alkali–aggregate reactivity, Cem. Concr. Res. 33 (2003) 1147–1153.
[11] R.F.M. Bakker, The influence of test specimen dimensions on the expansion of alkali reactive aggregate in concrete, in: G.M. Idorn, S. Rostam (Eds.), 6th International Conference on Alkali–Aggregate Reaction in Concrete, Denmark, 1983, pp. 369–375.
[12] C.A. Rogers, R.D. Hooton, Reduction in mortar and concrete expansion with reactive aggregates due to alkali leaching, Cem. Concr. Aggregates 13 (1991) 42–49.
[13] M.-A. Bérubé, B. Fournier, Canadian experience with testing for alkali–aggregate reactivity in concrete, Cem. Concr. Compos. 15 (1993) 27–47.
[14] M.-A. Bérubé, D. Chouinard, L. Boisvert, J. Frenette, M. Pigeon, Influence of wetting–drying and freezing–thawing cycles and effectiveness of sealers on ASR, in: A. Shayan (Ed.), 10th International Conference on Alkali–Aggregate Reaction in Concrete, Australia, 1996, pp. 1056–1063.
[15] B. Fournier, R. Chevrier, M. DeGrosbois, R. Lisella, K. Folliard, J. Ideker, M. Shehata, M. Thomas, S. Baxter, The accelerated concrete prism test (60 °C): variability of the test method and proposed expansion limits, in: M. Tang, M. Deng (Eds.), 12th International Conference on Alkali–Aggregate reaction in Concrete, International Academic Publishers—World Publishing Corporation, Beijing, China, 2004, pp. 314–323.
[16] J. Bokern, Concrete tests for ASR assessment: effects of testing environment on preconditions for an ASR and transferability of test results, in: M.A.T.M. Broekmans, B.J. Wigum (Eds.), 13th International Conference on Alkali–Aggregate Reactions in Concrete, Trondheim, Norway, 2008, pp. 511–520.
[17] P. Rivard, M.-A. Bérubé, J.-P. Ollivier, G. Ballivy, Decrease of pore solution alkalinity in concrete tested for alkali–silica reaction, Mater. Struct. 40 (2007) 909–921.
[18] K. Schmidt, Verwendung von Steinkohlenflugasche zur Vermeidung einer schädigenden Alkali-Kieselsäure Reaktion im Beton, Fak f Bauingenieur- u Vermessungswesen, München, 2009.
[19] S. Kamali, B. Gérard, M. Moranville, Modelling the leaching kinetics of cement-based materials—influence of materials and environment, Cem. Concr. Compos. 25 (2003) 451–458.
[20] S. Kamali, M. Moranville, S. Leclercq, Material and environmental parameter effects on the leaching of cement pastes: experiments and modelling, Cem. Concr. Res. 38 (2008) 575–585.
[21] T.C. Rilem, 106-AAR, 'Alkali Aggregate Reaction' A. TC 106-2—Detection of potential alkali-reactivity of aggregates—the ultra-accelerated mortar-bar test B. TC 106-3—Detection of potential alkali-reactivity of aggregates—method for aggregate combinations using concrete prisms, Mater. Struct. 33 (2000) 283–293.
[22] RILEM TC 219-ACS 'Alkali–silica reactions in Concrete Structures': RILEM AAR-4.1—Detection of potential alkali-reactivity of aggregates: accelerated (60 °C) concrete prism test, (unpublished draft), (2006).
[23] Norwegian Concrete Association, Alkali–aggregate Reactions in Concrete, Test methods and Requirements to Test Laboratories, NB32, 2005, p. 39.
[24] RILEM TC 219-ACS, 'Alkali–silica reactions in Concrete Structures': RILEM recommended test method: AAR-2, Detection of potential alkali-reactivity—Accelerated mortar-bar test method for aggregates, (unpublished draft), (September 2011).
[25] J. Lindgård, B. Pedersen, S.K. Bremseth, P.A. Dahl, T.F. Rønning, Experience using the Norwegian 38 °C concrete prism test to evaluate the alkali reactivity of aggregates, concrete mixes and binder combinations, Nordic Concr. Res. 42 (2010) 31–50.
[26] J. Lindgård, Alkali–silica reactions (ASR)—Performance testing, PhD thesis, NTNU, Norwegian University of Science and Technology Trondheim, (to be published).
[27] J. Lindgård, M. Haugen, N. Castro, M.D.A. Thomas, Advantages of using plane polished section analysis as part of microstructural analyses to describe internal cracking due to alkali–silica reactions, in: T. Drimalas, J.H. Ideker, B. Fournier (Eds.), 14th International Conference on Alkali–Aggregate Reactions in Concrete, Austin, Texas, 2012.
[28] P. Rivard, M.A. Bérubé, J.P. Ollivier, G. Ballivy, Experimental data on the alkalinity evolution of the pore solution in concrete affected by alkali–silica reaction, in: J. Weiss, K. Kovler, J. Marchand, S. Mindness (Eds.), International RILEM Symposium on Concrete Science and Engineering: A Tribute to Arnon Bentur, RILEM Publication SARL, 2004, p. 13.
[29] S. Diamond, in: K. Okada, S. Nishibayashi, M. Kawamura (Eds.), Mechanisms of Alkali–silica Reaction, 1989, pp. 83–94.
[30] J. Stark, D. Erfurt, E. Freyburg, C. Giebson, K. Seyfarth, B. Wicht, Alkali-Kieselsäure-Reaktion (Alkali–Silica Reaction), Series of publications No. 3, Bauhaus-University Weimar, F. A. Finger-Institute for building materials science, Weimar, 2008.
[31] R.C. Weast, M.J. Astle, W.H. Beyer, Handbook of Chemistry and Physics, CRC Press Florida, USA, 1986.
[32] K. De Weerdt, H. Justnes, Microstructure of binder from the pozzolanic reaction between lime and siliceous fly ash, and the effect of limestone addition, 1st International Conference on Microstructure Related Durability of Cementitious Composites, Nanjing, China, 2008, pp. 107–116.
[33] P.J. Nixon, R.J. Collins, P.L. Rayment, The concentration of alkalies by moisture migration in concrete—a factor influencing alkali aggregate reaction, Cem. Concr. Res. 9 (1979) 417–423.
[34] RILEM TC 191-ARP, Alkali-reactivity and prevention-Assessment, specification and diagnosis of alkali-reactivity, RILEM Recommended Test Method AAR-0: Detection of Alkali–Reactivity Potential in Concrete—Outline guide to the use of RILEM methods in assessments of aggregates for potential alkali-reactivity, Mater. Struct. 36 (2003) 472–479.
[35] Norwegian Concrete Association, Durable Concrete Containing Alkali Reactive Aggregates, NB21, 2004, p. 33.
[36] A.M. Neville, Properties of Concrete, 5th ed. Trans-Atlantic Publications Inc., 2011
[37] P.C. Aítcin, Does Concrete Shrink or Does it Swell? Concrete International, December 1999, American Concrete Institute, Farmington Hills, Michigan, 1999.
[38] J. Lindgård, P.J. Nixon, I. Borchers, B. Schouenborg, B.J. Wigum, M. Haugen, U. Åkesson, The EU "PARTNER" Project—European standard tests to prevent alkali reactions in aggregates: final results and recommendations, Cem. Concr. Res. 40 (2010) 611–635.
[39] B. Pedersen, Alkali-reactive and inert fillers in concrete, Rheology of Fresh Mixtures and Expansive Reactions, Norwegian University of Science and Technology, Trondheim, Norway, 2004, p. 292, (PhD-thesis).
[40] I. Sims, P.J. Nixon, Assessment of aggregates for alkali–aggregate reactivity potential: RILEM international recommendations, in: B. Fournier (Ed.), Marc-André Bérubé Symposium on Alkali–Aggregate Reactivity in Concrete, Montréal, Canada (part of the Proceedings of the 8th CANMET International Conference on Recent Advances in Concrete Technology), 2006, pp. 71–91.
[41] P. Rivard, G. Ballivy, Assessment of the expansion related to alkali–silica reaction by the Damage Rating Index method, Constr. Build. Mater. 19 (2005) 83–90.

Paper VI

Advantages of using plane polished section analysis as part of microstructural analyses to describe internal cracking due to alkali-silica reactions
J. Lindgård, M. Haugen, N. Castro, M.D.A. Thomas
in: T. Drimalas, J.H. Ideker, B. Fournier (Eds.) Proceedings of 14th International Conference on Alkali-Aggregate Reactions in Concrete (ICAAR), Austin, Texas, 2012

ADVANTAGES OF USING PLANE POLISHED SECTION ANALYSIS AS PART OF MICROSTRUCTURAL ANALYSES TO DESCRIBE INTERNAL CRACKING DUE TO ALKALI-SILICA REACTIONS

Jan Lindgård [1*], Marit Haugen [1], Nelia Castro [2], Michael D.A. Thomas [3]

[1]SINTEF Building and Infrastructure, Trondheim, NORWAY

[2]Norwegian University of Science and Technology, NO-7491 TRONDHEIM, Norway

[3]University of New Brunswick, Fredericton, CANADA

Abstract

Microstructural analysis is an important tool to diagnose and describe the extent of any ASR in concrete structures. Such analysis is additionally recommended to be performed in connection with laboratory testing of alkali reactivity to confirm that measured expansions are caused by ASR.

In a separate paper, a PhD study of the principal author on ASR performance testing is described. In order to confirm presence and extent of ASR after the exposure, microstructural analyses have been performed. These examinations included analysis of plane polished and thin sections, as well as SEM analysis. By using image analysis, the crack patterns in the plane polished sections were analysed to quantify the extent and distribution of cracks in concrete prisms. This paper presents some important findings from the microstructural analyses, with focus on the advantages of using plane polished section analysis as part of microstructural analysis to describe internal cracking due to ASR.

Keywords: alkali silica reaction, microstructural analysis, image analysis

1 INTRODUCTION

1.1 Background

Microstructural analysis as part of a condition survey

At SINTEF, microstructural analysis is a very important tool to diagnose and describe the extent of any ASR in a concrete structure. Such analysis includes macroscopic examination of fluorescent impregnated plane polished sections (in ordinary light and UV-light), examination of thin sections in a polarization microscope (with and without fluorescence filter) and occasionally Scanning Electron Microscopy (SEM) analysis, as well. The crack patterns are of particular importance in the ASR diagnosis.

Many petrographers only use microstructural analyses (i.e. analysis of thin sections and SEM) in their examinations. These analyses give a very good view of details in the interior of a structure, but they are less suited to give a sufficient overview of the extent of cracking in the concrete.

At SINTEF, more than 20 years of experiences have shown the importance and advantages of using larger samples to describe the crack intensity and crack pattern in drilled concrete cores by analysis of plane polished sections. Thus, a better correlation to what is observed in the field might be obtained. However, the presumption is that an experienced person performs the field survey, in addition to selecting representative

---

[*] Correspondence to: jan.lindgard@sintef.no

sampling locations on the structures. It is also important to carry out a comprehensive visual examination of the drilled cores when they arrive in the laboratory as a basis for detail planning of the laboratory program.

Normally, several complementary laboratory analyses are part of a survey of concrete structures with possible ASR damage, e.g. moisture state and mechanical properties (compressive strength and E-modulus).

Microstructural analysis as part of ASR laboratory testing

Several concrete prism tests (CPTs), e.g. RILEM AAR-3 [1], recommend that microstructural examinations are performed in connection with laboratory testing of alkali reactivity. If the expansion is judged to be deleterious, it is recommended to examine the internal features and crack patterns to confirm that the expansion is caused by ASR.

Description of the extent of internal cracking in concrete samples

In Canada, the DRI method developed by Dr. P.E. Grattan-Bellew [2] is frequently used to quantify internal deterioration caused by ASR. The method makes use of plane polished sections, but without impregnating them with any fluorescence. In the analysis, the following parameters are counted: cracks, precipitation of alkali gel, de-bonding and reaction rims. The different parameters are weighted as basis for calculating the DRI, i.e. a number describing the degree of damage in the plane polished section.

In Norway, the DRI method is rarely used, even though quantification of internal cracking has high focus. Instead, the extent of cracking is described verbally, in addition to describing type of cracks; e.g. whether cracks are running from the aggregates and into the cement paste, whether cracks connect aggregate particles or whether cracks appear parallel to the concrete surface (might indicate freeze/thaw damage). A more simple "cracking index" has, however, been used in a previous research project [3].

PhD study on performance testing – post-documentation of concrete prisms

In a separate paper [4], a PhD study of the principal author on laboratory ASR performance testing is described. A main aim of the PhD study, being part of the Norwegian COIN project (www.coinweb.no), has been to evaluate whether CPTs developed for assessment of alkali-silica reactivity of aggregates might be suitable for general ASR performance testing of concrete. In order to confirm the presence and extent of ASR after the exposure, microstructural analyses have been performed on selected concrete prisms. These examinations have included analysis of plane polished sections and thin sections, as well as SEM analysis.

The extent of internal cracking in the concrete prisms is documented in the plane polished sections that cover the whole prism (70x280 mm). In the photos taken in UV-light crack patterns appear clearly. By use of image analysis, the crack patterns were analysed to quantify the extent and spread in cracking in the concrete prisms. The image analysis is used as an alternative to the more time consuming DRI method [2].

This paper presents some important findings from the microstructural analyses, with focus on the advantages of using plane polished section analysis as part of microstructural analysis to describe internal cracking due to ASR.

2 THE TEST PROGRAMME

2.1 General

Of the 60 test series included in the PhD study [4], one prism from each of 15 test series was analysed by microstructural analysis after the ASR exposure in order to examine the presence and extent of ASR. The prisms were carefully selected to cover a wide range of concrete types and ASR exposure conditions, as well as a spread in expansion. Additionally, the visual descriptions were helpful in the selection.

In total 16 fluorescence impregnated polished sections were prepared (two polished sections were needed for the larger Norwegian concrete prism, 100x100x450 mm). From the same prisms, 25 fluorescence impregnated and polished thin sections for optical polarization microscopy were additionally prepared. 11 of these were also analysed by SEM.

2.2 Visual description

After the ASR exposure, one prism from each of the 60 test series was described visually. At first, any surface cracking and precipitation were registered and photographed. As part of further analyses of the prisms, each prism was cut in several pieces by use of a splitter [4]. Secondly, the cut faces of the prism ends were carefully examined to search for any internal gel exudation in cracks and pores.

2.3 Plane polished section analysis

In addition to give a general description of the extent of cracking and crack patterns in the 16 plane polished sections, the observed crack features were documented by taking photos in normal light and UV light. Examples of such photos are shown in Figure 1 and 2.

Measurement of cracking intensity by image analysis

In this study, the program Image SXM [5], a public domain image processing and analysing software, was used to create maps of the cracks in the polished sections through thresholding of the grey level histogram. The input images were acquired in fluorescent light, so the cracks were easily differentiated from the aggregates and the cement paste (Figure 2). The careful image acquisition (Figure 3) guaranteed that the brightness and contrast were reproducible and that the corresponding digital pixel values were stable. Thus, it was possible to use a fixed grey level threshold, effectively automating this step. A few images required additional minor manual corrections to erase relics of air voids that were not effectively avoided in the thresholding since their grey levels overlapped the crack's grey levels. After segmentation, the total *Area%* occupied by the cracks in each image, defined as the "cracking intensity", was analysed. This measure was further used to compare the cracking intensity in the various plane polished sections.

The prisms were stored with the same end facing upwards during the whole exposure time [4]. To measure any spread in internal cracking intensity over the prisms, the segmented images were divided in crosswise slices of 25 mm or lengthwise slices of 14 mm (12.5 mm in the larger Norwegian prisms) and the *Area%* occupied by the cracks in each slice was analysed. The values obtained for each slice were then normalized to the total *Area%*.

2.4 Thin section analysis

The 25 fluorescence impregnated thin sections were examined in a polarization microscope with a UV-filter. The following parameters were analysed: any reacting aggregate particles, any cracking, any precipitations (e.g. of ASR gel), porosity (w/cm ratio), distribution and size of air voids and any dissolution. During the analysis, emphasis was put on describing presence and extent of ASR by evaluating the amount of alkali-silica gel and the extent and location of cracks.

2.5 SEM analysis

The backscattered electron imaging (BEI) mode in SEM gives a picture of the different phases in the sample as a range of grey values [6]. The 11 samples analysed in the study were sputtered with carbon under vacuum to make them conductive before inspection by SEM. In addition to a brief visual examination of the polished thin sections, the composition of any precipitations (primarily ASR gel) was analysed by EDS (Energy Dispersive Spectrum of X-rays) or WDS (wavelength dispersive X-ray spectrometer).

Measurement of remaining alkali content

During an accelerated ASR laboratory test, the extent of alkali leaching and the depth influenced by alkali leaching is of importance for the prism expansion [7], [8]. In the PhD study, the extent of alkali leaching was documented by analysing the content of alkalis accumulated in the water in the bottom of each storage container [4]. Additionally, it was of interest to measure the remaining alkali content within the concrete prisms, but it is very difficult, maybe impossible, to squeeze out pore water from a concrete with a w/c ratio < 0.50, as applied for most test series. Alternative measuring procedures were thus included in the study.

To try to detect the depths influenced by alkali leaching and to check if any correlation exists between calculated remaining alkali content in the prisms and the extent of alkali leaching, WDS analysis was used in combination with the SEM analysis of the 11 polished thin sections. The content of alkalis, Na and K, in the binder was measured continuously from the outer surface to the centre of the prisms.

3 RESULTS

In this paper, only selected results from analyses of the plane polished sections are presented, with focus on description and quantification of the extent of internal cracking.

3.1 Visual description

The extent of surface cracking varied hugely between prisms exposed to various exposure conditions during the ASR performance testing and thus revealed different expansions [4]. The unwrapped prisms exposed to 60°C revealed the most extensive surface precipitation compared with corresponding prisms exposed to 38°C. Hardly any precipitation was registered on the surfaces of the prisms wrapped in damp cotton cloth and polyethylene according to the description in the RILEM AAR-3 CPT (2000) [9].

After splitting the prisms, white precipitation was observed in air voids in many of the samples, in particular in the prisms from the test series with highest expansion. An extensive content of such precipitation was also observed in many prisms after four weeks of exposure to 60°C.

3.2 Plane polished section analysis

Extent of cracking

The analyses of the plane polished sections showed a huge spread in extent of cracking, both internally within some of the prisms and between prisms from various test series. One example of the former is shown in Figure 2, showing a UV-photo of a prism from a test series with a relatively porous binder (CEM I, w/c 0.60) exposed to 100 % relative humidity (RH) and 60°C for 39 weeks. All prisms were stored with the same end facing upwards (right side of the picture) during the whole exposure time. As can be seen, the extent of cracking is low in the lower (0-30 mm) and the upper (80-100 mm) sections, while the medium section is rather heavily cracked. The 39-week expansion for this prism was measured to be 0.18 %.

Other examples, showing rather extensive cracking over a larger area of the prism is given in Figures 4 and 5. Figure 4 shows the UV-photo of a prism from a test series with a more dense binder (CEM I, w/c 0.45) exposed to 100 % RH and 38°C for 2 years, revealing a 2-years expansion of 0.30 %. Also for this prism the extent of cracking is somewhat less in the bottom and upper sections. Figure 5 shows the UV-photo of the lower part of a prism from a test series with a similar binder exposed to similar conditions for 2 years, but with larger prism size (100 mm cross sections instead of 70 mm). This prism revealed a 2-years expansion of 0.43 %. The cracks seem to be rather homogenously distributed in the prism.

Measurement of cracking intensity by image analysis

Results from the measurements of total cracking intensity (*Area%*) by image analysis of the 16 plane polished sections are presented in Figure 6. In this figure, the cracking intensities are plotted against the measured prism expansions. In all 16 prisms, the same aggregate combination, but four different binders (CEM I with three w/c ratios ranging from 0.30 to 0.60 and a CEM II-A/V fly ash cement with w/c ratio 0.45) were used.

Results from measurements of relative cracking intensity lengthwise from the bottom to the top of the prisms (the prisms were stored in this positions during the whole exposure time), after dividing each prism in crosswise slices of 25 mm, are shown in Figure 7 and 8.

Results from measurements of cracking intensity crosswise, after dividing each of the prisms in five lengthwise slices of 14 mm, are shown in Figure 9.

3.3 Thin section analysis

The analyses detected ASR in all the 25 examined thin sections. The extent of cracking varies, as well as the amount of alkali-silica gel present in air voids and cracks. The alkali-reactive Norwegian cataclasite has reacted in all the 16 test series examined by thin sectioning. However, no particles in the Årdal sand, classified as non-reactive according to the Norwegian ASR regulations [10], have shown any sign of reaction.

3.4 SEM analysis

The SEM analyses showed alkali-silica gel in all the 11 examined samples, occurring in air voids, in cracks in the cement paste, sometimes distributed within the cement paste, in the interface between aggregate particles and the cement paste or in cracks within the aggregate particles. The composition of the alkali-silica gel varied somewhat depending on the location within the concrete. As referred by several others [8], the alkali-silica gel tends to exchange alkalis with calcium when moving from the cracks inside an aggregate and out in the cement paste. Additionally, the extent of cracking in the thin sections varied.

4 DISCUSSION

Post-documentation after the ASR exposure – use of various analysing techniques

During the introductory visual examinations in the laboratory, the concrete samples were carefully checked as a basis to plan which samples were to be used for which analysis. During the preparation of the plane polished and thin sections, the first step was to saw the samples into two longitudinally halves. One half was used for preparation of the plane polished section, while one or two thin sections were prepared from the other half in locations where alkali-silica gel seemed to occur. As can be seen from Figure 2, the selected locations of the thin sections, only covering very limited parts of the concrete prisms, has a very high influence on the outcome and conclusion of the thin section analysis.

The thin section and SEM analyses documented as expected alkali-silica reactions to be the cause of expansion of the 16 concrete prisms examined after the ASR exposure. Even though these investigations are important tools to document that ASR really is the cause of expansion, none of these analysing techniques are well suited to assess the extent and variation in damage within larger concrete samples. For such evaluations, detection of crack pattern in plane polished sections gives a much better overview of the degree of damage, e.g. as shown in Figure 2, 4 and 5. However, the microscopy techniques are important tools for diagnosis and for detailed examinations, e.g. for measurement of the composition of alkali-silica gel by applying EDS or WDS analysis as part of the SEM analysis. The WDS analyses showed for instance that for various binders and both exposure temperatures (38 and 60°C), the alkali-silica gel picks up calcium (exchanged with Na and K) when moving from the cracks inside an aggregate and out in the cement paste.

Measurement of cracking intensity by image analysis

Image analysis is a less time consuming analysing technique compared with the DRI method [2]. It is also not necessary to use a microscope. Similar to the DRI method, the outcome of the image analysis is a number, representing the degree of damage (*area%* of cracks) in a plane polished section. On the other hand, the DRI method involves more parameters connected to an alkali-silica reaction, i.e. reaction products, reaction rims and de-bounding. However, as long as the same aggregate composition has been used in all the test series and the detailed analysing techniques documented that ASR was the cause of expansion, the image analyses could successfully be used in order to compare the extent of cracking, both internally within one plane polished section and between different test series.

A pretty good linear correlation was found between the cracking intensity (given as area% of cracks in the plane polished sections) and the measured prism expansion (Figure 6), even though four different binder qualities were used. The 28 days compressive strength ranged from 44 to 103 MPa. The aggregate composition was, however, identical in all test series. The good correlation found indicates that the accuracy of the image analysing technique is sufficiently good to use the method as a tool to analyse the degree of ASR damage in larger concrete samples. Rivard and Ballivy [11] have also previously found a rather good correlation between the measured expansion caused by ASR on laboratory-concrete prisms and the damage to concrete, as quantified by the DRI on polished sections prepared from these prisms.

For field samples from different structures with varying aggregate composition, the crack patterns are assumed to vary widely. As a consequence, the correlation between the cracking intensity and expansion is assumed to be reduced. Rivard and Ballivy [11] state that "DRI values are not absolute, but are a relative indicator for a particular aggregate or aggregate-cement combination of the extent of ASR damage". In most parts of a real concrete structure, the concrete is not free to expand, a matter that also is assumed to influence the correlation between internal cracking and expansion.

The lengthwise measurements of cracking intensity from the bottom to the top of the prisms, after dividing each prism in crosswise slices of 25 mm (Figure 8 and 9), show that the upper 25 mm of the prisms exhibit least cracking for most test series, followed by the lower 25 mm of the prisms. Further, in most cases the slices located 25-50 mm from the top of the prisms revealed less cracking than the slices located in correspondent distance from the bottom of the prisms. The mid parts of the prisms revealed significantly higher expansion compared with the upper 50 mm and lower 25 mm of the prisms. However, for some samples, and in particular the test series with binder CEM I, w/c 0.60 exposed to 60°C (Figure 2), a larger area of the upper half of the prism has minor cracking compared with the mid parts.

Also the crosswise measurements of cracking intensity, after dividing each prism in lengthwise slices (Figure 9) show that the outer 10-15 mm of the prisms get somewhat less cracking compared with the interior of the prisms.

The main reason for lower extent of cracking in the outer/upper/lower parts of the prisms compared with the interior of the prisms is assumed to be alkali leaching. The preliminary results from measurement of rate and extent of alkali leaching have shown a good correlation between expansion and extent of alkali leaching [4]. Since alkali leaching is connected to diffusion of ions from the interior of the prisms to the wet concrete surface, it is assumed that more porous concretes will have higher tendency to leach out alkalis. It is thus reasonable that the sample showing the least crack intensity in the upper third of the prism compared with the mid part is the most porous one with the highest w/c (see Figure 2).

Three of the 11 thin sections examined by WDS analysis were located in the top of the prisms, while one thin section was located in the bottom of the prism. In the three thin sections from the top of the prisms the mean alkali content in the upper 15 mm was 30-40 % lower compared with the mean alkali content in distance 20-35 mm from the top. For the thin section located in the bottom of one prism, the mean alkali content in the lower 15 mm was about 60 % lower compared with the mean alkali content in distance 20-35 mm from the bottom.

Of all the test methods included in the PhD study, the larger prisms used in the Norwegian CPT revealed highest expansion and least alkali leaching [4]. As can be seen in Figure 5, no distinct difference on cracking between outer and inner parts of the prism could be observed.

5 CONCLUSIONS

Based on microstructural analysis of 15 concrete prism test series after exposure to 100 % RH and 38 or 60°C, the following conclusions may be drawn:

- Image analysis could successfully be used in order to compare extent of cracking due to ASR in the concretes (with identical aggregate composition, but various binder qualities), both internally within one plane polished section and between different test series.
- A pretty good linear correlation was found between the cracking intensity (given as area% of cracks in the plane polished sections) and the measured prism expansion. The good correlation found indicates that the accuracy of the image analysing technique is sufficient good to use the method as a tool to analyse the degree of ASR damage in larger concrete samples.
- The main reason for lower extent of cracking in the outer/upper/lower parts of the prisms compared with the interior of the prisms is assumed to be alkali leaching.

6 REFERENCES

[1] RILEM TC 219-ACS (2011): 'Alkali-silica reactions in Concrete Structures': RILEM recommended test method: Detection of potential alkali-reactivity - 38°C test method for aggregate combinations using concrete prisms, (unpublished draft).

[2] Grattan-Bellew, PE, Danay, A (1992): Comparison of laboratory and field evaluation of alkali-silica reaction in large dam, in: International Conference on Concrete AAR in Hydroelectric Plants and Dams, Canadian Electrical Association in association with Canadian National Committee of ICOLD, Fredericton, Canada, pp. 23.

[3] Lindgård, J, Skjølsvold, O, Haugen, M (2004): Experience from evaluation of degree of damage in fluorescent impregnated plane polished sections of half-cores based on the "Crack index method", in: M. Tang, M. Deng (Eds.) 12th International Conference on Alkali-Aggregate Reactions in Concrete, Beijing, China, pp. 939-947.

[4] Lindgård, J, Rønning, TF, Thomas, MDA (2012): Development on an ASR performance test: preliminary result from a PhD study, in: 14th International Conference on Alkali-Aggregate Reactions in Concrete (submitted proceedings), Austin, Texas.

[5] Barret, SD (2008): Image SXM: http://www.ImageSXM.org.uk.

[6] Scrivener, KL (2004): Backscattered electron imaging of cementitious microstructures: understanding and quantification, Cement and Concrete Composites, (26) 935-945.

[7] Lindgård, J, Andiç-Çakır, Ö, Borchers, I, Broekmans, MTAM, Brouard, E, Fernandes, I, Giebson, C, Pedersen, B, Pierre, C, Rønning, TF, Thomas, MDA, Wigum, BJ (2011): RILEM TC219-ACS-P: Literature survey on performance testing, COIN project report 27, ISBN: 978-82-536-1209-6, pp. 164.

[8] Lindgård, J, Andiç-Çakır, Ö, Fernandes, I, Rønning, TF, Thomas, MDA (2011): Alkali-silica reactions (ASR): Literature review on parameters influencing laboratory performance testing, Cement and Concrete Research, in press.

[9] RILEM TC 106-AAR (2000): 'Alkali Aggregate Reaction' A. TC 106-2- Detection of Potential Alkali-Reactivity of Aggregates –The Ultra-Accelerated Mortar-Bar Test B. TC 106-3-Detection of Potential Alkali-Reactivity of Aggregates-Method for Aggregate Combinations Using Concrete Prisms, Materials and Structures, (33) 283-293.

[10] Norwegian Concrete Association (2004): Durable concrete containing alkali reactive aggregates, NB21, pp. 33.

[11] Rivard, P, Ballivy, G (2005): Assessment of the expansion related to alkali-silica reaction by the Damage Rating Index method, Construction and Building Materials, (19) 83-90.

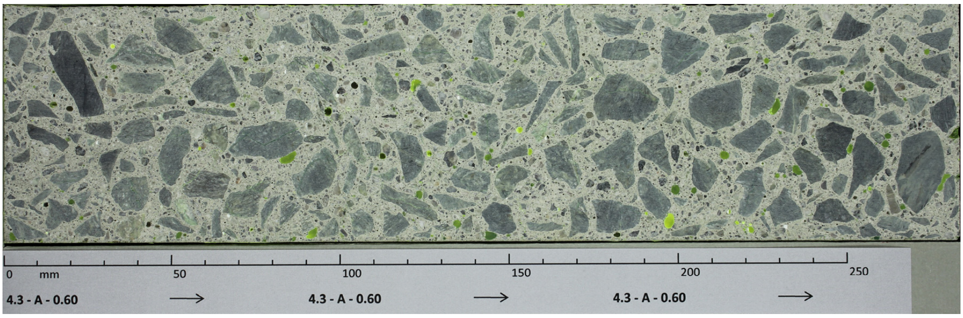

FIGURE 1: Photo in normal light of the plane polished section from test series 4.3-A-0.60.

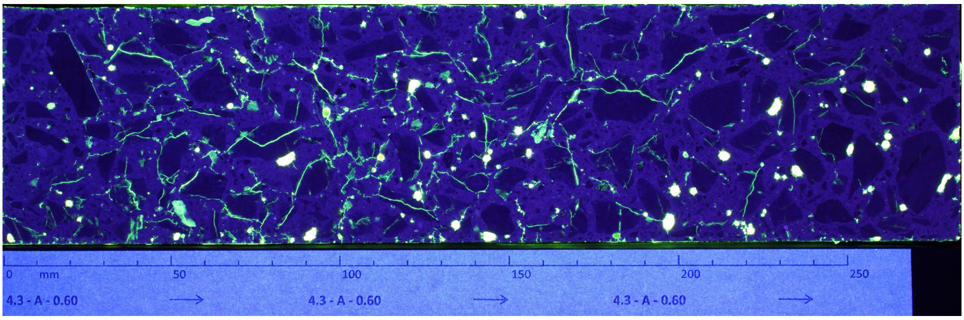

FIGURE 2: Photo in UV-light of the plane polished section shown in Figure 1.

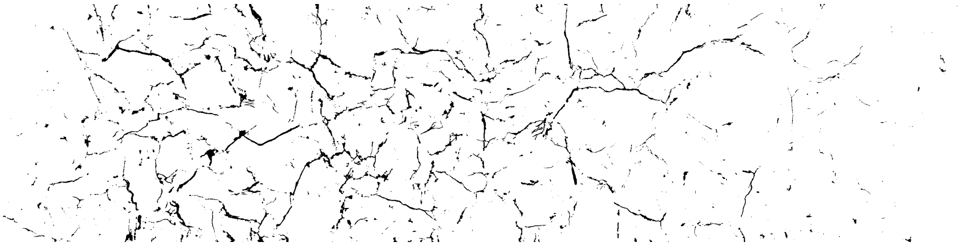

FIGURE 3: Map of the cracks in the plane polished section shown in Figure 1 and 2.

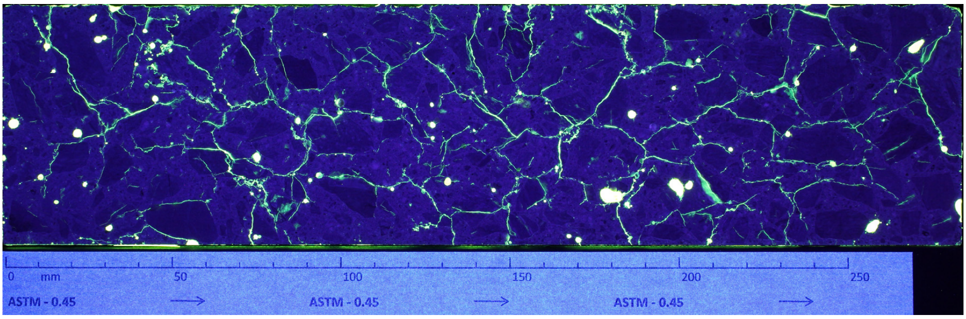

FIGURE 4: Photo in UV-light of the plane polished section from test series ASTM-0.45.

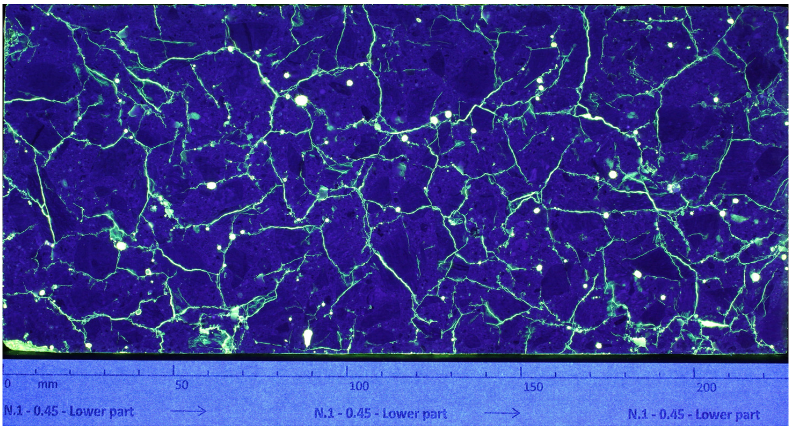

FIGURE 5: Photo in UV-light of the plane polished section from test series N1-0.45.

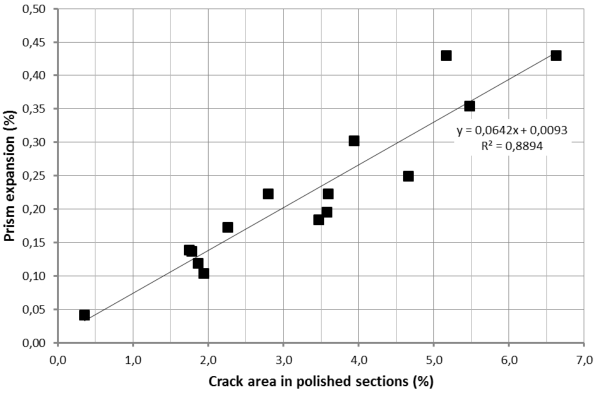

FIGURE 6: Total cracking intensity (Area%) in the 16 plane polished sections plotted against the measured prism expansions.

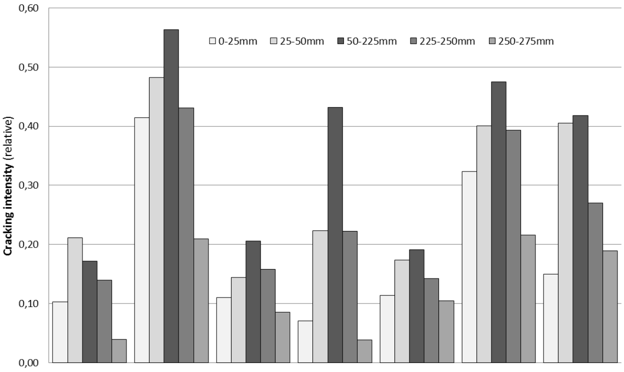

FIGURE 7: Relative cracking intensities in seven polished sections vs. height from the bottom (CEM I, w/c ratio 0.30 or 0.45, exposed to 38°C for 52 or 112 weeks). The test series to the right is the prism shown in Figure 4.

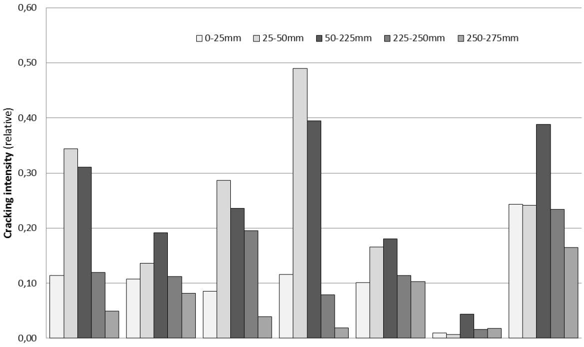

FIGURE 8: Relative cracking intensities in seven polished sections vs. height from the bottom (CEM I, w/c ratio ranging from 0.30 to 0.60, exposed to 60°C for 39 weeks). The test series in the middle is the prism shown in Figure 2.

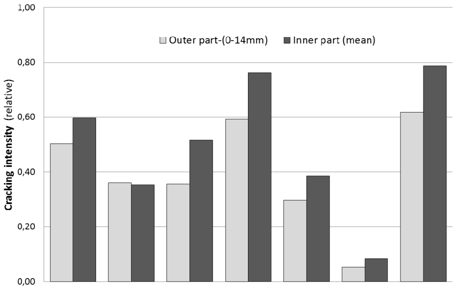

FIGURE 9: Relative cracking intensities in the same seven polished sections as shown in figure 8, but calculated crosswise, after dividing each of the prisms in five lengthwise slices of 14 mm. The test series in the middle is the prism shown in Figure 2.

Appendix 2: Complementary test procedures

- Alkali release from aggregates
- Dynamic E-modulus
- Alkali leaching: Procedure for sampling and measurement during concrete prism testing
- Relative diffusion coefficient: Supplementary test procedures plus calculation of results
- Electrical resistivity: Supplementary test procedures plus calculation of results
- Expansion: Detailed procedure for measuring length and weight without pre-cooling the prisms

Appendix 2

Alkali release from aggregates

In a pilot study, the alkali release from the two aggregate types used was measured; initially on powdered material (< 0.125 mm) made by crushing and grinding the aggregates and subsequently on the actual grading used in the concrete mixes (i.e. sand 0/4 mm and relative quantities of each of the three fractions of the coarse aggregate). The exposure conditions are similar to the method recommended by Berubé at al. [1], except that the solutions used are 1 M (0.7 M used by Berubé et al.) and that CH (calcium hydroxide) is added with the aggregate in order to enabling ion exchange between Ca^{2+} and alkalis of the aggregates and also to be in line with reality (i.e. the concrete pore water) where there is always an excess of $Ca(OH)_2$. The following test procedure was used for measurement of alkali release on the actual gradings:

- Two 1 M solutions (pH 14.0) were prepared, one with NaOH and one with KOH.
- 1000 g of each aggregate type was put in 8 alkali-resistant plastic bottles, before adding 50 g CH and either the NaOH solution or the KOH solution until the aggregates were submerged (the same amount was added to each of the bottles).
- [For the powdered material, 10 g powder, 1 g CH and 100 ml 1 M NaOH or 1 M KOH were used.]
- Four bottles (two of each solution) were stored at 38°C and four bottles were stored in the 60°C AAR-4.1 reactor for about one year. Additionally, one bottle with each of the blank solutions was stored at the same temperatures. A 20 ml sample was extracted from each of the bottles at three points in time (at 75, 150 and 405 days, respectively). The bottles were shaken once a week.
- [A similar procedure was used for the powdered material, but in this case the bottles were stored at 38°C for one week before sampling of 20 ml liquid. The samples were shaken periodically.]
- The alkali content of the aliquots removed from the bottles was determined by FAAS. In this method, the amount of sodium released by the aggregate is determined by measuring the Na content of the aliquot removed from the bottle containing KOH added CH and the amount of potassium is determined by measuring the K content of the aliquot removed from the bottle containing NaOH added CH. However, any alkalis measured in the reference solutions with NaOH or KOH added CH were subtracted.

For comparison, corresponding measurements were performed on some supplementary aggregate types (see Appendix 3).

Dynamic E-modulus

Internal cracks developed in the concrete prisms during the ASR exposure might be reflected in a reduced dynamic E-modulus. As a supplement to the expansion measurements and in order to check the sensitivity of such measurements for an early detection of internal cracking, the dynamic E-modulus was measured on all the unwrapped test series according to ASTM C 215-02 [2] (transverse mode) simultaneously with the expansion measurements (similarly as done in the German CPT [3]). The first measurements were performed after two weeks of exposure. To improve the accuracy of the measurements, the "receiver" was always placed on the same marked location on the prism surface.

Alkali leaching: Procedure for sampling and measurement during concrete prism testing

[The following procedure was developed and has been applied in the PhD study of Jan Lindgård. The procedure, excl. the calculation part (written in italic), is also included in the COIN (RILEM) literature review report [4] (Appendix 8).]

The principle is to sample water from the bottom of the concrete prism storage containers at given intervals and measure the content of alkalis present. At the end of the test, also the alkalis that may have been sucked up in any lining used should be measured.

Preparation of storage container

Before starting the test, make sure that the storage container, including the bottom grid, is clean. If needed, also apply a weak acid. After cleaning the container, wash with deionized water.

Always apply new lining (if applied). Only deionized water shall be used to wet the lining (if applied) and to fill the bottom of the storage container.

Avoid any contamination of the equipment used.

Measurement of volume water

At every sampling, the volume of the water in the bottom of the storage containers must be known. Due to sorption of water by the concrete prisms and by the lining (if applied), weighing of the containers will not be accurate. A more suitable procedure is to prepare a plot with volume water versus height of the water. After wetting the lining (if applied), fill up the container successively and measure the water depth in the center of the container bottom. At SINTEF, a wooden pin is applied for measuring, see Figure 2-1. If the bottom grid lies in the bottom at sampling of liquid, also place it in the bottom before preparing the height-volume plot.

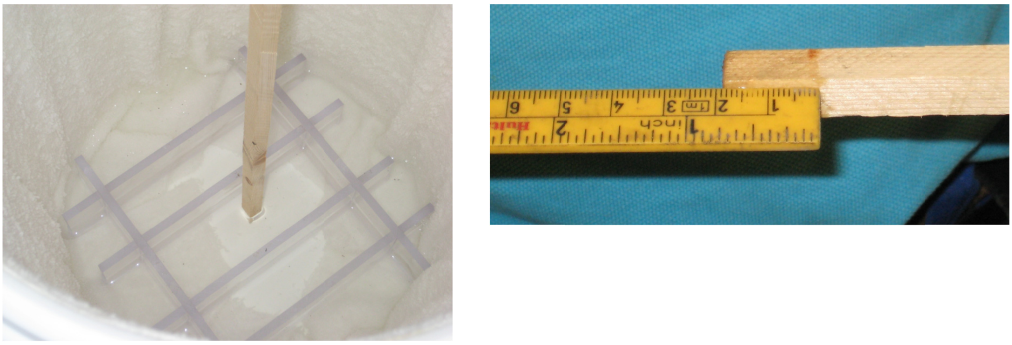

Figure 2-1 Measurement of height of the water in a container by use of a wooden pin.

Sampling of liquid

Make sure to measure the height of the water before each sampling as basis for calculating the volume of water. To homogenize the distribution of alkalis, stir the water before sampling. Apply a clean pipette (or similar) to suck up approximately 20 ml of water, see Figure 2-2. Fill the sample on a clean plastic bottle able to resist alkalis without disintegrate or contaminate the sample with supplementary alkalis. If a bottle has been used before, clean it by applying a weak acid solution, before washing it with de-ionized water. Before taking the next sample, clean the pipette with deionized water.

Figure 2-2. Sampling of water in a container by use of a pipette (left). Plastic bottle for storage of the water sample (right).

After sampling, add 20 ml deionized water to the container. Also add deionized water to compensate for any evaporation (i.e. add water up to the amount described in the test method).

<u>*Measurements, calculations and report*</u>

Measure the content of alkalis, [Na] and [K] (mg/l), in the 20 ml samples by use of flame atomic absorption spectroscopy (FAAS), inductively coupled plasma mass spectrometry (ICP-MS) or alternative equipment with comparable accuracy. Calculate the content of alkalis (mg/l) in the samples as [Na_2O], [K_2O] and [Na_2O_{eq}], respectively (*see Eq. 1*). Calculate the volume of the water (l) in the storage container on the basis of the measured water heights.

Comment: In this study, the content of alkalis was measured by a FAAS of type "SpectrAA-400". Beforehand, most samples were diluted to a concentration of 1:100. As a quality control, five of the samples were tested in parallel using inductively coupled plasma mass spectrometry (ICP-MS), a method regarded to be more accurate if only small quantities of alkalis are present in the samples. The correlation between the methods was satisfactory (the mean ICP-MS values were 3-9 % lower than the mean FAAS values).

The content of alkalis dissolved in the water in the bottom of each storage container (or in each of the alkali resistant plastic bottles in which the lining or the cotton wrapping was submerged) was calculated according to Eq. 1:

$$[Na_2O_{eq}] = ([Na] + [K] \times 23/39.1) \times 62 / (23 \times 2) \times 1000 \times V \qquad (g) \qquad (Eq.\ 1)$$

Where 23 = *molar weight of Na*
39.1 = *molar weight of K*
62 = *molar weight of* Na_2O
V = *volume (l) of the water in the bottom of the storage container (or in the plastic bottle in which the lining or the cotton wrapping was submerged)*

Calculate the cumulative amount of alkalis (g) leached out from the concrete prisms versus time. Account for the content of alkalis present in all previous 20 ml samples removed. Report the cumulative alkali leaching as reduction in the concrete alkali content, both expressed as *kg alkalis* *(i.e. Na_2O, K_2O and Na_2O_{eq}, separately) leached per m^3 concrete* and as % *alkalis (i.e. Na_2O, K_2O and Na_2O_{eq}, separately) leached* compared to the initial alkali content in the concrete at the time of mixing, see Figure 2-3.

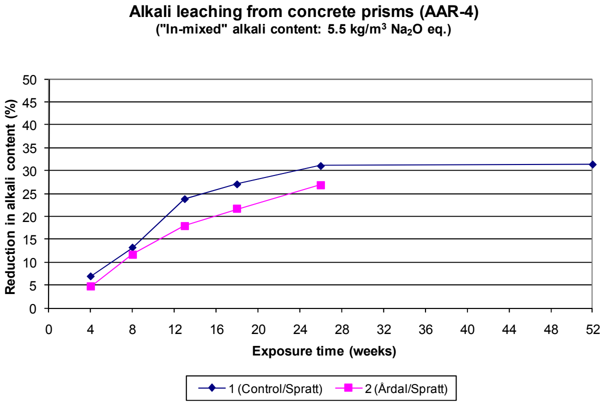

Figure 2-3 Example of presenting results from measurement of alkali leaching (comment: no lining was applied, thus the last reading represents the total alkali leaching).

Any alkalis present in the lining – total amount of alkalis leached

At the end of the test, also the alkalis present in the lining (if applied) should be measured. Either apply the whole lining, or divide the lining into representative samples. According to SINTEFs procedure, the lining is cut into three pieces; top, middle and bottom part, respectively. In this way, also the content of alkalis versus height above the water may be measured. The lowest part of the lining is slightly twisted inside the container to remove excess water.

After removing the lining, stir the water in the bottom of the container and sample 20 ml, before measuring the volume of the liquid by pouring the water into a separate container and weigh it (account for the 20 ml of water removed).

Submerge each lining sample in approximately 1.5-2 litres of deionized water (the exact volume of water must be measured) in a clean plastic container / plastic bottle able to resist alkalis without disintegrate or contaminate the sample with supplementary alkalis. If the container / bottle have been used before, clean it by applying a weak acid solution, before washing it with deionized water. Add a lid or screw cap to avoid evaporation. Stir or shake the liquid once a day for one week. After one week, stir once more, and sample 20 ml of the liquid by use of a similar procedure as applied for sampling from the containers (see above). Measure and calculate the amount of alkalis leached out (as described above). *(Comment: A similar procedure was used in this study to measure the alkalis present in any cotton wrapping used.)*

Calculate the total amount of alkalis leached out during the exposure period as the sum of alkalis present in the lining samples and the alkalis remaining in the bottom water after removing the lining. Account for the content of alkalis present in all previous 20 ml samples removed.

Relative diffusion coefficient: Supplementary test procedures plus calculation of results

The main procedure used for measurement and calculation of the relative diffusion coefficient (named "RelD" in the following) is described in paper IV, section 2.4.4 (corresponding to Eq. 6 – see later). However, measurements and calculations were also performed according to some supplementary procedures (these results are only presented in Appendix 3). All the procedures are described in the following:

After 4 weeks of ASR exposure, two of the six samples cut from each "extra prism" (as described in paper IV, section 2.4.1) were given special treatment during the "PF test procedure" (paper IV, section 2.4.2). After the initial submersion of the samples in water (i.e. before drying the samples at 105°C), one of the samples was dried for 6 months in a drying cabinet with temperature 50°C (but without any moisture control). The other sample was placed in a conditioning room at 20°C and 50 % RH in order to dry out slowly during the following 6 months. Additionally, each of the three "PF-samples" used for measurement of porosities and DCS (paper IV, section 2.4.2 and 2.4.3) was also given similar drying conditions for three weeks in the 20°C conditioning room before being fully dried in the 105°C oven. The relative diffusion coefficients were calculated in various ways as described in the following.

<u>"Calculation method I"</u>

Firstly, the relative diffusion coefficient was calculated by assuming it is equal to the ratio between the time it takes for a given concrete to dry to 50 % of its equilibrium value compared with the time it takes for a reference sample, i.e. RelD was calculated by comparing the time ($t_{c/2}$) various concrete samples need to dry out to a moisture state representing half of the amount of water lost (c) from saturated state to a moisture state in equilibrium with the surrounding environment. For both drying temperatures (20°C and 50°C, respectively), the mean calculated drying time for the ASTM samples (7 parallel test series) with the "basis" binder (CEM I, w/c of 0.45) was chosen as the reference drying time ($t_{ref.c/2}$). The relative diffusion coefficient ($RelD_{c/2}$) could then be calculated according to Eq. 2.

$RelD_{c/2} = t_{ref.c/2} / t_{c/2}$ (Eq. 2)

Most samples dried at 50°C became almost in moisture equilibrium with the air inside the drying cabinet during the six months drying period, while most samples dried at 20°C were still slowly drying (i.e. the drying versus time curve had not flattened out, in particular not for the most dense concretes with lowest w/cm). Thus, an estimation of the total water loss at equilibrium (c) was made in the following way (see Figure 2-4):

- The results were plotted as weight loss (weight-%) versus time and square root of time.
- For both curve types, the drying versus time curve was extrapolated to about 400 days (see typical drying curve in Figure 2-5). At this point in time it was simply assumed that the samples had reached a moisture state in equilibrium with the surrounding environment. The moisture loss to this assumed equilibrium (Eq. 3) was calculated as the mean moisture loss (c_{mean}) extrapolated from the two curve types, named c_{lin} and c_{scrt}, respectively.

$c_{mean} = (c_{lin} + c_{scrt}) / 2$ (Eq. 3)

For the samples dried at 50°C, the calculations of $c_{mean/2}$ and the time to reach this moisture state ($t_{c\text{-}mean/2}$) were done manually on prints of the drying versus time (in days) curves (after enlarging the first part of these curves).

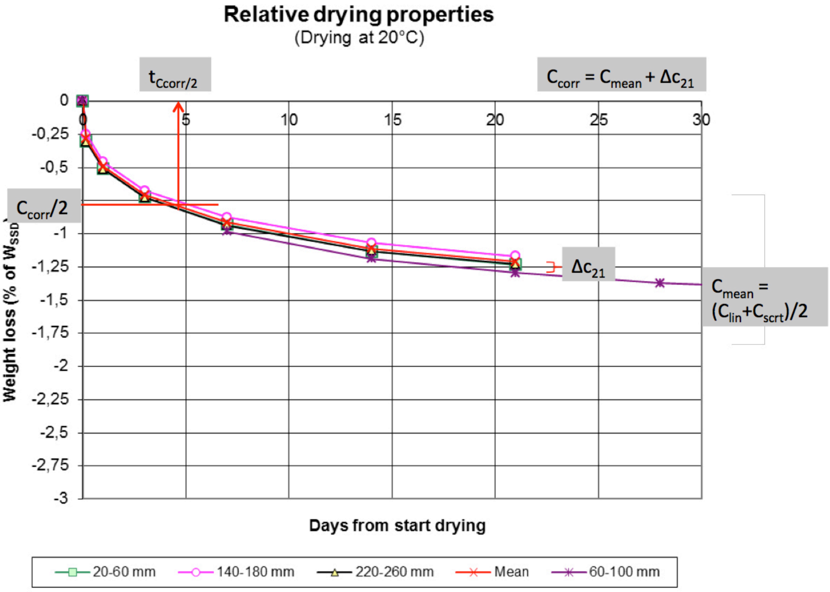

Figure 2-4 Calculation of relative diffusion coefficient based on drying of samples at 20°C / 50% RH.

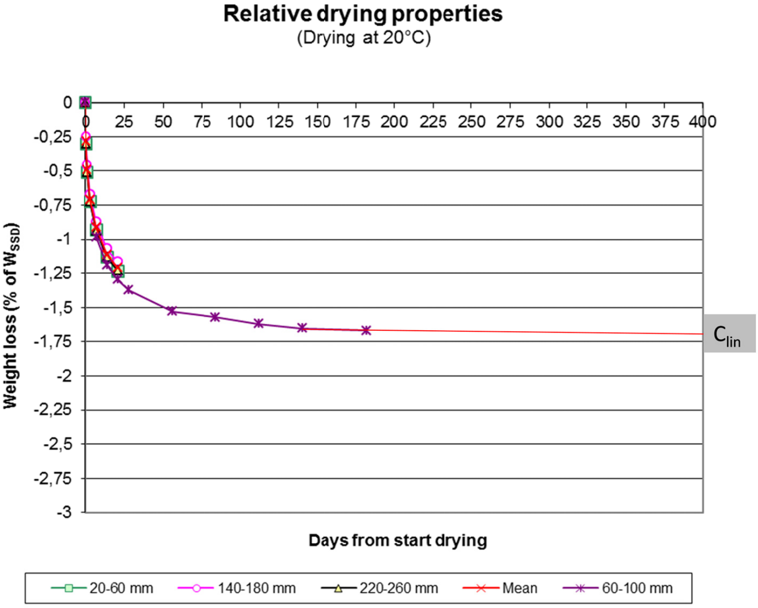

Figure 2-5 Typical drying curve extrapolated to 400 days.

If the concrete properties are homogenous in all the samples cut from the same prism, the samples should ideally dry out to the same moisture state and the drying versus time curves should in the end meet in the same point. However, due to heterogeneity (e.g. due to slight differences in cement paste / aggregate ratio) the 20°C drying curves for the four samples cut from the same prism might deviate slightly in the early drying phase as shown in Figure 2-4. However, the drying curves seem to be rather parallel from 4-5 days of drying until 21 days. By assuming that this difference is kept constant until the "assumed equilibrium point of time" (i.e. one assumes that the curves are parallel from 21 to 400 days of drying), the calculated mean weight loss (c_{mean}) was corrected (hopefully to improve the accuracy of the measurements) in the following way by taking advantage of the measured mean weight loss for the three "PF samples" from start drying until 21 days of drying ($c_{PF-mean21}$):

- The difference between this mean loss of moisture ($c_{PF-mean21}$) and the loss of moisture after 21 days for the single sample dried for six months (c_{21}) was calculated according to Eq. 4.
- The calculated mean c-value (c_{mean}) was corrected according to Eq. 5.

$\Delta_{c21} = c_{PF-mean21} - c_{21}$ (Eq. 4)

$c_{corr} = c_{mean} + \Delta c_{21}$ (Eq. 5)

Finally, the calculations of $c_{corr/2}$ and the time to reach this moisture state ($t_{Ccorr/2}$; see Figure 2-4) were done manually on prints of the drying versus time curves (similarly as for the samples dried at 50°C – see Eq. 6).

$RelD_{Ccorr/2} = t_{ref.Ccorr/2} / t_{Ccorr/2}$ (Eq. 6)

[Comment: The values for RelD$_{Ccorr/2}$ calculated based on slowly drying at 20°C are presented in paper IV, Table 14, section 3.4.2].

"Calculation method II"

For the samples dried at 20°C, similar calculations of the relative diffusion coefficient were additionally performed by comparing the corrected times ($t_{Ccorr/4}$) various concrete samples need to dry out to a moisture state representing ¼ of the amount of water lost (c_{corr}) from saturated state to a moisture state in "assumed equilibrium" with the surrounding environment – see Eq. 7. The purpose was to check if a comparison of the drying curves in an earlier stage of drying gave a similar rating of the relative diffusion coefficients for the various test series.

$RelD_{Ccorr/4} = t_{ref.Ccorr/4} / t_{Ccorr/4}$ (Eq. 7)

"Calculation method III"

For the samples dried at 20°C, calculation of the relative diffusion coefficients were additionally (based on the same measurements as described in the past) performed in a more simplified way. Instead of calculating a corrected drying time ($t_{Ccorr/2}$) for each test series and compare it with the corrected reference drying time ($t_{ref.Ccorr/2}$) (see Eq. 6), the mean time (t_{mean}) the four samples from each test series needed to lose a certain amount of water, defined as the "reference water loss" (in g/cm^2), was measured (read out from an enlarged drying versus time curve) and compared with the mean time the ASTM samples (t_{ref}) needed to lose the same amount of water. The surface area of the various samples was calculated based on the "PF-measurements" (paper IV, section 2.4.2). This "reference water loss" represents a weight loss close to *c/2* for the ASTM samples (see "Calculation method I"). In these calculations, the test series within each binder type were compared separately (due to varying amount of water lost at moisture equilibrium with the surroundings, controlled by the porosity and the quality of the binder). Thus, a separate reference time (t_{ref}) was calculated for each binder, by basing the calculations on the following "reference water losses":

- CEM I, w/c of 0.30: 0.015 g/cm^2
- CEM I, w/c of 0.60: 0.030 g/cm^2
- CEM I, w/c of 0.45: 0.020 g/cm^2 and 0.025 g/cm^2 (i.e. two separate calculations to slightly varying drying stages)
- CEM II/A-V, w/cm of 0.45: 0.020 g/cm^2 and 0.025 g/cm^2

The simplified calculations of relative diffusion coefficients were finally done according to Eq. 8.

$RelD_{Simplified} = t_{ref} / t_{mean}$ (Eq. 8)

These simplified calculations were not performed for the larger samples cut from prisms tested according to the Norwegian CPT.

Electrical resistivity: Supplementary test procedures plus calculation of results

The main procedure ("Procedure I") used for measurement of the electrical resistivity is described in paper IV, section 2.4.5. However, measurements were also performed according to two supplementary test procedures. The three procedures are described in the following:

- "Procedure I": After unpacking the prism from the tight polyethylene foil, but before splitting the "PF-samples" (paper IV, section 2.4.1), the electrical resistance (R, in ohm) across the prism cross section was measured by placing two 100x100 mm metal plates on two opposite sides (not the casting surface) of the mid part of the prism. A conductive gel was evenly distributed on the two plates to ensure good contact, before the readings of the electrical resistance (R, in ohm) were taken.
- "Procedure II": Immediately after splitting, brushing and weighing the "PF-samples" (paper IV, section 2.4.1 and 2.4.2), the electrical resistance across the sample cross section was measured for each of the samples (similarly as in "procedure I").
- "Procedure III": After submerging the "PF-samples" in water for seven days (paper IV, section 2.4.2) and removing excess surface water, the electrical resistance across the sample cross section was measured once more for all samples.

When calculating the electrical resistivity (ρ) according to Eq. 9 ([5], [6]), the following cross section widths (t) were used:

- 100 mm when measuring across the prisms (= the width of the metal plates)
- Mean thickness of each "PF-sample" (calculated based on the "PF-measurements")

$\rho = A \cdot R / L = L \cdot t \cdot R / L = t \cdot R \ (ohm \cdot m)$ (Eq. 9)

where $A = L \cdot t$ = area of the each of the two opposite sides of the sample (m^2)
L = length between the metal plates = length of the prism side (m)

Only results from measurements of electrical resistivity on whole prisms ("Procedure I") are presented in paper IV (section 3.4.3). These measurements and the "Procedure II" measurements are performed on samples with "in-situ" moisture state (i.e. same DCS as during the ASR exposure), and no further leaching of ions has taken place (as will happen during the 7 days submersion of the "PF-samples"). Even though the presented "Procedure I" results are somewhat lower than the "true" electrical resistivity (since some current can be transported through the concrete prisms outside the 100 mm zone used in the calculations), the internal ranking between the various test series is believed to be correct.

Results from measurements of electrical resistivity according to all the three procedures are presented in Appendix 3.

Expansion: Detailed procedure for measuring length and weight without pre-cooling the prisms

All readings in the modified versions of the various concrete prism tests were taken without pre-cooling the prisms. To secure accurate readings, i.e. reduce the influence of any weight loss and temperature variations from reading to reading, the following detailed test procedure was developed:

- The reference readings of the prisms measured without pre-cooling were taken the day after the prisms were exposed to their ASR exposure temperature (see Figure 1 in "paper IV").
- The three parallel prisms were always measured in the same sequence as for the reference readings.
- The next prism was taken out from the storage container exactly 2 minutes after the previous prism.
- For each prism, the length reading was taken exactly 45 seconds after removing the prism from the storage container, the weight reading after exactly 60 seconds, before the dynamic E-modulus was measured and the prism was put back into the container.
- The lid was only removed from the container for a short period when each prism as quickly as possible was taken out or later returned to the container.

Appendix 3: Complementary laboratory results

- Petrographic analysis of the two aggregate types
- Alkali release from aggregates
- Summary discussion of findings in paper IV
- Dynamic E-modulus
- Relative diffusion coefficient: Results from supplementary test procedures
- Electrical resistivity: Results from supplementary test procedures
- Supplementary comments to the "PF-measurements" and the DCS measurements
- Calculations based on the expansion measurements
  - Statistical analysis
  - Coefficient of thermal expansion
  - Length change in the "pre-reference phase"
- Mass increase of whole prisms: Supplementary results for the CEM I binders
- Microstructural analysis: Supplementary results, including WDS analysis of the ASR gel
- Photos
  - ASR test methods: ASR storage containers, wrapping of prisms and length measurements
  - Other measurements: DCS, RH and electrical resistivity
  - Visual inspection of prisms
  - Microstructural analyses
    - 16 plane polished sections (in UV-light)
    - Selected thin sections
    - Selected photos from the SEM analysis

Appendix 3

Petrographic analysis

The testing was performed by Marit Haugen, SINTEF Building and Infrastructure, according to the Norwegian ASR regulations [7]. The analyses were performed on the following fractions:

- "Årdal, 0/4": 1/2 and 2/4 mm, sieved out from the 0/4 mm fraction
- "Ottersbo, 4/8, 8/11, 11/16": Crushed 2/4 mm after blending the three fractions in equal amounts

Table 3-1: Petrographic analysis of the Årdal 0/4 mm sand.

Årdal, 0/4: mean of 1/2 and 2/4 mm	Volume %	Alkali reactivity evaluation
Feldspathic rock / feldspar particles	48	innocuous
Granite	44	innocuous
Quartzite, coarse grained / quartz particles	5	innocuous
Dark rock	3	innocuous

Table 3-2: Petrographic analysis of the Ottersbo coarse aggregate, blend of 4/8, 8/11 and 11/16 mm.

Ottersbo, 4/8, 8/11, 11/16: crushed 2/4 mm	Volume %	Alkali reactivity evaluation
Cataclasite	97	alkali reactive
Feldspathic rock	2	innocuous
Gneiss / granite	1	innocuous

Alkali release from aggregates

The results from the initially alkali release measurements performed on finely ground material from seven aggregate types are shown in Table 3-3.

Table 3-3: Measurement of alkali release from aggregate fines (< 125 µm) (storage for 7 days at 38°C and pH 14 - see description in Appendix 2).

Aggregate type	Net Na_2O_{eq} release (mass-%)
Limestone, UK	0.015
Impure limestone, Canada	0.013
Gneiss, Switzerland	0.061
Gneiss/Granitic sand[1], Norway	0.184
Granite, UK	0.093
Cataclasite[2], Norway	0.166
Gneiss/Granitic sand, Norway	0.145

[1] *Årdal sand*
[2] *Ottersbo coarse aggregate*

For the aggregate types used in the concrete mixes, 0.184 % by mass of Na_2O_{eq} alkalis was released from the ground Årdal sand (< 0.125 mm) and 0.166 % by mass from the powdered material produced from the coarse Ottersbo aggregate. If one assumes that these numbers are representative of the aggregate composition used, this alkali release corresponds to about 3.2 kg Na_2O_{eq} alkalis per m^3 of concrete. If such a high amount is released into the concrete pore water during the life time of a concrete structure, the impact on ASR will be considerable.

However, the later measurements performed on the aggregate grading used in the concrete and dispersed in solutions with pH 14 (1 M solutions) and temperature 38°C and 60°C, respectively, up to about one year (see Appendix 2) showed only a minor alkali release from the three Norwegian aggregate types (the other aggregate types were not tested further); less than 0.01 % by mass was released (rather stable values at all three points in time), corresponding to less than 0.2 kg Na_2O_{eq} alkalis per m^3 of concrete. This value is far less than that reported by Berubé at al. [1], in which measured alkali release in the range of 0.03-0.19 % for comparable aggregate types with size either in the range of 0.63-1 mm or 1-5 mm (not stated specifically). As a consequence of the measurements on the real aggregate fractions, it is not likely that the aggregate composition used has contributed significantly (< 5 %) to the alkali concentration in the concrete pore water.

One implication of the huge dependency of the aggregate grading on the results revealed, is that the influence of particle size on the amount of alkalis released by aggregates needs to be considered when developing a standardized test for measuring alkali contributions from aggregates (as is being done by RILEM TC-219 ACS). For example could introductory testing be performed on finely ground material. Further testing on real grading could then be performed if the alkali release from the powdered material is higher than a certain limit.

Summary discussion of findings in paper IV

(Comment: In the following, a summary discussion of the findings in paper IV is included. The text was originally included in paper IV (as section 4), but was later removed based on advice from the reviewer (in order to shorten the paper). However, since this text gives an easy-to-follow overview of the findings in paper IV (i.e. more readable than the details presented in section 3 of paper IV), it is included in this appendix (the numbering of the summary is kept as section 4). Where not mentioned specifically, the references to sections, tables and figures refer to paper IV).

4 SUMMARY OF FINDINGS IN PAPER IV

4.1 General

The detailed results presented and discussed in Section 3 clearly show that the internal moisture state and the concrete transport properties are significantly influenced by the "pre-treatment conditions", "ASR exposure conditions" and prism size. Additionally, the impact depends on the concrete quality, i.e. w/cm ratio and binder composition. Consequently, the conclusion from a concrete performance test will differ depending on the test procedure used.

In the following, the main findings are briefly summarized.

4.2 "Basis binder": Alteration of concrete porosity and moisture state during ASR exposure

The ASTM C-1293 38°C CPT [8] has been used as the reference test procedure. As a basis for the summary discussion, the observed alteration of the concrete properties of the prisms with the "basis" binder (CEM I, w/c of 0.45) during the ASR exposure according to this method is briefly summarized. After 4 weeks of exposure, no significant ASR expansion has taken place. However, primarily due to the on-going cement hydration, the concrete prisms have on average absorbed about 1.25 vol-% (corresponding to roughly 0.5 mass-%) of water after de-moulding (Figure 6). On average at 4 weeks, the measured evaporable water content is about 11.5 vol-% corresponding to DCS of 93-94 %. The internal RH is 93-94 % (Table 13).

From 4 to 52 weeks, the concrete properties are altered. The suction porosity increases on average 1.5 vol-% (Figure 4). The main mechanisms for the measured increase are assumed to be ASR induced micro-cracks that are able to suck water and the formation of ASR-gel in ASR induced cracks and air voids that will absorb water during the submersion period of the PF-measurements. A fair correlation exists between water uptake and expansion (lower part (black symbols) of Figure 5). Primarily due to the same mechanisms, the concrete prisms absorb on average 1.65 vol-% (corresponding to roughly 0.7 mass-%) of water (Figure 7). The change in macro porosity (air content) is negligible.

During the ASR exposure from 4 to 52 weeks, the internal moisture state increases on average as follows (Table 13); evaporable water content about 2 vol-%, DCS about 2-3 % and RH about 2-3 %. After 52 weeks of exposure, DCS is in the range of 95-97 % and the internal RH is in the range 96-96.5 % (Table 13, Figure 10).

Finally, there is a tendency to decreased electrical resistivity with increased ASR expansion (Figure 14). The reason might be that cracks generated during the ASR exposure are partly filled with ASR gel and water, making the transport of current easier than through concrete with less internal cracking.

4.3 Influence of specimen "pre-treatment"

For all test series, the moulds were stored at ambient temperature in the laboratory under plastic foil from casting until de-moulding the following day. The subsequent 0.5 h submersion of some of the prisms in water at 20°C (Tables 5-8) does not significantly influence the prism water uptake or the internal moisture state (evaporable water content, DCS and RH) measured after 4 and either 39 or 52 weeks of exposure, nor the transport properties measured after 4 weeks of exposure. From a "moisture point of view" this submersion thus seems unnecessary, since the water will be absorbed in any case later. Additionally, some have questioned if this early submersion might lead to significant leaching of alkalis from the concrete prisms (it does, to some extent, as discussed in paper V).

For all test series, the prisms were prepared for final exposure (e.g. wrapped) and put into the storage containers immediately after de-moulding (and after 0.5 h submersion for most test series) and the initial measurements of mass and length. Some storage containers were subsequently put into their ASR exposure conditions at 38 or 60°C, while other were kept at ambient temperature until age 7 or 28 days (Figure 1 and Tables 5-8). Additionally, a few test series were pre-cured 24 h at 60°C to simulate the curing temperature in a massive concrete structure (labeled "8FT" in Figure 1).

The test series exposed to elevated temperature directly after de-moulding, after 7 days of pre-storage at 20°C or after simulating curing conditions in a massive structure reveal equal internal moisture state at all ages. However, permanent exposure to 60°C directly after de-moulding significantly increases the relative diffusion coefficient compared with 7 or 28 days of pre-storage at 20°C (Table 14), making the internal transport of water and ions easier.

Extending the pre-storage period at 20°C to 28 days influenced the measured concrete properties as follows:

- The internal RH measured after 4 weeks of exposure is slightly reduced, especially for the "fly ash" test series exposed to 60°C. For some test series, DCS is slightly reduced as well (Tables 10 and 11). The main reason is probably a somewhat higher degree of hydration and consequently a higher degree of self-desiccation. For the "basis" binder exposed to 60°C, no influence on the internal RH of a prolonged storage at 20°C is observed.
- For the test series exposed to 38°C, a slightly lower relative diffusion coefficient is obtained after 4 weeks of exposure (Table 14), most likely due to a somewhat higher degree of hydration.
- In general, no significant influence of pre-storage length on the internal moisture state or the electrical resistivity is observed at the end of the exposure period (Tables 10 and 11 and Figure 14). The main reason is probably that during the exposure period, the extent of ASR becomes of more importance for the prism water uptake, the internal moisture state and the transport properties (see Section 4.2 above).

Wrapping of concrete prisms, by use of wet cotton cloths and plastic sheets, is applied in some test methods primarily with the aim to secure a high moisture content surrounding the prisms. Such wrapping generally leads to a higher water uptake in the first weeks of exposure compared with unwrapped prisms, in particular when exposed to 60°C (Figure 6). When exposed to 38°C, the water uptake is slightly higher also later in the exposure period. However, this is not true when exposed to 60°C; the wrapped prisms absorb significantly less water during the exposure period compared with the unwrapped prisms. The main reason is the considerably decreased amount of ASR obtained for the wrapped prisms (connected to alkali leaching - further discussed in paper V). Nevertheless, at both exposure temperatures wrapped prisms absorb significantly more water compared with unwrapped prisms for comparable expansions (Figure 5).

Furthermore, the wrapping generally leads to slightly higher DCS and internal RH after 4 weeks of exposure (Tables 10 and 11). This statement is not true for the internal RH of test series exposed to 60°C, where wrapped and unwrapped prisms obtain equal RH values. At the end of the ASR exposure, the wrapped 38°C test series still have roughly 1-1.5 % higher DCS and 0.5-1 % higher internal RH compared with the unwrapped prisms. However, due to the considerably higher expansion for unwrapped prisms exposed to 60°C compared with corresponding wrapped prisms, the unwrapped prisms generally reveal slightly higher evaporable water content and internal RH at the end of the exposure period.

At both exposure temperatures, the relative diffusion coefficients measured after 4 weeks of exposure are generally slightly lower for wrapped prisms compared with corresponding unwrapped prisms (Table 14). For the 38°C test series, this could be partly due to later exposure of wrapped prisms to elevated temperature (7 days versus 1 day). For the 60°C test series, the slightly lower expansion for the wrapped prisms after 4 weeks of exposure might be one of the reasons for this observation.

4.4 Influence of "ASR exposure conditions" and prism size

Temperature is the "exposure parameter" confirmed to have the highest impact on the internal moisture state and the transport properties of concrete. The prism size can also significantly influence the internal moisture state. For both parameters, the influence depends on the binder composition (see later in Section 4.5).

Generally for CEM I binders, exposure to 60°C leads to considerably higher water absorption in the first weeks of exposure compared with corresponding test series exposed to 38°C (Figure 6). The increased water uptake when the temperature raises is assumed to be mainly caused by the following two reasons: 1) Some of the 60°C test series have already started to expand somewhat after 4 weeks of exposure (up to 0.03 %), leading to suction of water into micro-cracks and ASR-gel; 2) As a rule, the relative diffusion coefficient increases with increasing exposure temperature (Section 3.4.2), because a coarser pore structure is produced at elevated temperature [9], making ingress of water easier. Additionally, the degree of hydration is assumed to be higher for the 60°C test series after 4 weeks of exposure, in particular for the "dense" binder, leading to sorption of slightly more water.

Somewhat surprisingly, the increased water uptake for the 60°C test series does not lead to increased evaporable water content or increased DCS after 4 weeks of exposure, implying that the water has been bound chemically. However, the internal RH is significantly higher for the test series exposed to 60°C. This RH-increase is probably primarily related to the coarsening of the pore structure produced by the elevated temperature as follows from the Kelvin-La Place equation giving the relation between pore sizes and RH, and as shown for cement pastes by Bray and Sellevold [9]. The denser the binder is, the more is the internal RH influenced. For the low w/c (0.30) CEM I binder, the test series exposed to 60°C reveal 4.5-8.5 % higher internal RH after 4 weeks of exposure compared with corresponding test series exposed to 38°C. For w/c of 0.45 and 0.60, the difference is in the range of 0.5-2.0 %. As discussed in paper IV, these differences in RH measured at 20°C after cooling the prisms will be even greater during the ASR exposure when the temperature is elevated to 38 and 60°C, respectively.

A similar influence of the exposure temperature is not observed for the test series with the "fly ash" binder, in which prism water uptake, evaporable water content, DCS and internal RH seems to be more or less independent of test method and exposure temperature, provided similar pre-storage at 20°C. One reason could be that the relative diffusion coefficient for the "fly ash" concrete seems to decrease with increasing exposure temperature (in contrast to the case for the CEM I binders), probably due to increased reaction of the fly ash and densification of the material for this reason.

At the end of the ASR exposure, the total prism water uptake and the internal moisture state is to a high extent influenced by the extent of ASR. It is thus difficult to separately point out the influence of the exposure temperature on the internal moisture state of the concrete, because other parameters such as the extent of alkali leaching also influence the results. The most marked differences should, however, be mentioned: Test series with the "dense" CEM I binder (w/c of 0.30) exposed to 38°C still reveals a considerably lower internal RH compared with test series exposed to 60°C, presumably due to a finer pore structure (leading to considerably lower relative diffusion coefficients – Section 3.4.2). The "fly ash" test series exposed to 60°C absorb considerably more water during the exposure period compared with the corresponding test series exposed to 38°C, most likely due to significantly higher ASR gel formation and prism expansion (and maybe also due to slightly higher degree of pozzolanic reaction). Additionally, the hydration products may be slightly different for concrete stored at 38°C compared with concrete stored at 60°C, as shown by De Weerdt and Justnes for the storage temperatures 38 and 80°C [10]. Finally, it should be remarked that the electrical resistivity is generally highest for the "fly ash" test series exposed to 60°C compared with 38°C exposure (Figure 14). The deviation is assumed to be connected to alkali leaching (higher extent of alkali leaching increases the electrical resistivity) and increased degree of pozzolanic reaction (Section 3.4.3).

In general for CEM I binders, the larger Norwegian prisms (100x100 mm) absorb less water per m^3 of concrete in the first weeks of exposure compared with the smaller (70x70 mm) ASTM prisms (Figures 6 and 7), indicating that the interior of the larger prisms have less access to water. Furthermore for the "dense" binder, the larger Norwegian prisms reveal slightly lower evaporable water content (0.4 mass-%) and a significantly lower internal RH (roughly 3.5 %) after 4 weeks of exposure compared with the smaller ASTM prisms. An internal moisture gradient (for DCS and RH) is evident in the larger Norwegian prisms (Figures 11). The RH gradient is most pronounced for the low w/c CEM I binder. For this "dense" binder, DCS and RH in the interior of the large Norwegian prism is equal to DCS and RH of sealed samples stored in airtight plastic bottles at 20°C until age 11-16 weeks (Figure 11).

At the end of the exposure period, both prism sizes reveal comparable internal moisture content. A substantial RH gradient is still observed in the Norwegian concrete prisms for the "dense" CEM I binder and the "fly ash" binder, see Figure 12 *(Comment: Such measurements were not performed for the 70x70 mm prisms*). For both binders, the RH gradient is higher than the corresponding gradients after 4 weeks of exposure. DCS is also slightly higher in the outer part of the prisms with these two binders compared with the interior. If one assumes that most alkalis are leached out from the outer part of the prisms, the lower ion concentration in the pore water in the outer part might have contributed to the observed RH gradient.

As expected, the extreme environments "sealed prisms" and "submerged prisms" (Table 4) significantly influence the prism water uptake at all ages by reducing and increasing it, respectively. All practical cases fall in between.

4.5 Influence of binder composition (w/c and addition of fly ash)

As expected, the concrete suction porosity, water absorption, internal moisture state and transport properties are strongly dependent on the nature of the binder, i.e. w/cm and binder composition. The impact of various "pre-treatment conditions" and "ASR exposure conditions" on these concrete properties also depend on the binder (comprehensively discussed in paper IV (section 3) and above in section 4.3 and 4.4). However, as stated previously, later in the ASR exposure period the extent of ASR and thus the extent of internal cracking become of more importance for these concrete properties.

Only minor differences in degree of capillary saturation (DCS) between the various binders were observed. Two other important concrete properties for initiation and progress of ASR, internal RH and relative diffusion coefficient, do however show substantially differences between various binders. The same is observed for the available (evaporable) water content.

Of the CEM I test series, those with the "dense" binder (w/c of 0.30) have, as expected, substantially lower suction porosity (i.e. far less capillary pores), evaporable water content and relative diffusion coefficient compared with the test series with higher w/c (0.45 and 0.60). Furthermore, the electrical resistivity is much higher. One of the most important differences between the CEM I binders is thought to be that the internal RH is much lower in prisms with the "dense" binder, primarily due to highest extent of self-desiccation and resistance to water uptake (maybe also partly due to a higher concentration of ion in the pore water). After 4 weeks of exposure, RH ranges from about 82-85 % for the 38°C "dense" binder test series and in the range of 90-92 % for corresponding test series exposed to 60°C (Figure 9). Corresponding values at the end of the exposure period is approximately 85-90 % (38°C) and 92-95 % (60°C) (Figure 10).

On the other hand, the internal RH in the test series with the CEM I binders with higher w/c (0.45 or 0.60) is always higher than 90 % after 4 weeks of exposure to both temperatures, the majority in the range of 93.5-96 % (Figure 9). Corresponding values at the end of the exposure period are in the range of 95.5-98 % (Figure 10).

Several important concrete properties of the test series with the "fly ash" binder deviate from the CEM I test series. Firstly, the relative diffusion coefficients (RelD) after 4 weeks of exposure varies far less (in the range of 0.4 to 0.6) compared with the values for the CEM I "basis" binder with equal w/cm (in the range of 0.5-4.1). In other words, the "fly ash" binder is more "robust" against any changes in specimen pre-treatment and exposure conditions compared with the CEM I "basis" binder. This is also noticeable on the water absorption and internal moisture state. For the "fly ash" test series, the prism water uptake, evaporable water content, DCS and internal RH seems to be more or less independent of test method and exposure temperature. One reason could be that the relative diffusion coefficient seems to decrease with increasing exposure temperature. Secondly, the addition of approximately 20 % of fly ash to the cement considerably reduces the "permeability" of the concrete (measured as lower RelD and higher electrical resistivity). This contributes to the generally lower water absorption by concrete prisms with the "fly ash" binder compared with prisms with the CEM I binders. Additionally, hydration products incorporating fly ash will most likely bind less water than hydration products of pure OPC, [11] and [12]. Thirdly, the internal RH is considerably lower in the "fly ash" test series compared with CEM I test series with equal w/cm. For the "fly ash" binder, RH varies in the range of 83-88.5 % for test series exposed to 38°C and in the range of 88-89 % for test series exposed to 60°C. Fourthly, the general increase in RH seen for the CEM I binders during the ASR exposure is not observed for the "fly ash" binder. On the contrary, the internal RH decreases (up to 4.5 %) for most of the "fly ash" test series.

To sum up: It is likely that the rather low RH found for the "dense" binder and probably also for the "fly ash" binder after 4 weeks of exposure contributes together with the measured lower relative diffusion coefficients to reduce the rate and extent of ASR. This is particularly true for the test series exposed to 38°C (further discussed in paper V). For all test series with the CEM I binders with higher w/c (0.45 or 0.60), RH is regarded to be sufficient for ASR to initiate. Thus, it appears that for these binders all the pre-treatments and test procedures provide sufficient moisture contents for ASR to proceed.

Dynamic E-modulus

The Figures 3-1 and 3-2 show the dynamic E-modulus for unwrapped test series with the ASTM C1293 CPT, the RILEM AAR-3 CPT and the RILEM AAR-4.1 CPT. Corresponding results for the Norwegian CPT test series is given in the thesis, section 5.3.3, Figure 6.

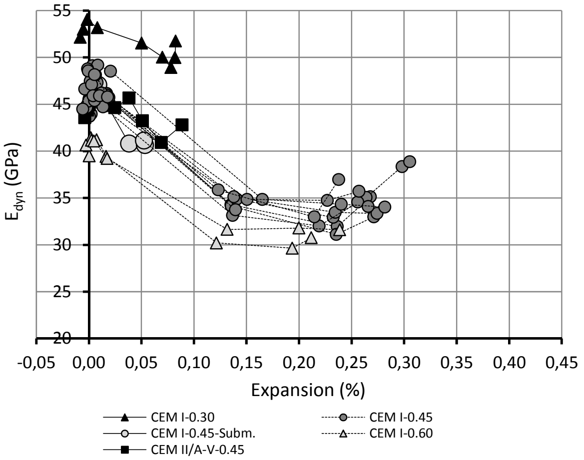

Figure 3-1 Dynamic E-modulus for the test series with the ASTM C1293 CPT and two unwrapped AAR-3 test series. (The first measurements were performed after two weeks of exposure. The abbreviations for the various test series are given in the Tables 5-8 in paper IV.)

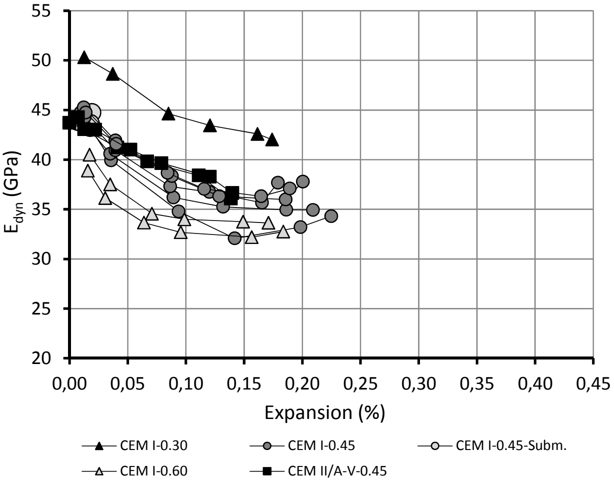

Figure 3-2 Dynamic E-modulus for the unwrapped test series with the AAR-4.1 CPT. (The first measurements were performed after two weeks of exposure. The abbreviations for the various test series are given in the Tables 5-8 in paper IV.)

Relative diffusion coefficient: Results from supplementary test procedures

The values for the relative diffusion coefficient (RelD) calculated based on slowly drying at 20°C (Appendix 2, Eq. 6) are presented in paper IV, Table 14, section 3.4.2. The results from the measurements and calculations performed according to the supplementary procedures described in Appendix 2 are presented in the Tables 3-4 to 3-6 (Table 3-4 includes the results presented in paper IV, while Table 3-5 represents drying at 50°C).

With a few exceptions, the different calculation procedures based on drying at 20°C give similar internal ranking of the relative diffusion coefficients for the various test series. Comparable results were also obtained when one "PF-sample" from each test series was dried in a drying cabinet at 50°C for 6 months (see Appendix 2).

However, slowly drying at 20°C and calculation according to Eq. 6 in Appendix 2 gives slightly more consistent results with respect to expected ranking between the "open" and "dense" CEM I binders tested according to similar exposure conditions, in addition to have the lowest internal spread between parallel test series. For this reason, only results from this procedure were included in paper IV.

Table 3-4: Relative diffusion coefficient (RelD) – dried at 20°C - calculated according to Eg. 6 and Eq. 7 (see Appendix 2). (Comment: The two test series in brackets are epoxy coated on the side faces, and thus reveal lower RelD than comparable test series).

Relative diffusion coefficients (**Reference** = mean of seven ASTM samples of the basis binder (in **bold**). Drying temp. = 20°C)										
Test series	$RelD_{c/2}$	$RelD_{c/4}$	Test series	$RelD_{c/2}$	$RelD_{c/4}$	Test series	$RelD_{c/2}$	$RelD_{c/4}$	Test series	$RelD_{c/2}$
4.1-U-A-0.45-1-S-1c	3.75	2.13	3.1-W-B-0.45-3-N-7c	0.70	0.82	**ASTM-U-A-0.45-1-N-1c**	**1.10**	**0.98**	N.1-U-A-0.45-3-S-1c	0.52
	2.81	1.48	3.2-W-B-0.45-4-N-8	0.90	1.14	**ASTM-U-A-0.45-2- N-1c**	**0.96**	**0.91**		0.64
	4.09	2.04	3.3-W-C-0.45-4-N-8	0.98	1.09	**ASTM-U-A-0.45-3-N-1c**	**1.50**	**2.33**	N.2-U-A-0.45-1-S-2	0.73
4.2-U-A-0.45-1-S-2	3.46	1.96	3.4-W-B-0.45-4-S-8	0.80	0.96	**ASTM-U-A-0.45-4-N-1c**	**0.98**	**0.96**		0.92
4.3-U-A-0.45-6-S-8	2.37	1.58	3.5- -E-0.45-5-N-8	(0.46)	0.39	**ASTM-U-A-0.45-5-N-1c**	**0.76**	**0.72**	N.3-U-A-0.45-4-S-8	0.58
4.4-U-A-0.45-2-S-29	2.25	1.63	3.6-W-D-0.45-6-S-8	0.54	0.60	**ASTM-U-A-0.45-6-N-1c**	**1.22**	**1.32**	N.3-U-A-0.30-7-S-8	0.11
	2.05	1.40	3.7-U-A-0.45-6-S-8	0.85	0.89	**ASTM-U-A-0.45-10-N-1c**	**0.82**	**0.80**	N.3-U-A-0.60-8-S-8	0.78
4.5-U-A-0.45-2-S-8FT	1.22	0.75	3.8-W-B-0.45-3-S-2	0.82	1.75	ASTM-U-A-0.30-7-N-1c	0.27	0.44	N.3-U-A-FA-0.45-9-S-8	0.39
4.7- -E-0.45-5-N-8	(0.70)	0.47	3.9-W-B-0.45-2-S-29	0.69	1.00	ASTM-U-A-0.60-8-N-1c	1.50	1.04		
4.8-W-B-0.45-1-S-2	1.88	1.44	3.10-W-B-0.45-2-S-8FT	0.90	0.73	ASTM-U-A-0.60-11-N-1c	1.41	1.00		
4.8-W-B-0.45-10-S-2	1.29	1.26	3.10-W-B-0.45-10-S-8FT	1.15	1.04	ASTM-U-A-FA-0.45-9-N-1c	0.56	0.45		
4.9-W-B-0.45-5-S-8	1.32	0.65	3.11-U-F-0.45-5-S-8	0.71	0.47					
4.10-W-C-0.45-6-N-8	1.61	1.29	3.4-W-B-0.30-7-S-8	0.16	0.26					
4.11-W-D-0.45-3-S-8	1.32	1.11	3.4-W-B-0.60-8-S-8	0.98	0.53					
4.3-U-A-0.30-7-S-8	0.52	0.83	3.8-W-B-FA-0.45-9-S-2	0.60	0.53					
4.9-W-B-0.30-7-S-8	0.44	0.79	3.9-W-B-FA-0.45-9-S-29	0.41	0.33					
4.3-U-A-0.60-8-I- S-8	3.00	1.53								
4.3-U-A-0.60-8-II-S-8	3.00	1.17								
4.9-W-B-0.60-11-S-8	2.32	1.36								
4.2-U-A-FA-0.45-9-S-2	0.40	0.37								
4.4-U-A-FA-0.45-9-S-29	0.41	0.35								

Table 3-5: Relative diffusion coefficient (RelD) – dried at 50°C - calculated according to Eg. 2 (see Appendix 2). (Comment: The two test series in brackets are epoxy coated on the side faces, and thus reveal lower RelD than comparable test series).

Relative diffusion coefficients (**Reference** = mean of seven ASTM samples of the basis binder (in **bold**). Drying temp. = **50°C**)							
Test series	$RelD_{c/2}$	Test series	$RelD_{c/2}$	Test series	$RelD_{c/2}$	Test series	$RelD_{c/2}$
4.1-U-A-0.45-1-S-1c	--	3.1-W-B-0.45-3-N-7c	0.82	**ASTM-U-A-0.45-1-N-1c**	**--**	N.1-U-A-0.45-3-S-1c	0.93
	--	3.2-W-B-0.45-4-N-8	0.81	**ASTM-U-A-0.45-2- N-1c**	**--**		1.60
	--	3.3-W-C-0.45-4-N-8	0.66	**ASTM-U-A-0.45-3-N-1c**	**0.75**	N.2-U-A-0.45-1-S-2	--
4.2-U-A-0.45-1-S-2	--	3.4-W-B-0.45-4-S-8	0.84	**ASTM-U-A-0.45-4-N-1c**	**1.12**		1.12
4.3-U-A-0.45-6-S-8	1.98	3.5- -E-0.45-5-N-8	(0.42)	**ASTM-U-A-0.45-5-N-1c**	**1.20**	N.3-U-A-0.45-4-S-8	0.96
4.4-U-A-0.45-2-S-29	1.98	3.6-W-D-0.45-6-S-8	0.66	**ASTM-U-A-0.45-6-N-1c**	**1.08**	N.3-U-A-0.30-7-S-8	0.29
	1.24	3.7-U-A-0.45-6-S-8	0.75	**ASTM-U-A-0.45-10-N-1c**	**0.99**	N.3-U-A-0.60-8-S-8	1.05
4.5-U-A-0.45-2-S-8FT	--	3.8-W-B-0.45-3-S-2	0.86	ASTM-U-A-0.30-7-N-1c	0.56	N.3-U-A-FA-0.45-9-S-8	0.34
4.7- -E-0.45-5-N-8	(0.67)	3.9-W-B-0.45-2-S-29	0.71	ASTM-U-A-0.60-8-N-1c	1.98		
4.8-W-B-0.45-1-S-2	--	3.10-W-B-0.45-2-S-8FT	--	ASTM-U-A-0.60-11-N-1c	1.34		
4.8-W-B-0.45-10-S-2	2.69	3.10-W-B-0.45-10-S-8FT	0.70	ASTM-U-A-FA-0.45-9-N-1c	--		
4.9-W-B-0.45-5-S-8	0.88	3.11-U-F-0.45-5-S-8	0.69				
4.10-W-C-0.45-6-N-8	1.60	3.4-W-B-0.30-7-S-8	0.49				
4.11-W-D-0.45-3-S-8	1.46	3.4-W-B-0.60-8-S-8	2.24				
4.3-U-A-0.30-7-S-8	0.47	3.8-W-B-FA-0.45-9-S-2	--				
4.9-W-B-0.30-7-S-8	0.34	3.9-W-B-FA-0.45-9-S-29	0.34				
4.3-U-A-0.60-8-I- S-8	1.12						
4.3-U-A-0.60-8-II-S-8	3.73						
4.9-W-B-0.60-11-S-8	1.68						
4.2-U-A-FA-0.45-9-S-2	--						
4.4-U-A-FA-0.45-9-S-29	0.36						

"--" = Due to a technical fault, the temperature in the drying cabinet was too low during the first days of drying. Thus, these results are discarded.

Table 3-6: Relative diffusion coefficient (RelD) – dried at 20°C - calculated according to Eg. 8 (see Appendix 2). (Comment: The two test series in brackets are epoxy coated on the side faces, and thus reveal lower RelD than comparable test series).

Relative diffusion coefficients (Calculated based on drying at 20°C to a certain *water loss* – see Appendix 2, Eq. 8). **Reference** = drying time for the ASTM test series; one reference for each binder type - in **bold** (the Norwegian CPT uses the two N.1 samples as reference)										
Test series	RelD		Test series	RelD		Test series	RelD		Test series	RelD
Water loss (g/cm^2):	*0.020*	*0.025*	*Water loss (g/cm^2):*	*0.020*	*0.025*	*Water loss (g/cm^2):*	*0.020*	*0.025*	*Water loss (g/cm^2):*	*0.018*
4.1-U-A-0.45-1-S-1c	5,42	6,89	3.1-W-B-0.45-3-N-7c	0,93	0,89	**ASTM-U-A-0.45-1-N-1c**	**1,05**	**1,16**	**N.1-U-A-0.45-3-S-1c**	**0,92**
	3,98	4,86	3.2-W-B-0.45-4-N-8	0,85	0,82	**ASTM-U-A-0.45-2-N-1c**	**0,75**	**0,83**		**1,10**
	4,35	5,12	3.3-W-C-0.45-4-N-8	0,99	0,90	**ASTM-U-A-0.45-3-N-1c**	**2,17**	**1,13**	N.2-U-A-0.45-1-S-2	0,81
4.2-U-A-0.45-1-S-2	6,08	7,51	3.4-W-B-0.45-4-S-8	0,84	0,87	**ASTM-U-A-0.45-4-N-1c**	**0,82**	**0,84**		1,02
4.3-U-A-0.45-6-S-8	4,09	4,62	3.5- -E-0.45-5-N-8	(0,59)	(0,57)	**ASTM-U-A-0.45-5-N-1c**	**1,09**	**1,16**	N.3-U-A-0.45-4-S-8	0,71
4.4-U-A-0.45-2-S-29	3,53	3,85	3.6-W-D-0.45-6-S-8	0,76	0,82	**ASTM-U-A-0.45-6-N-1c**	**1,20**	**1,27**		
	3,53	3,93	3.7-U -A-0.45-6-S-8	0,78	0,83	**ASTM-U-A-0.45-10-N-1c**	**0,79**	**0,82**		
4.5-U-A-0.45-2-S-8FT	1,69	2,40	3.8-W-B-0.45-3-S-2	2,50	1,15	Water loss (g/cm^2):	0.015	--		
4.7- -E-0.45-5-N-8	(1,24)	(1,72)	3.9-W-B-0.45-2-S-29	0,82	0,71	**ASTM-U-A-0.30-7-N-1c**	**1,00**	--		
4.8-W-B-0.45-1-S-2	3,83	4,30	3.10-W-B-0.45-2-S-8FT	1,20	1,59	*Water loss (g/cm^2):*	*0.030*	--		
4.8-W-B-0.45-10-S-2	3,90	4,62	3.10-W-B-0.45-10-S-8FT	1,86	2,14	**ASTM-U-A-0.60-8-N-1c**	**1,07**	--		
4.9-W-B-0.45-5-S-8	1,75	2,44	3.11-U -F-0.45-5-S-8	0,80	0,86	**ASTM-U-A-0.60-11-N-1c**	**0,94**	--		
4.10-W-C-0.45-6-N-8	3,27	3,93	*Water loss (g/cm^2):*	*0.015*	--	*Water loss (g/cm^2):*	*0.020*	*0.025*		
4.11-W-D-0.45-3-S-8	2,66	2,99	3.4-W-B-0.30-7-S-8	0,57	--	**ASTM-U-A-FA-0.45-9-N-1c**	**1,00**	**1,00**		
Water loss (g/cm^2):	*0.015*	--	*Water loss (g/cm^2):*	*0.030*	--					
4.3-U-A-0.30-7-S-8	5,57	--	3.4-W-B-0.60-8-S-8	0,70	--					
4.9-W-B-0.30-7- S-8	3,33	--	*Water loss (g/cm^2):*	*0.020*	*0.025*					
Water loss (g/cm^2):	*0.030*	--	3.8-W-B-FA-0.45-9-S-2	1,03	0,99					
4.3-U-A-0.60-8-I-S-8	2,20	--	3.9-W-B-FA-0.45-9-S-29	0,82	0,83					
4.3-U-A-0.60-8-II-S-8	1,67	--								
4.9-W-B-0.60-11-S-8	1,94	--								
Water loss (g/cm^2):	*0.020*	*0.025*								
4.2-U-A-FA-0.45-9-S-2	1,10	1,06								
4.4-U-A-FA-0.45-9-S-29	1,12	1,08								

Electrical resistivity: Results from supplementary test procedures

The results from measurements of electrical resistivity according to the three procedures described in Appendix 2 are given in the Tables 3-7 -- 3-10.

Table 3-7: Electrical resistivity (Ω) after 52 weeks of exposure of the RILEM AAR-3 test series (for abbreviations, see paper IV, Table 5).

Test series	I: Whole prism ("in-situ")	II: "PF-samples" ("in-situ")		III: "PF-samples" ("wet")	
	Ω (ohm·m)	Ω[1] (ohm·m)	c.o.v. (%)	Ω[1] (ohm·m)	c.o.v. (%)
3.1-W-B-0.45-3- N-7c	58	88	0.6	112	0.3
3.2-W-B-0.45-4- N-8	60	84	9.9	122	1.9
3.3-W-C-0.45-4- N-8	73	106	6.9	123	1.7
3.4-W-B-0.45-4- S-8	60	84	5.7	118	1.0
3.5- -E-0.45-5- N-8	1093	746	1.3	275	11.0
3.6-W-D-0.45-6- S-8	67	100	8.9	133	4.6
3.7-U -A-0.45-6- S-8	70	101	2.6	120	3.1
3.8-W-B-0.45-3- S-2	59	82	1.5	116	4.9
3.9-W-B-0.45-2- S-29	66	97	0.6	133	4.5
3.10-W-B-0.45-2- S-8FT	59	--	--	115	4.8
3.10-W-B-0.45-10- S-8FT	53	81	2.7	131	0.2
3.11-U -F-0.45-5- S-8	110	159	0.5	173	2.2
3.12-W-G-0.45-12- S-8	84	103	6.3	143	9.7
3.13-W-H-0.45-12- S-8	73	107	3.3	146	2.3
3.4-W-B-0.30-7- S-8	127	166	1.6	242	0.7
3.4-W-B-0.60-8- S-8	45	73	7.3	104	9.9
3.8-W-B-FA-0.45-9-S-2	435	--	--	663	4.9
3.9-W-B-FA-0.45-9-S-29	328	595	2.7	600	0.8

[1] Mean of two parallel samples

Table 3-8: Electrical resistivity (Ω) after 39 weeks of exposure of the RILEM AAR-4.1 test series (for abbreviations, see paper IV, Table 6).

Test series	I: Whole prism ("in-situ")	III: "PF-samples" ("wet")	
	Ω (ohm·m)	Ω[1] (ohm·m)	c.o.v. (%)
4.1-U -A-0.45-1- S-1c	87	139	5.8
4.2-U -A-0.45-1- S-2	98	146	2.5
4.3-U -A-0.45-6- S-8	104	141	3.9
4.4-U -A-0.45-2- S-29	106	152	2.0
4.5-U -A-0.45-2- S-8FT	97	159	6.4
4.6-U -F-0.45-5- S-8	158	230	3.8
4.7- -E-0.45-5- N-8	231	212	4.6
4.8-W-B-0.45-1- S-2	115	224	8.0
4.8-W-B-0.45-10- S-2	126	238	2.0
4.9-W-B-0.45-5- S-8	118	236	3.0
4.10-W-C-0.45-6- N-8	127	180	5.3
4.10-W-C-0.45-12- N-8	138	222	0.6
4.11-W-D-0.45-3- S-8	142	233	5.6
4.12-W-G-0.45-12- S-8	111	206	0.1
4.13-W-H-0.45-12- S-8	132	252	5.7
4.3-U -A-0.30-7- S-8	192	314	13.2
4.9-W-B-0.30-7- S-8	337	451	2.7
4.3-U -A-0.60-8-I S-8	72	115	6.9
4.3-U -A-0.60-8-II S-8	67	110	2.5
4.9-W-B-0.60-11- S-8	76	178	4.0
4.2-U -A-FA-0.45-9-S-2	637	938	1.2
4.4-U -A-FA-0.45-9-S-29	539	719	12.9

[1] Mean of two parallel samples

Table 3-9: Electrical resistivity (Ω) after 52 weeks of exposure of the Norwegian test series (for abbreviations, see paper IV, Table 7).

Test series	I: Whole prism ("in-situ")	II: "PF-samples" ("in-situ")		III: "PF-samples" ("wet")	
	Ω	Ω[1]	c.o.v.	Ω[1]	c.o.v.
N.1-U- A-0.45-3- S-1c	63	99	2.7	115	9.8
N.2-U- A-0.45-1- S-2	57	--	--	106	0.9
N.3-U- A-0.45-4- S-8	58	94	10.2	106	1.6
N.3-U- A-0.30-7- S-8	165	284	13.2	280	0.0
N.3-U- A-0.60-8- S-8	41	71	11.4	85	1.6
N.3-U- A-FA-0.45-9-S-8	486	--	--	548	27.2

[1] Mean of two parallel samples

Table 3-10: Electrical resistivity (Ω) after 52 weeks of exposure ASTM test series (for abbreviations, see paper IV, Table 8).

Test series	I: Whole prism ("in-situ")	II: "PF-samples" ("in-situ")		III: "PF-samples" ("wet")	
	Ω	Ω[1]	c.o.v.	Ω[1]	c.o.v.
ASTM-U-A-0.45-1- N-1c	67	--	--	108	0.4
ASTM-U-A-0.45-2- N-1c	63	--	--	114	2.9
ASTM-U-A-0.45-3- N-1c	68	99	2.0	112	1.5
ASTM-U-A-0.45-4- N-1c	71	--	--	118	2.0
ASTM-U-A-0.45-5- N-1c	78	117	0.4	121	7.6
ASTM-U-A-0.45-6- N-1c	67	97	3.5	111	6.2
ASTM-U-A-0.45-10- N-1c	60	88	1.3	123	4.7
ASTM-U-A-0.45-12- N-1c	69	100	5.4	121	4.1
ASTM-U-A-0.30-7- N-1c	177	219	0.4	243	0.8
ASTM-U-A-0.60-8- N-1c	53	--	--	88	0.8
ASTM-U-A-0.60-11- N-1c	48	70	3.4	91	1.1
ASTM-U-A-FA-0.45-9-N-1c	492	--	--	699	0.0

[1] Mean of two parallel samples

In general, the electrical resistivity measured on whole prisms with "in-situ" moisture state ("Procedure I"; the results are included in paper IV, section 3.4.3) is in the range 20-45 % lower than the corresponding results after splitting the prisms into several "PF-samples" ("Procedure II"). The main reason for this is that the calculated electrical resistivity over the cross section of the whole prisms is lower than the "true" electrical resistivity, since some current can be transported through the concrete prisms outside the 100 mm zone used in the calculations (see procedure described in Appendix 2). How much depends somewhat on the concrete properties. Additionally, applying the mean thickness of the "PF-samples" in the calculations (see Appendix 2) is a simplification that might influence the results significantly if the shape of the "PF-samples" varies over the cross section, since the measured electrical resistance (R) depends on the minimum thickness of the sample, not only the mean thickness. For a sample with a marked thinner mid part, the calculated electrical resistivity will be higher compared with a sample with equal mean thickness but with a more uniform thickness over the cross section. Despite these uncertainties, the internal ranking between the test series is in general similar for measurements performed on whole prisms and on split "PF-samples".

Furthermore, the electrical resistivity measured on "PF-samples" after 7 days of submersion in water ("Procedure III") is on average about 20 % higher (ranging from 0-60 %) than the corresponding results measured before submersion ("Procedure II"). However, the correlation between the two procedures is very good: R^2 for the trend line is 0.98 when the sealed test series are excluded. The observed increase in the electrical resistivity after submersion is somewhat surprising, since DCS will increase to 100 % during the 7 days submersion period and previous results have shown that the electrical resistivity decreases with increasing DCS [13]. This is due to a more continuous water phase after submersion. One implication of the measured increase in the electrical resistivity might be that the internal cracks induced by ASR (partly filled with ASR gel) do not form a continuous water phase through the samples. On the other hand, the electrical resistivity also strongly depends on the type and amount of ions dissolved in the pore water. During the 7 days submersion period in water many ions will leach out from the concrete samples, leading to increased electrical resistivity. In other words, the results strongly indicate that the reduced content of ions in the concrete pore water due to alkali leaching has higher influence on the electrical resistivity than the slightly increased DCS. However, the extent of alkali leaching is assumed to depend on the binder composition. The increase in electrical resistivity during the 7 days submersion in water is thus expected to be less for the "fly ash" binder and the "dense" binder. The revealed results confirm this assumption.

Supplementary comments to the "PF-measurements" and the DCS measurements

Suction porosity and air (macro) porosity

The standard procedure in the "PF-method" [14] (paper IV, section 2.4.2) is to calculate the suction porosity based on the water suction after drying at 105°C. Normally this suction porosity is slightly lower than the suction porosity calculated before drying the samples. The reason is believed to be that drying induces micro-cracks and slightly coarsen the pore structure of the cement paste. However, in the measurements performed on the "PF-samples" split from the ASR exposed prisms, the mean difference between the suction porosities measured before and after drying was on average about 0.3 % higher at the end of the ASR exposure compared with the measurements after 4 weeks of exposure. The main reason for this can be that ASR gel developed during the ASR exposure will absorb water when the "PF-samples" are submerged in water for one week (before drying the samples), and thus "be part of" the measured suction porosity. After drying, the ASR gel is not able to suck as much water as before drying. The result is that the "PF-samples" at the end of the ASR exposure have an apparent lower measured suction porosity after drying. Furthermore, the change in the suction porosity in the period beyond 4 weeks of exposure will be "apparently" lower compared with the results obtained if the data before drying the samples are used in calculations.

The suction porosities presented in paper IV are based on both "calculation procedures"; the results in Figure 4 are based on the values measured before drying the samples, while the detailed values for the suction porosities and the macro porosities given in the Tables 10-13 are calculated based on measurements after drying the samples.

For the two CEM I binders with highest w/c, the macro porosity (normally taken directly as the air content) in hardened concrete after 4 weeks of exposure is in general lower than the measured air content for the fresh concrete; on average 1.0 vol-% for the "open" binder and 0.7 vol-% for the "basis" binder. Of course some air is normally lost during transport, placement and compaction of the concrete. For the two remaining less permeable binders the deviations were almost negligible, in the range of -0.2 to 0.2 vol-%. The present differences are well within expected differences for independent methods. Similar differences were found by Sellevold and Farstad [14]; for 31 concretes with binder qualities in the same range as the test series in this paper, the measured fresh air contents were on average 0.5 to 1.0 vol-% higher than the air content measured in the "PF-method".

DCS over the prism height

To be able to document any changes in concrete properties over the prism height, each prism was always stored vertically in the storage container with the same prism end facing upwards during the whole ASR exposure period (as discussed in paper IV, section 3.3). Generally, no important differences in internal moisture state are recorded over the prism height. A few minor exceptions could though be mentioned: On average after 4 weeks of exposure, DCS is marginally higher in the bottom part of the wrapped 38°C prisms compared with the mid and upper part. Opposite, for the unwrapped 70x70x280 mm prisms stored at 38°C and 60°C, DCS is on average 0.5 % lower in the bottom part compared with the mid and upper part.

In the end of the ASR exposure period, the evaporable water content and DCS is on average approximately 0.5 %-point higher in the bottom part of the larger Norwegian concrete prisms compared with the mid and upper part. Finally, for the unwrapped 60°C RILEM AAR-4.1 prisms, DCS is on average roughly 1 % higher in the bottom part compared with the upper part. The latter could be connected to a higher extent of alkali leaching in the top part (see paper V), leading to less extent of ASR-gel that sucks water and thus increase the evaporable water content.

Statistical analysis

In order to document if the measured differences in prism expansion between various test series are statistically significant, all the expansion results are treated statistically as briefly described in paper V, section 3.3.3.

A more detailed description of the statistically analyses performed and the corresponding detailed results are given in the following (*comment: all these analyses are performed by one of the co-authors of paper V, Özge Andiç-Çakır from Ege University in Izmir, Turkey*):

<u>Coefficient of variations calculated for the various concrete prism tests are discussed in paper V</u> (section 3.3.3). Additional statistical analyses were performed in accordance to the methods described below, extracted from [15] and [16]. Statistical hypothesis testing is used in the statistical data analysis stage of comparative experiments, i.e. testing the equality of the mean of two different data series. Hypothesis testing procedures rely on using the information in a random sample from the population of interest. If this information is consistent with the hypothesis, the hypothesis will not be rejected. However, if this information is inconsistent with the hypothesis, the hypothesis can be rejected. The structure of hypothesis testing will be formulated with the use of the term *null hypothesis*, denoted by H_o. The rejection of H_o leads to the acceptance of an *alternative hypothesis*, denoted by H_1.

It should be emphasized that the truth or falsity of a particular hypothesis can never be known with certainty, because it is impossible to observe the whole population in most engineering cases. Rejecting the null hypothesis when it is true is defined as a type I error and its probability value is denoted by α. One way to report the result of a hypothesis test is to state that the null hypothesis to be rejected or not to be rejected at a specified α value. The other way is the P-value approach; the P-value is the smallest level of significance that would lead to rejection of the null hypothesis H_o with the given data. In constructing the hypothesis, the null hypothesis is always stated by equality, while, the alternate hypothesis might either be one-sided or two-sided. If the objective is to make a claim involving statements such as greater than or less than, one-sided alternative is appropriate. If no direction is implied by the claim, then the two-sided alternative is used.

For testing the equality of the mean of two different data series, A and B, the two-sided test hypothesis will become: H_o: $\mu_A = \mu_B$ and H_o: $\mu_A \neq \mu_B$. At the end of the hypothesis testing, i.e. t-test, two conclusions may be drawn: Either "Reject H_o: in favor of H_1 because of sufficient evidence in the data" or "Fail to reject H_o: because of insufficient evidence in the data". Note that the above conclusions do not involve a formal and literal “accept H_o”. The hypothesis testing is based on two *levels* of an experiment, where by using one-way ANOVA, more than two levels of a single factor can be compared.

In the present study, two sided t-test was used for the evaluation of two unpaired test series, assuming both populations are normally distributed and assuming equal variances (verified by f-test). For the tested series, if the inequality of variance is assumed, the p-values increase but the test results do not change. Unpaired tests are used if the data points do not match or the group of sample in question is tested twice, e.g. before-after treatment. In this study, the groups tested are completely different test series, not pairs. Due to the nature of experimental procedure, three specimens (n: 3) can be cast and cured for each mixture. Low number of specimens per test series seem to be a drawback for statistical analysis, however, the sample size was tried to be increased by including the available parallel test series expansion results. Prior to this, the equality of the mean of parallel test series was also tested (either by t-test or ANOVA). <u>The mean of *all* parallel test series cast in this study was found to be equal to each other at *all* ages.</u>

For this experimental study, all the eight test series cast and cured according to the ASTM C1293 CPT having w/c ratio of 0.45 ("basis" binder) reveal practically identical expansion after 52 weeks; the mean values ranging from 0.254 to 0.279% (paper V, Figure 11). In order to test the equality of mean expansion for these eight series, one-way ANOVA was performed. The difference between mean of the eight ASTM test series were found insignificant with a p-value of 0.5384; The difference between two mean values is considered significant if the p value is smaller than the chosen α value: 0.05. The mean of these eight series were used as the mean of the ASTM “basis” binder test expansion value for the following statistical tests performed – see the Tables 3-11, 3-12 and 3-13.

Table 3-11 Hypothesis test results for the 38°C CPT series. For abbreviations, see paper IV, Tables 5-8.

ASTM C1293 CPT (@52 weeks)		
Test Hypothesis (two-sided)	P-value	Comment*
$\mu_{ASTM1} = \mu_{ASTM2} = \mu_{ASTM3} = \mu_{ASTM4} = \mu_{ASTM5} = \mu_{ASTM6} = \mu_{ASTM10} = \mu_{ASTM12}$	0.538428	INSIGNIFICANT
$\mu_{ASTM1-6\&10\&12} = \mu_{ASTM0.30}$	4.85E-10	SIGNIFICANT
$\mu_{ASTM0.60-8} = \mu_{ASTM\ 0.60-11}$	0.17665	INSIGNIFICANT
$\mu_{ASTM1-6\&10\&12} = \mu_{ASTM0.60-8\&0.60-11}$	0.002576	SIGNIFICANT
$\mu_{ASTM1-6\&10\&12} = \mu_{ASTMFA0.45}$	1.33E-13	SIGNIFICANT
NORWEGIAN CPT (@52 weeks)		
Test Hypothesis (two-sided)	P-value	Comment*
$\mu_{N1-0.45} = \mu_{N2-0.45}$	0.51399065	INSIGNIFICANT
$\mu_{N1-0.45} = \mu_{N3-0.45}$	0.04858807	SIGNIFICANT
$\mu_{N2-0.45} = \mu_{N3-0.45}$	0.34597626	INSIGNIFICANT
$\mu_{N3-0.45} = \mu_{N3-0.30}$	0.00291008	SIGNIFICANT
$\mu_{N3-0.45} = \mu_{N3-0.60}$	0.19960707	INSIGNIFICANT
$\mu_{N3-0.45} = \mu_{N3-FA0.45}$	0.00206318	SIGNIFICANT
RILEM AAR- 3 CPT (@52 weeks)		
Test Hypothesis (two-sided)	P-value	Comment*
$\mu_{AAR3.1} = \mu_{AAR3.2}$	0.57846111	INSIGNIFICANT
$\mu_{AAR3.2} = \mu_{AAR3.3}$	0.02010381	SIGNIFICANT
$\mu_{AAR3.2} = \mu_{AAR3.4}$	0.17188231	INSIGNIFICANT
$\mu_{AAR3.2} = \mu_{AAR3.5}$	0.00039315	SIGNIFICANT
$\mu_{AAR3.4} = \mu_{AAR3.6}$	0.37201027	INSIGNIFICANT
$\mu_{AAR3.4} = \mu_{AAR3.7}$	0.07198399	INSIGNIFICANT
$\mu_{AAR3.4} = \mu_{AAR3.8}$	0.01999974	SIGNIFICANT
$\mu_{AAR3.4} = \mu_{AAR3.9}$	0.02001455	SIGNIFICANT
$\mu_{AAR3.8} = \mu_{AAR3.9}$	0.00321897	SIGNIFICANT
$\mu_{AAR3.10.2} = \mu_{AAR3.10.10}$**	0.77300508	INSIGNIFICANT
$\mu_{AAR3.4} = \mu_{AAR3.10.2\&3.10.10}$	0.88178739	INSIGNIFICANT
$\mu_{AAR3.4} = \mu_{AAR3.11}$	2.0066E-05	SIGNIFICANT
$\mu_{AAR3.4} = \mu_{AAR3.12}$	0.24641566	INSIGNIFICANT
$\mu_{AAR3.4} = \mu_{AAR3.13}$	0.42721516	INSIGNIFICANT
$\mu_{AAR3.4-0.45} = \mu_{AAR3.4-0.30}$	0.00105936	SIGNIFICANT
$\mu_{AAR3.4-0.45} = \mu_{AAR3.4-0.60}$	0.28859674	INSIGNIFICANT
$\mu_{AAR3.8FA} = \mu_{AAR3.9FA}$	0.01068493	SIGNIFICANT
$\mu_{AAR3.8FA} = \mu_{AAR3.9FA}$ (@112 weeks)	0.09588522	INSIGNIFICANT
$\mu_{AAR3.8} = \mu_{AAR3.8FA}$	4.9503E-06	SIGNIFICANT
$\mu_{AAR3.9} = \mu_{AAR3.9FA}$	0.00158437	SIGNIFICANT

* The difference between two mean values is considered significant if the p value is smaller than the chosen α value: 0.05.

** Two parallel test series

The following conclusions can be drawn from the analysis of unpaired test series (see Table 3-11):

ASTM C1293 CPT test results:

- Reducing w/c from 0.45 to 0.30 considerably reduces the expansion (ASTM 0.45 vs. ASTM 0.30; p-value: 4.85×10^{-10}).
- Increasing the w/c ratio from 0.45 to 0.60 seem to have an effect, but this effect is far less pronounced (ASTM 0.45 vs. ASTM 0.60; p-value: 0.0025).
- Adding FA to the binder considerably reduces the expansions (ASTM 0.45 vs. ASTM FA 0.45; p-value: 1.33×10^{-13}), even if the alkali content is increased considerably.

Norwegian CPT test results:

- Consistent with the ASTM test results, reducing w/c from 0.45 to 0.30 reduces the expansion (N3 0.45 vs. N3 0.30; p-value: 0.003). However, there is not enough proof for saying that altering w/c from 0.45 to 0.60 may change the expansion (N3 0.45 vs. N3 0.60; p-value: 0.1996).
- Adding FA to the binder considerably reduces the expansions (N3 0.45 vs. N3 FA 0.45; p-value: 0.002), even if the alkali content is increased considerably.

RILEM AAR-3 CPT test results:

- Adding less water to the cotton cloth wrapping affects the expansions (AAR 3.2 vs. AAR 3.3; p-value: 0.02).
- Sealed storage with no water access considerably reduces the expansion (AAR 3.2 vs. AAR 3.5; p-value: 0.0004).
- A pre-storage period of either 1-day or 28-days at 20°C alters the expansions; 1-day pre-storage increases and 28-day pre-storage decreases the expansions (AAR 3.4 vs. AAR 3.8; p-value: 0.0199 and AAR 3.4 vs. AAR 3.9; p-value: 0.02). There is a significant difference between the mean values of the series either pre-stored 1-day or 28-days at 20°C (AAR 3.8 vs. AAR 3.9, p-value: 0.0032).
- If the samples are submerged in deionized water continuously, this will considerably reduce the expansion (AAR 3.4 vs. AAR 3.11; p-value: 2x10-5).
- Similar to the Norwegian CPT results; reducing w/c from 0.45 to 0.30 considerably reduces the expansion (AAR 3.4-0.45 vs. AAR 3.4-0.30; p-value: 0.001), while there is not enough proof for saying that altering w/c ratio from 0.45 to 0.60 may change the expansion values (AAR 3.4-0.45 vs. AAR 3.4-0.60; p-value: 0.2886).
- After 52 weeks of exposure, there seems to be a significant difference between the mean values of FA incorporating samples cured for 1-day at 20°C versus 28-days at 20°C (AAR 3.8 FA vs. AAR 3.9 FA; p-value: 0.001). However, this difference seems to vanish after 112 weeks of exposure (AAR 3.8 FA vs. AAR 3.9 FA; p-value 0.0956). Obviously, there is a considerable difference between the expansion values of CEM I mixtures and FA incorporating ones measured at 52 weeks (AAR 3.8 vs. AAR 3.8 FA; p-value: 4.95 x 10-6 and AAR 3.9 vs. AAR 3.9 FA; p-value: 0.0016),), even if the alkali content is considerably increased for the FA mixes.

Table 3-12 Hypothesis test results for the 60°C RILEM AAR-4.1 CPT series.
For abbreviations, see paper IV, Tables 5-8.

RILEM AAR-4.1	13 weeks		26 weeks		39 weeks	
Test Hypothesis (two-sided)	P-value	Comment*	P-value	Comment*	P-value	Comment*
$\mu_{AAR4.1} = \mu_{AAR4.2}$	0.447515	INSIGNIFICANT	0.655301	INSIGNIFICANT	0.654179	INSIGNIFICANT
$\mu_{AAR4.2} = \mu_{AAR4.3}$	0.366956	INSIGNIFICANT	0.405679	INSIGNIFICANT	0.36836	INSIGNIFICANT
$\mu_{AAR4.3} = \mu_{AAR4.4}$	0.282238	INSIGNIFICANT	0.242377	INSIGNIFICANT	0.339177	INSIGNIFICANT
$\mu_{AAR4.3} = \mu_{AAR4.5}$	0.374642	INSIGNIFICANT	0.853354	INSIGNIFICANT	0.647754	INSIGNIFICANT
$\mu_{AAR4.3} = \mu_{AAR4.6}$	5.49E-05	SIGNIFICANT	0.000281	SIGNIFICANT	0.000591	SIGNIFICANT
$\mu_{AAR4.3} = \mu_{AAR4.7}$	0.004306	SIGNIFICANT	0.004845	SIGNIFICANT	0.005045	SIGNIFICANT
$\mu_{AAR4.8.1} = \mu_{AAR4.8.10}$ **	0.74274	INSIGNIFICANT	0.413663	INSIGNIFICANT	0.221764	INSIGNIFICANT
$\mu_{AAR4.8.1\&4.8.10} = \mu_{AAR4.2}$	6.59E-06	SIGNIFICANT	1.88E-05	SIGNIFICANT	5.1E-05	SIGNIFICANT
$\mu_{AAR4.8.1\&4.8.10} = \mu_{AAR4.9}$	0.26696	INSIGNIFICANT	0.399111	INSIGNIFICANT	0.663167	INSIGNIFICANT
$\mu_{AAR4.10.6} = \mu_{AAR4.10.12}$	0.39767	INSIGNIFICANT	0.516428	INSIGNIFICANT	---	----
$\mu_{AAR4.10.6\&4.10.12} = \mu_{AAR4.9}$	0.006809	SIGNIFICANT	0.007524	SIGNIFICANT	0.083702	INSIGNIFICANT
$\mu_{AAR4.9} = \mu_{AAR4.11}$	0.051694	INSIGNIFICANT	0.025392	SIGNIFICANT	0.030565	SIGNIFICANT
$\mu_{AAR4.9} = \mu_{AAR4.12}$	0.000124	SIGNIFICANT	1.75E-05	SIGNIFICANT	3.12E-05	SIGNIFICANT
$\mu_{AAR4.9} = \mu_{AAR4.13}$	0.103893	INSIGNIFICANT	0.164153	INSIGNIFICANT	0.224112	INSIGNIFICANT
$\mu_{AAR4.3\text{-}0.30} = \mu_{AAR4.9\text{-}0.30}$	0.000295	SIGNIFICANT	0.000118	SIGNIFICANT	0.000186	SIGNIFICANT
$\mu_{AAR4.3\text{-}0.45} = \mu_{AAR4.3\text{-}0.30}$	0.930037	INSIGNIFICANT	0.710334	INSIGNIFICANT	0.736977	INSIGNIFICANT
$\mu_{AAR4.9\text{-}0.45} = \mu_{AAR4.9\text{-}0.30}$	0.123161	INSIGNIFICANT	0.489567	INSIGNIFICANT	0.936053	INSIGNIFICANT
$\mu_{AAR4.3\text{-}0.60\text{-}I} = \mu_{AAR4.3\text{-}0.60\text{-}II}$ **	0.66922	INSIGNIFICANT	0.699055	INSIGNIFICANT	0.589138	INSIGNIFICANT
$\mu_{AAR4.3\text{-}0.60\text{-}I\&4.3\text{-}0.60\text{-}II} = \mu_{AAR4.9\text{-}0.60}$	3.04E-06	SIGNIFICANT	2.87E-05	SIGNIFICANT	3.78E-05	SIGNIFICANT
$\mu_{AAR4.3\text{-}0.45} = \mu_{AAR4.3\text{-}0.60\text{-}I\&4.3\text{-}0.60\text{-}II}$	0.006947	SIGNIFICANT	0.418462	INSIGNIFICANT	0.935251	INSIGNIFICANT
$\mu_{AAR4.9\text{-}0.45} = \mu_{AAR4.9\text{-}0.60}$	0.009308	SIGNIFICANT	0.01362	SIGNIFICANT	0.026211	SIGNIFICANT
$\mu_{AAR4.2FA} = \mu_{AAR4.4FA}$	0.056196	INSIGNIFICANT	0.241123	INSIGNIFICANT	0.876771	INSIGNIFICANT
$\mu_{AAR4.2} = \mu_{AAR4.2FA}$	0.002867	SIGNIFICANT	0.01584	SIGNIFICANT	0.045417	SIGNIFICANT
$\mu_{AAR4.4} = \mu_{AAR4.4FA}$	0.000485	SIGNIFICANT	0.00157	SIGNIFICANT	0.006013	SIGNIFICANT

* The difference between two mean values is considered significant if the p value is smaller than the chosen α value: 0.05.

** Two parallel test series

Conclusions for the RILEM AAR-4.1 test results (valid for 13, 26 and 39 weeks), see Table 3-12:

- If the samples are submerged in deionized water continuously or sealed with no access to water, these conditions affect the expansion values considerably (AAR 4.3 vs. AAR 4.6; p-value: 5.5x10-5 @13 weeks, 0.0002@ 26 weeks, 0.0006 @39 weeks and AAR 4.3 vs. AAR 4.7; p-value: 0.0043 @13 weeks, 0.0048 @26 weeks, 0.005 @39 weeks).
- Wrapping the prisms with moist cotton cloth considerably reduces the expansions (AAR 4.2 vs. AAR 4.8; p-values: 6.59x10-6 @13 weeks, 1.88x10-5 @26 weeks and 5.1x10-5@39 weeks). Similar conclusion is also valid for the AAR 4.3 vs. AAR 4.9 series at all ages.
- Adding less water to the wrapping affects the expansions; this effect diminishes at 39-weeks (AAR 4.9 vs. AAR 4.10; p-values: 0.0068 @13 weeks, 0.0075 @26 weeks and 0.0837 @39 weeks).
- Applying alkalis (pH 14.2) in the wrapping instead of water increases the expansion considerably (AAR 4.9 vs. AAR 4.12; p-values: 0.0001 @13 weeks, 1.75x10-5 @26 weeks and 3.12x10-5 @39 weeks).
- The effect of wrapping vs. unwrapping is similar at w/c 0.30 as for w/c 0.45 (AAR 4.3-0.30 vs. AAR 4.9-0.30; p-values: 0.0003 @13 weeks, 0.0001 @26 weeks and 0.0002 @39 weeks). Similar conclusion is also valid at w/c 0.60.
- Opposite as was found at exposure to 38°C, reducing w/c from 0.45 to 0.30 does not influence the expansion values when exposed to 60°C.
- Increasing w/c from 0.45 to 0.60 influences the expansion (AAR 4.9-0.45 vs. AAR 4.9-0.60; p-values: 0.0093 @13 weeks, 0.0136 @26 weeks and 0.0262 @39 weeks).
- Using wrapping without polyethylene bag affects the expansion values, especially at later ages (AAR 4.9 vs. AAR 4.11, p-value: 0.052 @13 weeks, 0.0254 @26 weeks, 0.0306 @39 weeks).

Results from comparing test series with identical concrete composition and similar pre-treatment conditions, but exposed according to different concrete prism test methods, are presented in Table 3-13. The conclusions are:

- After 52 weeks, there is a significant difference between the expansion of the N1 0.45 test series (large prisms) and ASTM 0.45 test series (smaller prism cross-section) (p-value: 0.0033), which is also valid for 112 weeks test results (p-value: 0.0476).
- Similarly, the N1 0.45 test series expansions are significantly higher than the AAR 3.4 expansion (p-value: 0.0006).
- There is no strong evidence to state that the ASTM CPT “basis” binder (CEM I, w/c of 0.45) test series' mean expansions (unwrapped prisms) differ from the RILEM AAR-3 CPT expansions (wrapped prisms) with similar pre-treatment conditions (p-values: 0.4578).
- Regarding the test series other than “basis” binder test mixtures; RILEM AAR 3.4 expansions are significantly higher than ASTM expansions at w/c 0.30 with the p-value of 0.048 @52 weeks and 0.0004 @112 weeks. Similarly, expansion values of the FA incorporating test series differ significantly (p-value: 0.0085 @52 weeks and 0.0291 @112 weeks).
- When the "Norwegian length readings" are taken without cooling and 7-days pre-storage at 20°C is applied, i.e. N3-0.45, the mean expansions are different from the AAR 3.4 expansions (p-value: 0.0118 @52 weeks); also valid at w/c 0.60 (p-value 0.0109 @52 weeks). However, this conclusion is not valid at w/c 0.30 (p-value: 0.097 @52weeks, 0.7289 @112weeks).
- At w/c 0.30, the mean expansions of the N3 test series are not equal to the corresponding ASTM test series (with smaller prism cross-section) (p-value: 0.0275 @52 weeks, 0.001 @112 weeks). This conclusion is also valid at w/c 0.60 (p-value: 0.003 @52weeks).

- For FA incorporating mixtures, the mean expansion values of the Norwegian CPT series vs. RILEM AAR-3 CPT series significantly differ with a p-value of 0.0305 @52 weeks, while this difference diminishes at 112 weeks (p-value: 0.2292).

Table 3-13 Comparison between different CPTs. For abbreviations, see paper IV, Tables 5-8.

NORWEGIAN CPT vs. ASTM C1293 CPT vs. RILEM AAR-3 CPT (@52 weeks)		
Test Hypothesis (two-sided)	P-value	Comment*
$\mu_{\text{N1-0.45}} = \mu_{\text{ASTM1-6\&10\&12}}$	0.003280903	SIGNIFICANT
$\mu_{\text{N1-0.45}} = \mu_{\text{AAR3.4}}$	0.000591732	SIGNIFICANT
$\mu_{\text{N3-0.45}} = \mu_{\text{AAR3.4}}$	0.01177097	SIGNIFICANT
$\mu_{\text{N3-0.30}} = \mu_{\text{ASTM-0.30}}$	0.027536629	SIGNIFICANT
$\mu_{\text{N3-0.30}} = \mu_{\text{AAR3.4-0.30}}$	0.097979165	INSIGNIFICANT
$\mu_{\text{N3-0.60}} = \mu_{\text{ASTM 0.60-8\&0.60-11}}$	0.003058784	SIGNIFICANT
$\mu_{\text{N3-0.60}} = \mu_{\text{AAR3.4-0.60}}$	0.010965273	SIGNIFICANT
$\mu_{\text{N3-FA0.45}} = \mu_{\text{ASTM-FA0.45}}$	0.056154807	INSIGNIFICANT
$\mu_{\text{N3-FA0.45}} = \mu_{\text{AAR3.8-FA\&AAR3.9-FA}}$	0.030543248	SIGNIFICANT
$\mu_{\text{AAR3.8}} = \mu_{\text{ASTM1-6\&10\&12}}$	0.457794495	INSIGNIFICANT
$\mu_{\text{AAR3.8}} = \mu_{\text{ASTM3}}$	0.588243146	INSIGNIFICANT
$\mu_{\text{AAR3.4-0.30}} = \mu_{\text{ASTM0.30}}$	0.048382442	SIGNIFICANT
$\mu_{\text{AAR3.4-0.60}} = \mu_{\text{ASTM0.60-8\&ASTM0.60-11}}$	0.323439063	INSIGNIFICANT
$\mu_{\text{AAR3.8FA\&AAR39FA}} = \mu_{\text{ASTMFA}}$	0.008495695	SIGNIFICANT
NORWEGIAN CPT vs. ASTM C1293 CPT vs. RILEM AAR-3 CPT (@112 weeks)		
Test Hypothesis (two-sided)	P-value	Comment*
$\mu_{\text{N1-0.45}} = \mu_{\text{ASTM3}}$	0.047579915	SIGNIFICANT
$\mu_{\text{N1-0.45}} = \mu_{\text{AAR3.8}}$	0.122903134	INSIGNIFICANT
$\mu_{\text{N3-0.30}} = \mu_{\text{ASTM0.30}}$	0.001052807	SIGNIFICANT
$\mu_{\text{N3-0.30}} = \mu_{\text{AAR3.4-0.30}}$	0.728969466	INSIGNIFICANT
$\mu_{\text{N3-FA0.45}} = \mu_{\text{ASTMFA0.45}}$	0.006691982	SIGNIFICANT
$\mu_{\text{N3-FA0.45}} = \mu_{\text{AAR3.8FA\&AAR3.9FA}}$	0.2292611	INSIGNIFICANT
$\mu_{\text{AAR3.8}} = \mu_{\text{ASTM3}}$	0.009135946	SIGNIFICANT
$\mu_{\text{AAR3.4-0.30}} = \mu_{\text{ASTM0.30}}$	0.000434079	SIGNIFICANT
$\mu_{\text{AAR3.8FA\&AAR3.9FA}} = \mu_{\text{ASTMFA}}$	0.029147691	SIGNIFICANT
38°C CPTs (@52 weeks) **vs. RILEM AAR-4.1 60°C CPT**(@26 weeks), "Temperature effect"		
Test Hypothesis (two-sided)	P-value	Comment*
$\mu_{\text{AAR4.1}} = \mu_{\text{ASTM1-6\&10\&12}}$	0.000168891	SIGNIFICANT
$\mu_{\text{AAR4.6}} = \mu_{\text{AAR3.11}}$	0.000428229	SIGNIFICANT
$\mu_{\text{AAR4.8-1\&AAR4.8.10}} = \mu_{\text{AAR3.8}}$	3.54262E-09	SIGNIFICANT
$\mu_{\text{AAR4.9}} = \mu_{\text{AAR3.4}}$	3.47016E-05	SIGNIFICANT
$\mu_{\text{AAR4.10.6\&4.10.12}} = \mu_{\text{AAR3.3}}$	5.50945E-06	SIGNIFICANT
$\mu_{\text{AAR4.11}} = \mu_{\text{AAR3.6}}$	7.25647E-05	SIGNIFICANT
$\mu_{\text{AAR4.12}} = \mu_{\text{AAR3.12}}$	0.068095505	INSIGNIFICANT
$\mu_{\text{AAR4.13}} = \mu_{\text{AAR3.13}}$	0.002828729	SIGNIFICANT
$\mu_{\text{AAR4.3-0.30}} = \mu_{\text{ASTM0.30}}$	0.000201264	SIGNIFICANT
$\mu_{\text{AAR4.9-030}} = \mu_{\text{AAR3.4-0.30}}$	0.003092083	SIGNIFICANT
$\mu_{\text{AAR4.3 0.60-I\&AAR4.3 0.60-II}} = \mu_{\text{ASTM 0.60-8\& ASTM 0.60-11}}$	0.000192056	SIGNIFICANT
$\mu_{\text{AAR4.9-0.60}} = \mu_{\text{AAR3.4-0.60}}$	6.3652E-06	SIGNIFICANT
$\mu_{\text{AAR4.2FA}} = \mu_{\text{ASTMFA}}$	2.34946E-05	SIGNIFICANT
$\mu_{\text{AAR4.2FA}} = \mu_{\text{AAR3.8FA}}$	0.000137616	SIGNIFICANT
$\mu_{\text{AAR4.4FA}} = \mu_{\text{AAR3.9FA}}$	0.002715451	SIGNIFICANT

* The difference between two mean values is considered significant if the p value is smaller than the chosen α value: 0.05.

There is quite a considerable difference between the mean expansion results of *similar* test series cured in accordance with RILEM AAR-3 conditions at 38°C for 52 weeks and RILEM AAR-4.1 conditions at 60°C for 26 weeks. Except for the AAR 4.12 vs. AAR 3.12 series (with alkalis added to the wrapping), all other mean expansions of pairwise comparisons are significant with quite low p-values ranging from 0.003 to 3.5426×10^{-9}, showing the considerable effect of the exposure temperature on the concrete prism expansions.

Coefficient of thermal expansion

Reference readings for most test series were carried out at 38°C and 60°C (see Figure 1 in paper IV). Additionally, pre-reference readings were performed for all prisms at 20°C prior to the start of exposure at higher temperature. Hence, the coefficient of thermal expansion, α_T, may be calculated (if neglecting the minor swelling that might occur during the first 24 h of exposure to elevated temperature).

For specimens stored 7 days at 20°C prior to exposure to higher temperature, the average α_T is $9.4\text{x}10^{-6}$ (*comment: see Table 3-14 on page 28*), with a standard deviation of $0.56\text{x}10^{-6}$ (c.o.v. = 5.9 %). These calculations include all CEM I test series, except those stored sealed or submerged in de-ionised water. This relatively low spread in α_T confirms the consistency of the expansion measurements. Furthermore, the measured α_T is in good agreement with the literature for concrete with similar aggregate types [17]. The calculated α_T for concretes with the "fly ash" binder is about 20 % higher than the values for the CEM I binders.

Length change in the "pre-reference phase"

(Comment: In order to shorten paper V, section 3.3.2 has been shortened in the final version. However, in the following, the original full text of that section is included, together with the detailed results from the calculations performed – see Table 3-14).

Length changes in the "pre-reference phase" (i.e. the period from de-moulding to the reference readings) may be in the form of shrinkage or swelling, depending on the composition of the concrete and the surrounding environment. Generally, continued hydration of concrete cured in water leads to minor swelling/expansion due to absorption of water by the cement hydrates [17]. The magnitude on the swelling might be in the order of 0.005 % or slightly higher according to Aítcin [18]. On the other hand, if the moisture supply to the hydrating cement paste is insufficient, shrinkage occurs due to withdrawal of water from capillary pores caused by the self-desiccation process. These effects are clearly shown by comparing the sealed prisms (paper V, Table 3), giving a net shrinkage of -0.011 % during the 6 days of pre-storage at 20°C after de-moulding, with the prisms stored in de-ionised water during the same period giving an expansion of 0.001 %. Both values are for CEM I concrete with w/c ratio of 0.45 ("basis" binder). The sealed storage represents an “extreme” variant in this study, but it is not unrealistic for the inner parts of massive concrete structures.

There is a marked effect of the w/c on length changes during the pre-storage period. Reduced w/c causes increased autogenous shrinkage due to higher self-desiccation, as expected. Of the same reason, there is a tendency to slightly more shrinkage when the prism size is increased. The maximum shrinkage (except the sealed test series) from de-moulding until after 6 days of pre-storage at 20°C was -0.006 % (CEM I test series with w/c of 0.30, Norwegian prisms). Also the test series with the "fly ash" binder (w/cm of 0.45) reveals minor shrinkage during the 6 days of pre-storage at 20°C: -0.005 % after 6 days for the Norwegian prism size.

Early-age shrinkage of a reversible nature may represent an “error” due to a resulting higher expansion when the prisms are placed in the ASR environment, provided the reference readings are taken after the pre-storage period at ambient temperature. However, if we assume that most of the early phase length changes may be reversible, a net shrinkage in the early phase may represent a “conservative approach”, i.e. a phenomenon that is likely to increase the amount of expansion that is attributed to ASR and vice-versa.

The maximum “conservative error” (if we exclude the extreme sealed variant) is 0.006 %. Consequently, if we use an acceptance criterion (critical expansion limit) of 0.040 %, this maximum "conservative error" constitutes about 15 % of the expansion limit (compared with taking the reference readings directly after de-moulding). However, most test series reveal less shrinkage than the "dense" binder test series. The average length change during the 6 days of pre-storage is -0.002 % (when excluding the sealed prisms), i.e. insignificant shrinkage, constituting about 5 % of a critical expansion limit of 0.040 %.

On the other hand, one comment should be given with respect to conditions that might increase the water uptake from de-moulding until the reference readings are taken, and consequently lead to a minor swelling of the concrete prisms. Such conditions might be use of any moist cotton cloth wrapping, pre-curing in a fog chamber or exposing the prisms to elevated temperature (as done in this study, when most reference readings were taken the day after the prisms were exposed to their storage environment – see paper V, section 2.3.1). If the reference readings are taken after a minor swelling, this will result in a slight "non-conservative error" in the expansion measurement, i.e. the expansion due to ASR will be slightly underestimated compared with taking the reference readings directly after de-moulding.

To sum up: For the binder types included in this study, only a few test series are significantly influenced by the time of the reference readings. The maximum length change that was observed prior to establishing the reference reading represented approximately 15 % of a critical expansion limit of 0.040 %. However, this will only influence the conclusion from a performance test if the final expansion is close to the acceptance criterion. For most of the test series included in this study, it is slightly conservative to take the reference readings after any pre-storage period at ambient temperature (i.e. a "conservative error"). The same is valid for any other binder type with equal or higher self-desiccation (e.g. low w/cm binders and any binder added higher quantities of SCMs). However, taking the reference readings without pre-cooling might be slightly "non-conservative" (see above). In any case, the time of the reference readings is of minor importance for the final prism expansions compared with the huge influence of the rate and amount of alkali leaching.

Table 3-14: Length changes in the "pre-reference phase" (see paper V, section 3.3.2).

		Pre-reference phase				
		Expansion (%) from de-moulding				
		Days from casting				
Norwegian 38°C CPT		2	7	8	28	29
N1-UA-0.45-3-S-1c	Standard Norwegian CPT (1 day, 0.5 h sub, cooled)					
N2-U-A-0.45-1-S-2	As N.1-U-0.45, but readings without pre-cooling	0,011				
N3-U-A-0.45-4-S-8	As N.2-U-0.45, but 7 days pre-storage at 20°C		-0,004	0,012		
N3-U-A-0.30-7-S-8	As N.3-U-0.45, but lower w/c ratio		-0,006	0,009		
N3-U-A-0.60-8-S-8	As N.3-U-0.45, but higher w/c ratio		-0,001	0,015		
N3-U-A-FA-0.60-9-S-8	As N.3-U-0.45, but fly ash binder with boosted alkali level		-0,005	0,016		
RILEM AAR-3 38°C CPT						
3.1-W-B-0.45-3-N7C	Standard RILEM AAR-3 (wrappping, cooled, 7 days)		0,001			
3.2-W-B-0.45-4-N8	As 3.1-W-B-0.45, but readings taken without pre-cooling		-0,002	0,015		
3.3-W-C-0.45-4-N8	As 3.2-W-B-0.45, but less water in wrapping		-0,002	0,016		
3.4-W-B-0.45-4-S8	As 3.2-W-B-0.45, but prisms 0.5h submerged after de-moulding		0,000	0,016		
3.5- - E-0.45-5-N8	Sealed storage (epoxy and aluminium foil) after de-moulding	Not measured at demoulding				
3.6-W-D-0.45-6-S8	As 3.4-W-B-0.45, but no polyethylene bag		-0,002	0,016		
3.7-U-A-0.45-6-S8	As 3.4-W-B-0.45, but no wrapping (one prism in each container)		-0,002	0,014		
3.8-W-B-0.45-3-S2	As 3.4-W-B-0.45, but 1 day pre-storage at 20ºC	0,017				
3.9-W-B-0.45-2-S29	As 3.4-W-B-0.45, but 28 days pre-storage at 20ºC	0,001			0,003	0,017
3.10-W-B-0.45-2-S8FT	As 3.4-W-B-0.45, but simulating “field curing temperature”		0,006	0,023		
3.10-W-B-0.45-10-S8FT	As 3.10-W-B-0.45-2, but repeated test series		0,004	0,019		
3.11.U-F-0.45-5-S8	Stored submerged in deionised water after de-moulding		0,001	0,015		
3.12-W-G-0.45-12-S8	As 3.4-W-B-0.45, but pH 14.2 in wrapping at start		0,000	0,018		
3.13-W-H-0.45-12-S8	As 3.4-W-B-0.45, but pH 13.2 in wrapping at start		-0,001	0,015		
3.4-W-B-0.30-7-S8	As 3.4-W-B-0.45, but lower w/c ratio		-0,004	0,012		
3.4-W-B-0.60-8-S8	As 3.4-W-B-0.45, but higher w/c ratio		0,004	0,020		
3.8-W-B-FA-0.45-9-S2	As 3.8-W-B-0.45, but fly ash binder with boosted alkali level	0,017				
3.9-W-FA-0.45-9-S29	As 3.9-W-B-0.45, but fly ash binder with boosted alkali level	-0,003			0,000	0,020
RILEM AAR-4.1 60°C CPT						
4.1-U-A-0.45-1-S1C	Standard RILEM AAR-4.1 (unwrapped, reactor, 1 day, 0.5 h sub)					
4.2-U-A-0.45-1-S2	As 4.1-U-A-0.45, but readings taken without pre-cooling	0,039				
4.3-U-A-0.45-6-S8	As 4.2-U-A-0.45, but 7 days pre-storage at 20ºC		-0,004	0,036		
4.4-U-A-0.45-2-S29	As 4.3-U-A-0.45, but 28 days pre-storage at 20ºC				0,000	0,039
4.5-U-A-0.45-2-S8FT	As 4.3-U-A-0.45, but simulating “field curing temperature”		0,000	0,037		
4.6-U-F-0.45-5-S8	Stored submerged in deionised water after de-moulding		0,001	0,039		
4.7--E-0.45-5-N8	Sealed storage (epoxy and aluminium foil) after de-moulding		-0,011	0,030		
4.8-W-B-0.45-1-S2	Standard RILEM AAR-4.1 Alt. test procedure	0,042				
4.8-W-B-0.45-10-S2	As 4.8-W-B-0.45-1, but repeated test series	0,042				
4.9-W-B-0.45-5-S8	As 4.8-W-B-0.45-1, but 7 days pre-storage at 20ºC		0,000	0,041		
4.10-W-C-0.45-6-N8	As 4.9-W-B-0.45, but less water in wrapping		-0,002	0,036		
4.10-W-C-0.45-12-N8	As 4.10-W-B-0.45-6, but repeated test series	Not measured at demoulding?				
4.11-W-D-S0.45-3-S8	As 4.9-W-B-0.45, but no polyethylene bag		0,001	0,040		
4.12-W-G-0.45-12-S8	As 4.9-W-B-0.45, but pH 14.2 in wrapping at start		-0,002	0,038		
4.13-W-H-0.45-12-S8	As 4.9-W-B-0.45, but pH 13.2 in wrapping at start		-0,001	0,039		
4.3-U-A-0.30-7-S8	As 4.3-U-A-0.45, but lower w/c ratio		-0,006	0,033		
4.9-W-B-0.30-7-S8	As 4.9-W-B-0.45, but lower w/c ratio		-0,002	0,036		
4.3-U-A-0.60-8-1-S8	As 4.3-U-A-0.45, but higher w/c ratio		-0,002	0,038		
4.3-U-A.0.60-11-S8	As 4.3-U-A-0.60-I, but repeated test series		-0,003	0,037		
4.9-W-B-0.60-11-S8	As 4.9-W-B-0.45, but higher w/c ratio		0,002	0,041		
4.2-U-FA-0.45-9-S2	As 4.2-U-A-0.45, but fly ash binder with boosted alkali level	0,037				
4.4-U-A-FA-0.45-9-S-29	As 4.4-U-A-0.45, but fly ash binder with boosted alkali level				-0,002	0,039

Mass increase of whole prisms: Supplementary results for the CEM I binders

The Figures 3-3 to 3-8 show the increase in net mass of whole prisms from de-moulding to 39 weeks (60°C) or 52 weeks (38°C) of exposure of the various test series (*comment: similar to Figure 8 in paper IV, apart from that the results in that figure was re-calculated from mass-% to volume-% water absorption*). For abbreviations, see Tables 5-8 and Figures 1-2 in paper IV.

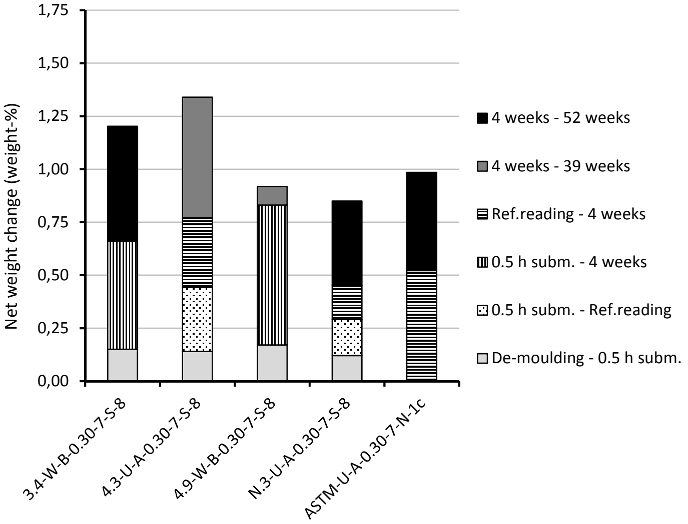

Figure 3-3 Increase in net mass of whole prisms from de-moulding to 39 weeks (60°C) or 52 weeks (38°C) of exposure of the five test series with the binder CEM I, w/c of 0.30.

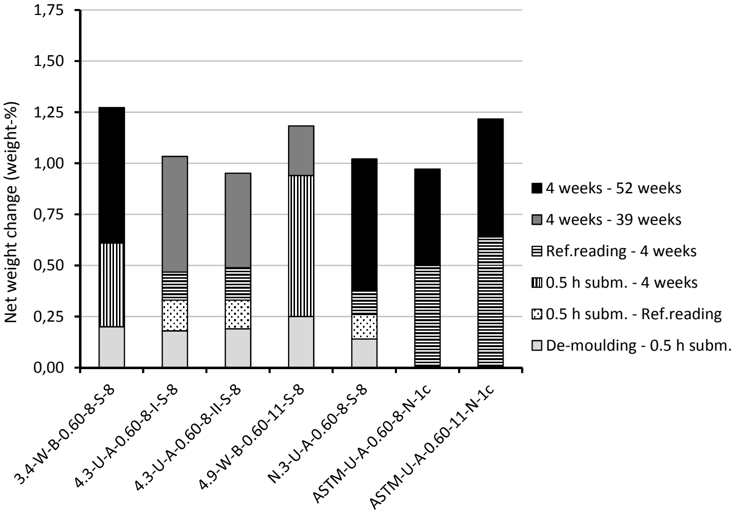

Figure 3-4 Increase in net mass of whole prisms from de-moulding to 39 weeks (60°C) or 52 weeks (38°C) of exposure of the seven test series with the binder CEM I, w/c of 0.60.

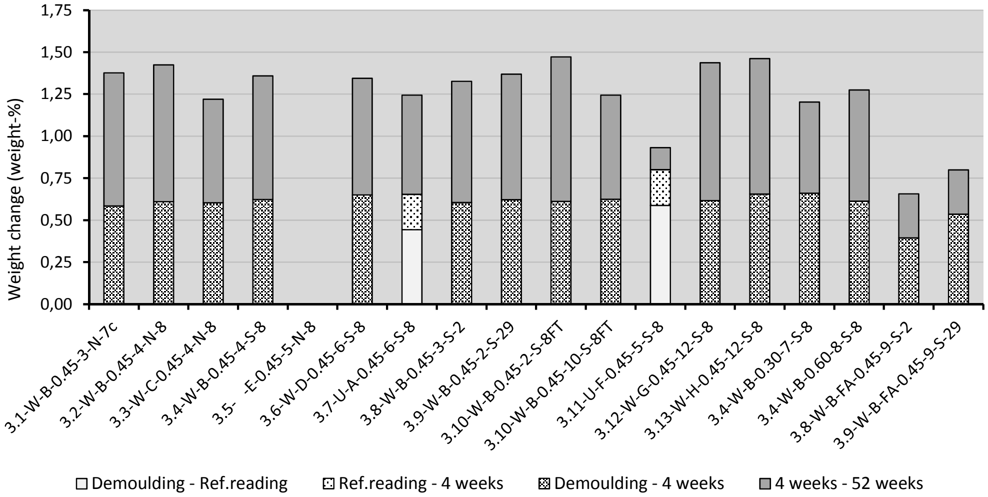

Figure 3-5 Increase in net mass of whole prisms from de-moulding to 52 weeks of exposure of the 18 RILEM AAR-3 test series.

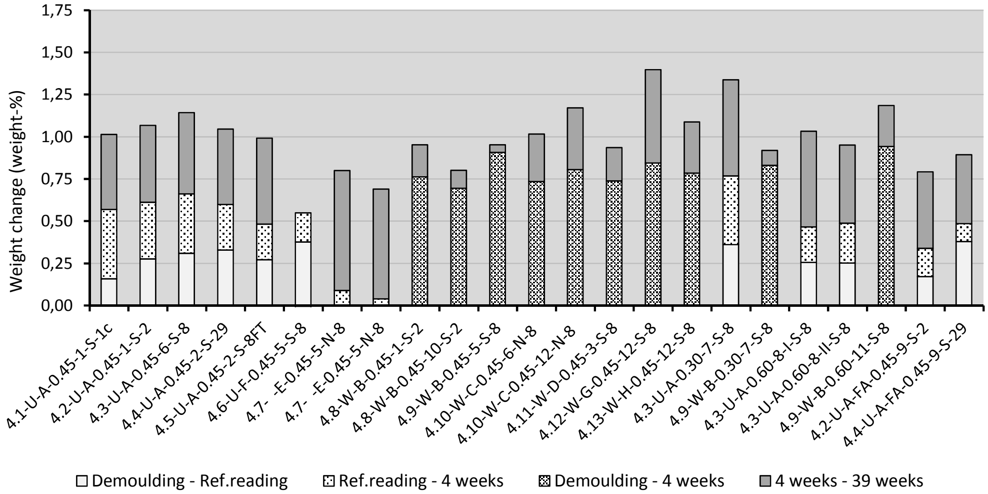

Figure 3-6 Increase in net mass of whole prisms from de-moulding to 39 weeks of exposure of the 22 RILEM AAR-4.1 test series.

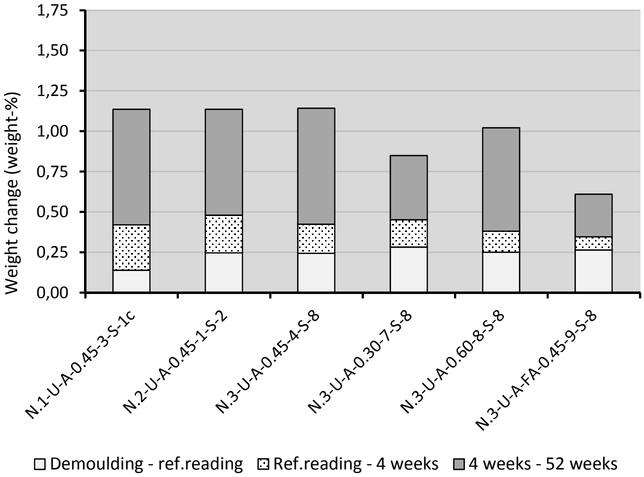

Figure 3-7 Increase in net mass of whole prisms from de-moulding to 52 weeks of exposure of the six test series with the Norwegian CPT.

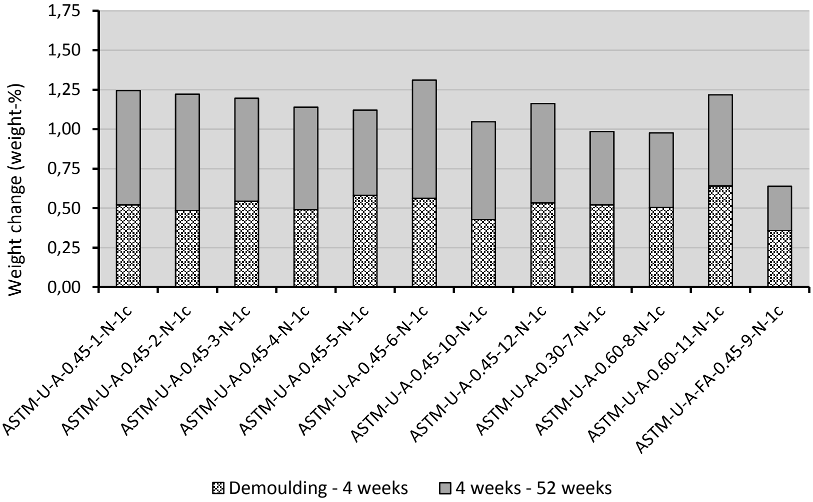

Figure 3-8 Increase in net mass of whole prisms from de-moulding to 52 weeks of exposure of the 12 ASTM C 1293 test series.

Microstructural analysis: Supplementary results, including WDS analysis of the ASR gel

(Comments: Results from microstructural analysis of selected concrete prisms after the ASR exposure are published in paper VI, including a brief evaluation of the various analysing techniques. Selected results are also presented in paper V, primarily plane polished sections analysis (section 2.5.2 and 3.4). In this appendix, some supplementary results from the microstructural analysis performed are presented. Photos from the microstructural analyses are presented later in this appendix).

Precipitation on the prism surfaces

During the ASR exposure, a white precipitation normally becomes visible on most of the concrete prisms (see paper V, section 3.4.1). As part of the pilot testing of alkali leaching, the precipitation was removed mechanically from the surface of two prisms (one at each of the two exposure temperatures) after finalising the ASR exposure. For both, the analyses of the dissolved precipitations showed a negligible content of alkalis. Thus, the minor alkali content in the precipitation stuck on the prism surfaces can be neglected in the alkali leaching calculations.

WDS analysis of the ASR gel

As stated in paper VI, the SEM analyses detected alkali-silica gel in all 11 samples examined, occurring in air voids, in cracks in the cement paste, sometimes distributed within the cement paste, in the interface between aggregate particles and the cement paste or in cracks within the aggregate particles. Figure 3-9 shows the composition of all the reaction products (measured by WDS analysis), presented as ratios between CaO/SiO_2 versus Na_2O_{eq}/CaO. A corresponding figure, with Na_2O_{eq}/SiO_2 on the vertical axes is shown in Figure 3-10. Generally, it seems like the composition of the reaction products is independent of the binder composition and the exposure temperature

The WDS analyses summarized in Table 3-15 show that the composition of the alkali-silica gel varies somewhat depending on the location within the concrete. As documented previously by several others [19], the alkali-silica gel picks up calcium (exchanged with Na and K) when moving from the cracks inside an aggregate and out in the cement paste. This finding is valid for all the binders and for both exposure temperatures (38 and 60°C). ASR-gel located in cracks inside the aggregates has higher content of SiO_2 and alkalis, and lower content of CaO (compared with ASR-gel in the cement paste).

Table 3-15 Mean results (mass-%) from 92 WDS analyses of reaction products (ASR-gel) in nine polished thin sections. (Comment: The test series analysed are shown in the Figures 3-9 -- 3-12).

Al_2O_3	Na_2O	SO_3	FeO	SiO_2	MgO	K_2O	CaO	Total	Location of the ASR-gel
1,10	0,65	0,16	0,11	38,46	0,05	1,13	29,98	71,63	ASR-gel in pores in the cement paste (27 points)
0,99	0,90	0,21	0,20	43,28	0,20	1,69	24,68	72,14	ASR-gel in pores close to aggregate particles (20 points)
1,18	0,94	0,17	0,20	47,17	0,09	1,53	25,60	76,89	ASR-gel in the tranzition zone (aggregate/cement paste) (21 points)
0,38	1,60	0,02	0,26	60,35	0,09	3,33	15,89	81,92	ASR-gel in cracks inside aggregate particles (24 points)

The Figures 3-11 and 3-12 show the same results as presented in the Figures 3-9 and 3-10, but in the Figures 3-11 and 3-12, the results are split into various locations inside the concrete, similar as summarized in Table 3-15.

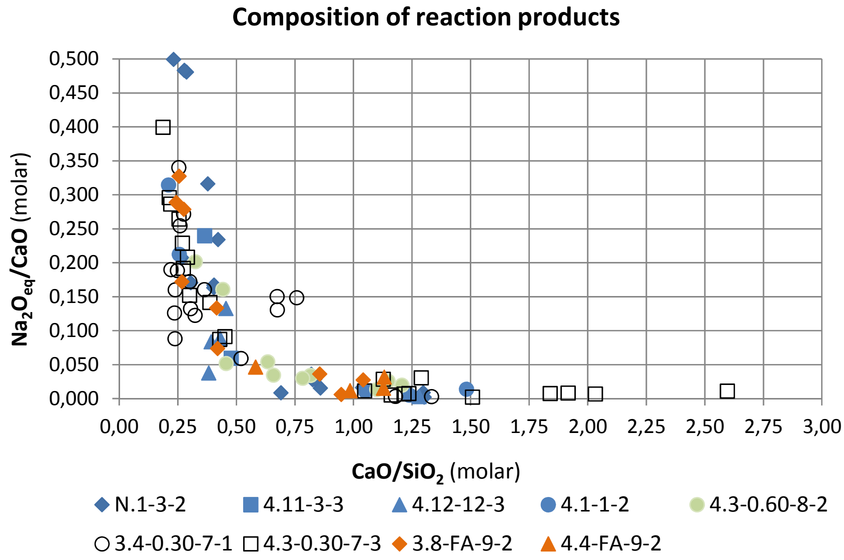

Figure 3-9 *Composition of reaction products for nine test series with varying binder composition and exposure conditions. (Comment: For abbreviations, see paper IV, Table 5-8).*

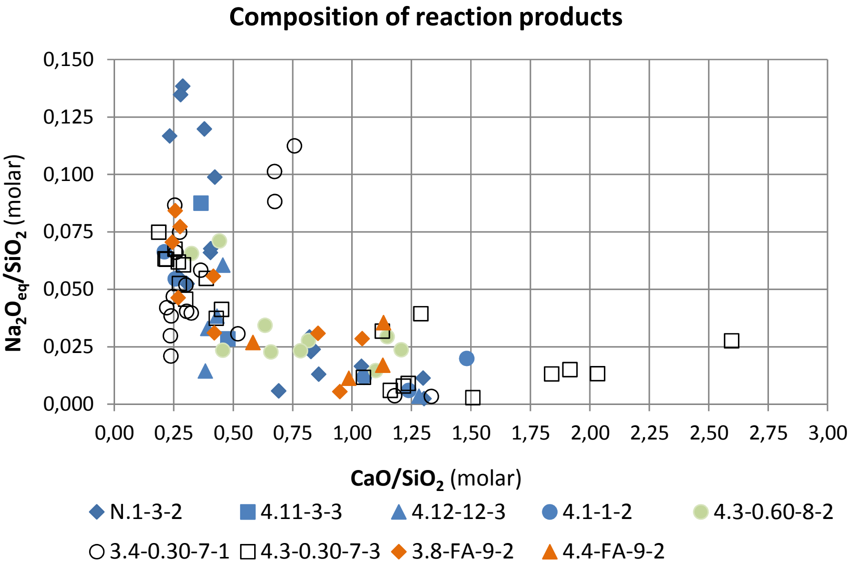

Figure 3-10 *Composition of reaction products for nine test series with varying binder composition and exposure conditions. (Comment: For abbreviations, see paper IV, Table 5-8).*

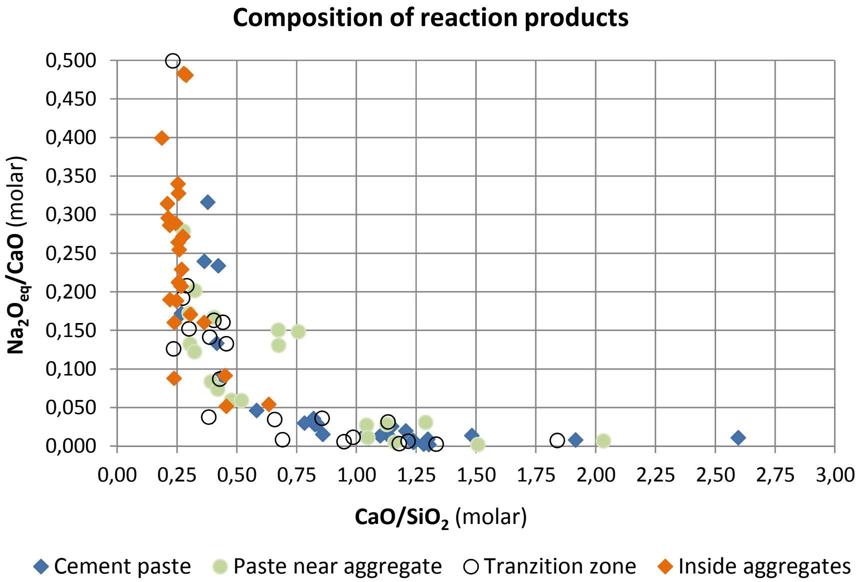

Figure 3-11 Composition of reaction products dependent on the location inside the concrete. (Comments: For abbreviations, see paper IV, Table 5-8. The test series analysed are shown in the Figures 3-9 and 3-10).

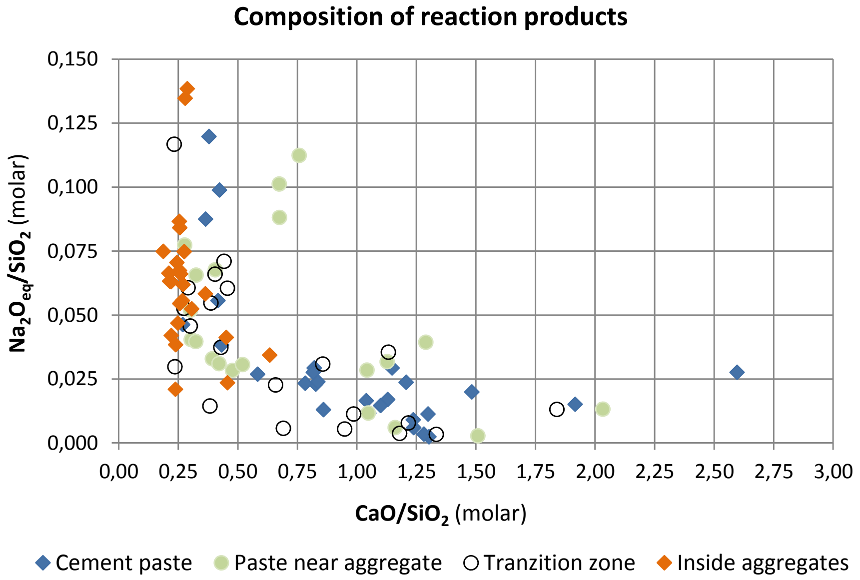

Figure 3-12 Composition of reaction products dependent on the location inside the concrete. (Comments: For abbreviations, see paper IV, Table 5-8. The test series analysed are shown in the Figures 3-9 and 3-10).

Photos: ASR storage containers, wrapping of prisms and length measurements

Photo 3-1—3-3 RILEM AAR-3: Storage container (left), wrapped prism (middle) and wrapped prism inside the prescribed polyethylene bag (right) (see details in paper IV, Table 3).

Photo 3-4—3-5 RILEM AAR-4.1: "Reactor" and storage container (see details in paper IV, Table 3). (Comment: Note the hot damp on the picture to the right when opening the lid of the "reactor". The stones to the right are used to press down the lid to get the new sealing completely tight – see photo 3-8).

Photo 3-6—3-9 RILEM AAR-4.1: Storage container with unwrapped prisms (left), the insulated box used during measuring (middle left), the new sealing system (middle right) and wrapped prisms (right) (Comment: The water on top of the prism (right) is the 5 ml added before closing the polyethylene bag - see details in paper IV, Table 3).)

Photo 3-10 *Storage containers for the Norwegian CPT (see details in paper IV, Table 3).*

Photo 3-11 *38°C storage room with containers for the RILEM AAR-3 CPT (top), the ASTM C1293 CPT (middle) and the Norwegian CPT (bottom).*

Photo 3-12 *Length measurements.*

Photos: DCS, RH and electrical resistivity

Photo 3-13—3-14 Cutting (left) and submersion (right) of "PF-samples".

Photo 3-15—3-16 RF measurements; crushing of concrete (left) and glass tubes with Vaisala sensors (right).

Photo 3-17 Measurement of electrical resistivity over the cross-section of a "PF-sample".

Photos: Visual inspection of prisms

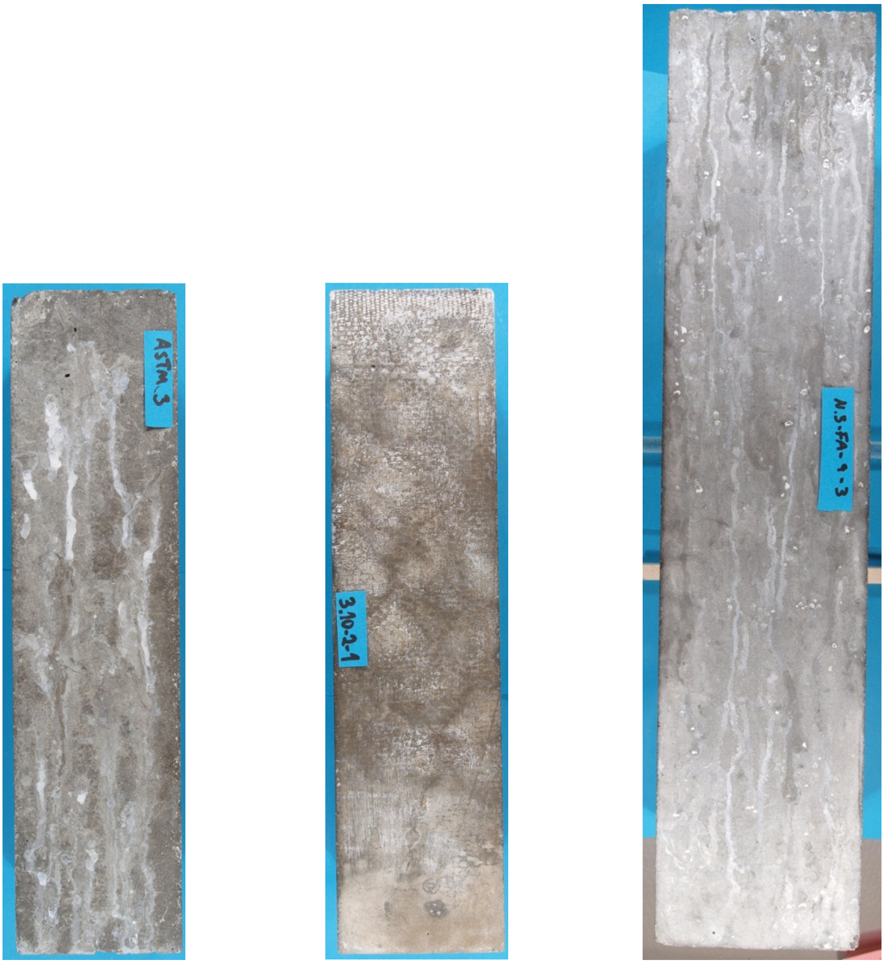

Photo 3-18—3-20 Surface of various prisms after 52 weeks of ASR exposure at 38°C: ASTM C1293 (left), RILEM AAR-3 (middle) and Norwegian CPT (right). (Comments: The prisms were stored in this vertical position during the entire exposure period. The RILEM AAR-3 prism was wrapped, the other unwrapped. For abbreviations, see paper IV, Tables 5-8).

Expansion = 0.261% Expansion = 0.217% Expansion = 0.055%

Photo 3-21—3-23 Cross-section of the same prisms as shown in the Figures 3-18—3-20. (Comments: Note some reaction products (white spots). For abbreviations, see paper IV, Tables 5-8).

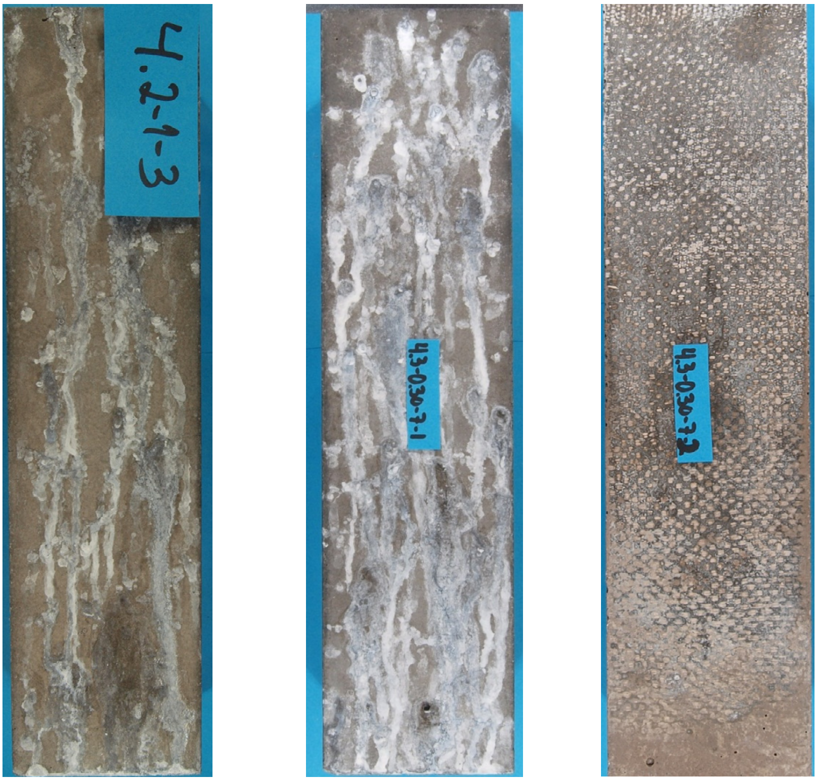

Photo 3-24—3-26 Surface of various prisms after 39 weeks of RILEM AAR-4.1 exposure at 60°C. (Comments: The prisms were stored in this vertical position during the entire exposure period. The prism to the right was wrapped, the other unwrapped. For abbreviations, see paper IV, Table 6).

Expansion = 0.209% Expansion = 0.173% Expansion = 0.060%

Photo 3-27—3-29 Cross-section of the same prisms as shown in the Figures 3-24—3-26. (Comments: Note some reaction products (white spots). For abbreviations, see paper IV, Tables 5-8).

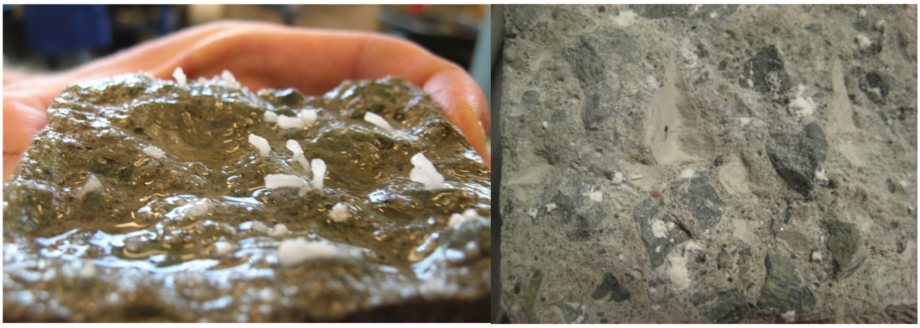

Photo 3-30—3-31 "Alkali worms" in a "PF-sample" (left) cut from a RILEM AAR-4.1 prism after 4 weeks of exposure and subsequently submerged in water for one week. Precipitations (reaction products) on a "PF-sample" during the subsequent drying period (right).

Photos: Plane polished sections

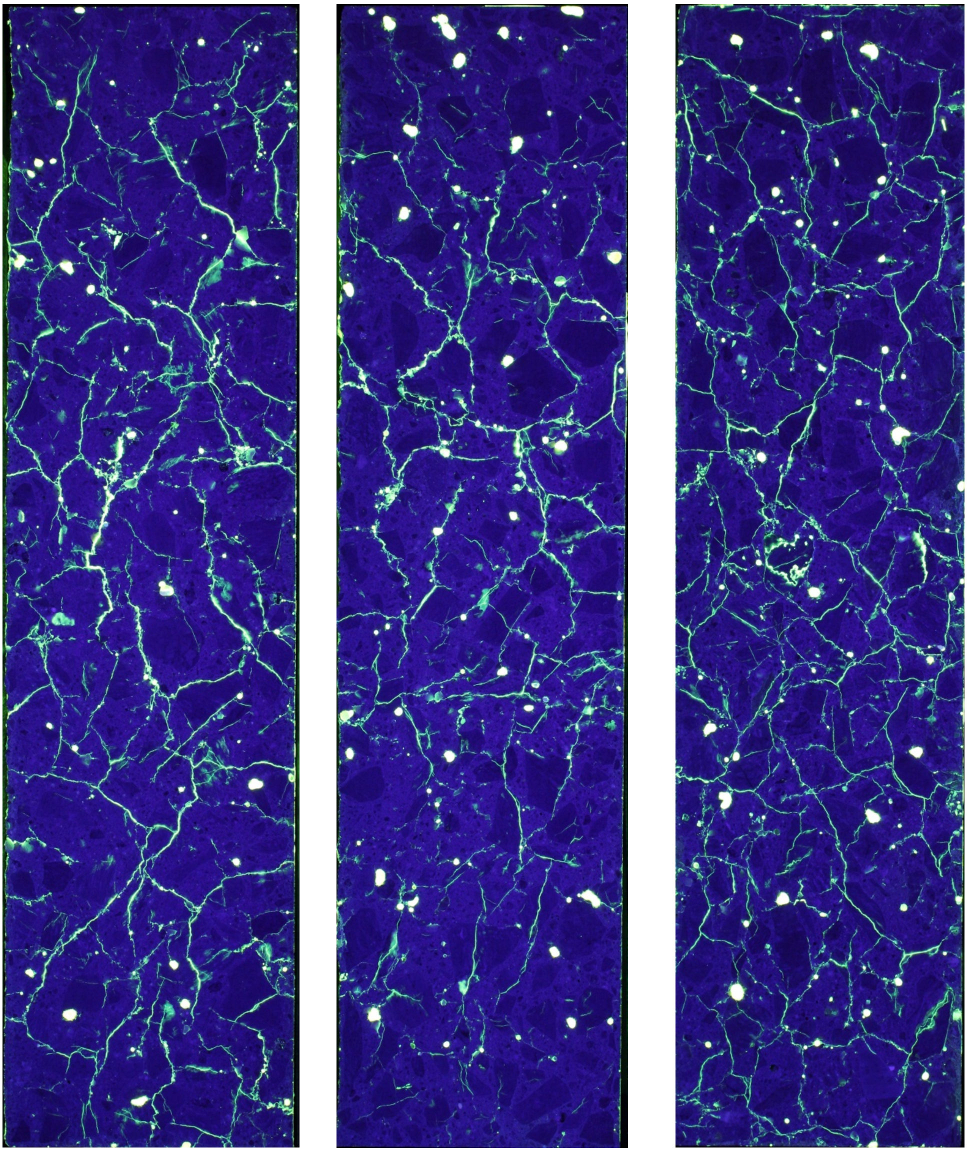

3.8-W-0.45
112 weeks
Expansion = 0.354 %
Cracking intensity = 5.5
Total alkali leaching: 12 %

3.9-W-0.45
112 weeks
Expansion = 0.195 %
Cracking intensity = 3.6
Total alkali leaching: 23 %

3.12-W-0.45
52 weeks
Expansion = 0.238 %
Cracking intensity = 4.7
Total alkali leaching: "< 0%"

Photo 3-32—3-34 Photo in UV-light of plane polished sections after ending the ASR exposure. (Comments: The prisms were stored in this vertical position during the entire exposure period. For abbreviations, see paper IV, Table 5).

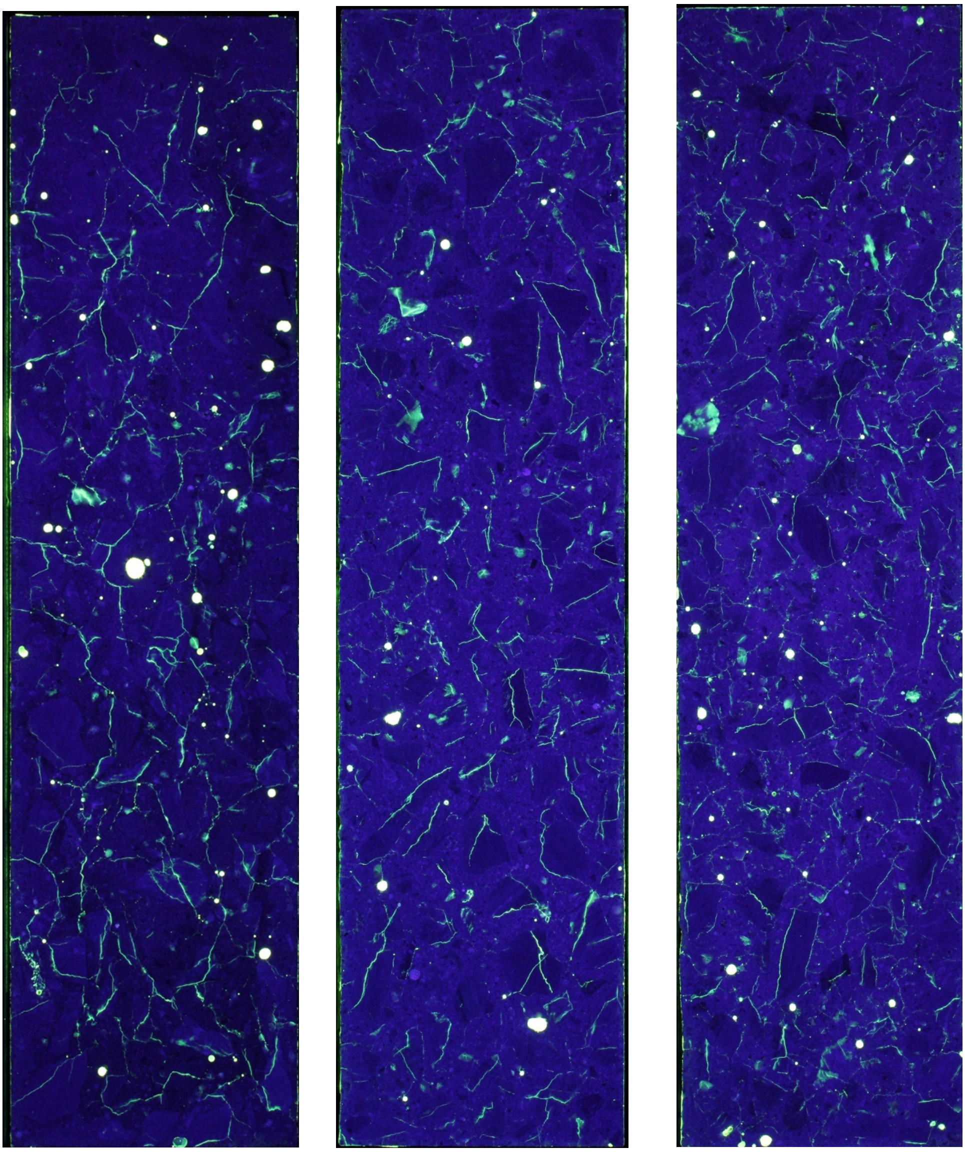

3.4-W-0.30
112 weeks
Expansion = 0.112 %
Cracking intensity = 1.7
Total alkali leaching: 25 %

3.8-W-FA-0.45
112 weeks
Expansion = 0.104 %
Cracking intensity = 1.9
Total alkali leaching: 9 %

3.9-W-FA-0.45
112 weeks
Expansion = 0.119 %
Cracking intensity = 1.9
Total alkali leaching: 12 %"

Photo 3-35—3-37 Photo in UV-light of plane polished sections after ending the ASR exposure. (Comments: The prisms were stored in this vertical position during the entire exposure period. For abbreviations, see paper IV, Table 5).

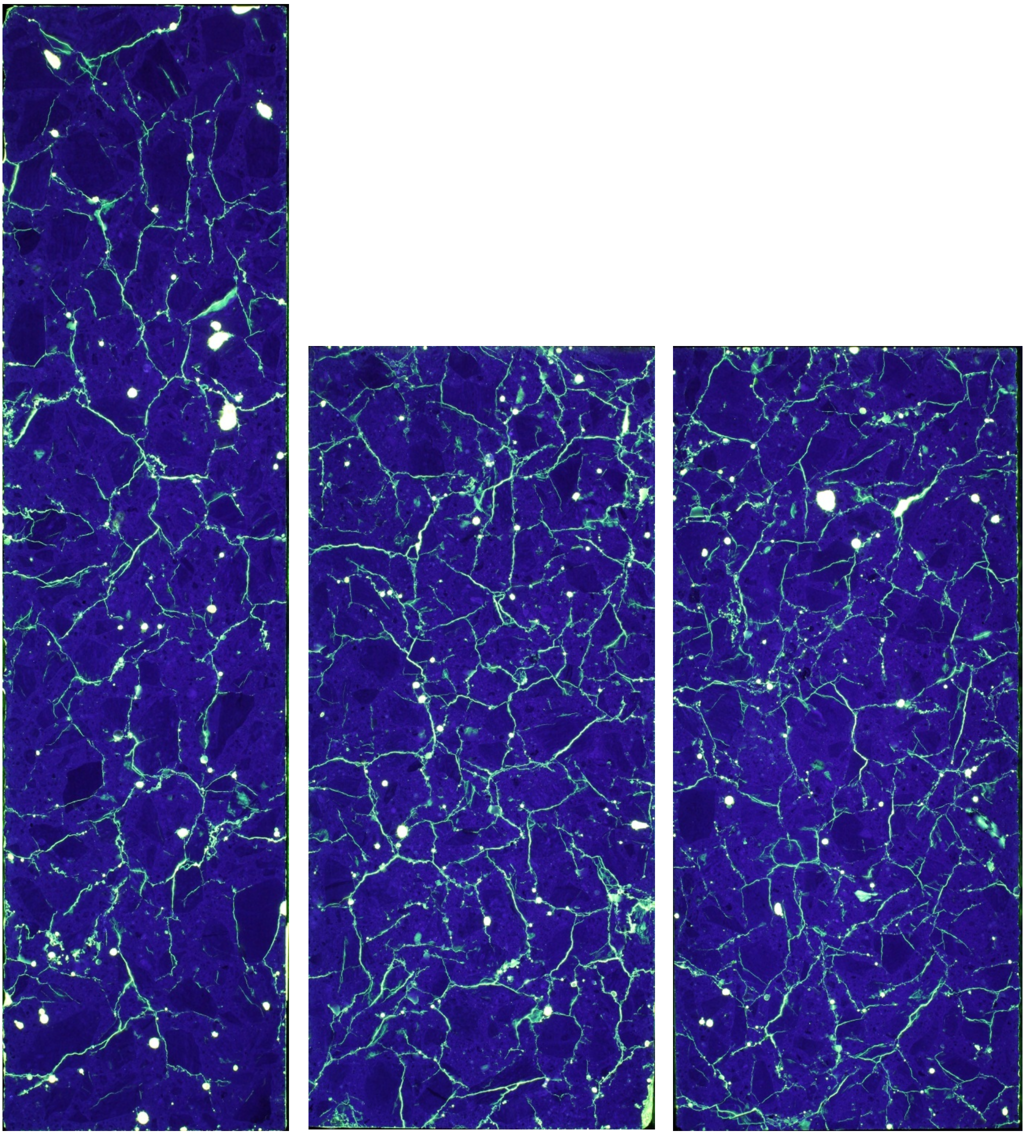

ASTM-3-U-0.45
112 weeks
Expansion = 0.302%
Cracking intensity = 3.9
Total alkali leaching: 45 %

N.1-U-0.45-lower part
112 weeks
Expansion = 0.430 %
Cracking intensity = 6.6
Total alkali leaching: 20 %

N.1-U-0.45-upper part
112 weeks
Expansion = 0.430 %
Cracking intensity = 5.2
Total alkali leaching: 20 %

Photo 3-38—3-40 Photo in UV-light of plane polished sections after ending the ASR exposure. (Comments: The prisms were stored in this vertical position during the entire exposure period. For abbreviations, see paper IV, Tables 7 and 8).

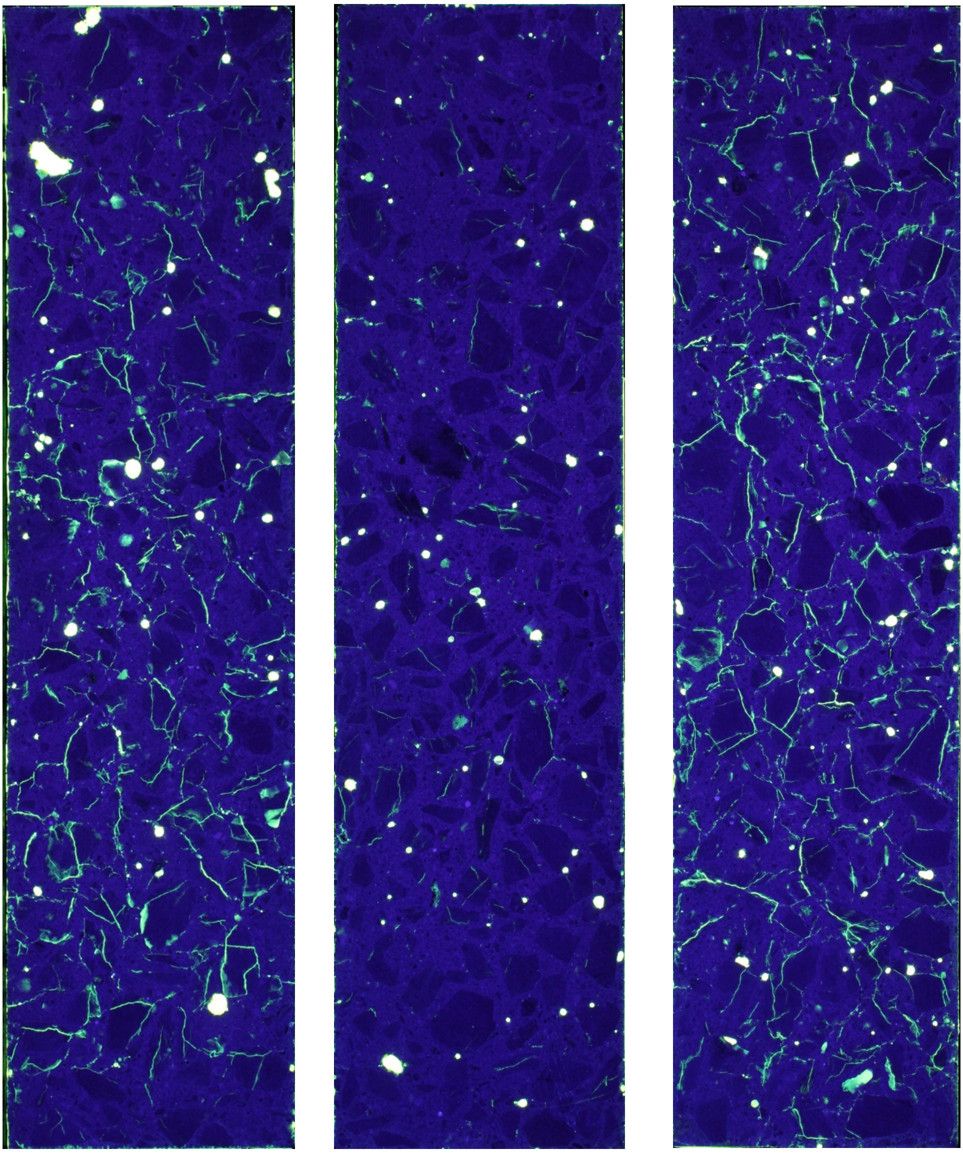

4.1-U-0.45
39 weeks
Expansion = 0.223 %
Cracking intensity = 2.8
Total alkali leaching: 35 %

4.11-W-0.45
39 weeks
Expansion = 0.041 %
Cracking intensity = 0.4
Total alkali leaching: 32 %

4.12-W-0.45
39 weeks
Expansion = 0.223 %
Cracking intensity = 3.6
Total alkali leaching: "< 0%"

Photo 3-41—3-43 Photo in UV-light of plane polished sections after ending the ASR exposure. (Comments: The prisms were stored in this vertical position during the entire exposure period. For abbreviations, see paper IV, Table 6).

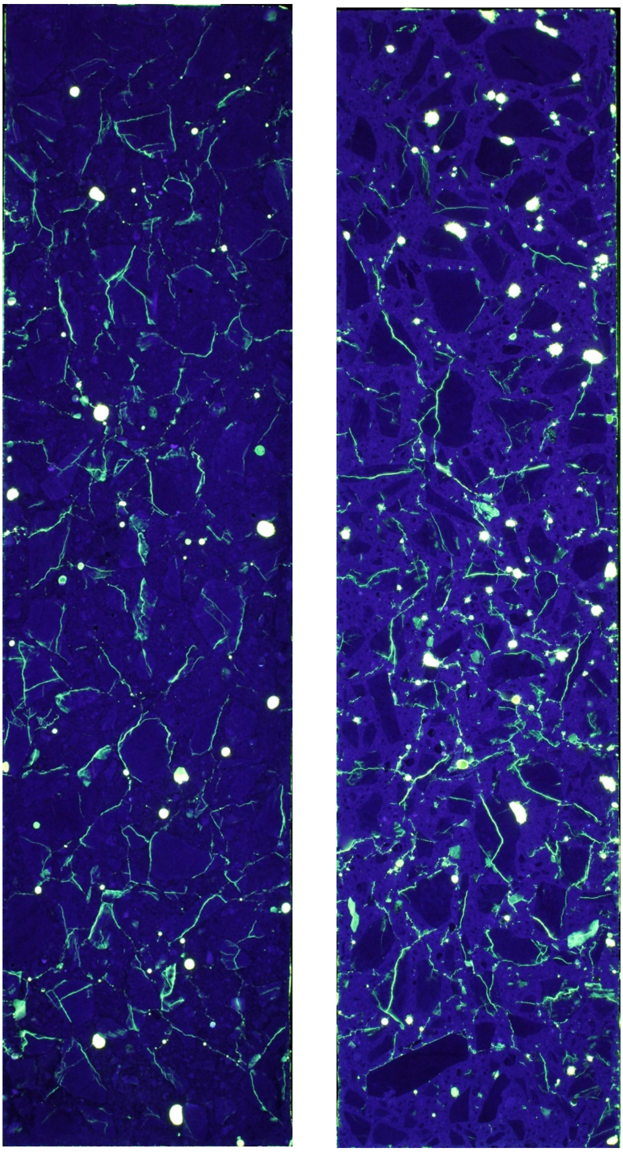

4.3-U-0.30
39 weeks
Expansion = 0.173 %
Cracking intensity = 2.3
Total alkali leaching: 29 %

4.3-U-0.60
39 weeks
Expansion = 0.184 %
Cracking intensity = 3.5
Total alkali leaching: 37 %

Photo 3-44—3-45 Photo in UV-light of plane polished sections after ending the ASR exposure. (Comments: The prisms were stored in this vertical position during the entire exposure period. For abbreviations, see paper IV, Table 6).

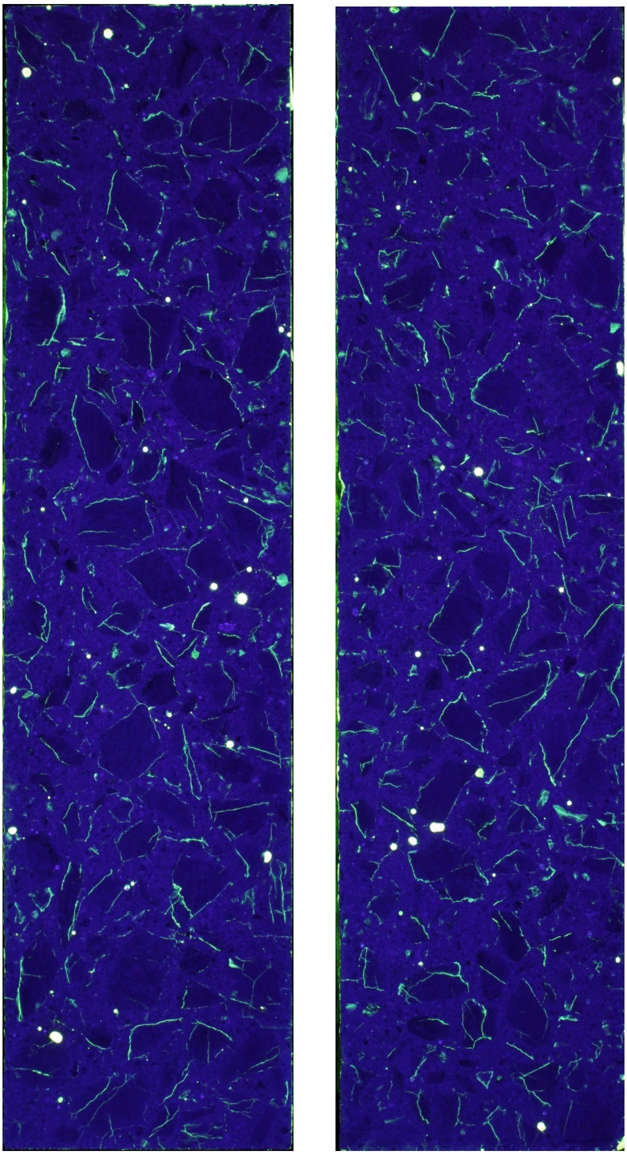

4.2-U-FA-0.45
39 weeks
Expansion = 0.137 %
Cracking intensity = 1.8
Total alkali leaching: 14 %

4.4-U-FA-0.45
39 weeks
Expansion = 0.139 %
Cracking intensity = 1.8
Total alkali leaching: 17 %

Photo 3-46—3-47 Photo in UV-light of plane polished sections after ending the ASR exposure. (Comments: The prisms were stored in this vertical position during the entire exposure period. For abbreviations, see paper IV, Table 6).

Photos: Thin sections

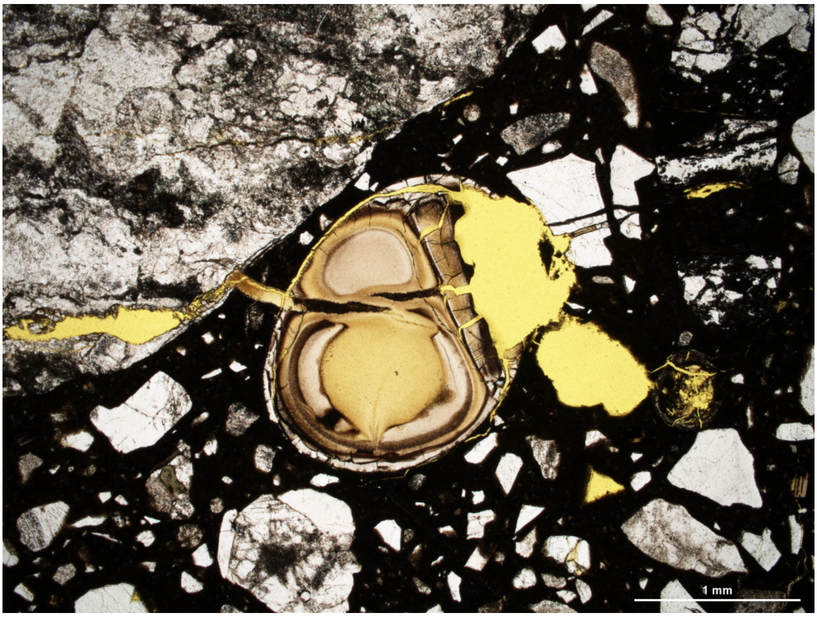

ASTM-3-U-0.45. Note: ASR-gel in a pore

Photo 3-48 Photo of a thin section after ending the ASR exposure.
(Comments: For abbreviations, see paper IV, Table 8)

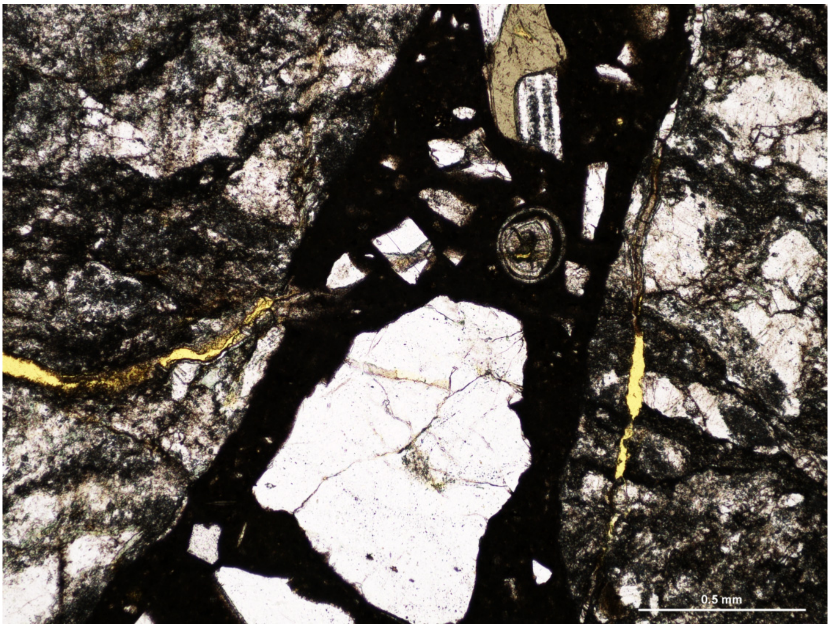

4.1-U-0.45. Note: ASR-gel in a pore and in a crack

Photo 3-49 Photo of a thin section after ending the ASR exposure.
(Comments: For abbreviations, see paper IV, Table 6)

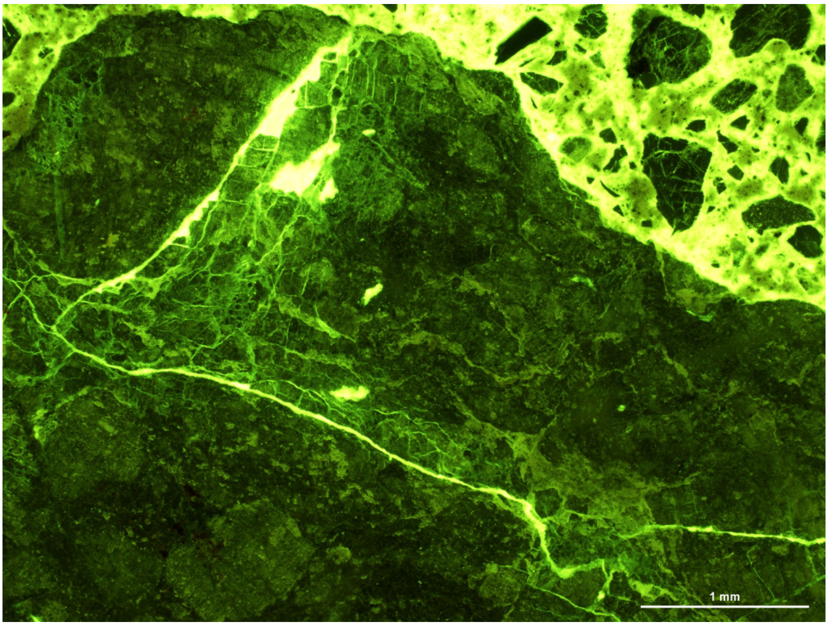

4.11-W-0.45. Note: Reacted cataclasite.

Photo 3-50 Photo of a thin section in UV-light after ending the ASR exposure.
(Comments: For abbreviations, see paper IV, Table 6)

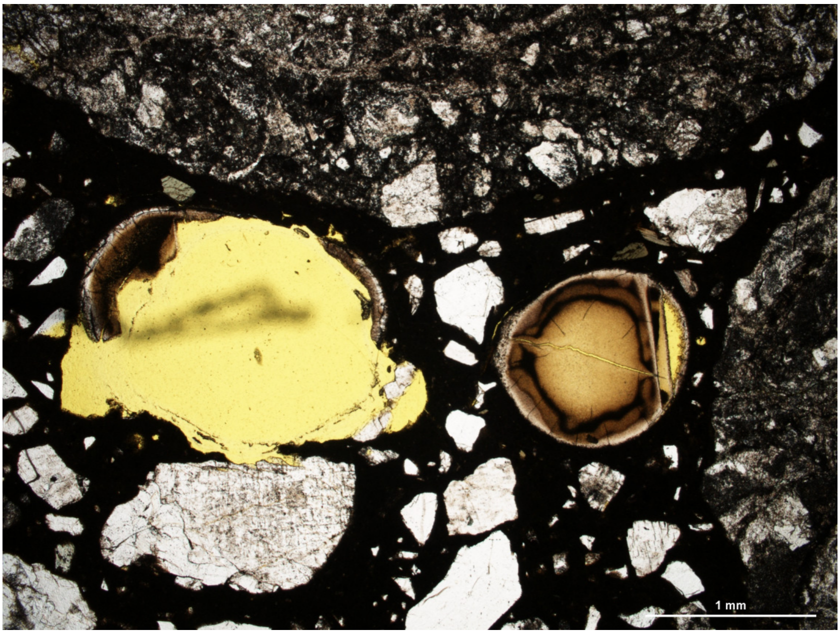

4.3-U-0.60. Note: ASR-gel in pores

Photo 3-51 Photo of a thin section after ending the ASR exposure.
(Comments: For abbreviations, see paper IV, Table 6)

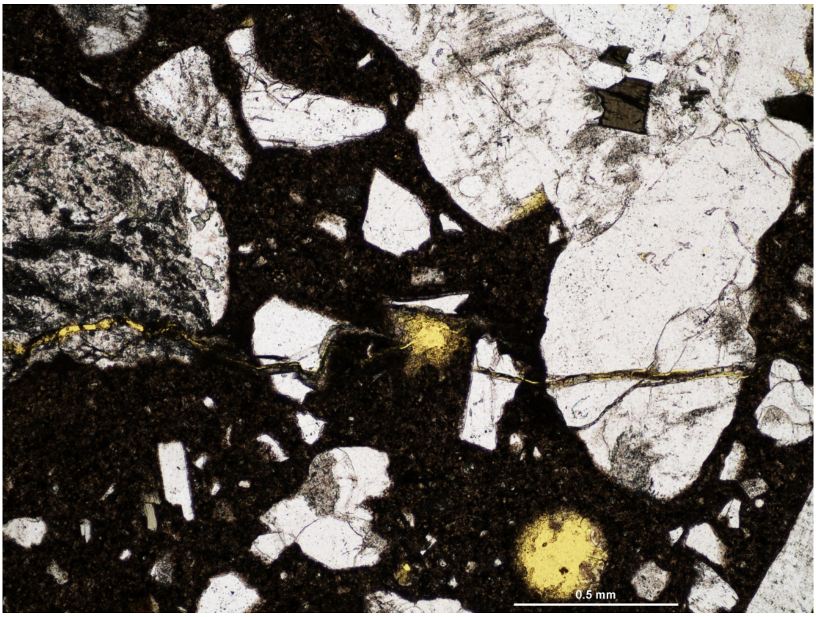

3.4-W-0.30. Note: ASR-gel in a crack and in pores

Photo 3-52 *Photo of a thin section after ending the ASR exposure.*
(Comments: For abbreviations, see paper IV, Table 5)

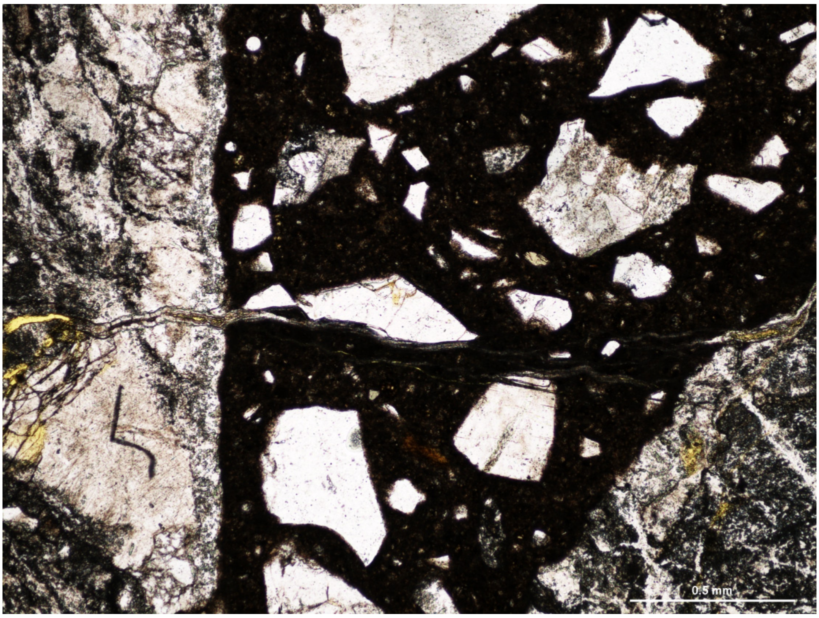

4.3-U-0.30. Note: ASR-gel in a crack between cataclasite particles

Photo 3-53 *Photo of a thin section after ending the ASR exposure.*
(Comments: For abbreviations, see paper IV, Table 6)

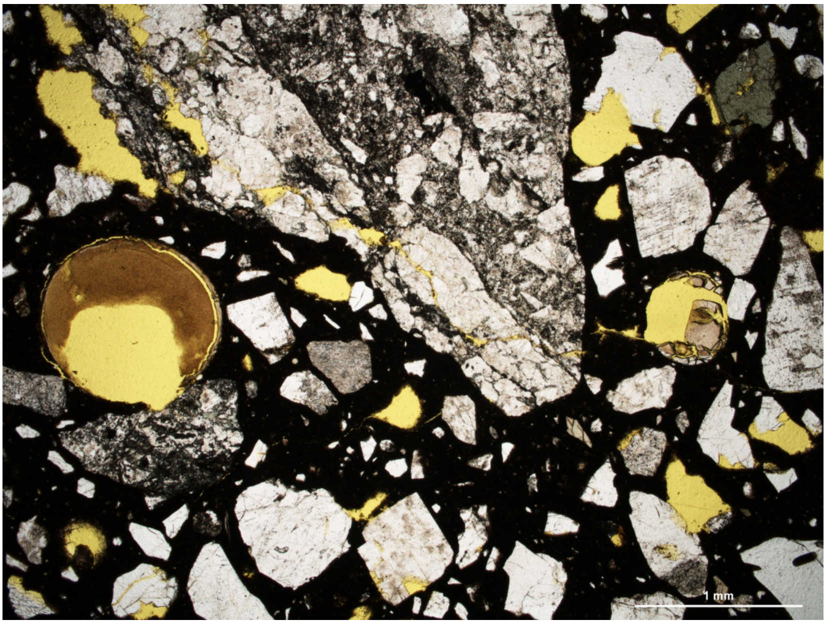

3.9-W-FA-0.45. Note: ASR-gel in pores

Photo 3-54 *Photo of a thin section after ending the ASR exposure.*
(Comments: For abbreviations, see paper IV, Table 5)

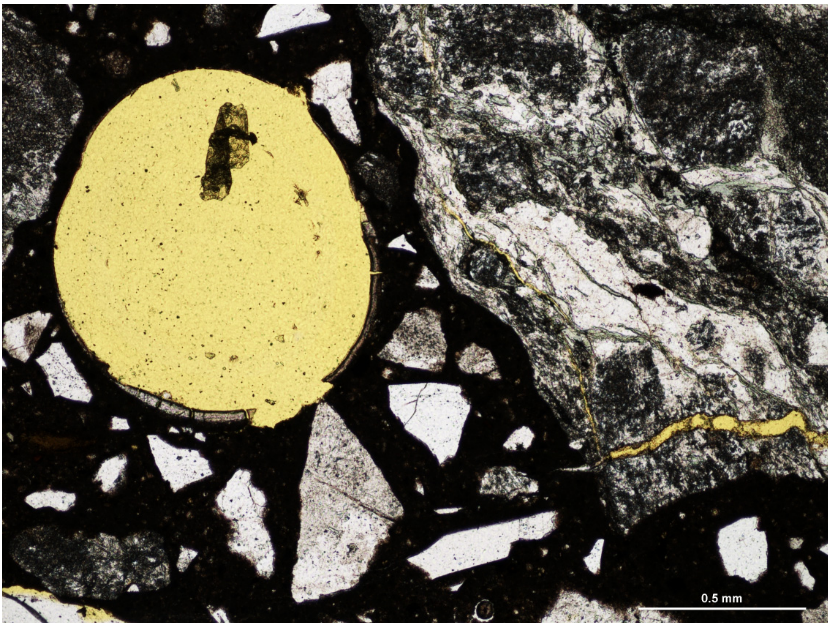

4.4-U-FA-0.45. Note: ASR-gel in a pore and in a crack in a cataclasite particle

Photo 3-55 *Photo of a thin section after ending the ASR exposure.*
(Comments: For abbreviations, see paper IV, Table 6)

Photos: SEM analysis

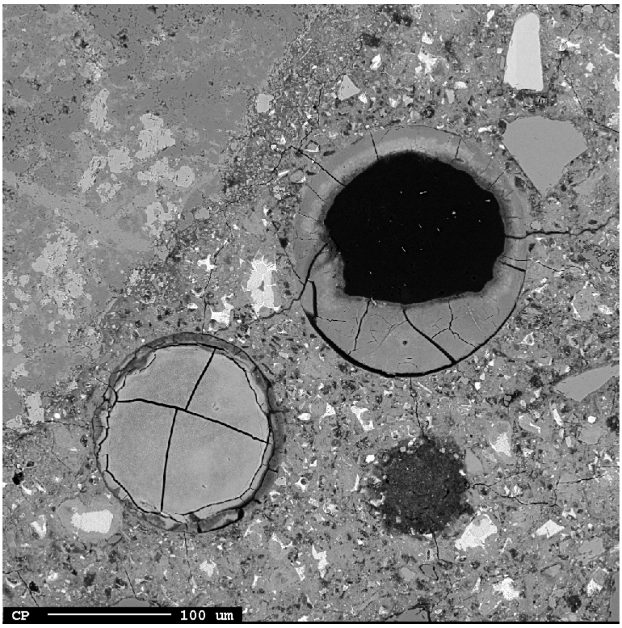

Photo 3-56 *Photo from SEM-analysis performed on a polished thin section of 4.1-U-0.45 after 39 weeks of ASR exposure. Note: ASR-gel in a pore close to an aggregate particle. (Comments: For abbreviations, see paper IV, Table 6)*

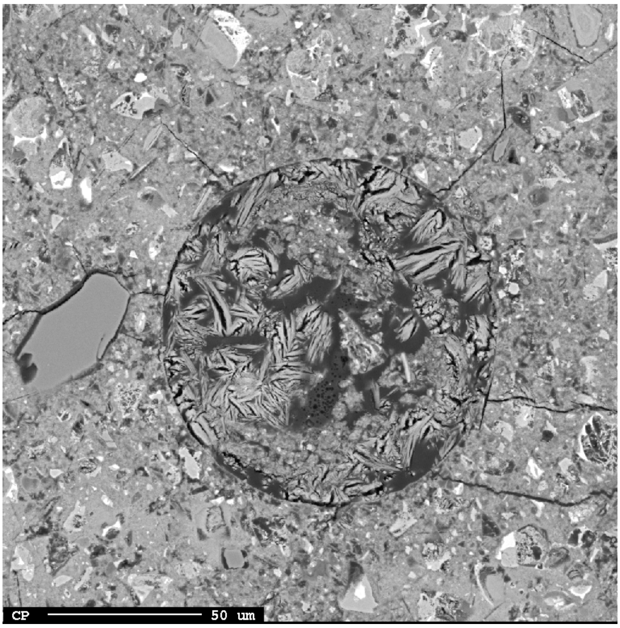

Photo 3-57 *Photo from SEM-analysis performed on a polished thin section of 4.3-U-0.60 after 39 weeks of ASR exposure. Note: Ettringite in a pore. (Comments: For abbreviations, see paper IV, Table 6)*

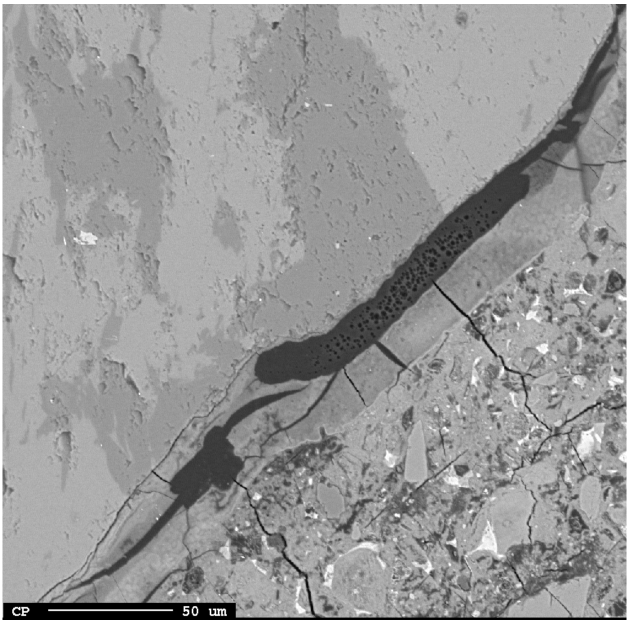

Photo 3-58 *Photo from SEM-analysis performed on a polished thin section of N.1-U-0.45 after 52 weeks of ASR exposure. Note: ASR-gel in the interfacial zone aggregate / cement paste. (Comments: For abbreviations, see paper IV, Table 7)*

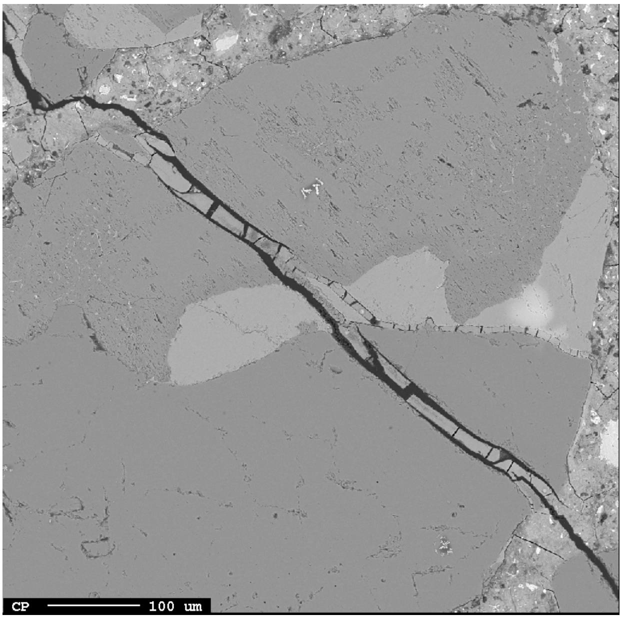

Photo 3-59 *Photo from SEM-analysis performed on a polished thin section of 3.4-W-0.30 after 112 weeks of ASR exposure. Note: ASR-gel in a crack in an aggregate particle. (Comments: For abbreviations, see paper IV, Table 5)*

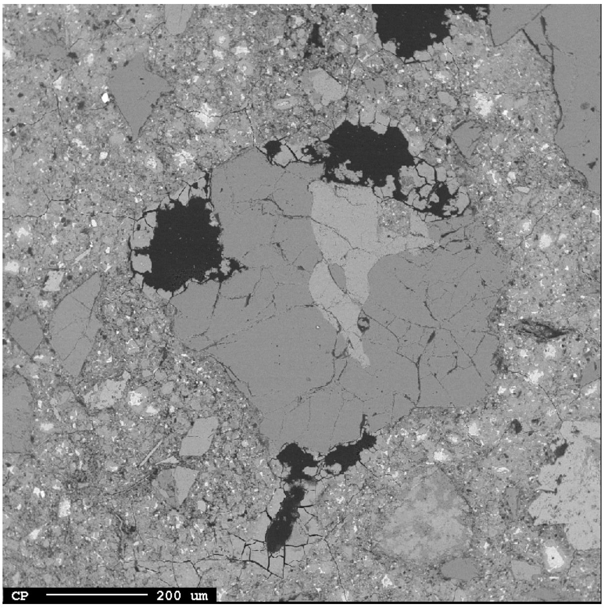

Photo 3-60 *Photo from SEM-analysis performed on a polished thin section of 4.12-W-0.45 after 39 weeks of ASR exposure. Note: Partly dissolved aggregate particle and some ASR-gel. (Comments: For abbreviations, see paper IV, Table 6)*

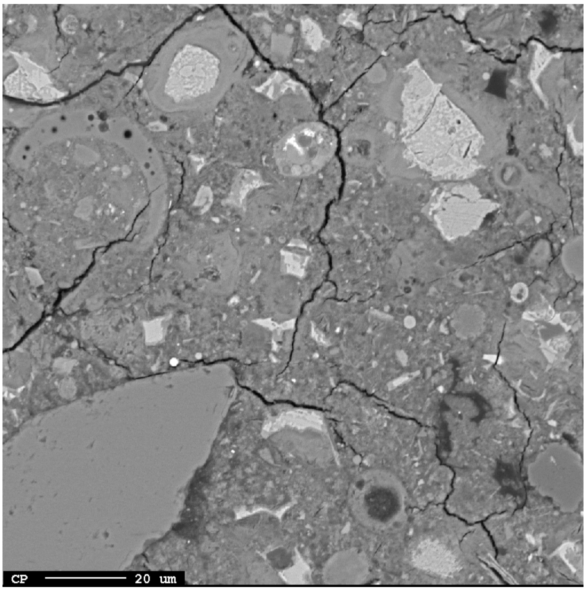

Photo 3-61 *Photo from SEM-analysis performed on a polished thin section of 4.4-U-FA-0.45 after 39 weeks of ASR exposure. Note: Remainder of a fly ash particle (curved – upper left corner). (Comments: For abbreviations, see paper IV, Table 6)*

Appendix 4: Comments on humidity and quality control during testing

Appendix 4

Appendix 4 Comments on humidity and quality control during testing

As discussed in the literature review paper [19], moisture will move from the warmer inner part to the colder outer parts of the concrete prisms during any overnight cooling before the measurements of length and weight. The outcome will be loss of some moisture during the cooling period (see results from the pilot testing discussed in paper IV, section 2.3.2). Despite that, no important differences in internal moisture state are observed at any time between pre-cooled prisms and prisms measured while being warm (see paper IV). However, before all the measurements of prism water uptake and internal moisture state, all the prisms were immediately sealed in tight polyethylene foil after being removed from their storage container, followed by an overnight cooling period before being unwrapped and prepared for the moisture measurements. This procedure hindered loss of water during the cooling-period. One minor exception with respect to effect of pre-cooling is observed: After 4 weeks of exposure, DCS and the internal RH is marginally lower in the pre-cooled prisms stored at 38°C compared with prisms measured warm. However, no deviations are observed at the end of the exposure period.

One important comment: If the periodic measurements are performed without pre-cooling the concrete prisms to ambient temperature, the high rate of evaporation and temperature loss during the measuring period will significantly influence the length and weight readings. Consequently, a detailed measuring procedure has to be strictly followed to secure that the reference readings and all the periodic measurements of length and mass are taken at the exact same time delay after removing each prism (one at the time) from the warm container (and the lid is put back on top). Immediately after each reading, the prism should be put back into the container. If some problems occur leading to a significant "time delay", the container should be put back into the storage room (or "reactor") before new measurements are performed the following day. In the present study, a detailed measuring procedure was developed (see Appendix 2). As part of this, each AAR-4.1 60°C steel container was immediately placed in an insulated box after removed it from the "reactor", while each 38°C container was placed on an insulating board. All the measurements of length and weight of the warm concrete prisms were performed without any kind of problems.

As discussed in the literature review paper [19], the type of container might significantly influence the internal moisture state of the prisms. The volume of the container, use of any cotton lining on the inside wall, the amount of water in the bottom and the tightness of the lid are important parameters in that respect. In the pilot study, RH inside the storage containers for the ASTM C-1293 CPT and the Norwegian CPT (see paper IV, Table 3) was measured to be close to 100 % when stored at 20°C. When inspected during testing, drops of water could be observed on the prism surfaces, indicating that the moisture content inside the containers is sufficient high. However, during testing at 38°C, all containers are stored in a dry room. Thus, the water level should be checked frequently and weight measurements should be used for quality control (see discussion on the next page).

RH inside the small AAR-4.1 60°C containers (see paper IV, Table 3 and photo in Appendix 3) has not been measured. However, even if no lining is used in these containers, inspections during pilot testing has shown that the prisms are completely covered with moisture due to condensation and water dripping and running along the prism surfaces. On the other hand, a possible source of error has been discovered for these containers placed inside the "reactor" with 100 % RH. During the pilot testing, the water level suddenly started to rise in some of the containers. In some cases, the lower part of the prisms was thus submerged in water. In such cases, the test series must be discarded due to the high extent of alkali leaching from the prisms that will result from partial immersion. Before starting the testing in the present study, a new sealing system was developed for these small AAR-4.1 storage containers (see Appendix 3, photo 3-8). After that, no similar problems have occurred.

Use of weight measurements as a quality control

As mentioned above, all containers are stored in a dry room during exposure to 38°C. If a lid develops a crack or if a screw cap (as used for the ASTM containers) is not sufficiently tightened, water may evaporate over time (as experienced in another project). The present study has shown that the RILEM AAR-3 containers (plastic tubes – see paper IV, Table 3 and photo in Appendix 3) are particularly vulnerable to drying due to the small amount of water in the bottom of the containers (only 350 ml). Consequently, to avoid any lack of water during testing, the water level should be controlled frequently. If at any time no water is left in the bottom of the container, the test series must be discarded.

The sealed 70x70x280 mm prisms stored in the 38°C dry room in single RILEM AAR-3 containers (without any water in the bottom – see paper IV, Tables 4 and 5) lost about 0.5 % weight (18-20 g) during the 52 weeks exposure period, meaning that the sealing (epoxy and aluminium foil) was not entirely tight. This led to about 0.015 % shrinkage of the prisms. In the RILEM CPTs, AAR-3 and AAR-4.1, a requirement is given to the recorded weight to ensure that sufficient water is present in the system. Until 2008, the draft method descriptions (e.g. the versions dated "30Sep07") stated that all the measurements related to a single test prism should be discarded if the weight loss recorded for the prism, with cross-section 75±5 mm and length 250±50 mm, was greater than 20 g. This means that a weight loss up to 0.4-0.8 w-% (depending on the prism size used) compared to the starting reference weight should be accepted. In light of the experience built up with the Norwegian CPT (where even prisms that exhibit minor shrinkage (e.g. if a non-reactive concrete mix with a binder with some self-desiccation is tested) normally increase at least 0.2 w-% in weight after the first 0.5 year of exposure - see paper II), and the recorded weight loss and shrinkage of the sealed prisms in the PhD test series (see above), this requirement to maximum allowed weight loss seems far too little restrict. Based on a suggestion from SINTEF to RILEM TC-219 ACS, the former requirement has now been sharpened. In the current method descriptions no weight reduction of the prisms, compared with the reference weight at start of testing, is allowed at the time of the final weight reading. If a net weight loss is recorded at the time of executing the last length readings, the measurements relating to these prisms shall be discarded. However, it might be more reasonable (for sure more conservative) to question (or at least re-check) test results showing less weight gain than 0.2 w-% in the end of the ASR exposure period.

One exception from this more restrict requirement might be if the moulds are stored in a fog room or similar high humid storage during the first 24 hours of curing. If so, the concrete prisms can suck water from the surroundings during the hydration phase, leading to a higher reference weight compared with storage under a tight plastic foil (as used in this study). One of the laboratories in the EU "PARTNER" project (see paper I) cured the prisms in a fog room at 20°C after casting (i.e. gave the prisms better curing conditions than the other laboratories). For some non-reactive mixtures tested according to the RILEM AAR-4.1 CPT, the prism hardly increased in weight at all. Some prisms even exhibited minor weight loss. Even though, the small expansions measured for these non-reactive mixtures were comparable with the results from other laboratories performing parallel test and that measured significantly higher weight gain during the ASR exposure period.

Appendix 5: Follow-up project – laboratory testing

- Materials: Aggregates and cement types
- Mixture proportions: Aggregate and binder compositions
- ASR test procedures
- Photo: Casting of concrete prisms

Appendix 5

Materials: Aggregates and cement type

Aggregate types:

- "Årdal" (gneiss/granitic) sand and coarse aggregate (Norwegian reference non-reactive aggregate [20], [7])
- "Ottersbo" (cataclasite) coarse aggregate (Norwegian reference reactive aggregate [20], [7]; reactive minerals are crypto- to microcrystalline quartz)
- Slowly reactive Norwegian natural sand and coarse aggregate (same as "N4" in the EU "PARTNER" project (see paper I); contain various aggregate types (dominated by gneiss/granite) - reactive minerals are crypto- to microcrystalline quartz in sandstones, siltstones and cataclastic rocks)
- "Spratt" (silicified limestone) coarse aggregate (used as reference reactive aggregate "worldwide"; reactive minerals are crypto- to microcrystalline quartz)
- Highly reactive German coarse aggregate (crushed river gravel containing limestone with impurities, marl, sandstone and a little content of cataclastic rocks) from Upper Rhine (used as "reference" reactive aggregate in some German ASR tests; reactive minerals are micro- to cryptocrystalline quartz)

The first two aggregates, i.e. Årdal sand and Ottersbo coarse aggregate, are the same as used in the PhD laboratory program.

Cement types:

- High alkali CEM I (alkali content 1.24 % Na_2O_{eq})
- Low alkali CEM I (alkali content 0.60 % Na_2O_{eq})
- Fly ash cement, CEM II/A-V (containing 21.6 % of a class F fly ash, co-grinded with the clinker; alkali content 1.25 % Na_2O_{eq} incl. alkalis in the fly ash)
- Slag cement, CEM III/B (incl. 68 % slag; alkali content 0.78 % Na_2O_{eq} incl. alkalis in the slag)

The first three cement types are the same as used in the PhD laboratory program (paper IV and V).

Mixture proportions: Aggregate and binder compositions

In total, 20 different concrete mixtures have been prepared with the aggregates and cement types listed above, see Table 5-1. In these mixtures, the following has primarily been varied (the motivation is given in brackets):

- Aggregate binder combination (document the alkali reactivity of different aggregate/binder combinations when tested according to the most promising test procedures used in the PhD study, and furthermore compare the results with field behaviour in the field exposure sites – see Appendix 6)
- Alkali content (determine the alkali threshold for various aggregate/binder combinations)

Table 5-1: Concrete mix design (the numbers represent the number of mixes performed).

	Cement type			
Aggregate type[1]	CEM I	Fly ash cement	Slag cement	Total alkali content (kg/m^3 Na_2O_{eq})
Årdal sand (F/C)	1	--	--	5.5
"N4" (F/C)	1	--	--	5.5
Ottersbo[2] (C)	3	2	1	2.0, 2.8 and 3.7 (CEM I); 5.0 and 6.5 (fly ash cement); 4.0[3] (50/50 CEM I/slag cement)
Spratt[2] (C)	3	2	1	1.5, 2.0 and 2.9 (CEM I); 5.0 and 6.5 (fly ash cement); 4.0[3] (50/50 CEM I/slag cement)
Upper Rhine[2] (C)	1	2	3	5.5 (CEM I); 5.0 and 6.5 (fly ash cement); 4.0[3] and 5.0[3] (50/50 CEM I/slag cement); 3.1 (slag cement; 68 % slag)

[1] *F=Fine fraction, C=Coarse fraction* [2] *Årdal sand was used as the fine fraction*
[3] *50/50 high alkali CEM I/slag cement (in total 34 % slag)*

ASR test procedures

The following ASR test procedures used in the PhD laboratory program are included in the follow-up project (see paper IV, Tables 5-8):

- Norwegian CPT (named "N.2" in the PhD study)
- ASTM C 1293 (1 and 28 days of pre-storage at ambient temperature)
- RILEM AAR-4.1 (1 and 28 days of pre-storage at ambient temperature, named "4.2" and "4.4" in the PhD study)
- RILEM AAR-3 (use of wrapping added alkalis with pH 14.2, named "3.12" in the PhD study)
- RILEM AAR-4.1 (use of wrapping added alkalis with pH 14.2, named "4.12" in the PhD study)

The reliability of these test procedures will be assessed against the behaviour of the concrete cubes stored at the two field exposure sites (see Appendix 6).

In total, 115 single test series are included in the follow-up project.

Photo: Casting of concrete prisms

Photo 5-1 Casting of concrete prisms.

Appendix 6: Follow-up project - field exposure sites

- Procedure for preparation and measuring of outdoor exposed cubes
- Photos: production of concrete cubes; two field exposure sites

Appendix 6

Procedure for preparation and measuring of outdoor exposed cubes

1. SCOPE

The "field site test" is aiming to provide a correlation between results obtained in accelerated concrete prism tests in the laboratory with "real behaviour" of identical concrete mixes stored outdoors under natural climatic conditions.

2. PRINCIPLE

Two 300 mm concrete cubes with the aggregate and binder under test are cast and stored outdoors under natural climatic conditions. The same principle and test setup as applied in the PARTNER project is applied, except the extra "wet stored" cube is omitted. In a sub-project within the COIN program (follow-up project based on the PhD study of Jan Lindgård), one cube is stored at SINTEF in Trondheim (A) and a parallel cube (B) is stored at LNEC in Lisbon. The cubes are stored on wood borders (see Figure 4) and exposed to the sun and ambient rainfall - for the SINTEF cubes, also freezing and thawing during the winter season. Measurements of changes in dimension are made periodically up to a concrete age of at least 5 years, but preferably as long as it takes to get reliable data from field (i.e. longer time for assumed non-reactive or very slowly reactive concrete mixes). Possible cracking has also to be assessed.

3. PREPARATION OF CUBES

Moulds

Two moulds suitable for casting 300 mm concrete cubes shall be used.

Casting and curing

The concrete used for the "field site test" should be of the same composition as the concrete to be compared with. To guarantee this, the best way is to cast the concrete specimens for the accelerated laboratory testing and for the "field site test" from the same concrete batch. However, in the COIN project, the cube mixes are added an air entraining agent to secure frost resistance. Thus, separate cubes batches are prepared.

Cast two cubes with a lateral length of 300 mm by filling each mould in three layers, with sufficient compaction of each layer by stamping with a steel bar and by applying a casting ladle along the sides. Cure the concrete in the moulds at 20±2 °C and relative humidity of not less than 90 % under moist covers for 24±0.5 hours. De-mould, before continuing the storage at similar humid storage conditions (at SINTEF, the cubes are stored under plastic sheets and covered with wet burlap sacks).

Monitoring

After sufficient curing, i.e. at least two weeks of humid laboratory storage, two pairs of non-corroding metallic measuring screws shall be glued in drilled holes on the top surface and on two adjacent side faces. The sketch in Figure 1 shows the measuring directions and the position of the 12 screws.

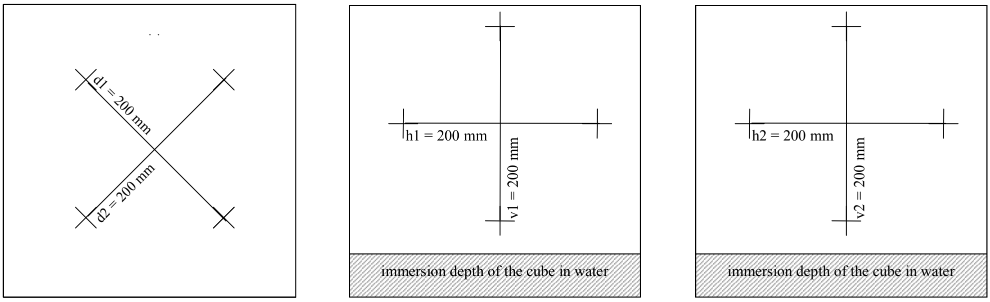

top surface

side face no. 1

side face no. 2
(adjacent to side face no. 1)

Figure 1. Positions of measuring screws on the concrete cube surfaces. *Comment: The figure is copied from the procedure applied in the PARTNER project. In the current PhD project, no water storage is applied. Thus, the screws on the side faces have a centric location on each side face.*

Before drilling the screw holes, with a drill diameter equal to the screw diameter and a hole depth 1-2 mm deeper than the length of the screws, drill the first hole and mark out the exact position of the other holes by applying the 200 mm "length marker bar" shown in Figure 2.

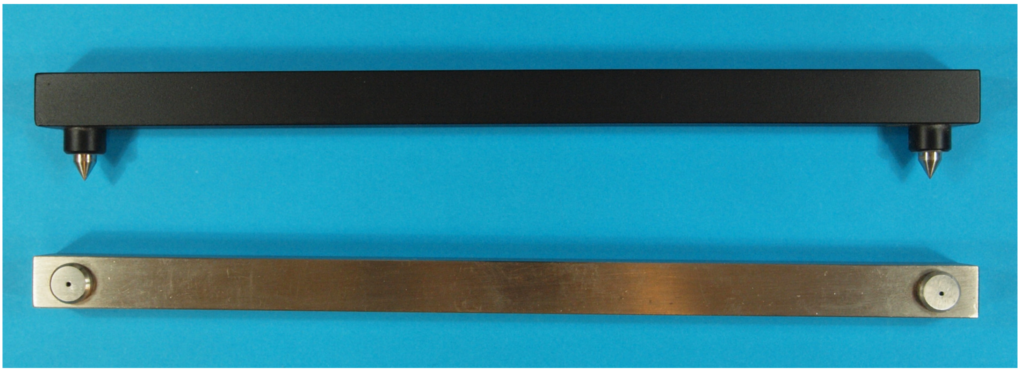

Figure 2. 200 mm "length marker bar" (black) and the 200 mm Invar reference bar.

At SINTEF, brass screws of dimension Φ x l = 8 mm x 10 mm are prepared by cutting a threaded brass bar (or alternatively a longer brass screw), see Figure 3. After cutting, the end faces of the screws are slightly grinded. A two components glue named ”Schnell-klebstoff X60” is applied to glue the screws. It can be ordered from: Hottinger Baldwin Measurements HBM (www.hbm.com). Supplement information (e.g. the nearest supplier or technical data) can be found at the website (search for “X60”).
At least one day after gluing the screws, a measuring hole is made in each screw by striking a bodkin with a hammer, before carefully drilling a hole with a 1.2 mm drill (see Figure 4).

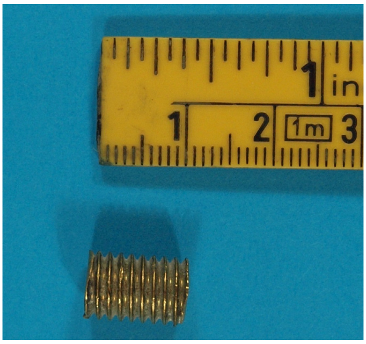

Figure 3. Brass screws of dimension Φ x l = 8mm x 10 mm applied at SINTEF.

Figure 4. Top surface with brass screws glued in drilled holes. The arrow shows a measuring hole.

4. OUTDOOR STORAGE

After sufficient curing in the laboratory, i.e. at least 14 days of moist curing (see above), the monitored cubes shall be stored outdoors on wood borders. The orientation of the cubes related to the sun is shown on the sketch in Figure 3 and in the enclosed measuring form.

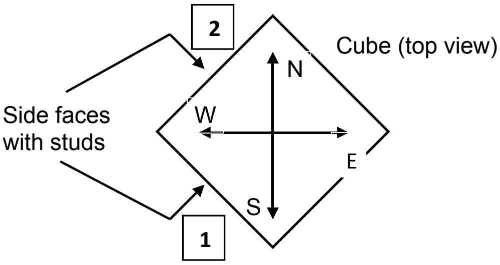

Orientation of the cubes;
N = North
S = South
W = West
E = East

Figure 3. Orientation of the cubes related to the sun.

5. MEASUREMENTS

Equipment

The length comparator shall be such as to accommodate the shape of the holes in the screws glued on the cubes. The standard gauge of the length comparator shall be 200 mm wide. The gradation of the comparator shall not be greater than 0.002 mm and the error throughout the range of traverse shall be no more than 0.005 mm. At SINTEF and LNEC, a digital Demec mechanical strain gauge with length 200 mm and gradation 0.001 mm is applied – see Figure 4.

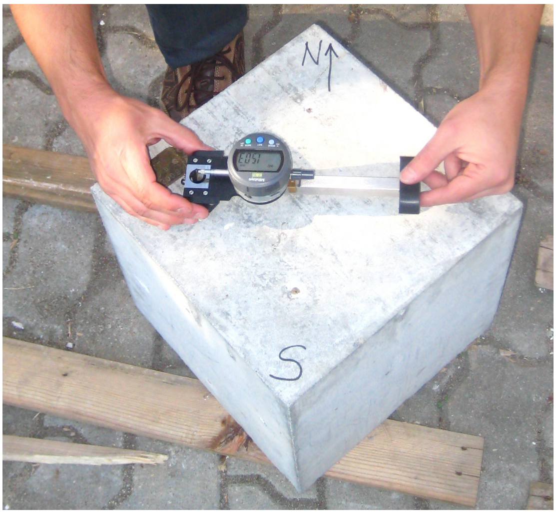

Figure 4. 200 mm digital Demec mechanical strain gauge.

Length readings

Measuring procedure

To avoid errors due to temperature movements of the concrete, all measurements (incl. the initial readings) should be executed at approximately the same internal concrete temperature. Preferably, the concrete temperature should not vary more than **±3°C** between each periodically measurement. It is recommended to do the readings in the morning, before the sun becomes too strong, and then in periods with rather stable temperature during the 24-hour period (to avoid temperature gradients in the concrete cubes). At SINTEF in Trondheim, the readings are normally taken at air temperatures between 10 and 15°C. The air temperature and the relative humidity have to be measured and reported on the enclosed measuring form.

At every measuring, make sure that the screws are clean to guarantee precise accommodation to the measuring device. One could benefit of placing an adhesive tape over each screw to avoid contamination during storage.

Before measuring each cube, adjust the strain gauge to zero while measuring the Invar rod that followed the Demec strain gauge ("reference zero reading", labelled "Invar, L_i" in the measuring form). For each cube, six length measures shall be taken - see below and Figure 1. At every measure, read the length, remove the strain gauge and measure once more. If the two following readings deviate more than **±0,002 mm**, read at least once more. If the readings still deviate more than ±0,002 mm, adjust to zero on the Invar rod and start all over again with the six readings.

If the accuracy of "each pair of readings" is acceptable, i.e. the two following readings deviate not more than ±0,002 mm, the mean values measured shall be noted in the measuring form. After taken the sixth and last length reading, the length of the Invar rod shall be read once more ("control measure"). If the length has changed more than **±0,003 mm** compared to the "reference zero reading", discard all the measurements on the actual cube, adjust to zero on the Invar rod and start all over again with the six readings.

Initial measurements

After the cubes have been placed at the exposure site and "acclimatized" to the actual "reading temperature", take the following initial length readings - see Figure 1 and the enclosed measuring form:

$L_{d1/0}$ = diagonal dimension no. 1 on the top surface (at time "0") (North-South)
$L_{d2/0}$ = diagonal dimension no. 2 on the top surface (East-West)
$L_{v1/0}$ = vertical dimension, side face no. 1
$L_{h1/0}$ = horizontal dimension, side face no. 1
$L_{v2/0}$ = vertical dimension side, face no. 2
$L_{h2/0}$ = horizontal dimension, side face no. 2

Periodically length measurements

The periodically length readings of each cube (i.e. $L_{d1/t}$, $L_{v1/t}$, etc.) should be repeated every 6 months, preferably in the spring and the fall in periods with rather stable temperature during the 24-hour period. In the measuring form, "t" is the time in months after the initial length readings were taken.

Visual control

Also the occurrence of cracking and gel exudations shall be noted at every measuring date. If cracks are visible, measure the crack width with a crack width gauge and document the figures in a separate form. Preferably, a photo should be taken and saved digitally.

6. EXPRESSION AND REPORTING RESULTS

Calculate the increase in dimensions of the cube for each period of measurement from the difference between the initial readings; $L_{xx/0}$. Differentiate thereby between the diagonal dimensions on the surface, the horizontal dimensions and the vertical dimensions on the side faces as follows.

Firstly calculate the following mean values:

Diagonal dimensions: $L_{dm/0} = (L_{d1/0} + L_{d2/0})/2$ $L_{dm/t} = (L_{d1/t} + L_{d2/t})/2$
Vertical dimensions: $L_{vm/0} = (L_{v1/0} + L_{v2/0})/2$ $L_{vm/t} = (L_{v1/t} + L_{v2/t})/2$
Horizontal dimensions: $L_{hm/0} = (L_{h1/0} + L_{h2/0})/2$ $L_{dm/t} = (L_{h1/t} + L_{h2/t})/2$

where "m" is the mean value and "t" the time in months after the initial length readings were taken.

Secondly calculate the change of dimensions in percent:

Diagonal change: $L_{dt} = ((L_{dm/t} - L_{dm/0}) / L_{dm/0}) \times 100\ \%$
Vertical change: $L_{vt} = ((L_{vm/t} - L_{vm/0}) / L_{vm/0}) \times 100\ \%$
Horizontal change: $L_{ht} = ((L_{hm/t} - L_{hm/0}) / L_{hm/0}) \times 100\ \%$

Finally report the dimension changes to the nearest 0.001 %.

In order to make the cracking assessable, give the cube marks according to the following table.

Stage of damage	Characteristic	Crack width
0	no damage	-
1	isolated fine cracks	< 0.2 mm
2	single fairly coarse cracks	0.2 – 0.5 mm
3	several fairly coarse cracks	0.2 – 1.0 mm
4	severe cracking	> 1 mm

Report the stage of damage e.g. as $C_t = 1$, where "t" is the time in months the concrete cubes have been exposed outdoors. Also the seasonable climatic data, i.e. the air temperature and the relative humidity, have to be reported. They are necessary to assess, whether upcoming expansion is caused by swelling or temperature changes or induced by ASR.

FIELD CUBES stored in Trondheim / Lisbon – dimension readings

Recipe: **Cube marked**: **Date of casting**: **Date placed in field**:

Time of reading	Date	Weather (temp? sunny or cloudy?)	Sign.	Storage time, t (months)	Readings (mm)							
					Invar	Top		Side face 1		Side face 2 (adjacent to side face 1)		Invar
					L_i	$L_{d1/t}$	$L_{d2/t}$	$L_{v1/t}$	$L_{h1/t}$	$L_{v2/t}$	$L_{h2/t}$	L_i
Zero reading (lab.) [1]		°C,		0								
Zero reading field [1]		°C,										
New zero reading field [2]		°C,										
New zero reading field [3]		°C,										
Annual reading		°C,										
Annual reading		°C,										
Annual reading		°C,										
Annual reading		°C,										
Annual reading		°C,										
Annual reading		°C,										
Annual reading		°C,										
Annual reading		°C,										
Annual reading		°C,										
Annual reading		°C,										
Annual reading		°C,										
Annual reading		°C,										
Annual reading		°C,										
Annual reading		°C,										

[1] SINTEFs new measuring device (measured in Trondheim)

[2] SINTEFs new measuring device (reading taken at LNEC, Lisbon, Portugal)

[3] LNECs measuring device (applied for the remaining readings at LNEC)

v = vertical
h = horisontal

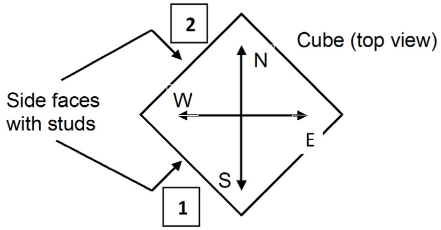

Jan Lindgård 2013-09-19

Photos: production of concrete cubes; two field exposure sites

Photo 6-1 Casting of concrete cubes.

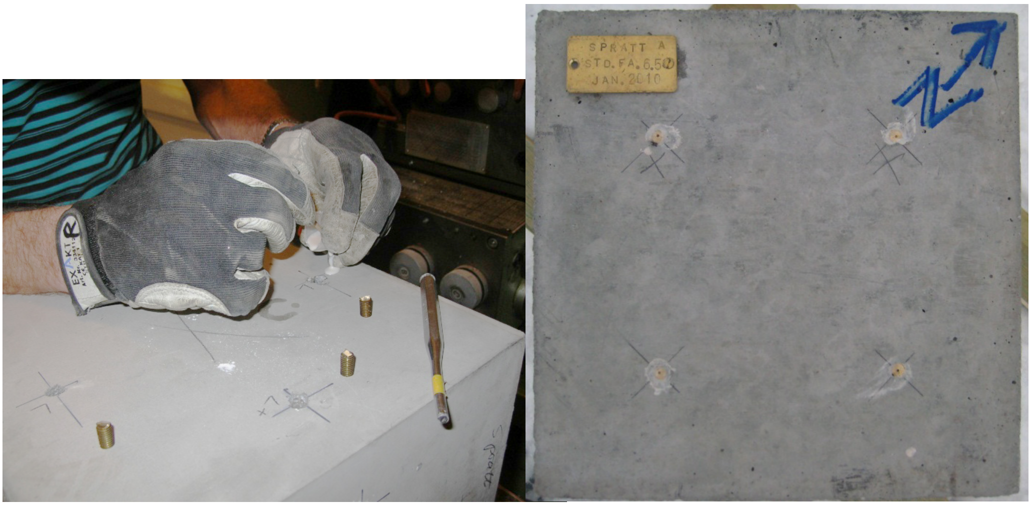

Photo 6-2—6-3 Preparation of measuring points (brass screws, glued in drilled holes; left) and final prepared cube including nameplate (right).

Photo 6-4 Field exposure site at SINTEF in Trondheim.

Photo 6-5 Field exposure site at SINTEF in Trondheim.

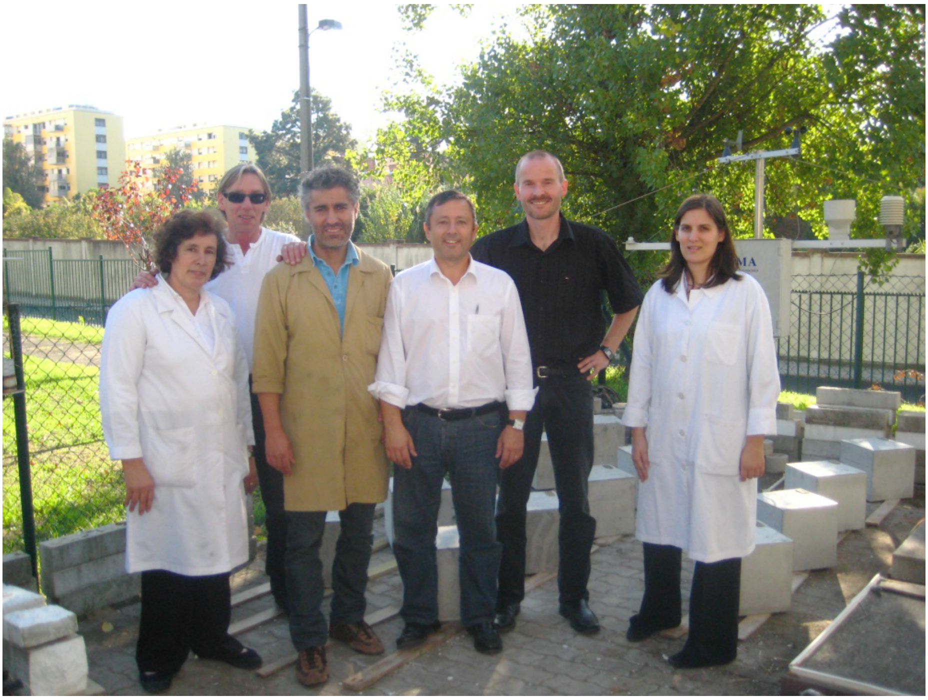

Photo 6-6 Field exposure site at LNEC in Lisbon, Portugal

Photo 6-7—6-8 Measurements of the cubes at the field exposure site at LNEC in Lisbon, Portugal.

References in appendices 1-6

References in Appendix 1-6

[1] M.-A. Bérubé, J. Duchesne, J.F. Dorion, M. Rivest, Laboratory assessment of alkali contribution by aggregates to concrete and application to concrete structures affected by alkali–silica reactivity, Cement and Concrete Research, 32 (2002) 1215-1227.
[2] ASTM C215-08 Standard Test Method for Fundamental Transverse, Longitudinal, and Torsional Frequencies of Concrete Specimens, in: American Society for Testing and Materials, Annual Book of ASTM Standards, 2008, pp. 7.
[3] Deutscher Ausschuss für Stahlbeton, DAfStb (Ed.) (2001): Vorbeugende Maßnahmen gegen schädigende Alkalireaktion im Beton: Alkali-Richtlinie. Beuth, Berlin, (DAfStb-Richtlinie).
[4] J. Lindgård, Ö. Andiç-Çakır, I. Borchers, M.T.A.M. Broekmans, E. Brouard, I. Fernandes, C. Giebson, B. Pedersen, C. Pierre, T.F. Rønning, M.D.A. Thomas, B.J. Wigum, RILEM TC219-ACS-P: Literature survey on performance testing, COIN project report 27, ISBN: 978-82-536-1209-6, 2011, pp. 164.
[5] D.A. Whiting, M.A. Nagi, Electrical resistivity of concrete - A literature review, PCA R&D Serial No. 2457, 2003, pp. 56.
[6] SINTEF internal procedure KS 14-05-04-128, Hardened concrete, Measurement of electrical resistivity, 2007.
[7] Norwegian Concrete Association: Alkali–aggregate reactions in concrete, Test methods and Requirements to Test Laboratories, NB32, 2005, pp. 39.
[8] ASTM C1293 - 08b Standard Test Method for Determination of Length Change of Concrete Due to Alkali-Silica Reaction, in, American Society for Testing and Materials, Annual Book of ASTM Standards, 2008, pp. 7.
[9] W. Bray, E.J. Sellevold, Water sorption properties of hardened cement paste cured or stored at elevated temperatures, Cement and Concrete Research, 3 (1973) 723-728.
[10] K. De Weerdt, H. Justnes, Microstructure of binder from the pozzolanic reaction between lime and siliceous fly ash, and the effect of limestone addition, in: 1st International Conference on Microstructure Related Durability of Cementitious Composites, Nanjing, China, 2008, pp. 107-116.
[11] K. De Weerdt, K.O. Kjellsen, E. Sellevold, H. Justnes, Synergy between fly ash and limestone powder in ternary cements, Cement and Concrete Composites, 33 (2011) 30-38.
[12] K. De Weerdt, M. Ben Haha, G. Le Saout, K.O. Kjellsen, H. Justnes, B. Lothenbach, The effect of temperature on the hydration of composite cements containing limestone powder and fly ash, Materials and Structures, 45 (2012) 1101-1114.
[13] E. Sellevold, Resistivity and humidity measurements of repaired and non-repaired areas in Gimsøystraumen bridge, in: International Conference: Repair of concrete structures, from theory to practice in a marine environment, Svolvær, Norway, 1993.
[14] E.J. Sellevold, T. Farstad, The PF-method - A simple way to estimate the w/c-ratio and air content of hardened concrete, in: ConMat'05 and Mindness Symposium ISBN 0-88865-810-9, The University of British Colombia, Vancouver, Canada, 2005.
[15] D.C. Montgomery, G.C. Runger, Applied Statistics and Probability for Engineers, Fourth ed., John Wiley and Sons, Inc., 2007.
[16] R.E. Walpole, Probability & Statistics for Engineers & Scientists, Business & Economics, Pearson Prentice Hall, 2007.
[17] A.M. Neville, Properties of concrete, 5 ed., Trans-Atlantic Publications, Inc., 2011.
[18] P.C. Aítcin, Does Concrete Shrink or Does it Swell?, in: Concrete International, December 1999, American Concrete Institute, Farmington Hills, Michigan, 1999.
[19] J. Lindgård, Ö. Andiç-Çakır, I. Fernandes, T.F. Rønning, M.D.A. Thomas, Alkali–silica reactions (ASR): Literature review on parameters influencing laboratory performance testing, Cement and Concrete Research, 42 (2012) 223-243.
[20] Norwegian Concrete Association: Durable concrete containing alkali reactive aggregates, NB21, 2004, pp. 33.